VOL. 704 NO. 1 2 JUNE 1995

JOURNAL OF CHROMATOGRAPHY A

INCLUDING ELECTROPHORESIS AND OTHER SEPARATION METHODS

ELSEVIER

JOURNAL OF CHROMATOGRAPHY A

INCLUDING ELECTROPHORESIS AND OTHER SEPARATION METHODS

Scope. The *Journal of Chromatography A* publishes papers on all aspects of **chromatography, electrophoresis** and related methods. Contributions consist mainly of research papers dealing with chromatographic theory, instrumental developments and their applications. In the *Symposium volumes*, which are under separate editorship, proceedings of symposia on chromatography, electrophoresis and related methods are published. *Journal of Chromatography B: Biomedical Applications* —This journal, which is under separate editorship, deals with the following aspects: developments in and applications of chromatographic and electrophoretic techniques related to clinical diagnosis or alterations during medical treatment; screening and profiling of body fluids or tissues related to the analysis of active substances and to metabolic disorders; drug level monitoring and pharmacokinetic studies; clinical toxicology; forensic medicine; veterinary medicine; occupational medicine; results from basic medical research with direct consequences in clinical practice.

Submission of Papers. The preferred medium of submission is on disk with accompanying manuscript (see *Electronic manuscripts* in the Instructions to Authors, which can be obtained from the publisher, Elsevier Science B.V., P.O. Box 330, 1000 AH Amsterdam, Netherlands). Manuscripts (in English; *four* copies are required) should be submitted to: Editorial Office of *Journal of Chromatography A*, P.O. Box 681, 1000 AR Amsterdam, Netherlands, Telefax (+31-20) 485 2304, or to: The Editor of *Journal of Chromatography B: Biomedical Applications*, P.O. Box 681, 1000 AR Amsterdam, Netherlands. Review articles are invited or proposed in writing to the Editors who welcome suggestions for subjects. An outline of the proposed review should first be forwarded to the Editors for preliminary discussion prior to preparation. Submission of an article is understood to imply that the article is original and unpublished and is not being considered for publication elsewhere. For copyright regulations, see below.

Publication information. *Journal of Chromatography A* (ISSN 0021-9673): for 1995 Vols. 683–714 are scheduled for publication. *Journal of Chromatography B: Biomedical Applications* (ISSN 0378-4347): for 1995 Vols. 663–674 are scheduled for publication. Subscription prices for *Journal of Chromatography A*, *Journal of Chromatography B: Biomedical Applications* or a combined subscription are available upon request from the publisher. Subscriptions are accepted on a prepaid basis only and are entered on a calendar year basis. Issues are sent by surface mail except to the following countries where air delivery via SAL is ensured: Argentina, Australia, Brazil, Canada, China, Hong Kong, India, Israel, Japan, Malaysia, Mexico, New Zealand, Pakistan, Singapore, South Africa, South Korea, Taiwan, Thailand, USA. For all other countries airmail rates are available upon request. Claims for missing issues must be made within six months of our publication (mailing) date. Please address all your requests regarding orders and subscription queries to: Elsevier Science B.V., Journal Department, P.O. Box 211, 1000 AE Amsterdam, Netherlands. Tel.: (+31-20) 485 3642; Fax: (+31-20) 485 3598. Customers in the USA and Canada wishing information on this and other Elsevier journals, please contact Journal Information Center, Elsevier Science Inc., 655 Avenue of the Americas, New York, NY 10010, USA, Tel. (+1-212) 633 3750, Telefax (+1-212) 633 3764.

Abstracts/Contents Lists published in Analytical Abstracts, Biochemical Abstracts, Biological Abstracts, Chemical Abstracts, Chemical Titles, Chromatography Abstracts, Current Awareness in Biological Sciences (CABS), Current Contents/Life Sciences, Current Contents/Physical, Chemical & Earth Sciences, Deep-Sea Research/Part B: Oceanographic Literature Review, Excerpta Medica, Index Medicus, Mass Spectrometry Bulletin, PASCAL-CNRS, Referativnyi Zhurnal, Research Alert and Science Citation Index.

US Mailing Notice. *Journal of Chromatography A* (ISSN 0021-9673) is published weekly (total 52 issues) by Elsevier Science B.V., (Sara Burgerhartstraat 25, P.O. Box 211, 1000 AE Amsterdam, Netherlands). Annual subscription price in the USA US$ 5389.00 (US$ price valid in North, Central and South America only) including air speed delivery. Second class postage paid at Jamaica, NY 11431. **USA POSTMASTERS**: Send address changes to *Journal of Chromatography A*, Publications Expediting, Inc., 200 Meacham Avenue, Elmont, NY 11003. Airfreight and mailing in the USA by Publications Expediting.

See inside back cover for Publication Schedule, Information for Authors and information on Advertisements.

0021-9673/95/$09.50

Printed in the Netherlands

VOL. 704, NO. 1 JOURNAL OF CHROMATOGRAPHY A 2 JUNE 1995

CONTENTS

(Abstracts/Contents Lists published in Analytical Abstracts, Biochemical Abstracts, Biological Abstracts, Chemical Abstracts, Chemical Titles, Chromatography Abstracts, Current Awareness in Biological Sciences (CABS), Current Contents/Life Sciences, Current Contents/Physical, Chemical & Earth Sciences, Deep-Sea Research/Part B: Oceanographic Literature Review, Excerpta Medica, Index Medicus, Mass Spectrometry Bulletin, PASCAL-CNRS, Referativnyi Zhurnal, Research Alert and Science Citation Index)

REVIEWS

REGULAR PAPERS

Column Liquid Chromatography

(Continued overleaf)

Contents (continued)

SHORT COMMUNICATIONS

Column Liquid Chromatography

Gas Chromatography

Electrophoresis

JOURNAL OF CHROMATOGRAPHY A

VOL. 704 (1995)

JOURNAL OF CHROMATOGRAPHY A

INCLUDING ELECTROPHORESIS AND OTHER SEPARATION METHODS

ELSEVIER

Amsterdam – Lausanne – New York – Oxford – Shannon – Tokyo

0021-9673/95/$09.50

Printed in the Netherlands

ELSEVIER

Journal of Chromatography A, 704 (1995) 1–25

JOURNAL OF CHROMATOGRAPHY A

Review

Laser-induced fluorescence detection of native-fluorescent analytes in column liquid chromatography, a critical evaluation

R.J. van de Nesse, N.H. Velthorst, U.A.Th. Brinkman, C. Gooijer*

Department of Analytical Chemistry, Free University, de Boelelaan 1083, 1081 HV Amsterdam, Netherlands

First received 14 November 1994; revised manuscript received 12 January 1995; accepted 12 January 1995

Abstract

This paper critically evaluates aspects that need to be considered when applying lasers instead of conventional lamps in fluorescence detection combined with column liquid chromatography (LC). To exclude the often underestimated role of chemical derivatization reactions as far as detection limits are concerned, emphasis is on analytes showing native fluorescence. First of all basic features of both continuous wave and pulsed lasers are considered, including a quantitative treatment of saturation and photodecomposition effects. Subsequently a detailed treatment on signal-to-noise in laser induced fluorescence (LIF) is presented, the various definitions of detection limits operative in the literature are compared and flow cell constructions are considered. The paper ends with a comparison between conventional fluorescence and LIF detection in LC, an overview of published data on detection limits and a discussion on future trends.

Contents

* Corresponding author.

0021-9673/95/$29.00
SSDI 0021-9673(95)00053-4

1. Introduction

Among the many spectroscopic methods that are applied in column liquid chromatography (LC), fluorescence spectroscopy has a prominent place because of its ability to detect analytes at trace levels [1,2]. Because, in general, the fluorescence signal intensity is directly proportional with the radiant power, the sensitivity of fluorescence detection can be improved by the use of lasers instead of conventional lamps as the excitation source [3]; however, it should be kept in mind that the crucial parameter is the signal-to-noise ratio. Proper excitation wavelength selection is an aspect of primary importance. Unfortunately, most lasers provide only a number of discrete lines, while there is a lack of output in the UV part of the spectrum, especially in the deep-UV region, i.e. below 300 nm. Since there are not many relevant native-fluorescent compounds that absorb radiation in the visible range, the applicability of visible laser-induced fluorescence (LIF) is limited. This readily explains the widespread attention devoted to derivatization procedures to convert analytes into fluorescent products that can be optimally excited by means of available laser lines [4]. Although standard solutions of pure fluorophores can be quantified by LIF at extremely low concentrations, derivatization of analytes at ultra-trace levels in complex matrices gives rise to various problems and achievable limits of detection (LOD) are often several orders of magnitude higher [5]. Fortunately, recent developments in laser technology have led to the design of systems that can provide deep-UV radiation and which are (or will soon become) commercially available. It is expected therefore, that in the near future studies on LIF of native-fluorescent analytes will see a notable increase.

This paper deals with aspects that need to be considered when applying lasers instead of conventional light sources with emphasis on UV excitation. In Section 2 various laser types are discussed that can be used in LIF detection. Attention is also paid to fluorescence saturation and photochemical decomposition, phenomena that can play a role in LIF because of the high incident light powers and tightly focused laser beams. LIF detection in LC is considered in Section 3 and includes a discussion on the parameters that influence signal intensity and noise, different flow cell constructions, and a comparison between LIF and conventional fluorescence detection. Besides, the literature on LC–LIF of native-fluorescent analytes, is reviewed. Finally, in Section 4 general conclusions are drawn and future developments are outlined.

2. Basic aspects of lasers in fluorescence detection

2.1. Laser types

Since the introduction of the ruby laser in 1960 [6], several laser types have been developed and commercialized, each one with its own unique properties. The preference of an analytical spectroscopist for a particular laser system will be determined by various criteria: wavelength availability, light power, pulsed/continuous-wave (CW) operation, output stability, lifetime, required facilities, robustness, size and, last but not least, costs. Some of these aspects are mutually related. For instance, deep-UV light is provided by a very expensive argon-ion laser that requires a high power line (e.g. 360 V, 3 phase, 50 A), a large cooling facility (e.g. 20 l water min^{-1}) and much laboratory space. On the other hand, the same laser type is available as a small size air-cooled version which produces only

visible light at low power, at a price which is a fraction of that of its big brother. It is therefore difficult to make general statements about the properties of a particular laser type because different versions are commercially available; for instance, Laser Focus World Buyers Guide 27 (1992) describes more than 360 argon-ion lasers that are on the market [7]. There is one aspect, however, that applies to all lasers: increasing light power (especially in the UV region) costs money.

In this section, technical details are described of various laser types important in analytical fluorimetry. Most information is derived from Laser Focus World, a magazine that appears monthly; especially the regular contributions of J. Hecht are worthwhile [7–9].

Laser output can be continuous or pulsed. In Table 1 the most popular CW lasers applied in analytical fluorimetry are summarized. It is clear that the number of available wavelengths is limited, especially in the UV region, which is a serious shortcoming in LIF. The wavelengths produced by the argon-ion laser depend on the electrical power input. Visible laser lines arise from the emission of singly ionized argon while doubly ionized argon provides lines in the UV part of the spectrum. The latter demand high power discharges and hence large cooling requirements, facilities that are usually not available in analytical laboratories. The high-power water-cooled lasers typically come in two sizes: a 1-m "small-frame" and a 2-m "large-frame" version. At the other end is the low-power air-cooled version of the argon-ion laser which only provides 488 and 514 nm output. These wavelengths generally are too long to be used for straightforward excitation of native fluorophores; in separation sciences analytically interesting analytes are indirectly detected by labeling with a fluorescent probe which efficiently absorbs the visible laser lines [3,4]. In the past two years, the excitation possibilities of commercially available argon-ion lasers in the UV have been increased considerably. The interesting deep UV emission at 275 nm recently became available by modification of the plasma tube and mirror coatings. Further, intra-cavity frequency doubling has been commercialized so that even shorter wavelengths, i.e. 229–257 nm, are available at hundreds of milliwatts. In the past years, laser tube lifetimes have increased considerably and now range from 2000 to 10 000 h. When the laser is operated in the UV mode, its lifetime decreases

Table 1
Characteristics of CW lasers used in analytical fluorimetry

Type	Wavelength (nm)		Total output power (mW)
Argon-ion	529, 514, 502,497, 488		10–30 000[a]
	477, 473, 466, 458, 455	also air-cooled	
	364, 351, 334		5000
	306, 302, 300, 275	only water-cooled	1.5
Krypton-ion	799, 752, 677, 647, 569		
	531, 521, 483, 476, 468	also air cooled	10–5000
	415, 413, 407		
	356, 351, 338	only water-cooled	2000
Helium–cadmium	325		1–100
	354[b]		20
	442		2–150
Diode (In:Ga:Al:P)	670		10
	635		3

Data adapted from Refs. [8,10].
[a] Upper value applies to water-cooled versions.
[b] Only recently on the market.

since much higher currents are needed. A typical feature of a deteriorating argon-ion laser is the sag of the cathode into the light beam. In our laboratory, we have extended the lifetime by turning the complete laser upside down so that gravity then acts on the other side of the cathode.

The krypton-ion laser basically uses the same construction as the argon-ion laser (mixed krypton–argon ion lasers are also available). Its output, however, is at higher wavelengths. Lasers operating on Kr^{3+} generate CW powers of 2.5 W at 242–266 nm and wavelengths as short as 219 nm, but they have not been commercialized as yet.

CW excitation in the UV part of the spectrum is provided by the compact helium–cadmium laser which is less expensive than a large-frame argon-ion laser and does not need extra facilities. A drawback is the limitation to two laser lines only, 325 and 442 nm; a second UV line at 354 nm became available recently. Lifetimes of HeCd lasers have been a problem in the past but nowadays specified lifetimes are 5000–6000 h. The most powerful commercially available version provides about 100 mW at 325 nm and 150 mW at 442 nm.

Diode lasers still typically deliver only red and infrared light; for the shortest-wavelength versions, the output is limited to a few milliwatts at wavelengths of 670 nm and 635 nm (not simultaneously provided by the same laser). For applications in analytical fluorimetry, special derivatization reagents have been developed which efficiently absorb the red light [11–14]. Low-power diode lasers are the cheapest lasers available (prices from US$ 100); they are compact and can be operated on a simple battery. The large spatial divergence of about 30° is compensated for by a lens that is incorporated in the assembly. The development towards shorter wavelengths, driven by the need for more compact information storage, has resulted in the production of diode lasers that deliver wavelengths in the green–yellow part of the spectrum, waiting to be commercialized.

Pulsed laser excitation combined with time-resolved detection can be used to discriminate between instantaneous processes such as Raman and Rayleigh scatter and the relatively long-living analyte fluorescence. Furthermore, a pulsed output is essential in non-linear processes where the efficiency of an n-photon process increases linearly with the n-th power of the irradiance (W cm^{-2}). In Table 2, the characteristics of pulsed lasers that are applied in analytical fluorimetry are summarized. Interesting aspects are the peak power, the pulse duration (important in fluorescence time-resolved detection), and the repetition rate (important for averaging pulse-to-pulse fluctuations). The nitrogen and the excimer laser usually provide a broad spatial beam of rectangular shape. As a result of the fast kinetics of the laser medium, the light amplification within one round trip is so large that in essence no mirrors are required; this behaviour is denoted as "super-radiant" emission. The laser radiation is generated by a high electrical

Table 2
Characteristics of pulsed lasers applied in analytical fluorimetry

Type	Wavelength (nm)	Average power (W)	Peak power (MW)	Pulse duration (ns)	Repetition frequency (Hz)
Excimer	308 (XeCl) 248 (KrF)	1–10	10–20	15	100–1000
Nitrogen	337	0.01–0.3	0.1–1	0.3–10	10–100
Nd:YAG[a]	1064[b]	1–10	100–200	5–10	10

Data adapted from Refs. [9,10].
[a] Flashlamp pumped.
[b] Can be frequency doubled, tripled and quadrupled to 532, 355 and 266, respectively.

discharge in a cavity filled with gas. As a result it produces large quantities of radio frequency interference (RFI) noise that is picked up by the detection system if not properly shielded. Excimer lasers are capable of producing very high average powers and are efficient for pumping dye lasers. The same laser assembly can be filled with different gases (F_2, ArF, KrCl, XeF, XeCl, KrF) so that excitation at several wavelengths is possible. Laser gas mixtures have to be replaced after, typically, one million shots. Gas cleaning equipment or gas replenishment can extend the lifetime.

The nitrogen laser provides a single line at 337 nm. It was one of the first commercially available UV lasers (1972); today it has been superseded by the excimer laser with its higher power levels and the neodymium laser with its third- and fourth-harmonic lines. The nitrogen laser has a simple construction, is easy to operate and inexpensive, and is available in very compact sizes. The pulse duration depends on the gas pressure and ranges from about 10 ns at 20 Torr (1 Torr = ca. 133 Pa) to about 300 ps at atmospheric pressure. The latter value is very suitable for time discrimination in fluorescence detection [15]. The neodymium laser, which consists of a host (often yttrium aluminium garnet, YAG) doped with Nd^{3+} ions, is a solid state laser that can be operated in the continuous mode although pulsed operation is often preferred because of the conversion efficiency in non-linear light generation; the 1064 nm output of the Nd:YAG is easily doubled, tripled, and quadrupled to 532, 355 and 266 nm, respectively. Neodymium lasers can be pumped by continuous lamps, pulsed flashlamps or the 810 nm diode laser. The latter has opened the way for compact size lasers with better output stability than the flashlamp-pumped versions.

The stability of the laser output is a critical parameter. Compared with conventional light sources lasers are, in general, more noisy which is important when the background is limiting the achievable detection limits (see Section 3). For CW lasers such as the argon- and krypton-ion lasers typical fluctuations are in the 0.5–1% range, while HeCd lasers are even less stable (1–2%). With feedback control devices the light power can be stabilized to 0.05%. Diode lasers offer extremely stable outputs and fluctuations of less than 0.005% can be reached [12]. Power reproducibility is a serious problem for pulsed lasers, especially in non-linear light generation where pulse fluctuations are further amplified. In the worst case, pulse-to-pulse fluctuations can be as high as 50% and signal averaging over a large number of pulses is needed to obtain a steady detector output. In these cases, a high repetition rate is favourable.

All the laser types mentioned above provide fixed wavelengths. Tunable wavelength selection (typically over a 50 nm range) is provided by dye lasers; because these are optically pumped, the shortest possible laser wavelength is limited by the pump source wavelength. When pumped by an argon- or krypton-ion laser, the shortest wavelength available is about 400 nm. A disadvantage of dye lasers is the photochemical decomposition of the dyes after prolonged pumping which causes a decrease in the output with time. Furthermore, the toxic nature of most dyes is an aspect of concern nowadays. Much more simple to operate are the tunable vibronic solid-state lasers such as the Ti:sapphire laser, which provides a continuous wavelength range of 660–1180 nm. Frequency doubling and tripling extends its applicability range into the UV region.

Finally, a critical survey of the available literature shows that, over the past decade, the robustness, versatility and application range of lasers have improved considerably. At the same time, prices have gone down. As a result, lasers have become a much more popular tool for analytical studies and application-orientated work.

2.2. *Influence of excitation power on fluorescence intensity*

The sensitivity of fluorescence detection can be increased by the high light intensity that lasers provide. The number of photons emitted per second by an illuminated sample that arrives at

the photocathode of a photomultiplier is given by:

$$n_f = 2.3\,\epsilon_\lambda\,[\text{analyte}]\,L\,\phi_f\,P_{ex}\,C \quad (1)$$

where ϵ_λ is the molar absorptivity ($l\,mol^{-1}\,cm^{-1}$), [analyte] the concentration of fluorophore ($mol\,l^{-1}$), L is the optical path length (cm), ϕ_f the fluorescence quantum yield, P_{ex} the incident radiant power (photons s^{-1}) and C the collection efficiency of the optical system of the detector. Eq. 1 holds if inner filter effects play no role so that the incident power, P_{ex}, is constant along the light path. The sensitivity of fluorescence detection can not be improved indefinitely by increasing laser power. At high incident radiation ground state depletion may occur and the fluorescence signal will no longer be proportional with the excitation power. Furthermore, the effect of photodestruction, which causes a decrease of the fluorescence signal with time, shows up more strongly at higher powers.

For CW lasers, the fluorescence intensity under saturation conditions can be calculated by assuming a steady state between the various molecular processes depicted in the kinetic scheme of Fig. 1. The number of photons emitted per second from an irradiated volume is:

$$n_f = k_f\,[S_1]\,V = \frac{k_f\,k_{ex}\,[\text{analyte}_{tot}]}{k_{ex} + k_f + k_{nr} + k_{ex}\,k_{isc}/k_T}\,V \quad (2)$$

where k_f is the fluorescence rate constant, k_{nr} is the sum of all non-radiative processes that depopulate the S_1 state (internal conversion, intersystem crossing and bimolecular quenching: $k_{ic} + k_{isc} + k_q[Q]$), k_T is the total decay rate constant for the T_1 state and V is the illuminated volume (cm^3); [analyte$_{tot}$] (molecules cm^{-3}) represents the total population of molecules in the three electronic states involved ($[S_0] + [S_1] + [T_1]$). The rate constant of excitation, k_{ex}, is determined by the light intensity and the molecular tendency for light absorption according to:

$$k_{ex} = \sigma_\lambda\,I = \frac{2300\,\epsilon_\lambda\,I}{N_A} = 3.8 \cdot 10^{-21}\,\epsilon_\lambda\,I \quad (3)$$

with σ_λ the absorption cross section (cm^2 molecule^{-1}), I the incident light intensity (photons $s^{-1}\,cm^{-2}$), ϵ_λ the molar absorptivity ($l\,mol^{-1}\,cm^{-1}$), and N_A Avogadro's number. At low irradiances (photons $s^{-1}\,cm^{-2}$), i.e. k_{ex} or $(k_{ex}\,k_{isc}/k_T) < (k_f + k_{nr})$, Eq. 2 reduces to the simpler Eq. 1. High irradiances occur when tight focusing is applied and/or with pulsed lasers as excitation source.

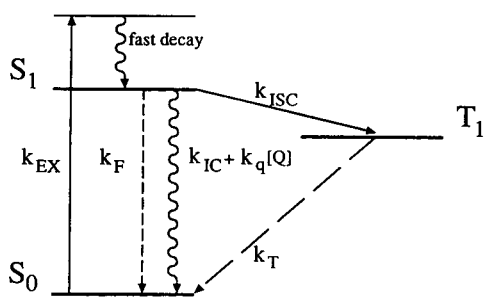

Fig. 1. Designation of intramolecular processes between singlet (S_0 and S_1) and triplet (T_1) states used in the kinetic equations in the text.

As an example, Table 3 shows calculated data which illustrate the effect of focusing, using molecular parameters that are typical for aromatic hydrocarbons. The number of photons that is emitted by one molecule irradiated during one second is calculated with Eq. 2 using an analyte concentration of one molecule per irradiated sample volume. The fluorescence signal from this volume is expressed by taking the illuminated area into account (photons mm^2 molecule^{-1} s^{-1}). For simplicity it was assumed that the light is uniformly distributed. The percent population distribution of the excited states is given by:

$$\%S_1 = \frac{k_{ex}}{k_{ex} + k_f + k_{nr} + k_{ex}\,k_{isc}/k_T} \times 100\% \quad (4)$$

$$\%S_0 = 100\% - \%S_1 \times (1 + k_{isc}/k_T) \quad (5)$$

$$\%T_1 = \%S_1 \times k_{isc}/k_T \quad (6)$$

The data on CW laser excitation show that with the numerical values used, saturation will occur for spot diameters smaller than 100 μm, dimensions that are typical for flow cells used in open-tubular LC and capillary electrophoresis

Table 3
Effect of focusing of CW and pulsed laser light on the population distribution of the three electronic states involved and the fluorescence intensity

Spot diameter (μm)	Continuous wave					
	k_{ex} (s^{-1})	$\%S_0$	$\%S_1$	$\%T_1$	Emitted photons (molecule^{-1} s^{-1})	Fluorescence intensity (photons mm^2 molecule^{-1} s^{-1})
1000	$9.6 \cdot 10^3$	99.90	0.009	0.09	$4.8 \cdot 10^3$	4800
100	$9.6 \cdot 10^5$	90.45	0.87	8.68	$4.4 \cdot 10^5$	4400
10	$9.6 \cdot 10^7$	8.65	8.30	83.05	$4.2 \cdot 10^6$	420
	100 Hz pulsed					
	k^a_{ex} (s^{-1})	$\%S^b_0$	$\%S^b_1$	$\%T^b_1$	Emitted photons (molecule^{-1} s^{-1})	Fluorescence intensity (photons mm^2 molecule^{-1} s^{-1})
1000	$9.6 \cdot 10^9$	0.85	89.88	9.27	92	92
100	$9.6 \cdot 10^{11}$	0.85	89.88	9.27	92	0.92
10	$9.6 \cdot 10^{13}$	0.85	89.88	9.27	92	0.0092

Excitation power ($\lambda_{ex} = 500$ nm): CW, 1 W; 100 Hz pulsed, 1 $W_{average}$, 1 MW_{peak} in rectangular 10 ns pulses. Molecular parameters: $\epsilon = 10\,000$ l mol^{-1} cm^{-1}, $\phi_f = 0.5$, $k_f = 5 \cdot 10^7$ s^{-1}, $k_{nr} = 5 \cdot 10^7$ s^{-1}, $k_{isc} = 10^7$ s^{-1}, $k_T = 10^6$ s^{-1}.
[a] In the pulse.
[b] Calculated at $t = 10$ ns.

(CE) (see Table 6). Obviously, for these micro-separation systems, excitation with a high-power laser is not efficient [16]. When the spot diameter is reduced from 1000 to 10 μm, which causes a 10 000-fold increase of the irradiance, the number of fluorescence photons emitted per molecule increases no more than 900-fold. The total fluorescence signal is determined by the number of molecules probed: as the illuminated area is 10 000-fold smaller, the net effect of saturation is an 11-fold lower fluorescence intensity (assuming the same optical path lengths). It should be noted that for this particular set of parameters, the main bottleneck in the saturation process is the relatively large k_{isc}/k_T ratio: at high irradiances a large part of the molecules is trapped in the triplet state.

Pulsed lasers provide about the same average power as CW lasers, but the light is typically concentrated in 10–100 pulses s^{-1} of about 10 ns. Consequently, the light power during the pulse is much higher and fluorescence saturation will occur more easily than with continuous excitation [17,18]. Because the pulse duration is on the same time scale as the inverse molecular rate constants denoted above, for pulsed laser-induced fluorescence the kinetics of fluorescence intensity can not be treated assuming steady-state conditions. For simplified temporal pulse profiles, the kinetic equations can be solved analytically although they are rather complicated [19]. An alternative approach is to use a numerical treatment of the problem [20]. The laser pulse is divided into small time intervals and the distribution between the molecular states at a particular time interval, t, is calculated by taking the values of the previous interval, $t - \Delta t$, as starting set. To illustrate the calculation procedure, which is simplified in this particular example by taking into account only two pathways, i.e. absorption and fluorescence, the number of molecules in the excited state at time t is given by:

$$[S_1]_t = [S_1]_{t-\Delta t} + k_{ex}[S_0]_t \Delta t - k_f[S_1]_t \Delta t \quad (7)$$

The total number of analyte molecules is constant, that is:

$$[S_0]_t = [\text{analyte}_{tot}] - [S_1]_t \quad (8)$$

By substituting Eq. 8 into Eq. 7 the problem can be solved. Every time increment is evaluated in a computer programme loop. With a more advanced programme, which takes into account the triplet state, the population distribution and the number of emitted photons of Table 3 were also calculated for a 1-W 100 Hz pulsed laser providing temporal rectangular 10 ns pulses. The result of these calculations shows that the number of emitted photons per molecule is independent of the irradiance, due to the fact that even for the largest spot size, i.e., 1000 μm diameter, the ground state is almost completely depleted. Fig. 2 gives the corresponding population distribution of the S_1 and T_1 states as a function of time. Initially, nearly all molecules are excited in S_1. Subsequently, inter-system crossing causes T_1 to be populated; after the pulse both excited states depopulate, S_1 much more rapidly than T_1. The number of fluorescence photons emitted per molecule per pulse is only 0.92 (Table 3). When taking into account the pulse frequency of 100 Hz it is evident that, for the present parameters, pulsed laser excitation yields low fluorescence intensity compared with CW excitation (92 vs. 4800 photons molecule^{-1} s^{-1} for 1000 μm beam diameter). When saturation conditions are met, further focusing of the laser beam will result in a decrease of the total fluorescence

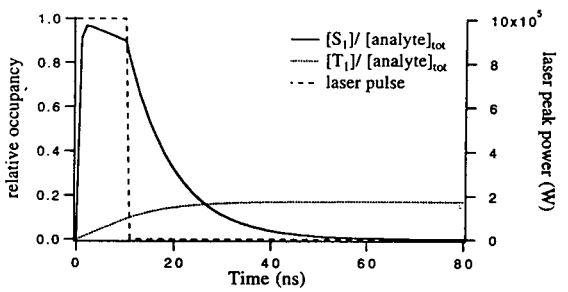

Fig. 2. Relative occupancy of the S_1 and T_1 states of a molecule (for intramolecular rate constants see Table 3) as a function of time upon excitation with a rectangular temporal 10 ns laser pulse having a peak power of $1 \cdot 10^6$ W and focused to a spot diameter of 1000 μm. Note that molecules excited to the triplet state will not decay to the ground state within the pulse duration; this decay typically takes 10 μs.

intensity since the number of probed molecules will become less. In fact fluorescence saturation with the 100 Hz pulsed laser occurs already at average irradiances as low as 1 mW mm^{-2} (occupancy of S_0: 94%). This value is in line with data in literature on fluorescence saturation with a 100 Hz excimer laser [17]. The above calculations indicate that the high light power of pulsed lasers can not be fully exploited in LIF detection. Of course the net effect of saturation on analyte detectability is also determined by the dependence of the background signal on the irradiance. For scatter processes, the background signal is linearly dependent on the applied laser power, which means that under saturation conditions, higher irradiances will lead to less favourable limits of detection. On the other hand, when the background is merely due to luminescence of impurities, saturation of the background signal may also occur and the LODs may occasionally improve.

Another point that should be considered is the photodegradation of analyte molecules upon prolonged laser excitation. Photodegradation may result from spontaneous decomposition of excited singlet or triplet states, or from a bimolecular reaction of these states with oxygen. When photodecomposition occurs from S_1, the loss of fluorophores can be written as:

$$-\frac{d[\text{analyte}]}{dt} = k_d[S_1]_t \quad (9)$$

where k_d is the pseudo first order decomposition rate constant. Since photodecomposition is a relatively slow process, steady-state conditions can be assumed for the faster molecular processes and integration of Eq. 9 yields:

$$\frac{[\text{analyte}]_t}{[\text{analyte}]_{t=0}} = \exp\left(\frac{-t\,k_d\,k_{ex}}{k_{ex} + k_f + k_{nr} + k_{ex}\,k_{isc}/k_T}\right) \quad (10)$$

Although the quantum yield of photodestruction is in general much smaller than the fluorescence quantum yield (values of 10^{-5} are reported [21,22]), its effect on the fluorescence intensity can be considerable because a molecule proceeds through many round trips during the transit

time. For instance, when a non-flowing sample containing molecules with photophysical parameters as in Table 3 and a photodestruction quantum yield of $5 \cdot 10^{-5}$ is illuminated at an irradiance of 1 W mm^{-2}, it can be calculated with Eq. 10 that 50% of the molecules will be destroyed after 1.4 s of irradiation time. In an LC system molecules are only exposed to laser light during the time interval Δt that is needed to cross the laser beam, which is often much less than 1 s. The number of fluorescent photons emitted per molecule traversing the illuminated volume, $n_{f,molecule}$, can be calculated by combining Eqs. 10 and 2 and integrating over time:

$$n_{f,molecule} = \frac{\phi_f}{\phi_d}\left[1 - \exp\left(\frac{-\Delta t\, k_d\, k_{ex}}{k_{ex} + k_f + k_{nr} + k_{ex}\, k_{isc}/k_T}\right)\right] \quad (11)$$

where ϕ_f and ϕ_d are the quantum yields of fluorescence and photodestruction, respectively. In an LC system there is a continuous transport of new of molecules in the light beam and molecules.

The impact of photodestruction for a CW and a pulsed laser is shown in Table 4, assuming a photodestruction quantum yield of $5 \cdot 10^{-5}$. Using the same molecular parameters as in Table 3, the number of fluorescent photons emitted per second in a probed area is calculated that arises from the illumination by 1-W laser light of a flowing sample having a linear velocity of 1 cm s^{-1}; the latter value corresponds to a typical flow-rate of 0.6 l min^{-1} in conventional-size LC with a 2–3 mm I.D. column. For simplicity the laser light is assumed to be uniformly distributed over a square-shaped spot. In order to distinguish between photodestruction and saturation effects, data calculated in the absence of photodestruction are also presented ($\phi_d = 0$). The fluorescence intensity is calculated by taking the illuminated area into account (photons mm^2 molecule^{-1} s^{-1}). The data of Table 4 indicate that with CW excitation the effect of photodestruction on analyte detectability is only marginal compared to saturation. The deviating percentage of destroyed molecules at the 10 μm spot size is caused by the fact that in this situation, most molecules are in T_1 from which, in this particular case, no photodecomposition was assumed to take place. Photodestruction and saturation can be distinguished experimentally by changing the flow-rate and hence, the transit time. From the dependence of the fluorescence intensity on the flow-rate, the quantum yield of photodestruction can be calculated [23]. The results in Table 4 apply for the standard geome-

Table 4
Effect of focusing and photodestruction on fluorescence intensity and percent molecules destroyed

Spot diameter (μm)	Continuous wave			100 Hz pulsed		
	Fluorescence intensity (photons mm^2 (molecule^{-1} s^{-1})		Molecules destroyed (%)	Fluorescence intensity (photons mm^2 molecule^{-1} s^{-1})		Molecules destroyed (%)
	$\phi_d = 0$	$\phi_d = 5 \cdot 10^{-5}$		$\phi_d = 0$	$\phi_d = 5 \cdot 10^{-5}$	
1000	4790	4680	5	92	92	0
500	4780	4550	9	23	23	0
250	4720	4290	17	5.8	5.8	0
100	4340	3510	35	0.92	0.92	0
50	3370	2440	49	0.23	0.23	0
25	1790	1270	51	0.058	0.058	0
10	420	340	34	0.0092	0.0092	0.01

Exposure of a streaming sample to 1 W 500 nm light from a CW laser and a 100 Hz laser providing 10 ns pulses. Linear flow-rate, 1 cm s^{-1}; molecular parameters are the same as in Table 3.

try with excitation perpendicular to the flow direction. In flow-cell assemblies where excitation light is pointed in the flow direction to achieve an increase of the optical path length, transit times are much longer and significant photodestruction has been reported [24,25].

With the pulsed laser, the number of emitted photons per molecule is constant since the ground state is almost completely depleted during the laser pulse. Because the number of probed molecules is directly proportional with the illuminated area a net decrease of signal intensity is observed. Photodestruction does hardly occur with the pulsed laser because the molecule proceeds through only 1.8 round trips during a pulse which is not much in view of the photodestruction quantum yield. It should be mentioned that the present model does not include photochemical pathways involving the triplet state or multi-photon processes, although especially the latter may be operative upon pulsed-laser irradiation.

3. LIF as detection method for LC

On account of the linear power dependence of fluorescence intensity (see Eq. 1), the introduction of lasers as excitation source for fluorescence detection in LC seems obvious. The high power of the light beam which, moreover, can be focused easily and efficiently, provides a much higher radiation yield in the flow cell than conventional light sources do. From an analytical point of view, two aspects are important to consider here; applicability to a wide range of analytes and detectability at trace levels. As regards the former aspect, new developments in laser technology keep increasing the freedom of choice of excitation wavelength, especially in the interesting UV region. The other aspect is a challenge for the analytical chemist: how does one "extract" as many fluorescent photons as possible from a sample while suppressing the background to a minimum. First, we consider important items such as the origin of background signals, signal-to-noise ratio (S/N) and the definition of the detection limit. Subsequently, applications of LIF in LC will be discussed, with emphasis on native-fluorescent analytes.

3.1. Signal-to-noise considerations

3.1.1. Background

The background is an important parameter in trace-level analysis. In general, in fluorescence detection it is the result of various contributions; the main ones are discussed below.

3.1.1.1. Laser light reflected and refracted at the flow cell

In principle, this light can readily be blocked by optical filters; however, because the laser light can be very intense, the optical density of the filter should be extremely high (transmittance $<10^{-4}$). Care should be taken to use filters that exhibit no luminescence on exposure to the laser light, as is often encountered when glass filters are applied. Chemical filters, which consist of a solution of an inorganic salt in distilled water, usually do not show unwanted luminescence. Stray light especially occurs at the boundaries of the flow cell walls and various cell configurations and assemblies have been tested to decrease its importance (see Section 3.2).

Although lasers provide optically pure lines, the output may contain low intensity light of non-selected wavelengths which arises from spontaneous emission. If these non-lasing lines are not blocked before they enter the flow cell and if the emission filter of the detector is transparent for the corresponding wavelengths, they may seriously contribute to the background.

3.1.1.2. Rayleigh and Raman scatter from the LC eluent

The intensity of both types of scatter varies inversely proportional with the fourth power of the excitation wavelength. This means that the scatter efficiency of the 257-nm line of the frequency-doubled argon-ion laser is 16-fold higher than that of the 514-nm line. Compared to refracted and reflected laser light, the contribution of Rayleigh scatter light is only of minor importance. Raman scatter, on the other hand, causes serious problems in detection because the

Raman spectrum can overlap with fluorescence spectrum of the analyte. The spectral width of a Raman line is at least as large as the spectral band width of the excitation source. The cross section of a Raman transition is typically on the order of 10^{-28} cm^2, which is about 12 orders of magnitude smaller than a typical absorption cross section of about 10^{-16} cm^2 (corresponding with a molar absorptivity ϵ of 26 000 $l\,cm^{-1}\,mol^{-1}$). Assuming parameters that are typical in fluorescence detection, such as an analyte with a 20% quantum yield present in 20 M solvent, and a 10-nm spectral detection window that selects the fluorescence light from the 100-nm broad emission spectrum, it can be calculated that Raman background signals are comparable to analyte fluorescence signals at an analyte concentration in the flow cell of 10^{-9} *M*.

Unlike fluorescence, Raman scatter is anisotropically distributed so that the signal-to-noise ratio (S/N), in principle, can be improved with polarized laser light and a proper choice of the angle of collection and emission polarizers [26].

Fig. 3 shows the Raman spectra of the three solvents mostly used in reversed-phase LC.

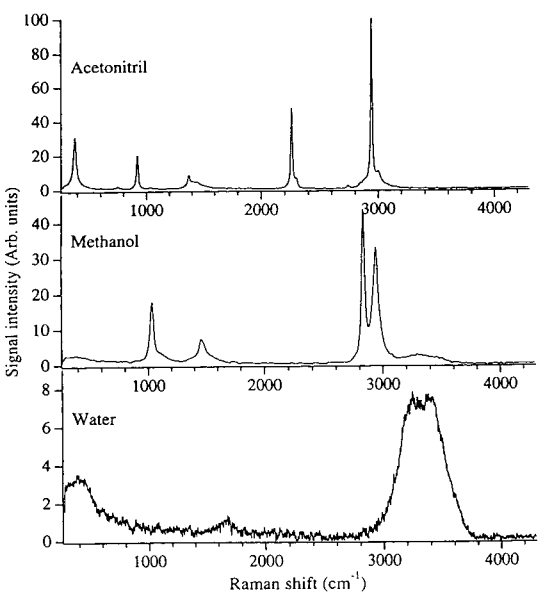

Fig. 3. Raman spectrum of solvents often used in reversed-phase LC.

When the Raman spectrum overlaps with the analyte fluorescence, interference filters can be used to select the analyte fluorescence in the spectral gaps between the baseline-resolved Raman peaks. It is often more convenient to select the optical region at the long-wavelength side of the highest Raman frequency with simple optical cut-off filters. Since the Raman bands shift with the excitation wavelength, short laser wavelengths can be used to prevent Raman interferences. In reversed-phase LC, the longest wavelength of the Raman spectrum results from the relatively broad OH-stretch band of water and methanol, which ranges from about 3000 to 3700 cm^{-1}. In Fig. 4 the minimal wavelength distance between excitation and emission settings is shown that is needed to prevent detection of this Raman scatter light. At long excitation wavelengths, such as the 670 nm light provided by diode lasers, it is only practicable to detect analyte fluorescence between the eluent Raman peaks since the OH stretch band extends to a wavelength region where common photomultipliers display no or little sensitivity.

Stray light and Rayleigh and Raman scatter are instantaneous processes, which allow time discrimination in favour of the slower fluorescence when pulsed laser sources are used. Unfortunately, this is much easier in frozen than in fluid solutions, since under the former conditions fluorescence lifetimes are usually significantly larger. In LC, lifetimes are often less than 10 ns,

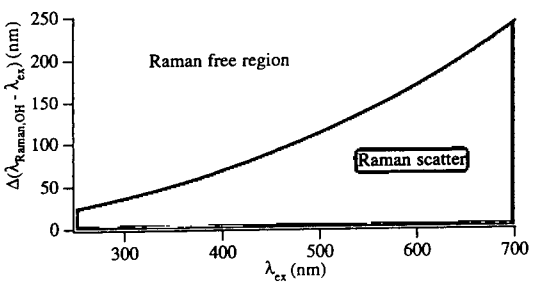

Fig. 4. Wavelength distance between excitation wavelength and the Raman OH-stretch vibration of water at 3700 cm^{-1} as a function of excitation wavelength. When analyte fluorescence is recorded at larger wavelength distances, Raman signals do not contribute to the observed background.

which means that only sharp laser pulses of about 1 ns allow effective discrimination.

3.1.1.3. Background luminescence

Background luminescence signals that are constant during a chromatographic run arise from the entire flow cell assembly —i.e. cuvette walls, flow-cell holder walls, collecting optics, optical filters and fibers— induced directly by laser light or indirectly by stray light and, last but not least, eluent impurities [27,28]. Luminescence from optical components can be decreased by using high spectral quality material; especially for the flow cell, which is exposed to the highest irradiance, Suprasil I quality quartz material is recommended. Eluent solvents that seem optically pure in conventional fluorimetry often need further purification such as distillation when LIF detection is used. Impurities that are present in the injected sample from the matrix and/or derivatization procedures, cause a varying background signal during chromatography which frequently —and unfortunately— plays the dominant role. In this case, clean-up procedures and optimization of the chromatographic system by choosing the proper column material and eluent conditions are necessary to decrease the effect of coeluting substances. In general, background luminescence is more intense at short wavelengths because the number of impurities that is excited increases.

The relative importance of the three types of background considered above strongly depends on the particular excitation and emission settings. When excitation is performed with, e.g., diode lasers at 670 nm, the analyte emission is measured in the spectral regions between the Raman peaks and the background is mainly determined by Raman scatter when native-fluorescent compounds are measured, despite its λ^{-4} intensity dependence; impurity fluorescence form matrix constituents often is negligible in this wavelength region [29]. On the other hand, excitation at 257 nm using a frequency-doubled argon-ion laser will cause relatively high backgrounds from luminescent impurities; the influence of intense Raman scatter can be reduced by recording fluorescence at longer wavelengths, i.e. above 290 nm [30].

3.1.2. Noise

The lowest signal intensity that can be detected is determined by the fluctuations of the background signal, denoted as noise. Usually, the assumption is made that the noise is normally distributed around a mean value according to a Gaussian function. However, noise may also include fluctuations which do not obey a regular distribution law, such as those produced by spikes on the line voltage or other disturbances from electrical equipment in the vicinity [31]. The noise intensity can be expressed as the standard deviation of the background signal measurements, denoted as the root-mean-square (RMS) noise, or the peak-to-peak value which is the difference between the minimum and maximum background signal. In Fig. 5 a typical time recording of a background signal is shown using an integration time of 1 s. For a normal distribution, 99.7% of all data points fall within ± 2.5 standard deviation ($\pm 2.5\ \sigma$) of the mean; in other words, for a chromatogram consisting of

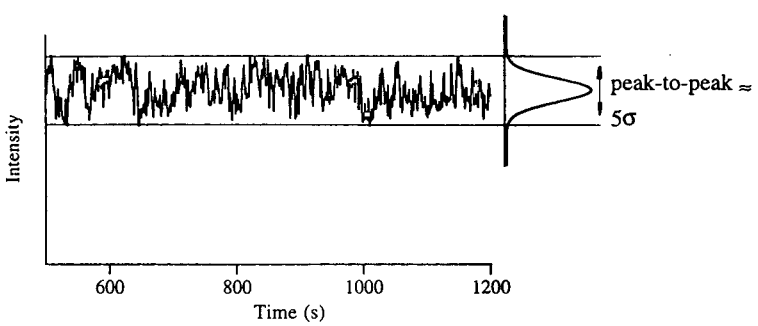

Fig. 5. Background recording showing the noise criterion.

1000 data points, only 3 points will be outside this range. It is therefore justified to estimate the RMS noise to be approximately 20% of the peak-to-peak value of a sufficiently long baseline recording.

Shot noise and flicker noise are the two major noise sources encountered in fluorescence detection. Shot noise is due to the random behaviour of light and matter. For instance, photons from a light source which impinge on a surface (e.g. the cathode of a photomultiplier) arrive randomly in time because they are not evenly spaced. The same random behaviour is observed for the thermal excitation of electrons from the photomultiplier cathode which leads to dark current. Shot noise follows the Poisson probability distribution function which means that the standard deviation or RMS noise of the number of events (e.g. photons or electrons) counted over time t, σ_{sn}, equals the square root of the number of events, n:

$$\sigma_{sn} = \sqrt{n} \tag{12}$$

Since the shot noise from background light (bl) and dark current (dc) photoelectrons are non-correlated, the total shot noise is given by [32]:

$$\sigma_{sn} = \sqrt{(\sigma_{bl})^2 + (\sigma_{dc})^2} \tag{13}$$

In analog signal processing, the relative standard deviation (R.S.D.) of the distribution of photoelectrons emitted from the cathode is preserved in the electrical signal output of the readout device since both signal and noise are multiplied by the same linear factors. After signal processing the output of the readout device is usually expressed in volts and registered by a recorder. When, during t seconds, n_{bl} background light photons arrive at the cathode with quantum efficiency θ and the dark current is generated by thermal excitation of n_{dc} photons, the background signal, $B_{total,volt}$, and the shot noise, $\sigma_{sn,volt}$, after processing by the readout device are:

$$B_{total,volt} = B_{bl,volt} + B_{dc,volt} = g(\theta n_{bl} + n_{dc}) \tag{14}$$

and

$$\sigma_{sn,volt} = g\sqrt{\theta n_{bl} + n_{dc}} = \sqrt{gB_{bl,volt} + gB_{dc,volt}} \tag{15}$$

respectively, where g(V) is the overall conversion factor that includes the gain of the photomultiplier, the signal processing and readout step.

Flicker noise is due to variations in the intensity of the light source or spatial vibrations in the experimental set-up. The magnitude of this type of noise, denoted as flicker noise, σ_{fn}, is directly proportional with the background signal. The flicker factor, ξ, is the experimentally observed R.S.D. of these instabilities for a given time constant or integration time, i.e.:

$$\sigma_{fn,volt} = \xi B_{bl,volt} \tag{16}$$

The total noise from the background light therefore is:

$$\sigma_{total,volt} = \sqrt{gB_{bl,volt} + gB_{dc,volt} + (\xi B_{bl,volt})^2} \tag{17}$$

The relative importance of shot and flicker noise is demonstrated in Fig. 6 where the peak-to-peak noise ($5\sigma_{total,volt}$) is plotted against the total background signal, B_{total}, assuming a dark current of 10 mV and $g = 10^{-6}$ V. The flicker factors (0.5% and 2.5%) are expressed as the percentage peak-to-peak noise of the background, so that $\xi_{p-p} = 5\xi \cdot 100\%$. From the figure

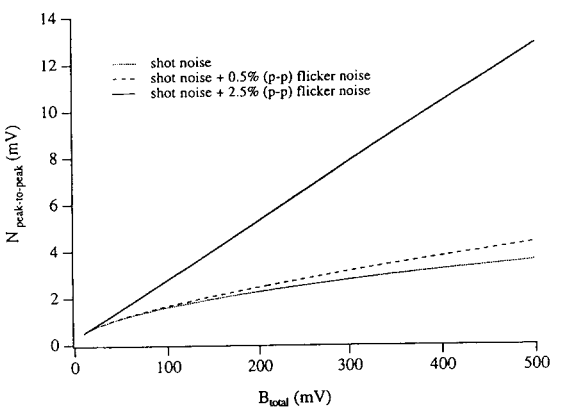

Fig. 6. Plot of peak-to-peak noise as a function of total background signal showing the effect of flicker noise.

it is noted that at low backgrounds ($B_{total,volt} < 20$ mV), the dark current noise ($N_{p-p} = 0.5$ mV) dominates. In this situation it is worth cooling the photomultiplier tube to decrease the release of thermally induced photoelectrons from the cathode. The relative contribution of the dark current compared to the other noise sources decreases rapidly with increasing background, especially if high flicker factors are encountered. For stable light sources ($\xi_{p-p} \leq 0.5\%$), shot noise is dominant over a wide background signal range and S/N can be improved by applying higher light powers because background as well as analyte signals increase linearly with the incident radiation in fluorescence detection. Under these conditions, the potential of laser excitation is obvious. A xenon-arc lamp in a conventional detector typically provides 100 μW focused in the flow cell, so that the use of a 1-W laser would yield 10 000-fold higher background and analyte signals and, under shot noise limited conditions, 100-fold better S/N ratios. In practice a gain of two decades is not readily achieved. Especially, when unstable light sources such as pulsed lasers and the non-stabilized HeCd laser are used, flicker noise already becomes dominant at low background values and noise increases linearly with the background. In this situation substituting a laser for a lamp and/or increasing the laser power will hardly or not improve S/N values.

Generally speaking, lasers provide a less stable light output than conventional sources and flicker noise limits analyte detectability. In order to decrease flicker noise, at the excitation side lasers can be stabilized by a feedback device consisting of a photodiode that monitors the intensity variations and is coupled to a light intensity regulator, for instance an electro-optical polarizer; on the detection side, fluctuations can be corrected for by ratioing the sample signal with the reference signal of, e.g., the above photodiode [30,33].

3.1.3. Detection limit

Although attempts have been made to introduce a standardized chromatographic limit of detection [31,34,35], a variety of definitions is used throughout literature. LODs are expressed in terms of injected concentration, C_{inj} (mol l^{-1}), injected mass, M_{inj} (kg), or the peak concentration present in the detector, C_{det} (mol l^{-1}). In the last instance, the dilution in the chromatographic system is taken into account. The three parameters are related as:

$$C_{det} = \frac{C_{inj} \cdot V_{inj}}{\sigma_v \sqrt{2\pi}} = \frac{M_{inj}}{\sigma_v \sqrt{2\pi}} \quad (18)$$

where σ_v is the (volume) standard deviation of the (Gaussian) chromatographic peak. The LOD is usually defined as the signal that is 2- or 3-fold higher than the noise. Unfortunately, some authors use the RMS noise whereas others take the peak-to-peak value. Furthermore, the signal and noise intensities depend on the detector integration or RC times, t_{det}; that is S/N increases linearly with $\sqrt{t_{det}}$.

As an example, in Table 5 two LODs are calculated using the same chromatographic system and detector, but different LOD definitions, noise criterions and time constants. The 250-fold difference in LOD that is found clearly shows the importance of reporting the experimental and mathematical conditions used in the determination and calculation of one's LOD values.

3.2. Detector flow cell constructions

Since the first application of LIF as a detection method in LC by Diebold and Zare [36], special attention has been paid to the optimization of the flow cell assembly, which is a critical part in the detection system. Because in LIF the incident light power is much higher than with conventional fluorescence detectors, refracted and reflected laser light and luminescence from the flow cell walls is also much higher and will often determine analyte detectability. Especially when flicker noise is present on the background, suppression of these unwanted light contributions may considerably improve the detection limits.

The illuminated volume in a flow cell must be small enough to maintain the chromatographic resolution. It should therefore match the scale of

Table 5
Comparison of two LOD values calculated using the same LC system but different LOD definitions, noise criterions and time constants

Assumptions			
Column	200 × 3.0 mm	Injected concentration	$1.5 \cdot 10^{-8}$ M
Flow-rate	0.5 ml min^{-1}	Analyte signal	90 mV
Analyte retention time	600 s	Rms noise (1 s integration)	2 mV
Injection volume	10 μl	LOD signal-to-noise criterion	S/N = 3
N (plates)	10 000		

Variables	*Experiment A*	*Experiment B*	*Effect on LOD_A/LOD_B*
Detector integration time	0.25 s	4 s	4 ×
Noise definition	peak-to-peak	RMS = 1/5 peak-to-peak	5 ×
LOD definition	injected concentration	peak concentration in cell	12.5 ×
Analyte LOD reported	$1 \cdot 10^{-8}$ *M*	$4 \cdot 10^{-11}$ *M*	250 ×

the separation technique that is used. In Table 6, different liquid-based separation methods and their typical flow cell volumes are listed. For large flow cell compartments, encountered in conventional-size LC, the introduction of the excitation light from a conventional lamp in general will not cause serious problems. In micro-separation techniques, however, it is not possible to focus all lamp excitation light into the detector cell compartment. Laser beams, on the other hand, can easily be adapted to the smallest flow cell diameters.

In most LIF assemblies, flow cell walls are removed from the field of view of the detector or even omitted at all. In Fig. 7 some well-known constructions used in LC–LIF are shown. In the flowing droplet cell, the surface tension forms a solvent bridge between the column outlet and a stainless-steel rod [36]. The development of a micro droplet of 0.4 μl, instead of the original 4 μl, has been reported [37]. Richardson et al. found 10-fold better LODs for a droplet cell compared with a conventional quartz cell using the 351/356 nm output of a Kr-ion laser [38]. A disadvantage of the droplet shape is that the curved surface works as a lens. Furthermore, changes in the eluent composition, for instance during gradient elution, will change the surface tension and, consequently, the shape of the droplet so that the optical alignment of the detector has to be adapted. The amount of refracted and reflected laser light that can reach the detector is reduced by a construction in which the stainless-steel rod is replaced by an optical fiber [39].

In the free falling jet approach of Folestad et al. the effluent from a conventional-size column is forced into a 120 μm internal diameter capillary to increase the linear velocity so that a jet of liquid emerges [40]. The laminar flow could only

Table 6
Typical flow cell volumes used for various separation methods

Separation system	Internal diameter of column (mm)	Typical flow cell volume (μl)
Conventional size LC	4.6/3.0	20
Small-bore LC	1.0	1.0
Packed-capillary LC	0.3	0.05
Open-tubular LC and CE	0.05	< 0.001

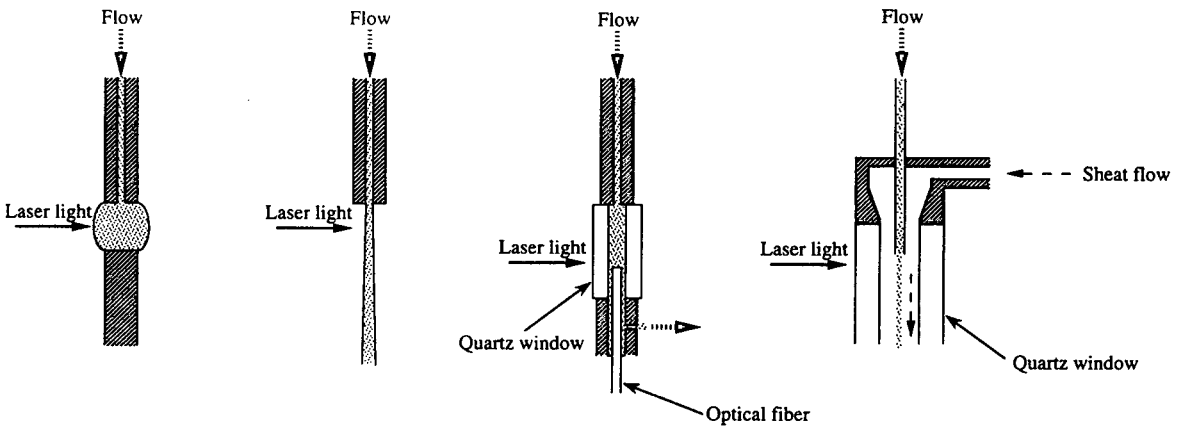

(A) Flowing Droplet (B) Free falling Jet (C) Fiber Flow Cell (D) Sheath Flow Cell

Fig. 7. Flow cell types used for LIF in LC (A–D) and CE (D).

be sustained for relatively high flow-rates (>1 ml min^{-1}). The same authors extended the applicability range to narrow-bore LC by using smaller capillaries at the column outlet; as a result a flow-rate of 45 μl min^{-1} could be used [41]. As with the flowing droplet, there is much reflected and refracted laser light but this is concentrated in the plane perpendicular to the flow direction. By collecting the fluorescence in an angle of 30° to this plane, scattered light could be decreased by 6 orders of magnitude. The free falling jet and the flowing droplet have been used only sporadically, presumably because of the inconvenience of the open cell construction.

A more practical design which is able to reject reflected and refracted laser light and flow cell wall luminescence by spatially filtering was achieved by Yeung and Sepaniak; here the fluorescence light is collected into a fiber that is put into the bore of the flow cell [42,43]. Transmittance of light through a fiber is only possible for light that enters the fiber within a certain acceptance angle:

$$\sin\theta \leqslant \frac{\sqrt{n_f^2 - n_c^2}}{n_e} \qquad (19)$$

where θ is the angle between the fiber axis and the light ray and n_f, n_c and n_e are the indices of refraction of the fiber core, fiber cladding and LC eluent, respectively. The fiber-cell assemblies can be adapted to micro-diameter columns by decreasing the sizes of flow cell and optical fiber [44]. Gluckman et al. reported a set-up with a cell volume of 92 nl, which was used for connection to a 250 μm I.D. capillary column [45].

Instead of utilizing the fiber for the collection of light, it can also be used to introduce the excitation light into the flow cell, while collecting the fluorescence light perpendicularly. In this way, the optical path length of the flow cell is increased to illuminate as much analyte inside the cell as is possible without significant loss of chromatographic resolution [21,33,46,47]. Apart from the rejection of unwanted light contributions, optical fibers offer flexibility of the detection system. Furthermore, time discrimination between light signals and the radio frequency noise, which is generated by the fast switching circuits of pulsed lasers and can be picked up by detection systems, is readily achieved. A 25-m fiber was used to cause a time delay of the emission light of about 125 ns, so that the RFI noise is no longer active [48].

When column diameters are very small, fused-silica capillaries are often used as flow cells; they are made transparent by removing a portion of the polyimide coating from the capillary. The flow cell usually is part of the separation column as coupling connections will destroy the chro-

matographic resolution [49,50]. The stray light contribution from capillaries often is so high that spatial filtering by means of microscope objectives is used and collecting optics are positioned out of the horizontal plane formed by the laser beam and the direction of the capillary [51,52]. Stray light intensity can be considerably decreased by immersing the capillary in an index-matching fluid having nearly the same refraction index as fused silica [53].

Detection volumes in the sub-nl range are achieved with the sheath-flow cell cuvette [54,55] and have been applied in "single-molecule" detection [21,56–58]. In this approach the column effluent is ensheathed by another flowing stream of similar refractive index. Under laminar flow conditions, the integrity of the small sample stream diameter is maintained. As the cuvette walls are far removed from the sample stream, flow cell wall luminescence and scattered stray light can easily be removed by spatial filtering. The cell can be incorporated in the electrical circuit of a capillary electrophoresis (CE) separation system, using an ensheating buffer stream.

3.3. Comparison between conventional fluorescence and LIF detectors

Applying LIF detection in LC is only useful when the analyte detectability obtained with conventional fluorescence detectors can be improved. For miniaturized systems, the light output of conventional sources can not be fully exploited because only a small part of the available excitation light can be directed into the flow cell. Recently, a filter fluorimeter has been described by Dovichi and co-workers which consists of a 75-W xenon-arc lamp and an efficient optical system; the excitation set-up was capable of delivering microwatts of optical power within a 10-nm spectral bandwidth and concentrated to a spot of about 180 mm in diameter [59]. On this scale (flow cell diameters typically are 50 μm), the spatial coherence of lasers is essential and LIF offers detection limits that are often more than three decades better than in conventional fluorimetry [60]. On the other hand, in conventional-size LC the introduction of light from a lamp into a flow cell diameter of 1 mm, generally will not be a problem. Then, the difference between LIF and conventional fluorimetry will be determined by four factors. A brief discussion, which partly repeats statements made earlier in this paper, is as follows.

3.3.1. The matching of the absorption spectrum of the analyte under study with the available laser line

Contrary to laser excitation sources, conventional fluorimeters equipped with a xenon-arc lamp and excitation monochromator, can be tuned readily to the absorption maximum of the analyte of interest. At first sight one might suspect that the lack of optimum excitation due to the limited tunability of the excitation source, as is the case with most lasers, can be counterbalanced by increasing the light power. However, the background signal also depends linearly on the excitation power. Consequently, even under shot-noise conditions, the gain in analyte detectability increases only with the square root of the incident radiation whereas it is directly proportional with the molar absorption coefficient. When flicker noise is dominant, increasing the laser power has no positive effect at all; tuning at a more favourable absorption wavelength is the only way to improve the detection limits. The influence of wavelength selection is clearly illustrated in Fig. 8, derived from a recent paper of Zare and co-workers [61]. In this figure, the electropherograms of phenanthrene obtained with near-UV excitation at 325 nm and deep-UV excitation at 257 nm are compared. In both situations the laser power at the capillary is 10 mW. Considering the 20-fold concentration difference, the improvement in sensitivity obtained by applying deep-UV excitation is remarkable.

3.3.2. The amount of radiation that can be introduced into the flow cell

For commercially available detectors equipped with a xenon-arc lamp and monochromator, the average output that reaches the flow cell compartment is limited to about 100 μW. In LIF detection a laser output of 1 W is about the maximum that can be used before saturation

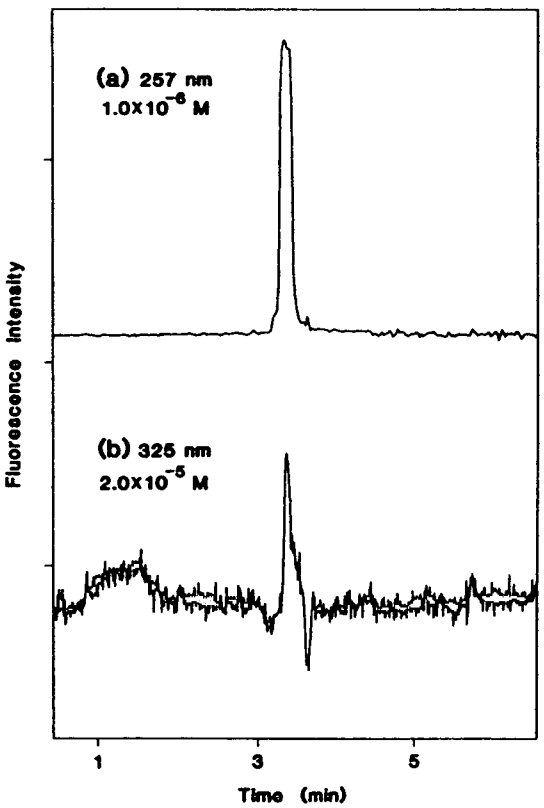

Fig. 8. Comparison of detection sensitivity for phenanthrene between near-UV and deep-UV laser excitations. (a) Electropherogram of $1.0 \cdot 10^{-6}$ *M* phenanthrene with deep-UV-LIF detection: laser wavelength 257 nm; laser power 10 mW; injection volume 0.5 nl. (b) Electropherogram of $2.0 \cdot 10^{-5}$ *M* phenanthrene with near-UV-LIF detection; laser wavelength 325 nm; laser power 10 mW; injection volume 0.5 nl. Note the 20-fold concentration difference. From Ref. [61].

occurs. This would imply that on the basis of excitation power only, the LODs measured with LIF will be two orders of magnitude better provided that shot-noise conditions are realized.

3.3.3. The stability of the output of the light source, especially important at high backgrounds

Whereas conventional light sources provide stable outputs, lasers are inherently less stabile and fluctuations on the order of 1–2% are not unusual for CW lasers; in other words, in various practical situations flicker noise dominates if no special measures are taken. For pulsed lasers, the pulse-to-pulse stability is even worse: deviations can be as large as 50% so that signal averaging over a substantial number of pulses is required to decrease the noise to acceptable levels.

3.3.4. The ability to measure in a window of the eluent Raman spectrum

If lasers are used, the Raman spectrum is highly resolved (see Fig. 3) and the analyte fluorescence can be detected in the spectral regions between the lines. As the Raman lines are at least as broad as the excitation band it is almost impossible for conventional fluorimeters with a typical 10–20 nm spectral band-pass to reject the Raman light completely. If the monochromators of the fluorimeter are equipped with a grating, the excitation and emission bandwidths expressed in wavelengths, are nearly constant over the whole spectrum. The possibility of measuring analyte fluorescence in a "Raman gap" is therefore optimal in the red part of the spectrum. To prevent the detection of excitation light transmitted by the grating in the second-order diffraction mode and stray radiation of wavelengths not selected by the monochromators, optical filters should be used in addition.

Only few authors have extensively compared their LIF results with data obtained using a conventional fluorescence detector under the same chromatographic conditions. In Table 7 literature data are assembled in which LODs obtained with LIF and conventional fluorimetry are compared. In all but one case, LIF yields better results; the average gain is 10–100 fold. The maximum (6000) and minimum (0.3) gain reported for fluorescein isothiocyanate and 9-methylanthracene can be interpreted using the arguments presented above. The absorption spectrum of fluorescein isothiocyanate has a perfect match with the high-power 488-nm line of the argon-ion laser. As the background due to luminescent impurities is relatively low upon excitation with visible light, shot noise is dominant which means that the available power can be fully exploited. On the other hand, under the

Table 7
Comparison of analyte detectability in LC using laser-induced (LIF) and conventional fluorescence (CF) detection

Analyte	LOD_{CF}/LOD_{LIF}	LIF system			
		Laser	λ_{ex} (nm)	Power (mW)	Ref.
Dansyl-analine	10	Ar-ion	351–364	0.85	70
OPA-amino acids[a,c]	45	Ar-ion	334–364	250	44
NDA-amino acids[b,c]	78	Ar-ion	458	900	44
Coumarin 7	6	HeCd	442	13	33
Benzo[*a*]pyrene	10	N_2/BBQ	386	15	69
NDA-amino acids	31	N_2/coumarin 1	454	2.4	39
9-Methylanthracene	0.15	HeCd	325	0.3	52
Adriamycin	30	Ar-ion	488	8	26
9-Hydroxymethylanthracene	250	Ar-ion	351–364	200	62
Fluorescein isothiocyanate	6000	Ar-ion	488	2000	62
Benzo[*a*]pyrene	5	Ar-ion	257	5	65

[a] OPA, *o*-phthalaldehyde.
[b] NDA, 2,3-naphthalenedialdehyde.
[c] Precolumn derivatisation at high analyte concentration, with subsequent dilution prior to injection.

experimental conditions applied in Ref. [52], 9-methylanthracene strongly absorbs the 365-nm line of a mercury arc lamp, while the 325-nm HeCd laser line is only weakly absorbed. Furthermore, the background encountered in UV-LIF is relatively high so that in combination with the unstable HeCd laser, flicker noise is the (undesired) limiting factor.

It should be emphasized that the data in Table 7 refer to the analysis of standard solutions. When analysing real samples by means of LC with LIF detection, the presence of interfering compounds usually determines the much higher detection limits that can be achieved. In such a situation, the gain that can be obtained by using LIF instead of conventional fluorescence detection is small when conventional-size LC is utilized and flicker noise dominates. The large gap existing between the ideal "standard" situation and real trace-level analysis is further discussed in the next section.

3.4. Applications

Although the number of compounds that exhibit native fluorescence is rather limited, there are highly interesting analytes within that group, such as, e.g., polynuclear aromatic hydrocarbons (PAHs) and their metabolites, aflatoxins, aromatic amino acids, and several vitamins and drugs such as alkaloids and steroids [1]. Unfortunately, most of these compounds require excitation with UV light, a part of the spectrum that is not easily covered by lasers, although major developments are taking place in this area today. This is also the reason why, since the introduction of LIF detection in LC, much attention has been devoted to the use of chemical derivatization procedures involving the reaction of the analyte with a strongly fluorescent label that can be excited by visible laser light (naphthalene-2,3-dialdehyde [44], fluorescein isothiocyanate [55,62]). Extremely low LODs have been reported in the literature, such as a value of 1.2 pM (injected concentration, $S/N_{peak} = 3$) for phenylalanine derivatized with fluorescein isothiocyanate [62]. However, such LODs generally do not reflect "real-life" situations because they are based on the analysis of standard solutions prepared by derivatizing the test analytes at high concentrations, with subsequent dilution prior to injection (cf. Table 7). In actual practice, when low analyte concentrations have to be determined, it is not exceptional to use a 10 000-fold excess of label, and improving analyte detectability often turns out to

be limited by the (slow) kinetics of the labelling reaction. Impurities that are present in the labelling reagent (even in very low amounts) and the formation of side-products, also adversely affect the final result [63]. This has been discussed in some detail by Kwakman et al. [5] for chemiluminescence detection in LC. It has also been emphasized by Mank et al. who have recently described a covalent labelling of thiols appropriate to utilize visible diode laser induced fluorescence detection [64]. Since the present review deals only with native-fluorescent analytes, such problems, of course, do not play any role at all.

Table 8 summarizes literature data on LC with LIF detection for some native-fluorescent analytes. All data apply for standard solutions, except the measurements of adriamycin, which were carried out in urine. In most studies attention has been paid to the determination of PAHs which can be excited by the shortest wavelengths of the argon-ion-, krypton-ion-, HeCd- and N_2 laser.

The data reported by different workers can not be compared directly because of differences in the experimental conditions (analytes, separation systems, lasers). Table 8 should therefore merely be used to extract some general conclusions on LIF detection in [conventional-size, micro and open-tubular (OT)] LC and CE.

(i) In general, the lowest concentration detection limits are found in conventional-size LC, where the optical path lengths are large and optically favourable flow cell assemblies can be used. Although the absolute detection limits in packed capillary and open tubular LC are extremely low, they require the injection of rather concentrated sample solutions.

(ii) Despite the fact that the light power of diode lasers is relatively low, analyte detectability often is very good. With the long excitation wavelengths used, the background is caused almost completely by Raman scatter, even though it is considerably less intense in the red part of the spectrum due to its λ^{-4} dependence. Furthermore, the light output of diode lasers is very stable so that the background contains only shot noise. Diode laser induced fluorescence (DIO-LIF) has shown to have interesting possibilities for the detection of photosensitizers in photodynamic therapy [29]. A well-known example is disulfonated aluminum phthalocyanine $AlPcS_2$ (see Fig. 9b), which comprises up to sixteen isomeric compounds. Applying DIO-LIF at 670 nm (power 10 mW), for the major component in the liquid chromatograms of spiked urine and faeces extracts, a detection limit of $7 \cdot 10^{-12}$ M could be obtained (20 times lower than achievable with a conventional fluorescence detector). This sensitivity is high enough to obtain detailed information about the excretion of the various isomers: Fig. 9a shows chromatograms of urine samples over 30 days after injection of the rat with 1 μmol/kg $AlPcS_2$. Evidently, such detailed information is highly relevant from a pharmacokinetic point of view.

In the green part of the spectrum impurity fluorescence is still relatively weak and high-laser powers can be applied [26,42]. An interesting example of LIF detection of a natively fluorescent analyte is the bioanalysis of the cytostatic drug doxorubicin (adriamycin) in human plasma [26], see Fig. 10. This compound can be appropriately excited with the 488 nm line of the Argon-ion laser; its emission maximum is at 595 nm. For sample clean-up, only a one-step protein precipitation was needed. Compared to conventional fluorescence detection the determination limit (200 pg/ml) was improved more than one order of magnitude even by using an air-cooled Argon-ion laser providing 8 mW at 488 nm. Presumably an additional gain of at least one decade will be obtained by applying a high-power laser giving about 1 W, but the low-power system suffices for the problem at hand.

(iii) When excitation is performed with UV light, the instability of the laser light source is a serious disadvantage. For the relatively unstable HeCd laser, a stabilizing circuit or a ratioing technique was used to suppress the amount of flicker noise [36,45,33,52]. The LODs measured with deep-UV LIF were all limited by the combination of high backgrounds and fluctuations in the laser output [61,65–68]. In these studies, only part of the available laser power was used.

Table 8
Detectability of native-fluorescent analytes using LC-LIF and CE-LIF

Analyte	Excitation			Separation system			LOD			Time constant (s)	Ref.
	Laser	λ_{ex} (nm)[a]	Power (mW)[a]	Column diameter (m-m)	Cell type	Optical path length (mm)	Injected concentration	Detector concentration	Injected mass		
Aluminium phthalocyanine	Diode	670	10	3.1	em fiber[b]	1.1	7 p*M*	480 f*M*	130 fg	0.5	29
Adriamycin	Ar-ion	488	1200	4.6	em fiber	1.0	n.i.a.[c]	19 p*M*	10 pg	2	43
Adriamycin	Ar-ion	488	1000	3.0	square quartz	1.5	140 p*M*	230 p*M*	8 pg	1	26
Coumarin 7	HeCd	442	13	4.6	ex fiber[d]	5	3 p*M*	n.i.a.	11 fg	0.2	33
Fluoranthene	N_2/PBD	366	2.5	CS[e]	droplet	2	3.7 n*M*	340 p*M*	15 pg	3	38
Fluoranthene	Kr-ion	351 + 356	1500	4.6	free-falling jet	0.12	3 p*M*	80 f*M*	6 fg	n.s.[f]	40
Fluoranthene	Kr-ion	351 + 356	200	CS	droplet	2	3.7 n*M*	340 p*M*	15 pg	3	38
Benzo[*a*]pyrene	N_2/BBQ	386	15	4.0	quartz	n.s.	90 p*M*	10 p*M*	1.1 pg	4	69
Aflatoxin B_{2a}	HeCd	325	8	CS	droplet	2	375 p*M*	9 p*M*	1.1 pg	3	36
Anthracene	XeCl	308	20	4.6	droplet	2	225 n*M*	11 n*M*	800 pg	n.s.	71
Benzo[*a*]pyrene	Ar-ion	257	5	3.0	em fiber	1.1	200 p*M*	9 p*M*	500 fg	1	65
Pyrene	HeCd	325	6.5	0.25 capillary	em fiber	0.050	3 n*M*	n.i.a.	120 fg	0.3	45
Perylene	N_2/BBQ	386	1	0.35 capillary	capillary	n.s.	60 n*M*	n.i.a.	850 fg	n.s.	72
Riboflavin	HeCd	442	4.1	0.025 OTLC	on-column	0.025	n.i.a.	4.8 n*M*	175 fg	1	52
Fluoranthene	HeCd	325	1.2	0.025 OTLC	on-column	0.025	500 n*M*	6 n*M*	100 fg	1	49
Conalbumin	Ar-ion	275	n.s.	0.050 CE	on-column	0.050	300 p*M*	n.i.a.	n.i.a.	n.s.	67
Tryptophan							5 n*M*	n.i.a.	n.i.a.	n.s.	67
Conalbumin	Ar-ion	257	9	0.050 CE	on-column	0.050	30 n*M*	n.i.a.	n.i.a.	n.s.	66
2-Methylanthracene	Ar-ion	257	10	0.025 CE	on-column	0.025	300 p*M*	n.i.a.	30 ag	n.s.	61
Tryptophan	KrF	248	12	0.075 CE	on-column	0.075	5 n*M*	n.i.a.	n.i.a.	0.05	68

Limits of detection from originally reported data were recalculated for S/N = 3 criterion (peak-to-peak noise). If neccessary, LOD detector concentrations (cf. CD_{det} in Eq. 8) were calculated from chromatogram figures

[a] For pulsed laser the average power is used.

[b] Emission light collected with fiber.

[c] No information available for recalculation.

[d] Excitation light coupled in via fiber.

[e] Conventional size, no information on exact column diameter available.

[f] Not stated in paper.

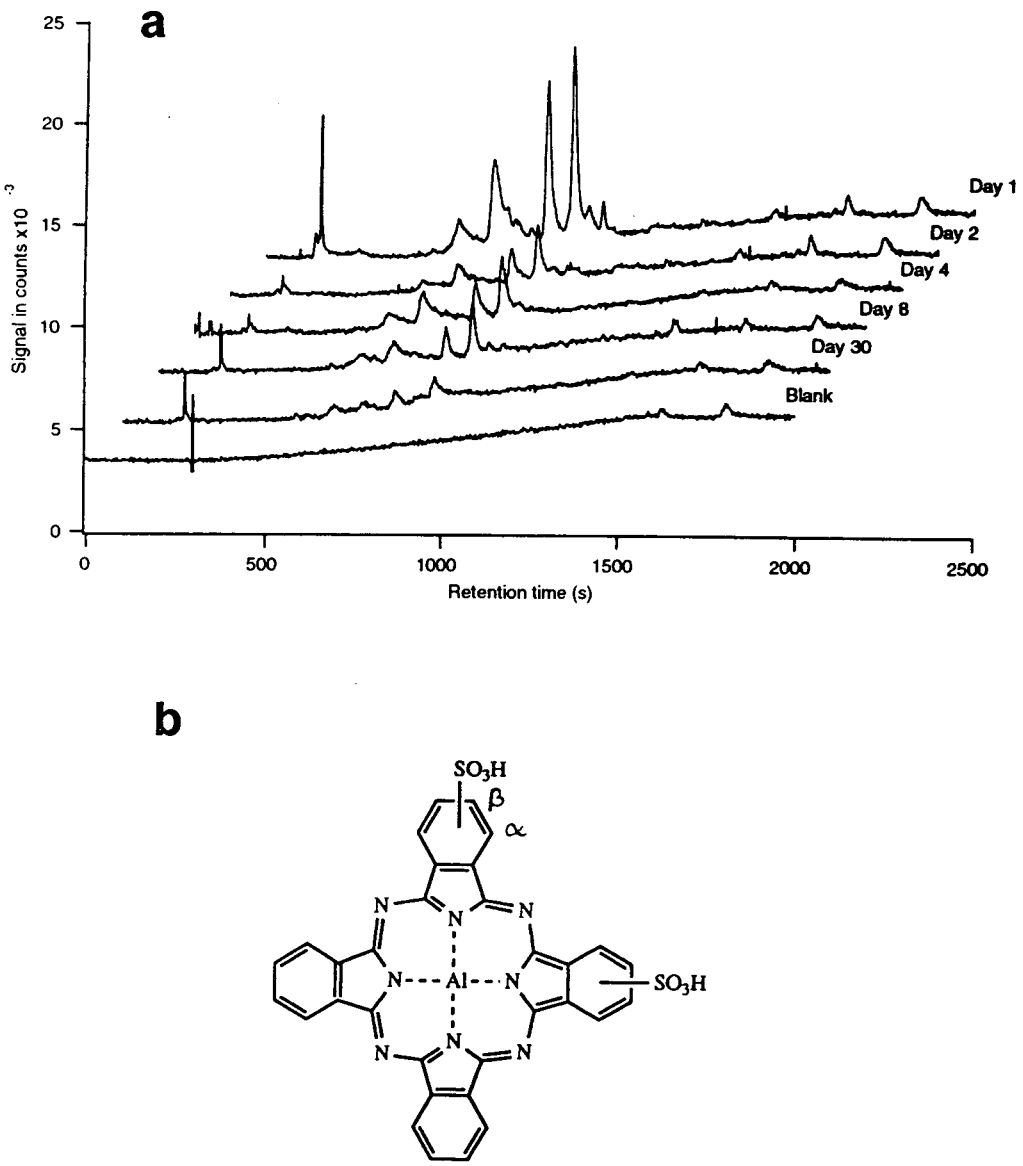

Fig. 9. (a) Chromatograms (performing linear gradient elution methanol–phosphate buffer, pH 5.0, from 25:75 to 90:10, v/v) of extracted urine samples after injection with 1 μmol/kg $AlPcS_2$; from Ref. [29]. (b) Structure of $AlPcS_2$.

(iv) As regards pulsed lasers it is remarkable that good LODs have been reported despite the well-known pulse-to-pulse instability [68,69]. Obviously, time discrimination is highly effective in decreasing background signals while pulse averaging diminishes the flicker noise.

(v) The LIF systems used for detection in CE demonstrate the potential of the new excitation possibilities in the deep-UV. Before the introduction of these laser lines, the analytes studied in the quoted work had to be determined using chemical derivatization of the amino group with subsequent analysis.

Deep-UV lines are not only useful for the

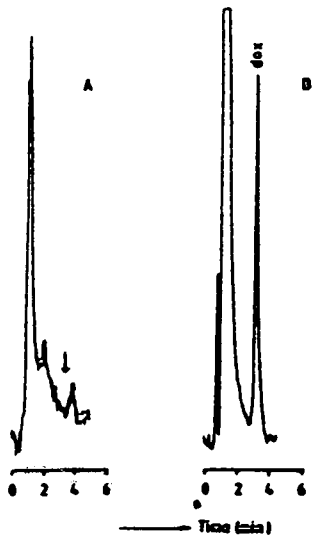

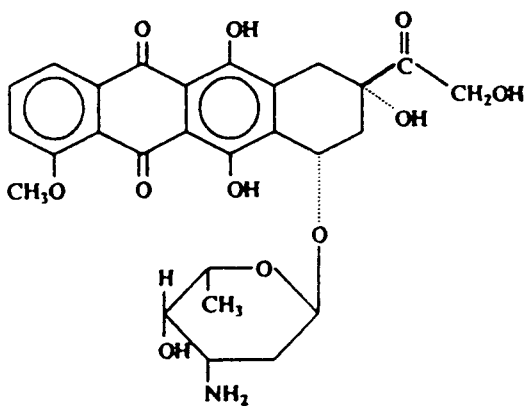

Fig. 10. Analysis of plasma samples pretreated by one-step protein precipitation. LIF detection was performed with an air-cooled Argon-ion laser (488 nm, 8 mW). The chromatograms were obtained using a conventional size RP-18 column; the mobile phase was a mixture of aqueous ortho-phosphoric acid solution (0.01 *M*) and acetonitrile (3:1, v/v). (A) Blank plasma sample; (B) plasma sample spiked with 4 ng/ml doxorubucin; (c) shows the chemical structure of doxorubicin (adriamycin). From Ref. [26].

detection of analytes which can not be excited by visible light. Since, at present, wavelength tuning of lasers over a large spectral range is not possible, the application range of a LIF system is determined by the coincidental match of the absorption spectrum of a particular analyte and the laser line. Because most analytes exhibit relatively high molar absorptivities at wavelengths shorter than 300 nm, a LIF detector operating in the deep-UV region has more potential than longer-wavelength systems. On the other hand its selectivity will be distinctly less, and the performance of such systems in real-life situations still has to meet the test.

4. Conclusions and future developments

The present review shows that LIF application in LC is not simply a matter of replacing a conventional light bulb, but that it involves adapting flow cells, optics, and detector instrumentation. Compared with laser excitation in the visible region, the problems encountered in deep-UV LIF are essentially different. In practice, background due to Raman scatter of the LC eluent can be readily excluded; on the wavelength scale it is so close to the laser line that it does not interfere with the analyte fluorescence and can be fully rejected by a simple cut-off filter. However, background luminescence from the flow cell assembly and impurities in the LC system show up strongly upon UV exposure. Eluents should therefore be purified and high-quality optical components should be used. As a result of the high background signal and instabilities in the laser output, flicker noise is already dominant at low excitation power. Under these conditions, the limit of detection can not be further improved because the noise amplitude and sample signal are both directly proportional with the laser power; the use of ratioing techniques and laser output stabilizers is of crucial importance.

As regards future developments, several new types of laser systems are now being developed. For detection of native-fluorescent analytes, the main interest will be on lasers which provide deep-UV light. An argon-ion laser producing these deep-UV lines already has been commercialized and hundreds of milliwatts are available.

Unfortunately, such a system is both expensive and large and requires high-power electrical facilities and extensive water cooling. The development of two other types of lasers seems more promising. Small-size excimer lasers are available today which operate on KrF gas and produce 248-nm light pulses at a frequency of 2000 Hz. Such a high repetition frequency enables efficient reduction of the noise caused by peak-to-peak fluctuations, by utilizing pulse averaging. Secondly, the use of diode lasers as pump source for neodymium lasers combined with a high-performance wavelength convertor has opened the way for an air-cooled and compact version that provides 266-nm light with low optical noise.

The above laser systems deliver only fixed wavelengths. For optimum excitation, tunability over a large spectral range is desirable. In this context, new developments in optical parametric oscillators (OPOs) combined with frequency mixing are interesting [7]. An OPO system, which is a tunable frequency converter based on an Nd:YAG laser, offers a "flat" spectral tuning curve in the deep UV. Although OPOs are still in the experimental stage, they bring us a step closer to the dream of every (analytical) spectroscopist: a versatile laser system providing tunable radiation from the visible region to the deep-UV.

References

[1] N. Ichinose, G. Schwedt, F.M. Schnepel and K. Adachi, in J.D. Winefordner (Editor), *Fluorimetric Analysis in Biomedical Chemistry*, Wiley, New York, 1991, Chs. 4 and 5.

[2] W.G.R. Bayens, D. de Keukeleire and K. Kordikis (Editors), *Luminescence Techniques in Chemical and Biomedical Analysis*, Marcel Dekker, New York, 1991.

[3] J.W. Hofstraat, C. Gooijer and N.H. Velthorst, in S.G. Schulman (Editor), *Molecular Luminescence Spectroscopy*, Part 3, Wiley, New York, Ch. 9, 1993.

[4] C.M.B. van den Beld and H. Lingeman, in W.G.R. Bayens, D. de Keukeleire and K. Korkidis (Editors), *Luminescence Techniques in Chemical and Biomedical Analysis*, Marcel Dekker, New York, 1991, Ch. 9.

[5] P.J.M. Kwakman, H. Koelewijn, I. Kool, U.A.Th. Brinkman and G.J. de Jong, *J. Chromatogr.*, 511 (1990) 155.

[6] T.H. Maiman, *Nature*, 187 (1960) 493.

[7] J.J. Ewing, *Laser Focus World*, November 1993, p. 105.

[8] J. Hecht, *Laser Focus World*, May 1992 p. 105, December 1992 p. 97, August 1993 p. 67.

[9] J. Hecht, *Laser Focus World*, April 1992 p. 77, June 1992 p. 63, May 1993 p. 87.

[10] J. Hecht, *The Laser Guidebook*, McGraw-Hill, New York, 2nd ed., 1992.

[11] J. Fabian, H. Nakazumi and M. Matsuoka, *Chem. Rev.*, 92 (1992) 1197.

[12] A.J.G. Mank, H. Lingeman and C. Gooijer, *Trends Anal. Chem.*, 11 (1992) 210.

[13] G. Patonay and M.D. Antoine, *Anal.Chem.*, 63 (1991) 321A.

[14] I. Imasaka, A. Tsukemoto and N. Ishibashi, *Anal. Chem.*, 61 (1989) 2285.

[15] R. Niessner, U. Panne and H. Schröder, *Anal. Chim. Acta*, 255 (1991) 231.

[16] S.H. Wu and N.J. Dovichi, *J. Chromatogr.*, 480 (1989) 141.

[17] S.A. Asher, R.W. Bormett, X.G. Chen, D.H. Lemmon, N. Cho, P. Peterson, M. Arrigoni, L. Spinelli and J. Cannon, *Appl. Spectrosc.*, 47 (1993) 628.

[18] P.A. Harmon, J. Teraoka and S.A. Asher, *J. Am. Chem. Soc.*, 122 (1990) 8789.

[19] I. Carmichael and G.L. Hug, *J. Phys. Chem.*, 89 (1985) 4036.

[20] R.R. Birge, in D.S. Kliger (Editor), *Ultrasensitive Laser Spectroscopy*, Academic Press, New York, 1983, Ch. 2.

[21] R.A. Mathies, K. Peck and L. Stryer, *Anal. Chem.*, 62 (1990) 1766.

[22] D.C. Nguyen, R.A. Keller, J.H. Jett and J.C. Martin, *Anal. Chem.*, 59 (1987) 2158.

[23] A.P. Larson, H. Ahlberg and S. Folestad, *Appl. Opt.*, 32 (1993) 794.

[24] A. Taylor and E.S. Yeung, *Anal. Chem.*, 64 (1992) 1741.

[25] J.H. Sugarman and R.K. Prud'homme, *Ind. Eng. Chem. Res.*, 26 (1987) 1449.

[26] C.M.B. van den Beld, *Ph.D. Thesis*, Leiden University, The Netherlands, 1991.

[27] T.G. Matthews and F.E. Lytle, *Anal. Chem.*, 51 (1979) 583.

[28] T.G. Matthews and F.E. Lytle, *Anal. Chem.*, 51 (1979) 583.

[29] A.J.G. Mank, C. Gooijer, H. Lingeman, N.H. Velthorst and U.A.Th. Brinkman, *Anal. Chim. Acta.*, 290 (1994) 103.

[30] R.J. van de Nesse, G.Ph. Hoornweg, C. Gooijer, U.A.Th. Brinkman, N.H. Velthorst and B. Law, *Anal. Chim. Acta*, 281 (1993) 373.

[31] J.E. Knoll, *J. Chromatogr. Sci.*, 23 (1985) 422.

[32] J.D. Ingle, Jr. and S.R. Crouch, *Spectrochemical Analysis*, Prentice-Hall, Englewood Cliffs, NJ, 1988, Ch. 5.

[33] J.M. Bostick, J.W. Strojek, T. Metcalf and T. Kuwana, *Appl. Spectrosc.*, 46 (1991) 1532.

[34] J.P. Foley and J.G. Dorsey, *Chromatographia*, 18 (1984) 503.

[35] ACS Committee on Environmental Improvement, *Anal. Chem.*, 52 (1980) 2242.
[36] G.J. Diebold and R.N. Zare, *Science*, 196 (1977) 1439.
[37] K.H. Milby and R.N. Zare, *Int. Lab.*, March/April (1984) 10.
[38] J.H. Richardson, K.M. Larson, G.R. Haugen, D.C. Johnson and J.E. Clarkson, *Anal. Chim. Acta*, 116 (1980) 407.
[39] K.-I. Tsunoda, A. Nomura, J. Yamada and S. Nishi, *Anal. Chim. Acta*, 229 (1990) 3.
[40] S. Folestad, L. Johnson, B. Josefsson and B. Galle, *Anal. Chem.*, 54 (1982) 925.
[41] S. Folestad, B. Galle and B. Josefsson, *J. Chromatogr. Sci.*, 23 (1985) 273.
[42] E.S. Yeung and M.J. Sepaniak, *Anal Chem.*, 52 (1980) 1465A.
[43] M.J. Sepaniak and E.S. Yeung, *J. Chromatogr.*, 190 (1980) 377.
[44] M.C. Roach and M.D. Harmony, *Anal. Chem.*, 59 (1987) 411.
[45] J. Gluckman, D. Shelly and M. Novotny, *J. Chromatogr.* 317 (1984) 443.
[46] H. Todiriki and A.Y. Hirakawa, *Chem. Pharm. Bull.*, 32 (1984) 193.
[47] S.A. Soper, S.M. Lunte and T. Kuwana, *Anal. Sci.*, 5 (1989) 23.
[48] K.-I. Tsunoda, A. Nomura, J. Yamada and S. Nishi, *Anal. Chim. Acta*, 229 (1990) 3.
[49] H.P.M. van Vliet and H. Poppe, *J. Chromatogr.*, 346 (1985) 149.
[50] M. Verzele and C. Dewaele, *J. High Resolut. Chromatogr. Chromatogr. Commun.*, 10 (1987) 248.
[51] K.J. Miller and F.E. Lytle, *J. Chromatogr.*, 648 (1993) 245.
[52] E.J. Guthrie, J.W. Jorgenson and P.R. Dluzneski, *J. Chromatogr. Sci.*, 22 (1984) 171.
[53] Y. Kurosu, T. Sasaki and M. Saito, *J. High Resolut. Chromatogr.*, 14 (1991) 186.
[54] L.W. Hersberger, J.B. Callis and G.D. Christian, *Anal. Chem.*, 51 (1979) 1444.
[55] Y.F. Cheng and N.J. Dovichi, *Science*, 242 (1988) 562.
[56] D.C. Nguyen, R.A. Keller, J.H. Jett and J.C. Martin, *Anal. Chem.*, 59 (1987) 2158.
[57] N.J. Dovichi, J.C. Martin, J.H. Jett, M. Trkula and R.A. Keller, *Anal. Chem.*, 56 (1984) 348.
[58] J.H. Hahn, S.A. Soper, H.L. Nutter, J.C. Martin, J.H. Jett and R.A. Keller, *Appl. Spectrosc.*, 45 (1991) 743.
[59] E. Arriaga, D.Y. Chen, X.L. Cheng and N.J. Dovichi, *J. Chromatogr. A*, 652 (1993) 347.
[60] M. Albin, R. Weinberger, E. Sapp and S. Moring, *Anal. Chem.*, 63 (1991) 417.
[61] S. Nie, R. Dadoo and R.N. Zare, *Anal. Chem.*, 65 (1993) 3571.
[62] C.M.B. van den Beld, H. Lingeman, G.J. van Ringen, U.R. Tjaden and J. van der Greef, *Anal. Chim. Acta*, 205 (1988) 15.
[63] C.M.B. van den Beld, U.R. Tjaden, N.J. Reinhoud, D.S. Stegehuis and J. van der Greef, *J. Control. Rel.*, 13 (1990) 129.
[64] A.J.G. Mank, E.J. Molenaar, H. Lingeman, C. Gooijer, U.A.Th. Brinkman and N.H. Velthorst, *Anal. Chem.*, 65 (1993) 2197.
[65] R.J. van de Nesse, G.Ph. Hoornweg, C. Gooijer, U.A.Th. Brinkman and N.H. Velthorst, *Anal. Chim. Acta*, 227 (1989) 173.
[66] D.F. Swaile and M.J. Sepaniak, *J. Liq. Chromatogr.*, 14 (1991) 869.
[67] T.T. Lee and E.S. Yeung, *J. Chromatogr.*, 595 (1992) 319.
[68] K.C. Chan, G.M. Janini, G.M. Muschik and H.J. Issaq, *J. Liq. Chromatogr.*, 6 (1993) 1877.
[69] N. Furuta and A. Otsuki, *Anal. Chem.*, 55 (1983) 2407.

ELSEVIER

Journal of Chromatography A, 704 (1995) 27–36

JOURNAL OF CHROMATOGRAPHY A

Review

Selective determination of peptides containing specific amino acid residues by high-performance liquid chromatography and capillary electrophoresis

Hua Cui, J. Leon, E. Reusaet, Auke Bult*

Department of Pharmaceutical Analysis, Faculty of Pharmacy, Utrecht University, Sorbonnelaan 16, 3584 CA Utrecht, Netherlands

First received 9 January 1995; revised manuscript received 6 February 1995; accepted 6 February 1995

Abstract

HPLC and CE methods for the selective determination of peptides containing cysteine, arginine, tryptophan, tyrosine and proline are reviewed. Chemical derivatization combined with UV–visible and fluorescent detection is the most often used method. The derivatization conditions, sensitivities, advantages, disadvantages and applications of these methods are discussed. Related methods are also considered.

Contents

* Corresponding author.

0021-9673/95/$29.00
SSDI 0021-9673(95)00167-0

1. Introduction

There is increasing interest in the investigation of bioactive peptides related to most areas of life sciences. For their identification, quantification and purification, a number of methods have been developed. High-performance liquid chromatography (HPLC) is a powerful technique for the separation and determination of peptides owing to the good recovery, high resolution and considerable experimental flexibility [1]. It has been widely used in peptide chemistry. Recently, capillary electrophoresis (CE) [2,3] has made great progress as a complementary method to HPLC. It permits rapid and efficient separations of charged components present in small sample volumes. Increasing numbers of papers have been published about separation and determination of peptides by CE.

A variety of detection techniques in HPLC and CE have been applied to the determination of peptides, including radioimmunoassay, mass spectrometry (MS), ultraviolet (UV)–visible absorption, electrochemical detection and fluorescence measurements. According to Kai et al. [4], radioimmunoassay as an off-line detection method in HPLC generally offers high sensitivity and selectivity for peptides, but it is difficult to obtain specific antibodies, especially for oligopeptides. In addition, the methodology does not provide any structural information about unknown peptides. Mass spectrometric detection coupled with HPLC and CE needs expensive instrumentation and refined operation, although the method shows good structural specificity for peptides. UV detection at wavelengths between 200 and 280 nm is the most frequently used method for the detection of peptides. The detection does not require derivatization of peptide. However, UV detection is not selective for peptides, and UV-absorbing components in crude samples and/or in the mobile phase may interfere with the sensitive determination of peptides. Fluorescence detection is far superior to UV detection in both sensitivity and selectivity, because there are relatively few fluorescent interfering substances. However, introduction of a fluorescent label in the peptide is necessary. Electrochemical detection usually offers better sensitivity and selectivity than UV detection, but is influenced by oxidizing or reducing components in samples and in the mobile phase.

There is a need for the sensitive and selective determination of peptides containing specific amino acid residues in complex samples such as enzymatic digests, degradation products and parent compounds and metabolites of peptide drugs in biological samples. For this purpose, chemical derivatization combined with UV–visible and fluorescent detection in HPLC and CE is the most often used method. A selected number of reagents can react selectively with particular amino acid residues in peptides and proteins under mild conditions and form derivatives with characteristic spectral features that are detectable by UV–visible and/or fluorescent detection. Ideal chemical derivatization should meet the following requirements: (a) the derivatization reagent is selective for a specific amino acid residue; (b) the peptides of interest are rapidly and quantitatively derivatized under mild conditions with a minimum of manipulations, while no degradation of peptides occurs; (c) the label introduces a high degree of sensitivity; (d) the derivatization reagent and its possible degradation products formed during the reaction are either non-detectable or well separable from the derivatized peptides of interest; and (e) for precolumn derivatization, the derivatives should be stable.

The derivatization can take place at the precolumn or postcolumn stage. Both techniques have their own limitations [5]. Precolumn derivatization is the simplest and most commonly used procedure. Because the sample is labelled prior to separation, no modification of the instrument is needed to incorporate the derivatization step. However, the derivative produced has to be stable, otherwise postcolumn derivatization is indicated.

Electrochemical detection without derivatization has been used for the selective determination of tyrosine-containing peptides, but the selectivity of the method is lower than that of the fluorescent derivatization method.

There may be as many as twenty different native amino acids in peptides. It is not yet possible to derivatize selectively amino acid

residues such as asparagine, aspartic acid, glutamic acid, glutamine, glycine, isoleucine, leucine, serine, threonine and valine because of the absence of characteristic side-chains, suitable for selective derivatization. On the other hand, although many chemical reagents for the specific modification of proteins and peptides have been described [6], some of them are not suitable for analytical purposes. Therefore, to date, only methods for the selective determination of peptides containing cysteine, arginine, tryptophan, tyrosine and proline have been reported. We review advances in this area. Some methods for the selective determination of specific amino acid residues in intact proteins are also briefly discussed. These methods are limited for the determination of a single protein without combination with HPLC and CE.

2. Selective determination of cysteine-containing peptides

Various thiol-specific reagents has been described for the selective determination of thiol-containing compounds [6–8]. They consist of chromogenic and fluorigenic reagents. Chromogenic reagents, 5,5′-dithiobis(2-nitrobenzoic acid) (DTNB) and its analogues, have been reported for the selective determination of biologically important thiols (including small cysteine-containing peptides) through precolumn and postcolumn derivatization [7]. Several types of fluorigenic reagents have been developed for the selective determination of thiol-containing compounds, including dansylaziridine, N-substituted maleimides, bimanes and halogenobenzofurazans. Each reagent has its own merits [8]. Dansylaziridine produces highly fluorescent adducts, but is also fluorescent itself, which results in an interfering peak in the chromatogram. N-substituted maleimides have no blank fluorescence and give highly fluorescent adducts, but form multiple fluorescent products because of hydrolysis of the fluorophores. The reaction of bimanes with thiols is fast, but bimanes produce several reagent peaks in the chromatogram and may also react with non-thiolic functional groups. Halogenobenzofurazans present optimum fluorigenic and physico-chemical features, including lack of native fluorescence, high reactivity towards thiols and excellent solubility and stability of the reagents and their thiol derivatives, but require drastic derivatization conditions. Dansylaziridine, maleimides and bimanes have been applied for the selective detection of cysteine residues in proteins. Halogenobenzofurazans, ammonium 7-fluorobenzo-2-oxa-1,3-diazole-4-sulfonate (SBD-F) and 4-(aminosulfonyl)-7-fluoro-2,1,3-benzoxadiazole (ABD-F) have been used for the selective determination of cysteine-containing peptides. The selective determination of cysteine-containing peptides focuses mainly on the study of small peptides such as glutathione, cysteinylglycine and γ-glutamylcysteine that occur naturally in human body fluids. DTNB, SBD-F and ABD-F will be discussed in more detail.

2.1. DTNB and its analogues

DTNB (Ellman's reagent) reacts with thiol-containing compounds, resulting in the release of a mixed disulfide and 2-nitro-5-mercaptobenzoic acid (Fig. 1). Precolumn HPLC methods have

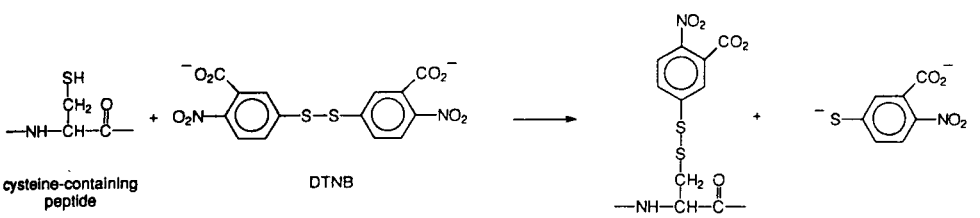

Fig. 1. Reaction of a cysteine-containing peptide with DTNB.

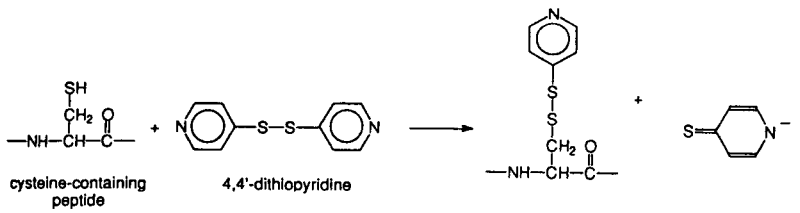

Fig. 2. Reaction of a cysteine-containing peptide with 4,4′-dithiopyridine.

been developed for the selective determination of small cysteine-containing peptides in biological samples [9,10]. The derivatization must be carried out at pH > 8.0. The mixed disulfide is detected at 280 or 330 nm. The methods have been applied for the determination of glutathione in rat liver [9] and of cysteine, γ-glutamylcysteine and glutathione in mouse liver [10]. The weakness of the methods based on DTNB derivatization is that the derivatization reaction requires a high pH.

4,4′-Dithiopyridine, similarly to DTNB, can derivatize thiol-containing compounds (Fig. 2). Andersson et al. [11] developed a postcolumn derivatization HPLC method for the determination of cysteine, glutathione, cysteinylglycine and γ-glutamylcysteine in plasma. The derivatization was carried out at pH 7.3 and the thione anion was detected at 324 nm. The detection limit is 50 nmol/l in plasma. 4,4′-Dithiopyridine was compared with DTNB. DTNB may be preferable to dithiopyridine for precolumn derivatization, whereas postcolumn derivatization with 4,4′-dithiopyridine gives better sensitivity owing to the higher absorbance coefficient of the thione anion.

Other aromatic disulfides such as 2,2′-dithiodipyridine and 6,6′-dithiodinicotinic acid have lower absorptivities, making them less attractive sulfhydryl reagents than 4,4′-dithiopyridine and DTNB.

2.2. SBD-F

SBD-F was described in 1983 as a fluorigenic reagent for the determination of thiol-containing compounds [12]. Small cysteine-containing peptides such as glutathione and other biological thiols in blood and plasma are typically derivatized at pH 9.5 and 60°C for 1 h and determined by HPLC [13–16] and CE [17] with fluorescence detection at 515 nm with excitation at 385 nm. The derivatization scheme is shown in Fig. 3. Sueyoshi et al. [18] used SBD-F as a precolumn derivatization reagent for the selective detection of cysteine-containing peptides in RP-HPLC. A peptide containing a disulfide bond was reduced and cleaved with tributylphosphine, and then reacted with SBD-F at pH 8.5 and 60°C for 1 h. The range of quantification was 100 pmol to 10 nmol. The method has been applied to the selective detection of cysteine-containing fragments in an enzymatic digest of bovine high-molecular-mass kininogen.

Ling and Baeyens [19] carried out a comparative study of micro-LC and capillary zone electrophoresis for the analysis of thiols (including small peptides containing cysteine) using SBD-F as a precolumn derivatization reagent. Both systems have been applied to the specific detection of reduced glutathione in human whole blood.

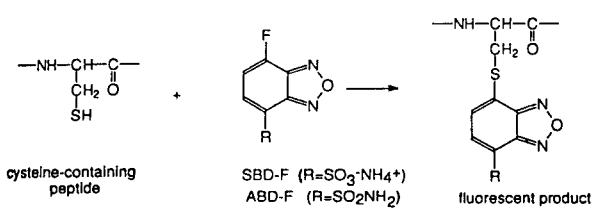

Fig. 3. Reaction of a cysteine-containing peptide with SBD-F and ABD-F.

In conclusion, the methods based on SBD-F are simple, sensitive and reliable and there are no interfering reagent peaks in the chromatogram. Disadvantages include the low reactivity of SBD-F, the long reaction time and alkaline pH.

2.3. ABD-F

ABD-F is similar to SBD-F. It was designed and synthesized in order to obtain milder derivatization conditions than with SBD-F and to overcome possible thiol degradation [20]. The derivatization reaction is typically carried out at pH 8.0 and 50°C for 5 min (Fig. 3). The fluorescence is monitored at 510 nm with excitation at 380 nm. ABD-labelled small peptides such as glutathione and other biological thiols were separated by HPLC and detected fluorimetrically with a detection limit of 0.4 pmol. ABD-F is also used for the differentiation of cysteine residues in proteins of large molecular mass. Toyo'oka and Imai [21] isolated and characterized cysteine-containing regions of proteins using ABD-F and HPLC. Egg albumin as a model for thiol-containing proteins was treated with ABD-F. In the presence of 0.5% sodium dodecyl sulfate (SDS) at pH 8.0 and 60°C for 1 h, all four cysteine residues (Nos. 11, 30, 367 and 382) were specifically labelled. In the absence of SDS at pH 8.0 and 40°C for 1 h, however, selective labelling of only one cysteine residue (No. 367) occurred.

It is concluded that ABD-F is a useful reagent for the sensitive and selective determination of cysteine-containing peptides by HPLC because of its excellent reactivity, selectivity to the thiol group, low fluorescence background, and good fluorophore stability. Moreover, its solubility in water may be also advantageous for reaction with native proteins.

3. Selective determination of arginine-containing peptides

The specific determination of arginine-containing peptides is relatively difficult to achieve. The high pK_a of the guanidine functional group ($pK_a = 12–13$) necessitates fairly drastic reaction conditions (pH 12) to generate an effective nucleophile. Most proteins and peptides are not stable to extremely alkaline pH. However, benzoin as a fluorescent derivatization reagent has been reported for the selective determination of arginine-containing peptides by HPLC and CE. Although 9,10-phenanthrenequinone [22,23] and ninhydrin [24] have been used as fluorescent derivatization reagents for the determination of monosubstituted guanidino compounds by HPLC, they have not been applied to the selective determination of arginine-containing peptides by HPLC. In principle, they are applicable to the determination of arginine-containing peptides, although the derivatization conditions may need to be modified. However, the sensitivity of methods for monosubstituted guanidino compounds using 9,10-phenanthrenequinone and ninhydrin is lower than with benzoin. In addition, 9,10-phenanthrenequinone is insoluble in water and must be dissolved in dimethylformamide, which often causes incompatibility with the mobile phase in HPLC.

3.1. Benzoin

Benzoin was found to react selectively with guanidine and monosubstituted guanidino compounds (including arginine containing peptides) in alkaline solution (Fig. 4). The adduct 2-substituted amino-4,5-diphenylimidazole shows strong fluorescence at 435 nm with excitation at 325 nm [25–27]. Several HPLC methods based on this reaction have been developed for the selective determination of arginine-containing peptides.

Ohno et al. [28] proposed a reversed-phase HPLC method coupled with on-line postcolumn derivatization with benzoin and fluorescence detection for the selective determination of arginine-containing peptides. The arginine-containing peptides kyotorphin, kallidin, bradykinin, angiotensin (ANG) I, II and III, substance P and β-melanocyte stimulating hormone (β-MSH) could be determined with detection limits of 5–15 pmol. The facile detection of arginine-con-

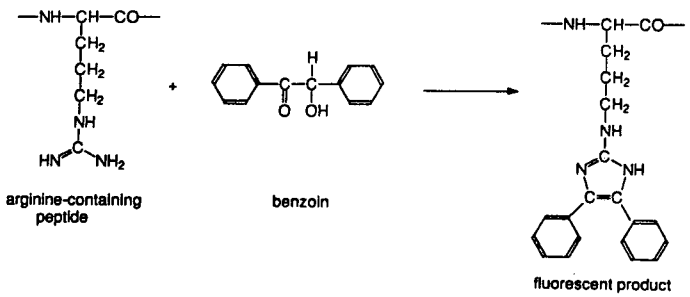

Fig. 4. Reaction of an arginine-containing peptide with benzoin.

taining fragments in the tryptic digest of β-melanocyte stimulating hormone as a model compound showed satisfactory result.

Precolumn fluorescence derivatization is more sensitive than postcolumn derivatization, which allows detection levels in the femtomole range for arginine-containing peptides [29]. The derivatization reaction is typically carried out at 100°C for 90 s in 0.2 *M* potassium hydroxide containing 3 m*M* benzoin. The HPLC method allows the determination of ANG I, II and III. The benzoin derivatives of ANGs and their analogues can be successfully resolved on a reversed-phase column with isocratic elution. This HPLC method can be applied not only to enzyme assays in the renin–angiotensin system but also to the investigation of the enzymatic degradation of various ANGs in biological samples [30]. The disadvantage of this method is that the column slowly deteriorates because of the alkaline mobile phase (pH 8–9).

Cobb and Novotny [31] proposed a CE method with laser-induced fluorescence detection for the selective determination of arginine-containing peptides using the reaction with benzoin. ANG I, II and III and their analogues were used as model arginine-containing peptides. Derivatization was performed prior to separation under the conditions used in precolumn derivatization HPLC. A detection limit of 270 amol was achieved for model arginine-containing peptide. The selective detection of arginine-containing fragments in the tryptic digest of chicken egg white lysozyme also demonstrates the applicability of the method for high-sensitivity peptide mapping. The use of CE permits rapid and highly efficient separations with minimal sample volumes, while the laser-based fluorescence detection system yields three orders of magnitude lower detection limits than HPLC with conventional fluorescence detection [27].

Tomori [32] investigated the fluorescence derivatization of DLL-MePhe-Pro-Arg-H (LY-DLL, LY-294468) with benzoin. It was found that the guanidino group of the arginine residue was not converted into a fluorescent derivative by reaction with benzoin. However, if the LY-DLL was first converted into an LY-DLL–Tris adduct with Tris–HCl buffer (pH 8.5) for 3–24 h at room temperature, the LY-DLL–Tris adduct could be derivatized by benzoin at 65°C for 5 min in 0.8 *M* sodium hydroxide. The HPLC method based on the modification has been proposed for the determination of LY-DLL in biological fluids.

Recently, we studied the precolumn fluorescence derivatization of antagonist [Arg^6, D-$Trp^{7,9}$, $MePhe^8$]–substance P {6–11} (antagonist G) with benzoin by HPLC (unpublished results). It was found that under the derivatization conditions used in the literature [29] antagonist G was partly degraded so that several peaks were observed in the chromatogram. Therefore, milder conditions for antagonist G were chosen. Under the conditions used (0.067 *M* NaOH, heating at 100°C for 10 s), good results were obtained and degradation was negligible. The detection limit was 0.21 nmol/ml. The method has been successfully applied to the selective detection of arginine-containing fragments in

chemical degradation products of antagonist G. One and three fragments were found in acidic and alkaline solution, respectively.

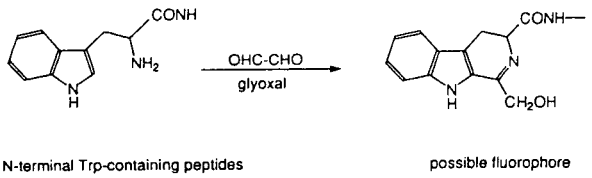

Fig. 5. Reaction of an N-terminal trypophan peptide with glyoxal.

4. Selective determination of tryptophan-containing peptides

There are few reports on the selective determination of tryptophan-containing peptides. However, some papers have been published on the determination of tryptophan in intact proteins, by a direct spectrophotometric determination or a spectrophotometric determination based on colour reactions of intact protein with a variety of reagents, such as sulfenyl halides, 2-hydroxy-5-nitrobenzyl bromide and acid ninhydrin. Direct spectrophotometric determination is based on the absorption of the aromatic group of tryptophan, tyrosine and phenylalanine in the UV region between 250 and 300 nm. Each amino acid has its own characteristic absorption pattern. Derivative spectrophotometric techniques have been introduced to measure tryptophan in the presence of tyrosine and phenylalanine [33–38]. The methods need a considerably large amount of sample proteins and are affected by other absorbing components. Spectrophotometric determinations based on colour reactions with sulfonyl halides [39–41], 2-hydroxy-5-nitrobenzyl bromide [42,43] and acid ninhydrin [44] are not strictly selective for tryptophan and the reagents also react with cysteine. In principle, these methods are applicable as a basis for the selective determination of tryptophan-containing peptides. However, the methods have not so far been combined with HPLC and CE and measure only one peptide or protein in a single analysis. Only the fluorescence derivatization reagent glyoxal has been reported for the selective determination of tryptophan-containing peptides.

4.1. Glyoxal

It was found that phenylglyoxal and glyoxal react selectively with N-terminal tryptophan-containing peptides and form highly fluorescence derivatives (Fig. 5). However, the reaction of phenylglyoxal with the N-terminal tryptophan peptide results in several fluorescent products, whereas the reaction of glyoxal gives a single fluorescence product [45]. Kai et al. [4] proposed an HPLC method for the sensitive and selective determination of N-terminal tryptophan peptides using glyoxal as a precolumn fluorescence derivatization reagent. The derivatization takes place in acidic medium (pH 4.5) at 100°C for 30 min. The fluorescence was detected at 465 nm with excitation at 275 nm. The detection limits for N-terminal tryptophan-containing peptides Trp-Gly-Gly, Trp-Gly, Trp-Ala, Trp-Leu and Trp-Met-Asp-Phe-NH_2 were 55–382 fmol per 100-μl injection volume. The method also allowed the facile detection of an N-terminal tryptophan fragment in the enzyme reaction mixture of dynophin A with trypsin.

5. Selective determination of tyrosine-containing peptides

Derivative spectrophotometry can also be used for the determination of tyrosine in intact proteins [33–38]. Several good methods have been reported for the selective determination of tyrosine-containing peptides by HPLC and CE by use of the fluorescence derivatization reagents 1,2-diamino-4,5-dimethoxybenzene and borate–hydroxylamine–cobalt(II). In addition, HPLC combined with electrochemical detection has been used for this purpose.

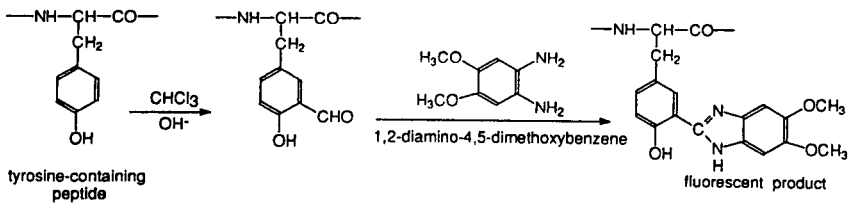

Fig. 6. Reaction of a tyrosine-containing peptide with 1,2-diamino-4,5-dimethoxybenzene.

5.1. 1,2-Diamino-4,5-dimethoxybenzene

A precolumn fluorescence derivatization method has been described for the HPLC determination of tyrosine-containing peptides [46]. The tyrosine residue in the peptide is first formylated in 0.6 *M* potassium hydroxide at 60°C for 10 min in the presence of 50% (v/v) chloroform, and the resulting formylaldehyde is then converted into a fluorescent derivative by reaction with 1,2-diamino-4,5-dimethoxybenzene at 60°C for 18 min in a weakly acidic solution (pH 3–4). The derivatization scheme is shown in Fig. 6. The peptide derivatives fluoresce most intensely at pH 1.3–3.5. The derivatives were separated on a reversed-phase column by isocratic elution and detected at 425 nm with excitation at 350 nm. The detection limits for the tyrosine-containing peptides tested (Tyr-Gly, Gly-Tyr, Tyr-Arg, Tyr-Phe, Tyr-Gly-Gly, Tyr-Gly-Gly-Phe, methionine enkephalin, leucine enkephalin and ANG (I, II and III)) are in the range 3.4–26.2 pmol.

1,2-Diamino-4-methoxybenzene, resembling 1,2-diamino-4,5-dimethoxybenzene, has also been utilized for the selective determination of tyrosine-containing peptides in a combination with CE and laser-induced fluorescence detection [31]. The model tyrosine-containing peptides Gly-Leu-Tyr, Tyr-Arg, ANG II, methionine enkephalin and leucine enkephalin were detected at 438 nm with excitation at 330 nm. The detection limit for leucine enkephalin was 390 amol, which is four orders of magnitude lower than with HPLC and conventional fluorescence detection. This method has been applied to the detection of tyrosine-containing peptides in the chymotryptic digest of horse heart cytochrome *c* for peptide mapping purposes.

5.2. Borate–hydroxylamine–cobalt(II)

Kai and Ohkura [47] described a fluorescence derivatization method for N-terminal tyrosine-containing peptides. The derivatives of the peptide are formed by heating at 100°C for 1–5 min in a weakly alkaline (pH 8–9) solution containing 3.3 m*M* hydroxylamine, 17 μM Co^{2+} and 0.1 *M* borate. The fluorescence is most intense at 440 nm with excitation at 330 nm in a weakly alkaline solution. The structure of the fluorescent product is unknown. The method can be applied to both precolumn and postcolumn derivatization systems for HPLC. Precolumn HPLC has been applied to endogenous enkephalins in a tissue extract at the 300-fmol level [48].

5.3. HPLC–electrochemical detection

Some amino acids have electroactive substituents. The most important of these are the phenol, indole and thiol substituents of tyrosine, tryptophan and cysteine, respectively. Peptides containing these amino acids should be detectable by electrochemical detection (ED). White [49] developed an HPLC method for the determination of tyrosine-containing peptides (oxytocin, Leu-enkephalin, ANG II and Lys-vasopressin) with ED (electrode potential +0.9 V). Although most peptides are probably electroactive by virtue of the terminal amino group, selectivity is reached by selection of a suitable electrode potential. ED is more selective than UV detection, but oxidizing and/or reducing compounds in biological samples should be removed before subjecting the samples to HPLC. Mousa and Couri [50] applied an HPLC–ED

method for the determination of enkephalins, β-endorphins, tyrosine, tyrosylglycine and tyrosylglycylglycines (electrode potential +1.25 V). The detection level was in the 10–100-pg range. This method can be used to determine tissue levels and to study pharmacodynamics of enkephalins and β-endorphin. A highly specific measurement of the different enzymes involved in the metabolism of enkephalin has been achieved.

6. Selective determination of proline-containing peptides

Only one paper has been published on the selective determination of proline-containing peptides [51]. Short-chain peptides with an N-terminal proline were determined by HPLC with laser-induced fluorescence (LIF) detection. The peptides were derivatized with 4-(N,N-dimethylaminosulfonyl) - 7 - fluoro - 2,1,3 - benzoxadiazole (DBD-F) at 50°C for 1 h in 0.1 *M* borax (pH 9.3)–acetonitrile (Fig. 7). The rate of reaction decreases with increase in the molecular mass of the peptide. The proline peptides, including bioactive peptides such as Pro-Leu-Gly-NH_2, Pro-Thr-Pro-Ser-NH_2 and Pro-Asp-Val-Asp-His-Val-Phe-Leu-Arg-Phe-NH_2, were well separated by reversed-phase HPLC. The detection limits with a 15-mW argon ion laser at 488 nm were in the 6–28-fmol range. The detection limits were improved to 2–5 fmol with a microbore column, which was two orders of magnitude higher than with a conventional fluorescence detector using a xenon arc lamp.

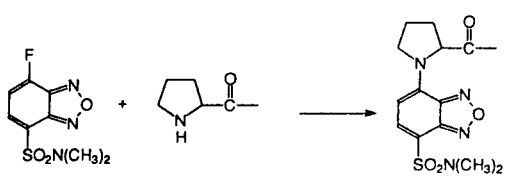

Fig. 7. Reaction of an N-terminal proline peptide with DBD-F.

7. Conclusions and future trends

Only a limited number of amino acids in peptides can be derivatized selectively. Extension of this number will be difficult and may be feasible only for the functional groups thiol–ether (methionine), primary aliphatic amino (lysine) and imidazole (histidine).

Development of more sensitive and selective detection methods can improve the future determination of peptides. Especially HPLC and CE combined with MS detection or LIF detection together with selective derivatization are expected to be fruitful.

The selective derivatization of amino acids in proteins is even more complicated compared with peptides because of steric hindrance by the three-dimensional structure of proteins. On the other hand, sometimes it is possible to differentiate between "outer" and "inner" amino acids in proteins.

The methods discussed can be applied to the analysis of complex mixtures such as enzyme digests, degradation products and biological fluids. Determination of peptides and proteins in biological fluids is of paramount interest for pharmacological studies of these compounds. Extensive application studies will be needed for different purposes.

References

[1] M.T.W. Hearn, in C. Horvath (Editor), High Performance Liquid Chromatography, Advances and Perspectives, Vol. 3, Academic Press, New York, 1983 pp. 87–155.
[2] D.M. Goodall, D.K. Lloyd and S.J. Williams, LC·GC Int., 3 (1990) 28–30, 32–36, 38, 40.
[3] Z. Deyl, F. Tagliaro and I. Miksik, J. Chromatogr. B, 656 (1994) 3–27.
[4] M. Kai, E. Kojima and Y. Ohkura, J. Chromatogr. A, 653 (1993) 235–240.
[5] H. Lingeman and W.J.M. Underberg, in H. Lingeman and W.J.M. Underberg (Editors), Detection-Oriented Derivatization Techniques in Liquid Chromatography, Marcel Dekker, New York, 1990, pp. 1–11.
[6] R.L. Lundblad and C.M. Noyes, Chemical Reagents for Protein Modification, CRC Press, Boca Raton, FL, 2nd ed., 1991.

[7] P.M. Ueland, H. Refsum, S.P. Stabler, M.R. Malinow, A. Anderson and R.H. Allen, Clin. Chem., 39 (1993) 1764–1779.
[8] W.R.G. Baeyens, K. Imai and B.L. Ling, in D. Eastwood and L.J. Cline Love (Editors), Progress in Analytical Luminescence, American Society for Testing and Materials, Philadelphia, 1988, pp. 83–99.
[9] J. Reeve and J. Kuhlenkamp, J. Chromatogr., 194 (1980) 424–428.
[10] C. Komuro, K. Ono, Y. Shibamoto, T. Nishidai, M. Takahashi and M. Abe J. Chromatogr., 338 (1985) 209–212.
[11] A. Andersson, A. Isaksson, L. Brattstrom and B. Hultberg, Clin. Chem., 39 (1993) 1590–1597.
[12] K. Imai, T. Toyo'oka and Y. Watanabe, Anal. Biochem., 128 (1983) 471–473.
[13] T. Toyo'oka and K. Imai, J. Chromatogr., 282 (1983) 495–500.
[14] T. Toyo'oka and K. Imai, Analyst, 109 (1984) 1003–1007.
[15] A. Araki and Y. Sako, J. Chromatogr., 422 (1987) 43–52.
[16] B.L. Ling, C. Dewaele and W.R.G. Baeyens, J. Chromatogr., 553 (1991) 433–439.
[17] B.L. Ling, W.R.G. Baeyens and C. Dewaele, Anal. Chim. Acta, 255 (1991) 283–288.
[18] T. Sueyoshi, T. Miyata, S. Iwanaya, T. Toyo'oka and K. Imai, J. Biochem. 97 (1985) 1811–1813.
[19] B.L. Ling and W.R.G. Baeyens, J. High Resolut. Chromatogr., 14 (1991) 169–173.
[20] T. Toyo'oka and K. Imai, Anal. Chem., 56 (1984) 2461–2464.
[21] T. Toyo'oka and K. Imai, Anal. Chem., 57 (1985) 1931–1937.
[22] Y. Yamamoto, A. Saito, T. Manji, K. Maeda and K. Ohta, J. Chromatogr., 162 (1979) 23–29.
[23] Y. Yamamoto, T. Manji, A. Saito, K. Maeda and K. Ohta, J. Chromatogr., 162 (1979) 327–340.
[24] Y. Hiraga and T. Kinoshita, J. Chromatogr., 226 (1981) 43–51.
[25] Y. Ohkura and M. Kai, Anal. Chim. Acta, 106 (1979) 89–94.
[26] M. Kai, M. Yamaguchi and Y. Ohkura, Anal. Chim. Acta, 120 (1980) 411–414.
[27] M. Kai, T. Miura, K. Kohashi and Y. Ohkura, Chem. Pharm. Bull., 29 (1981) 1115–1120.
[28] M. Ohno, M. Kai and Y. Ohkura, J. Chromatogr., 392 (1987) 309–316.
[29] M. Kai, T. Miyuzaki, Y. Sakomoto and Y. Ohkura, J. Chromatogr., 322 (1985) 473–477.
[30] Y. Sakamoto, T. Miyazaki, M. Kai and Y. Ohkura, J. Chromatogr., 380 (1986) 313–320.
[31] K.A. Cobb and M.V. Novotny, Anal. Biochem., 200 (1992) 149–155.
[32] E. Tomori, Chromatographia, 36 (1993) 105–109.
[33] C. Balestrieri, G. Colonna, A. Giovane, G. Irace and L. Servillo, Eur. J. Biochem., 90 (1978) 433–440.
[34] C. Balestrieri, G. Colonna, A. Giovane, G. Irace and L. Servillo, Anal. Biochem., 106 (1980) 49–54.
[35] L. Servillo, G. Colonna, C. Balestrieri, R. Ragone and G. Irace, Anal. Biochem., 126 (1982) 251–257.
[36] Y. Nozaki, Arch. Biochem. Biophys., 277 (1990) 324–333.
[37] L. Servillo, G. Colonna, C. Balestrieri, R. Ragone and G. Irace, Anal. Biochem., 126 (1982) 251–257.
[38] J. Bertini, C. Mannucci, R. Noferini, A. Perico and P. Rovero, J. Pharm. Sci., 82 (1993) 179–182.
[39] A. Fontana and E. Scoffone, Methods Enzymol., 25 (1972) 482–494.
[40] E. Boccu, F.M. Veronese, A. Fontana and C.A. Benassi, Eur. J. Biochem., 13 (1970) 188–192.
[41] A. Fontana, E. Scoffone and C.A. Benassi, Biochemistry, 7 (1968) 980–986.
[42] H.R. Horton and D.E. Koshland, Jr., J. Am. Chem. Soc., 87 (1965) 1126–1132.
[43] T.E. Barman and D.E. Koshland, Jr., J. Biol. Chem., 242 (1967) 5771–5776.
[44] I. Molnar-Perl and M. Pinter-Szakacs, Anal. Biochem., 177 (1989) 16–19.
[45] E. Kojima, Y. Ohba, M. Kai and Y. Ohkura, Anal. Chim. Acta, 280 (1993) 157–162.
[46] J. Ishida, M. Kai and Y. Ohkura, J. Chromatogr., 356 (1986) 171–177.
[47] M. Kai and Y. Ohkura, Anal. Chim. Acta, 182 (1986) 177–183.
[48] M. Kai and Y. Ohkura, Trends Anal. Chem., 6 (1987) 116–120.
[49] M.W. White, J. Chromatogr., 262 (1983) 420–425.
[50] S. Mousa and D. Couri, J. Chromatogr., 267 (1983) 191–198.
[51] T. Toyo'oka, M. Ishibashi and T. Terao, J. Chromatogr. A, 661 (1994) 105–112.

ELSEVIER

Journal of Chromatography A, 704 (1995) 37–44

JOURNAL OF CHROMATOGRAPHY A

NMR imaging of the chromatographic process. Deposition and removal of gadolinium ions on a reversed-phase liquid chromatographic column

Ernst Bayer, Edgar Baumeister, Ulrich Tallarek, Klaus Albert, Georges Guiochon*

Institut für Organische Chemie, Universität Tübingen, Auf der Morgenstelle 18, D-72076 Tübingen, Germany

Received 16 December 1994; accepted 13 February 1995

Abstract

NMR imaging permits the visualization of the adsorption processes which take place in chromatographic columns during the adsorption and concentration of strongly retained analytes from their solutions in weak solvents and during the desorption of these compounds as more concentrated bands in a strong mobile phase. The results obtained demonstrate that the surface of stationary phases is not homogeneous and that column beds are not homogeneously packed. These deviations from an idealized behavior must be taken into account in the interpretation of the results.

1. Introduction

The techniques of NMR imaging constitute powerful tools for the investigation of the various processes involved in the migration of bands along chromatographic columns. Previous publications have illustrated this phenomenon and investigated various aspects of the mechanism of band broadening [1,2]. In another implementation of the method, local values of the axial and transverse dispersion coefficients have been measured [3]. For the visualization of the various effects which take place inside the column, however, the use of Gadolinium(III) chelates is the simplest and most fruitful approach. This method is noninvasive and it allows the continuous monitoring of the bands of compounds injected in the column and the real-time analysis of these chromatographic bands directly inside the column. The method takes advantage of the enhancement by the gadolinium(III) atoms or ions of the rate of relaxation of the protons which are in their immediate neighborhood [4–6].

In spite of thirty years of intense investigations, there are still areas in chromatography which remain poorly understood. The most important includes the phenomena involved in band broadening [1–3] whose understanding is critical for improvement of the performance of columns and which are the topic of ongoing investigations. Other phenomena of importance are those related to analytical applications in which a compound contained in a solution is adsorbed at the column inlet where it is concentrated because the solution is a weak mobile

* Corresponding author. Address for correspondence: Department of Chemistry, University of Tennessee, Knoxville, TN, 37996-1600, USA.

0021-9673/95/$09.50
SSDI 0021-9673(95)00200-6

phase. A change in the mobile phase composition towards a stronger solution allows the migration of the analyte. This procedure is common in trace analysis. Here we present a study of this phenomenon of adsorption from a weak mobile phase followed by the desorption into a stronger eluent.

2. Experimental

The equipment and experimental design used in the present study are the same as described in our previous study on the migration and separation of gadolinium bands [2]. Thus, they are only briefly described.

2.1. Liquid chromatography

A Merck Superformance (Darmstadt, Germany) glass column (12 cm bed length × 2.6 cm I.D.) was packed with Lichrospher RP18 (Merck), 15 μm average particle size, by sedimentation of a concentrated slurry of the adsorbent. The system was completed by a SYKAM S 1100 pump (Gilching, Germany), a Rheodyne sampling valve (Cotati, CA. USA) and a Linear UVIS 204 detector (Reno, NE. USA). These devices were connected to the column by plastic tubings. Care was taken to avoid the presence of even nonmagnetic metals close to the column, because they could perturb the image, and in the same time to limit the extent of the extra-column contribution to band broadening. The mobile phase was a buffer solution (see below). The water and buffer solution were not filtered before use.

2.2. NMR system

The column was placed inside a solenoid coil (transmitter/receiver coil length, 10 cm), which was positioned horizontally in the middle of the superconducting whole body imager (Magnetom 63, Siemens, Erlangen, Germany) of the University of Tübingen. This imager operates at 1.5 Tesla, corresponding to a frequency of approximately 63.6 MHz for proton imaging. A set of three mutually orthogonal coil groups can produce any desired gradient, in any direction respective to the axis of the main magnetic field, with a maximum gradient strength of 10 mT/m. The column and the solenoid which surrounds it are positioned orthogonal to the tunnel axis, i.e., to the direction of the main magnetic field. The system permits the acquisition of images of the distribution of the gadolinium concentration in any planar direction. The direction is chosen by appropriately directing the magnetic field gradient. The image can be updated every 7 s. The image of the column cross-section (26 × 120 mm) is given in a 166 × 166 mm field of view, as a 256 × 256 matrix, the individual pixel corresponding to a 0.65 × 0.65 mm rectangle of column packing. In the construction of the image, the signal is averaged over a thickness of ca. 1 mm.

2.3. Analytes

The analytes are solutions of Gd(III) and of its complexes with ethylenediaminetetraacetic acid (EDTA), *trans*-1,2-cyclohexanediaminetetraacetic acid (CDTA), 1,4,7,10-tetraazacyclododecane-1,4,7,10-tetraacetic acid (DOTA), and diethylenetriaminepentaacetic acid (DTPA).

3. Results and discussion

As explained previously [2], the relationship between the intensity of the signal acquired during the imaging experiments and the local concentration of gadolinium is not linear. The signal increases with increasing concentration of gadolinium at low concentrations because the relaxation of the protons is enhanced by gadolinium (T_1 effect). The regions of the column where the concentration of gadolinium is low or moderate appear in shades of gray to white. However, at high concentrations, the relaxation is so fast that there is no signal [4–6]. Thus, the regions where the concentration of gadolinium is high appear black. The nonlinear behavior of the calibration curve explains the

images obtained and the change in appearance of the bands when their concentration varies.

In solution in pure water, Gd^{3+} associates with water molecules and forms a weakly stable complex, $[Gd(H_2O)_9]^{3+}$ or aquo complex. This complex is retained on the C_{18} bonded silica adsorbents used in reversed-phase chromatography, via silanophilic interactions with the residual silanols. Fig. 1 shows a 2D-FLASH image [7] of a longitudinal slice of the column in a horizontal plane shortly after an injection has been made. Note that in all figures, the direction of the mobile phase stream is from left to right. The sample injected is a solution of Gd^{3+}, Gd(III)EGTA, Gd(III)CDTA, and Gd(III)-DTPA. Under the conditions of the experiment (15% acetonitrile in the eluent), the concentration of Gd^{3+} is high enough to saturate the residual silanols and its retention time on chemically bonded C_{18} silica is negligible [8]. Thus, the Gd^{3+} band elutes as an unretained band. This band is seen in Fig. 1 as a thin dark black band. No signal is observed for the water protons in the vicinity of the Gd^{3+} band whose concentration is high. This is because the gadolinium ion has a very strong and efficient "inner sphere relaxation" effect [9–12] on up to the nine water molecules in the aquo complex, $[Gd(H_2O)_9]^{3+}$. Note that in Gd(III)DTPA there is one coordination site left for one water molecule. The rapid exchange with the surrounding water molecules explains the very low signal intensity in the region occupied by the band [13]. The signal is now determined by relaxation time T_2 rather than by T_1. The anomalies in the band profile have been previously explained [2].

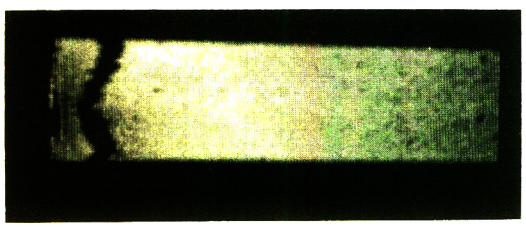

Fig. 1. 2D-FLASH image of a longitudinal, central slice of the column bed (26 mm wide, 95 mm long). The dark band in front is $[Gd(H_2O)_9]^{3+}$. Mobile phase, water–acetonitrile (85:15), 5 m*M* KH_2PO_4 and 4 m*M* octylamine, pH 5.0; flow-rate 3 ml/min (left to right). Acquisition parameters: flip angle $\theta = 90°$; repetition time, $T_R = 0.03$ s; echo time, $T_E = 10$ ms; slice thickness, 4 mm; image matrix, 256×256.

If the aquo complex is unretained on C_{18} silica, it is rather strongly retained on the residual silanols [14]. Thus, part of the gadolinium ions remain adsorbed on the surface for a certain time-period after passage of the band. When the concentration of gadolinium is moderate, the enhancement it causes to the relaxation of the water protons is significant but no longer as dramatic observed with the band of concentrated aquo complex. The T_1 effect dominates, leading to a higher signal [13]. As a consequence of the local presence of gadolinium, the contrast between the band of organic complexes and the column background is markedly reduced, as exemplified in Fig. 2.

To demonstrate the actual influence of the gadolinium adsorbed on the stationary phase on the separation between bands of organic complexes, the column was opened and the first centimeter of packing material was removed from the bed. Then the column was filled with an equivalent amount of virgin material from the same batch, flushed with pure acetonitrile, then with pure water. An injection of a solution of $[Gd(H_2O)_9]^{3+}$, Gd(III)CDTA, Gd(III)DOTA, and Gd(III)DTPA [15] leads to the band profiles illustrated in Fig. 3. When the mixture of chelates reaches the beginning of the column (frames 2–4), they begin to separate on the new packing material. The bands are rather concentrated at this stage and appear in black (see above, T_2 effect). They become progressively bright bands as they dilute (dominating T_1 effect). When they reach the unchanged part of the column, which is loaded with gadolinium, the bands merge into a black zone (frames 4–9). Most of the amount of analytes contained in this band seems to remain immobile, as if sticking to the old, unreplaced, packing material, while only part of it migrates slowly along the column (frames 11–16). The passage of this band darkens the column bed, meaning probably that part of the migrating chelates are strongly adsorbed on the Gd^{3+}-treated C_{18} packing materi-

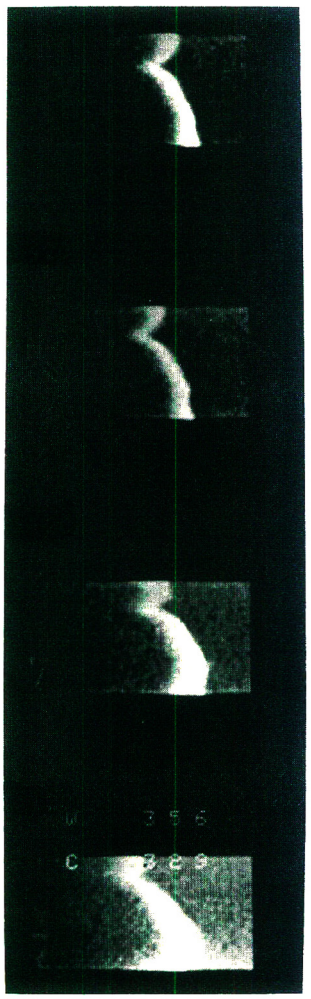

Fig. 2. 2D-FLASH images of the initial part (26 × 52 mm) of longitudinal, central slices comparing Gd(III)DTPA bands obtained at the same migration distance, for increasing amounts of gadolinium deposited on the column. Same acquisition parameters as for Fig. 1.

al. This strong retention is a combined result of the presence of residual silanols and adsorbed gadolinium ions. When the elution is over, the region at the beginning of the old material (i.e., the part of the bed not removed) is dark while the new material added has become bright (compare frames 1 and 16). The interface between new and old material is underlined by a nearly straight black line, suggesting that a certain amount of chelates has remained strongly adsorbed there (frame 10, arrow).

The simplest explanation for this behavior is a secondary retention mechamism due to electrostatic interactions with the Gd^{3+} ions adsorbed on the stationary phase of the negatively charged chelates (with formulas $[Gd(III)CDTA]^{-}$, $[Gd(III)DOTA]^{-}$, and $[Gd(III)DTPA]^{2-}$). This would explain why they exhibit a stronger retention on the stationary phase modified by the adsorption of the Gd^{3+} ions on the residual silanols than on the untreated adsorbent. Note that there is no *n*-octylamine present in the mobile phase used for these experiments (pure water), in contrast to the experimental conditions used for the data in Figs. 1 and 2 and in our previous study [2]. When present, this compound could mask the residual silanols (since it is basic), or the adsorbed gadolinium ions (because of its nucleophilic character [16]). As a matter of fact, metallic adsorption sites, apart from the residual silanol groups have been shown to be responsible also for the strong adsorption of nucleophilic organic compounds [14,17].

The washing of undesired impurities from stationary-phase surfaces has been investigated [18], with special attention to metallic ions [18–20]. It has been claimed that EDTA removes all metallic impurities from surfaces [19]. Others have found acid washing to be more effective [20]. We attempted to extract the gadolinium ions adsorbed on the C_{18} bonded silica with injections of a dilute solution of EDTA. Fig. 4 illustrates typical results obtained after the injection of a 40-μl solution. This compound is not visible. Only its effect on the local concentration of gadolinium can be recognized on the figures. When it comes into contact with the gadolinium ions adsorbed on the old stationary phase, EDTA reacts to form the complex $[Gd(III)EDTA]^{-}$ which is much less retained and migrates along the column. As a result, gadolinium is entirely and easily leached from the beginning of the column (new material) which darkens again (compare frames 1 and 16). It is also removed partly from the beginning of the old material section which turns from black (T_2 effect) to intense white (T_1 effect). The end

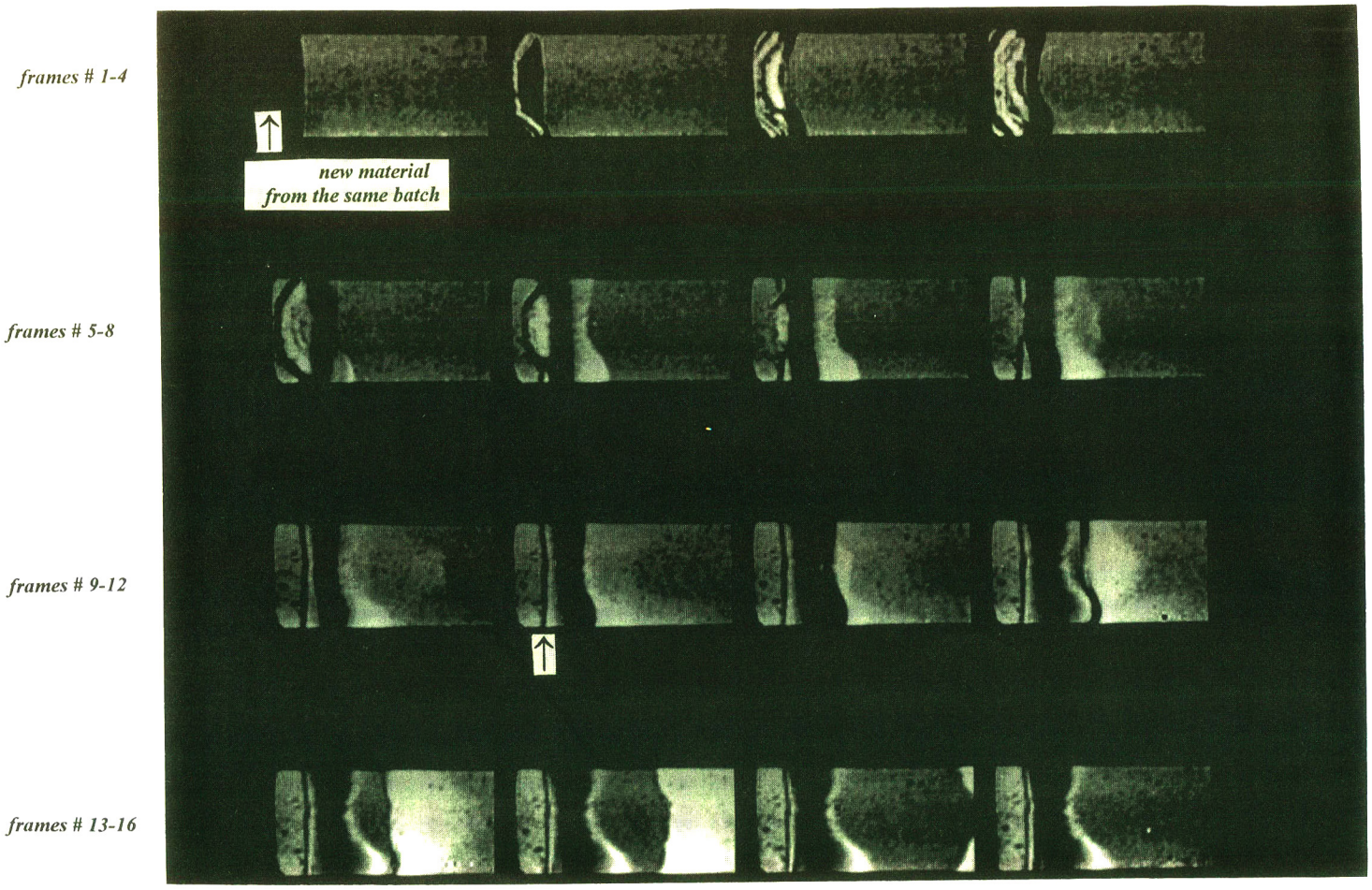

Fig. 3. 2D-FLASH images of the initial part (26 × 52 mm) of a longitudinal, central slice obtained after the injection of 50 μl of a mixture of Gd^{3+} and of its complexes with CDTA, DOTA, and DTPA. Mobile phase: pure water, flow-rate 3 ml/min. Time elapsed, 15 min between frames 2 and 9, 30 min between frames 9 and 16. Same acquisition parameters as for Fig. 1.

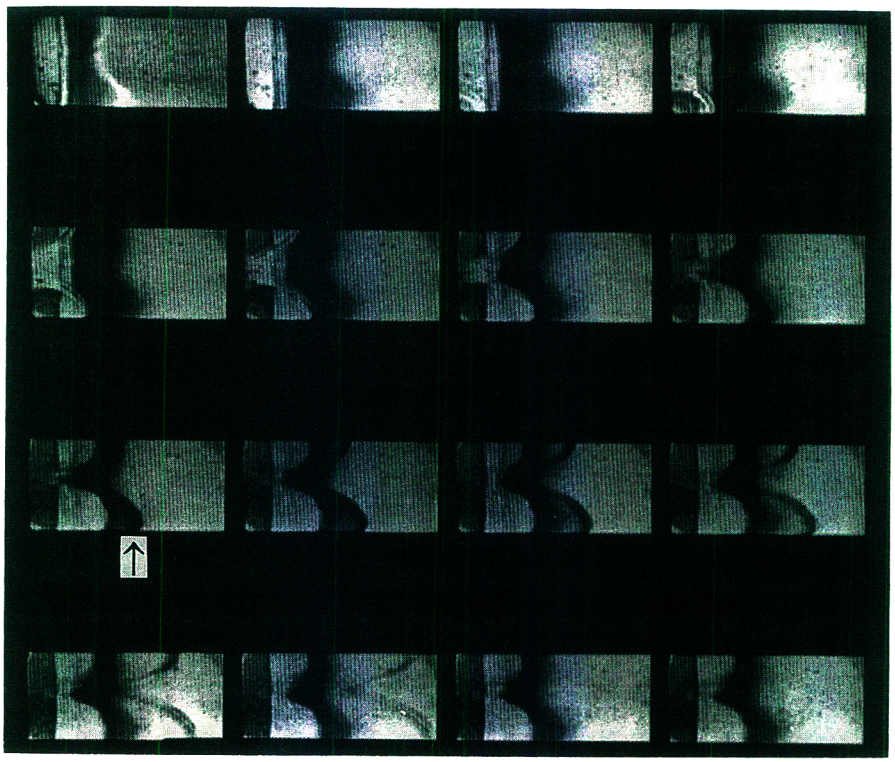

Fig. 4. 2D-FLASH images of the initial part (26 × 52 mm) of a longitudinal, central slice obtained after the injection of a dilute solution of EDTA. Flow-rate, 3 ml/min. Same acquisition parameters as for Fig. 1.

of the dark region in the old packing material remains unmodified because there was not enough EDTA in the sample. The band of newly formed complex migrates slowly across the black zone of modified material on which it is strongly retained (see above, Fig. 3). It emerges from that zone at frames 8–9 (see arrow) as a narrow concentrated band. It is much less retained on the unmodified adsorbent, migrates rapidly and disperses. Thus, it fades to gray, then disappears (frames 13–16).

Comparison of frames 2 and 16 shows the substantial removal of gadolinium by EDTA. The unexpected shape of the bands has been explained previously [2]. The center part of the inlet frit is obstructed by an accidental deposit.

Fig. 5 illustrates the washing of gadolinium from the column by flushing it with a solution of EDTA of constant concentration (0.01 *M*). The EDTA band reacts with the gadolinium ions adsorbed on the modified adsorbent, forming the less adsorbed complex which migrates slowly and accumulates, forming an intense black band which appears in frames 5 and 6 (see arrow). The sequence of images in Fig. 5a shows that there are several stages in the removal. The black part, corresponding to the zone heavily loaded with gadolinium, has disappeared in frame 6, but several fronts are seen in frames 9 and 10 and, although the material appears to be homogeneous in frame 12, the image darkens progressively until frame 16. Even then, some trace amount of gadolinium remains in the first 15 mm of old packing material, as shown by the light gray area.

Fig. 5b illustrates the kinetics of the phenomenon. The signal intensity integrated in the selected spot during the washing of the column

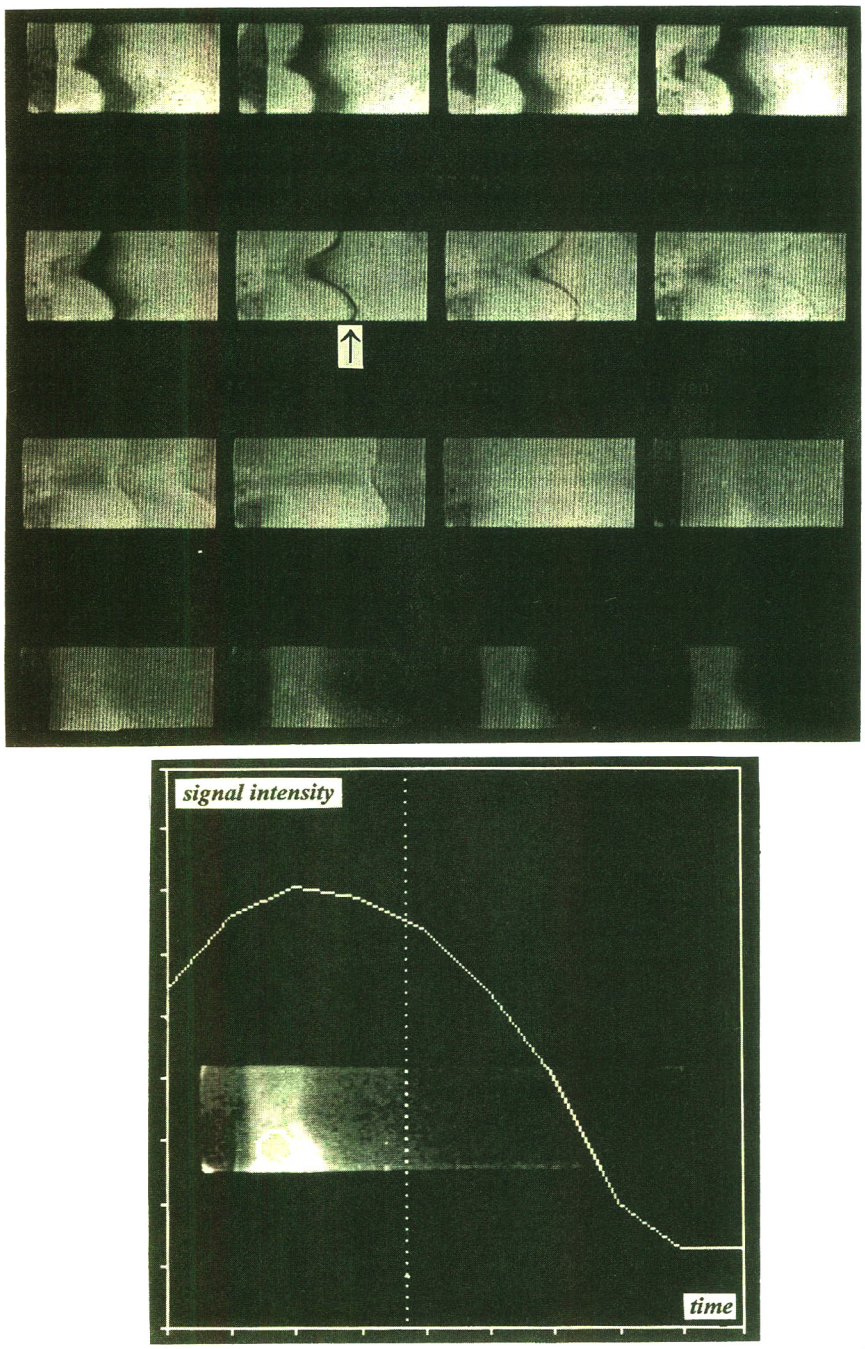

Fig. 5. Concentration distribution of gadolinium during washing of the column by a dilute EDTA solution (flow-rate, 3 ml/min). (a) 2-DFLASH images of the column bed. Time evolved between frames 1 and 13, 40 min. (b) Plot of the total signal intensity of the area marked on the image versus time. For the relationship between signal and gadolinium concentration, see text and Ref. [2]. Same acquisition parameters as for Fig. 1.

with the solution of EDTA is plotted versus time. The curve has a maximum, as does the calibration curve relating the signal intensity and the concentration of gadolinium (see explanation of the T_1 and T_2 effects, at the beginning of this section).

Washing small amounts of a strongly retained compound from a chromatographic column is not the simple process that the simplistic assumptions of linear chromatography would suggest. Stationary phases are not homogeneous. There is a wide distribution of adsorption energy on their surface. Even if we elect to assume that the retention mechanism is unique, compounds adsorbed on sites of different adsorption energies are washed out at different velocities.

References

[1] M. Ilg, J. Maier-Rosenkranz, W. Müller, K. Albert, E. Bayer and D. Höpfel, J. Magn. Reson., 96 (1992) 335.
[2] U. Tallarek, E. Baumeister, K. Albert, E. Bayer and G. Guiochon, J. Chromatogr. A, 696 (1995) 1.
[3] E. Baumeister, U. Klose, K. Albert, E. Bayer and G. Guiochon, J. Chromatogr. A, 694 (1995) 321.
[4] V.M. Runge (Editor), Enhanced Magnetic Resonance Imaging, Mosby, St. Louis, MO, 1989, Ch. 5.
[5] S. Aime, M. Botta and G. Ermondi, J. Magn. Reson., 92 (1991) 572.
[6] D.G. Gadian, J.A. Payne, D.J. Bryant, I.R. Young, D.H. Carr and G.M. Bydder, J. Comput. Assist. Tomogr., 9 (1985) 242.
[7] A. Haase, J. Frahm, D. Matthaei, W. Hänicke and K.-D. Merboldt, J. Magn. Reson., 67 (1986) 258.
[8] M.M. Vora, S. Wukovnig, R.D. Finn, A.M. Emran, T.E. Boothe and P.J. Kotari, J. Chromatogr., 369 (1986) 187.
[9] R.B. Lauffer, Chem. Rev., 87 (1987) 901.
[10] S.H. Koenig, C. Baglin, R.D. Brown and C.F. Brewer, Magn. Reson. Med., 1 (1984) 496.
[11] S.H. Koenig and R.D. Brown III, Progress in NMR Spectroscopy, *22* (1990) 487.
[12] C.A. Chang, H.G. Brittain, J. Telser and M.F. Tweedle, Inorg. Chem., 29 (1990) 4468.
[13] W. Grodd and R.C. Brasch, Fortschr. Röntgenstr., 145 (1986) 130.
[14] J. Nawrocki, Chromatographia, 31 (1991) 177, 193.
[15] K. Kumar, K.V. Sukumaran and M.F. Tweedle, Anal. Chem., 66 (1994) 295.
[16] G. Szepesi, How to Use Reversed-Phase HPLC, VCH Publishers, New York, 1992, Ch. 4.
[17] B. Buszewski, Chromatographia, 34 (1992) 573.
[18] J. Nawrocki, D.L. Moir and W. Szczepaniak, Chromatographia, 28 (1989) 143.
[19] J. Köhler, D.B. Chase, R.D. Farlee, A.J. Vega and J.J. Kirkland, J. Chromatogr., 352 (1986) 275.
[20] M. Verzele, M. de Potter and J. Ghysels, J. High Resolut. Chromatogr., 2 (1979) 151.

ELSEVIER

Journal of Chromatography A, 704 (1995) 45–53

JOURNAL OF CHROMATOGRAPHY A

Preparation and evaluation of magnesia-coated silica as column packing material for high-performance liquid chromatography

Kazunori Nobuhara[a], Mikio Kato[a], Motoshi Nakamura[b,*], Masayoshi Takami[b], Shoji Kaneko[b]

[a]*Fuji-Silysia Chemical, Ltd., Kozoji, Kasugai 487, Japan*

[b]*Department of Materials Science and Technology, Shizuoka University, Johoku, Hamamatsu 432, Japan*

First received 16 August 1994; revised manuscript received 25 January 1995; accepted 25 January 1995

Abstract

The preparation of a mixed oxide gel composed of silica and magnesia was attempted by a coating method in order to develop a useful column packing material for liquid chromatography. The physical properties of the gels obtained remained almost the same as those of the native silica gel, but the surface silanol groups and the acid strength both changed, depending on the preparation conditions. The chromatographic behaviour of the gels was tested using benzene, dimethyl phthalate, pyridine and phenol as solutes. The magnesia-coated silicas calcined at temperatures between 600 and 800°C exhibited the excellent separation abilities for these compounds.

1. Introduction

Oxides such as silica and alumina have been widely used adsorbents and column packing materials for liquid chromatography. Recently other metal oxides such as titania and zirconia have been studied as alternative column packings material to silica, because these new ceramics have chemical stability and a different separation ability to silica. These interesting surface properties and chromatographic applications have been studied in detail by various workers [1–12].

In our investigations on mixed oxide gels as adsorbents, it has been found that they exhibited different and specific properties from each component of the oxides [13–16]. We have also reported that they could be used as adsorbents for the recovery of trace and novel elements [17] and for the removal of environmental pollutants [18]. Based on our results on adsorbents, four mixed oxide gels, silica–titania, silica–alumina, silica–zirconia and silica–magnesia, were tested as column packing materials for liquid chromatography. For this purpose, first the four mixed oxide gels, which were prepared by a coprecipitation method, were examined with respect to their surface characteristics and separation abilities. It was found that silica–magnesia had an excellent separation ability for basic solutes such as pyridine, the separation of which is difficult with silica gel [19,20]. However, silica–magnesia obtained by the coprecipitation method was neither spherical nor uniform and had a wide range of particle size distribution. These characteristics are unfavourable for column packing materials.

* Corresponding author.

0021-9673/95/$09.50
SSDI 0021-9673(95)00118-2

In this work, coating for commercially available spherical silica gel with magnesia was attempted in order to avoid the above-mentioned problems with regard to particle morphology and size distribution. The surface characteristics of the magnesia-coated silica gels obtained were evaluated to assess their use as column packing materials for liquid chromatography.

2. Experimental

2.1. Chemicals

The spherical silica gel Super Microbead silica gel 100A-10 (Fuji-Silysia Chemical) was used as a matrix. Magnesium chloride hexahydrate and other reagents (Wako) were of analytical-reagent grade.

2.2. Preparation of magnesia-coated silica gel

To magnesium chloride solution of a given concentration, 10 g of the commercially available spherical silica was added. With stirring, 6 *M* ammonia solution was added dropwise to adjust the pH to the appropriate value. After stirring for 30 min, the solution was filtered by suction. The resultant gel was washed with 100 ml of distilled water and 100 ml of methanol. The gel was then dried overnight at 110 °C, followed by calcining at 400–1000°C for 2 h.

2.3. Determination of amount of magnesia coated on silica gel

Magnesia-coated silica gel (about 0.1 g) was placed in a platinum vessel that had been accurately weighed. After heating at 1000°C in an electric furnace and cooling to room temperature in a desiccator, the vessel was again weighed accurately to determine the mass loss of the gel. Subsequently, 20 ml of concentrated HF were added to the platinum vessel, then the mixture evaporated to dryness on a heated sand-bath. The same operation was repeated after adding 5 ml of concentrated HF to the residue in the vessel. The residue was dissolved in 1 *M* nitric acid and the resulting solution was transferred into a 100-ml calibrated flask and diluted to volume with 1 *M* nitric acid. An aliquot of the solution was diluted to an appropriate concentration. The final working solution for the determination contained 0.5% of lanthanum. The lanthanum solution was prepared by dissolving lanthanum oxide in hydrochloric acid.

The content of magnesium was determined using a Japan Jarrel-Ash Model AA-880 Mark II atomic absorption spectrometer and converted into magnesia (MgO) concentration.

2.4. Measurement of physical properties

The nitrogen adsorption isotherms of the gels at 77 K were measured. From the result, the specific surface areas and pore volumes were determined. The specific surface area was calculated from the BET equation. The pore volume was obtained from the liquid nitrogen volume evaluated from the nitrogen adsorption volume at $P/P_0 = 0.97$ [20]. Scanning electron micrographs were taken using a JEOL Model T330A scanning electron microscope.

2.5. Acid strength of gel surface

The surface acid strengths of gels were determined using the visual colour change method as follows [21]. The sample gel (0.1 g) was placed in a 50-ml flask containing 10 ml of dried benzene, then one by one up to seven Hammett's indicators were added successively in order of their pK_a values until the added indicator showed the colour of the acid form. The acid strength of the gel was taken to be between its pK_a value and that of the former. The Hammett's indicators used and their pK_as were anthraquinone ($pK_a = -8.2$), benzalacetophenone (−5.6), dicinnamalacetone (−3.0), 4-benzenazodiphenylamine (1.5), *p*-dimethylaminoazobenzene (3.3), phenylazonaphthylamine (4.0) and methyl red (4.8).

2.6. Chromatographic test

The gel was packed into a stainless-steel column (250 mm × 4.6 mm I.D.) by a slurry method as follows [22]. To a solvent mixture of glycerol and methanol, 3 g of the gel were added, then the slurry was well dispersed by ultrasonic vibration for 20 min in vacuo. The slurry was transferred to a packing reservoir and packed into a column filled using methanol as a solvent under a pressure of 300 kg/cm^2.

Benzene, dimethyl phthalate, pyridine and phenol as test solutes were used to evaluate the gels as packing materials for HPLC, the concentrations of which were 8.0, 8.0, 3.6 and 18.0 mg/ml, respectively. An aliquot of 10 μl of the methanol solution was injected into a Nippon Bunko LC-800 HPLC system. The mobile phase was *n*-hexane containing 1% methanol at a flow-rate of 1 ml/min at room temperature. Detection was carried out at 254 nm with a UV detector. Using the retention time of benzene as the dead time, the capacity factors of other solutes were estimated.

3. Results and discussion

3.1. Effect of preparation conditions on amount of magnesia coated

The effect of the pH of the solution on the amount of magnesia coated was investigated by adjusting the pH of 100 ml of the solution containing 10 g of silica gel and 0.12 *M* magnesium chloride with 6 *M* ammonia solution. The higher the pH, the more magnesia was coated on silica gel (Fig. 1). However, above pH 10 the amount of magnesia coated became almost constant. Also, the amount of magnesia coated increased with increasing concentration of $MgCl_2$, but above 0.4 *M* it remained almost constant, as shown in Fig. 2. Generally, the dissociation or ionization of $MgCl_2$ occurs in a solution of lower pH, but magnesium hydroxide [$Mg(OH)_2$] precipitates from a solution of higher pH owing to hydrolysis under conditions above the solubility product, reported as 10^{-9}–10^{-11}. In fact, a white suspension in addition to silica gel was observed in solutions with higher concentrations of $MgCl_2$ after adjusting the pH to 9, but the amount of magnesia coated was almost constant. This suggests that magnesia is coated not by the simple deposition of $Mg(OH)_2$ but by the adsorption of magnesium species on the silica surface.

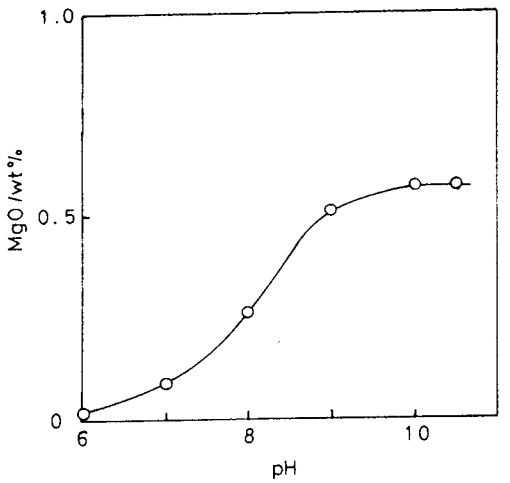

Fig. 1. Effect of pH on amount of magnesia coated on silica Matrix silica, 10 g; $MgCl_2$ concentration, 0.12 *M*.

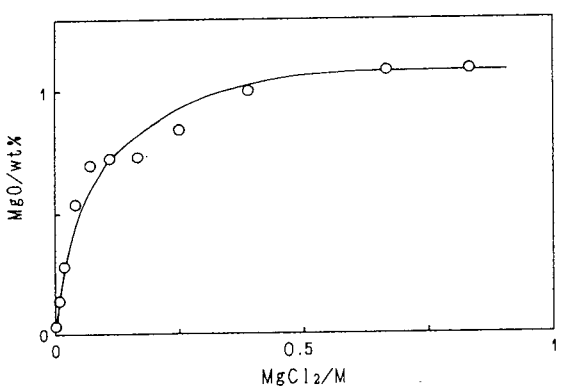

Fig. 2. Effect of concentration of magnesium chloride. Preparation pH = 9.

Table 1
Relationship between surface characteristics and amount of magnesia coated

Gel	Amount of magnesia (ppm)	Specific surface area (m^2/g)	Pore volume (ml/g)
Silica (untreated)	–	344	1.14
Magnesia-coated silica[a]	1400	322	1.15
	2800	327	1.16
	5400	322	1.16
	7400	317	1.14
	11000	319	1.13

[a] Dried at 110°C.

3.2. Physical properties of the surface of gels

The specific surface areas and the pore volumes of untreated and magnesia-coated silicas are given in Tables 1 and 2, respectively. The specific surface areas have a tendency to decrease only slightly with increase in the amount of magnesia coated, but the pore volumes were constant, independent on the magnesia coating. The calcining temperature did not influence the specific surface area and the pore volume of magnesia-coated silica. Fig. 3 shows that the morphology and grain size of untreated silica were very close to those of magnesia-coated silica.

The FT-IR spectra of untreated and magnesia-coated silicas are shown in Fig. 4. The isolated silanol group was assigned from the spectrum and was observed at around 3750 cm^{-1} in both gels [23]. The hydrogen-bonded silanol group, which was assigned from the spectrum observed at around 3400 cm^{-1}, existed only on untreated silica. Stout and DeStefano [24] reported a similar observation on a zirconia-treated silica surface by means of NMR. Neither the specific surface area nor the pore volume was influenced, but the surface silanol groups changed in quality with the magnesia coating.

3.3. Surface acid strength

Using the visual colour change method [21], the acid strength of the gels was investigated (Table 3). The introduction of basic magnesia on silica by coating had a tendency to weaken the surface acid strength; the untreated silica had the strongest acid strength. Further, the effect of calcining on the surface acid strength of the gels is summarized in Table 4. Magnesia-coated silicas dried at 110°C and calcined at 400°C showed weaker acid strengths than untreated silica. The acid strengths of the gels calcined at 600 and 800°C were the same as that of untreated silica. The gel calcined at the highest temperature of

Table 2
Relationship between surface characteristics and calcining temperature

Gel	Drying or calcining temperature (°C)	Specific surface area (m^2/g)	Pore volume (ml/g)
Silica (untreated)	–	344	1.14
Magnesia-coated silica[a]	110	322	1.16
	400	327	1.15
	600	330	1.16
	800	330	1.15

[a] Coated with 5400 ppm magnesia.

Fig. 3. Scanning electron micrographs of matrix silica and magnesia-coated silicas: (a) untreated silica; (b) 5400 ppm magnesia-coated silica dried at 110°C; (c) 5400 ppm magnesia-coated silica calcined at 800°C.

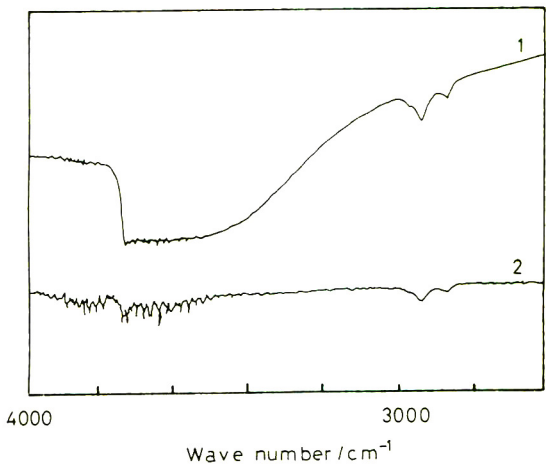

Fig. 4. FT-IR spectra. 1 = Untreated silica; 2 = magnesia-coated silica (5400 ppm).

Table 3
Acid strength of magnesia-coated silica

Gel	Amount of magnesia (ppm)	Acid strength (H_0)
Silica (untreated)	–	$1.5 < H_0 < 3.3$
Magnesia-coated silica[a]	1400	$1.5 < H_0 < 3.3$
	2800	$3.3 < H_0 < 4.0$
	5400	$3.3 < H_0 < 4.0$
	7400	$4.0 < H_0 < 4.8$
	11000	$4.0 < H_0 < 4.8$

[a] Dried at 110°C.

1000°C exhibited the greatest strength in the gels examined.

From Fig. 4 and Table 5, it is suggested that the magnesia coating contributes to weakening the surface acid strength by diminishing the hydrogen-bonding silanol groups. However, the effect of the thermal treatment on the surface acid strength was not clearly explained from the above results, because it is considered that the surface silanol groups are decreased by calcining, resulting in the lowering of the acid strength. As an example, the investigation of Okamoto et al. [25] made it clear that the number of the hydrogen-bonded silanol groups was decreased on thermal treatment of silica, but the number of isolated silanol groups unchanged. Mause and

Table 4
Acid strength of magnesia-coated silica

Gel	Drying or calcining temperature (°C)	Acid strength (H_0)
Silica (untreated)	–	$1.5 < H_0 < 3.3$
Magnesia-coated silica[a]	110	$3.3 < H_0 < 4.0$
	400	$3.3 < H_0 < 4.0$
	600	$1.5 < H_0 < 3.3$
	800	$1.5 < H_0 < 3.3$
	1000	$-3.0 < H_0 < 1.5$

[a] Coated with 5400 ppm of magnesia.

Engelhardt [26] also reported that the hydrogen-bonded silanol groups were removed by thermal treatment, whereas the number of the isolated silanol group increased. In addition, Malinowski et al. [27] demonstrated that the acid strength of magnesia increased as the heat treatment temperature was raised., Hence the increase in the acid strength of the magnesia-coated silica by thermal treatment may be caused not by silica but magnesia. The relationship between the surface acid strength and the thermal treatment must be clarified by further investigations on the type and amount of the surface acid and base sites.

It is interesting that in the proposed method, without changing the favourable physical characteristics as a column packing material, the species of silanol groups and the surface acid strength of silica can be changed.

3.4. Chromatographic behaviour

Chromatographic tests were carried out by using neutral dimethyl phthalate, acidic phenol and basic pyridine as solutes, and benzene for the dead time determination. The chromatograms obtained with magnesia-coated silica gels are shown in Fig. 5. The neutral dimethyl phthalate was not influenced by the magnesia coating and was separated successfully with a sharp and symmetrical peak, because the material had adequate physical characteristics for this separation such as a specific surface area and pore volume much the same as those of untreated silica. In contrast, the elution behaviours of pyridine and phenol changed considerably after the magnesia coating. Pyridine was not eluted at all using untreated silica because of the specific interaction with surface silanol groups, but it could be separated successfully without tailing on magnesia-coated silica. The capacity factors decreased slightly depending on the amount of magnesia coated. Hence, it is evident that the separation ability for pyridine is changed con-

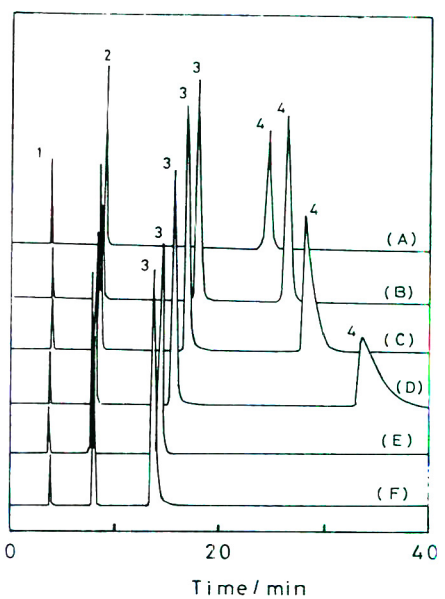

Fig. 5. Chromatograms obtained with magnesia-coated silica. Amount of magnesia coated on silica by drying at 110°C: (A) 0 (untreated silica); (B) 1400; (C) 2800; (D) 5400; (E) 7400; (F) 11 000 ppm. Solutes: 1 = benzene; 2 = dimethyl phthalate; 3–pyridine; 4 = phenol. Mobile phase, 1% methanol–n-hexane; flow-rate, 1 ml/min; detection at 254 nm.

siderably by the magnesia coating. The elution behaviour of phenol was different to that of pyridine. The magnesia coating caused a strong retention of phenol, although the untreated silica exhibited a good separation ability. The 1400 ppm gel-coated magnesia still retained a good separation ability, but other gels lost this ability with increase in the amount of magnesia and caused distinct peak tailing. With the 7400 ppm coated gel, phenol could not be eluted at all within 60 min.

The effect of calcining on the separation behaviour of the magnesia-coated silica gels for these four solutes is shown in Fig. 6. The retention of dimethyl phthalate on the gels increased with increase in calcination temperature. This tendency has also been shown on silica [25]. The calcining of the magnesia-coated gels considerably affected the elution of pyridine and phenol. The retention of pyridine, which could be improved by the magnesia coating, had a tendency also to be strengthened with calcining, whereas, the elution of phenol was facilitated.

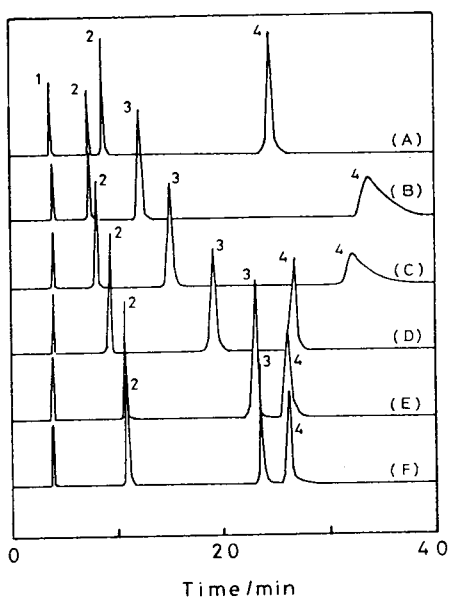

Fig. 6. Chromatograms obtained with calcined magnesia-coated silica. Treated silicas contained 5400 ppm of magnesia. Calcining temperature; (A) untreated; (B) 110; (C) 400; (D) 600; (E) 800; (F) 1000°C. Solutes and conditions are the same in Fig. 5.

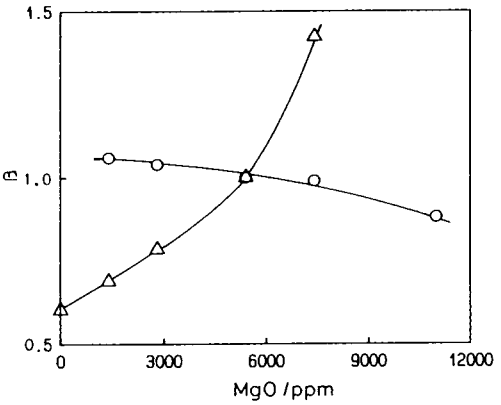

Fig. 7. Effect of amount of magnesia coated on capacity factor. ○ = Pyridine; △ = phenol.

Figs. 7 and 8 show the effects of the magnesia coating of silica and the calcining of magnesia-coated silica on the retention. The ratio of the capacity factor of pyridine or phenol to that of dimethyl-phthalate ($k'_{\text{pyridine}}/k'_{\text{DMP}} = \alpha_{\text{pyridine}}$ or $k'_{\text{phenol}}/k'_{\text{DMP}} = \alpha_{\text{phenol}}$) can be regarded as a measure of the interaction between the solute and the stationary phase. In Figs. 7 and 8, β is estimated as the relative value of α in each gel when α in the gel with 5400 ppm magnesia and dried at 110°C is defined as unity. These two graphs illustrate more clearly than the chromatograms the effects of magnesia coating and calcining on the retention behaviour of pyridine and

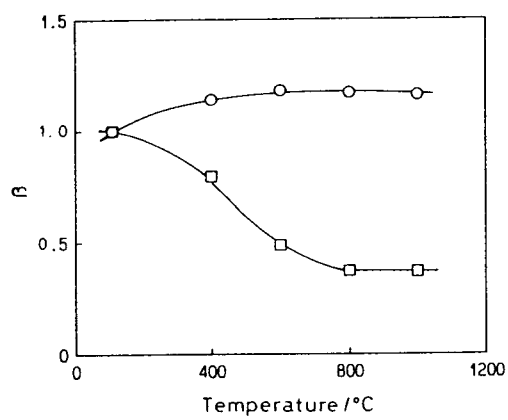

Fig. 8. Effect of calcining temperature on capacity factor. ○ = Pyridine; □ = phenol.

phenol. From these results, it is considered that (1) the specific interaction between silica and basic solutes such as pyridine is considerably improved by coating magnesia on the silica surface, but the dependence on the amount of magnesia coated is not very great, (2) coating with magnesia has a tendency lead to the loss of the excellent separation ability of silica for acidic compounds such as phenol, depending on the amount coated, (3) the lost separation ability for acidic compounds on coating can be recovered by calcining without a great influence on the separation of other solutes and (4), the separation of pyridine is not affected as much as that of phenol by the calcining.

The elution behaviour of pyridine and phenol is related to the surface acid strength. As described above, the coating of magnesia on silica diminishes the surface silanol groups, and consequently the acid strength of the gel is weakened. This would result in a better separation for pyridine, because of the lowering of both the solid acid–base interactions and the interactions between the surface silanol groups and pyridine. Conversely, the gel with a weakened surface acid strength would interact more strongly with phenol by acid–base interaction. The effect of calcining on the chromatographic behaviour can also be explained by the same interactions as those of coating. The relationship may be made clearer by the measurement of total acid and base amounts of the gel.

4. Conclusion

Magnesia-coated silica could be easily obtained by the proposed method, and retained the same physical properties as the commercially available silica used as the silica matrix. However, the separation ability of magnesia-coated silica was very different from that of the silica matrix, depending on both the amount of magnesia coated and the thermal treatment. The difference in the separation ability for the basic solute pyridine is noticeable. The separation ability for phenol was improved by calcining the gel, although the retention of the acidic phenol was unfavourably influenced by the magnesia coating.

References

[1] M.P. Rigney, T.P. Weber and P.W. Carr, J. Chromatogr., 484 (1989) 273.
[2] M. Kawahara, H. Nakamura and T. Nakajima, Anal. Sci., 5 (1989) 485.
[3] M. Kawahara, H. Nakamura and T. Nakajima, Anal. Sci., 5 (1989) 763.
[4] M.P. Rigney, E.F. Funkenbusch and P.W. Carr, J. Chromatogr., 499 (1990) 291.
[5] M. Kawahara, H. Nakamura and T. Nakajima, J. Chromatogr., 525 (1990) 149.
[6] H. Matsuda, H. Nakamura and T. Nakajima, Anal. Sci., 6 (1990) 911.
[7] U. Trudinger, G. Muller and K.K. Unger, J. Chromatogr., 535 (1990) 111.
[8] J.A. Blackwell and P.W. Carr, J. Liq. Chromatogr., 14 (1991) 2875.
[9] J.A. Blackwell and P.W. Carr, J. Chromatogr., 549 (1991) 43.
[10] H. Matsuda, H. Nakamura, T. Nakajima, Y. Asai and J. Sawa, Anal. Sci., 7 (1991) 813.
[11] L.T. Kubota and Y. Gushiken, Analyst, 116 (1991) 281.
[12] J. Nawrocki, M.P. Rigney, A. McCormick and P.W. Carr, J. Chromatogr. A, 657 (1993) 292.
[13] S. Kaneko, M. Mikawa and S. Yamagiwa, Chem. Lett., (1989) 209.
[14] S. Kaneko, M. Mikawa and S. Yamagiwa, Colloids Surf., 46 (1990) 203.
[15] S. Kaneko and W. Takahasi, Colloids Surf., 47 (1990) 69.
[16] S. Kaneko, S. Ohmori, M. Mikawa, T. Yamazaki, M. Nakamura and S. Yamagiwa, Chem. Lett., (1992) 2249.
[17] M. Nakamura, H. Saitoh, Y. Maejima, S. Yamagiwa and S. Kaneko, Fresenius' Z. Anal. Chem., 335 (1989) 573.
[18] S. Kaneko, S. Okuda, M. Nakamura and Y. Kubo, Chem. Lett., (1980) 1621.
[19] S. Kaneko, T. Mitsuzawa, S. Ohmori, M. Nakamura, K. Nobuhara and M. Masatani, Chem. Lett., (1993) 1275.
[20] S. Kaneko, T. Mitsuzawa, S. Ohmori, M. Nakmura, M. Nakamura, K. Nobuhara and M. Masatani, J. Chromatogr. A, 669 (1994) 1.
[21] K. Tanabe, Solid Acids and Bases, Academic Press, London, 1970.
[22] R.P.W. Scott, Silica Gel and Bonded Phases. Their Production, Properties and Use in LC, Wiley, New York, 1993.
[23] S.G. Bush, J.W. Jorgenson, M.L. Miller and R.W. Linton, J. Chromatogr., 260 (1983) 1.

[24] R.W. Stout and J.J. DeStefano, J. Chromatogr., 326 (1985) 63.
[25] M. Okamoto, K. Nobuhara and K. Jinno, J. Chromatogr., 556 (1991) 407.
[26] M. Mauss and H. Engelhardt, J. Chromatogr., 371 (1986) 235.
[27] S. Malinowski, S. Szczepanskaya, A. Bielanski and J. Sloczynski, J. Catal., 4 (1965) 324.

ELSEVIER

Journal of Chromatography A, 704 (1995) 55–65

JOURNAL OF CHROMATOGRAPHY A

Egg yolk riboflavin binding protein as a new chiral stationary phase in high-performance liquid chromatography

G. Massolini[a,*], E. De Lorenzi[a], M.C. Ponci[a], C. Gandini[a], G. Caccialanza[a], H.L. Monaco[b]

[a]*Department of Pharmaceutical Chemistry, University of Pavia, Via Taramelli 12, 27100 Pavia, Italy*
[b]*Department of Genetics, University of Pavia, Via Abbiategrasso 207, 27100 Pavia, Italy*

First received 6 October 1994; revised manuscript received 10 January 1995; accepted 10 January 1995

Abstract

A chiral stationary phase for high-performance liquid chromatography based on hen egg yolk riboflavin binding protein is introduced. The purified protein was immobilized on activated $5NH_2$ Nucleosil silica. Chiral acidic, basic and uncharged drugs were chromatographed and the influence of the mobile phase parameters on the retention times and enantioselectivity was studied. Thirteen out of the twenty compounds tested were partially or baseline resolved. These encouraging preliminary results suggest that this chiral stationary phase may be applicable to a wide range of drug enantiomers in the reversed-phase mode.

1. Introduction

Several proteins, such as α_1-acid glycoprotein (AGP) [1], bovine and human serum albumin (BSA [2] and HSA [3]) and ovomucoid (OVM) [4] have been shown to have stereospecific binding interactions with chiral entities of pharmaceutical interest. This recognition process has been successfully exploited to develop protein-based chiral stationary phases (CSPs), useful in the chromatographic resolution of pharmaceutically active enantiomers in the reversed-phase mode. However, there are still many enantiomers that have not been resolved by protein-based CSPs and, moreover, from the point of view of the pharmaceutical industry, the commercially available CSP technology does not appear to be as robust as might be desired. For these reasons, more efforts should be made to establish which type of proteins can be used in the resolution of racemic compounds and to prepare stable and reproducible protein-based chiral columns. In order to find proteins with the property of chiral recognition and broad applicability, we undertook a wide project for the purification and immobilization of proteins from different sources such as the riboflavin binding proteins (RFBP), fatty acid binding proteins (FABP) and β-lactoglobulin (BLG).

The name riboflavin binding protein is applied to several molecular species that are thought to be involved in the transport and storage of the vitamin [5]. The first protein of this family to be isolated and studied was hen egg white RFBP [6]. The molecule has been well characterized; it has a molecular mass of 32 000, which corre-

* Corresponding author.

0021-9673/95/$09.50
SSDI 0021-9673(95)00043-7

sponds to 219 amino acids, it is phosphorylated in a maximum of nine positions and has a carbohydrate content of about 14%. Its isoelectric point is about 4, depending on the exact isoforms studied. Different isoforms are believed to have different phosphate contents and/or deamidated asparagines and glutamines. Subsequently, three other hen proteins were isolated and characterized to various extents: egg yolk, serum and liver RFBP [7]. Egg white, yolk and serum RFBP appear to be the product of the same gene but to have undergone different post-translational modifications. The amino acid sequence is the same but it is between eleven and thirteen amino acids shorter in the case of yolk RFBP [7]. Yolk and serum RFBP share the same type of asparagine-linked oligosaccharide chains, which are different from the carbohydrates linked to egg white RFBP [8]. All the RFBPs are highly cross-linked molecules, presenting nine disulfide bridges, which explains their very high stability. Only one of the members of this protein family has so far been used as a CSP, viz., egg white RFBP [9]. As the differences among the members of this protein family have been shown to be substantial, we anticipated that the behaviour of a yolk RFBP CSP would be likely to be different from that of egg white RFBP.

This paper reports the results of chromatographic experiments carried out using a column of egg yolk RFBP bound to $5NH_2$ Nucleosil silica. Acidic, basic and uncharged analytes were chromatographed on yolk RFBP silica and the influence of mobile phase pH and percentage of organic modifier on the enantioselective retention was studied. Whenever there were data on the behaviour of the analytes on the egg white RFBP CSP, the two sets of results were compared and are discussed.

2. Experimental

2.1. Apparatus

A Hewlett-Packard HP 1050 liquid chromatograph with a Rheodyne sample valve (20-μl loop) equipped with a Hewlett-Packard HP 1050 variable-wavelength detector connected to an HP Vectra Q5/165 workstation was used. A stainless-steel column (100 mm × 4.6 mm I.D.) was packed with yolk RFBP-conjugated silica gel by Shandon HPLC (Runcorn, Cheshire, UK).

2.2. Reagents and materials

Ibuprofen (IB), ketoprofen (KE), flurbiprofen (FL), indoprofen (IN), suprofen (SU), fenoprofen (FE), carprofen (CA), warfarin (WA), tryptophan (TR), lormetazepam (LM), oxazepam (OX), lorazepam (LO), verapamil (VE), bepridil (BE) and nicardipine (NC) were purchased from Sigma (St. Louis, MO, USA) and gallopamil (GA) from Schiapparelli (Turin, Italy). Isradipine (IS) was kindly donated by Sandoz (Milan, Italy), amlodipine (AM) by Pfizer (Sandwich, UK), nimodipine (NM) by Bayer (Milan, Italy) and manidipine (MA) by Takeda (Osaka, Japan). KH_2PO_4 and ethanol (HPLC grade) were purchased from Merck (Darmstadt, Germany). DEAE-cellulose was purchased from Whatman (Maidstone, UK) and Sephadex G-100 from Pharmacia (Uppsala, Sweden). All the reagents used in protein purification were of analytical-reagent grade.

2.3. Purification of yolk RFBP

The hen egg yolk RFBP was purified as follows: after separating the whites from the yolks and adding riboflavin to saturate the protein, the latter were homogenized in a blender with 3 volumes of sodium acetate buffer (0.1 *M*, pH 5.3). The diluted yolks were centrifuged to remove the insoluble material and the supernatant was loaded on a DEAE-cellulose column (50 × 3 cm I.D.) that had been equilibrated with the same buffer. After washing the column extensively until all the bound protein was removed with the same buffer, yolk RFBP was eluted, adding 0.2 M NaCl to the buffer. RFBP is easily detected during the purification by its intense yellow colour and its absorbance at 455 nm. The pooled fractions containing the protein of interest were run through a Sephadex G-100 column using as eluent 0.05 *M* Tris–HCl (pH 7.5). The bound riboflavin was removed by

extensive dialysis at pH 3.0 to prepare the apoprotein that was used in the experiments.

2.4. Preparation of yolk RFBP column

Immobilization was carried out by Shandon HPLC following a previously described method [9]: $5NH_2$ Nucleosil (3 g) was slurried in HPLC-grade acetonitrile and N,N-disuccinylimidyl carbonate (4.5 g) was added. This mixture was stirred gently for 18 h (using a rotary evaporator). The silica was filtered and washed with acetonitrile and 50 m*M* potassium phosphate buffer (pH 7.5). A 300-mg amount of RFBP was suspended in 50 m*M* potassium phosphate buffer and the activated silica was added. After 2 h of gentle mixing using the rotary evaporator the product was collected by filtration and washed with sterile water and 2-propanol–water (1:2). The stationary phase was packed in a stainless-steel column (100 mm × 4.6 mm I.D.).

2.5. Chromatographic conditions

All the experiments were performed at ambient temperature (24–25°C) and the flow-rate was set at 0.8 ml/min. The operating UV wavelength was fixed at the corresponding maximum for each compound. Sample preparation was carried out by dissolving known amounts of chiral drugs in *n*-propanol, each solution was diluted with buffer to a concentration of 0.1 m*M* and 20 μl were injected into the HPLC column. Normally 2–4 nmol of analyte are recommended.

3. Results and discussion

Seven arylpropionic anti-inflammatory drugs, eight calcium channel antagonists with different structures, three benzodiazepines, tryptophan and warfarin were chromatographed on the yolk RFBP column. The structures of all the compounds tested are depicted in Fig. 1. In Table 1 the k', α and *Pi* values corresponding to the best chromatographic results are summarized; the enantioselectivity is expressed by α and *Pi*, where *Pi* is the ratio between the average valley depth and the average peak height (Kaiser's peak separation factor [10]). This parameter was found to give excellent discrimination between good and bad responses and is much more easily measurable than the resolution, R_s. Fig. 2 shows the best resolution obtained for some of the chiral compounds tested. The pH and percentage of organic modifier were changed in order to study the effect on retention and enantioselectivity.

3.1. Influence of pH and mobile phase composition on retention

pH

The influence of mobile phase pH on the enantioselective retention of charged and neutral analytes on the yolk RFBP column was systematically investigated. In general, the affinity for the stationary phase increased as the compounds became less ionized.

For the arylpropionic anti-inflammatory drugs (Fig. 3), increasing the pH above 4.6 decreases k' for most compounds. As the isoelectric point of yolk RFBP is about 4, under these conditions the protein has a net negative charge. Moreover, these compounds have all pK_a values in the range 4.0–5.0 and therefore electrostatic repulsion phenomena between stationary phase and analyte can occur. The fact that the trend is slightly different for the strongly retained IN and CA, where the decrease in k' starts at pH 5.5, may indicate the prevalence of hydrophobic interactions over ionic binding for such bulky structures.

The k' values of dihydropyridines (Fig. 4) are highly influenced by pH variation except for IS and NM. The extent of retention is directly dependent on the hydrophobicity of the substituents, MA being the most strongly retained compound, followed by NC and AM. Further, the very short retention times at pH 3.8 are ascribable to ionic repulsion as both the amines and RFBP are positively charged. The phenylalkylamines VE, GA and BE (Fig. 5) both follow a trend similar to the other calcium channel antagonists, although the latter shows a much more dramatic increase in the k' value as the pH is raised.

For benzodiazepines and TR the pH does not significantly influence the k' values. The fact that WA shows a decrease in retention time above pH 4.6 might be explained by the delocalized negative charge located at the centre of a largely non-polar molecule which could be responsible for electrostatic repulsion (Fig. 6).

Organic modifier

As expected in a system which works similarly to a reversed-phase mode, the influence of the percentage of organic modifier on the k' parameter is dependent on the hydrophobicity of the molecular structure of the analyte. An increase in the percentage of ethanol results in a large retention time decrease, especially for those compounds which are more retained in the absence of the organic modifier. For example, increasing the ethanol concentration from 5% to 10% (pH 5.5) causes a decrease in k' from 79.44 to 33.25 for IN whereas for the simpler SU the decrease in k' is only from 3.21 to 2.95. The same trend is observed for dihydropyridines.

For arylpropionic acids (Fig. 7), the elution

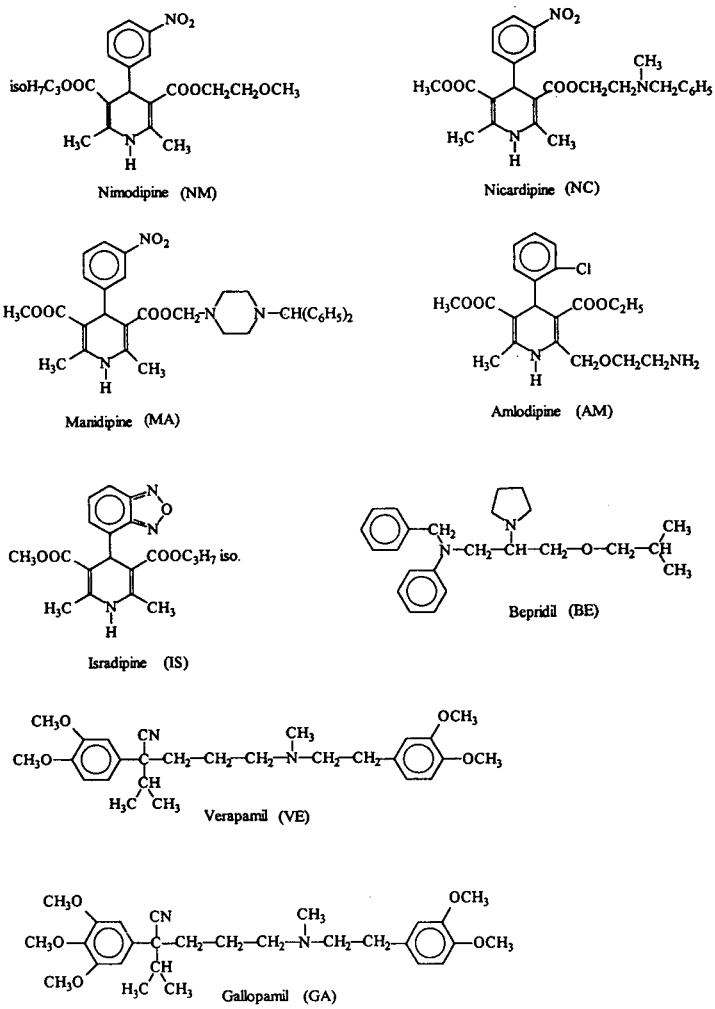

Fig. 1.

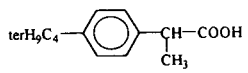

Ibuprofen (IB)

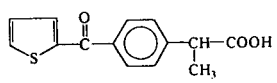

Suprofen (SU)

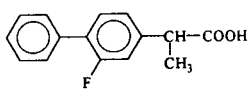

Flurbiprofen (FL)

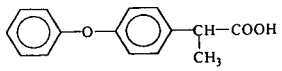

Fenoprofen (FE)

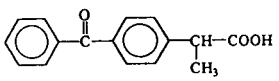

Ketoprofen (KE)

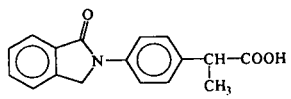

Indoprofen (IN)

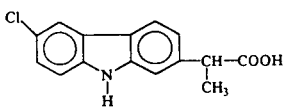

Carprofen (CA)

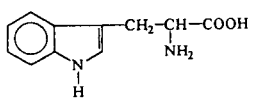

Tryptophan (TR)

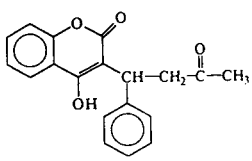

Warfarin (WA)

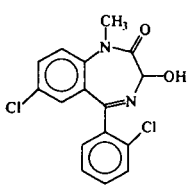

Lormetazepam (LM)

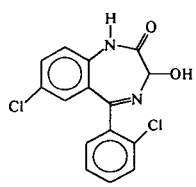

Lorazepam (LO)

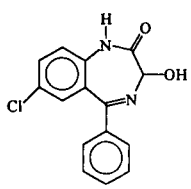

Oxazepam (OX)

Fig. 1. Structures of the compounds tested.

Table 1
Best mobile phase compositions obtained for the compounds tested and corresponding chromatographic parameters (k', α and Pi)

Compound	k'	α	Pi	Mobile phase
Ibuprofen	1.32	1	–	–[a]
Ketoprofen	2.56	1.22	0.61	50 m*M* KH_2PO_4 (pH 5.5)
Flurbiprofen	6.10	1.13	0.40	50 m*M* KH_2PO_4 (pH 5.5)
Indoprofen	9.84	1.16	0.77	50 m*M* KH_2PO_4 (pH 6.5)–ethanol (90:10, v/v)
Suprofen	8.27	1.08	0.20	50 m*M* KH_2PO_4 (pH 5.5)
Fenoprofen	1.82	1	–	–[a]
Carprofen	22.09	2.01	1	50 m*M* KH_2PO_4 (pH 5.5)–ethanol (95:5, v/v)
Warfarin	4.67	1.39	0.98	50 m*M* KH_2PO_4 (pH 4.6)–ethanol (90:10, v/v)
Tryptophan	0.31	1	–	–[a]
Lormetazepam	4.35	1	–	–[a]
Lorazepam	4.02	1.63	0.94	50 m*M* KH_2PO_4 (pH 5.5)–ethanol (95:5, v/v)
Oxazepam	3.92	4.55	1	50 m*M* KH_2PO_4 (pH 5.5)–ethanol (95:5, v/v)
Gallopamil	3.20	1	–	–[a]
Verapamil	3.55	1	–	–[a]
Bepridil	11.96	1.21	0.36	50 m*M* KH_2PO_4 (pH 5.5)–ethanol (95:5, v/v)
Isradipine	8.57	1.28	0.76	50 m*M* KH_2PO_4 (pH 5.5)
Amlodipine	5.49	1	–	–[a]
Nimodipine	0.72	1.11	0.08	50 m*M* KH_2PO_4 (pH 5.5)
Nicardipine	10.61	1.32	0.76	50 m*M* KH_2PO_4 (pH 5.5)–ethanol (95:5, v/v)
Manidipine	232.94	1.32	0.50	50 m*M* KH_2PO_4 (pH 5.5)–ethanol (95:5, v/v)

[a] No separation was obtained with any of the mobile phases considered.

order is IN > CA > SU > KE > FL > FE > IB. IN is not shown because in the absence of organic modifier it is not eluted after 3 h. It is likely that the additional carbonyl function present in some of the structures is responsible for a further hydrogen bond with a hydrogen-donating group at the binding site of the protein, and this is clearly demonstrated by the k' values for KE and FE. A further indication of the important role played by the carbonyl function in KE comes from the fact that this compound shows at least a hint of separation in all the chromatographic conditions tested whereas the enantiomers of FE have not been resolved so far. In the dihydropyridine family, with an increase in the percentage of organic modifier the retention times decrease, as expected; the presence of aromatic rings in the MA and NC structures appears to be responsible for their high k' values (followed by NM, IS and AM) (Fig. 8). MA is not shown in Fig. 8 as it was not eluted after 7 h.

Benzodiazepines, TR and WA follow the same rule.

3.2. Influence of pH and mobile phase composition on enantioselectivity

Thirteen out of the twenty compounds tested were partially or baseline resolved, as shown by the chromatographic parameters α and Pi in Table 1. Nevertheless no optimization was carried out and the results are to be considered as preliminary. Data obtained by the systematic study on the influence of the mobile phase parameters on the enantioselectivity showed that on increasing the pH in the range 3.8–6.5 (ethanol concentration 10%) the separation is not generally influenced to a great extent for most of the compounds tested. In contrast, the percentage of organic modifier provided to play an important role with respect to the enantioselective mechanism.

Among the arylpropionic anti-inflammatory drugs, the compounds with bulkier structures are those that showed higher retention together with better enantioselectivity. Keeping the ethanol concentration constant (10%), the best sepa-

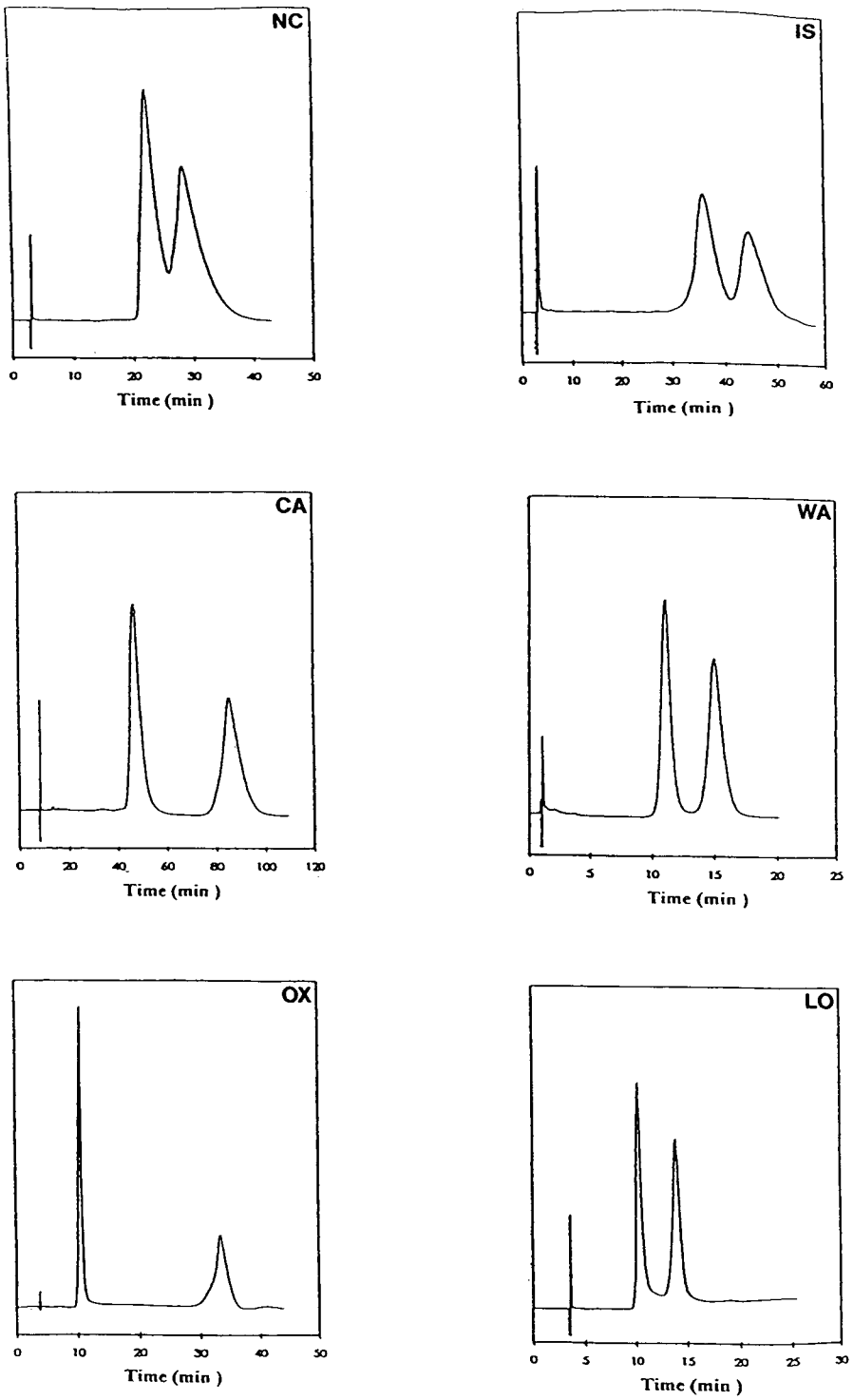

Fig. 2. Chromatograms of some of the compounds tested. The corresponding chromatographic conditions are given in Table 1.

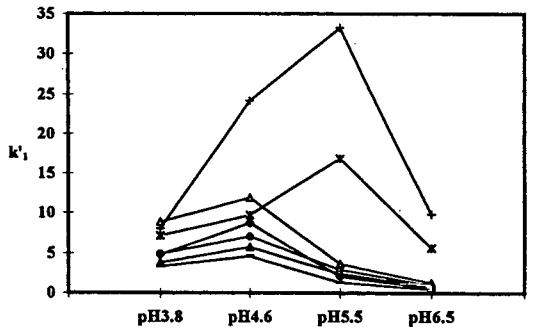

Fig. 3. Influence of pH on k'_1 for arylpropionic acids (ethanol content kept constant at 10%). Sample: – = IB; ▲ = KE; △ = FL; O = SU; ◆ = FE; * = CA; + = IN.

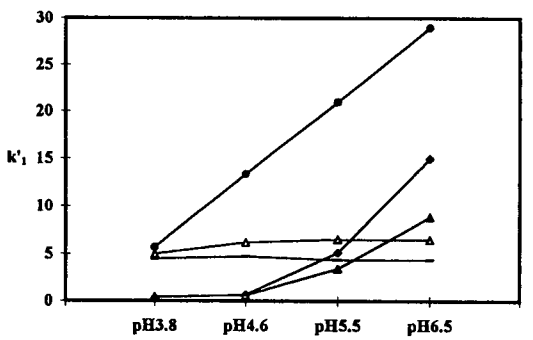

Fig. 4. Influence of pH on k'_1 for dihydropyridines (ethanol content kept constant at 10%). Sample: – = IS; ▲ = AM; △ = NM; O = MA; ◆ = NC.

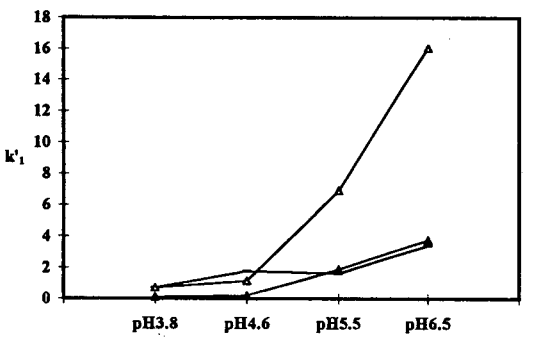

Fig. 5. Influence of pH on k'_1 for phenylalkylamines (ethanol content kept constant at 10%). Sample: – = GA; ▲ = VE; △ = BE.

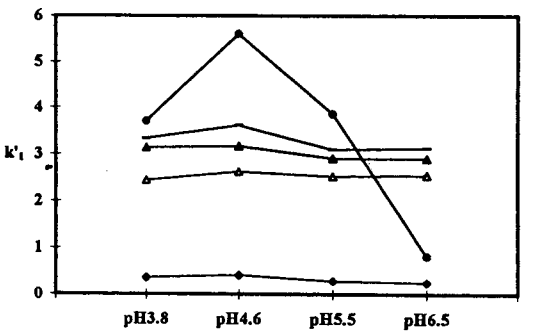

Fig. 6. Influence of pH on k'_1 for benzodiazepines, TR and WA (ethanol content kept constant at 10%). Sample: – = LM; ▲ = LO; △ = OX; O = WA; ◆ = TR.

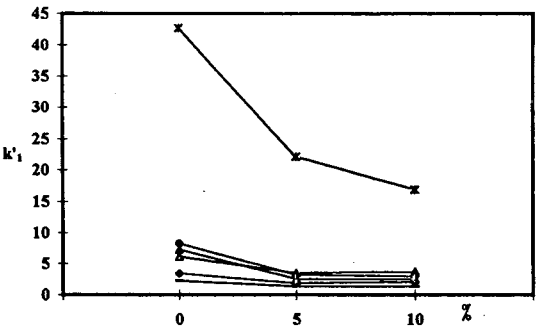

Fig. 7. Influence of percentage of organic modifier on k'_1 for arylpropionic acids (pH kept constant at 5.5). Sample: – = IB; ▲ = KE; △ = FL; O = SU; ◆ = FE; * = CA.

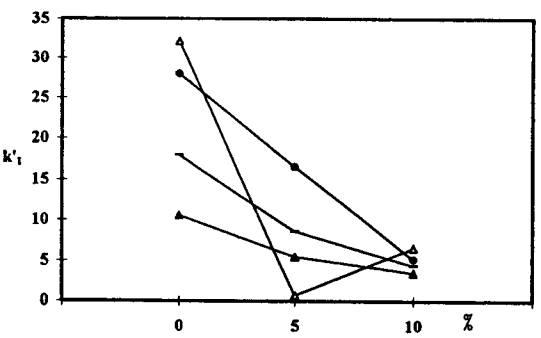

Fig. 8. Influence of percentage of organic modifier on k'_1 for dihydropyridines (pH kept constant at 5.5). Sample: – = IS; ▲ = AM; △ = NM; O = NC.

ration was obtained for CA, which shows a *Pi* value higher than 0.98 at pH > 4.6; IN was resolved with a *Pi* value of 0.77 at pH > 3.8. A decrease in the percentage of organic modifier results in baseline resolution for CA and in a too strong protein–solute interaction, which leads to unacceptable retention times (no peaks eluted after 3 h in the absence of ethanol in the mobile

phase). The presence of multiple points of attachment to the protein in the IN structure (aromatic ring and carbonyl group) could explain the observed chromatographic behaviour. SU, FL and KE, which were unresolved or partially resolved at all pH values with 10% of ethanol present, showed a slight improvement in enantioselectivity on reducing the concentration of ethanol. FE and IB have not been resolved so far, probably because these compounds do not have the structural prerequisites for obtaining three-point interactions with the binding site of yolk RFBP.

The calcium channel antagonists GA, VE and AM did not show any enantioselectivity, whereas for BE and all the other dihydropyridines the percentage of ethanol was the parameter that influenced the separation most. On decreasing the ethanol concentration from 10% to 5% (at pH 5.5), BE, IS, NC and MA are partially resolved with *Pi* values of 0.36, 0.34, 0.76 and 0.50, respectively. A further improvement in the peak separation function is observed in the absence of the organic modifier (pH 5.5): for example, the *Pi* changes from 0.34 to 0.76 and from 0.76 to 1.0 for IS and NC, respectively, but the long retention times and the low efficiency obtained are not desirable for analytical purposes.

Both benzodiazepines LO and OX gave very good enantioselectivity with 5% of ethanol (pH 5.5) and *Pi* values of 0.90 and 0.94, respectively. Increasing the pH leads to a dramatic increase in the retention time of the second-eluted enantiomer for OX. The fact that LM has not been separated so far under any of the conditions tested clearly demonstrates that small changes in the molecular structure (a methyl group) can influence the separation substantially. The weak acid WA was found to be the best resolved compound so far on the yolk RFBP column. The best separations were achieved in the pH range (4.5–5.5) where this analyte is mainly uncharged, and this leads to the conclusion that the hydrophobic interactions of this bulky and rigid molecule are necessary in the enantioselective interactions with the protein-binding site.

Tryptophan was never separated on the yolk RFBP column and its retention times were very short under any of the chromatographic conditions tested. This is surprising as its indole moiety confers on this molecule a hydrophobicity comparable to that of the anti-inflammatory drugs considered. It can be hypothesized that the amino group which is protonated in the operating pH range is responsible for repulsion phenomena with a positive charge located in the protein hydrophobic binding site.

3.3. Influence of type of uncharged modifier on retention and enantioselectivity

Different organic modifiers, namely methanol, ethanol, *n*-propanol and acetonitrile, were tested with respect to the enantioselective retention of all analytes. The variations in chromatographic parameters observed are shown in Table 2 for a constant concentration of organic modifier of 5% and a pH of 5.5. The alkanols cause a weakening of the hydrophobic interactions between the solute and the protein surface. For a series of 1-alkanols, the effect increases rapidly with increasing length of the alkyl chain. Although acetonitrile gives k' values even lower than *n*-propanol, the enantioselectivity is comparable to that obtained with ethanol.

The small number of compounds tested so far on the egg white RFBP CSP, namely KE, IB, FL, WA, benzoin and α,ε-dibenzoyllysine, makes the comparison between the chromatographic performances of hen egg yolk and egg white RFBP CSPs difficult. The effect of pH and percentage of organic modifier on k' follows a similar trend for both CSPs, that is, with increase in pH, k' decreases for acidic analytes (i.e., KE). For the basic compounds tested on egg yolk RFBP, the pH effect is reversed but comparison with egg white RFBP is not possible as no basic drugs have yet been tested on this phase. The influence of organic modifiers on k' is similar to that of a reversed-phase mode for both columns, but the retention times were generally found to be shorter on egg yolk RFBP under the same conditions.

As far as the enantioselectivity is concerned, KE, IB, FL and WA showed different behaviour

Table 2
Influence of type of uncharged modifier on retention and enantioselectivity

Compound	Methanol		Ethanol		*n*-Propanol		Acetonitrile	
	k'_1	α	k'_1	α	k'_1	α	k'_1	α
Ibuprofen	1.38	1.13	1.32	1	1.12	1	1.07	1
Ketoprofen	3.01	1.22	2.56	1.14	1.52	1	1.36	1.06
Flurbiprofen	3.08	1.14	3.46	1	2.32	1	2.34	1
Indoprofen	115.29	1	79.44	1	12.72	1	7.25	1.06
Suprofen	3.36	1.07	3.21	1	1.58	1	1.44	1
Fenoprofen	1.85	1	1.82	1	1.38	1	1.36	1
Carprofen	30.42	2.20	22.09	2.01	14.45	1	6.67	1.14
Warfarin	6.77	1.99	4.67	1.26	3.11	1	1.97	1.33
Tryptophan	0.38	1	0.31	1	0.27	1	0.26	1
Lormetazepam	5.81	1	4.35	1	3.58	1	0.22	1
Lorazepam	4.91	1.87	4.02	1.63	3.28	1.12	3.07	1.25
Oxazepam	4.87	6.68	3.92	4.55	2.61	1.69	2.5	3.08
Gallopamil	6.42	1	3.2	1	2.91	1	1.13	1
Verapamil	8.28	1	2.55	1	4.32	1	1.32	1
Bepridil	–[a]	–[a]	11.96	1.21	10.02	1.08	16.95	1
Isradipine	10.58	1.18	8.57	1.17	5.21	1	5.07	1
Amlodipine	11.41	1	5.49	1	6.14	1	6.05	1
Nimodipine	21.8	1	14.68	1	8.37	1	6.8	1
Nicardipine	23.71	1.34	16.61	1.32	9.73	1	7.72	1.11
Manidipine	–[a]	–[a]	232.94	1.32	–[a]	–[a]	–[a]	–[a]

Mobile phase: 50 m*M* KH_2PO_4 (pH 5.5)–organic modifier (95:5, v/v)
[a] Not eluted within 5 h.

on egg white and egg yolk RFBP. On egg white RFBP, baseline resolution was obtained for KE and WA and only partial resolution for IB and FL. On egg yolk RFBP, baseline resolution was achieved for WA, with shorter retention times than those on egg white RFBP. On the egg yolk column KE showed only a modest separation and IB and FL were not enantioseparated. On the other hand, IN, CA, LO, OX, IS and NC, not yet tested on the egg white stationary phase, gave very good enantioseparations within reasonable retention times on the egg yolk column. It should be noted that the positive results obtained with IN and CA, in contrast to those obtained with IB and KE, lead us to think that a bulky and rigid structure rather than a simpler molecule is required in order to establish more easily the hydrophobic interactions that seem to be crucial for enantioselectivity. Moreover, the small amount of egg yolk RFBP used for the preparation of this column compared with that used for the egg white RFBP [9], AGP [11] and OVM [12] CSPs could be responsible for the poor resolution of some of the compounds tested. It has already been pointed out for the AGP CSP [13] that a low protein content gives, for hydrophilic drugs, bad resolution owing to a low separation factor, tailing peaks and low separation efficiency.

In order to obtain reproducible results, a very important aspect is the column stability and robustness, which were evaluated on the egg yolk RFBP CSP using WA as the probe. After 250 injections and with the wide changes in mobile phase composition and pH that were required in method development, the stereoselective performance and the efficiency of the column were unaffected. This is consistent with the chromatographic parameters reported in Table 3.

Table 3
Chromatographic parameters of warfarin (A) for initial injection and (B) after 250 injections.

Parameter	A	B
k'_1	4.9	4.64
k'_2	8.5	7.92
α	1.73	1.70
R_s	2.81	2.49
Plates/m	15 020	11 980

Mobile phase: 50 m*M* KH_2PO_4 (pH 5.5)–ethanol (95:5, v/v).

4. Conclusions

The encouraging preliminary results obtained on the egg yolk RFBP CSP suggest its applicability to a reasonably wide range of drug enantiomers in the reversed-phase mode. Further optimization of the chromatographic conditions and a higher protein loading of the column could further improve its applicability, efficiency and selectivity. Although it is well known that egg yolk RFBP has a specific binding site for riboflavin, the data reported here can neither confirm nor disprove whether the drugs tested interact with this protein binding site. Displacement studies are necessary in order to confirm this possibility and to attempt to elucidate the enantioselective mechanisms.

Acknowledgements

We are grateful to Angela McGann of Shandon HPLC (Runcorn, Cheshire, UK) for kindly providing the packing of the yolk RFBP column and to Massimiliano Perduca for help with the protein purification.

References

[1] J. Hermansson, *Trends Anal. Chem.*, 8 (1989) 251.
[2] S. Allenmark, *J. Liq. Chromatogr.*, 9 (1986) 425.
[3] Domenici, C. Bertucci, P. Salvadori, G. Felix, I. Cahagne, S. Mottellier and I.W. Wainer, *Chromatographia*, 29 (1990) 170.
[4] T. Miwa, T. Miyakawa, M. Kayano and J. Miyake, *J. Chromatogr.*, 408 (1987) 316.
[5] H.B. White, III, and A.H. Merril, Jr., *Annu. Rev. Nutr.*, 8 (1988) 279.
[6] M.B. Rhodes, P.R. Azari and R.E. Feeney, *J. Biol. Chem.*, 230 (1958) 399.
[7] N. Norioka, T. Okada, Y. Hamazume, T. Mega and T. Ikenaka, *J. Biochem. (Tokyo)*, 97 (1985) 19.
[8] M.S. Miller, E.G. Buss and C.O. Clagett, *Biochim. Biophys. Acta*, 677 (1981) 225.
[9] N. Mano, Y. Oda, N. Osakawa, Y. Yoshida, T. Sato and T. Miwa, *J. Chromatogr.*, 623 (1992) 221.
[10] R.E. Kaiser, *Gas Chromatographie*, Geest und Portig, Leipzig, 1960.
[11] J. Hermansson, *J. Chromatogr.*, 269 (1983) 71.
[12] T. Miwa, M. Ichikawa, M. Tsuno, T. Hattori, T. Miyakawa, M. Kayano and Y. Miyake, *Chem. Pharm. Bull.*, 35 (1987) 682.
[13] J. Hermansson, *J. Chromatogr.*, 298 (1984) 67.

ELSEVIER

Journal of Chromatography A, 704 (1995) 67–74

JOURNAL OF CHROMATOGRAPHY A

Cationic β-cyclodextrin: a new versatile chiral additive for separation of drug enantiomers by high-performance liquid chromatography

Christian Roussel[a,*], Anita Favrou[b]

[a]*CNRS URA 1410, Centre National de la Recherche Scientifique, ENSSPICAM, Faculté Sciences St. Jérôme, F-13397 Marseille, Cedex 20, France*

[b]*Société Roquette Frères, 62136 Lestrem, France*

First received 9 November 1994; revised manuscript received 3 February 1995; accepted 3 February 1995

Abstract

The chromatographic separations of the enantiomers of a series of eight phenylhydantoin and methylhydantoin derivatives of amino acids are described, using reversed-phase HPLC with a chiral additive in the mobile phase: native β-cycodextrin (β-CD), carboxymethylated β-CD and a cationic β-CD derivative. Retentions time and selectivities obtained with these three chiral additives are compared. As the cationic β-CD gave promising results, its usefulness in the resolution of several drugs of particular interest (chlorthalidone, terbutaline, mephobarbital and hexobarbital) is demonstrated.

1. Introduction

The examination of drug enantiomers is currently accepted as one of the most important steps when studying the pharmacokinetic and pharmacodynamic properties of drugs with chiral centres [1]. However, in order to study these properties, the initial step involves the development of a suitable method for their separation. High-performance liquid chromatography (HPLC) has played a large part in this work, for which a number of chiral selectors, chemically bound to the stationary phase [chiral stationary phase (CSP)] or added to the mobile phase, have been investigated.

When a chiral selector is introduced into the mobile phase used with an achiral column, it offers the advantage of flexibility, a wide range of possible additives and often lower cost compared with the equivalent CSP [2]. One of the widely used chiral mobile phase additives is the cyclodextrin group (CDs). CDs are cyclic, non-reducing oligosaccharides consisting of D-glucose units bonded through α-1,4-linkages. According to the number of glucose units forming the cyclodextrin-ring (six, seven or eight), one differentiates between α-, β- and γ-cyclodextrins. β-Cyclodextrin, the most readily available of the cyclodextrins and generally the best sized complex former, shows an anomalously low solubility [3,4] in aqueous–organic solvents (1.85 g per 100 ml water). In this respect, chiral chromatograph-

* Corresponding author.

SSDI 0021-9673(95)00166-2

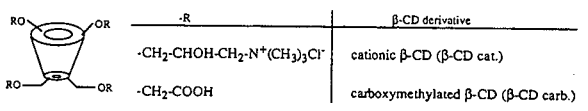

Fig. 1. β-CD derivatives used in the study.

ic separations require relatively high concentrations of CD to move complexation toward its maximum [5]. The use of urea in the eluent to enhance solubility, as recommended by Pharr et al. [6], is not a viable option in most experimental protocols as it leads to problems with baseline stability and high viscosity [7]. An alternative route to improve the solubility of CDs is available through derivatization of the CD structure at the hydroxyl groups. Several CD derivatives, such as methylated, hydroxyethyl, hydroxypropyl and acetylated β-CD, have already been produced and utilized industrially [8,9]; others have been prepared only on a laboratory scale and used for analytical or research purposes, with promising results.

In this work, carboxymethylated β-CD and a new cationic β-CD derivative (Fig. 1) were examined as chiral additives in the separation of the enantiomers of a group of eight amino acid derivatives in the form of phenylthiohydantoins (PTH) and methylthiohydantoins (MTH) and of several chiral drugs of current interest.

2. Experimental

2.1. Chemicals

PTH- and MTH-amino acids, chlorthalidone, terbutaline, hexobarbital and mephobarbital were obtained from Sigma (St. Louis, MO, USA) and were used without further purification (Fig. 2).

Acetic acid and triethylamine (TEA) were purchased from Carlo Erba (Rueil-Malmaison, France) and Janssen Chimica (Geel, Belgium), respectively. Ethanol (95%) was purified by distillation.

CDs (Fig. 1) were obtained from Roquette Frères (Lestrem, France). Cationic β-CD is characterized by an average molar degree of substitution (MS), i.e., number of substituents per glucose units, of 0.45. The sample contains less than 2% of free β-CD. It was used as an aqueous solution of pH 8.4 at a concentration of $2.80 \cdot 10^{-4}$ torus/g (i.e. number of cyclodextrin torus equivalents per gram of solution). Carboxymethylated β-CD is characterized by an MS value of 0.38. The sample contains less than 3% of native β-CD and is used as an aqueous solution of pH 5.18 at a concentration of

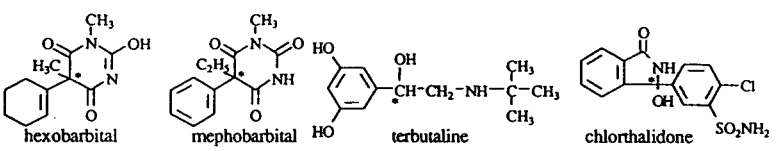

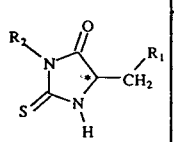

compound	R_1	R_2	abbreviations
MTH-Tyrosine	p-hydroxyphenyl	methyl	MTH-Tyr
PTH-Tyrosine	p-hydroxyphenyl	phenyl	PTH-Tyr
MTH-Phenylalanine	phenyl	methyl	MTH-Phe
PTH-Phenylalanine	phenyl	phenyl	PTH-Phe
MTH-Norvaline	ethyl	methyl	MTH-Nva
PTH-Norvaline	ethyl	phenyl	PTH-Nva
MTH-Leucine	iso-propyl	methyl	MTH-Leu
PTH-Leucine	iso-propyl	phenyl	PTH-Leu

Fig. 2. Structures of solutes studied.

$2.93 \cdot 10^{-4}$ torus/g. These MS values only indicate the average degree of substitution, without a precise localization on the torus.

2.2. Equipment

HPLC was performed with a Merck Hitachi LiChroGRAPH L-6000 HPLC pump, a Merck Hitachi LiChroGRAPH L-4000 UV detector and a Merck D2000 recorder. Separations were carried out with a Merck LiChroCART 250-4 Superspher 100 RP-18 column (4 μm, 250 × 4 mm I.D.).

Acetate buffer used in the mobile phases is an aqueous solution of 0.8% (v/v) of TEA, the pH of which is adjusted with acetic acid. Phosphate buffer is obtained by dissolution of 1.776 g/l of NaH_2PO_4 in water and the pH is adjusted with orthophosphoric acid. All the mobile phases were filtered through a Millipore HV membrane filter (0.45 μm) and were degassed prior to use by a vacuum ultrasonic method. Sample solutions were prepared so as to give a concentration of 8 mg/l for each solute. The amount of the sample injected was 20 μl. All chromatograms were obtained at 22.5°C. UV detection was performed at 264 nm for the amino acid derivatives, at 254 nm for chlorthalidone and barbiturates and at 275 nm for terbutaline. The dead volume was determined by injection of sodium nitrate.

2.3. Determination of the elution orders

The elution orders were determined by injection of partially resolved mixtures obtained by preparative chromatography on a microcrystalline cellulose triacetate column [10]. The elution order of the enantiomers of terbutaline, which is not resolved with this chromatographic system, was not determined.

2.4. Calculation of the stability constants

The determination of the stability constants, K_s, using the HPLC method with addition of cyclodextrin to an aqueous mobile phase has already been described [11]. For a neutral solute, Eq. 1, which expresses the stability constant K_s of a complex from chromatographic data, has been established theoretically [12,13]:

$$\frac{1}{k'} = \frac{1}{k'_0} + \frac{K_s[CD]_T^n}{k'_0} \quad (1)$$

where k'_0 is the capacity factor obtained in the absence of CD, k' is the capacity factor of the sample solute with a concentration $[CD]_T$ of cyclodextrin in the mobile phase and n is the stoichiometry of the complex. It is clear from Eq. 1 that k' shows a hyperbolic dependence on $[CD]_T$ and a plot of $1/k'$ vs. $[CD]_T^n$ gives a straight line whose slope is equal to K_s/k'_0. For the determination of the stoichiometries of CD complexes, several chromatographic runs with different CD concentrations are needed. When the stoichiometry of the complexes is known or assumed, only two chromatographic analyses are useful: one to determine k'_0 and the other to determine k' at a known CD concentration.

3. Results and discussion

Chromatographic separations, using CDs as mobile phase modifiers, are largely the result of selectivity in the formation of inclusion complexes. The elution time of a given solute is a function of the strength of these complexes. These two driving forces act synergistically and are directly related to the properties of the guest and to the interactions that may be engaged with the CD [14–16]. Hence, it is important to consider that in the derivatized cationic or carboxymethylated β-CD, the apparent diameter of the toroidal cone rim can be modified with the introduction of a more bulky group, by the selective substitution of some of the hydroxyl groups. Moreover, the effect of substitution would be expected to affect the extent of interaction with the side-chain of the analyte. These interaction modifications with the derivatization of the CD rim may be evaluated through the determination of the stability constants of the complexes.

The stability constants K_s of the complexes formed with the eight MTH- and PTH-amino acids were determined with β-CD, cationic β-CD and carboxymethylated β-CD, and are reported with the corresponding chromatographic data in Table 1. K_s values were calculated according to Eq. 1 on the basis of the chromatographic results from one concentration in the case of carboxymethylated β-CD (25 m*M*) and from two different concentrations in the case of cationic β-CD (25 and 40 m*M*). In the latter instance, the stoichiometry of the complexes was controlled by inspection of the plots $1/k'$ vs. cationic β-CD concentration for compounds that have maximum steric hindrance either in position R_1 (MTH-phenylalanine) or R_2 (PTH-norvaline), or in both of these positions (PTH-tyrosine). Obtaining a good linear correlation demonstrates the 1.1 stoichiometry of the complexes, as the occurrence of higher order of complexation would give a non-linear correlation between $1/k'$ and cationic β-CD concentration.

According to the results in Table 1, the use of carboxymethylated β-CD does not lead to a change compared with the use of native β-CD: the retention times are similar. The separations with carboxymethylated β-CD of compounds that are baseline separated with β-CD (MTH-tyrosine and MTH-phenylalanine) are not improved. All the other analyte separations are simply maintained or become worse. This may be explained by very weak stability constants: the inclusion is hindered by the carboxymethylation of the CD. However, a significant linear correlation (Fig. 3) is found between the complexing capacities of β-CD and carboxymethylated β-CD, if we do not consider the singular K_s value obtained with the laevorotatory enantiomer of MTH-tyrosine. This demonstrates that when inclusion may occur, it is governed by the same factors with the two chiral additives.

The K_s values obtained in presence of cationic β-CD (Table 1), if we do not consider the (−)-enantiomer of MTH-Tyr, are also well correlated with those determined with β-CD (Fig. 4, $R = 0.958$). The slope value ($s = 0.759$) and the intercept, which deviate significantly from unity and zero, respectively, indicate a weak complex-forming ability of cationic β-CD compared with native β-CD. The cationic groups modify the accessibility of the CD cavity and hinder the inclusion of the solute, which in turn results in decreased complex stability. Nevertheless, when inclusion occurs, new and more selective interactions take place, which result in a sufficiently large difference between the stability constants of the complexes formed with each enantiomer. This results in either an improved selectivity (MTH-Tyr) or emergence of selectivity (PTH-Phe and MTH-Leu).

Further, according to the high solubility of cationic β-CD in reversed mobile phases, a selectivity decrease may be compensated for with an increase in chiral additive concentration; for instance, with MTH-Phe enantiomers, the selectivities obtained with 25 and 40 m*M* cationic β-CD concentrations ($\alpha = 1.149$ and 1.188) straddle the value obtained with β-CD (25 m*M*; $\alpha = 1.177$).

Following the promising results obtained in the previous chiral chromatographic separations, it was of interest to establish the usefulness of cationic β-CD in the resolution of different drugs. The resolutions of the diuretic and hypertensive chlorthalidone and the bronchodilator terbutaline were reproduced according to Walhagen and Edholm [17] in the presence of

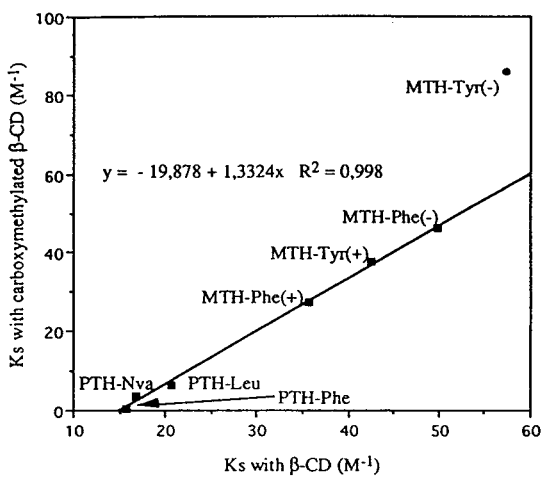

Fig. 3. Correlation between K_s values obtained with β-CD and carboxymethylated β-CD.

Table 1
Study of the influence of β-CD, cationic β-CD and carboxymethylated β-CD

Compound	Parameter	Without CD	25 m*M* β-CD	Cationic β-CD		25 m*M* carboxymethylated β-CD	K_s (l/mol)
				25 m*M*	40 m*M*		
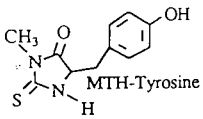 MTH-Tyrosine	t_r	13.12	6.38(−) 7.07(+)	6.68(−) 7.88(+)	5.52(−) 6.56(+)	6.06(−) 7.78(+)	β-CD: 57.4(−); 42.6(+)
	k'	3.46	1.50(−) 1.77(+)	1.61 2.08	1.16 1.57	1.24 1.88	β-CD cat.: 50.9(−); 30.3(+)
	α	1.000	1.180	1.291	1.356	1.517	β-CD carb.: 86.1(−); 37.8(+)
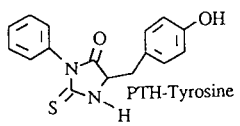 PTH-Tyrosine	t_r	24.71	18.32	20.51	18.42	24.27	β-CD: 5.4
	k'	7.41	6.18	7.01	6.22	7.99	β-CD cat.: 0.1
	α	1.000	1.000	1.000	1.000	1.000	β-CD carb.):—
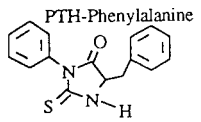 PTH-Phenylalanine	t_r	164.64	90.29	106.64(−) 111.18(+)	88.19 93.04	130.00 131.87	β-CD: 15.7
	k'	55.00	34.41	40.66 42.43	33.58 35.49	47.15 47.84	β-CD cat.: 7.1(−); 5.2(+)
	α	1.000	1.000	1.044	1.057	1.015	β-CD carb.: 0.6; 0.05
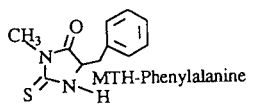 MTH-Phenylalanine	t_r	60.42	23.51(−) 27.21(+)	31.31(−) 35.58(+)	24.36 28.46	26.66(−) 33.26(+)	β-CD: 49.9(−); 35.7(+)
	k'	19.55	8.22(−) 9.67(+)	11.23(−) 12.90(+)	8.55 10.16	8.87 11.32	β-CD cat.: 28.0(−); 19.2(+)
	α	1.000	1.177	1.149	1.188	1.276	β-CD carb: 46.1(−)27.5(+)
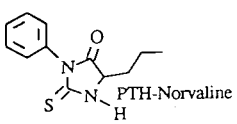 PTH-Norvaline	t_r	75.74	45.91(−) 47.10(+)	58.30	50.94	58.24	β-CD: 16.8(−); 15.6(+)
	k'	24.76	17.00(−) 17.47(+)	21.77	18.98	20.57	β-CD cat.: 1.3
	α	1.000	1.027	1.000	1.000	1.000	β-CD carb.: 3.7
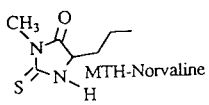 MTH-Norvaline	t_r	24.84	18.56	24.79	24.46	24.60	β-CD: 7.0
	k'	7.45	6.28	8.68	8.59	8.11	β-CD cat.:—
	α	1.000	1.000	1.000	1.000	1.000	β-CD carb.:—
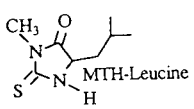 MTH-Leucine	t_r	46.88	30.44	42.43(+) 43.79(−)	39.20(+) 41.23(−)	41.79	β-CD: 11.4
	k'	14.95	10.94	15.57(+) 16.11(−)	14.37(+) 15.17(−)	14.48	β-CD cat.:—
	α	1.000	1.000	1.034	1.056	1.000	β-CD carb.:—
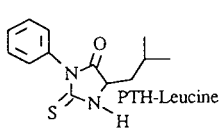 PTH-Leucine	t_r	151.70	79.12(−) 81.25(+)	105.47(−) 107.66(+)	88.19(−) 91.02(+)	108.35	β-CD: 20.6(−); 19.0(+)
	k'	50.60	30.03(−) 30.86(+)	40.20(−) 41.05(+)	33.58(−) 34.69(+)	39.13	β-CD cat.: 5.3(−); 4.4(+)
	α	1.000	1.028	1.021	1.033	1.000	β-CD carb.: 6.6

Chromatographic conditions: LiChroCART 250-4 Superspher 100 RP-18 column (4 μm, 250 × 4 mm I.D.); mobile phase, ethanol–acetate buffer (pH 4.1) (20:80, v/v) + 25 m*M* torus CDX; flow rate, 0.8 ml/min; temperature, 22.5°C.

native β-CD and attempted with cationic β-CD. The chromatographic data and the chromatograms are reported in Table 2 and Fig. 5, respectively. The two compounds are well resolved with each chiral additive. However, the elution of chlorthalidone enantiomers, which is similar in the two cases, results in a decrease in resolution with cationic β-CD. This decrease is not significant for the terbutaline enantiomers, in spite of a great difference in elution time.

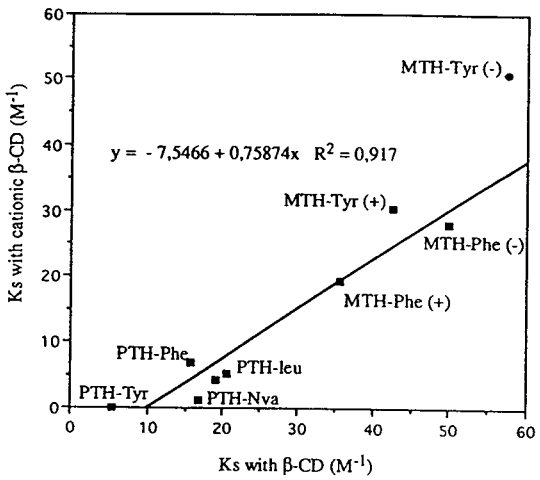

Fig. 4. Correlation between K_s values obtained with β-CD and cationic β-CD.

Barbiturates, which are widely used as anaesthetics, sedatives, hypnotics, anticonvulsants, etc., may be resolved into enantiomers of different pharmacological activity. Differences in the pharmacological effectiveness of these compounds have been widely investigated [18–23] since the synthesis and resolutions of optically active barbiturates were reviewed. However, chromatographic resolution in the presence of β-CD [14,24,25] requires a concentration near the solubility limit, whereas the use of methylated β-CD [26,27] needs a long time to reach the equilibrium of a dynamic coating of the stationary phase. These drawbacks do not occur when using cationic β-CD: (i) it is far more soluble in water than free β-CD and (ii) no dynamic coating is required. Moreover, the chromatographic data reported in Table 2 for hexobarbital and mephobarbital show a decrease in retention with an increase in resolution and selectivity, leading to shorter and better analysis conditions. These two compounds are baseline resolved in presence of cationic β-CD (Fig. 5).

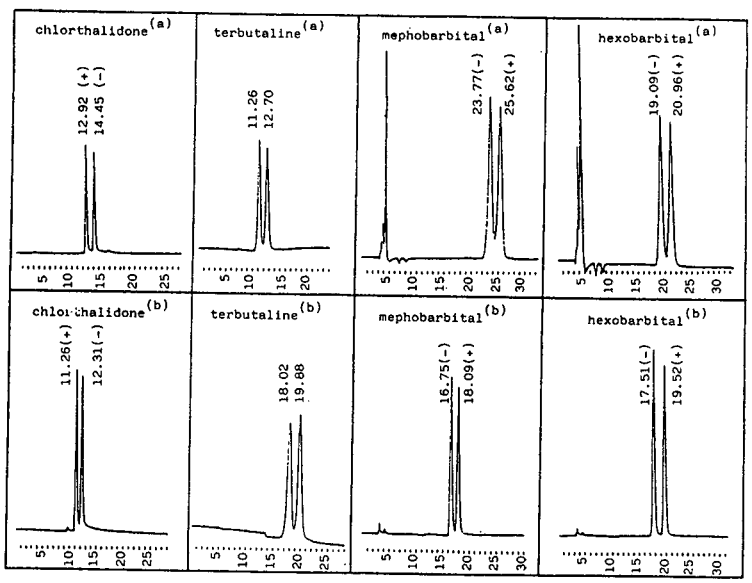

Fig. 5. Chromatograms of drugs obtained with (a) native β-CD and (b) cationic β-CD. Chromatographic conditions as described in Table 2.

Table 2
Influence of native β-CD and cationic β-CD on the enantiomeric separation of different drugs

Compound	Parameter	With β-CD	With cationic β-CD
Chlorthalidone[a]	t_r	12.92 min (+); 14.45 min (−)	11.26 min (+); 12.31 min (−)
	k'	3.857 (+); 4.432 (−)	3.504 (+); 3.924 (−)
	α	1.149	1.120
	R_s	2.5	1.5
Terbutaline[b]	t_r	11.26 min; 12.70 min	18.02 min; 19.88 min
	k'	2.657; 3.123	3.551; 4.020
	α	1.176	1.132
	R_s	1.6	1.4
Mephobarbital[c]	t_r	23.77 min (−); 25.62 min (+)	16.75 min (−); 18.09 min (+)
	k'	6.053 (−); 6.602 (+)	4.030; 4.432
	α	1.091	1.100
	R_s	1.4	1.7
Hexobarbital[c]	t_r	19.09 min (−); 20.96 min (+)	17.51 min (−); 19.52 min (+)
	k'	4.665 (−); 5.220 (+)	4.258 (−); 4.862 (+)
	α	1.119	1.142
	R_s	1.6	2.5

[a] EtOH–acetate buffer (pH 4.1) (20:80, v/v) + [CD] = 25 m*M*; flow-rate, 0.8 ml/min; temperature, 22.5°C; detection at 254 nm.
[b] Acetate buffer (pH 5.9) + 10 m*M* CD; flow-rate, 0.8 ml/min; temperature, 22.5°C; detection at 275 nm.
[c] EtOH–phosphate buffer (pH 2.5) (20:80, v/v) + 25 m*M* CD; flow-rate, 0.6 ml/min; temperature, 22.5°C; detection at 254 nm.

4. Conclusion

The use of cationic β-CD as a chiral additive in the mobile phase presents definite advantages over the use of other, commonly used, cyclodextrin chiral additives such as native β-CD or methylated cyclodextrin. The retention time and resolution may be controlled owing to the wide range of solubility of the cationic β-CD. In general, the enantioselectivities observed are at least as good as those for native β-CD under the same conditions and are potentially improved by using higher concentrations. In this work we have not taken advantage of the presence of charged nitrogen, which we believe might be used for chiral ion-pair chromatography in the future.

References

[1] E.J. Ariens, *Trends Pharmacol. Sci.*, May (1986) 200.
[2] D.W. Armstrong, *J. Liq. Chromatogr.*, 3 (1980) 895.
[3] A.K. Chatjigakis, C. Donzé and A.W. Coleman, *Anal. Chem.*, 64 (1992) 1632.
[4] M. Taghvaei and G.H. Stewart, *Anal. Chem.*, 63 (1991) 1902.
[5] T. Takeuchi, H. Asai and D. Ishii, *J. Chromatogr.*, 357 (1986) 409.
[6] D.Y. Pharr, Z.S. Fu, T.K. Smith and W.L. Hinze, *Anal. Chem.*, 61 (1989) 275.
[7] C. Pettersson, T. Arvidsson, A.L. Karlsson and I. Marle, *J. Pharm. Biomed. Anal.*, 4 (1986) 221.
[8] J. Szejtli, *J. Inclus. Phenom. Mol. Recognit. Chem.*, 14 (1992) 25.
[9] J. Szeman and J. Szejtli, in D. Duchêne (Editor), *Minutes 5th Int. Symp. Cyclodextrins, Paris, 1990*, Editions de la Santé, Paris, 1990, p. 672.
[10] C. Roussel, J.L. Stein, M. Sergent and R. Phan Tan Luu, in D. Stevenson and I.D. Wilson (Editors), *Recent Advances in Chiral Separations*, Plenum Press, New York, 1991, p. 105.
[11] K. Uekama, F. Hirayama, S. Nasu, N. Matsuo and T. Irie, *Chem. Pharm. Bull.*, 26 (1978) 2477.
[12] J. Zukowski, D. Sybilska and J. Jurczak, *Anal. Chem.*, 57 (1985) 2215.
[13] K. Fujimura, T. Ueda, M. Kitagawa, H. Takayanagi and T. Ando, *Anal. Chem.*, 58 (1986) 2668.
[14] K. Cabrera and G. Schwinn, *Kontakte (Darmstadt)*, 3 (1989) 3.
[15] K. Cabrera and G. Schwinn, *Int. Lab.*, July–August (1990) 28.
[16] A. Favrou and C. Roussel, in A.R. Hedges (Editor), *Minutes 6th Int. Symp. Cyclodextrins, Chicago, April 1992*, Editions de la Santé, Paris, 1992, p. 603.

[17] A. Walhagen and L.-E. Edholm, *Chromatographia*, 32 (1991) 215.
[18] J. Knabe, W. Rummel, H.P. Buech and N. Frang, *Arzneim.-Forsch.*, 28 (1978) 1048.
[19] I.K. Ho and R.A. Harris, *Annu. Rev. Pharmacol. Toxicol.*, 21 (1981) 83.
[20] M.K. Ticku, *Biochem. Pharmacol.*, 30 (1981) 1579.
[21] J. Baldauf, H. Wibert and H.P. Buech, *Arzneim.-Forsch.*, 32 (1982) 1281.
[22] P. Scolnick, K.C. Rice, J.L. Barker and M.S. Paul, *Brain Res.*, 233 (1982) 143.
[23] N.P.E. Vermeulen and D.D. Breimer, in E.J. Ariens, W. Soudijn and B.M. Timmermans (Editors), *Stereochemistry and Biological Activity of Drugs*, Blackwell, Oxford 1983, p. 33.
[24] D. Sybilska, J. Zukowski and J. Bojarski, *J. Liq. Chromatogr.*, 9 (1986) 591.
[25] J. Zukowski, D. Sybilska and J. Bojarski, *J. Chromatogr.*, 364 (1986) 225.
[26] J. Zukowski and N. Nowakowski, *J. Liq. Chromatogr.*, 12 (1989) 1545.
[27] J. Zukowski, J. Sybilska, J. Bojarski and J. Szejtli, *J. Chromatogr.*, 436 (1988) 381.

ELSEVIER

Journal of Chromatography A, 704 (1995) 75–81

JOURNAL OF CHROMATOGRAPHY A

Resolution of gram quantities of racemates by high-speed counter-current chromatography

Ying Ma[a], Yoichiro Ito[a,*], Alain Foucault[b]

[a]*Laboratory of Biophysical Chemistry, National Heart, Lung, and Blood Institute, National Institutes of Health, Bethesda, MD 20892, USA*

[b]*Laboratoire de Bioorganique et Biotechnologies ESR 71, Centre National de la Recherche Scientifique, 16 Rue Pierre et Marie Curie, 75005 Paris, France*

First received 13 December 1994; revised manuscript received 27 January 1995; accepted 31 January 1995

Abstract

Gram quantities of (±)-dinitrobenzoyl amino acids were separated by high-speed counter-current chromatography (CCC) using N-dodecanoyl-L-proline-3,5-dimethylanilide as a chiral selector (CS). Standard and pH-zone-refining CCC techniques were compared. By using the standard technique, 10 mg to a maximum of 1 g of samples was resolved in 2–9 h simply by increasing the concentration of the CS in the stationary phase. By using pH-zone-refining CCC, even more sample (2 g) was efficiently separated in less time (3 h). In both techniques, leakage of CS from the column was negligible. The method requires no solid support and the same column can be used repeatedly to separate a variety of enantiomers by dissolving appropriate chiral selectors in the stationary phase.

1. Introduction

Because of increasing demands for chiral purity, there is intensive interest in techniques for the separation of enantiomers. Direct separation of enantiomers by high-performance liquid chromatography (HPLC) is now widely used and more than one hundred chiral stationary phases are commercially available for analytical-scale separations [1]. However, few preparative applications using HPLC [2] have been reported because of the limited capacity of the standard-size columns and the high cost of solid stationary phases for large columns. Counter-current chromatography (CCC) [3–7] is an excellent alternative since the column requires no solid support and can be used to separate a variety of enantiomers by adding a suitable chiral selector to the stationary liquid phase.

In the past, CCC separations of chiral compounds have been described using various techniques such as droplet CCC [8], rotation locular CCC [9] and centrifugal partition chromatography [10,11]. None of these techniques, however, was suitable for preparative-scale separations in terms of sample size, resolution or separation time.

In our laboratory, highly efficient preparative-scale separations of chiral compounds were achieved by high-speed CCC using both standard [12] and pH-zone-refining CCC [13–16] techniques. We have chosen a chiral selector, N-

* Corresponding author.

0021-9673/95/$09.50
SSDI 0021-9673(95)00148-4

dodecanoyl-L-proline-3,5-dimethylanilide, described by Pirkle and Murray [17] for use in HPLC, and recently introduced as a free molecule for chiral resolution in centrifugal partition chromatography by Oliveros et al. [10]. A series of (±)-3,5-dinitrobenzoyl (DNB) amino acids was used to evaluate the CCC procedures.

2. Experimental

2.1. Reagents

Glass-distilled HPLC-grade organic solvents including methyl *tert.*-butyl ether, hexane, ethyl acetate, methanol and trifluoroacetic acid (TFA) were purchased from Burdick & Jackson Labs., Muskegon, MI, USA. Hydrochloric acid (Fisher Scientific, Fair Lawn, NJ, USA) and aqueous ammonia (>28%) (Baker, Phillipsburg, NJ, USA) were analytical grade. (±)-DNB-leucine and (±)-DNB-phenylalanine were purchased from Aldrich, Milwaukee, WI, USA. Other DNB-amino acids and N-dodecanoyl-L-proline-3,5-dimethylanilide (chiral selector or CS) were synthesized according to the method described by Oliveros et al. [10].

2.2. Apparatus

The experiments were performed using a commercial high-speed CCC centrifuge (Ito multilayer coil separator/extractor; P.C. Inc., Potomac, MD, USA; a comparable instrument is available from Pharma-Tech Research Corp., Baltimore, MD, USA. General features of the apparatus are described elsewhere [12]. The apparatus holds a multilayer coil separation column on the rotary frame at a distance of 10 cm from the central axis of the centrifuge. A counterweight is mounted on the opposite side for balancing the column. The desired planetary motion of the column was produced by coupling a plastic gear mounted on the column holder to an identical stationary gear on the centrifuge axis; the column holder undergoes a synchronous planetary motion, i.e. one rotation about its own axis during one revolution around the central axis of the centrifuge.

The column was prepared in our laboratory by winding a single piece of 160 m × 1.6 mm I.D. polytetrafluoroethylene (PTFE) tubing around the holder hub making 11 coiled layers between a pair of flanges spaced 5 cm apart. The total column volume measured 330 ml. The ends of the coil were connected to flow tubes (0.85 mm I.D. PTFE) that enter and exit the centrifuge through its hollow central stationary pipe. As described earlier [12], these flow tubes are twist-free when the column is rotated so that the elution can be performed through the rotating column without the use of rotary seals.

2.3. Preparation of two-phase solvent systems and sample solutions

Three different solvent systems were prepared, two for the standard CCC and one for pH-zone-refining CCC. For standard CCC, solvent systems consisting of hexane–ethyl acetate–methanol–10 m*M* hydrochloric acid (8:2:5:5 and 6:4:5:5, v/v) were used. Each solvent mixture was thoroughly equilibrated in a separatory funnel, and the two phases were separated shortly before use. The chiral selector (CS) was added to the organic stationary phase at various concentrations ranging from 10 to 60 m*M*.

For pH-zone-refining CCC, the desired volumes of methyl *tert.*-butyl ether and water were equilibrated in a separatory funnel. After the two phases were separated, both TFA (20 m*M*) and CS (10–60 m*M*) were added to the organic stationary phase and aqueous ammonia (20 m*M*) was added to the aqueous mobile phase.

The sample solutions were prepared by dissolving a desired amount of the sample in the two-phase solvent system used for separation.

2.4. Separation procedure

Both standard and pH-zone-refining CCC were performed using an apparatus schematically illustrated in Fig. 1. In each separation, the column (a) was entirely filled with the organic stationary phase as follows: about 150 ml of

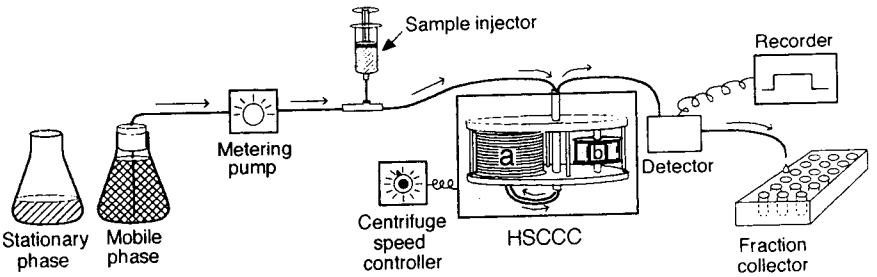

Fig. 1. Elution system for high-speed counter-current chromatography.

CS-free organic phase was first pumped into the inlet of the column (330 ml capacity). Then, 200 ml of the CS-containing organic phase were pumped into the column, discharging ca. 20 ml of excess CS-free stationary phase from the column outlet. The column therefore contained 130 ml of CS-free stationary phase at its outlet. (During the separation, a portion of this CS-free stationary phase was retained in the column to absorb any CS that may be carried over by the mobile phase, thus preventing contamination of the fractions with the CS). After the sample solution was injected through the sample port, the aqueous mobile phase was pumped into the column at a flow-rate of 3.3 ml/min while the column was rotated at 800 rpm regulated by the speed controller. The absorbance of the effluent was continuously monitored at 254 nm (standard CCC technique) or 206 nm (pH-zone-refining CCC) (Uvicord S; LKB, Bromma/Stockholm, Sweden) and 3.3-ml fractions were collected (Ultrorac, LKB).

2.5. Analysis of CCC fractions

Each peak fraction obtained from the standard CCC elution was analyzed by circular dichroism (CD) and/or optical rotation apparatus to determine the chirality. The analytical standard CCC technique thus developed was in turn used for determining optical purity and chirality of fractions obtained from the pH-zone-refining CCC technique. The pH of the fractions from the pH-zone-refining CCC separation was measured (Accumet portable laboratory pH meter, Fisher Scientific, Pittsburgh, PA, USA).

3. Results and discussion

Fig. 2A shows the separations of enantiomers of four different (±)-DNB-amino acids using the standard CCC technique. With a two-phase solvent system composed of hexane–ethyl acetate–methanol–10 m*M* hydrochloric acid (8:2:5:5, v/v), the separations were performed on an analytical scale (5–10 mg for each racemic mixture) to investigate the mechanism of enantioselectivity of the chiral selector. These chromatograms were obtained from left to right by injecting racemic mixtures of DNB-phenylglycine, DNB-phenylalanine, DNB-valine and DNB-leucine, respectively. All of these separations were carried out by injection of successive samples, without renewing the column phases containing the chiral selector. The results indicate that the enantioselectivity of DNB-amino acids is closely related to the side chain (R) of the molecule. Within a class (aliphatic or aromatic) the chromatographic separation factor (α) increases with the increasing size of R as shown in Table 1.

The preparative capability of the present system was investigated with the separation of (±)-DNB-leucine by varying the concentration of the chiral selector from 10 to 60 m*M* in the stationary phase using a similar two-phase solvent system composed of hexane–ethyl acetate–methanol–10 m*M* HCl (6:4:5:5, v/v). The results

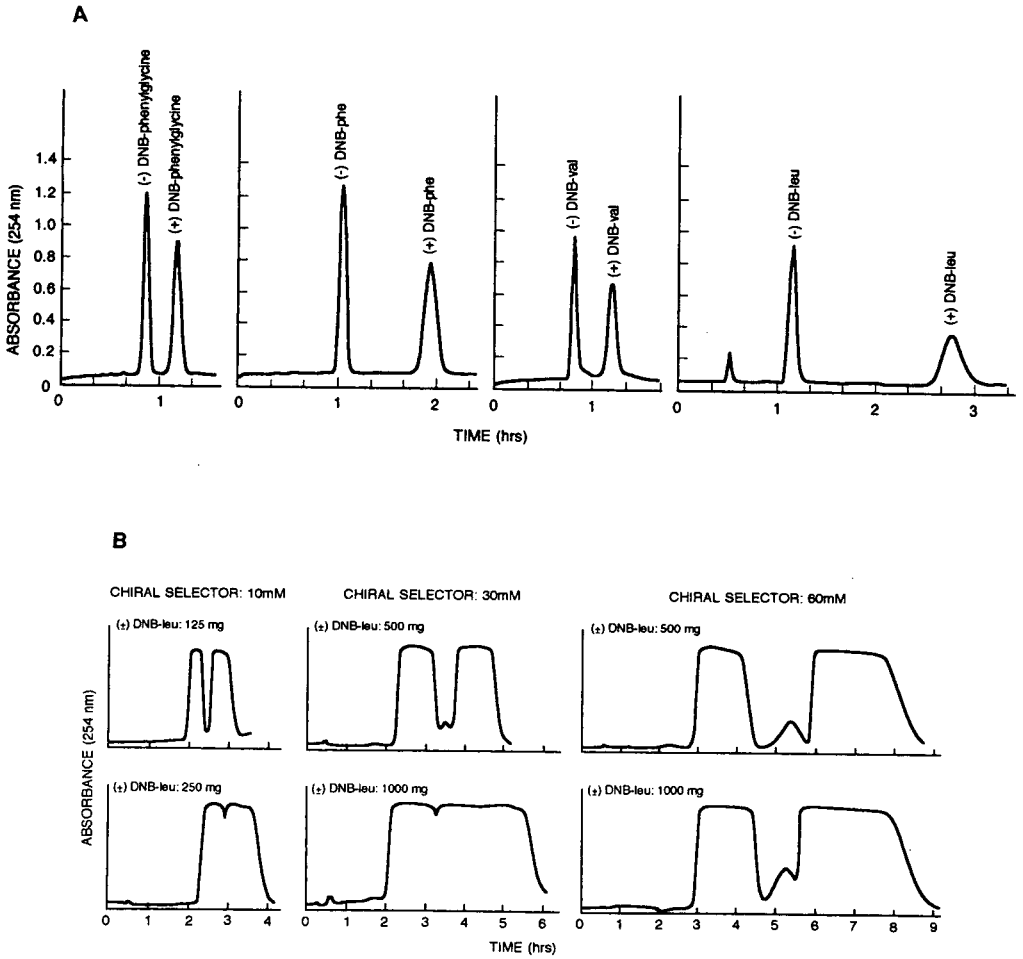

Fig. 2. Separations of (±)-DNB-amino acids by the standard CCC technique in analytical (A) and preparative (B) scales. Experimental conditions: apparatus: multilayer coil high-speed CCC centrifuge with a semipreparative column of 1.6 mm I.D. and 330 ml capacity; solvent system: (A) hexane–ethyl acetate–methanol–10 m*M* HCl (8:2:5:5), N-dodecanoyl-L-proline-3,5-dimethylanilide (2 g) was added to the organic stationary phase (200 ml) as a chiral selector (CS), (B) hexane–ethyl acetate–methanol–10 m*M* HCl (6:4:5:5) where the organic stationary phase containing CS at 10 to 60 m*M* as indicated. Samples: (A) from left to right: (±)-DNB-phenylglycine, (±)-DNB-phenylalanine, (±)-DNB-valine and (±)-DNB-leucine, 5–10 mg of each dissolved in 5 ml of solvent consisting of equal volumes of each phase; (B) (±)-DNB-leucine, 125–1000 mg dissolved in 10–45 ml of solvent. Flow-rate: 3.3 ml/min in the head-to-tail elution mode; revolution: 800 rpm; analysis of fractions: optical rotation and CD; stationary phase retention: 65% of the total column capacity.

indicate that the sample loading capacity is largely determined by the concentration (or net amount) of the chiral selector in the stationary phase (Fig. 2B): The higher the concentration of the chiral selector, the greater the peak resolution. The maximum sample size of 1 g was completely resolved in 9 h. Further increasing the sample size to 2 g, however, resulted in extensive carryover of the stationary phase apparently due to the formation of solid precipitate in the column. This problem was greatly alleviated by the pH-zone-refining CCC technique which allows use of more polar solvent systems.

pH-Zone-refining CCC [13–16] is a powerful preparative technique that is comparable to displacement chromatography [18] and isotacho-

Table 1
Separation factors of enantiomers of DNB-amino acids

Sample	R[a]	$D_{(\pm)}$[b]	$D_{(-)}$[c]	$D_{(+)}$[d]	α[e]
DNB-Phenylglycine	C_6H_5	0.17	0.19	0.41	2.13
DNB-Phenylalanine	$CH_2C_6H_5$	0.20	0.31	0.72	2.33
DNB-Valine	$CH(CH_3)_2$	0.18	0.19	0.43	2.27
DNB-Leucine	$CH_2CH(CH_3)_2$	0.30	0.37	1.36	3.43

[a]R = Side chain.
[b]$D_{(\pm)}$ = Distribution ratio (analyte concentration in the stationary phase divided by that in the mobile phase measured before the chiral selector was added to the solvent system).
[c]$D_{(-)}$ = Distribution ratio of (−)-enantiomer.
[d]$D_{(+)}$ = distribution ratio of (+)-enantiomer.
[e]α = Separation factor.

phoresis [19]. It yields a succession of highly concentrated rectangular solute peaks with minimum overlap where impurities are concentrated at the peak boundaries. Recently, the technique has been successfully applied to separations of wide varieties of compounds including amino acid derivatives [20,21], oligopeptide derivatives [22], a variety of hydroxyxanthene dyes [23–27], alkaloids [28], indole auxins [14], structural [29] and geometrical [30] isomers, etc.

In the present study this technique was used to resolve (±)-DNB-leucine using a binary two-phase solvent system composed of methyl *tert.*-butyl ether and water where a retainer acid (trifluoroacetic acid) and the chiral selector (same as that used in the standard CCC technique) were added to the organic stationary phase and an eluent base (ammonia) to the aqueous mobile phase.

Fig. 3 shows a typical chromatogram obtained by pH-zone-refining CCC, where two gram of (±)-DNB-leucine was eluted in a single rectangular UV peak in about 3 h. The pH of each fraction (dotted line) revealed that the peak was evenly divided into two pH zones with a sharp transition. When peak fractions were analyzed by the analytical-scale standard CCC technique described earlier, the first zone (pH 6.5) was almost entirely composed of (−)-DNB-leucine and the second zone (pH 6.8) of (+)-DNB-leucine while the narrow zone boundary contained both isomers and an impurity (see the upper diagram). This mixing zone is estimated to be no more than 5% of each peak.

In the absence of a complexing agent, as reported elsewhere [14,16], the separation of the analytes and their elution order in pH-zone-refining CCC are based on the zone pH which is expressed by the following equation

$$\mathrm{pH}_z = \mathrm{p}K_a + \log\left(\frac{K_D}{D_r} - 1\right) \quad (1)$$

where K_D is the partition ratio of the neutral analyte $\{[AH]_{org}/[AH]_{aq}\}$, and D_r is the distribution ratio for the retainer acid or analytes (formerly called apparent partition coefficient or K_r). In the present method, however, the organic phase contains the chiral selector CS that binds to AH with a formation constant, $K = [AHCS]_{org}/[AH]_{org}[CS]_{org}$. Consequently, Eq. 1 must be modified to

$$\mathrm{pH}_z = \mathrm{p}K_a + \log\left\{\frac{K_D}{D_r}\cdot(1 + [CS]_{org}K) - 1\right\} \quad (2)$$

provided that CS and its complexes are insoluble in the aqueous phase ($D_{CS} > 100$ for the present solvent system). Since both pK_a and K_D values of the two enantiomers are identical and D_r is common, the separation of the two pH zones must be derived from the difference in term $[CS]_{org}K$ for the two isomers. Eq. 2 clearly indicates that resolution of two enantiomers is improved by increasing CS concentration and/or

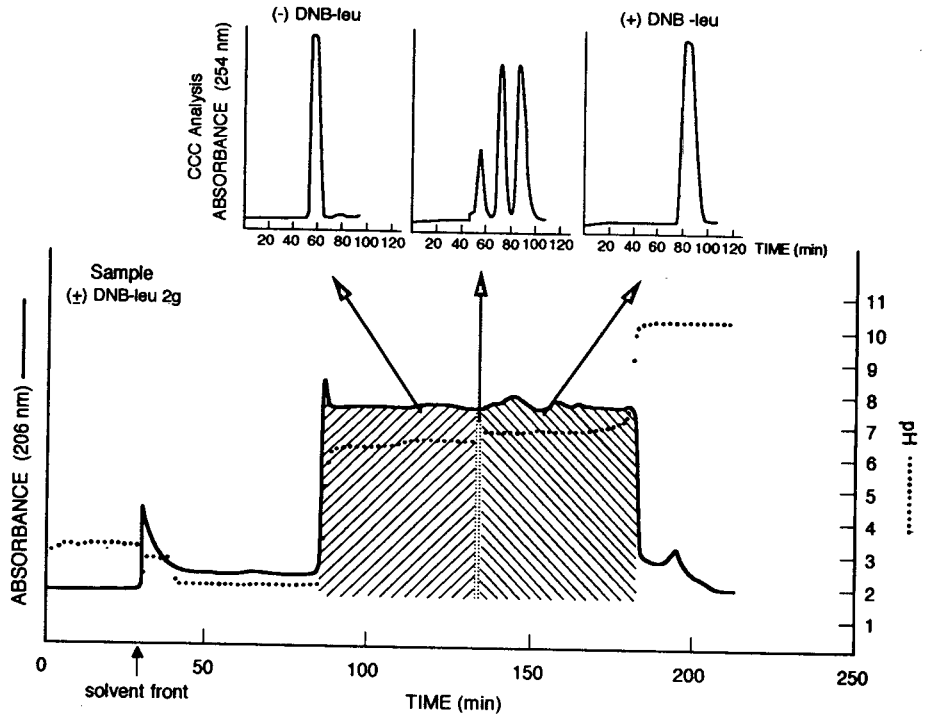

Fig. 3. Separation of (±)-DNB-leucine by pH-zone-refining CCC. Experimental conditions for pH-zone-refining CCC: Apparatus as in Fig. 2; solvent system: methyl *tert.*-butyl ether–water; stationary phase: upper organic phase to which TFA (40 m*M*) and CS (40 m*M*) were added; mobile phase: lower aqueous phase to which aqueous ammonia was added at 20 m*M*; sample: (±) DNB-leucine 2 g; flow-rate: 3.3 ml/min; revolution: 800 rpm; analysis: chirality by analytical high-speed CCC and pH by a portable pH meter. Experimental conditions for the analytical CCC as in Fig. 2A. Note that the analysis of the fraction from the mixing zone (middle chromatogram) shows three peaks corresponding to (−)-DNB-leucine, impurity and (+)-DNB-leucine from left to right.

the formation constant, K, for one of the isomers relative to the other.

Compared with the standard CCC technique described earlier, the pH-zone-refining CCC technique allows separation of larger amounts in shorter times. In addition, the method uses relatively polar solvent systems which can hold the chiral selector for much longer reducing contamination in the purified fractions. In both techniques, however, leakage of the chiral selector into the eluate can be completely eliminated by filling the outlet of the column with a suitable amount of CS-free stationary phase so that any chiral selector in the flowing mobile phase is retained.

Although our studies only show chiral separations of (±)-DNB-amino acids, it is obvious that the method may be extended to the separation of other racemic mixtures by choosing appropriate chiral selectors.

Acknowledgements

The authors wish to thank Drs. H. Ziffer and X.-K. Zhang for their kind help in structural analyses and Drs. Henry M. Fales and Alan L. Scher for editing the manuscript with valuable suggestions. A.F. fully acknowledges L. Oliveros and C. Minguillon for their helpful contribution in chiral chromatography.

References

[1] C.J. Welch, *J. Chromatogr. A*, 666 (1994) 3.
[2] E. Francotte and A.J. Junker-Buchheit, *J. Chromatogr.*, 576 (1992) 1.
[3] Y. Ito and R.L. Bowman, *Science*, 167 (1970) 281.
[4] Y. Ito, in N.B. Mandava and Y. Ito (Editors), *Countercurrent Chromatography: Theory and Practice*, Marcel Dekker, New York, 1988, Ch. 2, p. 79.
[5] W.D. Conway, *Countercurrent Chromatography: Apparatus, Theory and Applications*, VCH, New York, 1990.
[6] Y. Ito, in E. Heftmann (Editor), *Chromatography, 5th Edition, Part A: Fundamentals and Techniques (Journal of Chromatography Library*, Vol. 51A), Elsevier, Amsterdam, 1992, Ch. 2, p. A69.
[7] A. Berthod and D.W. Armstrong, *J. Liq. Chromatogr.*, 11 (1988) 1187.
[8] T. Takeuchi, R. Horikawa and T. Tanimura, *J. Chromatogr.*, 284 (1984) 285.
[9] B. Domon, K. Hostettmann, K. Kovacevic and V. Prelog, *J. Chromatogr.*, 250 (1982) 149.
[10] L. Oliveros, P. Franco Puertolas, C. Minguillon, E. Camacho-Frias, A. Foucault and F. Le Goffic, *J. Liq. Chromatogr.*, 17 (1994) 2301.
[11] D.W. Armstrong, R. Menges and I.W. Wainer, *J. Liq. Chromatogr.*, 13 (1990) 3571.
[12] Y. Ito, *CRC Crit. Rev. Anal. Chem.*, 17 (1986) 65.
[13] A. Weisz, A.L. Scher, K. Shinomiya, H.M. Fales and Y. Ito, *J. Am. Chem. Soc.*, 116 (1994) 704.
[14] Y. Ito, K. Shinomiya, H.M. Fales, A. Weisz and A.L. Scher, in W.D. Conway and R. Petroski (Editors), *Countercurrent Chromatography*, American Chemical Society, Washington, DC, in press.
[15] A.L. Scher and Y. Ito, in W.D. Conway and R. Petroski (Editors), *Countercurrent Chromatography*, American Chemical Society, Washington, DC, in press.
[16] Y. Ito, in Y. Ito and W.D. Conway (Editors), *High-Speed Countercurrent Chromatography*, Wiley-Interscience, New York, Ch. 9, in press.
[17] W.H. Pirkle and P.G. Murray, *J. Chromatogr.*, 641 (1993) 11.
[18] Cs. Horváth, A. Nahum and J.H. Frenz, *J. Chromatogr.*, 218 (1981) 365.
[19] P. Boček, M. Deml, P. Gebauer and V. Dolnik, in B.J. Radola (Editor), *Isotachophoresis*, VCH, Weinheim, 1988.
[20] Y. Ito and Y. Ma, *J. Chromatogr. A*, 672 (1994) 101.
[21] Y. Ma and Y. Ito, *J. Chromatogr. A*, 678 (1994) 233.
[22] Y. Ma and Y. Ito, *J. Chromatogr. A*, in press.
[23] A. Weisz, D. Andrzejewski, R.J. Highet and Y. Ito, *J. Chromatogr. A*, 658 (1994) 505.
[24] A. Weisz, D. Andrzejewski and Y. Ito, J. *Chromatogr. A*, 678 (1994) 77.
[25] A. Weisz, D. Andrzejewski, K. Shinomiya and Y. Ito, in W.D. Conway and R. Petroski (Editors), *Countercurrent Chromatography*, American Chemical Society, Washington, DC, in press.
[26] K. Shinomiya, A. Weisz and Y. Ito, in W.D. Conway and R. Petroski (Editors), *Countercurrent Chromatography*, American Chemical Society, Washington, DC, in press.
[27] A. Weisz, in Y. Ito and W.D. Conway (Editors), *High-Speed Countercurrent Chromatography*, Wiley-Interscience, New York, Ch. 10, in press.
[28] Y. Ma, Y. Ito, E. Sokolosky and H.M. Fales, *J. Chromatogr. A*, 685 (1994) 259.
[29] Y. Ma, Y. Ito, D. Torok and H. Ziffer, *J. Liq. Chromatogr.*, 17 (1994) 3507.
[30] C. Denekamp, A. Mandelbaum, A. Weisz and Y. Ito, *J. Chromatogr. A*, 685 (1994) 253.

ELSEVIER

Journal of Chromatography A, 704 (1995) 83–87

JOURNAL OF CHROMATOGRAPHY A

Direct high-performance liquid chromatographic separation of the enantiomers of methoxy and hydroxy derivatives of 3,4-dihydro-3-(dipropylamino)-2*H*-1-benzopyrans with dopaminergic activity

Salvatore Caccamese[a,*], Grazia Principato[a], Marie-Claude Viaud[b], Gérald Guillaumet[b]

[a]*Dipartimento di Scienze Chimiche, Università di Catania, Viale A. Doria 6, 95125 Catania, Italy*

[b]*Laboratoire de Chimie Bioorganique et Analytique, URA CNRS 499, Université d'Orléans, BP 6759, 45067 Orléans Cedex 2, France*

First received 2 November 1994; revised manuscript received 17 January 1995; accepted 17 January 1995

Abstract

The direct HPLC resolution of the enantiomers of methoxy and hydroxy derivatives of 3,4-dihydro-3-(dipropylamino)-2*H*-1-benzopyrans and of unsubstituted amino compounds was achieved using Chiralcel OD and/or Chiralpak AD stationary phases. The position of the substituent (methoxyl or hydroxyl) in the aromatic ring has a strong effect on the enantioselectivity. Circular dichroism spectra of the single enantiomers of one compound were measured.

1. Introduction

Dopamine is an important neurotransmitter both in the central nervous system and in peripheral tissues. Malfunction of the dopaminergic system has been suggested to play a major role in diseases such as schizophrenia and parkinsonism [1]. Although treatment is available with drugs influencing the dopaminergic system, the therapy of these diseases is far from satisfactory [2].

Recently, we demonstrated that isosteric replacement of the methylene group at C-4 in the 2-aminotetralins by oxygen may play an important role in the selective recognition of the serotoninergic or dopaminergic receptors in relation to the position of the substituent (hydroxyl or methoxyl) on the aromatic ring [3,4]. The effect of the replacement of the C-4 in several mono- and dihydroxytetralins by oxygen on the dopaminergic activity has also been investigated by other groups [5,6].

An efficient synthesis of the compounds in Fig. 1 has been described [4] and its advantage lies in

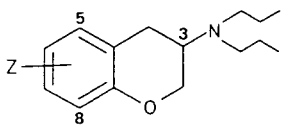

Fig. 1. Structure of compounds **1–6**, where Z = OH or OCH_3 at position 5, 6 or 8.

* Corresponding author.

0021-9673/95/$09.50
SSDI 0021-9673(95)00087-9

the possibility of preparing both dipropylic or diallylic derivatives. From the diallylic derivatives, by enantioselective crystallization with optically pure binaphtylphosphoric acid both enantiomers of 8-hydroxy-3,4-dihydro-3-(dipropylamino)-2*H*-1-benzopyran (Z = OH) were subsequently obtained. In vitro assays of dopaminergic activity indicated highly enantioselective recognition of the D-2 sites by the (−)-enantiomer [4]. Apart from this result, the reported pharmacological evaluations refer only to racemic compounds [5,6].

This prompted us to search for a direct method of enantiomeric separation in order to obtain sizeable amounts of individual enantiomers of dipropylic or unsubstituted amino derivatives which can be submitted to pharmacological assays. Indeed, recent guidance has been given for toxicity and activity testing during the development process of chiral drugs [7].

In this paper we report the first HPLC resolution of the enantiomers of 3,4-dihydro-3-(dipropylamino)-2*H*-1-benzopyrans and of unsubstituted amino compounds.

Among various HPLC chiral stationary phases (CSPs) used by us, only polysaccharide-derived types were able to resolve the enantiomers of this class of compounds and the chiral separation depended strongly on the position of the substituent (methoxyl or hydroxyl) in the aromatic ring. The resolution factors (R_s) of some compounds were fairly good and afforded milligram separation and circular dichroism (CD) measurement of the single enantiomers.

For completeness of information, it is useful to mention the following direct methods of enantiomeric resolution of isosteric tetralin derivatives. A Chiralcel OD column was used to determine directly the enantiomeric purity of the dopamine agonist 2-(N-propyl-N-2-thienylethylamino)-5 hydroxytetralin [8]. The enantiomers of 5-hydroxy-2-(dipropylamino) tetralin were resolved by chiral ion-pair chromatography, using N-benzyloxycarbonylglycyl-L-proline as the counter ion on a carbon column [9]. The enantiomeric purity of 5,6- and 6,7-dihydroxy-2-aminotetralins was determined using an 18-crown-6 chiral crown ether coated on a silica gel column [10].

2. Experimental

2.1. Apparatus

The HPLC system consisted of a Varian Model 5060 liquid chromatograph with Valco sample loops (10 or 50 μl), a Jasco Uvidec 100-III UV spectrophotometric detector operating at 240 nm and a Varian CDS 401 data system or an Omniscribe Houston recorder for fraction collection. CD spectra were recorded on a Jasco Model 600 spectropolarimeter. The mobile phases were HPLC-grade *n*-hexane–2-propanol mixtures. The columns (25 cm × 4.6 mm I.D.) used for the experiments reported in Table 1 were packed with Chiralcel OD (cellulose tris-3,5-dimethylphenylcarbamate) and with Chiralpak AD (amylose tris-3,5-dimethylphenylcarbamate), both coated on 10-μm silica gel from Daicel (Tokyo, Japan). The columns used for some unsuccessful experiments reported in the next section were another helical phase column, Chiralpak OP(+) from Daicel, and three Pirkle phase columns, (*R*)-α-Burke 1, (*R*)-DNBPG and (*R*,*R*)-Whelk O-1, all from Regis Chemical (Morton Grove, IL, USA). The column void time (t_0) was measured by injection of 1,3,5-tri-*tert.*-butylbenzene as a non-retained sample. Retention times were mean values of two replicate determinations. All separations were carried out at ambient temperature.

2.2. Chemicals

The syntheses of compounds **1**, **2**, **4**, **5**, **7** and **8** have been described elsewhere [4]. They start from readily available or commercial 2-hydroxybenzaldehydes and proceed in six steps. Compounds **3**, **6** and **9** were synthesized similarly, starting from 2-hydroxy-5-methoxybenzaldehyde, as intermediate products of a unique synthetic pathway [11].

3. Results and discussion

The chromatographic results for six compounds of the general formula in Fig. 1 and for

three compounds bearing an unsubstituted NH_2 group (**7–9**) are presented in Table 1.

Among the isomeric hydroxy derivatives, two of them (**2** and **3**) were resolved on Chiralcel OD, whereas the isomeric **1** was not resolved on this phase, as reported in Table 1 and from other trials with various percentages of 2-propanol in hexane as eluent. The composition of the mobile phase was in fact critical for obtaining baseline R_s, as shown for **2** and **3**. However, the enantiomeric resolution of **1** was achieved by using a Chiralpak AD column, as shown in Fig. 2. This phase was also efficient in the resolution of **2** and **3**, although to a lesser extent by comparing the α and R_s values.

Among the isomeric methoxy derivatives, **5**

Table 1
HPLC resolution of enantiomeric compounds **1–9** on chiral stationary phases

Compound	Z[a]	R[b]	CSP	A(%)[c]	k'[d]	α	R_s
1	5-OH	$CH_2CH_2CH_3$	OD	5	1.15	NS[e]	
			AD	10	0.58	1.13	0.8
2	8-OH	$CH_2CH_2CH_3$	OD	5	1.65	1.19	1.3
			OD	10	0.99	1.15	0.8
			OD	20	0.52	1.27	0.6
			AD	10	0.67	1.09	0.8
3	6-OH	$CH_2CH_2CH_3$	OD	5	1.89	1.50	3.3
			OD	10	0.88	1.69	3.1
			OD	30	0.27	1.49	1.0
			AD	10	1.02	1.12	1.3
4	5-OCH_3	$CH_2CH_2CH_3$	OD	5	0.19	NS	
			AD	10	0.04	NS	
			AD	0	0.16	1.43	0.8
5	8-OCH_3	$CH_2CH_2CH_3$	OD	3	3.04	1.34	2.0
			OD	3[f]	2.99	1.24	1.8
			OD	5	1.60	1.26	1.7
			AD	0	0.75	NS[g]	
6	6-OCH_3	$CH_2CH_2CH_3$	OD	10	0.29	NS	
			AD	10	0.23	1.35	1.4
7	5-OCH_3	H	OD	5	4.34	1.06	0.6
			OD	5[h]	4.70	1.19	1.6
			AD	10	1.84	NS[i]	
8	8-OCH_3	H	OD	10	8.42	1.20	1.7
			OD	10[h]	7.73	1.19	1.8
			OD	20[h]	3.64	1.20	1.4
			AD	10	2.11	NS[i]	
9	6-OCH_3	H	OD	10	1.25	NS	
			OD	30	1.81	NS	
			OD	30[f]	1.62	NS	
			AD	10	2.28	1.35	5.0[j]

[a] See the general formula in Fig. 1.
[b] Substituents on the nitrogen atom.
[c] Percentage of 2-propanol in *n*-hexane at a flow-rate of 1 ml/min for Chiralcel OD (t_0 = 3.3 min) and at a flow-rate of 0.5 ml/min for Chiralpak AD (t_0 = 7.2 min), unless specified otherwise.
[d] Capacity factor of the first-eluted enantiomer.
[e] Not separated.
[f] Flow-rate 1.3 ml/min, t_0 = 2.7 min.
[g] Shoulder on the rising edge.
[h] 2-Propanol doped with 0.5% of diethylamine.
[i] Flat-topped peak.
[j] Tailed peaks.

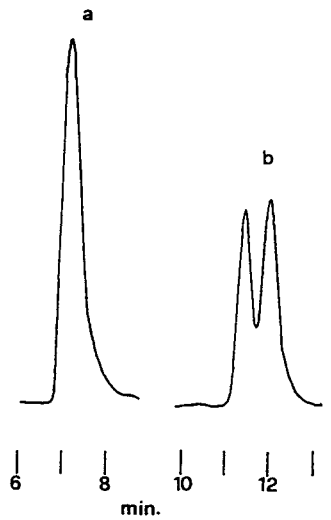

Fig. 2. HPLC behaviour of **1** on (a) Chiralcel OD with mobile phase *n*-hexane–2-propanol (95:5) at a flow-rate of 1 ml/min and (b) Chiralpak AD with mobile phase *n*-hexane–2-propanol (9:1) at a flow-rate of 0.5 ml/min.

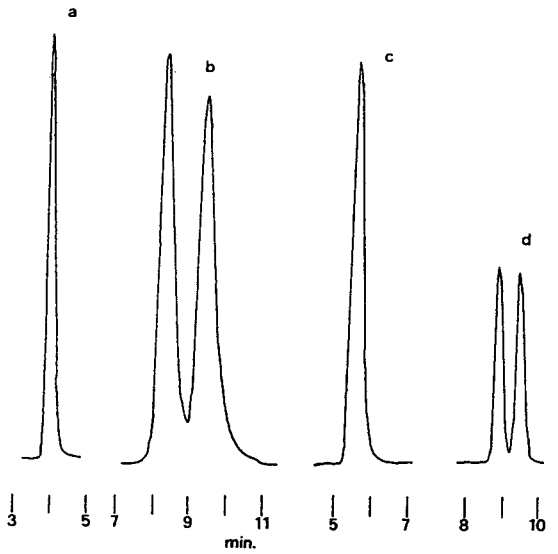

Fig. 3. HPLC separation of (a) **4**, (b) **5** and (c) **6** on Chiralcel OD with mobile phase *n*-hexane–2-propanol (95:5) at flow-rate of 1 ml/min and (d) **6** on Chiralpak AD with mobile phase *n*-hexane–2-propanol (9:1) at a flow-rate of 0.5 ml/min.

was efficiently resolved into its enantiomers by the Chiralcel OD column but the isomers **4** and **6** were not separated, as shown in Table 1 and Fig. 3. The enantiomeric resolution of the latter compounds was instead obtained using a Chiralpak AD column. The good resolution factor obtained for **5** afforded a separation of its enantiomers by repeated 50-μl injections of racemic **5** and collection of the eluates from the chromatographic peaks. The CD spectra of both eluates were measured and they were mirror images of each other, as shown in Fig. 4, indicating that the two eluates are optical isomers. Analytical HPLC re-runs on the eluates indicated an enantiomeric purity of 100% for the first peak and 95% for the second peak. Their UV spectra were also identical.

Among the isomeric methoxy derivatives of the primary amines, again we note a marked difference in the enantiomeric selectivity of the two CSPs on the same compound. Compound **9** was in fact resolved only by using a Chiralpak AD phase, as reported in Table 1 and in Fig. 5. The isomers **7** and **8** were instead better resolved by using the Chiralcel OD column. Addition of diethylamine to the mobile phase was effective in

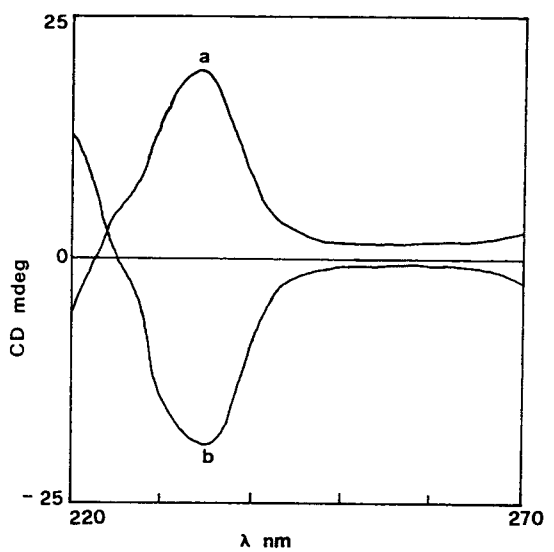

Fig. 4. CD spectra of the enantiomers of **5** obtained from (b) the first and (a) the second HPLC-eluted peaks.

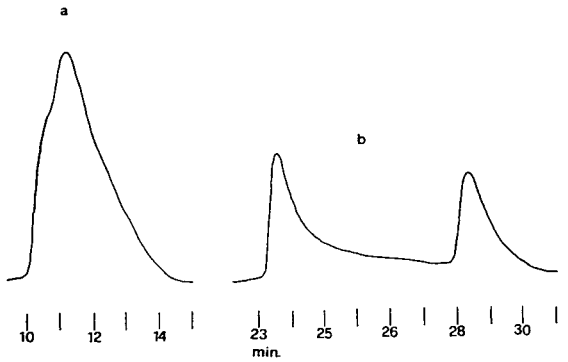

Fig. 5. HPLC behaviour of **9** with two CSPs: (a) Chiralcel OD and (b) Chiralpak AD. Mobile phase, *n*-hexane–2-propanol, (a) 7:3 at a flow-rate 1 ml/min and (b) 9:1 at a flow-rate 0.5 ml/min.

the enhancement of the enantiomeric resolution of **7–9**, as expected for primary amines. The effect is very strong for **7**, as shown in Fig. 6.

Hence very fine effects tune the interaction of the enantiomers of these derivatives of 3,4-dihydro-3-amino-2*H*-1-benzopyrans with the polar carbamate moiety of the Chiralcel OD and Chiralpak AD phases. This isomeric effect was also found in other classes of chiral compounds [12]. Also, the difference in the size of the helical cavity of the cellulose- and amylose-derived phases plays a significant role in the chiral recognition of the same compound.

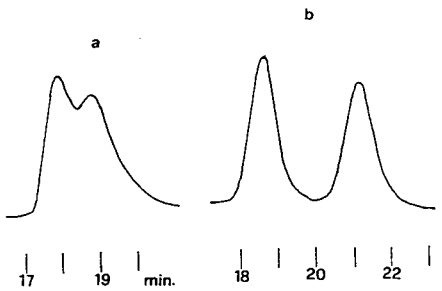

Fig. 6. HPLC resolution of **7** on Chiralcel OD at a flow-rate of 1 ml/min with mobile phase (a) *n*-hexane–2-propanol 95:5 and (b) *n*-hexane–2-propanol doped with 0.5% of diethylamine (95:5).

The good values of the resolution factors open the way to the rapid semi-preparative HPLC isolation of individual enantiomers and subsequent in vitro dopaminergic activity assays on them.

Finally, we should mention that several trials were made to obtain enantiomeric resolution of **2**, **3**, **6** and **9** using various Pirkle CSPs, reported under Experimental. However, although these phases differ in the kind and number of stereogenic centres, unsatisfactory results were obtained.

References

[1] C. Kaiser and T. Jain, Med. Res. Rev., 5 (1985) 145.
[2] H. Bottcher, G. Barnickel, H.H. Hausberg, A.F. Haase, C.A. Seyfried and V. Eiermann, J. Med. Chem., 35 (1992) 4020.
[3] J.M. Cossery, H. Gozlan, U. Spampinato, C. Perdicakis, G. Guillaumet, L. Pichat and M. Hamon, Eur. J. Pharmacol., 140 (1987) 143.
[4] M. Al Neirabeyeh, D. Reynaud, T. Podona, L. Ou, C. Perdicakis, G. Coudert, G. Guillaumet, L. Pichat, A. Gharib and N. Sarda, Eur. J. Med. Chem., 26 (1991) 497.
[5] L.D. Wise, H.A. Dewald, E.S. Hawkins, D.M. Reynolds, T.G. Heffner, L.T. Meltzer and T.A. Pugsley, J. Med. Chem., 23 (1988) 688.
[6] A.S. Horn, B. Kaptein, N.A. Vermue, J.B. De Vries and T.B.A. Mulder, Eur. J. Med. Chem., 23 (1988) 325.
[7] FDA's Policy Statement for the Development of New Steroisomeric Drugs, Food and Drug Administration, Washington, DC, 1992.
[8] D.T. Witte, J.P. Franke, P.J. Swart and R.A. De Zeeuw, Chirality, 4 (1992) 62.
[9] A. Karlsson, L. Bjork, C. Petterson, N. Anden and U. Hacksell, Chirality, 2 (1990) 90.
[10] P. Castelnovo, Chirality, 5 (1993) 181.
[11] M.C. Viaud and G. Guillaumet, manuscript in preparation.
[12] S. Caccamese, G. Principato, U. Gruss, G. Hagele and S. Failla, Tetrahedron: Asymmetry, 5 (1994) 141.

ELSEVIER

Journal of Chromatography A, 704 (1995) 89–97

JOURNAL OF CHROMATOGRAPHY A

Determination of the cyanobacterial osmolyte glucosylglycerol by high-performance liquid chromatography

A. Schoor*, N. Erdmann, U. Effmert, S. Mikkat

Department of Plant Physiology, University of Rostock, Doberaner Str. 143, Rostock 18051, Germany

First received 1 November 1994; revised manuscript received 1 February 1995; accepted 8 February 1995

Abstract

A combination of reversed-phase chromatographic (RPC) [octadecyl silica (ODS)] and ion-moderated partition chromatographic (IMPC) (Ca^{2+}) stationary phases with water as mobile phase provides separation of the cyanobacterial osmolyte glucosylglycerol (2-O-α-D-glucopyranosylglycerol, GG) from other ubiquitous osmolytes (sucrose, trehalose, glycinebetaine) and major natural carbohydrates, also in the presence of common osmotic stressors (mannitol, sorbitol). The method allows investigations of GG biosynthesis in vitro where glucose and glycerol can be released. The separate use of RPC or IMPC columns is restricted to samples containing no significant amounts of sucrose and glucose, respectively. Amino-bonded silica and acetonitrile–water mixtures provide excellent separation of GG from disaccharides but separation from important hexoses is limited.

1. Introduction

Cyanobacteria are able to compensate hyperosmotic stresses by synthesis of low-molecular-mass organic solutes exhibiting osmotic and protective functions, e.g. trehalose, sucrose, glucosylglycerol and glycinebetaine [1]. The salt-dependent accumulation of GG was first detected in the cyanobacterium *Synechococcus* in 1980 [2] and meanwhile found in numerous freshwater and marine cyanobacteria [1,3–10]. Similar glucosylglycerols were found in some higher plants [11,12].

Detection and quantification of GG were performed by three different techniques: ^{13}C NMR spectroscopy [1,2,4,5,7], gas-liquid chromatography [8,9] and enzymatic determination [3,10]. All methods are time-consuming and, partly, need harmful chemicals or high sample amounts [8,13]. Additionally, the enzymatic estimation of glucose after acid hydrolysis of GG leads to overestimation since other soluble glucose-containing compounds (sucrose, trehalose) may interfere [3]. To overcome many of these disadvantages it seemed promising to introduce HPLC methods for the practical estimation of GG. Recently, the biochemical pathway of GG biosynthesis has been discovered [19]. Also for studies of the regulation of this pathway HPLC should be promoted.

HPLC methods have been already used for the separation of macroalgal organic osmolytes [13,14]. However, research of microalgal salt adaptation includes some special problems, as availability of biomass and the high salt load of cells. Additionally, studies of salt adaptation need a rapid and inexpensive assay technique for the osmolytes which does not suffer from inter-

* Corresponding author.

0021-9673/95/$09.50
SSDI 0021-9673(95)00181-6

ference by salt and addition of biochemical precursors, activators and inhibitors.

Karsten et al. [13] reported on an HPLC method for the determination of macroalgal organic solutes using IMPC columns. Resolution of several polyols, carbohydrates and the most important heteroside of red algae (floridoside) was superior. However, selectivity of IMPC (Ca^{2+}, H^+, Pb^{2+}) is often insufficient for disaccharides [20]. Usually, IMPC columns require periodic regeneration of the ionic phase or extensive employment of guard columns during determinations of samples containing non-compatible salts. Common polystyrene-based columns need more attention to prevent obstruction.

The use of silica columns and addition of small amounts of an aliphatic silica amine modifier in the mobile phase were shown to be valuable tools in the general screening of various macroalgal osmolytes, but common steel columns were unsuitable for long-term use [14]. In addition, the carry-over of salt results in a tailing peak in the region of hexitols and hexoses and may produce difficulties in peak integration.

Resolution of hexoses and hexitols is often problematic. Finally, the mobile phase acetonitrile is hazardous and disadvantageous for the detection of carbohydrates without derivatization.

In this paper, an HPLC method is described which results from the comparison of three standard separation techniques and which is intended for determinations of GG in the presence of common osmolytes and metabolites in living cells as well as in bioassays. The method should be helpful, both in biochemical and ecological research.

2. Experimental

2.1. Apparatus

All chromatographic experiments were performed with a chromatograph consisting of LC-9A pumps, SIL-9A autoinjector (sample loop: 1–50 μl), CTO-6A column oven, DGU-4A solvent degasser and RID-6A refractive index detector (Shimadzu Corp., Kyoto, Japan). Data processing and integrations were performed by the chromatographic software ChromStar Vers. 3.12 (Bruker-Franzen Analytik, Bremen, Germany).

The following columns were used: LiChrosorb/HibarRT ODS (5 μm, 250 × 4 mm I.D.) from Merck (Darmstadt, Germany), HPX-87C (250 × 4 mm I.D.) connected with a corresponding Carbo-C guard column (30 × 4.6 mm I.D.) from Bio-Rad (Richmond, USA), Nucleosil/100 NH_2 column (5 μm, 250 × 3 mm I.D.) with guard column (11 × 3 mm I.D.) of identical material, and Nucleosil/100 ODS columns (5 and 10 μm, 250 × 4 mm I.D.) with corresponding guard columns (11 × 4 mm I.D.) from Machery-Nagel (Oensingen, Germany).

2.2. Reagents

All chromatographic solvents (HPLC grade) used were obtained from J.T. Baker (Deventer, Netherlands). Carbohydrates and inorganic chemicals were purchased from Merck (Darmstadt, Germany). Hexitols, glycinebetaine and the glucose determination kit (510-A) were from Sigma (St. Louis, MO, USA). Polystyrene-based ion-exchange resins (Wofatit KPS-H^+ and SBW-Cl^-) were from VEB Farbenfabrik (Wolfen, Germany). Cellulose (300MN) was obtained from Serva (Heidelberg, Germany). Floridoside was purified from the red alga *Palmaria palmata* by HPLC according to the procedure described in Ref. [13] using the HPX-87C column.

2.3. Extraction, sample preparation and purification of GG

GG was extracted from the axenic unicellular cyanobacterium *Synechocystis* PCC 6803 grown at 20 W/m^2 (continuous light), 29°C and continuous aeration with CO_2-enriched air (5% v/v) in NaCl-enriched (10–40 g/l) basal medium (according to Ref. [15]).

Cells were harvested by centrifugation. A simple treatment of all pellets with 80% ethanol (v/v) results in nearly complete extraction of

low-molecular-mass compounds [8]. All extractions were performed within 4 h at 65°C. The residue of freeze-dried ethanol extracts was redissolved in water (HPLC grade). Usually, GG containing solutions were cleared by membrane filtration (0.45 μm) before injecting 10-μl samples. Further special sample preparations and injection volumes will be described in the text.

Higher amounts of nearly pure GG (~98% w/w) were prepared by use of polystyrene-based cationic and anionic ion-exchange columns and thin-layer chromatography (cellulose, acetonitrile–water, 85:15, v/v). The concentration of purified GG was determined by enzymatic estimation of glucose after acid hydrolysis [3].

3. Results and discussion

3.1. Octadecyl silica phase column

Reversed-phase HPLC enables principally the separation of carbohydrate oligomers [16–18]. According to the molecular structure of GG, its separation from hexoses and disaccharides was assumed.

Samples could be used without desalting because salts rapidly eluted near the dead time. GG showed retention using water or 50 m*M* boric acid as mobile phase. It separated from the monosaccharides glucose and fructose which have lower, but equal retention times, and from the disaccharides trehalose and maltose. Unfortunately, GG nearly coeluted with the disaccharide sucrose which is a widespread osmolyte in cyanobacteria, algae and higher plants (Table 1). Use of various aqueous inorganic buffers at different pH values, variation of temperature, and addition of organic solvents provided no resolution of GG and sucrose (data not shown). Sodium chloride solutions (0.5 and 1 *M*) as mobile phase gave slightly enhanced retention times without remarkably better resolution. Differences between chromatograms of the three ODS stationary phases tested (see Apparatus) were insignificant (data not shown).

With respect to investigations of GG biosynthesis in vitro, precursors were tested. They showed different retention behaviour under standard conditions (Table 1). Glycerol 3-phosphate (G3P) and the common sugar intermediate uridine diphosphate glucose (UDPG) eluted before the dead time. Under the same conditions, adenosine diphosphate glucose (ADPG) eluted near the hexoses and hexitols tested whereas glycerol showed markedly enhanced retention (Table 1). Glycerol could be released during GG biosynthesis experiments in vitro due to hydrolysis of added glycerol phosphate and should be monitored for exact characterization of the GG synthesizing enzyme system [19].

Table 1
Capacity ratios of compounds relevant to osmo-acclimation studies

Substance	k'
UDPG	(−0.20)
G3P	(−0.18)
NaCl	0.03
Sorbitol/mannitol	0.15
ADPG	0.16
Glucose/fructose	0.16
Glycerol	0.21
Trehalose	0.25
Maltose	0.27
Glycinebetaine	0.33
GG	0.42
Sucrose	0.43

Merck ODS column, 250 × 4 mm I.D.; solvent, 0.05 *M* boric acid; flow-rate, 1.0 ml min^{-1} (μ = 0.20 cm s^{-1}); temperature, 30°C.

Due to its limited resolution, RPC (ODS) is only recommended for GG determinations of biochemically well characterized cyanobacterial strains since coelution with various substances cannot be excluded. Nevertheless, simple sample preparation, fast elution of precursors, and use of water as mobile phase make this method attractive. Additionally, RPC allows nearly complete purification of samples with severe salt contamination. Recovery experiments with osmolyte additions (50 μg, injection volume: 50 μl) to 0.85 m*M* NaCl solutions showed only 0.4% of the NaCl peak overlapping with the GG peak (0.8% in the case of glycinebetaine). This method may be helpful when desalting proce-

dures with mixed-bed ion-exchange resins are impracticable (low amounts of GG, estimation of the charged osmolyte glycinebetaine).

3.2. Ion-moderated partition chromatography column

The usefulness of cation-binding stationary phases for determinations of carbohydrates in diverse fields is well documented, e.g. [13,20–25]. In the widely used Ca^{2+}-form, desalting of samples could be ignored. However, high salt contaminations should be eliminated to prevent extensive utilization of guard columns and anionic interferences [13]. The separation of GG from sucrose and fructose was excellent (Table 2). Surprisingly, GG did not show a retention time between those of the glucose containing disaccharides tested and glucose. GG and glucose eluted as a single peak.

Generally, modifications of the separation conditions are limited for polystyrene-based columns. Variation of column temperature and ionic strength of the mobile phase (5–50 m*M* calcium nitrate) or additions of the organic modifier acetonitrile up to 30% (v/v) brought about no resolution of glucose and GG. GG showed slightly lower retention times than glucose without chromatographic significance (data not shown). The macroalgal heteroside floridoside which is structurally related to GG emerged also in the region of glucose. But separation of this heteroside and its corresponding sugar (galactose) seems to involve fewer problems since resolution of galactose and glucose is usually high.

In the case of GG determination, the coelution of GG and glucose prevents a wide application of the Ca^{2+}-moderated stationary phase although osmotic significant production of glucose in vivo has not been documented. But artificial modifications during in vivo and in vitro experiments (heterotrophic growth on glucose, additions of glucose-containing precursors, screening of mutants with defects in C-metabolism) could lead to enhanced concentrations of free glucose. Apart from this restriction and due to the selectivity for a wide range of known osmolytes (disaccharides, polyols, heterosides) [13,20,25], IMPC (Ca^{2+}) is a valuable tool also

Table 2
Relative retention times of selected sugars, polyols and heterosides in comparison to that of sucrose for two Ca^{2+}-moderated partition chromatography phases

Substance	Relative retention times		
	Aminex HPX-87C[a]	Aminex HPX-87C[b]	Polysphere CHCA[c]
Sucrose	1.00	1.00	1.00
Maltose	1.02	1.01	–
Floridoside	–[d]	–	1.23
GG	1.17	–	–
Glucose	1.17	1.21	1.26
Galactose	–	1.37	–
Fructose	1.46	1.52	1.49
Mannitol	1.77	–	1.71
Sorbitol	2.07	–	2.04

Retention times were made comparable by transformation with respect to column dimensions assuming insignificant external dead volumes and similar physical properties of the stationary phases because exact informations from the producers were not available.

[a] 250 × 4.0 mm I.D., (Bio-Rad); solvent, water; flow-rate, 0.25 ml min^{-1}; temperature, 85°C; own measurements.

[b] 300 × 7.8 mm I.D., (Bio-Rad); solvent, water; flow-rate, 0.6 ml min^{-1}; temperature, 85°C; according to the producer [20].

[c] 300 × 6.5 mm I.D., (Merck); solvent, water; flow-rate, 0.5 ml min^{-1}; temperature, 90°C; according to Ref. [13].

[d] not determined or data not available.

to characterize low-molecular-mass substances of cyanobacteria.

3.3. Aminopropyl silica phase column

Chromatography of sugars and polyols by amino-bonded silica as stationary phase and acetonitrile–water mixtures as mobile phase is widely used and characterized just as in situ modification of silica phases with amines [14,22,26–29].

Using amino-bonded silica and acetonitrile–water mixtures of 72.5 up to 87.5% (v/v) acetonitrile, sufficient separations of disaccharides and some important monosaccharides were obtained. Major results were similar to those of the IMPC column: GG showed retention times more comparable to those of hexoses than to the expected intermediate retention between mono- and disaccharides. A mobile phase of 75% (v/v) acetonitrile gave separation from fructose and glucose, but resolutions were insufficient for quantitative determinations (Fig. 1). Higher proportions of acetonitrile improved the selectivity for GG/fructose but, simultaneously, lowered the selectivity for GG/glucose (Fig. 2). Linear detector response was achieved for purified GG over the range tested (1–500 μg, $n = 7$, $r =$ 0,998, peak-height method). However, exact peak integrations of samples containing only a few micrograms of GG were complicated or impossible due to carry over of salt and unknown impurities.

Amino-bonded silica showed instability after injection of several hundred samples simply purified by filtration and not deionized. This led to a rapid decrease of capacity ratios. In Table 3 capacity ratios of a new and an old column (loss of about 40% of column efficiency) are compared. Substantial loss of retention power can be seen, especially for the late eluting disaccharides. Furthermore, peak symmetry became poor ($\tau =$ 1.07 and $\tau = 1.80$ for the new and old column, respectively). Interestingly, capacity ratios of

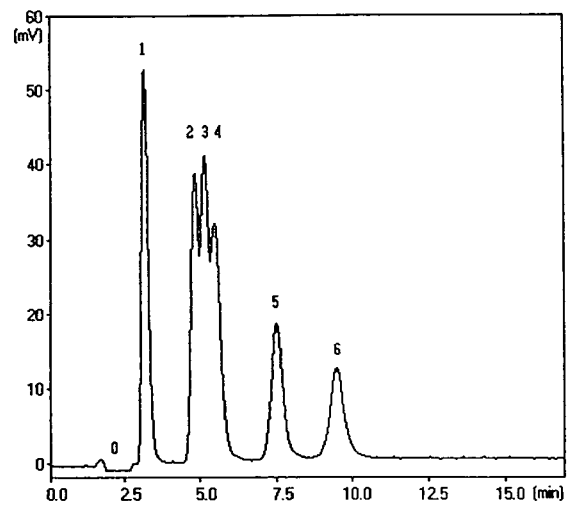

Fig. 1. Chromatogram of standard compounds. Peaks: 0 = injection solvent (water, inverts), 1 = glycerol, 2 = fructose, 3 = GG, 4 = glucose, 5 = sucrose, 6 = trehalose. NH_2 column (new), 250 × 3 mm I.D.; solvent, acetonitrile–water (75:25); flow-rate, 0.8 ml min^{-1} ($\mu = 0.25$ cm s^{-1}); temperature, 30°C.

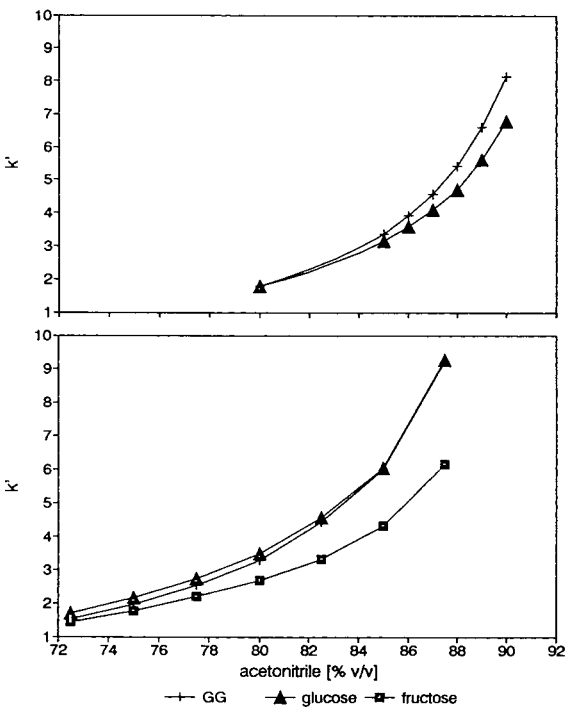

Fig. 2. Dependence of capacity ratios (critical compounds) on acetonitrile content of the mobile phase and column age (upper figure, old column; lower figure, new column). Further analytical conditions as in Table 3.

Table 3
Dependence of capacity ratios of selected compounds on age of amino-bonded silica

Substance	k' (old)[a]	k' (new)
Glycerol	1.35	1.62
Fructose	3.68	6.14
Glucose	4.84	9.26
GG	5.53	9.22
Floridoside	5.87	9.41
Sucrose	11.18	23.75
Trehalose	19.98	45.11

NH_2 column, 250 × 3 mm I.D.; solvent, acetonitrile–water (87.5:12.5); flow-rate, 0.8 ml min^{-1} (μ = 0.25 cm s^{-1}); temperature, 30°C.
[a] The old column suffered from a loss of 7000 theoretical plates per metre (GG, injection volume: 30 μl).

GG became markedly higher compared to glucose (Fig. 2). With high acetonitrile contents (87–90%, v/v) acceptable resolution (R_s = 1.10–1.25) of glucose and GG was obtained. Finally, an acetonitrile–water mixture of 87.5% (v/v) was chosen to reduce separation times of sucrose containing samples to 25 min (analytical conditions as in Table 3). Solvent peaks could be reduced by use of a sample solvent comparable to the mobile phase (usually acetonitrile–water, 80:20, v/v). This injection solvent was a good indicator for sample purity. Highly purified samples containing no salts and charged compounds gave clear solutions. Light scattering was visible in low contaminated samples and high salt contaminated samples provided a biphasic system (acetonitrile in the upper layer and sample and salts in the lower water layer), unsuitable for injection.

Sample cleaning by use of cationic and anionic ion-exchange resins provided excellent baseline stability and prevented further inactivation of the stationary phase. Only a slight loss of retention and selectivity was detected after injection of several hundred samples cleaned by deionization. However, use of controlled degraded amino-bounded silica is not recommended since it is difficult to obtain reproducible degradations. Improvements of the chromatographic system should be directed to in situ modifications of (aminopropyl) silica by amines.

3.4. Combination of octadecyl silica phase column and ion-moderated partition chromatography column

A combination of RPC (ODS) and IMPC (Ca^{2+}) columns was investigated to improve the low selectivity of the IMPC column with respect to GG and glucose. At the same time separation from important polyols should be conserved and water as advantageous mobile phase favoured.

Capacity ratios of carbohydrate oligomers could be controlled by temperature during RPC [16] whereas temperature effects (60–85°C) on the IMPC column were low (data not shown). Temperatures below 55°C were not suitable for IMPC because α- and β-D-glucose seemed to be partly resolved. Separations were specified by resolution (R_s; measurement of peak width at half-height) because compounds showed different peak width at comparable retention times. The IMPC column was set to 60°C and installed behind the ODS column (28°C, ambient).

The most important cyanobacterial disaccharides, GG and some potential metabolites of in vitro studies (glucose, glycerol [19]) separated with acceptable resolutions at the optimal flow-rate of 0.3 ml min^{-1} (Fig. 3, Table 4). Complete separation from common osmotic stressors (mannitol, sorbitol) was also conserved. But resolutions of trehalose and glucose as well as of GG and fructose almost disappeared.

If RPC was also performed at 60°C, resolution between GG and fructose was enhanced mostly at the costs of resolution between GG and glucose just as those between disaccharides (Table 4). This can be helpful especially for samples cleaned by strong ion-exchange resins where breakdown of sucrose and release of fructose may occur.

3.5. Biochemical application

Using the two configurations of combined RPC–IMPC, GG was determined in both salt-

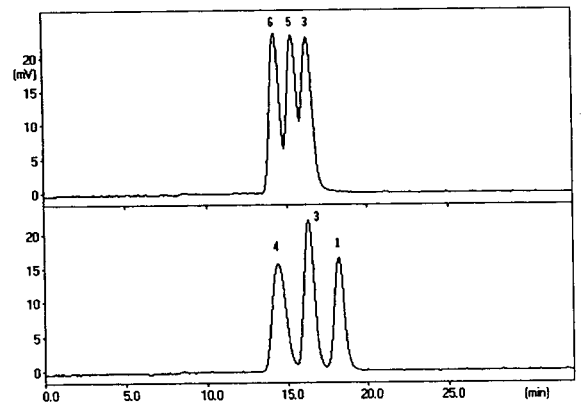

Fig. 3. Chromatograms of standard compounds relevant to in vivo (upper figure) and in vitro (lower figure) studies. Numbers as in Fig. 1. Merck ODS column, 250 × 4 mm I.D.; temperature, (ambient) 28°C; combined with an HPX-87C column, 250 × 4 mm I.D.; temperature, 60°C; solvent, water; flow-rate, 0.3 ml min^{-1}; injection volume: 30 μl.

adapted cells and cell-free extracts of *Synechosystis* PCC 6803 (Fig. 4) with high reproducibility (retention times, all compounds tested, $n = 3$, C.V. $< 0.4\%$). GG gave a linear detector response over the range tested (1–500 μg, $n = 6$, $r = 0.9996$, peak-height method) and a detection limit of about 150 ng was obtained (signal-to-noise ratio of 3).

Sucrose showed low significance in *Synechocystis* PCC 6803 and peak integrations were no problem in spite of the limited resolution between GG and this compound. Free fructose was never detected if samples were quickly desalted by ion-exchange resin. Fructose may become a problem for algal strains containing high amounts of sucrose. Careful desalting prevents release of fructose. Unknown substances interfering with GG were not detected. Significant amounts of unknown substances as well as sub-

Table 4
Dependence of chromatographic resolutions during RPC/IMPC on temperature of RPC

Substance	Sucrose	Trehalose	Glycine-betaine	Glycerol	Glucose	Fructose	Mannitol	Sorbitol	Maltose	Proline
GG	0.98	1.74	8.50	1.74	1.52	0.20	2.40	4.76	1.60	9.29
	1.07	1.42	8.58	2.27	0.85	0.79	2.94	5.14	1.17	9.39
Sucrose	x	1.02	9.46	2.76	0.74	1.05	3.34	5.67	0.71	11.19
		0.38	9.67	3.40	0.06	1.80	4.01	6.18	0.20	12.13
Trehalose	x	x	10.38	3.81	0.09	1.93	4.31	6.58	0.24	12.01
			9.94	3.75	0.37	2.14	4.34	6.48	0.14	12.37
Glycine-betaine	x	x	x	7.25	8.64	7.43	5.99	3.38	9.58	2.60
				6.73	8.24	7.41	5.66	3.19	9.06	2.76
Glycerol	x	x	x	x	3.03	1.33	0.83	3.37	3.32	9.29
					2.81	1.33	0.81	3.19	3.29	9.39
Glucose	x	x	x	x	x	1.55	3.50	5.45	0.11	10.21
						1.49	3.36	5.25	0.22	10.44
Fructose	x	x	x	x	x	x	1.95	4.08	1.62	9.20
							2.01	4.14	1.84	9.84
Mannitol	x	x	x	x	x	x	x	2.40	3.82	8.03
								2.30	3.86	8.26
Sorbitol	x	x	x	x	x	x	x	x	5.99	5.61
									5.86	5.79
Maltose	x	x	x	x	x	x	x	x	x	11.21
										11.37

Merck ODS column, 250 × 4 mm I.D.; temperature, (ambient) 28°C (upper values) and 60°C (lower values); combined with an Aminex HPX-87C column, 250 × 4 mm I.D.; temperature, 60°C; solvent, water; flow-rate, 0.3 ml min^{-1}.

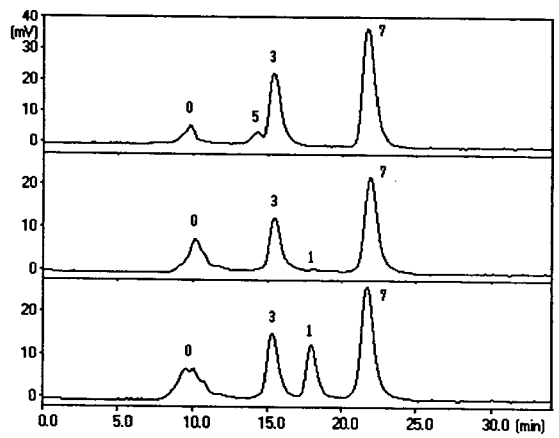

Fig. 4. Elution profiles of GG containing samples cleaned by ion-exchange resin (upper profile, extract of whole cells adapted to 684 m*M* NaCl; middle profile, GG synthesized in vitro by a protein extract according to Ref. [19]; lower profile, as middle profile, sample treated with alkaline phosphatase before desalting). Peaks: 0 = unknown compounds, 7 = sorbitol (internal standard), further numbers as in Fig. 1. Analytical conditions as in Fig. 3.

strates of GG biosyntheses in vitro eluted near the estimated dead time (data not shown).

For samples containing disaccharides and GG, separations can be completed within 18 min whereas in the presence of hexitols, glycinebetaine or proline separation times of up to 32 min are needed. The latter charged compounds can be easily removed by ion-exchange resin. Glutamic acid is one of the most important amino acids accumulated in *Synechocystis* under osmotic stress (unpublished data). Retention time of this compound was controlled by ionic strength of the mobile phase (2–50 m*M* calcium nitrate) and appeared in the region of disaccharides and GG. Glutamic acid was not retained using water as mobile phase. Ionic strength slightly influenced retention times of the other compounds tested (data not shown).

The RPC column provided additional protection of the IMPC column. Although chromatography was stable the RPC column was cleaned after injection of about 150 samples by rinsing with methanol or acetonitrile.

4. Conclusions

Separation of GG by three HPLC methods commonly used for carbohydrate detection is unsatisfactory because its retention behaviour is similar to that of important osmolytes (sucrose) or monosaccharides (glucose, fructose).

Using reversed-phase mechanisms (ODS), capacity ratios are low and more comparable to disaccharides. During chromatography on amino-bonded silica with acetonitrile–water mixtures capacity ratios are similar to common hexoses. Controversy over the mechanisms of that chromatography exists [14]. Interestingly, separation of GG from hexoses was improved after partial degradation of amino-bounded silica. Altogether, amino-bonded silica allows rapid determination of ubiquitous cyanobacterial osmolytes including GG if significant amounts of glucose or fructose are absent. In samples carefully prepared from whole cells without breakdown of sucrose this is mostly the case in contrast to samples where GG is synthesized in vitro. Deionization is necessary to prevent baseline shift and rapid inactivation of the stationary phase. Loss of reducing sugars [22] and the disadvantageous use of acetonitrile has to be taken into account.

Also IMPC (Ca^{2+}) provides insufficient resolution of GG and glucose. However, a combination of RPC and IMPC results in sufficient resolution of major (cyanobacterial) osmolytes, monosaccharides and polyols depending on temperature of RPC. It allows detection of GG synthesized in vivo and in vitro within acceptable time and using water as mobile phase. Desalting is recommended to prevent extensive use of guard columns. This method can be further optimized by variation of column dimensions, particle size and independent temperature setting for both IMPC and RPC and may be applicable for the determination of samples containing charged osmolytes (glycinebetaine), disaccharides and GG in the presence of high amounts of salt by switching the flow of the mobile phase between RPC and IMPC automatically. The combination of RPC and IMPC

may also be helpful for determinations of unusual carbohydrates without testing sets of expensive IMPC columns or doubling chromatographies due to column change, though advantages and common disadvantages of a column combination have to be weighted.

Acknowledgement

This work was supported by a grant from the Deutsche Forschungsgemeinschaft, Germany.

References

[1] R.H. Reed, L.J. Borowitzka, M.A. Mackay, J.A. Chudek, R. Forster, S.R.C. Warr, D.J. Moore and W.D.P. Stewart, *FEMS Microbiol. Rev.*, 39 (1986) 51.
[2] L.J. Borowitzka, S. Demmerle, M.A. Mackay and R.S. Norton, *Science*, 210 (1980) 650.
[3] N. Erdmann, *Z. Pflanzenphysiol.*, 110 (1983) 147.
[4] S.R.C. Warr, R.H. Reed, J.A. Chudek, R. Forster and W.D.P. Stewart, *Planta*, 163 (1985) 424.
[5] E. Tel-Or, S. Spath, L. Packer and R.J. Mehlhorn, *Plant Physiol.*, 82 (1986) 646.
[6] R.H. Reed, S.R.C. Warr, N.W. Kerby and W.D.P. Stewart, *Enzyme Microb. Technol.*, 8 (1986) 101.
[7] M.A. Mackay and E.S. Norton, *J. Gen. Microbiol.*, 133 (1987) 1535.
[8] H. Reed, in L. Packer and A.N. Glazer (Editors), *Methods in Enzymology*, Academic Press, London, 1988, Ch. 56, p. 528.
[9] F.A.A. Mohammad, R.H. Reed and W.D.P. Stewart, *FEBS Microbiol. Lett.*, 16 (1983) 287.
[10] V.V. Kevbrin, A.V. Dubinin and G.A. Osipov, *Mikrobiologiya*, 60 (1991) 596.
[11] M. Kaneda, K. Mizutani and K. Tanaka, *Phytochemistry*, 21 (1982) 891.
[12] G. Bianchi, A. Gamba, R. Limiroli, N. Pozzi, R. Elster, F. Salamini and D. Bartels, *Physiol. Plant.*, 87 (1993) 223.
[13] U. Karsten, D.N. Thomas, G. Weykam, C. Daniel and G.O. Kirst, *Plant Physiol. Biochem.*, 29 (1991) 373.
[14] N. Kerby, R.H. Reed and P. Rowell, *J. Chromatogr.*, 479 (1989) 353.
[15] M.B. Allen and D.J. Arnon, *Physiol. Plant.*, 8 (1955) 653.
[16] P. Vrátný, J. Čoupek, S. Vozka and Z. Hostomská, *J. Chromatogr.*, 254 (1983) 143.
[17] L.A.Th. Verhaar, B.F.M. Kuster and H.A. Claessens, *J. Chromatogr.*, 284 (1984) 1.
[18] E. Andriamboavonjy, E. Flaschel and A. Renken, *J. Chromatogr.*, 587 (1991) 288.
[19] M. Hagemann and N. Erdmann, *Microbiol.*, 140 (1994) 1427.
[20] Bio-Rad, HPLC Columns, Methods and Applications, 1993, p. 55.
[21] J.C. Kuo and E.S. Yeung, *J. Chromatogr.*, 223 (1981) 321.
[22] C. Brons and C. Olieman, *J. Chromatogr.*, 259 (1983) 79.
[23] R. Pecina, G. Bonn, E. Burtscher and O. Bobleter, *J. Chromatogr.*, 287 (1984) 245.
[24] A.G.J. Voragen, H.A. Schols, M.F. Searle-van Leeuwen, G. Beldman and F.M. Rombouts, *J. Chromatogr.*, 370 (1986) 113.
[25] P. Adams, J.C. Thomas, D.M. Vernon, H.J. Bohnert and R.G. Jensen, *Plant Cell Physiol.*, 33 (8) (1992) 1215.
[26] K. Aitzetmüller, *J. Chromatogr.*, 156 (1978) 354.
[27] B.B. Wheals and P.C. White, *J. Chromatogr.*, 176 (1979) 421.
[28] H. Binder, *J. Chromatogr.*, 189 (1980) 414.
[29] N.L. Wade and S.C. Morris, *J. Chromatogr.*, 240 (1982) 257.

ELSEVIER

Journal of Chromatography A, 704 (1995) 99–111

JOURNAL OF CHROMATOGRAPHY A

Stereospecific analysis of the major triacylglycerol species containing γ-linolenic acid in Evening Primrose oil and borage oil

Peter R. Redden*, Xiaorong Lin, John Fahey, David F. Horrobin

Efamol Research Institute, Kentville, Nova Scotia B4N 4H8, Canada

First received 6 December 1994; revised manuscript received 1 February 1995; accepted 8 February 1995

Abstract

Evening Primrose oil (EPO) and borage oil (BO) are used frequently in nutritional and clinical studies involving a disease condition with an impaired or inadequate Δ^6-desaturase enzyme activity. This impairment may be bypassed by supplementation with γ-linolenic acid (GLA, 18:3n-6), an intermediate metabolite of linoleic acid (LA, 18:2n-6). The major individual triacylglycerol (TG) species comprising all potential positional isomers (molecular species) from both EPO and BO were separated, isolated by reversed-phase HPLC and subjected to HPLC stereospecific analysis as naphthylethyl urethane derivatives. The method of analysis is useful since only small quantities of the individual TG species are required and prior experimentally demanding fractionation steps are eliminated. Over 90% of the important clinical fatty acid, GLA, present in EPO and over 80% of the GLA in BO have been identified and quantified in the molecular species of their respective analyzed TG fractions. Generally, within the individual GLA-containing TG species from both oils, GLA is distributed asymmetrically among the three positions, preferentially at the sn-2 and sn-3 positions, although more so for the TG species in BO. The positional isomers of the diacid TG species were determined directly from the stereospecific analysis. For the triacid TG species computer aided linear regression was used to determine the positional isomers. The predicted positional isomeric distributions for the individual TG species calculated using the 1-random, 2-random, 3-random distribution theory from the stereospecific analysis of the native oils were in good agreement with the experimentally determined values. In contrast to other seed oils the pairs of individual TGs possessing chirality do not exist as racemic mixtures in either oil.

1. Introduction

EPO and BO are used most frequently in nutritional and clinical studies where it has been shown clinically that diseases are possibly associated with an impaired or inadequate Δ^6-desaturase activity. This impairment may be alleviated by dietary supplementation with γ-linolenic acid (GLA, 18:3n-6) an intermediate Δ^6-desaturation product of linoleic acid (LA, 18:2n-6) [1–5]. A number of animal and human studies have suggested, however, that the biological activities of these two oils are quite different [6–12].

Therefore, BO and EPO do not have equivalent effects, which however can not be explained on the basis of the GLA content alone. There are several possible explanations for this. Apart from GLA there are substantial differences in

* Corresponding author.

0021-9673/95/$09.50
SSDI 0021-9673(95)00182-4

the overall fatty acid compositions of the two oils (see Table 2). There may be minor non-triglyceride components of the oils which exert pharmacological effects. Alternatively, the association of GLA with other fatty acids in the triacylglycerol (TG) species of the oils may modulate GLA potency in exerting its beneficial effects. Indeed, fats with similar or even identical fatty acid composition, but different TG structures, have already been shown to exert different biological activities. Peanut oil in its native state is relatively atherogenic; however, when randomized so that all the fatty acids are equally distributed among the three positions of the TG, peanut oil loses its atherogenicity [13,14]. Moreover, in rats given a structured TG, the absorption into the lymph was enhanced for fatty acids that were located in the sn-2 position of the TG [15]. In addition, there is evidence suggesting that the TG structure of human breast milk, as compared to that of formula, affects infant plasma TG and phospholipid fatty acid composition [16]. Thus it appears that the structure of the TGs in fats and oils may play an important part in the absorption, biological action and distribution of the fatty acids into tissue lipids.

Previously, the stereospecific distribution of the fatty acids in native EPO [17,18] and BO [17,19] have been determined. The GLA in both oils was distributed asymmetrically and was preferentially located at the sn-2 and sn-3 positions although more so for BO. The stereospecific distribution of individual TG fractions cannot be assumed on the basis of the analysis of the total oil. This applies to all fats and oils and the TG structures can only be determined by first fractionating the fat or oil into the individual TG species and carrying out a stereospecific analysis on each of them [20].

Previously we have described the HPLC separation and quantification of the TG species of both EPO and BO [21]. In this report we have isolated the major TG species of both EPO and BO by reversed-phase HPLC, subjected them to stereospecific analysis, and compared the positional isomer distribution ratio of the individual GLA containing TG species. There are several different methods available to determine the fatty acid stereospecific or positional distribution of TGs based on TLC, chiral-phase or normal-phase HPLC [22–27]. For our study the latter approach is the most convenient [27]. Smaller quantities of TGs can be analyzed since no intermediate TLC purification step is required and numerous samples can be handled at the same time. Moreover, this method is considered robust for the stereospecific analysis of the fatty acids in fats and oils. Recently, a comparison between the classical TLC procedure and this HPLC method demonstrated that there was no significant difference between the two methods using the TGs from olive oil [28].

2. Experimental

All solvents were HPLC grade and were obtained from BDH (Toronto, Ont., Canada). 1,3-Dioleoyl-2-palmitoyl-sn-glycerol (sn-OPO), 1,2-dioleoyl-2-linoleoyl-*rac*-glycerol (*rac*-OLL) and 1-palmitoyl-2-oleoyl-3-stearoyl-*rac*-glycerol (*rac*-POS) were purchased from Sigma (St. Louis, MO, USA). BF_3–methanol (14%) was supplied by Pierce Chemical Co. (St. Louis, MO, USA). *S*-(+)-1-(1-Naphthyl)ethyl isocyanate, 4-pyrrolidinopyridine, ethyl bromide and magnesium turnings were purchased from Aldrich (Milwaukee, WI, USA). Bakerbond Octadecyl SPE (500 mg) cartridges were obtained from J.T. Baker (Toronto, Ont., Canada) The TGs of Evening Primrose oil (Efamol, Guildford, UK) and borage oil (Callanish, Breasclete, UK) were purified on 20×20 cm silica TLC plates with hexane–diethyl ether–formic acid (80:20:2, v/v) as the developing solvent and extracted from the silica gel with chloroform–methanol (1:1, v/v).

The TG species of EPO and BO (~ 500 μg injected) were separated and identified by reversed-phase HPLC as previously described [21]. Individual TG species were collected manually (up to ten injections were made to ensure enough material was collected) for the stereochemical analysis in duplicate. An aliquot of

each individual TG fraction was kept for total fatty acid composition.

The standard TGs, the isolated individual TG species as well as samples of native EPO and BO were each dissolved in diethyl ether (2 ml) previously dried over molecular sieves (4 Å). Freshly prepared 0.5 *M* ethyl magnesium bromide (Grignard reagent) in dry diethyl ether (0.5 ml) was added and the mixture shaken for 30–40 s before glacial acetic acid (50 μl) and water (2 ml) were added to stop the reaction. The products were extracted with diethyl ether (5 ml) and washed with 2% sodium bicarbonate and distilled water. To minimize isomerization of the fatty acids within the diacyglycerols (DGs), the solvent was evaporated at room temperature and the residue derivatized immediately. The Grignard hydrolysis mixture was dissolved in toluene (0.5 ml) previously dried over molecular sieves (4 Å). (*S*)-(+)-1-(1-Naphthyl)ethyl isocyanate (12.5 μl) and 4-pyrrolidinopyridine (4 mg) were added and the mixture heated overnight at 50°C. After evaporation of the solvent, the products were dissolved in warm methanol–water (95:5, v/v, 6 ml) and added to a Bakerbond ODS solid-phase extraction column previously solvated with methanol–water (95:5, v/v, 10 ml). An additional 15 ml of this solvent was washed through and the required products were then eluted with acetone (10 ml).

The HPLC separation of the diastereomeric sn-1,2(2,3)-DG urethane derivatives was carried out with the Beckman HPLC system described above. Two columns of silica gel (Supelcosil, Supelco, Bellefonte, PA, USA, 3 μ, 15 cm × 4.6 mm I.D. and Hypersil, HiChrom, Reading, UK, 3 μ, 25 cm × 4.6 mm I.D.) were used in series with 0.3% 1-propanol (containing 2% water) in iso-octane as the mobile phase at a flow-rate of 1 ml/min and UV detection at 280 nm. The solvent system was prepared fresh daily and the sample was injected in a minimum amount of solvent. The corresponding sn-1,2- and sn-2,3-DG naphthylethyl urethane derivatives were collected manually and subsequently transmethylated [27]. In practice the diastereomeric sn-1,2- and sn-2,3-DG urethane derivatives were each collected, usually as a group of peaks, and there was baseline separation of these two groups of derivatives with the exception of samples containing long chain fatty acids (see Results section). Although the sn-1,3-DG urethane derivatives can be collected, they are usually contaminated as a result of acyl migration of the sn-1,2(2,3)-DG urethanes, and hence do not give accurate results for the sn-2 position. The individual TG species and the collected diastereomeric sn-1,2- and sn-2,3-DG urethane derivatives were methylated with 14% BF_3–methanol (2 ml) for 30 min, extracted with hexane (5 ml), concentrated and the entire sample injected.

GLC analysis was carried out using a Hewlett-Packard Model 5890 chromatograph equipped with a flame ionization detector. Separation of the methyl esters was achieved using a fused capillary Omegawax 320 column (Supelco, 30 m × 0.32 mm, 0.25 μm film thickness) at a split ratio of 1:25, injection port temperature of 200°C, detector temperature of 220°C and an oven temperature programmed at 165°C for 2 min then 6°C/min to 180°C and then held at 180°C for 3 min then 1°C/min to 190°C and held for 5 min then 0.8°C/min to 200°C then held for 5 min.

3. Results

To ensure that our methodology was reliable, three standard TGs, sn-OPO, *rac*-POS and *rac*-OLL were subjected to stereospecific analysis. After collection and methylation of the sn-1,2-DG and sn-2,3-DG urethane derivatives, the fatty acids at the three positions (expressed as mol%) within all the TGs were determined from the following equations (the brackets are meant to represent mol% values):

$$\text{Position[sn-1]} = 3 \times [\text{TG}] - 2 \times [\text{sn-2,3-DG urethanes}]$$

$$\text{Position[sn-3]} = 3 \times [\text{TG}] - 2 \times [\text{sn-1,2-DG urethanes}]$$

$$\text{Position[sn-2]} = 3 \times [\text{TG}] - [\text{sn-1}] - [\text{sn-3}]$$

Assuming these standard TGs were positionally pure, we found about 4% of the fatty acids had migrated to the outside sn-1 and sn-3 positions (Table 1) indicating a 4% absolute error associated with our methodology. This error most probably arises from acyl migration within the diacylglycerols prior to or during the derivatization procedure but is comparable to the error associated with this method of stereospecific analysis [27].

The HPLC separation of the TG species of BO and EPO is shown in Fig. 1. The identities or probable identities of the peaks have been reported previously [21]. The individual TG fractions collected from BO for stereochemical analysis were the major peaks labelled 2, 3, 4, 5,

Table 1
Positional fatty acid analysis of standard TGs and the individual TG fractions isolated from EPO and BO (expressed as mole%)

Fatty acid[a]	TG species[b]	All	sn-1[c]	sn-2[d]	sn-3[e]	Fatty acid[a]	TG species[b]	All	sn-1[c]	sn-2[d]	sn-3[e]
	sn-OPO					*Borage oil*					
16:0		33.3	3.6	92.8	3.6		LGG				
18:1[f]		66.7	96.5	7.1	96.5	18:2		33.9	88.8	5.6	7.2
	rac-POS					18:3		66.1	12.0	93.5	92.8
16:0		32.4	48.2	−0.9	49.8		LGL				
18:0		33.9	48.7	7.0	46.1	18:2		65.4	92.1	60.8	43.3
18:1[f]		33.7	3.9	93.3	4.1	18:3		34.8	8.4	38.8	57.2
	rac-OLL						OGG				
18:1[f]		33.7	46.6	4.0	50.6	18:1[f]		27.5	65.4	2.8	14.2
18:2		66.3	53.4	96.1	49.4	18:2		12.2	14.5	47.1	79.7
EPO						18:3		60.4	20.2	10.1	6.1
	LGG						PGG				
18:2		35.2	59.8	25.5	20.5	16:0		30.4	57.4	38.4	−4.6
18:3		64.8	39.5	75.3	79.6	18:2		3.3	3.9	9.3	−3.3
	LGL					18:3		66.3	38.5	53.0	107
18:2		66.8	79.8	68.9	51.7		OGL				
18:3		33.2	20.2	32.4	47.0	18:1[f]		33.0	20.2	23.4	55.4
	OGL					18:2		33.9	68.1	19.5	14.1
18:1[f]		34.4	36.8	32.6	33.8	18:3		33.0	11.2	57.4	30.4
18:2		35.8	46.8	41.8	18.8		PGL				
18:3		29.9	16.7	25.3	47.7	16:0		31.3	43.7	27.3	22.9
	PGL					18:2		33.4	44.0	27.6	28.6
16:0		28.5	59.1	1.5	24.9	18:3		35.3	12.5	44.9	48.5
18:2		36.8	24.6	52.0	33.8		OLL				
18:3		34.6	16.2	49.6	38.0	18:1[f]		33.6	15.4	21.0	64.4
	OLL					18:2		66.4	84.6	30.0	35.5
18:1[f]		33.6	27.2	41.4	32.2		SGL and PGO				
18:2		66.4	72.8	58.6	67.8	16:0		18.6	36.5	11.3	8.0
	PLL					18:0		13.5	2.4	22.2	15.6
16:0		30.0	48.2	6.4	35.4	18:1[f]		19.1	8.5	24.3	24.5
18:1[f]		2.0	nd	nd	nd	18:2		15.5	32.9	1.7	11.9
18:2		67.0	42.8	103	55.6	18:3		33.4	19.8	40.6	39.8
18:3		1.0	nd	nd	nd						

Abbreviations: nd = not detected, P = palmitic, S = stearic; O = oleic, L = linoleic, G = γ-linolenic acid.
[a] Unless otherwise indicated the unsaturated fatty acids are from the n-6 family.
[b] Each TG species analyzed in duplicate.
[c] 3 × [TG] − 2 × [sn-2,3-DG urethanes].
[d] 3 × [TG] − [sn-1] − [sn-3].
[e] 3 × [TG] − 2 × [sn-1,2-DG urethanes].
[f] n-7 and n-9.

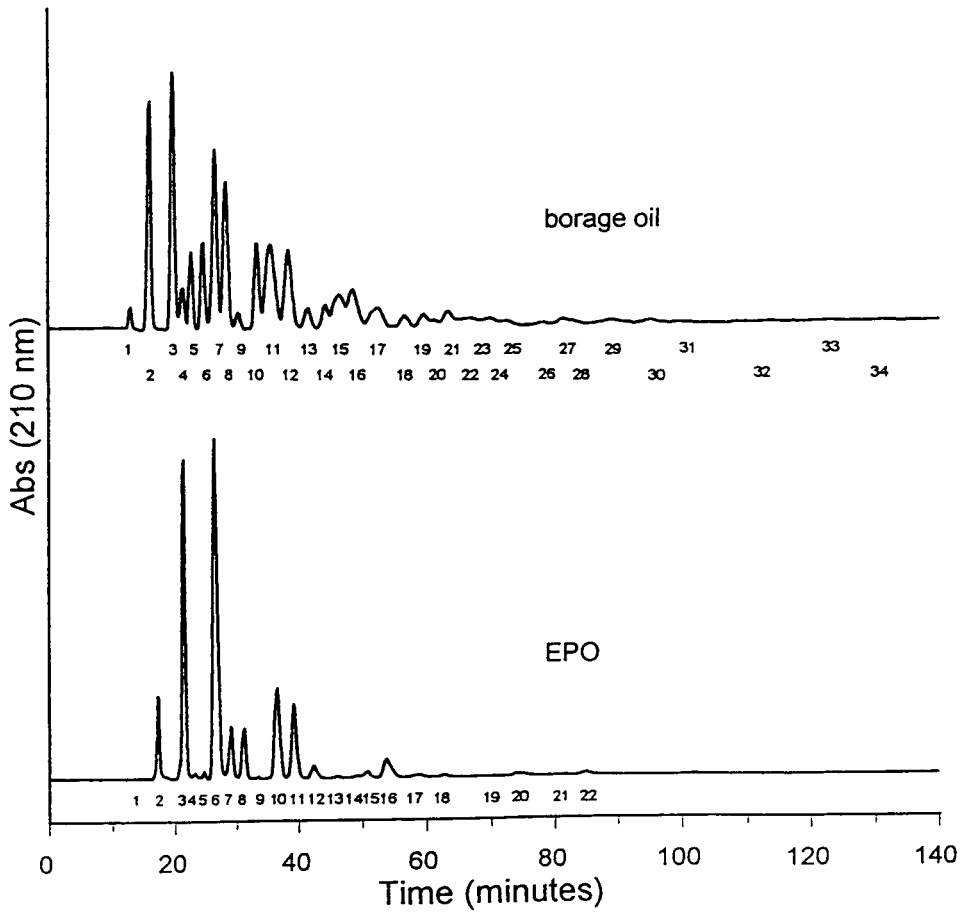

Fig. 1. Reversed-phase HPLC profile of the triacylglycerols of EPO and borage oil. Reproduced from Ref. [21].

7, 8, 10, 11, and 12 corresponding to LGG [1], LGL, OGG, PGG, OGL, PGL, OLL, a mixture of OGO, GaGL and PLL, and a mixture of SGL and PGO, respectively. For EPO the TG fractions collected were 2, 3, 7, 8, 10, and 11 corresponding to LGG, LGL, OGL, PGL, OLL, and a mixture of PLL and OGO, respectively.

The HPLC profiles of the sn-1,2(2,3)-DG urethane derivatives of native BO and EPO are shown in Fig. 2 with the results of the stereospecific analysis given in Table 2. Example HPLC profiles of the sn-1,2(2,3)-DG urethane derivatives of the individual diacid species, LGL, from BO and EPO are shown in Fig. 3. Similarly the profiles from the individual triacid species, OGL from both BO and EPO, are shown in Fig. 4. Since the mobile phase was prepared daily, differences in day-to-day retention times were observed, however, there was nearly baseline resolution of sn-1,2-DG urethanes from the sn-

[1] Note that the abbreviations (P = palmitic; S = stearic; O = oleic; L = LA; G = GLA and Ga = gadoleic or 20:1n-9) used for the TGs are meant to mean all positional isomers of a particular TG and according to a rule often used in reversed-phase HPLC are named with the shortest or most saturated fatty acid chain first and the most highly unsaturated fatty acid chain in the middle. When discussing positional isomers within an individual TG species the notation, sn (stereochemical numbering), will be used to indicate positional specificity. For example sn-OGL refers to a TG with oleic acid located at the sn-1 position, GLA at the sn-2 position and LA at the sn-3 position.

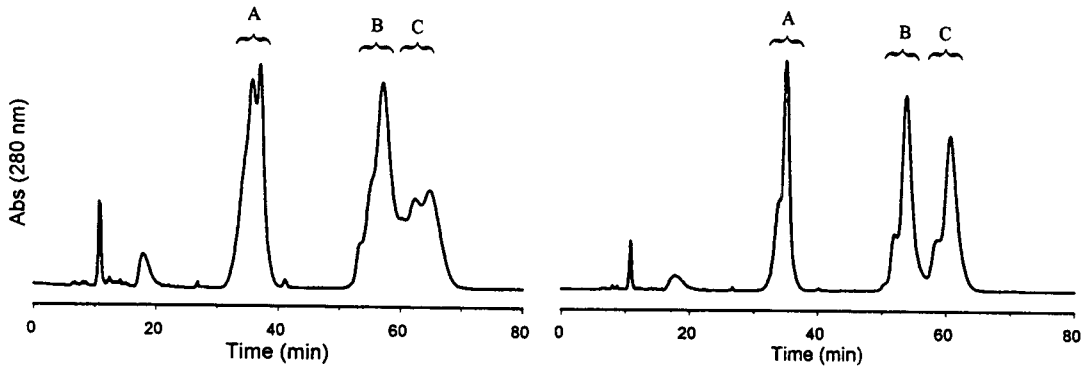

Fig. 2. HPLC profiles of the sn-1-3-, sn-1,2- and sn-2,3-DG naphthylethyl urethane derivatives obtained from BO (left) and EPO (right). The peaks under the letter A represent the sn-1,3-DG derivatives, under the letter B, the sn-1,2-DG derivatives and under the letter C the sn-2,3-DG derivatives. Conditions: two silica columns in series (150 × 4.6 mm I.D., 3-μm and 250 × 4.6 mm I.D., 3-μm); mobile phase, iso-octane–2-propanol (containing 2% water) (99.7:0.3, v/v) at 1 ml/min and UV detection at 280 nm.

2,3-DG urethane derivatives with the exception of samples containing long chain fatty acids. It was not possible to obtain baseline resolution for samples containing long chain fatty acids, most probably because the retention times of the sn-1,2-DG urethane derivatives containing long chain fatty acids overlap with the sn-2,3-DG urethane derivatives containing the normal range of fatty acids [27].

The results of the stereospecific analysis for the above TG samples and all the other isolated individual TG species are given in Table 1. Additionally for all the diacid TG species the results from the stereospecific analysis give the TG positional isomer ratios (normalized to 100%) and these are shown in Tables 3 and 4. With regards to the diacid TG species containing GLA there are some empirical observations worthy of comment. There is a significantly greater proportion of the positional isomers

Table 2
Borage oil and EPO positional fatty acid composition (expressed as mol%)

	16:0	18:0	18:1	18:2n-6	18:3n-6	20:1n-9	22:1n-9	24:1n-9
Borage Oil								
Total	11.5	4.2	18.0	42.0	17.7	3.3	2.0	1.2
sn-1[a]	20.2	4.9	17.5	38.5	3.5	5.9	6.1	3.5
sn-2[b]	−3.1	1.4	18.9	53.4	32.2	0.0	−1.7	−0.9
sn-3[c]	17.5	6.4	17.5	34.2	17.4	4.0	1.7	0.9
EPO								
Total	6.0	2.2	9.0	74.4	8.5			
sn-1[a]	11.3	3.9	9.8	70.0	4.9			
sn-2[b]	−0.4	0.7	7.8	81.5	10.3			
sn-3[c]	7.1	2.0	9.4	71.6	10.2			

[a] 3 × [TG] − 2 × [sn-2,3-DG urethanes].
[b] 3 × [TG] − [sn-1] − [sn-3].
[c] 3 × [TG] − 2 × [sn-1,2-DG urethanes].

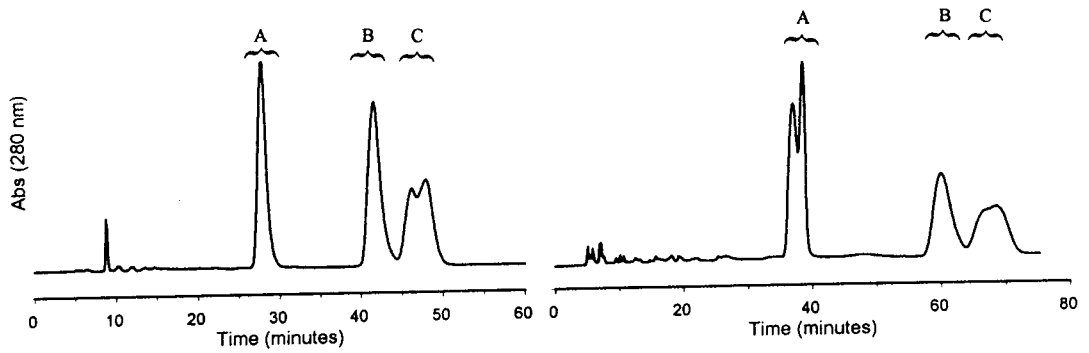

Fig. 3. HPLC profiles of the sn-1,3-, sn-1,2- and sn-2,3-DG naphthylethyl urethane derivatives obtained from the diacid TG species, LGL, isolated from BO (left) and EPO (right). The conditions and letters as described in Fig. 2.

containing GLA at the sn-1 and sn-2 positions in EPO than in BO. For example for the LGG species in EPO, sn-GGL and sn-GLG correspond to 19.4% and 24.1%, respectively, of the three possible isomers compared to only 7.1% and 5.5%, respectively, for BO. Similarly for the LGL species, sn-GLL in EPO accounts for 20.7% of the three isomers compared to only 8.0% in BO.

Within the triacid OGL and PGL species, GLA was distributed throughout the three positions slightly more in EPO than in BO. For the OGL species from EPO the percentages of the sn-GXX, sn-XGX and sn-XXG isomers are 20.1, 28.9 and 51.1%, respectively, compared to 11.6, 57.6 and 30.7%, respectively, for BO. For the PGL species from EPO the percentages of the sn-GXX, sn-XGX and sn-XXG isomers are 15.3, 49.4 and 35.6%, respectively, compared to 10.4, 43.9 and 45.7%, respectively, for BO. The different molecular species or positional isomers present in the individual triacid TG species can be mathematically determined by solving a set of equations. The equations are derived from the data in Table 1. Examples for the *rac*-POS TG and the OGL TG species isolated from EPO are given in Table 5. There are nine independent equations with a total of six unknowns. Although there are more equations than unknowns none of the equations are exactly mathematically redundant because of the small experimental inaccuracies. Consequently an exact solution using

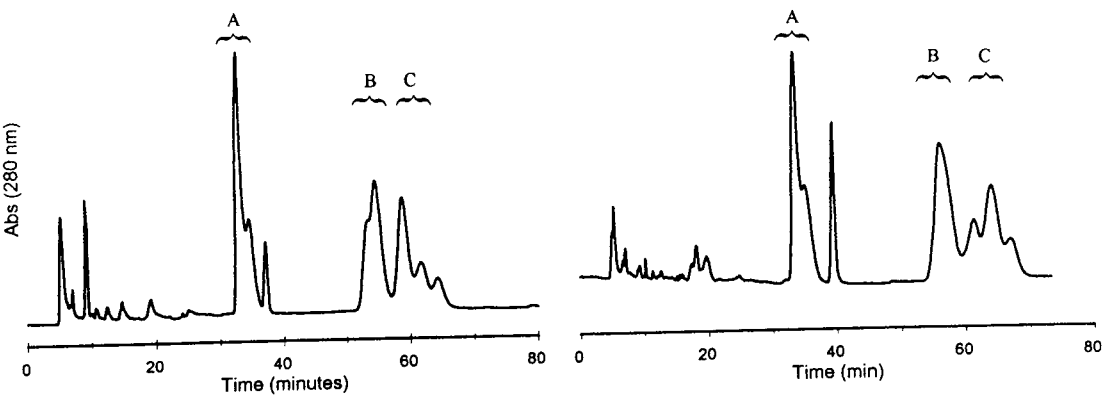

Fig. 4. HPLC profiles of the sn-1,3-, sn-1,2- and sn-2,3-DG naphthylethyl urethane derivatives obtained from the triacid TG species, OGL, isolated from BO (left) and EPO (right). The conditions and letters as described in Fig 2.

Table 3
Positional isomer distribution for the individual TG species isolated from BO

TG mol%[a]		LGG 4.7 mol%			LGL 8.3 mol%			OGG 1.0 mol%	
		TG[b]	Oil[c]		TG[b]	Oil[c]		TG[b]	Oil[c]
	sn-LGG	87.4	4.1	sn-GLL	8.0	0.7	sn-OGG	79.4	0.8
	sn-GLG	5.5	0.3	sn-LGL	37.2	3.1	sn-GOG	3.4	0.03
	sn-GGL	7.1	0.3	sn-LLG	54.8	4.5	sn-GGO	17.2	0.2
TG mol%[a]		PGG 1.9 mol%			OGL 7.4 mol%			PGL 6.1 mol%	
		TG[b]	Oil[c]		TG[b]	Oil[c]		TG[b]	Oil[c]
	sn-PGG	59.9	1.1	sn-OGL	13.5	1	sn-PGL	23.3	1.4
	sn-GPG	40.1	0.8	sn-LGO	44.1	3.3	sn-LGP	20.6	1.3
	sn-GGP	nd	nd	sn-GLO	11.6	0.9	sn-GLP	4.3	0.3
				sn-OLG	7.1	0.5	sn-PLG	22.4	1.4
				sn-LOG	23.6	1.7	sn-LPG	23.3	1.4
				sn-GOL	0	0	sn-GPL	6.1	0.4
TG mol%[a]		OLL 5.1 mol%			SGL and PGO 5.6 mol%				
		TG[b]	Oil[c]		TG[b]	Oil[c]			
	sn-OLL	15.3	0.8	sn-SGL	3.3	0.2			
	sn-LOL	20.8	1.1	sn-LGS	16.2	0.9			
	sn-LLO	63.9	3.2	sn-GLS	0.5	0.03			
				sn-SLG	0.2	0.01			
				sn-LSG	15.6	0.9			
				sn-GSL	7.7	0.4			
				sn-PGO	17.9	1.0			
				sn-OGP	3.1	0.2			
				sn-GOP	5.2	0.3			
				sn-POG	18.8	1.1			
				sn-OPG	5.2	0.3			
				sn-GPO	6.4	0.4			

[a] mol% of total oil TGs; from reference [21], [b]mol% of the individual TGs, [c]mol% of the total oil TGs.

elementary linear algebra is not possible. These slight inconsistencies resulting from the experimental inaccuracies can be resolved either by ignoring some of the equations, by making simplifying assumptions (See Ref. [26]), or by calculating an approximate solution to this overdetermined system using linear regression. To eliminate any further error that may arise from simplifying assumptions the latter approach was used. Linear regression was carried out with the numerical values in column 4 of Table 5 as the dependent variables and six independent indicator variables, A–F, corresponding to the six positional isomers of *rac*-POS or OGL. The

Table 4
Positional isomer distribution for the individual TG species isolated from EPO

TG mol%[a]		LGG 2.7 mol%			LGL 14.7 mol%			OGL 3.3 mol%	
		TG[b]	Oil[c]		TG[b]	Oil[c]		TG[b]	Oil[c]
	sn-LGG	56.5	1.5	sn-GLL	20.3	3.0	sn-OGL	10.3	0.3
	sn-GLG	24.1	0.7	sn-LGL	32.5	4.8	sn-LGO	18.6	0.6
	sn-GGL	19.4	0.5	sn-LLG	47.2	6.9	sn-GLO	14.1	0.5
				sn-OLG	25.4	0.8			
				sn-LOG	25.7	0.8			
				sn-GOL	6.0	0.2			
TG mol%[a]		PGL 3.2 mol%			OLL 12.3 mol%			PLL 10.9 mol%	
		TG[b]	Oil[c]		TG[b]	Oil[c]		TG[b]	Oil[c]
	sn-PGL	33.0	1.1	sn-OLL	27.0	3.3	sn-PLL	53.6	5.8
	sn-LGP	16.4	0.5	sn-LOL	41.1	5.1	sn-LPL	7.1	0.8
	sn-GLP	14.8	0.5	sn-LLO	31.9	3.9	sn-LLP	39.3	4.3
	sn-PLG	30.9	1.0						
	sn-LPG	4.7	0.2						
	sn-GPL	0.5	0.02						

[a] mol% of total oil TGs; from Ref. [21].
[b] mol% of the individual TGs.
[c] mol% of the total oil TGs.

solution values A–F that were obtained are given in Table 5, column 6. This method gives reasonable answers in most cases but can yield solution values that are negative when one of the fatty acid positional mol% values from Table 1 is small or close to zero. To prevent this, instead of minimizing the sum of squared differences between columns 4 and 5 of Table 5, as is done in routine linear regression, we minimized this sum with a large penalty added for any elements of column 6 that were negative. This minimization can be done easily using the iterative capabilities of non-linear regression software. The macros for implementing such a scheme in SPlus for Windows (Version 3.1, Statistical Sciences, Seattle, WA, USA) are available from the third author. The results obtained for *rac*-POS demonstrate that the linear regression analysis is in agreement with that expected for a 50:50 mixture of sn-POS and sn-SOP. The error of about 4% is a result of the error associated with the positional fatty acid stereospecific analysis. A check of the solution values by substituting them into the nine equations demonstrates that good matches were obtained. Analogous sets of equations and solutions were obtained for the OGL species isolated from BO and the PGL species isolated from both oils with the positional isomer results given in Tables 3 and 4. Fraction 11 isolated from BO contains P, O, L, G and Ga and corresponds to a mixture of PLL, OGO and GaGL based on its fatty acid composition and relative retention time [21]. No positional analysis is reported for this fraction because of errors associated with the stereospecific analysis that occur as a result of the presence of the long chain fatty acid 20:1n-9. Fraction 12 from BO contains P, S, O, L and G and corresponds to a mixture of SGL and PGO based on its fatty acid composition and relative retention time [21]. As

Table 5
Linear regression determination of the positional isomer distribution for *rac*-POS and the OGL TG species isolated from EPO

TG	sn-1,2,3-TG	Mol%	Equations[a]	Check[b]	Solution[c]	Theoretical[d]
rac-POS	PSO	A	A + B = 48.2	48.8	A = 3.2	A = 0
	POS	B	C + D = 0	0.17	B = 45.6	B = 50.0
	SPO	C	E + F = 49.8	50.7	C = 0.07	C = 0
	OPS	D	C + E = 48.7	47.47	D = 0.1	D = 0
	SOP	E	A + F = 7.0	6.5	E = 47.4	E = 50.0
	OSP	F	B + D = 46.1	45.7	F = 3.3	F = 0
			D + F = 3.9	3.4		
			B + E = 93.3	93.0		
			A + C = 4.1	3.21		
OGL	OLG	A	A + B = 36.8	35.7	A = 25.4	A = 23.8
	OGL	B	C + D = 32.6	31.7	B = 10.3	B = 21.1
	LOG	C	E + F = 33.9	32.7	C = 25.7	C = 16.3
	GOL	D	C + E = 46.8	44.3	D = 6.0	D = 8.0
	LGO	E	A + F = 41.8	39.5	E = 18.6	E = 19.8
	GLO	F	B + D = 18.8	16.3	F = 14.1	F = 11.0
			D + F = 16.7	20.1		
			B + E = 25.3	28.9		
			A + C = 47.7	51.1		

[a] Values from Table 1.
[b] Substitute solution into equations.
[c] Computer-aided non-linear least squares regression, see Results.
[d] Based on 50:50 mixture for *rac*-POS or on the data in Table 2 for EPO and using the 1-random, 2-random, 3-random distribution theory.

with the triacid TG species the positional isomer distribution for this mixture can be determined by linear regression of the set of equations derived from the data in Table 1. In this case there were 15 equations and 12 unknowns with the positional isomer distribution results given in Table 3.

The six TG species analyzed from EPO represent 47.1% of the total TGs. If trilinolein (38.0% of the total TGs) is included then over 85% of the molecular species (or positional isomers) in EPO and over 50% of the molecular species in BO have been identified and quantified. More importantly, over 90% of the GLA present in EPO and over 80% of the GLA in BO can be accounted for in their respective analyzed TG fractions.

4. Discussion

In this study the stereospecific analysis of native EPO agrees with previous analyses [17,18]. The results for BO are also in broad agreement with those obtained previously [17,19], although differences regarding the long chain fatty acids, 22:1n-9 and 24:1n-9, are evident. We found that these long chain fatty acids were almost exclusively located at the sn-1 position whereas previously 22:1n-9 was found almost exclusively at the sn-3 position [17]. However, it has been noted that fats or oils containing fatty acids greater than C_{18} in length are not suitable for stereospecific analysis by the present HPLC method, hence the results presented here for BO should be viewed with caution [27]. Indeed, the HPLC profile of the sn-1,2(2,3)-DG urethane derivatives from BO shown in Fig. 2 shows that there was no baseline separation between these two groups of diastereomeric DG urethane derivatives meaning there was overlap during their collection. A similar problem was encountered for fraction 11 isolated from BO that contains the long chain fatty acid, 20:1n-9. As mentioned earlier the most probable reason is the overlap of the sn-

1,2-DG urethanes containing long chain fatty acids with the sn-2,3-DG urethanes containing the normal range of fatty acids.

The stereospecific analysis of the individual TG species isolated by reversed-phase HPLC was relatively easy accomplished, although more than 10 injections of ~500 μg of BO or EPO were required to provide enough of the individual TG species for the stereospecific analysis. As can be seen from Figs. 3 and 4 the diastereomeric sn-1,2-DG urethane derivatives were virtually baseline resolved from the sn-2,3-DG urethane derivatives. Moreover, these profiles and the profiles of the sn-1,2- and sn-2,3-DG urethane derivatives for the other individual TGs isolated from the two oils are qualitatively different suggesting that the positional isomeric distributions are different between the same individual TG species from the two oils. Indeed, Tables 3 and 4 clearly show that the positional isomeric distributions are different for the same individual TG species in the two oils.

The TGs of plant seed oils which are rich in oleic, linoleic and α-linolenic acids have a relatively low degree of asymmetry based on the stereospecific analysis of the total oil. In maize, soybean, linseed, and olive oils position sn-2 is almost exclusively occupied by unsaturated fatty acids, while saturated as well as unsaturated fatty acids occur to the same extent at the sn-1 and sn-3 positions [23]. The isolated TG classes from the monounsaturated TGs of cocoa butter were also found to be racemic [29]. However, in this report, examination of the individual TG species possessing chirality shows that they do not exist, either in BO or EPO, as racemic mixtures. In general, there is a substantial enantiomeric excess (ee) defined as

$$\text{Enantiomeric excess (ee)} = \frac{\%\text{difference between enantiomers}}{\%\text{total of enantiomers}} \cdot 100\%$$

which is larger in BO than in EPO. For the LGG species in EPO there was 49% ee for the sn-LGG optical isomer compared to 85% in BO. For the LGL species in EPO there was 40% ee for the sn-LLG optical isomer compared to 74% in BO. With regards to the three individual pairs of optical isomers in the OGL and PGL species, while there was an excess of one enantiomer, no striking differences were evident comparing the two oils. In contrast, the stereospecific analysis of the PLO TG species isolated from peanut and cottonseed oils showed that there was an enantiomeric excess within the pairs of optical isomers of PLO from peanut oil whereas the individual pairs of optical isomers occurred nearly to the same extent in cottonseed oil [26]. Although it has been shown that GLA is resistant to pancreatic lipase in vitro [17] it is uncertain whether the enzymes involved in the hydrolysis of TGs in vivo have a preference for one enantiomer.

The positional isomeric distribution for the individual TG species were also predicted using the 1-random, 2-random, 3-random distribution theory by multiplying the stereospecific results obtained for the native oils. For example, within EPO (Table 2) one would predict for sn-GLL, $0.049 \times 0.815 \times 0.716$, or 2.86 mol%; similarly 5.16 mol% for sn-LGL, and 5.82 mol% for sn-LLG. These values when converted to a percentage of the three possible isomers are 20.7%, 37.3% and 42.1%, respectively, which are in very good agreement with the values determined experimentally (Table 4). Similarly the predicted percentages of the three isomers for the LGG species from EPO are 24.0%, 27.1% and 48.9%, corresponding to sn-GGL, sn-GLG and sn-LGG, respectively. Again these predicted values are in good agreement with the values determined experimentally. The predicted positional distribution for the OGL species from EPO is given in Table 5 and broadly compares to the values determined experimentally by linear regression. A similar comparison was observed for the PGL species from EPO.

The values predicted for the isomeric distribution of the LGG and LGL species from BO do not agree as well with the experimental values. The differences in these cases are most probably a result of the errors associated with our stereospecific analysis of native BO as discussed earlier. However, using the data from Ref. [17], even though in that report there was significantly more GLA present, the predicted values for the isomeric distribution of the diacid LGG and

LGL species and triacid OGL and PGL species of BO are in much closer agreement to the values determined experimentally.

The agreement between the predicted (calculated) and experimentally determined positional isomeric distribution for individual TG species suggests that as long as the stereospecific analysis of an intact fat or oil is carried out with reasonable precision the results can be used as a guide to estimate the isomeric composition of individual TG species within a fat or oil. The exact composition, however, can only be determined by fractionating the fat or oil and analyzing the isolated individual TG species. In animal tissues where the TG species can be markedly asymmetric the 1-random, 2-random, 3-random distribution theory has been used to calculate the amounts of various positional isomers with precision [22,30]. Recently the major individual TG species of olive oil have been isolated by silver-ion HPLC and subjected to stereospecific analysis. Again, using the stereospecific analysis results for the intact olive oil and the 1-random, 2-random, 3-random distribution, there was very good agreement between the predicted and experimental positional isomer distributions for the isolated OLO and POO TG species [31].

The advantage of the present method for the stereospecific analysis of individual TG species is that they were isolated by HPLC directly from the oils. While it may be time-consuming to collect enough material, prior experimentally-demanding fractionation steps are eliminated. The positional isomer analysis of isolated diacid TG species was very straightforward, but for the triacid TG species computer-aided linear regression was utilized to solve the positional isomer equation set. Others utilizing a slightly different approach have, with regard to the isolated PLO species from peanut and cottonseed oils, assumed that the percentage of P at the sn-2 position was negligible as an approximation in solving their equation set [26]. This assumption was valid in their case, however, it would not be prudent to make any assumption in our case especially because of the asymmetric distribution of GLA. Moreover, while in this study only the sn-1 and sn-3 positions are determined directly with the sn-2 position calculated and, thus, subject to cumulative error, it has been demonstrated that no significant difference exists between the classical TLC and HPLC stereospecific methods of analyses for oils containing a normal range of fatty acids [28]. Further refinements are, however, required for fats and oils containing the full range of fatty acids.

In summary this study has established that there are substantial differences in positional isomerism of the major GLA-containing individual TG species between BO and EPO. Whether these differences can account for the demonstrated differences in biological activity is not known. A final explanation of the biological differences between the whole oils will require the specific biological testing of either the isolated individual TG positional isomers or the non-triglyceride fractions.

References

[1] S. Wright and J. L Burton, Lancet II, (1982) 1120.
[2] J. Chaintreuil, L. Monnier, C. Colette, P. Crastes de Paulet, A. Orsetti, D. Speilmann, F. Mendy and A. Craste de Paulet, Hum. Nutr. Clin. Nutr., 38C (1984) 121.
[3] J.K. Pye, R.E. Mansel and L.E. Hughes, Lancet II, (1985) 373.
[4] J. Poulakka, L. Makarainen, L. Viinikka and O. Ylikorkala, J. Reprod. Med., 30 (1985) 149.
[5] D.F. Horrobin, Rev. Contemp. Pharmacother., 1 (1990) 1.
[6] Y.-Y. Fan and R.S. Chapkin, J. Nutr., 122 (1992) 1600.
[7] M.M. Engler, Prostaglandins, Leukotrienes and Essential Fatty Acids, 49 (1993) 809.
[8] D.E. Barre, B.J. Holub and R.S. Chapkin, Nutr. Res., 13 (1993) 739.
[9] L. Monner, S. El boustani and A. Crastes de Paulet, B. Descomps and F. Mendy, Corps. Gras, in press.
[10] N.E. Cameron, M.A. Cotter, K.C. Dines, S. Robertson and D. Cox, Br. J. Pharmacol., 109 (1993) 972.
[11] K.C. Dines, M.A. Cotter and N.E. Cameron, Presented at *The Phisiological Society* meeting, Aberdeen, UK, 1994.
[12] D.K. Jenkins, J.C. Mitchell, M.S. Manku and D.F. Horrobin, Med. Sci. Res., 16 (1988) 526.
[13] D. Kritchevsky, Arch. Pathol. Lab. Med., 112 (1988) 1041.
[14] D. Kritchevsky, S.A. Tepper, D. Vesselinovitch and R.W. Wissler, Atheroscler., 17 (1973) 225.

[15] M.M. Jensen, M.S. Christensen and C.-E. Hoy, Ann. Nutr. Metab., 38 (1994) 104.
[16] S.M. Innis, R. Dyer and C.M. Nelson, Lipids, 29 (1994) 541.
[17] L.D. Lawson and G.B. Hughes, Lipids, 23 (1988) 313.
[18] P. Laakso and W.W. Christie, Lipids, 25 (1990) 349.
[19] G. Griffiths, A.K. Stobart and S. Stymne, Biochem. J., 252 (1988) 641.
[20] H. Brockerhoff and M. Yurkowski, J. Lip. Res., 7 (1966) 62.
[21] P.R. Redden, Y.-S. Huang, X. Lin and D.F. Horrobin, J. Chromatogr. A, 694 (1995) 381.
[22] W.W. Christie, in R.J. Hamilton and J.B. Rossell (Editors), Analysis of Oils and Fats, Elsevier Applied Science Publishers, London, UK, 1986, p. 313.
[23] W.C. Breckenridge, in A. Kuksis (Editor), Handbook of Lipid Research, Vol. 1, Plenum Press, New York, NY, 1978.
[24] Y. Itabashi, A. Kuksis, L. Marai and T. Takagi, J. Lip. Res., 31 (1990) 1711.
[25] T. Takagi and Y. Ando, Lipids, 26 (1991) 542.
[26] G. Sempore and J. Bezard, J. Am. Oil Chem. Soc., 68 (1991) 702.
[27] W.W. Christie, B. Nikolova-Damyanova, P. Laakso and B. Herslot, J. Am. Oil Chem. Soc., 68 (1991) 695.
[28] P. Damiani, F. Santinelli, M.S. Simonetti, M. Castellini and M. Rosi, J. Am. Oil Chem. Soc., 71 (1994) 1157.
[29] J. Sampugna and R.G. Jensen, Lipids, 3 (1968) 519.
[30] W.W. Christie and J.H. Moore, Biochim. Biophys. Acta, 210 (1970) 46.
[31] F. Santinelli, P. Damiani and W.W. Christie, J. Am. Oil Chem. Soc., 69 (1992) 552.

ELSEVIER

Journal of Chromatography A, 704 (1995) 113–120

JOURNAL OF CHROMATOGRAPHY A

Isolation of low-molecular-mass hydrophobic bitter peptides in soybean protein hydrolysates by reversed-phase high-performance liquid chromatography☆

I. Lovšin Kukman*, M. Zelenik-Blatnik, V. Abram

Department of Food Science and Technology, Biotechnical Faculty, University of Ljubljana, Jamnikarjeva 101, 61000 Ljubljana, Slovenia

First received 1 November 1994; revised manuscript received 27 December 1994; accepted 30 December 1994

Abstract

The molecular mass distribution of peptides in isoelectric soluble soybean protein hydrolysates and their hydrophobic peptide fractions was determined by gel permeation HPLC on a Zorbax Bio Series GF-250 column. The hydrophobic bitter peptide fraction of isoelectric soluble soybean protein hydrolysate with degree of hydrolysis 15% was fractionated on a Sephadex G-25 Fine column. The most bitter low-molecular-mass fraction of the peptides was separated by reversed-phase HPLC on a Spherisorb ODS-2 column. Fourteen low-molecular-mass hydrophobic bitter peptides containing three to six amino acid residues were isolated. They are predominantly composed of hydrophobic amino acids and have leucine, valine or tyrosine at their C-terminal position

1. Introduction

It has been known for a long time that enzymatic hydrolysis of proteins frequently leads to the production of a bitter taste, which is due to the presence of strongly hydrophobic bitter peptides arising as natural degradation products of the proteolytic reaction [1]. Numerous bitter peptides have been isolated from enzymatic hydrolysates of casein [2,3], soybean protein [4,5], cheese [6,7] and some other foods, and their structures determined. The bitterness of peptides can be predicted by calculation of the Q value of a peptide, which depends on the amino acid composition. The Q value represents the average hydrophobicity of a peptide and is calculated by summing the Δf values of the amino acid residues of a peptide and dividing by the number of amino acid residues as described by Ney [8]. When the Q value is greater than 1.4 kcal mol^{-1}, bitterness is likely to appear [9]. To avoid bitterness in this case, the relative molecular mass of a peptide must be as high as possible and more than 6000 [10]. The results of enzymatic hydrolysis of casein show that for larger peptides, neither hydrophobicity nor size alone is responsible for bitter potency, but that conformational parameters must be of greater im-

* Corresponding author.

☆ Presented at the *International Symposium on Chromatographic and Electrophoretic Techniques, Bled, Slovenia, 10–13 October 1994.*

0021-9673/95/$09.50
SSDI 0021-9673(95)00014-3

portance. Further, it was concluded that only a part of the structure is responsible for contact with the taste receptor [2,11].

Different types of chromatographic methods have been developed for the separation of proteins and their hydrolysates. Among the various HPLC systems, including gel permeation [12,13], reversed-phase (RP-HPLC) [14–16] and ion exchange [17–19] modes, RP-HPLC has been most extensively used. There have been many studies of the separation of milk proteins, especially casein digest [20,21], but there are no published studies documenting the RP-HPLC separation of hydrophobic bitter peptides in soybean protein hydrolysates.

The aim of this work was to isolate small hydrophobic bitter peptides and to determine the molecular mass distribution of peptides in soybean protein hydrolysates using gel permeation HPLC, gel chromatography and RP-HPLC.

2. Experimental

2.1. Materials

Soybean protein isolate, Purina 500 E, was purchased from Protein Technologies International (Ypres, Belgium). Alcalase 2.4 l (a commercial preparation of subtilisin Carlsberg from *Bacillus licheniformis*) was obtained from Novo Nordisk (Bagsvaerd, Denmark). The protein molecular mass calibration standards used were carbonic anhydrase, cytochrome *c*, angiotensin II, angiotensinogen fragment 11–14 (Sigma, St. Louis, MO, USA) and the B-chain and A-chain of insulin (Serva, Heidelberg, Germany). Ammonium acetate and sodium dodecyl sulphate (SDS) were also obtained from Sigma, acetonitrile from Rathburn Chemicals (Walkerburn, UK) and trifluoroacetic acid (TFA) from Applied Biosystems (Warrington, UK). All other chemicals were of analytical-reagent grade.

2.2. Methods

Preparation of isoelectric soluble soybean protein hydrolysates (ISSPHs)

Five isoelectric soluble soybean protein hydrolysates were produced in the laboratory according to the standard procedure [22]. Hydrolysis was carried out under the following standard conditions: substrate concentration $S = 8\%$ protein (calculated from Kjeldahl N × Kjeldahl conversion factor for soy protein isolate, f_N, 6.25); enzyme/substrate concentration ratio $E/S = 12$ AU kg^{-1} (Anson units per kg substrate), pH = 8.0, temperature 50°C. One Anson unit (AU) is the amount of enzyme which under the given reaction conditions digests haemoglobin at an initial rate such that there is liberated per 10 min an amount of trichloroacetic acid-soluble product which gives the same colour with phenol reagent as 1 μmol of tyrosine [23]. The course of the reaction was followed by the pH-stat technique, and when the desired degree of hydrolysis (DH value) had been reached, the enzyme was inactivated by lowering the pH to 4.0–4.2 for 30 min, and the separation of the isoelectric soluble soybean protein hydrolysates from the insoluble matter was carried out at the same pH by centrifugation (1 h at 8000 *g*). All the hydrolysates were then freeze-dried, analysed for Kjeldahl N and stored in closed containers.

Isolation of the hydrophobic bitter peptide fractions (HPFs)

The hydrophobic bitter peptide fractions (HPFs) were extracted from the isoelectric soluble soybean protein hydrolysates (ISSPHs) with 2-butanol according to the procedure of Adler-Nissen [24], freeze-dried, analysed for Kjeldahl N and stored in closed containers.

Gel permeation high-performance liquid chromatography

The molecular mass distribution of the hydrolysates and the hydrophobic peptide fractions (ISSPHs and their HPFs) were determined by gel permeation high-performance liquid chromatography (GP-HPLC) on a Zorbax Bio Series GF-250 column (250 × 9.4 mm I.D., particle size 6 μm) with a separation range of M_r 4000–400 000 using an LDC Analytical HPLC system. The mobile phase was 0.1 *M* phosphate buffer (pH 8.0) containing 0.1% SDS at a flow-rate of 1.0 ml min^{-1}. Peptides were monitored at 215 nm with an absorbance range of 0.02 AUFS. The

column was calibrated with six peptide standards (carbonic anhydrase, cytochrome *c*, A- and B-chains of insulin, angiotensin II and angiotensinogen fragment 11–14) and the molecular masses of peptides were determined from the calibration plots log M_r vs. t_r (min): log $M_r = 7.81 - 0.45t_r$ ($r = 0.98$). Samples were dissolved in 0.1 *M* phosphate buffer, (pH 8.0) containing 0.1% SDS and filtered through a 0.45-μm filter (Millipore). The injection volume was 20 μl.

Preparative gel chromatography of the hydrophobic bitter peptide fraction

The hydrophobic bitter peptide fraction of isoelectric soluble soybean protein hydrolysate (HPF-ISSPH-DH 15%, 70 mg) was dissolved in 1.5 ml of water and filtered through a 0.45-μm filter (Millipore). The filtrate was applied to a Sephadex G-25 Fine column (78 × 3 cm I.D.) and eluted with distilled water at 8°C at a flow-rate of 15 ml h^{-1}. The effluent was collected in 5-ml fractions. The absorbance was measured at 215 nm and the collected fractions were sensorially analysed for bitterness. The column was calibrated with cytochrome *c*, angiotensin II and L-leucine.

Reversed-phase chromatography

The most bitter low-molecular-mass peptide fraction obtained by preparative gel chromatography on the Sephadex G-25 Fine column was separated on a Spherisorb ODS-2 column (250 × 4 mm I.D., particle size 5 μm) using an LDC Analytical HPLC system. After equilibration of the column with 0.1% (v/v) TFA (solvent A) at a flow-rate of 1.0 ml min^{-1}, peptides were eluted by linearly increasing the concentration of solvent B [0.1% (v/v) TFA in acetonitrile] as follows: 0–2 min, 0% B; 2–5 min, 0–10% B; 5–65 min, 10–40% B; 65–70 min, 40–70% B; 70–71 min 70–0% B. The re-equilibration time was 10 min. Peptides were monitored at 220 nm with an absorbance range of 0.1 AUFS. The injection volume was 20 μl and the injection was repeated twenty times in order to obtain substantial amounts for further analysis. The eluates were divided into fractions 1–18 as shown in Fig. 3. The peptide fractions were concentrated under a nitrogen atmosphere, dried in a Speed-Vac concentrator and tasted for bitterness.

Peptide material that was not well-separated into individual peaks was subjected to chromatography with a second solvent system, consisting of 25 m*M* amonium acetate (pH 6.0) (A) and 60% (v/v) acetonitrile in 50 m*M* ammonium acetate (pH 6.0) (B), with the following gradient: 0–2 min, 0% B; 2–62 min, 0–100% B; 62–63 min, 100–0% B. All other conditions were the same as above.

The ammonium acetate was removed from the isolated peptides to facilitate amino acid and sequence analysis with an elution system consisting of 0.1% (v/v) TFA (A) and 0.1% (v/v) TFA in acetonitrile (B) with the following gradient: 0–6 min, 0–15% B; 6–26 min, 15–25% B; 26–36 min, 25–50% B; 36–37 min, 50–80% B; 37–38 min, 80–0% B. The isolated peptides were evaporated in a Speed-Vac concentrator.

Amino acid analysis

Amino acid analysis of peptide hydrolysates, obtained after hydrolysis for 24 h in 6 *M* HCl at 110°C, was performed on an Applied Biosystems 421A amino acid analyser.

Sequence analysis

An Applied Biosystems Model 475A liquid-pulsed protein sequencer, connected on-line to a Model 120A phenylthiohydantoin–amino acid analyser from the same manufacturer, was used for amino acid sequence determinations.

Calculation of hydrophobicity

The hydrophobicities (the *Q* values) of the peptides were calculated according to Ney [8] on the basis of the Δf values of Tanford [25].

Sensorial analysis

The bitterness of the hydrolysates ($c = 3\%$ N × 6.25), their hydrophobic peptide fractions ($c = 0.5\%$ N × 6.25) and gel chromatographic fractions was estimated by scoring on a scale from zero to five (0, no bitterness; 1, weak bitter after-taste; 2, weakly bitter; 3, bitter; 4, strongly bitter; 5, extremely bitter) by a panel of three persons.

3. Results and discussion

The elution profiles obtained for five ISSPHs and their HPFs on the Zorbax Bio Series GF-250 column are given in Fig. 1A and B. A high-molecular-mass fraction (fraction I; M_r 30 000–3000), a medium-molecular-mass fraction (fraction II; M_r 3000–1000) and a low-molecular-mass fraction (fraction III; $M_r < 1000$) of ISSPHs were obtained (Table 1). Fraction III is mainly composed of low-molecular-mass peptides and free amino acids. Some of them were retained on the column and eluted with an elution time of more than 12 min (Fig. 1A and B). The high-molecular-mass fraction of ISSPHs and HPFs consists of peptides of M_r 30 000–3000 (Fig. 1A) and 10 000–3000 (Fig. 1B). In peptides with $M_r >$ 10 000 present in the ISSPHs and having a longer chain length, the hydrophobic chains are generally directed towards the interior part of the molecule. Thus they are long enough to allow conformations such as hair-pin loops or clusters. Therefore, these peptides were not extracted from the hydrolysates with 2-butanol. As can be seen from Table 1, ISSPHs and their HPFs contain mainly low-molecular-mass peptides. Their content varies from 55.6 to 82.2% for ISSPHs and from 72.3 to 89.2% for their HPFs. The bitterness of ISSPHs rises as the degree of hydrolysis increases (Table 1). A slight decrease in bitterness was observed at DH 15%. HPFs of all ISSPHs give an extremely bitter taste even at a concentration of 0.5% N × 6.25 (all the hydrolysates were tasted at a concentration of 3% N × 6.25, as described under Experimental). From these results, we can conclude that the bitterness of ISSPHs is mainly due to low-molecular-mass peptides.

The elution profile of HPF-ISSPH-DH 15% obtained on a Sephadex G-25 Fine column (Fig. 2) shows a good correlation with the elution profile of the same sample subjected to GP-HPLC on the Zorbax Bio Series GF-250 column (Fig. 1B). As shown in Fig. 2, bitterness appeared at the end of the high-molecular-mass fraction of HPF (elution volume from 180 to 220

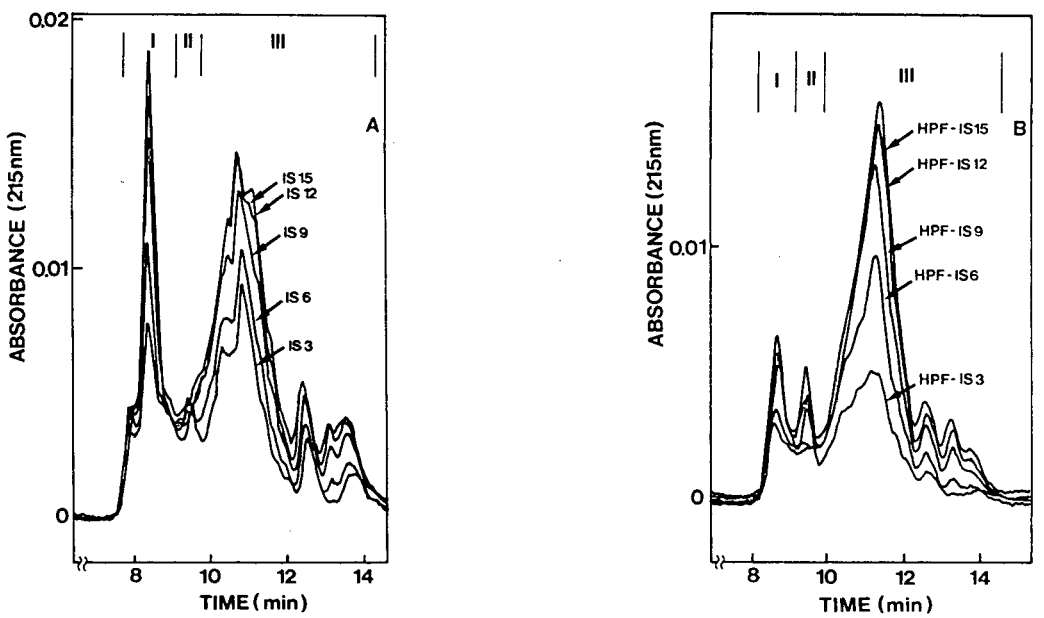

Fig. 1. Elution profiles of (A) five ISSPHs and (B) their HPFs on a Zorbax Bio Series GF-250 column (250 × 9.4 mm I.D.). The molecular mass fractions are designated I, II and III; I = high-molecular-mass fraction; II = medium-molecular-mass fraction; III = low-molecular-mass fraction.

Table 1
Bitterness and molecular mass distribution of ISSPHs and their HPFs obtained by GP-HPLC on a Zorbax Bio Series GF-250 column (250 × 9.4 mm I.D.)

Sample	Bitterness (score)	Area (%)		
		Fraction I: M_r 30 000–3000	Fraction II: M_r 3000–1000	Fraction III: M_r < 1000
ISSPH-DH 3%	0	37.3	7.1	55.6
ISSPH-DH 6%	2	31.5	6.2	62.3
ISSPH-DH 9%	3	23.0	5.8	71.2
ISSPH-DH 12%	3	16.3	5.2	78.5
ISSPH-DH 15%	2	13.9	3.9	82.2
HPF-ISSPH-DH 3%	5	17.2[a]	10.5	72.3
HPF-ISSPH-DH 6%	5	14.2[a]	10.3	75.5
HPF-ISSPH-DH 9%	5	10.7[a]	6.9	82.4
HPF-ISSPH-DH 12%	5	8.3[a]	3.9	87.8
HPF-ISSPH-DH 15%	5	6.7[a]	4.1	89.2

[a] M_r 10 000-3000.

ml), increased gradually in the medium-molecular mass fraction (elution volume from 250 to 290 ml) and reached a maximum intensity in the low-molecular-mass fraction of peptides (elution volume from 290 to 340 ml). The most bitter low-molecular-mass fraction of peptides (M_r < 1000) obtained after GPC on a Sephadex G-25 Fine column was separated into a large number of peptides on the Spherisorb ODS-2 column (Fig. 3) by a gradient of 0.1% (v/v) TFA (A) and 0.1% (v/v) TFA in acetonitrile (B). The eluate from RP-HPLC was divided into eighteen fractions, which were dried and tasted for bitterness. The straight line represents the gradient profile used. Generally, peptides appeared to be separated by RP-HPLC according to their hydrophobicity. Peptides with lower retention times are either small or hydrophobic and less strongly adsorbed on the stationary phase. They tasted slightly bitter in addition to a sour, burning or salty taste (fractions 1–7 and 9). The results of sensorial analysis are in agreement with many statements in the literature that peptides can elicit bitter, sweet, sour, umami, salt, astringent or tickling sensations [26,27]. Expressive bitter tasting fractions of insufficiently separated peptide material (fractions 8, 10, 11–15 and 18) were rechromatographed using a second solvent system consisting of 25 m*M* ammonium acetate (pH 6.0) (A) and 60% (v/v) acetonitrile in 50 m*M* ammonium acetate (pH 6.0) (B) (Figs. 4 and 5). The elution conditions using ammonium acetate in the RP system have been studied previously with casein digests and found to be suitable for peptide separations [20].

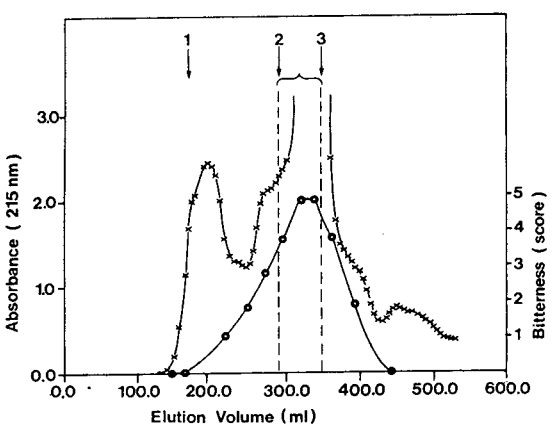

Fig. 2. Chromatogram of the hydrophobic bitter peptide faction from isoelectric soluble soybean protein hydrolysate (HPF-ISSPH-DH 15%) on a column of Sephadex G-25 Fine × = Absorbance at 215 nm; ○ = bitterness. The most bitter low-molecular-mass peptide fraction from 290 to 340 ml (shown with a brace) was rechromatographed by RP-HPLC. The numbers denote elution positions of the following compounds: 1 = cytochrome c; 2 = angiotensin II; 3 = L-leucine.

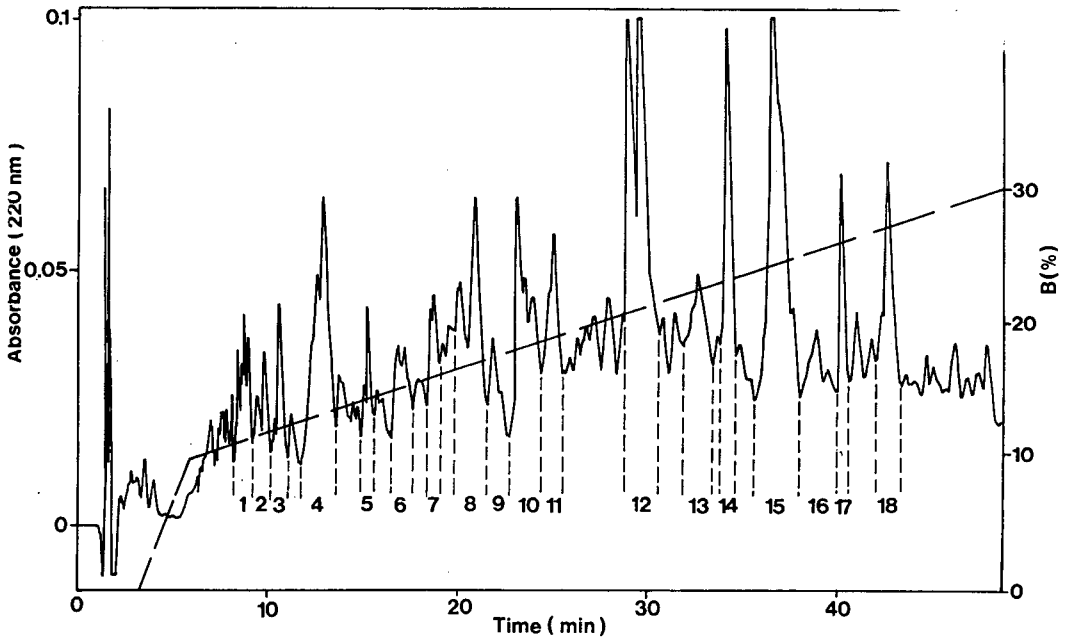

Fig. 3. RP-HPLC of the most bitter low-molecular-mass peptide fraction on a Spherisorb ODS-2 column (250 × 4 mm I.D.) with (A) 0.1% (v/v) TFA and (B) 0.1% (v/v) TFA in acetonitrile. The co-eluted peptide material is divided into fractions 1–18.

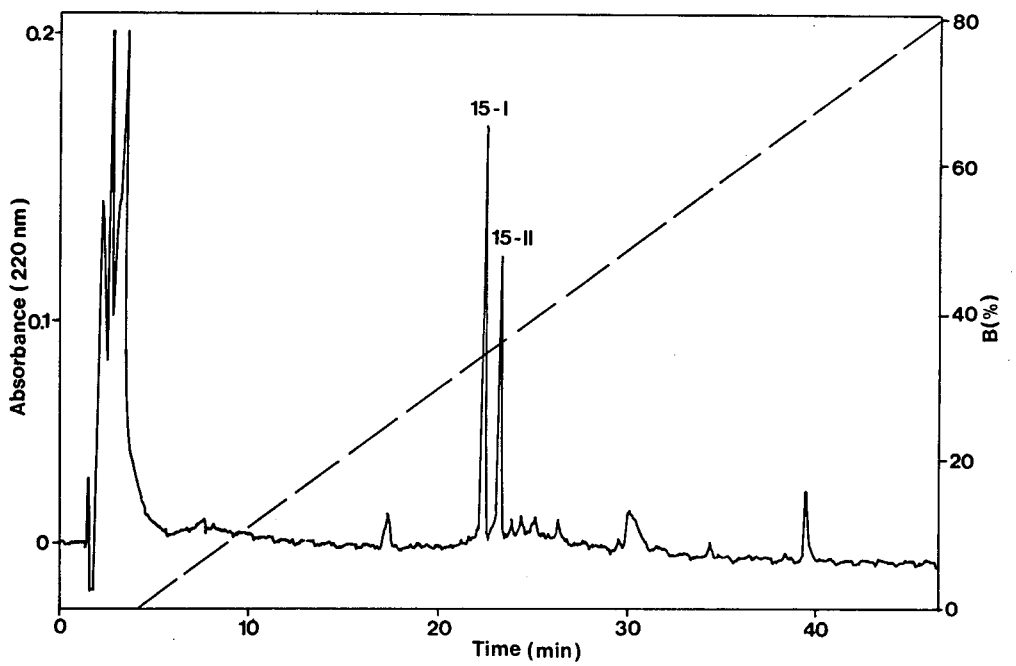

Fig. 4. Elution profile of rechromatographed fraction 15 from Fig. 3, obtained on a Spherisorb ODS-2 column by utilization of a second solvent system (peptides 15-I and 15-II).

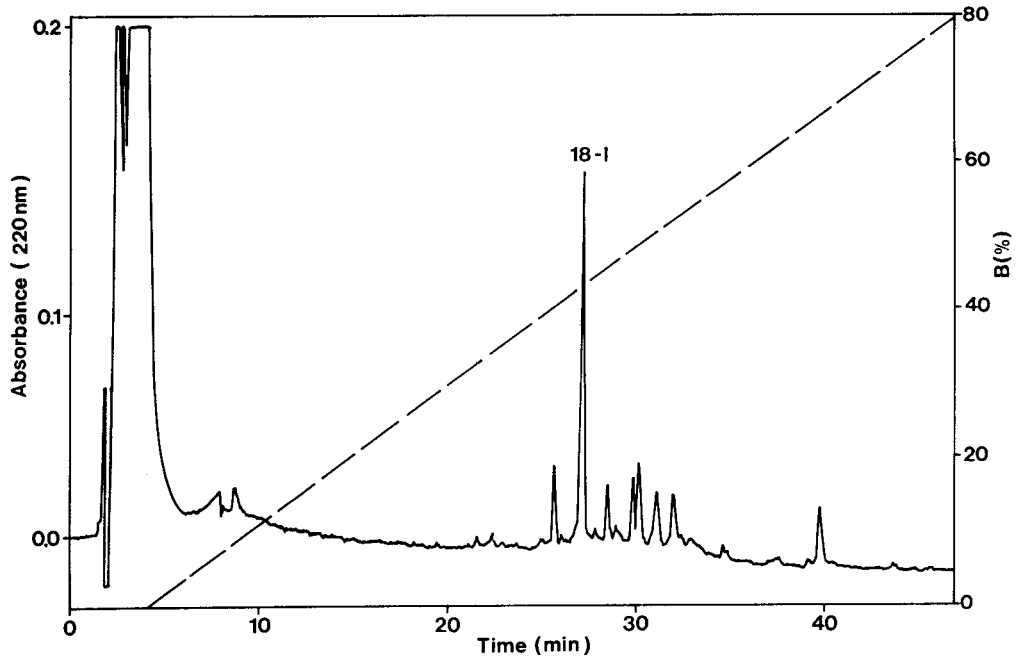

Fig. 5. Elution profile of rechromatographed fraction 18 from Fig. 3, obtained on a Spherisorb ODS-2 column by utilization of a second solvent system (peptide 18-I).

Table 2
Bitter-tasting low-molecular mass peptides isolated from the hydrophobic peptide fraction of isoelectric soluble soybean protein hydrolysate DH 15% (HPF-ISSPH-DH 15%)

RP-HPLC Fraction No.	Peptide	Eluent B (%)[a]	Hydrophobicity, Q (kcal mol^{-1})[b]	Hydrophobic residue	Sequence	M_r
8	8-I	19.65	1.46	2/3	FLS	365.41
	8-II	19.96	1.99	3/4	LLPH	478.57
10	10-I	20.77	1.75	3/4	LVGY	450/52
	10-II	20.54	2.34	3/4	IYIG	464.54
11	11-I	21.37	1.70	3/4	VYDV	494.53
	11-II	21.08	1.90	3/4	SVIY	480.54
12	12-I	22.67	2.23	4/4	VYFV	526.62
	12-II	22.84	2.21	3/4	ISIY	494.56
13	13-I	24.17	2.17	4/4	VVLY	492.60
14	14-I	24.50	2.05	2/3	DIF	392.42
	14-II	24.75	1.77	4/5	GYPVV	533.61
15	15-I	25.75	2.17	4/4	YVVL	492.60
	15-II	26.00	1.60	3/5	SGFTL	509.54
18	18-1	28.64	1.44	3/6	SNLNFL	678.72

[a] Eluent B = 0.1% TFA in acetonitrile.
[b] From Ref. [25].

The isolated peptides, the percentage of eluent B in the mobile phase, hydrophobicity, Q (kcal mol^{-1}), ratio of hydrophobic residues, amino acid sequences and the relative molecular masses of the peptides are given in Table 2. Fourteen bitter-tasting hydrophobic peptides with 3–6 amino acid residues and Q values from 1.44 to 2.34 kcal mol^{-1} were isolated. They are all predominantly composed of hydrophobic amino acids and with leucine, valine or tyrosine at the C-terminal part, which is in good agreement with the specificity of Alcalase, which cleaves predominantly at the carbonyl side of hydrophobic amino acids [22].

4. Conclusion

RP-HPLC has been demonstrated to be a reliable method with a high resolving power for the separation of hydrophobic bitter peptides from soybean protein hydrolysates. Peptides that co-eluate in the first mobile phase were easily separated using a second solvent system on the same RP-HPLC column.

Acknowledgements

The authors thank Dr. Igor Križaj (Jožef Stefan Institute, Ljubljana) for amino acid and sequence analyses of peptides. Many thanks are due to A. Plestenjak, T. Golob and B. Nahtigal for their contributions to the taste evaluations. This work was supported by a grant from the Ministry of Science and Technology of Slovenia.

References

[1] T. Nagodawithana, in S.L. Taylor (Editor), Enzymes in Food Processing, Academic Press, San Diego, 1993, pp. 159–199.
[2] E. Bumberger and H.D. Belitz, Z. Lebensm.-Unters.-Forsch., 197 (1993) 14–19.
[3] K.-H. Sohn and H.-J. Lee, Korean J. Food Sci. Technol., 20 (1988) 659–665.
[4] M. Fujimaki, M. Yamashita, Y. Okazawa and S. Arai, J. Food Sci., 35 (1970) 215–218.
[5] K.-H. Sohn and H.-J. Lee, Agric. Biol. Chem., 32 (1968) 794–795.
[6] J. Edwards and F.V. Kosikowski, J. Dairy Sci., 66 (1983) 727.
[7] A.J. Cliffe, J.D. Marks and F. Mulholland, Int. Dairy J., 3 (1993) 379–387.
[8] K.H. Ney, Z. Lebensm.-Unters.-Forsch., 147 (1971) 64.
[9] K.H. Ney, Z. Lebensm.-Unters.-Forsch., 149 (1972) 321.
[10] K.H. Ney, Fette Seifen Anstrichm., 8 (1978) 323–325.
[11] N. Ishibashi, K. Kouge, J. Shinoda, H. Kanehisa and H. Okai, Agric. Biol. Chem., 52 (1988) 819–827.
[12] H.G. Barth, Anal. Biochem., 124 (1982) 191–200.
[13] N. Chikazumi and T. Ohta, J Liq. Chromatogr., 14 (1991) 403–425.
[14] P.A. Hartman, J.D. Stodola, G.C. Harbour and J.G. Hoogerheide, J. Chromatogr., 360 (1986) 385.
[15] S. Visser, C.J. Slangen and H.S. Rollema, J. Chromatogr., 548 (1991) 361–370.
[16] J.E. Haky, A.R. Raghani, B.M. Dunn and L.F. Wieserman, Chromatographia, 32 (1991) 49–55.
[17] R.J. Benson, Am. Lab., 17 (1985) 30.
[18] R.G. Elkin and J.E. Griffith, J. Assoc. Off. Anal. Chem., 68 (1985) 1028.
[19] K. Yao and S. Hjerten, J. Chromatogr., 385 (1987) 87.
[20] L. Lemieux and J. Amiot, J. Chromatogr., 473 (1989) 189–206.
[21] L. Lemieux and J. Amiot, J. Liq. Chromatogr., 13 (1990) 4023–4035.
[22] J. Adler-Nissen, Enzymatic Hydrolysis of Food Proteins, Applied Science, London, 1986.
[23] M.L. Anson, J. Gen. Phys., 22 (1938) 79.
[24] J. Adler-Nissen, in Frontiers of Flavour, Proceedings of the 5th International Flavor Conference, Porto Karras, Chalkidiki, Greece, 1987, pp. 63–77.
[25] C. Tanford, J. Am. Chem. Soc., 84 (1960) 4240.
[26] T. Nishimura and H. Kato, Food Rev. Int., 4 (1988) 175–194.
[27] N. Ishibashi, J. Ono, K. Kato, T. Shigenaga, J. Shinoda, H. Okai and S. Fukui, Agric. Biol. Chem., 52 (1988) 91–94.

ELSEVIER

Journal of Chromatography A, 704 (1995) 121–130

JOURNAL OF CHROMATOGRAPHY A

Optimization of an analytical procedure for the determination of triazine herbicides in environmental samples☆

Helena Prosen*, Lucija Zupančič-Kralj, Jože Marsel

Department of Chemistry and Chemical Technology, University of Ljubljana, Aškerčeva 5, 61000 Ljubljana, Slovenia

First received 5 November 1994; revised manuscript received 15 December 1994; accepted 30 December 1994

Abstract

A clean-up procedure and high-performance liquid chromatographic conditions were optimized for the determination of triazines in drinking and surface water. Two extraction systems were tested: off-line solid-phase extraction (SPE) with C_{18}-bonded silica gel cartridges and on-line SPE with PLRP-S (styrene–divinylbenzene copolymer) preconcentration cartridges. The on-line SPE procedure was chosen for further work. Chromatographic conditions were optimized for UV absorbance and particle beam (PB) MS detection. The LC–UV analytical system with on-line preconcentration showed excellent linearity over the concentration range tested and low detection limits (below 0.05 μg/l) for drinking water. With preconcentration from large volumes of water, some triazines and other pesticide pollutants could be detected in drinking and river water by PB-MS. Quantification was achieved by means of the standard addition method. For soil samples, the extraction procedure was off-line and more elaborate.

1. Introduction

Environmental pollution with pesticides is of major public concern and maximum allowable concentrations have been set for drinking water and for surface water, which is often a source of drinking water. In the European Community, the upper limit for the presence of an individual pesticide in drinking water is set at 0.1 and at 0.5 μg/l for the total pesticide content [1]. In surface water, these limits are about an order of magnitude higher (1–3 μg/l). Such strict limits imply lower limits of detection for analytical methods used for pesticide determination in waters. Recommended limits of detection for drinking water are in the 0.01–0.02 μg/l range [1].

Although capillary gas chromatography (GC) is the method most often used for pesticide determinations in environmental samples, it is not a suitable technique for some analytes because of their thermal lability or polarity. Therefore, liquid chromatography (LC) is becoming a method of choice in many instances, particularly for the determination of polar compounds and for screening purposes [2]. The most common mode of detection is with a UV–visible absorbance detector, preferably a diode-array detector, which offers the advantage of recording the UV spectrum of each compound and comparing it with those from a library [2,3].

Unfortunately, LC cannot be as easily coupled

* Corresponding author.

☆ Presented at the *International Symposium on Chromatographic and Electrophoretic Techniques, Bled, Slovenia, 10–13 October 1994.*

0021-9673/95/$09.50
SSDI 0021-9673(95)00015-1

as GC with MS. There are various different LC–MS interfaces available, but so far three types have proved to be the most useful in environmental analysis: thermospray (TSP), particle beam (PB) and atmospheric pressure ionization (API) [1]. Among these, only PB offers the advantage of both the electron impact (EI) and chemical ionization (CI) modes, and therefore the possibility of direct comparison of the recorded spectrum with library spectra, as is commonly accomplished in GC–MS analysis. Although there are some drawbacks to the use of PB, such as its reported non-linearity, matrix effects and lack of sensitivity, procedures employing LC–PB-MS analysis have recently been included in US Environmental Protection Agency (EPA) analytical protocols for pesticide analysis [4].

Another important advantage of LC determination of water contaminants is the ease of coupling with on-line preconcentration techniques for water samples [5]. These techniques have gained in popularity in the last few years because they can readily be automated [6] and offer greater sensitivity, less contamination and analyte loss than off-line solid-phase extraction techniques or even classical liquid–liquid extraction of water samples [7]. Although most of the papers dealing with on-line SPE–LC analysis use UV absorbance detection for pesticides, recently there have appeared several applications using PB-MS [8] or TSP-MS detection [9].

In this work, the target compounds were triazines, which are well known herbicides. Their structures together with some chemical constants important for their behaviour are shown in Fig. 1. Some of them, especially atrazine, have become major pollutants of ubiquitous presence owing to their widespread use in agriculture and for other purposes [2]. Besides environmental waters, most pollution with triazines occurs in soil. The higher residual concentrations in soils after spraying of crops prevent crop rotation in successive years [10], and also represent a threat to ground waters. Atrazine especially has a high leaching potential [2]. Triazines are sufficiently volatile and thermally stable enough to be determined by GC, but LC has also proved to be

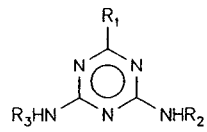

Name	R_1	R_2	R_3	M_w	pK_a	P_{ow}
atrazine	—Cl	$-CH(CH_3)_2$	$-CH_2CH_3$	215,7	1,7	2,57
simazine	—Cl	$-CH_2CH_3$	$-CH_2CH_3$	201,7	1,7	2,00
cyanazine	—Cl	$-C(CH_3)_2$ | CN	$-CH_2CH_3$	240,7	1,0	1,73
terbutylazine	—Cl	$-C(CH_3)_3$	$-CH_2CH_3$	229,7	2,0	3,04
ametryn	$-SCH_3$	$-CH_2CH_3$	$-CH(CH_3)_2$	227,3	4,1	3,07
prometryn	$-SCH_3$	$-CH(CH_3)_2$	$-CH(CH_3)_2$	241,4	4,1	3,41
dipropetryn	$-SC_2H_5$	$-CH(CH_3)_2$	$-CH(CH_3)_2$	255,4	NA	NA

Fig. 1. Structures, molecular masses, ionization constants (pK_a) and *n*-octanol–water partition coefficients (P_{ow}) for target triazine herbicides.

equally applicable [11]. Some papers have been published dealing with the determination of triazines in water with on-line preconcentration coupled to LC and with UV absorbance [12,13] and TSP detection [14,15], whereas the possibility of detecting triazines by PB-MS has been only partially examined [16, 17].

The aim of this work was to compare the off-line and on-line SPE of triazines from water samples and to optimize the extraction procedure for soil samples. Subsequent analysis was performed by LC with UV absorbance detection and PB-MS detection was also tested. Combining these two modes of detection is useful because of the low detection limits that can be achieved with UV absorbance detection, while PB-MS detection offers confirmation of the presence of a pesticide in unknown samples.

2. Experimental

2.1. Materials

Triazine standards of 98–99% purity were obtained from Riedel-de Haën (Seelze, Germany). A stock standard solution of a mixture of triazines was prepared in acetonitrile at a con-

centration of 50 mg/l every 2 months and kept in a refrigerator. No decomposition of triazines was observed during that time. Methanol and acetonitrile were of LC-gradient grade from Merck (Darmstadt, Germany). Ethyl acetate was 99.5% pure from Carlo Erba (Milan, Italy). Acetone was ≥99.7% pure "Baker analysed" HPLC reagent grade from J.T. Baker (Deventer, Netherlands). LC-grade water was obtained by purifying distilled water with a Milli-Q water purification system (Millipore, Bedford, MA, USA). Other reagents used, such as ammonium acetate, sodium sulphate, dilute ammonia solution and dilute hydrochloric acid solution, were of analytical-reagent or prepared from analytical-reagent grade reagents.

Solid-phase extraction cartridges used for off-line extraction were Bakerbond disposable cartridges from J.T. Baker packed with 3 g of C_{18} Polar Plus silica gel. SP extraction precolumns for on-line use were 10 × 2.0 mm I.D. cartridges packed with styrene–divinylbenzene (PLRP-S) copolymer of 15–25-μm particle size from the Prospekt method development set from Spark Holland (Emmen, Netherlands). The cartridge holder was purchased from Spark Holland. Anion-exchange cartridges were 3-ml Supelclean LC-SAX SPE tubes (Supelco, Bellefonte, PA, USA).

The LC analytical column was 150 × 3.0 mm I.D., laboratory packed with 5-μm particle size Hypersil ODS from Hewlett-Packard (Palo Alto, CA, USA). Helium used for PB operation was 99.996% pure from Messer Griesheim (Gumpoldskirchen, Austria).

For calibration a tap water sample and weakly polluted river water were spiked with triazines. River water was filtered before extraction through a dense-pore laboratory filter-paper.

2.2. Off-line SPE sample preparation

The SPE cartridge was preconditioned with 10 ml of methanol and 10 ml of LC-grade water. A 250-ml volume of water sample was loaded on the cartridge. The pH of the sample was adjusted before extraction with dilute HCl or dilute ammonia solution. After sample loading, the cartridge was rinsed with 10 ml of LC-grade water and partially dried by passing air through it. Analytes were eluted with 10 ml of ethyl acetate. Residual water in the eluate was removed by drying with sodium sulphate. The ethyl acetate eluate was evaporated under a stream of nitrogen on a water-bath (ca. 50°C). The analytes were redissolved in 0.1 ml of acetonitrile and injected into the LC system.

2.3. On-line SPE sample preparation

The experimental set-up used for on-line SPE was comparable to similar systems [2,7,8]. The cartridge was conditioned with 10 ml of acetonitrile and rinsed with the mobile phase prior to preconcentration in order to avoid initial loss of analytes. The sample delivery pump and attached tubes were first rinsed with sample and then 200 ml of sample were passed through the cartridge at a flow-rate of 6 ml/min. After preconcentration, the analytes were eluted from the cartridge to the analytical column with mobile phase in the backflush mode.

2.4. Chromatographic conditions

The mobile phase pump and sample delivery system consisted of a ConstaMetric III pump from LDC Analytical, Milton Roy (Riviera Beach, FL, USA). The mobile phase was acetonitrile–0.1 *M* ammonium acetate solution (pH 7) (1:1) and the flow-rate was set to 0.4 ml/min. The variable-wavelength UV–visible absorbance detector was a SpectroMonitor 3100 from LDC Analytical, Milton Roy and was set to 240 nm. The manual injection valve equipped with a 20-μl sample loop and a six-port switching valve were obtained from Rheodyne (Cotati, CA, USA). Chromatograms were recorded with a computing integrator (Model 4100, Milton Roy). For quantification, peak areas were used.

2.5. Particle beam and mass spectrometer conditions

For coupling of LC with MS, a particle beam interface was used (Model 59980B, Hewlett-

Packard). Its operating conditions were optimized by flow injection of 1 μg of atrazine and monitoring the response with a mass spectrometer in the electron impact (EI) ionization mode and selected-ion monitoring (SIM) at m/z 200. Parameters optimized were helium pressure, nebulizer position, desolvation chamber temperature and ion source temperature. Their values were set to 50 psi (345 kPa), position 9, 60°C and 250°C, respectively.

The mass spectrometer was an HP 5989A MS-Engine (Hewlett-Packard). The instrument was operated in the EI ionization mode at a filament emission of 300 mA and an electron energy of 70 eV. Spectra of triazines were recorded in the scan mode from m/z 50 to 400. For quantification, areas of the base peaks in the extracted ion chromatograms were measured.

2.6. Soil extraction procedure

All soil samples were provided by the Agricultural Institute, Ljubljana. Soils were air-dried, finely ground and homogenized.

Uncontaminated soil from the Slovenian Alps was suspended in an acetone solution of an appropriate amount of triazines. The suspension was then allowed to air-dry for ca. 24 h.

A 10-g amount of soil (spiked or sample) was mixed with 20 ml of LC-grade water and extracted on an ultrasonic bath for 15 min. To the suspension, 20 ml of acetone were added and the mixture was ultrasonically extracted for 15 min. The suspension was centrifuged for 10 min. The clear, brown-yellow supernatant was evaporated under a stream of nitrogen until less than 20 ml of aqueous solution was left (partial adsorption of water on the soil particles). The residual aqueous solution was loaded on a preconditioned C_{18} disposable SPE cartridge. The cartridge was rinsed with 10 ml of LC-grade water and partially dried. Triazines were eluted with 10 ml of ethyl acetate. Part of the brown substances (presumably humic acids) retained on the cartridge was also eluted. The eluate was dried with sodium sulphate and cleaned on an SAX disposable SPE cartridge, preconditioned with 2 ml of LC-grade water, 2 ml of methanol and 2 ml of ethyl acetate. Coloured ionic substances were retained, while triazines passed through the cartridge. The colourless eluate was evaporated under a stream of nitrogen on a water-bath (ca. 50°C) and the residue was dissolved in 0.1 ml of acetonitrile and injected into the LC system.

3. Results and discussion

3.1. Chromatographic conditions

The target compounds were triazines differing minimally in chemical structure and properties, as shown in Fig. 1. It was necessary to find a suitable isocratic mobile phase for their separation, recommended also for the PB interface to the MS system.

Recently, the RP chromatographic behaviour of triazines was investigated [11]. It was stated that a mobile phase with an ion-pairing reagent (sodium dodecyl sulphate) gave a better separation than a buffer–organic solvent mobile phase. Owing to its insufficient volatility for use with the PB, an ion-pairing reagent could not be used, but we found a much better separation of almost the same set of triazines with an acetonitrile–buffer system. If no buffer was added to the mobile phase, the compounds were less well separated.

Ammonium acetate solution was added to the mobile phase because it reportedly increased the transport of analytes through the PB interface [18]. In previous work [17], the addition of ammonium acetate did not significantly contribute to the noise in MS-generated chromatograms when an EI scan was performed above m/z 64. In our case, the noise was very high, thus increasing the limits of detection, whereas the noise was significantly lower when using LC-grade water–acetonitrile as the mobile phase. The pH of the mobile phase did not have any significant impact on the separation of compounds and was set to neutrality.

3.2. Optimization of off-line SPE conditions

The initial off-line SPE conditions were those recommended by the cartridge producer. The elution solvent was methanol and the cartridge

Table 1
Triazine recoveries from tap water: influence of sample pH and NaCl addition (2 g/l)

Compound	Recovery (%)						
	Off-line SPE			On-line SPE			
	pH 3–4	pH 6–7	pH 9–10	pH 3–4	pH 6–7	pH 9–10	Salt added
Atrazine	89	87	93	50	68	96	83
Ametryn	36	79	140	60	79	77	80
Terbutylazin	90	126	133	89	110	94	93

Off-line SPE: C_{18} cartridge, theoretical amount on analytical column 100 ng. On-line SPE: PLRP-S cartridge, theoretical amount on analytical column 200 ng.

was to be thoroughly dried prior to elution. However, we found drying of the cartridge to be very time consuming and not entirely successful. The elution solvent was therefore changed to ethyl acetate, which is immiscible in water and thus amenable to drying of residual water by means of sodium sulphate addition. A similar procedure has already been used by other workers [10,19].

The influence of the sample pH on the analyte recovery was also tested. The pH of the samples was adjusted to ca. 3, 7 and 9. The recoveries at neutral and basic pH were essentially the same, but those from acidic samples were lower for certain triazines, as shown in Table 1. This implies decreased retention of protonated species on the C_{18}-bonded silica gel material. Breakthrough of compounds was also tested with up to 500 ml of sample and no loss of analytes at this volume was found. Breakthrough volumes for simazine and atrazine on a C_{18} cartridge have been reported to be more than 1 l [10]. The usual volume of sample preconcentrated was set to 250 ml as a compromise between time and sensitivity.

3.3. Optimization of on-line SPE conditions

The conditions for on-line SPE are strongly influenced by the chromatographic conditions previously adjusted. In our case, the recoveries of less polar analytes such as prometryn and dipropetryn were lower than those using off-line SPE cartridges, as can be seen from Table 2. Although a different sorbent was used, we explain these lower recoveries by incomplete elution of these less polar analytes from the cartridge owing to an insufficient percentage of organic solvent in the mobile phase. If the same on-line SPE cartridge was used several times, a

Table 2
Comparison of extraction recoveries and repeatabilities for target triazines in tap water using off-line and on-line SPE ($n = 4$).

Compound	Off-line SPE		On-line SPE	
	Recovery (%)	Repeatability (%)	Recovery (%)	Repeatability (%)
Cyanazine	86	±7	102	±6
Simazine	102	±6	93	±9
Atrazine	124	±10	96	±10
Ametryn	85	±14	82	±6
Terbutylazin	128	±18	97	±2
Prometryn	113	±21	74	±3
Dipropetryn	100	±8	74	±6

Sample volume: 250 ml off-line SPE, 200 ml on-line SPE. Triazine concentration in sample: 1 μg/l.

regeneration step following the elution with mobile phase was necessary. Pure acetonitrile was passed through the cartridge before the next preconcentration in order to ensure complete removal of residual substances.

The influence of the sample pH and the addition of a neutral salt (sodium chloride) to the sample before extraction was also studied. There was a decrease in recoveries for some compounds at acidic sample pH, while NaCl addition had no significant effect on the recoveries, as shown in Table 1. Neutral pH was chosen for further work, as it was also advisable in order to avoid interferences from humic substances [20].

No breakthrough of analytes was observed up to a volume of 500 ml, and 200 ml of sample were found to be sufficient for quantification purposes with a UV absorbance detector.

3.4. Comparison of off-line and on-line sample preparation procedures

The two most commonly used sorbent materials for both types of extraction were compared. Although C_{18}-bonded silica gel is sometimes used in on-line SPE, its use has been widely superseded by styrene–divinylbenzene copolymer material, mainly because of its higher breakthrough volumes for more polar compounds [20]. In off-line extraction procedures, this polymer is less often used and has only recently gained in popularity [1].

The recoveries and repeatabilities for both types of extraction are compared in Table 2. The recoveries for prometryn and dipropetryn are lower with PLRP-S cartridges for the reasons discussed above but, in general, the recoveries are higher for PLRP-S cartridges and also the repeatability is better, as there is less sample manipulation in the on-line process. Triazines are moderately volatile compounds and some loss may occur during the evaporation step in the off-line SPE procedure.

In order to reach the same detection limit with both sample preparation methods, higher volumes of water sample should be preconcentrated in the off-line SPE procedure, as only part of the final extract is injected on to the LC column, which implies a longer sample preparation process. Even with very similar sample volumes for preconcentration (250 ml off-line and 200 ml on-line), the off-line procedure was found to be more time consuming and tedious, as it required the attention of the operator, which was not necessary in the on-line process, although it was not automated. Ease of automation is one of the main advantages of on-line SPE [7], although off-line SPE can also be automated by means of robotization [10]. The advantage of off-line SPE is its greater flexibility in the choice of elution solvents and in impurity removal [7].

Owing to its inherent simplicity of operation and better repeatability, on-line SP extraction was used for further work. However, the modified off-line procedure was applied for isolation and clean-up of triazines from soil samples, which will be discussed later.

3.5. UV detection of triazines in water

The performance of the method was checked by analysing spiked tap water. Fig. 2a shows a typical chromatogram of tap water spiked with triazines. The linearity was very good ($r^2 = 0.9986–1.000$) and the limits of detection (signal-to-noise ratio = 3) were below 0.05 μg/l and most of them were in the range recommended [1].

For river water, the interference peak at the beginning of the chromatogram was much higher and therefore strongly interfered with the determination of cyanazine and simazine, which elute first, as can be seen from Fig. 2b. Other triazines also showed higher limits of detection, while dipropetryn could not be determined in river water because of its co-elution with an impurity present in the water. Better limits of detection could be achieved by including an additional clean-up step in the preconcentration procedure, but this implied a much more complicated system with additional pumps and valves.

3.6. Particle beam-mass spectrometric results

Although it has been reported that some triazines can be determined by PB-MS [16,17], in our case the performance of the PB-MS system for the detection of triazines was not satisfactory.

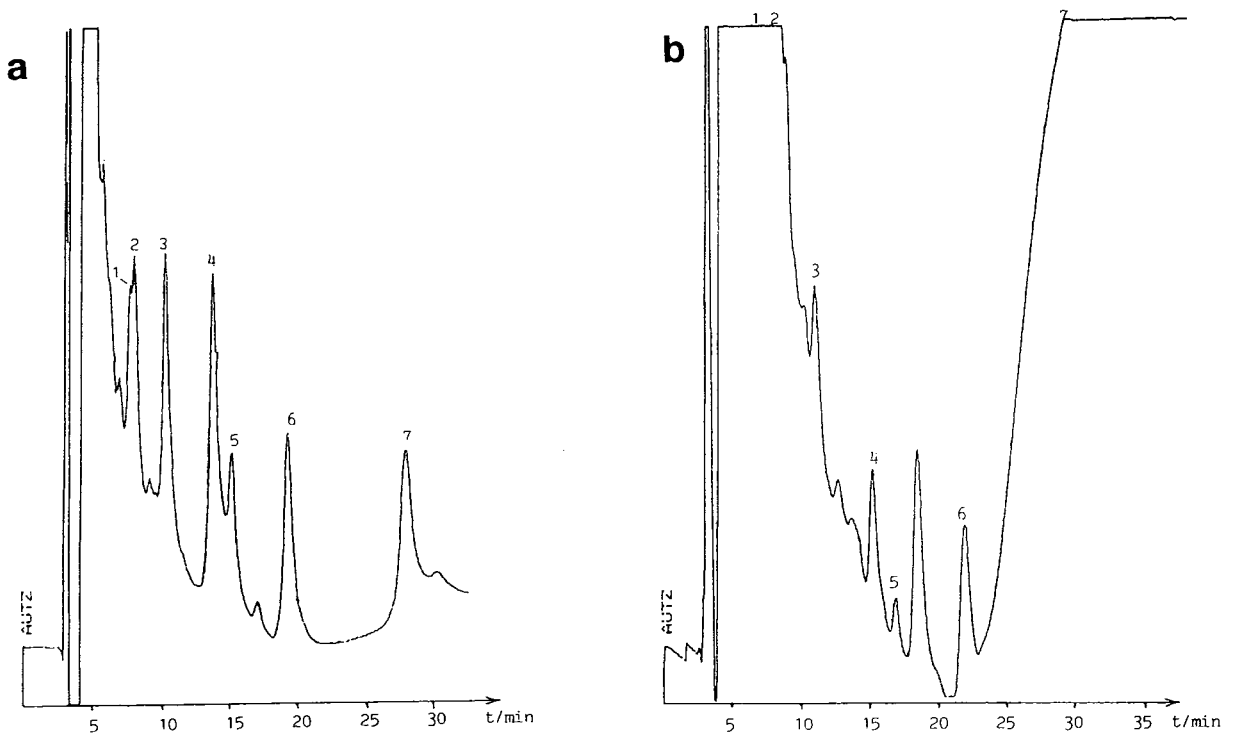

Fig. 2. UV absorbance chromatograms of preconcentrated spiked water samples. (a) Tap water, 0.2 μg/l triazines, 200 ml; sensitivity 0.005 AUFS, detector attenuation 6. (b) River water, 0.2 μg/l triazines, 200 ml; sensitivity 0.02 AUFS, detector attenuation 6. Peaks: 1 = cyanazine; 2 = simazine; 3 = atrazine; 4 = ametryn; 5 = terbutylazin; 6 = prometryn; 7 = dipropetryn.

There was significant peak broadening, as can be observed in Fig. 3, for an injected standard solution compared with the chromatograms in Fig. 2a and b recorded with a UV absorbance detector. The sensitivity was low, typical limits of detection when injecting standard solutions being in the range 2–5 mg/l. Addition of ammonium acetate to the mobile phase did not significantly improve the transport of analytes through the PB interface.

However, when analyses were performed with on-line SPE–LC connected to the PB-MS system, a significant matrix effect could be observed when processing preconcentrated water samples. Quantification was thus best achieved by the standard addition method.

River and drinking water samples were analysed with the on-line SPE–HPLC–PB-MS coupled system. In Table 3, calibration parameters, ranges of linearity and limits of detection are given for the target compounds in drinking water. It is evident that because of high limits of detection, higher volumes of water, typically 300–600 ml, had to be preconcentrated in order to achieve sufficient sensitivity with PB-MS detection for real samples.

In water from a highly polluted stream flowing through an agricultural area, atrazine was detected at the level of 0.3 ± 0.1 μg/l.

In drinking water, an unknown peak was detected, which was subsequently identified as the herbicide bromacil. In Fig. 4, an extracted ion chromatogram of bromacil and a comparison of spectra are shown. The presence of this compound was further confirmed with a bromacil standard. The concentration measured was 0.2 ± 0.1 μg/l.

3.7. Soil analysis results

For pesticide separation from soil before clean-up procedures (including SPE), Soxhlet

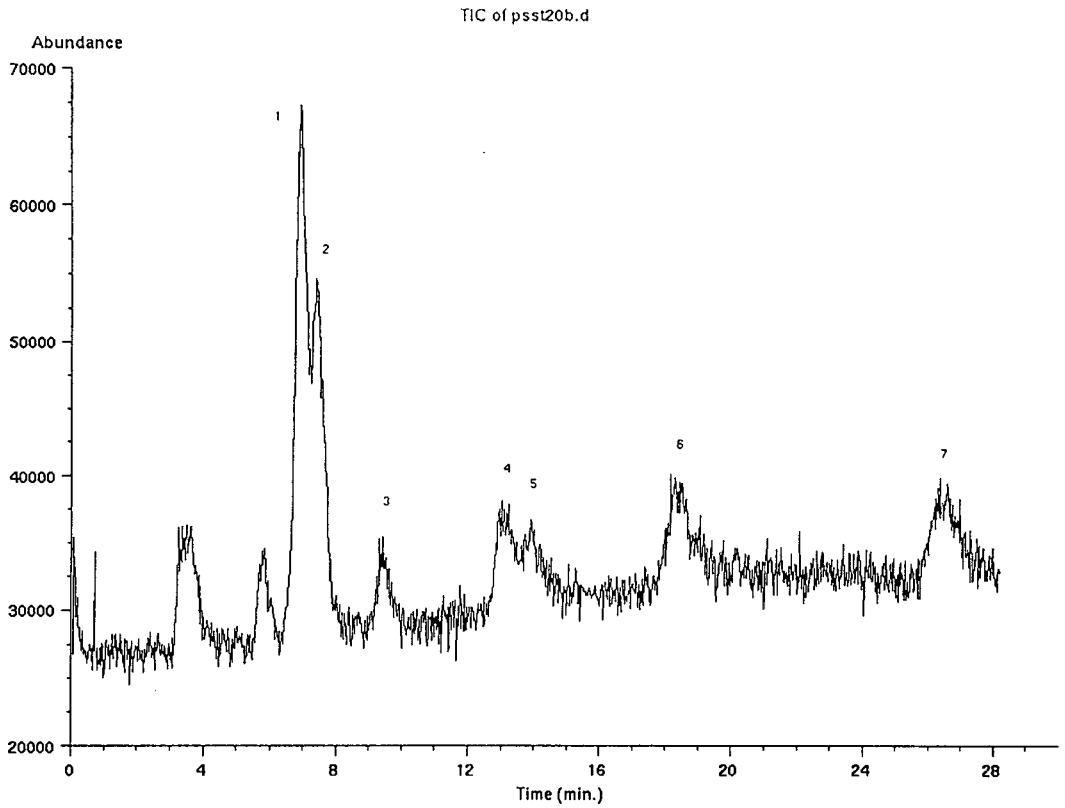

Fig. 3. Total ion chromatogram (scan range from m/z 50 to 400) of a standard solution of pesticides in acetonitrile, 400 ng injected. Peaks as in Fig. 2.

extraction, ultrasonic extraction and supercritical fluid extraction are mostly used. They were found to be comparable in recoveries, while the repeatability was best with supercritical fluid extraction [21]. However, in Soxhlet and ultrasonic extraction, the choice of solvent is very

Table 3
Calibration parameters, ranges of linearity and limits of detection (LOD) (signal-to-noise ratio = 3) for the determination of target triazines by LC–PB-MS

Compound	m/z for quantification	Calibration graph[a]	r	Linearity range (μg/l)	LOD (μg/l)
Cyanazine	225	$y = 39.8x - 1.6$	0.9987	0.2–5.0	0.2
Simazine	201	$y = 160.2x - 49.2$	0.9906	0.2–2.0	0.4
Atrazine	200	$y = 29.9x - 10.4$	0.9866	0.2–5.0	0.7
Ametryn	227	$y = 21.9x + 6.1$	0.9995	0.5–5.0	0.2
Terbutylazin	214	$y = 15.0x - 2.7$	0.9996	0.2–5.0	0.2
Prometryn	184	$y = 26.4x - 1.7$	0.9877	0.2–5.0	0.7
Dipropetryn	255	$y = 23.3x - 4.5$	0.9625	0.2–5.0	1.2

On-line preconcentration of 200 ml of spiked drinking water. Full-scan conditions (m/z from 50 to 400), base peak quantification.
[a] y = in arbitrary units; x = in μg/l.

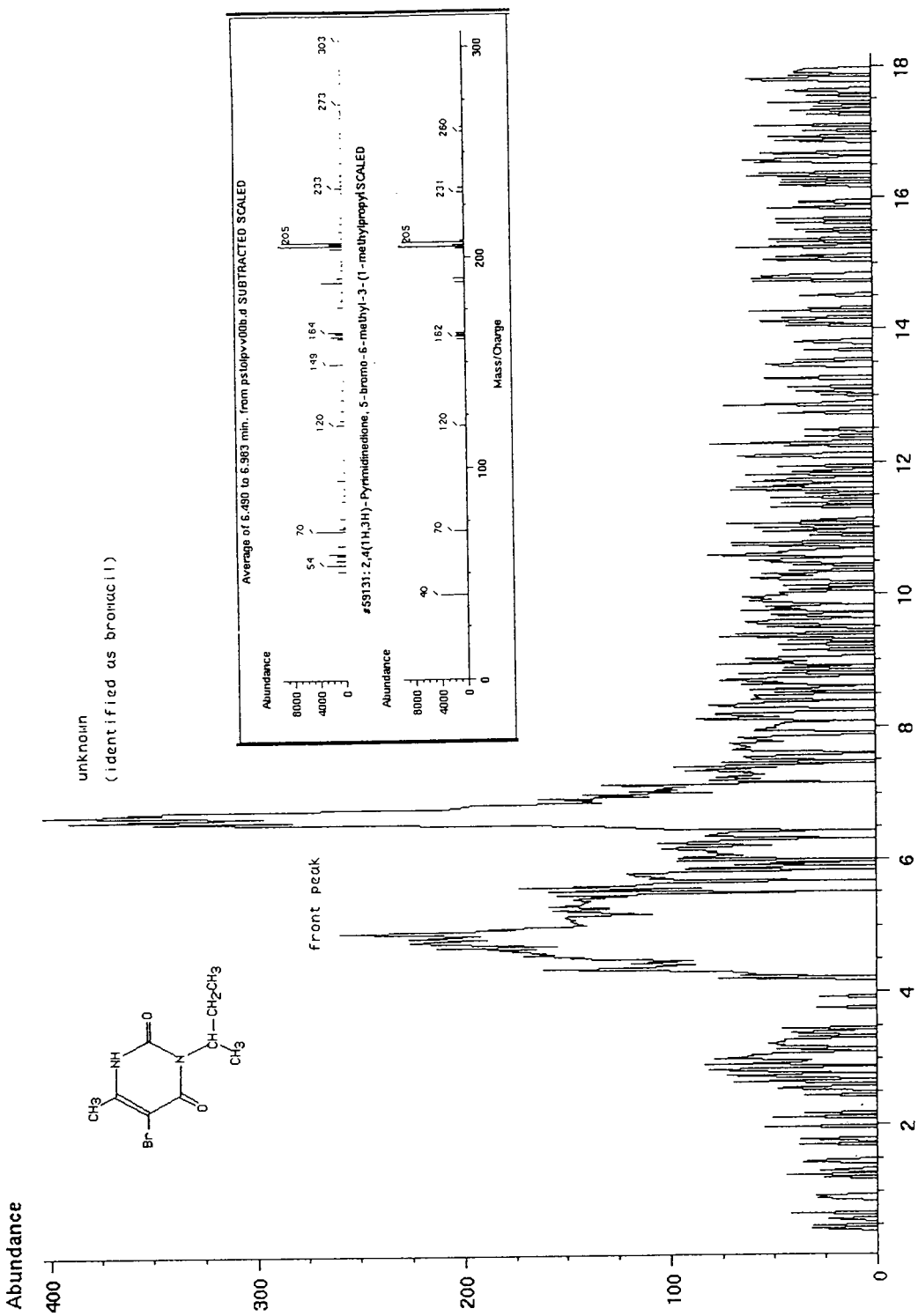

Fig. 4. Extracted ion chromatogram (m/z 207) of an on-line preconcentrated 500-ml sample of drinking water. Inset: comparison of unknown peak spectrum (scan range from m/z 50 to 400) with the spectrum of the herbicide bromacil from a library.

important. As we decided to use C_{18} SPE cartridges for further clean-up of the sample extract, the percentage of organic solvent in the extract applied to the cartridge should be as low as possible in order to allow complete retention of analytes on the C_{18} cartridge [10]. Therefore, all traces of organic solvent should be evaporated before the SPE procedure.

Methanol is the solvent most frequently used for soil extraction, either alone or in mixtures with other solvents or water. However, we decided to use acetone–water, which has been reported to be successful when extracting soil by sonication [19]. The main advantage of acetone over methanol is its greater volatility.

The SPE procedure was the same as for water samples. The ethyl acetate eluate was light brown, indicating a moderate content of other soil components, presumably humic acids. These compounds were removed by passing the ethyl acetate eluate through a strong anion-exchange cartridge, where triazines were not retained.

In spite of several clean-up steps, many interferences were still present in the UV absorbance chromatogram, and therefore some of the triazines could not be quantified in this way. In the PB-MS analysis, the detection limits were too high to detect triazines in soil extracts. Recoveries of the overall extraction procedure ranged from 45% (terbutylazine) to 120% (atrazine).

In the PB-MS analysis of cornfield soil samples, we were not able to detect any triazines, but some other pesticides were identified, e.g., chloromethylaniline and the herbicide chlorotoluron.

4. Conclusions

On-line solid-phase extraction demands less sample manipulation and is simpler than off-line SPE. It is more convenient for the analysis of water samples, while soil samples are better processed using off-line SPE. UV absorbance detection of triazines is sensitive enough, but lacks confirmation, while PB-MS detection lacks sensitivity for triazines, as typical limits of detection for drinking water samples are in the 0.2–1.2 μg/l range. This can be overcome by preconcentrating higher volumes of sample or, alternatively, by using SIM. However, this implies losing information about other pollutants present in environmental samples, as the LC–PB-MS system serves also as a powerful tool for the detection and identification of unknown contaminants.

References

[1] D. Barceló, J. Chromatogr., 643 (1993) 117.
[2] I. Liska, E.R. Brouwer, A.G.L. Ostheimer, H. Lingeman and U.A.Th. Brinkman, Int. J. Environ. Anal. Chem., 47 (1992) 267.
[3] C. Schlett, Fresenius' J. Anal. Chem., 339 (1991) 344.
[4] C.S. Creaser and J.W. Stygall, Analyst, 118 (1993) 1467.
[5] D. Barceló, Analyst, 116 (1991) 681.
[6] J. Slobodnik, E.R. Brouwer, R.B. Geerdink, W.H. Mulder, H. Lingeman and U.A.Th. Brinkman, Anal. Chim. Acta, 268 (1992) 55.
[7] I. Liska, J. Chromatogr., 655 (1993) 163.
[8] H. Bagheri, J. Slobodnik, R.M. Marcé Recasens, R.T. Ghijsen and U.A.Th. Brinkman, Chromatographia, 37 (1993) 159.
[9] S. Chiron, E. Martinez and D. Barceló, J. Chromatogr. A, 665 (1994) 283.
[10] M.S. Mills and E.M. Thurman, Anal. Chem., 64 (1992) 1985.
[11] G. Sacchero, S. Apone, C. Sarzanini and E. Mentasti, J. Chromatogr. A, 668 (1994) 365.
[12] V. Coquart and M.-C. Hennion, J. Chromatogr., 585 (1991) 67.
[13] V. Coquart and M.-C. Hennion, J. Chromatogr., 553 (1991) 329.
[14] H. Bagheri, E.R. Brouwer, R.T. Ghijsen and U.A.Th. Brinkman, J. Chromatogr., 647 (1993) 121.
[15] S. Chiron, S. Dupas, P. Scribe and D. Barceló, J. Chromatogr. A, 665 (1994) 295.
[16] A. Cappiello, G. Famiglini and F. Bruner, Anal. Chem., 66 (1994) 1416.
[17] R.M. Marcé, H. Prosen, C. Crespo, M. Calull, F. Borrull and U.A.Th. Brinkman, J. Chromatogr. A, 696 (1995) 63.
[18] J.S. Ho, T.D. Behymer, W.L. Budde and T.A. Bellar, J. Am. Soc. Mass Spectrom., 3 (1992) 662.
[19] M.J. Redondo, M.J. Ruiz, R. Boluda and G. Font, Chromatographia, 36 (1993) 187.
[20] I. Liska, E.R. Brouwer, H. Lingeman and U.A.Th. Brinkman, Chromatographia, 37 (1993) 13.
[21] J.L. Snyder, R.L. Grob, M.E. McNally and T.S. Oostdyk, Anal. Chem., 64 (1992) 1940.

ELSEVIER

Journal of Chromatography A, 704 (1995) 131–139

JOURNAL OF CHROMATOGRAPHY A

Thermospray ionization liquid chromatography–mass spectrometry and chemical ionization gas chromatography–mass spectrometry of hexazinone metabolites in soil and vegetation extracts

Joseph B. Fischer*, Jerry L. Michael

USDA Forest Service, Southern Forest Experiment Station, George W. Andrews Forestry Sciences Laboratory, Devall Drive, Auburn, AL 36849, USA

First received 4 October 1994; revised manuscript received 27 January 1995; accepted 6 February 1995

Abstract

We have used thermospray LC–MS to confirm three highly polar metabolites (A, B, and G) of the herbicide hexazinone [3-cyclohexyl-6-(dimethylamino)-1-methyl-1,3,5-triazine-2,4(1H,3H)-dione], and chemical ionization GC–MS to confirm two other metabolites (D and E) in extracts of soil and vegetation from a forest in the Central Alabama Piedmont. Selected-ion monitoring (SIM) of the protonated molecular ions of metabolite A [3-(4-hydroxycyclohexyl)-6-(dimethylamino)-1-methyl-1,3,5-triazine-2,4(1H,3H)-dione] at mass-to-charge ratio (m/z) 269 and metabolite B [3-cyclohexyl-6-(methylamino)-1-methyl-1,3,5-triazine-2,4(1H,3H)-dione] at m/z 239 gave matrix detection limits (MDLs) of 25 ppb (ng/g) and 50 ppb, respectively, in 10 g vegetation samples. MS quantitation for A and B generally confirmed high-performance liquid chromatography data. SIM of the protonated molecular ion of metabolite G [3-cyclohexyl-6-(methylamino)-1,3,5-triazine-2,4(1H,3H)-dione] at m/z 225 afforded an MDL of 5 ppb in 50 g topsoil samples. Metabolite G was not confirmed above the MDL in any of the soils tested. Chemical ionization GC–MS using methane reagent gas gave strong ion signals for metabolite D [3-cyclohexyl-1-methyl-1,3,5-triazine-2,4,6(1H,3H,5H)-trione] at m/z 226 and 144 and metabolite E [3-(4-hydroxycyclohexyl)-1-methyl-1,3,5-triazine-2,4,6(1H,3H,5H)-trione] at m/z 242, 224, and 144. SIM at these masses afforded MDLs of 50 ppb for D and 400 ppb for E in 10 g vegetation samples.

1. Introduction

The herbicide hexazinone [3 - cyclohexyl - 6 - (dimethylamino) - 1-methyl - 1,3,5 - triazine - 2,4(1H,3H) - dione], marketed by E.I. DuPont de Nemours and Co., under the trade name of Velpar®, is widely used for pine growth release in the Southeastern United States. We recently completed an environmental fate study in the Central Alabama Piedmont in support of reregistration of hexazinone for forestry use in accordance with regulations set forth by the United States Environmental Protection Agency under the Federal Insecticide, Fungicide and Rodenticide Act (40CFR, Part 158.540). Samples from this study were analyzed for ppb (ng/g) levels of the applied herbicide and for all major known metabolites of the parent compound in those

* Corresponding author.

SSDI 0021-9673(95)00168-9

matrices where previous work [1–4] had shown them to occur. All vegetation samples were analyzed for hexazinone and metabolites A [3 - (4 - hydroxycyclohexyl) - 6 - (dimethylamino) - 1 - methyl - 1,3,5 - triazine - 2,4(1H,3H)dione], B [3 - cyclohexyl - 6 - (methylamino) - 1 - methyl - 1,3,5 - triazine - 2,4(1H,3H)dione], C [3 - (4 - hydroxycyclohexyl) - 6 - (methylamino) - 1 - methyl - 1,3,5 - triazine - 2,4(1H,3H)dione], D [3 - cyclohexyl - 1 - methyl - 1,3,5 - triazine - 2,4,6(1H,3H,5H)trione], and E [3 - (4 - hydroxycyclohexyl) - 1 - methyl - 1,3,5 - triazine - 2,4,6(1H,3H,5H)trione]. All soil samples were analyzed for the above and for metabolite G [3-cyclohexyl - 6 - (methylamino) - 1,3,5 - triazine - 2,4(1H,3H)dione], a suspected soil metabolite [5]. The structures of these compounds are shown in Fig. 1.

Our initial analytical challenge was to develop a rugged chromatographic separation giving baseline resolution of all seven analytes. The published method of Holt [6] used packed-column GC coupled with a nitrogen–phosphorus detector, required derivatization with trifluoroacetic anhydride (TFAA), and did not include metabolite G. Attempts to adapt this procedure to capillary GC conditions revealed the production of complex mixtures of products which had not been observed on packed-column GC, possibly due to irreversible adsorption of the partially derivatized byproducts by active sites on the stationary support.

Isocratic reversed-phase HPLC methods have been reported for the analysis of residues of the parent hexazinone in water [7–10], soil [8–10], and plant tissue [10,11], but in these studies no

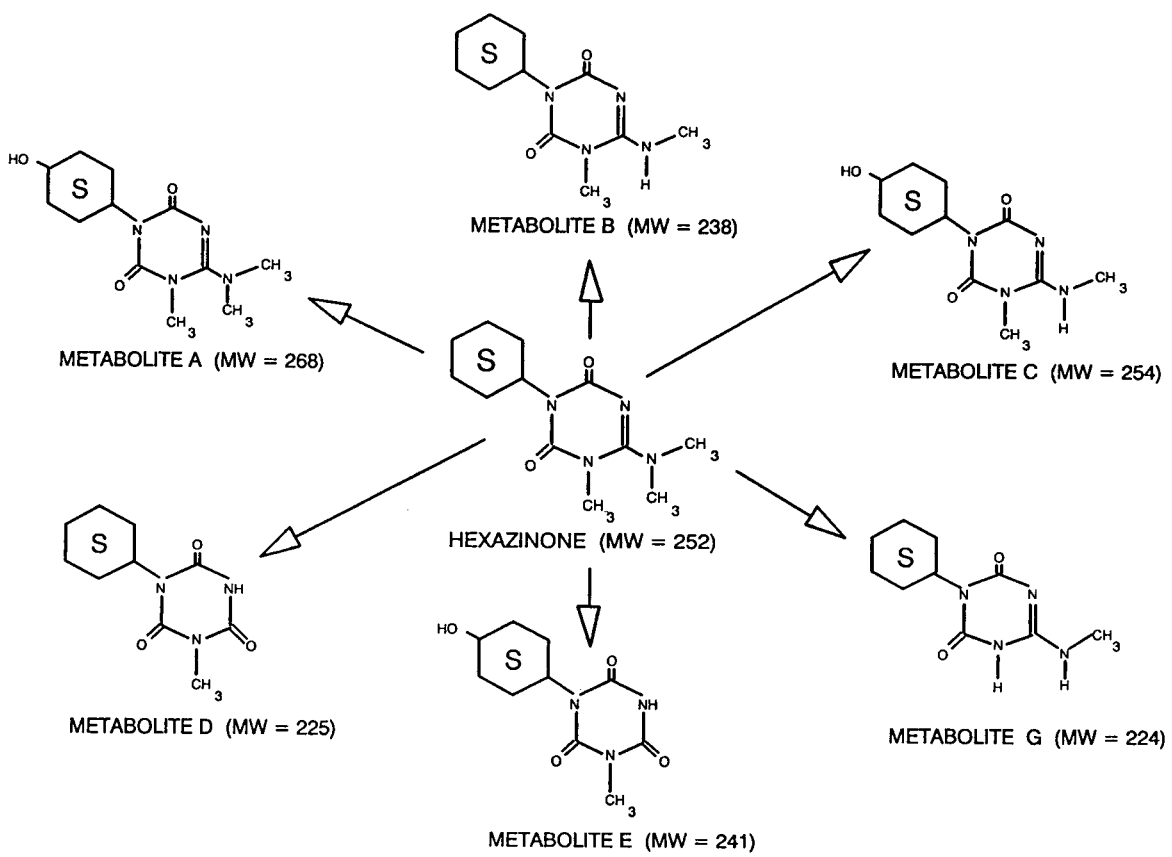

Fig. 1. Hexazinone and its primary soil and vegetation metabolites A through E and G.

attempt was made to simultaneously quantify any metabolites. Earlier work in our laboratory revealed that the range of polarities encompassed by these metabolites is too broad for isocratic elution and that their UV absorbance maxima differ too much for all of them to be detected efficiently at a single wavelength [12]. We therefore developed a reversed-phase gradient elution HPLC separation with time-programmed variable-wavelength UV absorbance detection. A typical chromatogram of a standard mixture of 100 ng each of hexazinone and metabolites A through E and G is shown in Fig. 2. The highly polar 4-hydroxylated cyclohexyl metabolites C, E, and A elute first, followed by the doubly-demethylated metabolite G, then by the singly-demethylated metabolite B, the parent compound, and finally the deaminated metabolite D, which exists almost entirely as the keto-tautomer (i.e., the 1,3,5-trione).

This gradient reversed-phase HPLC separation with programmed variable-wavelength UV absorbance detection, when used in conjunction with a cleanup of the soil and vegetation extracts by treatment with divalent lead [14], was adequate to permit reliable quantitation of most of the analyte components in both matrices.

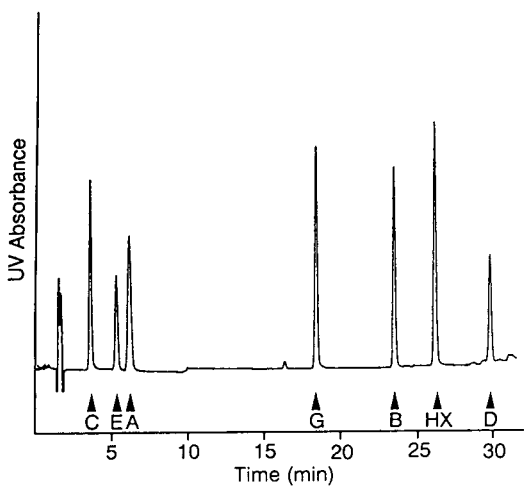

Fig. 2. Gradient HPLC separation of hexazinone and its metabolites with programmed variable-wavelength ultraviolet absorbance detection (chromatographic conditions given in text).

Some uncertainties remained, particularly regarding sporadic high results for metabolite G, which did not correlate with levels of the other analytes and which occurred mainly in surface soil extracts from mid- and toe-slope positions on the Velpar ULW-treated watershed.

Characterization of hexazinone and metabolites A, B, C, D, and E by electron-impact (EI) MS was reported by Reiser et al. [13], but no data was reported for metabolite G. The mass spectra reported were obtained by direct probe or by packed-column GC at the microgram level–lower levels being undetectable except by derivatization with TFAA. Preliminary studies in our laboratory using capillary GC–EI-MS with splitless injection confirmed poor sensitivity for all underivatized metabolites except G, which was not detectable in any amount, even by SIM.

In an effort to avoid derivatization and utilize the power of the reversed-phase HPLC separation already developed, we investigated thermospray ionization as an alternative interface technique for MS confirmation of hexazinone metabolites in soil and vegetation samples. We report on the initial development of thermospray LC confirmation methods for metabolite G in soil samples and for metabolites A and B in forest vegetation samples, as well as their application to actual environmental residue samples from our field study. We also report on the development of a chemical ionization (CI) GC–MS method for the confirmation of metabolites D and E in forest vegetation samples, and the results of its application to the samples from our field study.

2. Experimental

2.1. Materials and methods

Gradient HPLC components

LDC CM4000 multiple solvent delivery system and SM4000 programmable variable-wavelength absorbance detector (LDC Analytical, Riviera Beach, FL, USA), WISP 710B autoinjector (Waters Chromatography Div., Millipore Corp., Milford, MA, USA), Shimadzu CTO-6A column

oven (Shimadzu Scientific Instruments, Columbia, MD, USA), Spectra-Physics SP4400 Chrom-Jet integrator (Spectra-Physics Analytical, Fremont, CA, USA), and Beckman Ultrasphere ODS 150 cm × 4.6 mm I.D. column (Beckman Instruments, San Ramon, CA, USA).

HPLC mobile phases

Solutions: (A) acetonitrile–water (8.5:91.5, v/v); (B) acetonitrile–water (30:70, v/v); (C) acetonitrile–water (70:30, v/v). Gradient: 100% A (0–4 min); 100% A to 100% B (4–26 min); 100% B to 100% C (28–29 min); flush with 100% C (29–38 min); 100% C to 100% A (38–39 min); reequilibrate with 100% A (39–50 min). Total flow-rate, 1.0 ml/min; column temperature, 40°C.

HPLC ultraviolet absorbance detection wavelength program

Wavelengths: 230 nm (0–4.5 min) for metabolite C; 200 nm (4.5–10 min) for metabolites E and A; 230 nm (10–25 min) for metabolites G and B; 245 nm (25–28.5 min) for hexazinone; 200 nm (28.5–33 min) for metabolite D; 0.01 AUFS; plot speed, 0.5 cm/min.

Mass spectrometer

Finnigan MAT 4510B quadrupole mass spectrometer with 9611 gas chromatograph, pulsed positive-ion/negative-ion chemical ionization option, SuperIncos data system, and Finnigan thermospray LC interface. Vaporizer tube fitted with laser-drilled sapphire spray tip (0.0025 inch I.D.).

LC components

Waters M6000A solvent pump with pulse dampener, Rheodyne 7125 loop injector with 20-μl loop, Beckman Ultrasphere-ODS guard column (4.5 cm × 4.6 mm I.D.).

Mobile phases

Metabolite G: methanol–water (30:70, v/v) (0.05 *M* ammonium acetate) pumped at 1.0 ml/min at room temperature (21°C); back pressure 1600–1800 psi.

Metabolites A and B: acetonitrile–water (15:85, v/v) (0.05 *M* ammonium acetate) pumped at 1.0 ml/min at room temperature (21°C); back pressure 1300–1500 psi.

Thermospray operating conditions

Ion source block, 230°C; vaporizer tube, 90°C; aerosol spray, 264°C; repeller electrode, + 30 V; filament off.

MS acquisition parameters

Full scan; mass range 120–300; 0.95 s/scan + 0.05 s bottom settling time; 600 scans/run (10.0 min).

SIM, metabolite G; total scan time, 1.000 s; mass interval 224.567–225.567 acquire 0.839 s; 600 scans/run (10.0 min).

SIM, metabolites A and B; total scan time, 1.000 s; mass intervals 238.572–239.572 acquire 0.419 s, 268.580–269.580 acquire 0.426 s; 600 scans/run (10.0 min).

Gas chromatographic conditions for metabolites D and E

Finnigan 9611 gas chromatograph with heated pass-through capillary MS interface; J&W fused-silica capillary column, 14 m × 0.25 mm I.D., 0.25 μm SE-54 film (J&W Scientific, Folsom, CA, USA); carrier gas, helium at 3.5 psi head pressure, 53 cm/s at 120°C; 1 μl splitless injection at 120°C, purge on at 0.7 min; oven temperature 120°C (1.0 min) to 250°C at 20°C/min, hold to 10.0 min; transfer oven temperature, 250°C; manifold temperature, 90°C.

GC–CI-MS acquisition parameters

Electron energy, 110 eV; ion source temperature, 150°C; source pressure, 1.0 mm Hg.

Full scan; mass range 100–300, 0.95 s/scan + 0.05 s bottom settling time; 500 scans/run (8.33 min).

SIM, metabolites D and E; total scan time 1.000 s, scanning mass intervals 143.543–144.543 (acquire 0.213 s), 223.567–224.567 (acquire 0.210 s), 225.568–226.568 (acquire 0.213 s), and 241.572–242.572 (acquire 0.210 s); 500 scans/run (8.33 min).

Analytical standards

Hexazinone metabolites A (Lot no. T3937-2, 98.4%), B (Lot no. A3928-4, 98.8%), D (Lot no. B2838-6, 99.97%), E (Lot no.T3936-3, 99.9%), and G (Lot no. T4916-2, 99.1%) all supplied courtesy of E.I. DuPont de Nemours and Co. (Wilmington, DE, USA).

Solvents

Acetonitrile, chloroform, methanol, and HPLC grade water (Burdick and Jackson Div., Baxter Diagnostics, Muskegon, MI, USA).

Reagents

Ammonium acetate, 99 + % (Aldrich Chemical Co., Milwaukee, WI, USA) stored in a desiccator over anhydrous calcium sulfate (Drierite, W.A. Hammond Co., Xenia, OH, USA) until ready for use; anhydrous powdered sodium sulfate and granular lead(II) acetate trihydrate (J.T. Baker, Phillipsburg, NJ, USA).

Solid-phase extraction (SPE) columns

Bakerbond SPE no. 7189-07 light load octadecyl (C_{18}), 6-ml HC, Lot no. E13502, packed with 1000 mg reversed-phase octadecylsilane bonded to silica gel (40 μm APD, 60 Å) (J.T. Baker, Phillipsburg, NJ, USA).

2.2. Sample preparation, determination and quantitation

One watershed of 76 hectares (ha) was treated with the liquid formulation Velpar-L at 6 kg active ingredient per hectare (ai/ha). An adjacent watershed of 75 ha was treated with the pellet formulation Velpar-ULW at 6 kg ai/ha. A third watershed (96 ha) was left untreated as a control. Over 1200 soil core samples, and 600 vegetation samples from each of 4 species (blueberry, bracken fern, dogwood, and bunchgrass) were collected from a gridwork of sites throughout these three adjacent watersheds during the 12-month period following application. Soil samples (50 g) were dried, pulverized, extracted with 3–68 ml portions of methanol–water (4:1), evaporated, treated with 2 ml of 1 *M* lead(II) acetate, filtered through GF/B glass fibre paper, concentrated on 1000 mg C_{18} SPE columns, and eluted with methanol. Vegetation samples (10 g) were pulverized with dry ice, dried by blending intimately with 20 g of anhydrous powdered sodium sulfate, extracted with 3–68 ml portions of chloroform, filtered through GF/B glass fibre paper, rotoevaporated into water, treated with 2 ml of 1 *M* lead(II) acetate, filtered through GF/B paper, concentrated on C_{18} SPE columns, and eluted with methanol [14].

Every sample extract injected into the mass spectrometer was compared to a set of external standards of the analyte(s) of interest run the same day. These standards were made up in methanol at concentrations spanning the range from the detection limit to the highest anticipated sample level. Typical calibration standard levels for thermospray analyses of metabolite G in soil samples were 0.5, 2, 5, 20, and 50 ng/g. Typical calibration levels for thermospray analyses of metabolites A and B in vegetation were 1, 10, 100, 200, and 400 ng/g. Typical calibration levels for GC–CI-MS analyses of metabolites D and E in vegetation were 0.5, 1, 2, 5, 10, 20, 50, and 100 ng/g. A full calibration curve was run at the beginning of each day, followed by random single standards after every 4 samples. Minimum matrix detection levels (MDLs) were estimated based on a peak height of three times the background noise level. Responses were nonlinear, especially for CI of metabolites D and E. Calculations assumed quantitative recovery in the extracts.

3. Results and discussion

3.1. Metabolite G in soil samples

Metabolite G has been identified as a potential metabolite of hexazinone in soil [5], but there are no published chromatographic or mass spectral data. A typical HPLC–UV chromatogram of a soil extract appearing to contain metabolite G is shown in Fig. 3. Close examination of many such chromatograms revealed that the retention time of the "G" peak was always 0.1–0.2 min

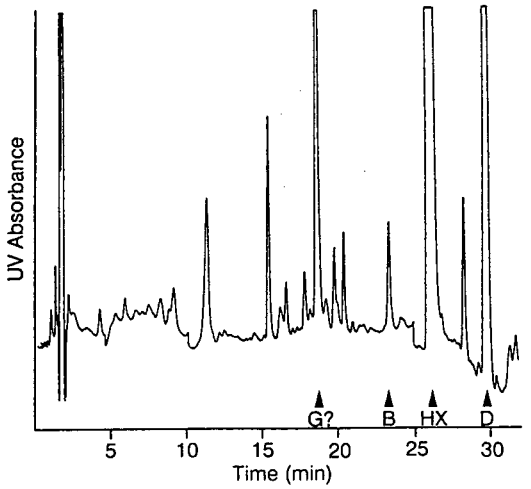

Fig. 3. Extract of hexazinone-treated surface soil. Same chromatographic conditions as Fig. 2.

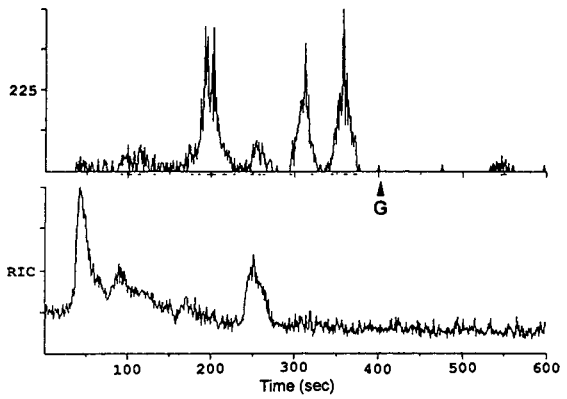

Fig. 4. Full scan thermospray ion chromatogram (1.0 s/scan) of surface soil extract (10-μl injection). Lower trace full scan (mass range 120–300); upper trace single-ion chromatogram (m/z 225). Chromatographic conditions given in Experimental section.

later than that of metabolite G standards chromatographed before and after the sample extract. Reanalysis of some of these samples with detection at a different UV wavelength (200 nm vs. 230 nm) produced a ratio of absorbances (A_{200}/A_{230}) that was about 1.2 as opposed to 2.9 for an authentic metabolite G standard. These facts led to questioning the authenticity of the "G" peak in these soil extracts and called for identity confirmation by an independent technique. As noted above, metabolite G cannot be analyzed by GC–MS without derivatization. It chromatographs well, however, under reversed-phase HPLC conditions, making it a natural candidate for thermospray LC–MS. Under thermospray conditions with a vaporizer tube temperature of 90°C and a repeller voltage of +30 V, metabolite G produces only one ionic species, the protonated molecule at m/z 225. The high noise and low sensitivity characteristic of full scan thermospray operation can be largely eliminated by SIM at m/z 225 only. Metabolite G is insoluble in water and soluble in methanol at room temperature (1 mg/ml), partially reprecipitating at 4°C. Its tendency to reprecipitate may account for the pronounced tailing under thermospray conditions using methanol–water (30:70) (0.05 M NH_4OAc). Less tailing is evident using acetonitrile–water, but interferences appear in soil extracts at m/z 225 which do not occur with methanol–water. A typical full scan thermospray chromatogram of a surface soil extract is shown in Fig. 4 together with the selected-ion scan at m/z 225. No trace of metabolite G is seen at its retention time of 405 s (6.75 min), even though the original HPLC chromatogram (Fig. 3) showed a 630 ppb peak. A rechromatograph of this sample under SIM conditions confirmed that metabolite G is not present above the MDL of 5 ppb. Nearly 200 soil samples that had shown levels of metabolite G greater than 20 ppb under gradient HPLC conditions were reanalyzed using thermospray LC–MS with SIM at 225 m/z. Metabolite G was not detected above the MDL of 5 ppb in any of these samples, even though QC soil samples spiked at 50 ppb consistently gave 60% recoveries. Thus we have not been able to confirm its natural occurrence as a metabolite of hexazinone in soil.

3.2. Metabolites A and B in vegetation samples

Metabolites A and B are the primary metabolites of hexazinone, resulting from hydroxylation (A) or demethylation (B) of the parent compound. They are the easiest of the metabolites to analyze as they can be gas chromatographed without derivatization. Using modifications of the Holt procedure, J.C. Feng and co-workers [15–20] have reported levels of A and B in

Canadian soil and vegetation [20] which track residual hexazinone levels fairly closely. Metabolite B is consistently the most abundant metabolite. We were able to reliably quantify A and B in our soil extracts using gradient HPLC, but vegetation extracts often contained high levels of coextracted coeluting interferences. Metabolites A and B differ greatly in polarity, but can be chromatographed isocratically with an acetonitrile–water (15:85, v/v) (0.05 *M* NH_4OAc) mobile phase. At a vaporizer tube temperature of 90°C and a repeller voltage of +30 V, metabolites A and B, like G, exhibit no decomposition and produce only their protonated molecules at *m/z* 269 for A and *m/z* 239 for B (Fig. 5). SIM at only these two masses affords MDLs of 25 ppb for A and 50 ppb for B. A full scan thermospray LC–MS chromatogram of a typical grass extract is shown in Fig. 6. Calculated levels of metabolites A and B in this sample by HPLC with UV absorbance detection were 4.1 ppm (mg/g) and 14.5 ppm, respectively. Reanalysis of this sample by thermospray-SIM confirmed the presence of both metabolites at roughly these levels. Almost 60 vegetation samples showing high levels of A and/or B on gradient HPLC were reanalyzed by thermospray LC–MS. Quantitation by LC–MS generally confirmed levels quantitated by gradient HPLC. In all cases the presence of metabolite B was confirmed. The presence of metabolite A was confirmed in all samples but two.

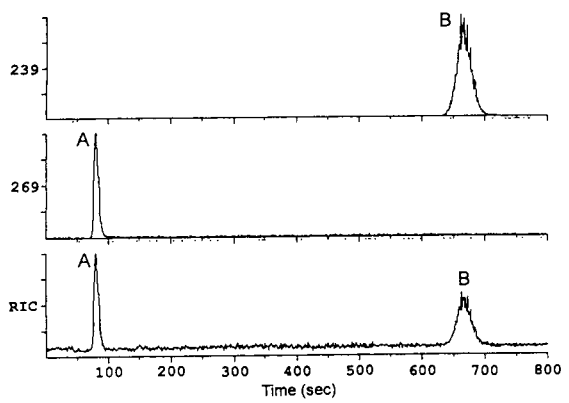

Fig. 5. Full scan thermospray total-ion chromatogram (1.0 s/scan) of a mixed standard of 200 ng each metabolites A and B (conditions given in text). Lower trace full scan (mass range 120–300); middle trace single-ion chromatogram of A (*m/z* 269); upper trace single-ion chromatogram of B (*m/z* 239).

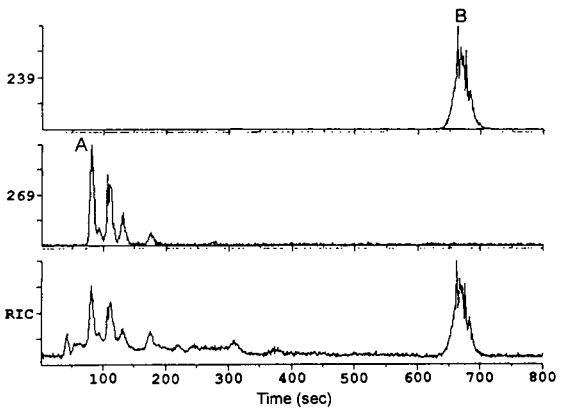

Fig. 6. Full scan thermospray total-ion chromatogram of grass extract with single-ion traces at *m/z* 269 (metabolite A) and *m/z* 239 (metabolite B). All conditions same as Fig. 5.

3.3. Metabolites D and E in vegetation samples

The two deaminated metabolites D and E are exceptionally difficult to detect selectively due to their highly stable 1,3,5-triazine-2,4,6-trione ring structures. Their UV absorbance maxima lie below 200 nm, necessitating detection at this unselective wavelength where many plant coextractives absorb strongly. This places heavy demands on sample cleanup procedures and virtually guarantees coeluting interferences from one or more plant species. Their stable ring structures also make D and E unresponsive to the NPD rubidium bead nitrogen-selective GC detector. We found that D and E exhibit no response to thermospray LC–MS, presumably due to their failure to form association complexes with protons or ammonium ions in aqueous solution. Metabolites D and E can be analyzed by capillary GC–MS but we found that they exhibit very low sensitivities under EI conditions. Neither compound gives a detectable molecular ion. The base peak in both cases is the resonance-stabilized double hydrogen rearrangement ion at *m/z* 144, which was described by Reiser et al. [13]. Full scan EI–MS of splitless

1-μl injections gives on-column detection limits of 10 ng for D and 25 ng for E, corresponding to MDLs of 5000 ppb and 12 500 ppb, respectively, in 10 g vegetation samples–too high for confirmation purposes. SIM at m/z 144 only improves the MDLs to 1000 ppb and 5000 ppb, respectively. We therefore investigated CI as an alternative ionization mode for metabolites D and E because the high ion source pressures and confinement times of CI should greatly increase the probability of ion-yielding collisions. Full scan CI using methane reagent gas at a source pressure of 1.0 mm Hg gave two major ions for metabolite D, the protonated molecule at m/z 226 and the m/z 144 rearrangement ion (see Table 1). CI of metabolite E gave the protonated molecule at m/z 242, the base peak at m/z 224 $[242 - H_2O]^+$, and the m/z 144 rearrangement ion. SIM at masses 144, 224, 226, and 242 afforded MDLs of 50 ppb for D and 400 ppb for E, just adequate for confirmation.

GC–MS-CI-SIM was applied to 56 vegetation samples that had shown high levels of metabolites D and/or E. Fig. 7 shows a typical gradient HPLC chromatogram of a suspect vegetation sample, which exhibited 18.3 ppm of metabolite D and 1.5 ppm of metabolite E. Fig. 8 shows the corresponding CI-SIM chromatogram of this sample, which confirms the presence of both metabolites. Metabolite D was confirmed in all vegetation samples tested, although usually at a lower concentration than observed with HPLC, suggesting the presence of coeluting interferences absorbing at the UV detection wavelength of 200 nm. Metabolite E was confirmed in 23 of the 56 samples tested.

Table 1
Chemical ionization positive-ion mass spectra of hexazinone metabolites D and E

Compound	m/z	Relative abundance	Assignment
Metabolite D	226	100	$[M+H]^+$
	144	25	Rearrangement
Metabolite E	242	36	$[M+H]^+$
	224	100	$[M+H-H_2O]^+$
	144	30	Rearrangement

Conditions: methane reagent gas at source pressure 1.0 mm Hg. Filament ionization at 110 eV. Full scan m/z 100–300 at 1.0 s/scan.

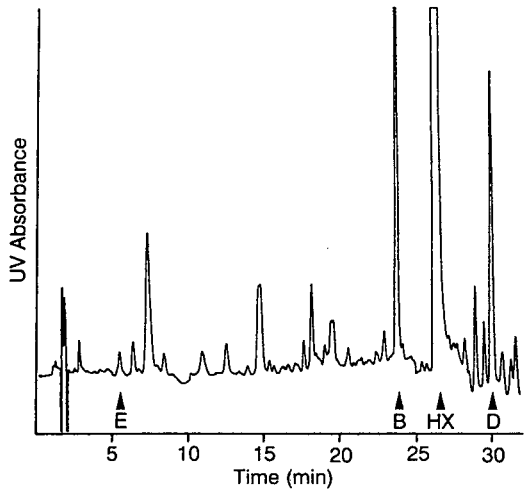

Fig. 7. Gradient HPLC chromatogram of an extract of blueberry leaves and branches from a hexazinone-treated site. Chromatographic conditions same as Fig. 2.

4. Conclusions

We have developed selective, sensitive, and reliable thermospray LC–MS methods for identi-

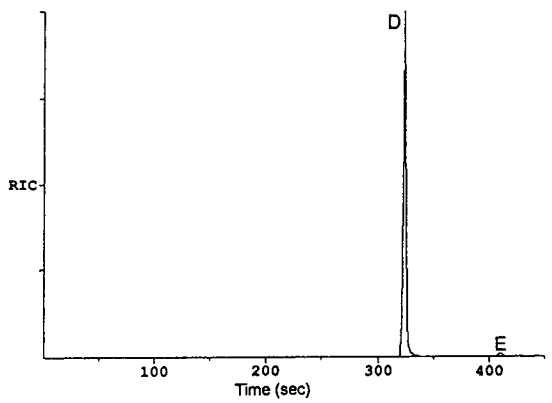

Fig. 8. GC–CI-SIM chromatogram of a 1-μl splitless injection of the same blueberry extract as in Fig. 7. Temperature-programmed GC conditions given in text. Methane reagent gas (1.0 mm Hg) with filament ionization at 110 eV. Acquisition at m/z 144, 224, 226, and 242 (0.21 s each; 1 s/scan).

ty confirmation of three highly polar metabolites of hexazinone (A, B, and G) in samples of forest soil and vegetation from the Southeastern United States. Metabolites A and B were confirmed in four plant species using thermospray LC–MS-SIM at m/z 269 and 239, respectively. MDLs of 25 ppb for A and 50 ppb for B were achieved in 10 g vegetation samples.

Thermospray LC mass spectra are presented for the first time for metabolite G, a suspected metabolite of hexazinone in soil. Soil samples were identified by HPLC with UV detection to contain metabolite G at concentrations above 20 ppb, but when these samples were reanalyzed by thermospray LC–MS-SIM at m/z 225 metabolite G was not detected above an MDL of 5 ppb. Therefore, we were unable to confirm the existence of metabolite G in soil. Metabolites D and E, which have resisted detection by other means including thermospray LC–MS, were confirmed in vegetation samples by GC–MS-CI-SIM at m/z 144, 224, 226, and 242 with MDLs of 50 and 400 ppb respectively. No derivatization was required for any of these procedures.

While thermospray LC–MS has been eclipsed by newer techniques, such as electrospray and atmospheric pressure ionization, we have found thermospray to be a rugged, sensitive, and selective technique for the confirmation of polar and/or thermally-labile small molecules, like herbicide metabolites, in extracts of complex environmental matrices, especially when used in the selected-ion monitoring mode.

Acknowledgements

We wish to thank the E.I. DuPont Agricultural Products Department and the USDA Forest Service Southern Forest Experiment Station for their support of this work.

References

[1] R.C. Rhodes, J. Agric. Food Chem., 28 (1980) 311.
[2] R.C. Rhodes, J. Agric. Food Chem., 28 (1980) 306.
[3] R.C. Rhodes and R.A. Jewell, J. Agric. Food Chem., 28 (1980) 303.
[4] R.C. Rhodes, R.L. Krause and M.H. Williams, Soil Sci., 129 (1980) 311.
[5] E.I. DuPont de Nemours and Co., private communication.
[6] R.F. Holt, J. Agric. Food Chem., 29 (1981) 165.
[7] P.B. Bush, J. Michael, D.G. Neary and K.V. Miller, in W.W. Witt (Editor), Proc. Southern Weed Sci. Soc. 43rd Ann. Mtg., January, 1990, Atlanta, Georgia, p. 184.
[8] D.C. Bouchard and T.L. Lavy, J. Chromatogr., 270 (1983) 346.
[9] D.C. Bouchard, T.L. Lavy and E.R. Lawson, J. Environ. Qual., 14 (1985) 229.
[10] T.L. Lavy, J.D. Mattice and J.N. Kochenderfer, J. Environ. Qual., 18 (1989) 507.
[11] A.E. Smith, J. Agric. Food Chem., 37 (1989) 358.
[12] M.J.M. Wells, in K.C. Van Horne (Editor), Proc. 2nd Ann. Int. Symposium, Sampling Preparation and Isolation Using Bonded Silicas, January 1985, Philadelphia, Pennsylvania, p. 63.
[13] R.W. Reiser, I.R. Belasco and R.C. Rhodes, Biomed. Mass Spectrom., 10 (1983) 581.
[14] J.L. Michael and J.B. Fischer, in press.
[15] J.C. Feng, J. Environ. Sci. Health (Part B), 22 (1987) 221.
[16] J.C. Feng and C.C. Feng, Can. For. Serv. Inf. Rep. FPM-X-81 (1988).
[17] J.C. Feng, C.C. Feng and S.S. Sidhu, Can. J. For. Res., 19 (1989) 378.
[18] R. Prasad and J.C. Feng, Weed Technol., 4 (1990) 371.
[19] D.N. Roy, S.K. Konar, D.A. Charles, J.C. Feng, R. Prasad and R.A. Campbell, J. Agric. Food Chem., 37 (1989) 443.
[20] J.C. Feng, Can. J. Chem., 70 (1992) 1087.

ELSEVIER

Journal of Chromatography A, 704 (1995) 141–148

JOURNAL OF CHROMATOGRAPHY A

Simultaneous determination of twelve constituents of I-tzu-tang, a Chinese herbal preparation, by high-performance liquid chromatography and capillary electrophoresis

Shuenn-Jyi Sheu*, Hong-Ren Chen

Department of Chemistry, National Taiwan Normal University, 88, Sec. 4, Tingchow Road, Taipei, Taiwan

First received 17 November 1994; revised manuscript received 23 January 1995; accepted 15 February 1995

Abstract

A high-performance liquid chromatographic method and a capillary electrophoretic method for the separation of four anthraquinoids, five flavones, two carboxylic acids and one saponin in I-tzu-tang were developed. Detection at 254 nm with a linear gradient elution system of tetrabutylammonium bromide and dihydrogenphosphate buffer or with micellar electrokinetic chromatography with sodium dodecyl sulphate and sodium cholate buffer was found to be the most suitable approach for this analysis. The contents of these components in an unpretreated I-tzu-tang extract could be easily determined within 50 min by HPLC or 14 min by CE. The effect of buffers on this separation and the validation of these methods are discussed.

1. Introduction

Chinese herbal preparations are widely used in eastern Asia and suitable assay methods are therefore needed urgently for quality control purposes. Recently, high-performance liquid chromatography (HPLC) [1–4] and capillary electrophoresis (CE) [5–8] have been employed to establish the optimum conditions for examining two or three constituents of the preparations. However, as our knowledge of the effective components of Chinese herbal preparations is still limited and their chemical compositions are very complicated, to determine accurately the contents of Chinese herbal preparations is very difficult. Efforts to develop simpler and more rapid methods that can assay as many bioactive constituents as possible are therefore necessary.

I-tzu-tang (Cimicifuga Combination) is a herbal prescription often used to treat those having constipation with bleeding and severe local pain, and is composed of six herbs, Cimicifugae Rhizoma, Bupleuri Radix, Angelicae Radix, Glycyrrhizae Radix, Scutellariae Radix and Rhei Rhizoma [9]. In this study, twelve bioactive components, sennoside A (SA), sennoside B (SB), emodin (E) and aloe-emodin (AE) in Rhei Rhizoma, baicalin (BG), baicalein (B), wogonin (W), oroxylin A 7-O-glucuronide (OG) and wogonin 7-O-glucuronide (WG) in Scutellariae Radix, glycyrrhizin (GZ) in Glycyrrhizae Radix, ferulic acid (FA) in Angelicae Radix and caffeic acid (CA) in Cimicifugae Rhizoma [10] were selected for analysis; their structural formulae are shown in Fig. 1. Using these compounds,

* Corresponding author.

0021-9673/95/$09.50
SSDI 0021-9673(95)00211-1

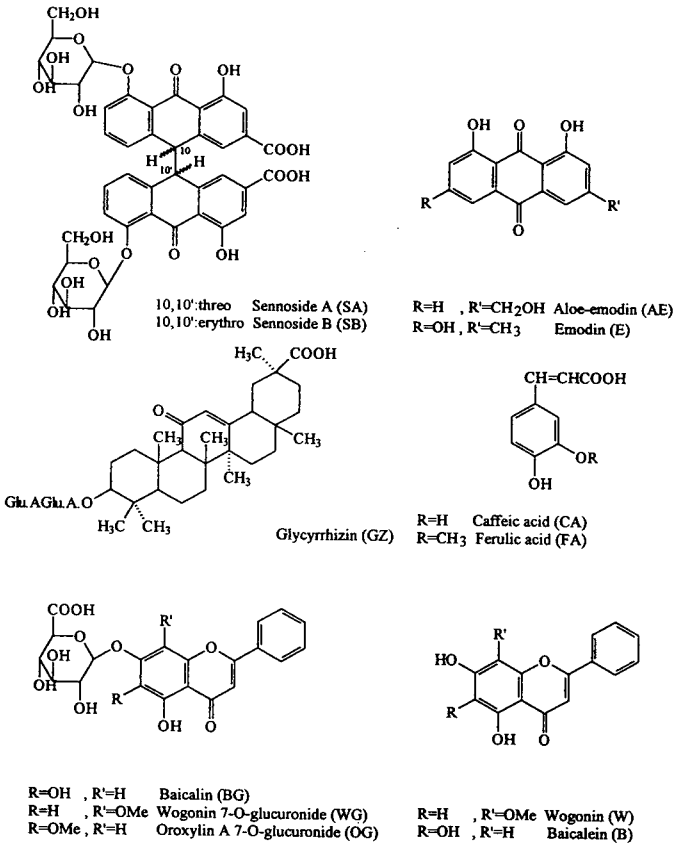

Fig. 1. Structures of the twelve marker substances.

consisting of four anthraquinoids, five flavones, two carboxylic acids and one saponin as marker substances, an HPLC and a CE method for determining the quality of I-tzu-tang were developed. The suitabilities of these two methods were compared and are discussed.

2. Experimental

2.1. Reagents and materials

Baicalin, baicalein, wogonin, sennoside A and sennoside B were purchased from Yoneyama (Osaka, Japan), tetrabutylammonium bromide (TBA), potassium dihydrogenphosphate, sodium dihydrogenphosphate, sodium borate and salicylic acid from Kanto (Tokyo, Japan), glycyrrhizin, tetralin (tetrahydronaphthalene), ferulic acid and caffeic acid from Tokyo Kasei (Tokyo, Japan), emodin and aloe-emodin from Extrasynthese (Genay, France) and sodium dodecyl sulphate (SDS) and sodium cholate (SC) from Sigma (St. Louis, MO, USA). Methanol and acetonitrile were of the LC grade (Mallinkrodt, St. Louis, MO, USA) and phosphoric acid was of analytical-reagent grade (Merck, Darmstadt, Germany). Oroxylin A 7-O-glucuronide and wogonin 7-O-glucuronide were isolated from Scutellariae Radix [11–14]. Three I-tzu-tang samples were purchased from two Chinese pharmaceutical companies in Taiwan. Peak identification and purity checking of all marker substances and test samples were done with a photodiode-array detector or a variable wavelength UV detector.

2.2. Preparation of Chinese herbal preparation extracts

A 1.0-g sample of I-tzu-tang was extracted with 70% methanol (7.5 ml) by stirring at room temperature for 15 min, then centrifuged at 1500 g for 5 min. Extraction was repeated three times. The extracts were combined and filtered through a No. 1 filter-paper. After addition of internal standard solution (for HPLC, 0.5 mg of tetralin in 1 ml of 70% methanol was prepared and 1.25 ml were taken each time; for CE, 1 mg of salicyclic acid in 1 ml of 70% methanol was prepared and 2.5 ml were taken each time), the Chinese herbal preparation extract was diluted to 25 ml with 70% methanol. This solution was passed through a 0.45-μm filter and the filtrate was injected into the HPLC or CE systems.

2.3. Apparatus and conditions

HPLC system

HPLC was performed on a Shimadzu LC-6AD apparatus equipped with a Shimadzu SCL-6B system controller and a Shimadzu SPD-M6A photodiode-array detector (254 nm). Satisfactory separation of the marker substances was obtained with a reversed-phase column (Cosmosil $5C_{18}$-AR, 5 μm, 25 cm × 4.6 mm I.D.) (Nacalai Tesque, Kyoto, Japan) eluted at a flow rate of 0.8 ml/min with a linear solvent gradient of A–B [A = buffer–CH_3OH–CH_3CN (8:1:1, v/v), adjusted to pH 3.5 with phosphoric acid; B = buffer–CH_3OH–CH_3CN (1:2:2, v/v), adjusted to pH 4.2 with phosphoric acid; buffer = aqueous solution consisting of 3.0 m*M* TBA and 7.3 m*M* KH_2PO_4 (0.1 g of KH_2PO_4 was made into a 100 ml aqueous solution)] varying as follows: 0 min, 95:5; 5 min, 85:15; 10 min, 80:20; 20 min, 60:40; 35 min, 25:75; and 40–50 min, 0:100.

CE system

The electrophoretic experiments were carried out on a Spectra Phoresis 1000 capillary electrophoresis system equipped with a UV detector set at 254 nm and a 70 cm × 75 μm I.D. fused-silica capillary tube (Polymicro Technologies, Phoenix, AZ, USA) with the detection window placed at 62.5 cm. The conditions were as follows: injection mode, 2 psi s (hydrodynamic); cartridge temperature, 30°C; run time, 15 min; applied voltage, 20 kV (constant voltage, positive to negative polarity). The electrolyte was a buffer solution consisting of 18 m*M* SDS, 2 m*M* SC, 12.5 m*M* $Na_2B_4O_7$ and 10 m*M* NaH_2PO_4.

3. Results and discussion

3.1. Analytical conditions for HPLC method

All twelve marker substances contain either carboxylic or phenolic groups and are able to be separated by optimizing the pH and concentrations of tetrabutylammonium and dihydrogenphosphate in the eluent. Buffers of pH 3.5 and 4.2 in the two solvent reservoirs of a high-pressure gradient system were chosen, because with a pH higher or lower than these values, acceptable separation was not obtained.

A primary experiment was first conducted at 7.3 m*M* KH_2PO_4 without TBA. In this case, E, WG, OG and BG could be separated, but other compounds were partially or completely overlapped. With TBA, however, the formation of an ion pair not only enhanced the separation of the sample components but also shortened the running time of the whole analysis.

Dihydrogenphosphate concentration

Several KH_2PO_4 buffer solutions with pH 3.5 and 4.2 at different concentrations ranging from 0 to 15 m*M* were used in order to study the effect of dihydrogenphosphate on the separability. In Fig. 2, the capacity factors for the marker substances obtained at different KH_2PO_4 concentrations are shown. From the results it can be seen that by using the mobile phase without KH_2PO_4, a good resolution was obtained only for E, WG, OG and BG. With the addition of KH_2PO_4 to the mobile phase, a much better separation was obtained, especially for highly polar compounds such as CA, SB, SA, BG, OG, WG, FA and GZ. Increasing the buffer concentration from 0 to 15 m*M* not only varies the retention time but also narrows peaks of the

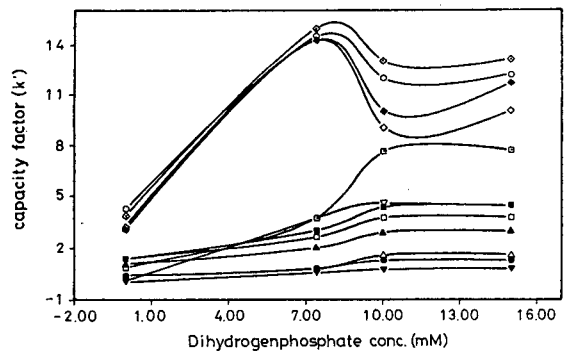

Fig. 2. Effect of KH_2PO_4 concentration on capacity factor (k'). (▼) CA = caffeic acid; (□) OG = oroxylin A 7-O-glucuronide; (◇) B = baicalein; (●) SB = sennoside B; (■) WG = wogonin 7-O-glucuronide; (◆) W = wogonin; (△) SA = sennoside A; (▽) FA = ferulic acid; (○) AE = aloe-emodin; (▲) BG = baicalin; (⊡) GZ = glycyrrhizin; (◈) E = emodin.

components in I-tzu-tang. As shown in Fig. 2, satisfactory resolution was obtained at 10 m*M* KH_2PO_4. However, when the chromatogram was closely examined, it was found that the separation of FA from WG and SA from SB was somewhat incomplete, and the peak of AE was too broad.

TBA concentration

Three buffer systems (prepared by mixing 7.3 m*M* KH_2PO_4 with 0, 3 and 6 m*M* TBA) were used in order to study the effect of TBA on the separability. The results obtained are shown in Fig. 3, where the capacity factors are plotted against TBA concentration. There was an increase in the retention times of carboxylic acids and glycosides but a decrease in those of the less polar compounds when the TBA concentration in the buffer solution increased. From the results, a buffer solution of 7.3 m*M* KH_2PO_4 and 3 m*M* TBA was found to produce the best resolution.

The running time for the separation of all twelve authentic compounds was about 50 min (Fig. 4). As a methanol–water extract of the I-tzu-tang sample was injected directly and analysed, the results were as good as those obtained with pure chemical samples, except for SB, FA, CA and AE, the concentrations of which were either to low to be detected or to be subject to serious interference by other components, as shown in Fig. 5.

3.2. Analytical conditions for CE method

According as the method for determining anthraquinones [15] (a buffer solution consisting of 10 m*M* SDS, 12.5 m*M* NaH_2PO_4 and 15 m*M* $Na_2B_4O_7$ and acetonitrile in the ratio 3:1), we used a buffer solution of 20 m*M* SDS, 12.5 m*M* NaH_2PO_4 and 15 m*M* $Na_2B_4O_7$ in our primary study and found that there was a well separated electropherogram for eight of the twelve components, but it was difficult to separate B from

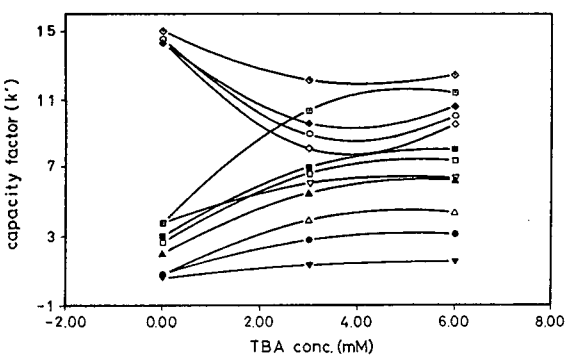

Fig. 3. Effect of TBA concentration on capacity factor (k'). Symbols as in Fig. 2.

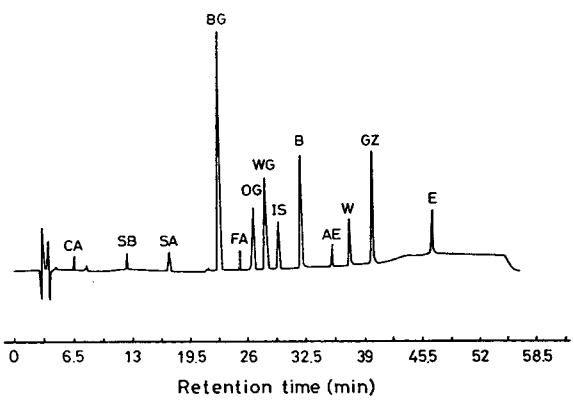

Fig. 4. HPLC of the twelve authentic compounds of marker substances. IS = internal standard (tetralin); other symbols as in Fig. 1.

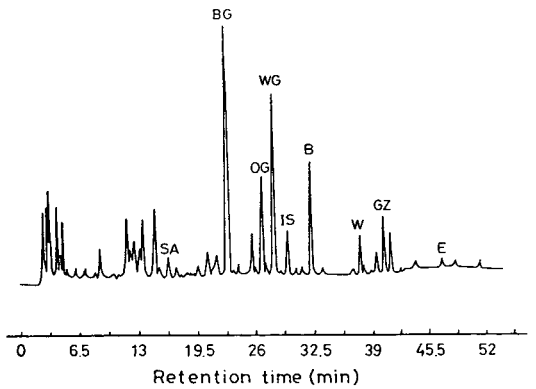

Fig. 5. HPLC of I-tzu-tang.

WG and BG from FA. Substituting sodium cholate for SDS, it was found that the separation of B from WG and BG from FA was complete, but the separation of OG from WG and W from BG failed. Therefore, a buffer system consisting of SDS, SC, borate and dihydrogenphosphate was chosen.

Effect of SDS and SC

Seven electrolyte systems containing different molar ratios of SDS to SC ranging from 1:0 to 0:1 (A:B = 1:0, 9:1, 5:1, 2:1, 1:2, 1:5 and 0:1; A = buffer solution of 20 m*M* SDS, 15 m*M* $Na_2B_4O_7$ and 12.5 m*M* NaH_2PO_4; B = buffer solution of 20 m*M* SC, 15 m*M* $Na_2B_4O_7$ and 12.5 m*M* NaH_2PO_4) were used to study the effect of SDS to SC ratio on the separability. The results obtained are shown in Fig. 6, where the effective mobilities (U_e) are plotted against mole-ratio of SDS to SC. There was first a decrease and then a gradual increase in the effective mobilities of the marker substances, especially those of W, B and WG, when the SDS to SC ratio in the electrophoretic solution decreased. This change can be explained by the fact that there was great difference in the critical micelle concentration between SDS and SC. From Fig. 6, it is clear that analysis carried out at a buffer solution consisting of 18 m*M* SDS, 2 m*M* SC, 15 m*M* $Na_2B_4O_7$ and 12.5 m*M* NaH_2PO_4 could offer a good separation.

Effect of pH

Seven electrolyte systems containing 18 m*M* SDS and 2 m*M* SC at different pH values ranging from 8.14 to 9.74 (prepared by mixing 10 m*M* NaH_2PO_4 with different concentrations of $Na_2B_4O_7$) were used in order to study the effect of pH on the separability. In Fig. 7, the effective mobilities for the components obtained at different pH values are shown. The effective mobilities of these twelve compounds varied with the pH of the buffer, especially those of W, B, E and AE. From the results, a buffer solution of pH 9.35 (12.5 m*M* $Na_2B_4O_7$) was found to produce the best resolution.

The running time for the separation of the twelve marker substances was 14 min (Fig. 8) when using an electrolyte of 18 m*M* SDS, 2 m*M* SC, 12.5 m*M* $Na_2B_4O_7$ and 10 m*M* NaH_2PO_4. As a methanol–water extract of the I-tzu-tang

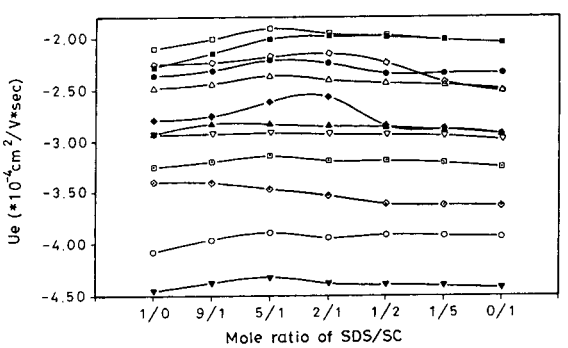

Fig. 6. Effect of SDS-to-SC mole-ratio on effective mobility. Symbols as in Fig. 2.

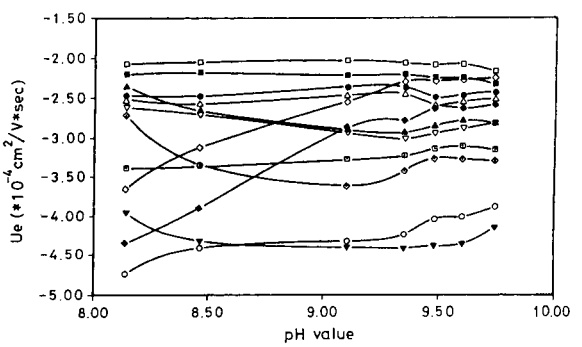

Fig. 7. Effect of pH on effective mobility. Symbols as in Fig. 2.

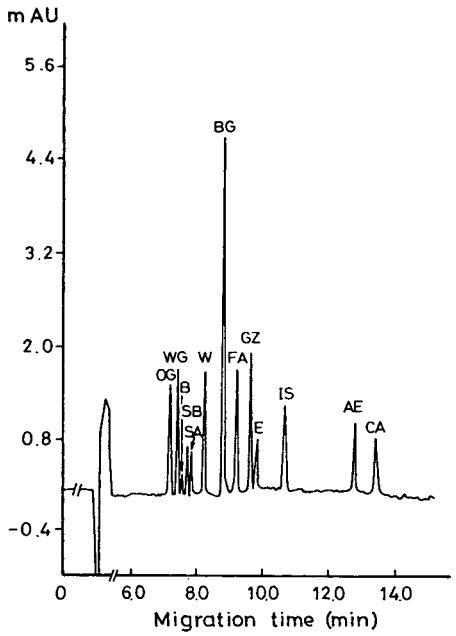

Fig. 8. CE of the twelve authentic compounds. IS = internal standard (salicylic acid); other symbols as in Fig. 1.

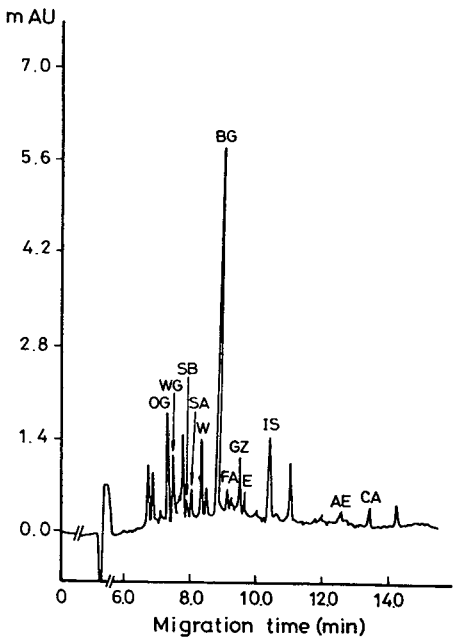

Fig. 9. CE of I-tzu-tang.

sample was injected directly and analysed, the results were as good as those obtained with authentic compounds, except for B, which suffered serious interference by the components of rhubarb, as shown in Fig. 9.

3.4. Method validation

The marker substances in the samples were identified by comparing the retention times or migration times of authentic standards with those obtained in the sample chromatograms or electropherograms and the UV spectra obtained from the photodiode-array detector, and also were checked with the blank test solutions. The detection limit ($S/N = 3$) of each marker substances in HPLC varied from 0.08 to 0.50 ng (0.008–0.050 μg/ml, flow cell length 10 mm) and in CE from $2.25 \cdot 10^{-3}$ to $8.00 \cdot 10^{-3}$ ng (0.45–1.60 μg/ml, column I.D. 75 μm).

Linearity

The linearity of the plot of peak-area ratio (X) vs. concentration (Y, mg/ml) for each of the marker substances in HPLC and CE was investigated. The regression equations of the graphs and the correlation coefficients for these compounds are given in Table 1.

Precision

The reproducibility (relative standard deviation) of the proposed methods, on the basis of peak-area ratios for six replicate injections, was 0.84–1.20% for HPLC and 0.94–2.01% for CE. The relative standard deviation of the retention time or migration time of each peak for six replicate injections was less than 0.45% (HPLC) or 2.64% (CE). The detailed data for individual constituents are given in Table 2.

Accuracy

Suitable amounts (0.10–0.20 mg) of the marker substances were added to a sample of I-tzu-tang of known component contents and analysed using the two proposed procedures. The recoveries of all constituents determined by either method were around 98–103%. The tailing factors of all peaks were very close to unity.

Table 1
Data for linear ranges and correlation coefficients

Constituent	HPLC				CE			
	Linear range (μg/ml)	Slope	Intercept	r	Linear range (μg/ml)	Slope	Intercept	r
SA	1.0–18.0	0.283	$1.50 \cdot 10^{-3}$	0.9995	1.0–18.0	0.569	$2.60 \cdot 10^{-3}$	0.9996
BG	12.6–226.8	0.245	$4.57 \cdot 10^{-2}$	0.9997	7.8–140.4	0.405	$1.71 \cdot 10^{-2}$	0.9996
OG	1.6–28.3	0.182	$7.91 \cdot 10^{-3}$	0.9992	1.6–28.3	0.259	$4.40 \cdot 10^{-3}$	0.9994
WG	2.8–50.0	0.182	$1.37 \cdot 10^{-2}$	0.9994	2.8–50.0	0.384	$1.16 \cdot 10^{-2}$	0.9994
B	1.2–21.6	0.134	$7.40 \cdot 10^{-3}$	0.9996				
W	0.8–13.7	0.113	$3.90 \cdot 10^{-3}$	0.9994	1.3–22.5	0.151	$1.50 \cdot 10^{-3}$	0.9995
GZ	8.6–154.1	0.294	$1.71 \cdot 10^{-2}$	0.9999	5.1–91.8	0.597	$2.93 \cdot 10^{-2}$	0.9998
E	0.5–9.0	0.095	$1.18 \cdot 10^{-3}$	0.9995	0.6–10.8	0.132	$1.80 \cdot 10^{-3}$	0.9991
SB					0.8–13.7	0.527	$4.30 \cdot 10^{-3}$	0.9992
AE					0.8–13.7	0.235	$1.75 \cdot 10^{-2}$	0.9993
FA					1.3–22.5	0.119	$1.00 \cdot 10^{-3}$	0.9994
CA					2.5–45.0	0.190	$1.48 \cdot 10^{-2}$	0.9995

3.5. Determination of marker substances in I-tzu-tang

When the test solution of I-tzu-tang was analysed by HPLC and CE under the selected conditions, the calculated contents of marker substances given in Table 3 were obtained. These data indicate that both of the proposed methods are relatively suitable for the determination of a large number of anthraquinone, flavone, carboxylic acid and saponin type compounds in a complicated system.

In conclusion, by optimizing the pH, buffer composition and buffer concentration of the eluent or carrier, eight components of I-tzu-tang extract could be determined by HPLC within 50 min and eleven of the twelve marker substances could be determined by CE within 14 min. Although the HPLC method had difficulty in separating FA, CA and SA owing to serious

Table 2
Reproducibility of separation of marker substances

Constituent	HPLC		CE	
	R.S.D. (%) ($n = 6$)		R.S.D. (%) ($n = 6$)	
	Retention time	Amount measured	Migration time	Amount measured
SA	0.08	0.92	1.54	1.82
BG	0.09	1.01	2.15	1.09
OG	0.11	1.10	1.31	1.45
WG	0.17	0.87	1.32	1.56
B	0.20	0.94		
W	0.24	0.84	2.45	1.14
GZ	0.40	0.95	2.08	0.94
E	0.45	1.20	2.51	1.73
SB			1.67	2.01
FA			1.95	1.56
AE			2.64	1.72
CA			2.45	1.24

Table 3
Contents of marker substances in commercial I-tzu-tang[a] (mg/g)

Constituent	Sample I		Sample II		Sample III	
	HPLC	CE	HPLC	CE	HPLC	CE
SA	0.62	0.60	0.79	0.74	0.68	0.64
BG	5.23	5.54	8.06	8.21	7.14	7.48
OG	0.81	0.86	1.83	1.95	1.50	1.62
WG	1.04	1.10	2.24	2.24	2.13	2.25
B	0.76		1.15		0.98	
W	0.20	0.21	0.28	0.29	0.26	0.27
GZ	0.54	0.55	0.77	0.78	0.99	0.97
E	0.09	0.08	0.11	0.10	0.12	0.11
SB		0.47		0.57		0.55
AE		0.03		0.09		0.10
FA		0.05		0.07		0.07
CA		0.07		0.08		0.09

[a] Composition of I-tzu-tang (amount in grams) Cimicifugae Rhizoma, 1.5; Bupleuri Radix, 5.0; Angelicae Radix, 6.0; Glycyrrhizae Radix, 2.0; Scutellariae Radix, 3.0; and Rhei Rhizoma, 1.0.

interference from some impurities and the CE method failed to determine B owing to interference from the components of rhubarb, the two proposed methods showed good linear relationships between the peak-area ratio and concentration, acceptable reproducibilities and high recoveries, and should therefore be useful for the analysis of herbal preparations. Compared with the HPLC method, the CE method is more attractive, especially owing to its shorter running time, and therefore should be useful for large numbers of samples and for quality control in pharmaceutical plants.

Acknowledgement

Financial support from the National Science Council, Republic of China, is gratefully acknowledged.

References

[1] M. Harada, Y. Ogihara, Y. Kano, A. Akahori, Y. Ichio, O. Miura and H. Suzuki, Iyakuhin Kenkyu, 19 (1988) 852.
[2] M. Harada, Y. Ogihara, Y. Kano, A. Akahori, Y. Ichio, O. Miura, K. Yamamoto and H. Suzuki, Iyakuhin Kenkyu, 20 (1989) 1300.
[3] K.C. Wen, C.Y. Huang and F.S. Liu, J. Chromatogr., 593 (1992) 191.
[4] K.C. Wen, C.Y. Huang and F.L. Lu, J. Chromatogr., 631 (1993) 241.
[5] Y.M. Liu and S.J. Sheu, J. Chromatogr., 637 (1993) 219.
[6] Y.M. Liu and S.J. Sheu, J. Chromatogr., 639 (1993) 323.
[7] H.R. Chen and S.J. Sheu, J. Chromatogr. A, 653 (1993) 184.
[8] Y.M. Liu and S.J. Sheu, J. High Resolut. Chromatogr., 17 (1994) 559.
[9] H.Y. Hsu and C.S. Hsu, Commonly Used Chinese Herb Formulas with Illustrations, Oriental Healing Arts Institute, Los Angeles, 1980, pp. 613–614.
[10] H.Y. Hsu, Y.P. Chen, S.J. Sheu, C.S. Hsu, C.C. Chen and H.C. Chang, Chinese Material Medica—A Concise Guide, Modern Drug Press, Taipei, 1985, pp. 47–48, 61–62, 120–121, 410–411 and 416–417.
[11] T. Tomimori, Y. Miyaichi and H. Kizu, Yakugaku Zasshi, 102 (1982) 388.
[12] T. Tomimori, Y. Miyaichi, Y. Imoto, H. Kizu and Y. Tanabe, Yakugaku Zasshi, 103 (1983) 607.
[13] T. Tomimori, Y. Miyaichi, Y. Imoto, H. Kizu and Y. Tanabe, Yakugaku Zasshi, 104 (1984) 524.
[14] T. Tomimori, Y. Miyaichi, Y. Imoto, H. Kizu and C. Suzuki, Yakugaku Zasshi, 104 (1984) 529.
[15] S.J. Sheu and H.R. Chen, Anal. Chim. Acta, in press.

ELSEVIER

Journal of Chromatography A, 704 (1995) 149–156

JOURNAL OF CHROMATOGRAPHY A

Salt effect on size-exclusion chromatography of partially sulfonated alternating copolymers of maleic acid and styrene in a polar solvent ☆

N. Šegudović*, S. Sertić, M. Kovač-Filipović, V. Jarm

INA-Industrija Nafte, Research and Development, Savska c. 41/X, Zagreb, Croatia

First received 13 October 1994; revised manuscript received 28 December 1994; accepted 11 January 1994

Abstract

The molecular mass distributions of poly[(maleic acid)-alt-styrene] (SMA) and poly[(maleic acid)-alt-(*p*-sulfostyrene, styrene)] (SSMA) were measured by size-exclusion chromatography (SEC) in N,N-dimethylformamide (DMF) and in DMF containing different amounts of LiBr. The degree of sulfonation of SSMA varies from 18.3 mol% (SSMA I), to 44.8 mol% (SSMA II) and to 83 mol% (SSMA III). Measurements were made at 40°C using a μBondagel set of columns. SEC measurements were followed by viscosity measurements at 25°C in the same media and by light scattering measurements only for the SSMA I sample. The concentrations of LiBr added to DMF were 0.025, 0.075 and 0.10 *M*, at which concentrations of counter ions the viscosity effect of polyelectrolyte was suppressed in all samples. The addition of LiBr to DMF shifted the chromatograms towards longer elution volumes (lower molecular mass); however, this shift was not significant in the case of the SSMA III sample, although the concentration of LiBr was 0.1 *M*. With the highest concentration of LiBr there was a problem with solubility of the sample. The M_w values vary from $24.1 \cdot 10^6$ (SSMA III in DMF) to $5.7 \cdot 10^4$ (SSMA I in DMF–0.10 *M* LiBr). Light-scattering data showed that SEC measurements using the polystyrene calibration graph afford only relative values for the molecular mass distribution.

1. Introduction

The structure and consequently the solution properties of polytlectrolytes in a polar medium with and without added salt are radically different. Coulombic interactions between charges fixed along the macromolecule backbone or side groups are responsible for the most unusual properties of polyelectrolytes, and these interactions are very sensitive to the presence of counter ions in solution. The presence of small electrolytes in polar media, which determines the solution ionic strength, screens out charges and the repulsive interactions between identical charges along the chain. The competition between repulsive forces along the fixed charges on the chain (or side group), and the screening effects brought about by the excess of counter ions (from the added salt) are manifested in a complex dependence of solution properties on

* Corresponding author.

☆ Presented at the *International Symposium on Chromatographic and Electrophoretic Techniques, Bled, Slovenia, 10–13 October 1994.*

0021-9673/95/$09.50
SSDI 0021-9673(95)00048-8

these parameters (charge density and counter ion excess).

One of the most commonly employed solvents for studying the solution properties of polar polymers and polyelectrolytes is N,N-dimethylformamide (DMF) [1–4], and this solvent has found widespread application in the size-exclusion chromatographic (SEC) analysis of polyelectrolytes. The existence of polar groups in a polymer coil causes some specific problems in interpreting the results of SEC because, in addition to size exclusion, some additional mechanisms might be involved. As SEC separation is greatly dependent on solution properties, such as hydrodynamic volume or intrinsic viscosity, a thorough understanding of how the charge of the polymer and the polarity of the solvent influence these parameters is of utmost importance. According to the aforementioned, it is difficult to believe that the universal approach of Benoit et al. [5] is valid for solutions of polyelectrolytes, and comparison of molecular mass data obtained by methods, e.g., light scattering (LS) is necessary.

Many small electrolytes act as "non-solvents" when added to aqueous polar solutions of polyelectrolytes. Increasing amounts of these electrolytes tend to diminish the solvent quality of the media until finally, at some critical concentration of salt, phase separation occurs. The 1:1 electrolytes are generally the least effective of the simple salts for promoting phase separation in polyelectrolyte solutions. The tendency of low-molecular-mass electrolytes to salt out polyelectrolytes from polar media is probably a consequence of both an ionic atmosphere and site-binding phenomena [6].

In a second paper [7] we dealt with solutions of non-sulfonated poly[(maleic acid-alt-styrene] (SMA) and sulfonated poly[(maleic acid)-alt-(p-sulfostyrene, styrene)] (SSMA) copolymers in DMF and DMF–0.05 *M* LiBr as media. The conclusion was that SMA was a weak polyelectrolyte and SSMA behaved as a strong polyelectrolyte. The concentration of added LiBr (0.05*M*) was not sufficient to suppress completely the additional separation mechanisms for SEC of polyelectrolytes.

In this work, we extended the concentration range of LiBr from 0.025 to 0.10 *M*, i.e., from low to moderate concentrations [8].

2. Experimental

2.1. Materials, intrinsic viscosity and high-performance SEC (HPSEC)

The preparation of samples, intrinsic viscosity measurements and HPSEC measurements have been described elsewhere [7].

The concentration range of copolymers for all viscosity measurements was 0.15–0.5 g/100 ml, but in the media containing 0.05 *M* LiBr the copolymer concentration ranged from 0.3 to 0.65 g/100 ml.

2.2. Light scattering

The average molecular mass, M_W, of copolymers was determined using a KMX-6 laser low-angle light-scattering photometer (LLALS) (Chromatix, Mountain Valley, CA, USA) [9] with a helium–neon laser as a light source (λ = 633 nm) and a standard static 15-mm measuring cell. All measurements were made at room temperature and the measuring angle was 6–7° with a field stop of 0.2 mm. Copolymer solutions, usually of five different concentrations, ranging from 1 to 5 mg/ml, were filtered before use through 0.5-μm membrane filters (Millipore, Bedford, MA, USA).

2.3. Differential refractometry

For the measurements of specific refractive index increment (SRII), a Brice-Phoenix differential refractometer was used. Measurements were performed at wavelengths of 436 and 546 nm at 25°C. The differential refractometer was calibrated with sodium chloride solutions of known concentration and refractive index [10]. Sample solutions, usually at five different concentrations ranging from 2 to 10 mg/ml, were filtered before use through 1-μm Millipore filters.

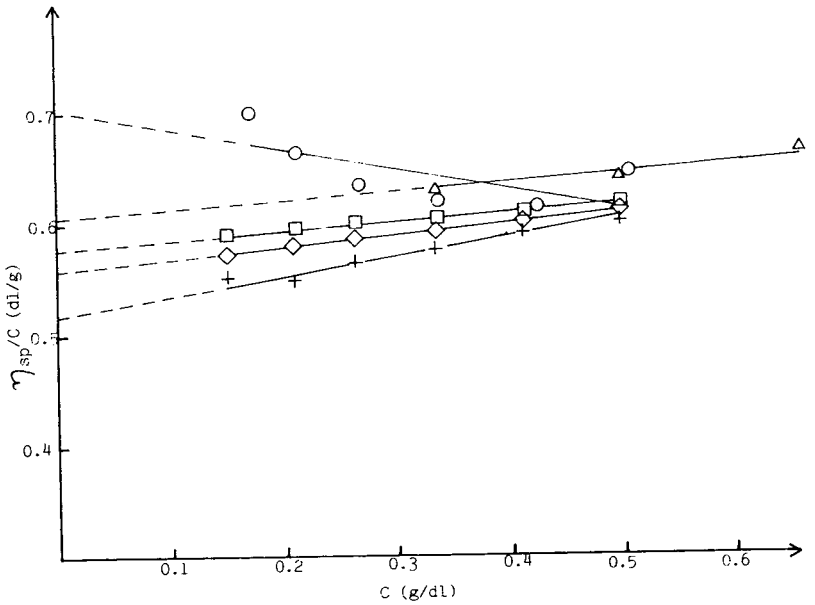

Fig. 1. Reduced viscosity *vs.* concentration of SMA copolymer in (○) DMF, (+) DMF–0.025 *M* LiBr, (△) DMF–0.05 *M* LiBr, (◇) DMF–0.075 *M* LiBr and (□) DMF–0.1 *M* LiBr.

3. Results and discussion

In a second study [7] we observed significant differences in intrinsic viscosity and molecular mass data for SMA and SSMA copolymers in DMF and DMF–0.05 *M* LiBr. Therefore, in this work we extended the measurements in the media with LiBr concentrations from 0.025 to 0.1 *M*.

Fig. 1 shows the results for the reduced viscosity of SMA in DMF and DMF containing various amounts of LiBr. As can be seen, a concentration of 0.025 *M* LiBr suppressed the weak polyelectrolyte effect observed in salt-free DMF. In DMF of higher ionic strength (0.075 and 0.10 *M* LiBr concentrations) the reduced viscosity was higher than in DMF containing 0.025 *M* LiBr, which cannot be explained. Some discrepancies in the case of a 0.05 *M* LiBr concentration could be ascribed to small differ-

Table 1
Dependence of intrinsic viscosity data on the degree of sulfonation and the concentration of LiBr added to DMF

Degree of sulfonation (mol-%)	LiBr added (*M*)				
	0	0.025	0.05	0.075	0.1
0 (pure SMA)	0.701	0.526	0.608	0.557	0.578
18	1.408	0.539	0.621	0.490	0.501
44.8	2.439	0.688	0.640	0.573	
83	3.246	0.888	0.812	0.682	0.584

ences in the concentration range of the copolymer in solution. The intrinsic viscosity calculated by first-order linear regression analysis is presented in Table 1 for all concentrations of added LiBr and for the salt-free DMF.

Fig. 2 shows the reduced viscosities for SSMA I (degree of sulfonation 18.3 mol-%) in salt-free DMF and in DMF containing various concentrations of LiBr. A significant difference between salt-free DMF and DMF with the smallest amount of added LiBr is evident. The reduced viscosity of SSMA I in 0.025 *M* LiBr is close to that of SMA. Moreover, with a high concentration of LiBr (0.075 and 0.10 *M*), the reduced

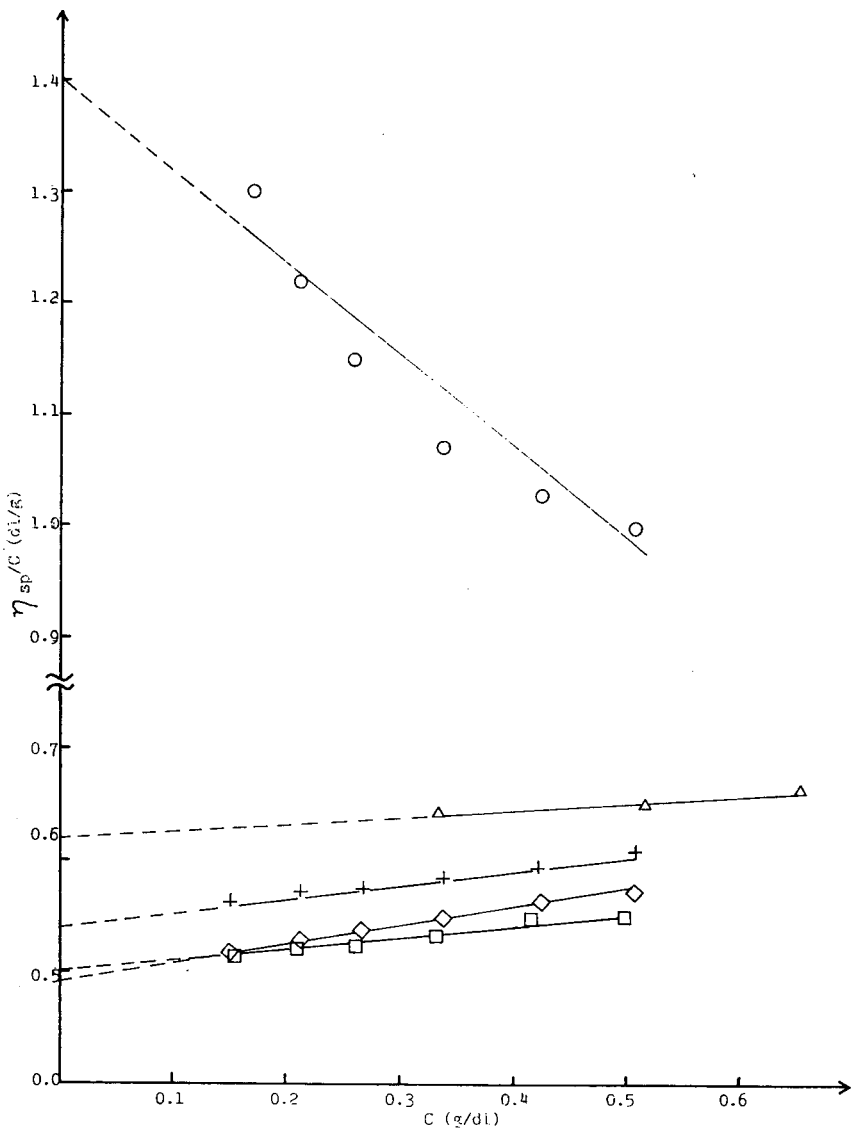

Fig. 2. Reduced viscosity *vs.* concentration of SSMA I copolymer in (○) DMF, (+) DMF–0.025 *M* LiBr, (△) DMF–0.05 *M* LiBr, (◇) DMF–0.075 *M* LiBr and (□) DMF–0.1 *M* LiBr.

viscosity is actually slightly lower than in the case of SMA. The calculated [η] values of SSMA I are presented in Table 1.

Fig. 3 illustrates the reduced viscosities of the SSMA II sample with a moderate degree of sulfonation (44.8 mol-%) in the same media. A significant difference is observed between the reduced viscosity in DMF and in LiBr-containing media. With the lowest concentration of LiBr, the reduced viscosity of SSMA II is slightly higher in comparison with that of SMA, but with a higher concentration of added LiBr (0.075 *M*), the reduced viscosities are much closer to each other. The calculated intrinsic viscosity (Table 1) confirms the aforementioned results.

Reduced viscosities of SSMA III (degree of sulfonation 83 mol-%) are presented in Fig. 4. Differences between the reduced viscosity in salt-free DMF and in DMF containing LiBr are much more evident. Addition of 0.025 *M* LiBr to DMF significantly reduces the viscosity, but the value is still higher in comparison with SMA. Neither a concentration of 0.05 nor 0.075 *M* LiBr in DMF decreases the viscosity to that of SMA.

Only with the solution of DMF containing 0.1 *M* LiBr does the value of the reduced viscosity of SSMA III approach that of SMA. Corresponding [η] values are also shown in Table 1. Fig. 5 presents the size-exclusion chromatograms for three sulfonated copolymers (SSMA I, II, and III) in the measured media. The chromatograms of SSMA I and II are almost the same with DMF–0.025 *M* LiBr (Fig. 5a), but the chromatogram of SSMA III is still shifted toward lower elution volumes. Calculated values of M_w and M_n are given in Table 2.

The polystyrene calibration graph was used for

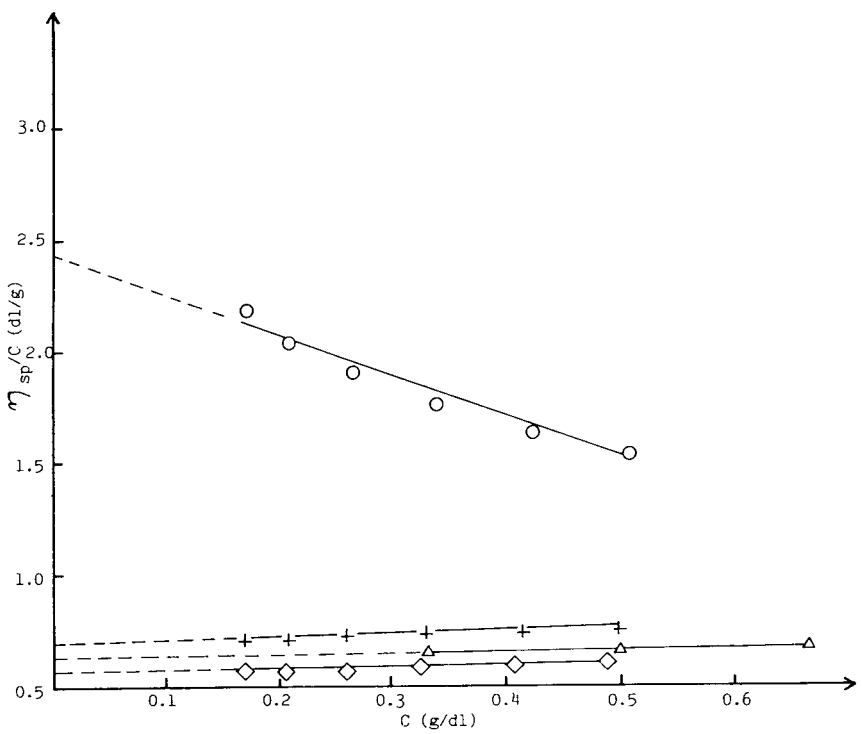

Fig. 3. Reduced viscosity *vs.* concentration of SSMA II copolymer in (○) DMF, (+) DMF–0.025 *M* LiBr, (△) DMF–0.05 *M* LiBr, and (◇) DMF–0.075 *M* LiBr.

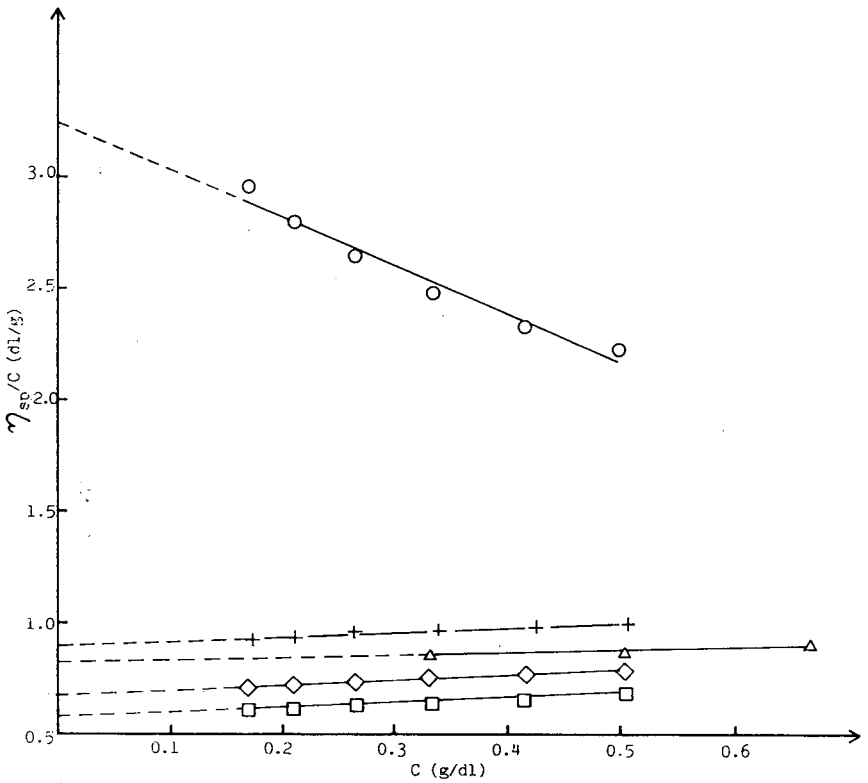

Fig. 4. Reduced viscosity *vs.* concentration of SSMA III copolymer in (○) DMF, (+) DMF–0.025 *M* LiBr, (△) DMF–0.05 *M* LiBr, (◇) DMF–0.075 *M* LiBr and (□) DMF–0.1 *M* LiBr.

calculation of molecular mass distribution data and M_W and M_n values. Fig. 5b shows chromatograms of copolymers with DMF–0.075 *M* LiBr eluent. SSMA I and II again show very close results and almost the same as for SMA with DMF–0.05*M* LiBr eluent [7]. Earlier elution for SSMA III is still evident. The molecular mass data (Table 2) confirm the aforementioned. With DMF–0.10 *M* LiBr eluent (Fig. 5c), all the chromatograms are more similar to each other and at the same time to the chromatogram of SMA with, DMF–0.05 *M* LiBr [7]. The calculated molecular mass data for SSMA I and II are lower than those for SMA. Only the molecular mass for SSMA III is higher than that for SMA, but this difference is smaller than that in DMF with a lower content of LiBr. Comparing Fig. 5a, b and c, it is evident that the detector response decreases with increasing amount of LiBr in DMF and with increasing degree of sulfonation.

During the preparation of solutions in DMF–0.10 *M* LiBr, a problem occurred in filtration through a 0.5-μm filter, and the baseline stability during SEC analyses was worse in comparison with DMF solutions containing lower concentrations of LiBr. This was the reason why we did not try to perform measurements with a higher concentration of LiBr to check the behaviour of SSMA III. This might mean that the addition of higher amounts of LiBr diminishes the solvent power of DMF, and causes the precipitation of part of the solute in DMF–0.10 *M* LiBr or in solutions with a higher content of LiBr. To check the correct molecular mass for all samples we performed light-scattering measurements. Table 3 gives M_W data and refractive index increment

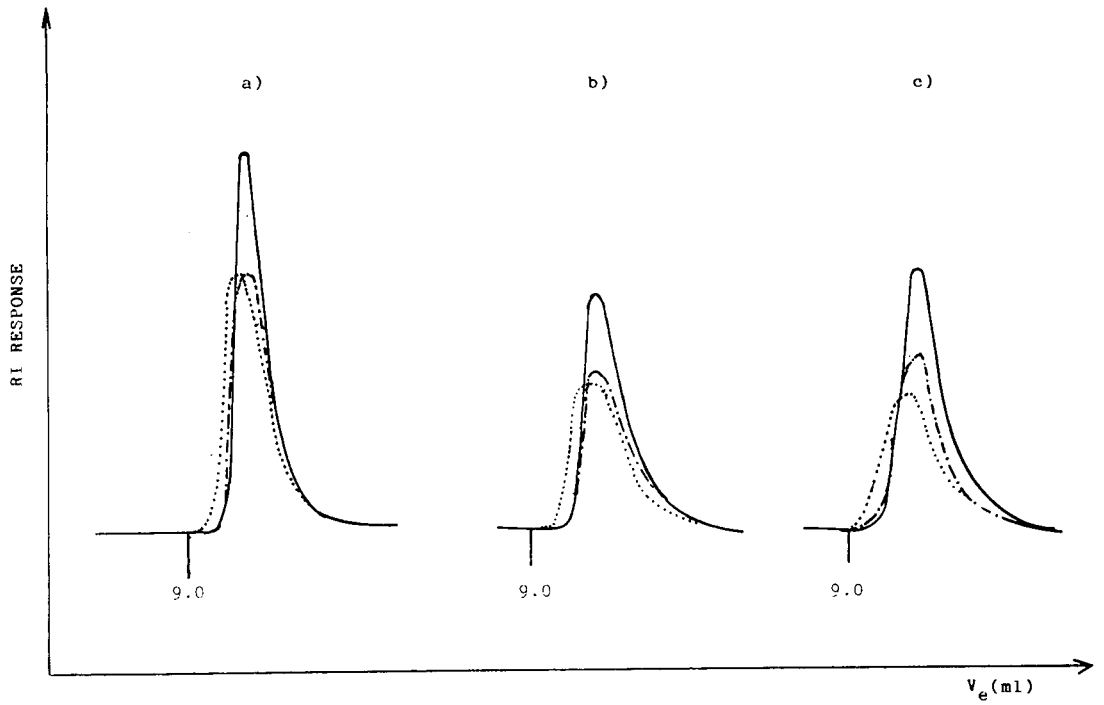

Fig. 5. HPSEC on μBondagel column set (E-high and two E-linear) at 40°C and a flow-rate of 0.5 ml/min in (a) DMF–0.025 *M* LiBr (b) DMF–0.075 *M* LiBr and (c) DMF–0.1 *M* LiBr for (——) SSMA I, (– · – · –) SSMA II and (· · · · ·) SSMA III.

data, d*n*/d*c*, for SSMA I in all four copolymer solutions of different ionic strength. For comparison, M_W and d*n*/d*c* for SMA in DMF were $1.62 \cdot 10^5$ and 0.124 ml/g, respectively.

The measured M_W values are "apparent" because the refractive index increment, d*n*/d*c*, for a multi-component system is complex and comprises all components in solution [11]. These effects may be more important for a higher concentration of salt (>0.5 *M*). Because of the relatively modest salt concentration (<0.10 *M*), the effects of measured parameters may be neglected and no measurements of d*n*/d*c* at a constant chemical potential were performed,

Table 2
Dependence of M_W and M_n, determined by HPSEC, on the degree of sulfonation and concentration of LiBr added to DMF

Degree of sulfonation (mol-%)	LiBr added (*M*)									
	0		0.025		0.05		0.075		0.1	
	M_W	M_n	M_W	M_n	M_W	M_n	M_W	M_n	M_W	M_n
0 (pure SMA)	$4.06 \cdot 10^6$	$0.49 \cdot 10^6$			$7.33 \cdot 10^4$	$3.03 \cdot 10^4$				
18	$11.1 \cdot 10^6$	$1.21 \cdot 10^6$	$1.12 \cdot 10^5$	$5.54 \cdot 10^4$	$7.2 \cdot 10^4$	$3.67 \cdot 10^4$	$5.86 \cdot 10^4$	$3.25 \cdot 10^4$	$5.67 \cdot 10^4$	$3.03 \cdot 10^4$
44.8	$23.1 \cdot 10^6$	$1.38 \cdot 10^6$	$1.08 \cdot 10^5$	$5.47 \cdot 10^4$	$1.03 \cdot 10^5$	$5.16 \cdot 10^4$	$7.27 \cdot 10^4$	$3.42 \cdot 10^4$	$6.24 \cdot 10^4$	$3.25 \cdot 10^4$
83	$24.1 \cdot 10^6$	$1.25 \cdot 10^6$	$3.04 \cdot 10^5$	$7.81 \cdot 10^4$	$2.30 \cdot 10^5$	$4.72 \cdot 10^4$	$1.71 \cdot 10^4$	$4.72 \cdot 10^4$	$1.37 \cdot 10^4$	$4.36 \cdot 10^4$

Table 3
M_w determined by LLALS for SSMA I in different media

Concentration of LiBr added (M)	M_w	dn/dc (ml/g)
0.025	$1.82 \cdot 10^5$	0.122
0.05	$2.08 \cdot 10^5$	0.116
0.075	$2.28 \cdot 10^5$	0.115
0.1	$2.54 \cdot 10^5$	0.111

$A_2 = (5.0\text{–}4.7) \cdot 10^{-4}$ mol ml/g^2.

even though we observed a small decrease in dn/dc values on increasing the LiBr concentration (Table 3). At the same time, there is a small increase in M_w with increased concentration of LiBr. The second virial coefficients decrease slightly with increasing concentration of LiBr ($A_2 = 5.0 \cdot 10^{-4}$ mol ml/g^2 at 0.025 M and $4.75 \cdot 10^{-4}$ mol ml/g^2 at 0.10 M LiBr), indicating again a decrease in solvent quality. Light-scattering data showed that the calculated M_w and M_n values from SEC measurements using the polystyrene calibration graph have only a relative meaning. This should be taken into account for the absolute molecular mass distribution.

4. Conclusion

The results obtained by SEC measurements in solutions of different ionic strength have shown that in polar media SSMA samples behave as strong polyelectrolytes. Introduction of a sulfo group in the *para* position of the styrene unit of copolymers is responsible for a strong polyelectrolyte effect in comparison with a weak polyelectrolyte in the case of the non-sulfonated copolymer SMA. The polyelectrolyte effect depends on the degree of sulfonation. In the case of a copolymer with a low degree of sulfonation (SSMA I, 18.3 mol-%), a low concentration of LiBr is almost enough to screen out the charge and suppress the expansion of macromolecular coils caused by intramolecular repulsive forces. The effect of a higher degree of sulfonation could be eliminated by increasing the concentration of LiBr (0.075 or 0.10 M). Only for the copolymer with the highest degree of sulfonation (SSMA III, 83 mol-%) is the concentration of 0.10 M insufficient for the complete suppression of macromolecular expansion, but at this concentration the solvent quality decreases and copolymer becomes partially insoluble. SEC measurements in the mentioned eluent using the polystyrene calibration graph gave only relative values for molecular masses. Comparing the viscosity data and SEC data there is some doubt whether the separation process in SEC measurements is based only on size or if some additional processes are involved (ion inclusion and ion exclusion).

All the results observed have shown that SEC measurements are affected by the polarity and ion strength of the eluent and by the degree of sulfonation, i.e., charge density of copolymers.

References

[1] G. Coppola, P. Fabri and B. Pallesi, J. Appl. Polym. Sci., 16 (1972) 2829.
[2] N.D. Hann, J. Polym. Sci. Polym. Chem. Ed., 15 (1977) 1331.
[3] N. Šegudović, F.E. Karasz and W.J. MacKnight, J. Liq. Chromatogr., 13 (1990) 2581.
[4] N. Šegudović, S. Sertić, M. Kovač-Filipović and V. Jarm, J. Appl. Polym. Sci., Appl. Polym. Symp., 48 (1991) 185.
[5] H. Benoit, Z. Grubišić and R. Rempp, J. Polym. Sci., B5 (1967) 753.
[6] R.W. Armstrong and U.P. Strauss, Encyclopedia of Polymer Science and Technology, Vol. 10, Interscience, New York, 1969, p. 781.
[7] N. Šegudović, S. Sertić, M. Kovač-Filipović and V. Jarm, in preparation.
[8] H. Mattoussi, S. O'Donohue and F.E. Karasz, Macromolecules, 42 (1992) 743.
[9] S.H. Kim and P.M. Cotts, J. Appl. Polym. Sci., 42 (1991) 217.
[10] A. Kruis, Z. Phys. Chem., B34 (1936) 13.
[11] M. Nagasawa and A. Takahashi, in M.B. Huglin (Editor), Light Scattering from Polymer Solutions, Wiley, New York, 1972, Ch. 16.

ELSEVIER

Journal of Chromatography A, 704 (1995) 157–162

JOURNAL OF CHROMATOGRAPHY A

Permeation tube approach to long-term use of automatic sampler retention index standards

Thomas J. Bruno

Thermophysics Division, Chemical Science and Technology Laboratory, National Institute of Standards and Technology, Boulder, CO 80303, USA

First received 29 December 1994; revised manuscript received 3 February 1995; accepted 9 February 1995

Abstract

A permeation tube that is sealed internally in a commercially-available automatic sampler vial provides a simple and convenient method of preparing, using, and storing standard retention index samples for long periods of time. The approach is especially suited to the handling of volatile organic compounds that are very important in fuels research, alternative refrigerant research and in many environmental analyses. It also provides the very desirable feature of dispensing sample that is at very low concentration or even at infinite dilution, since no commercial automatic sampler is currently capable of doing this for the analyst. The device is very simple, and can be constructed and prepared with a liquid sample in a few minutes. It requires the use of minimal quantities of sample, and substantially decreases the hazards associated with handling volatile organics in the laboratory.

1. Introduction

Automatic samplers are a vital tool for the chromatographic analysis of a wide variety of samples. They greatly reduce the time and labor required for analyses, and reduce the potential for operator exposure to potentially dangerous chemicals. The typical commercially available automatic sampler container, consisting of a glass vial and a crimped septum cap, performs only marginally when used with volatile organic compounds (VOCs), however. Leakage through the septum and around the seal is very common, and after the septum has been pierced by a syringe needle, leakage through the septum is inevitable and rapid. While this is of little consequence for VOCs that are sampled and analyzed quickly, it is a serious problem for sample vials that the analyst desires to retain and use on a long-term basis. While it is possible to replace the crimped septum cap after each use, this approach is extremely inconvenient and time consuming. It also increases the risk of operator exposure to the sample, and the potential for accidental sample spillage. Moreover, leakage around the seal will persist even if the cap is replaced after each use.

Long-term samples include retention time and retention index standards and markers [1–5]. Such samples are used extensively in chromatographic qualitative analysis and peak assignment/identification. It is very desirable to package such samples in order to minimize material loss and handling, and to minimize the initial quantity of material that is required for their preparation. Moreover, retention index standards are usually used at very low concentrations (often approaching infinite dilution), or even as head-

0021-9673/95/$09.50
SSDI 0021-9673(95)00184-0

space vapors. This is also true for samples used in physicochemical chromatographic measurements [6–8]. It is therefore helpful to package such standards in a way that facilitates drawing and delivering a very dilute aliquot.

In this paper, we present an approach to the application of automatic sampler vials to long-term retention index standards. The method is based on permeation tubes, well known devices that have been used for the preparation of gaseous mixtures for many years [9–12]. A permeation tube is a short length (usually between 5 and 20 cm) of a polymeric tubing through which a fluid may pass at a relatively slow, constant rate (at a given temperature). Numerous polymers have been used for the preparation of the tubes used for such permeation devices. These polymers include polyethylene, polyvinyl acetate, polyamide, polyester, silicones, polyvinylidene chloride and polyethylene terephthalate. The most common materials are fluorinated ethylene propylene (FEP Teflon[1]) and tetrafluoroethylene (TFE Teflon). The most common use of permeation tubes is for the preparation of gas mixtures.

Such a permeation device is typically prepared by filling the inside of the tube (with one end plugged) with the desired fluid until approximately 80 percent of the tube volume is occupied with liquid. For more volatile fluids, this must be done in a pressurized manifold. Most permeation tube devices are two-phase (vapor + liquid) systems, however single-phase high-pressure gaseous tubes have been prepared occasionally. The tube is then "conditioned" at a constant suitable temperature to saturate the polymer with the fluid. At that point, the permeation rate of the fluid will be constant at a given temperature. If the temperature is changed, some time will be required for the constant rate to be reestablished at the new temperature.

Permeation tubes are commonly used for the preparation of gas mixtures using dynamic techniques in which the tube containing the desired fluid is held in the slip stream of a flowing diluent gas. A knowledge of the diluent flow-rate and temperature allows the calculation of the concentration of the fluid in the diluent gas.

2. Theory

The operation of a polymeric permeation tube device is described fundamentally by Fick's law [9–11]:

$$q_d = (p_g A \Delta P)/L \quad (1)$$

$$p_g = D \cdot S \quad (2)$$

where q_d is the amount of sample material (fluid) that passes through the permeation material (in mass units per unit area per unit time), p_g is the fluid permeability constant, D is the diffusion coefficient (in area per unit time), S is the solubility constant of the fluid in the polymer (in concentration units divided by fugacity or pressure), A is the area of the material, ΔP is the pressure difference across the polymer, and L is the thickness of the polymer. The pressure difference ΔP is in practice usually taken as the difference between the vapor pressure of the permeating fluid and the pressure within the sampling area. As these equations demonstrate, the main factors that affect passage of a gaseous material through a polymeric permeation tube are (1) the vapor pressure of the permeating fluid and (2) the solubility of the permeating fluid in the polymer. At constant temperature, the solubility of the permeating fluid in the polymer is constant. In the great majority of permeation tube applications, the fluid is contained (usually under its head pressure) in the inside of a sealed tube made from the polymer, and the desired concentration of fluid is achieved by appropriate mixing with a diluent flowing outside the tube. The concentration of the fluid in the diluent can be approximated by:

[1] Certain commercial equipment, instruments or materials are identified in this paper in order to adequately specify the experimental procedure. Such identification does not imply recommendation or endorsement by the National Institute of Standards and Technology, nor does it imply that the materials or equipment identified are necessarily the best available for that purpose.

$$[c] = \frac{(v \cdot 10^6)(T/273)(P/0.101\,325)q_d}{q_D M} \quad (3)$$

where [c] is the concentration expressed in parts per million (that is, 0.0001 percent), T is the temperature of the permeation tube (in K), P is the pressure of the diluted gas stream (in MPa), q_D is the volumetric flow-rate of the diluent (in l/min), v is the molar volume of the permeating fluid (in l) and M is the relative molecular mass of the permeating fluid. A common approximation is to replace v with 22.4 l, the molar volume of an ideal gas. In the present case, with the permeation tube functioning in reverse, the diluted sample vapor is on the inside of the tube.

For purposes of Eq. (3), the flow-rate q_D for the current apparatus is taken as the sampling rate (in μl/min), done by syringe on an automatic sampler. This allows the approximate concentration of fluid inside of the permeation tube insert to be calculated.

3. Experimental

A standard wide-mouth commercial automatic sampler vial can be fitted with a permeation tube insert as shown in Fig. 1 to provide long-term sample storage and availability, and also to dispense the samples at low concentrations or in the infinite dilution range. The permeation tube insert consists of a short length of TFE (tetrafluoroethylene) or FEP (fluorinated ethylene propylene) Teflon permeation tubing (0.48 cm O.D., 0.32 cm I.D.). The typical length of exposed permeation tube is 1.9 cm. In general, the TFE material will provide a higher permeation rate for hydrocarbons than will the FEP material [13]. This rule of thumb appears not to hold for halogenated hydrocarbons, however. Branched hydrocarbons will have a much lower permeation rate than straight chain hydrocarbons. These considerations will affect the choice of permeation tube material.

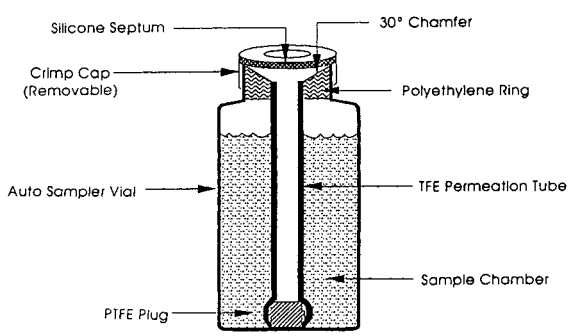

Fig. 1. Schematic diagram of an automatic sampler vial fitted with a permeation tube insert.

The permeation tube is held in place in the neck of the vial by a collar made from a short length (0.48 cm) of flexible polyethylene tubing (0.64 cm O.D., 0.32 cm I.D.) that is press-fitted on the top end of the permeation tube. The relative sizes of the polyethylene ring (expanded with the permeation tube inserted) and the inside diameter of the neck of the vial (0.64 cm) provide an interference fit that allows for an excellent seal to the automatic sampler vial. An interference fit exists when the outside diameter of the insert exceeds the available inside diameter of the vial. The bottom of the permeation tube is securely plugged by a small disk of 25 percent glass-filled Teflon (PTFE-glass, 0.4 cm maximum diameter) machined to provide an interference fit with three points of contact.

To assemble the insert, the permeation tube, with one end plugged with the glass-filled Teflon disk, is fitted with the polyethylene collar. The liquid sample is then added to the vial, and the insert is press-fitted into the neck on a small laboratory hydraulic press or an arbor press. The collar and permeation tube are sized to be flush with the top of the vial, thus allowing a standard crimped septum cap to be fastened onto the vial. Before the septum cap is installed, a 30° chamfer is cut concentrically into the top surface of the collar and permeation tube, to help guide a syringe needle into the permeation tube. This is easily done with a hand-held carbide cutter that is commonly used to dress the ends of tubing used for packed chromatographic columns.

After the septum cap is crimped on the vial, the unit is placed in a laboratory oven and maintained between 50 and 100°C to allow

conditioning and induction of the permeation tube. The choice of the induction temperature depends on the boiling point of the fluid. The typical induction period for commercial permeation tubes is approximately 3 weeks to achieve a constant permeation rate [10]. We have found that for use as low concentration retention standards, a high level of concentration reproducibility is of secondary importance, and induction periods of 5–7 days are adequate.

4. Results and discussion

Automatic sampler vials containing a permeation tube insert have been prepared for a variety of VOC samples, and several of the more instructive examples will be described. The hydrocarbon samples have included *n*-hexane, *n*-octane, *n*-decane and 2,3-dimethyl pentane. Halocarbon samples have included fluorotrichloromethane (R-11), 1,1-dichloro-1-fluoroethane (R-141b) and 1,2-difluoroethane (R-152). The last compound is particularly illustrative of the advantages of this approach for sampling. R-152 is very toxic because its potential metabolic products include monofluoroacetic acid, even after exposure to moderate concentrations [14]. Moreover, the intermediate volatility (normal boiling temperature of 30.7°C) of this material makes it somewhat difficult to handle in a conventional automatic sampler vial.

A significant challenge associated with the preparation of permeation tubes has always been the prevention of leakage through the tube closure(s) [9,12]. For this reason, a number of experiments were done to verify the integrity of the plug at the bottom of the tube in the automatic sampler vial. Two sets of vials were prepared (with TFE permeation tubes) containing *n*-hexane, and were maintained at 70°C for 5 days after an initial induction period. One set of vials had crimped septum caps in place (the configuration shown in Fig. 1), and the other set was left uncapped. Although this temperature is slightly above the normal boiling temperature of *n*-hexane, there was no measurable decrease in the liquid levels of the vials. If leakage through the plug had occurred, some decrease in the liquid level would have been noted. Similar observations were made with other hydrocarbons (straight chain and branched) that were maintained at relatively high temperatures.

Vials were also prepared with permeation tubes that were fitted with multiple plugs, some plugs having multiple barbs and some being simple cylindrical plugs. No change in tube performance was noted with any combination. As a final check, a vial was prepared in which a plug such as that shown in Fig. 1 was inserted, but the polyethylene tube used to form the collar extended throughout the length of the permeation tube. This sheath covered the entire active (that is, permeating) surface of the insert. This tube showed no permeation activity; no vapor could be detected inside the tube. We can therefore conclude that the material that enters the interior of the tube has in fact permeated from the liquid space, and has not leaked through a properly prepared and installed plug.

Because of differences in permeation rates of different fluids in the TFE and FEP materials, two different sampling modes (steady-state and dynamic) are noted for the performance of the vials. The steady-state mode is obtained when the sampling rate (removal of vapor sample) is balanced by the permeation rate (replenishment of fluid). This behavior is illustrated in Fig. 2a, with *n*-hexane as the sample drawn from a vial fitted with a TFE insert. This figure shows raw area counts from a flame ionization detector that were obtained from 7-μl injections of the interior space of the permeation tube. These samples were injected into a polymethyl siloxane coated capillary column (1 μm thickness, 50:1 split ratio). The concentration of sample is approximately constant (within approximately 6.5 percent) for a sampling rate of approximately once every 1.5 min. No attempt was made to control the temperature of the vial for these measurements. Temperature control would undoubtedly increase the reproducibility of the area measurements, but, as was noted earlier, this is a secondary concern for retention index samples. The dynamic mode occurs when the sampling rate exceeds the replenishment rate. This behavior is illustrated in Fig. 2b, with *n*-octane as the sample with an FEP insert. Here we note a

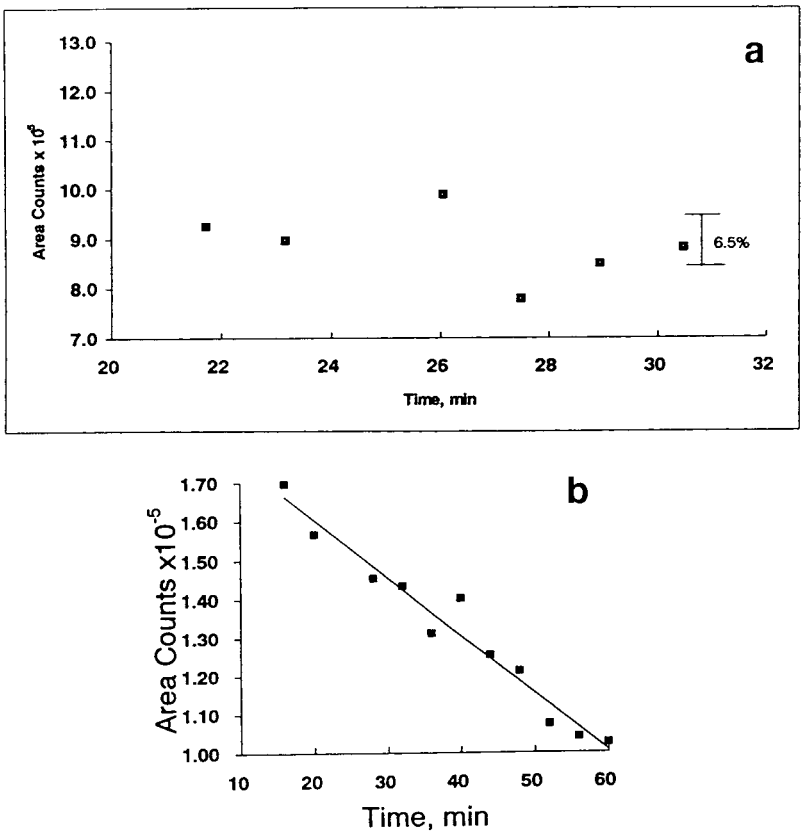

Fig. 2. (a) Plot of FID raw area counts against sampling time for *n*-hexane sampled through a TFE insert. (b) Plot of FID raw area counts against sampling time for *n*-octane sampled through a FEP insert.

steady decrease in the area counts for a sampling rate of once every 4 min.

Another potential use for automatic sampler vials equipped with permeation tubes is for the evaluation of permeation tubes themselves. One can use chromatographic instrumentation to sample the interior of the permeation tube at an increasing rate, rather than the uniform rate that was used here. One can then determine the transition from steady-state mode to dynamic mode. The permeation through the tube at this transition is characteristic for the sample for a given permeation tube material.

5. Conclusions

In this note, we have explored the application of permeation tube inserts to extend the utility of automatic sampler vials, especially as applied to the measurement of retention index standards. The combination of these two components can provide a chromatographic sampling method that is safe, convenient and widely applicable. In addition, the approach is potentially useful as a method of characterizing the performance of permeation tube materials.

Acknowledgements

The financial support of the Gas Research Institute, Chicago Il. (Contract No. 5093-260-2720), and the United States Environmental Protection Agency, Stratospheric Ozone Protection Branch (Contract No. DW13935632-01-0), is gratefully acknowledged. The assistance of

T.G. Waldorf with some aspects of the fabrication is gratefully acknowledged.

References

[1] E.sz. Kovats, Helv. Chim., 41 (1958) 1915.
[2] M.B. Evans, J.K. Haken, J. Chromatogr., 472 (1989) 93–127.
[3] T.J. Bruno, M. Caciari, J. Chromatogr. A, 672 (1994) 149–158.
[4] T.J. Bruno, M. Caciari, J. Chromatogr. A, 679 (1994) 123–132.
[5] T.J. Bruno, M. Caciari, J. Chromatogr. A, 686 (1994) 245–251.
[6] J.R. Conder, C.L. Young, *Physicochemical Measurement by Gas Chromatography*, John Wiley and Sons (Wiley-Interscience), Chichester, 1979.
[7] R.J. Laub, R.L. Pecsok, *Physicochemical Applications of Gas Chromatography*, John Wiley and Sons (Wiley-Interscience), New York, 1978.
[8] T. Cserhati, K. Valko, *Chromatographic Determination of Molecular Interactions*, CRC Press, Boca Raton, FL, 1994.
[9] G.O. Nelson, *Gas Mixtures: Preparation and Control*, Lewis Publishers, Boca Raton, FL, 1992.
[10] J. Namiesnik, J. Chromatogr., Chromatogr. Revs., 300 (1984) 79–108.
[11] D.R. Paul, Y.P. Yampol'ski (Editors), *Polymeric Gas Separation Membranes*, CRC Press, Boca Raton, FL, 1994.
[12] C.F. Cullis, J.G. Firth (Editors), *Detection and Measurement of Hazardous Gases*, Heinemann Educational Books, London, 1981.
[13] D. Williams, VICI Metronics, personal communication, 1994.
[14] T.J. Bruno (Editor), *Handbook for the Identification and Analysis of Alternative Refrigerants*, CRC Press, Boca Raton, FL, 1995.

ELSEVIER

Journal of Chromatography A, 704 (1995) 163–172

JOURNAL OF CHROMATOGRAPHY A

Solid-phase microextraction of nitrogen-containing herbicides

Anna A. Boyd-Boland*, Janusz B. Pawliszyn

The Guelph–Waterloo Centre for Graduate Work in Chemistry, University of Waterloo, Waterloo, Ontario N2L 3G1, Canada

First received 22 November 1994; revised manuscript received 26 January 1995; accepted 31 January 1995

Abstract

A solid-phase microextraction (SPME) method, coupled with GC–MS, GC–NPD and GC–FID has been developed for the analysis of 22 nitrogen-containing herbicides in water. A polar poly(acrylate) coated fiber was used to extract the analytes directly from the samples over the concentration range 0.1 to 1000 ng/ml. Limits of detection with each of the detectors were determined to be in the ng/l, to sub ng/l levels. Some applications of the method have been demonstrated for soil samples and wine samples with GC–MS and the latter was quantified by standard addition.

1. Introduction

The analysis of herbicides and pesticides in natural waters is an area of increasing importance not only because of their potential toxicity, persistence and water solubility but also because of their universal application. This paper focuses on the analysis of nitrogen-containing herbicides which are currently investigated by US EPA methods 507 and 508, and some other related herbicides. These herbicides are widely used as pre- and post-emergent weed control agents for a wide variety of crops, including corn, sorghum, wheat, rice and sugar cane, and for fruits, vegetables and vineyards. Consequently they are found in river water [1–5], ground water [6,7] and soils [8–10] in Europe, the United States and Canada. A 1988 survey of pesticide residues in Ontario drinking water found that atrazine (one of the herbicides under investigation) was the most common pesticide detected [11]. It has also been identified as one of the most widely used herbicides, over $90 \cdot 10^6$ kg was consumed in 1980 alone [2].

Current methods of analysis for aqueous or solid samples involve either liquid–liquid extraction [1–3,11], solid-phase extraction (SPE) [2,3,7,12–14] or supercritical fluid extraction (SFE) [8]. The disadvantages of liquid–liquid extraction are the use of large quantities of often toxic and environmentally unfriendly solvents, the time consuming procedures and the need for concentration of analytes before analysis. SPE methods have eliminated many of these disadvantages by decreasing the amount of solvent required and shortening, somewhat, the extraction process. However, there are still disadvantages to SPE: the presence of particulate matter in samples can cause plugging of the cartridges, breakthrough is sometimes experienced for highly concentrated samples and dedicated instruments are required for subsequent analysis. SFE

* Corresponding author.

0021-9673/95/$09.50
SSDI 0021-9673(95)00151-4

methods are generally non-portable and require large quantities of high purity CO_2.

An alternative technique is solid-phase microextraction (SPME), a solvent-free analytical process which overcomes most of the disadvantages of the conventional methods while maintaining the advantages [15]. It involves direct extraction of the analytes with the use of a small diameter optical fiber that has been coated with a polymeric stationary phase and housed in a syringe assembly for protection. Analytes in an aqueous sample, or the headspace above a sample, partition into the polymeric phase according to their distribution coefficient. They are subsequently thermally desorbed in the injection port of a gas chromatograph (GC) for analysis. The polymeric phase essentially behaves in the same way as the organic solvent in the liquid–liquid extraction process but has the advantage of being bonded to the fiber so that after desorption of the analytes, it is ready for the next extraction.

SPME has already been successfully applied to the analysis of a variety of analytes in solid, liquid and gas phases [16]. The method has been shown to be applicable to both polar and non-polar analytes, including, volatile organic compounds [17–19], phenols [20], and PAHs/PCBs [21]. This paper presents the first application of SPME to this important class of herbicides, the nitrogen-containing herbicides. A polar poly(acrylate) coated fiber was used to extract analytes from aqueous and soil samples.

2. Experimental

2.1. Fiber preparation

The coated fiber selected for the analysis of the nitrogen-containing herbicides was fused silica coated to a thickness of 95 μm with poly(acrylate) and 1 cm in length. Preliminary experiments were conducted to compare a 15 μm poly(dimethylsiloxane) coated fiber, a 55 μm poly(dimethylsiloxane) coated fiber and the 95 μm poly(acrylate) coated fiber. The poly(dimethylsiloxane) fibers were conditioned in the injection port of the GC for 3 hours at 250°C. However, to obtain consistent analytical results with the poly(acrylate) coated fiber, it must be conditioned before initial application by the procedure described in detail by Buchholz and Pawliszyn [22] and briefly outlined here. The coated fibers are placed inside a stainless-steel tube through which a stream of helium flows. The stainless-steel tube is then placed inside a muffle furnace and held at 300°C for four hours. After mounting the fibers in the needle assembly, further conditioning under He at 250°C in the injection port of a GC was required to remove impurities which may be present from the epoxy.

2.2. Reagents

Two separate standard mixtures of herbicides (herbicide mix 1 and herbicide mix 2, Supelco, Canada, catalogue numbers 4-9136 and 4-9138, respectively, 100 μg/ml) were purchased. The herbicides present were Atrazine, Benfluralin, Bromacil, Metolachlor, EPTC, Oxyfluorofen, Hexazinone, Molinate, Oxadiazon, Isopropalin, Propachlor, Propazine, Pendimethalin, Cycloate, Metribuzin, Simazine, Butylate, Terbacil, Pebulate, Profluralin, Trifluralin and Vernolate. The stock standards were used to prepare 50-ml aqueous solutions containing 0.1 mg/l of each analyte. Stock solutions were freshly prepared every two weeks and used to prepare 4-ml standards at the required concentration.

All solutions were prepared with NANOpure water (Barnstead ultrapure water system). Blank analyses were performed regularly to ensure that no herbicides were present in laboratory reagents, or fibers.

2.3. Instrumentation

Initial analysis was performed using both a Varian 3500 gas chromatograph (GC) equipped with a septum programmable injector (SPI) and a flame ionisation detector (FID) and a Varian 3400CX GC with an FID and a nitrogen–phosphorous detector (TSD or NPD). Analytes were separated with a Supelco PTE-5 column, 30 m × 0.25 mm with a phase thickness of 0.25 μm. The temperature program used for the analysis of

each herbicide mixture was: 100°C, hold for 5 min, then to 300°C at 10°C/min, and hold for 5 min. The carrier gas was ECD grade helium, maintained at a flow-rate of 1.0 ml/min. The SPI injector was isothermally programmed at 250°C for SPME extractions and direct solvent injections. The FID was held at 300°C, with a nitrogen make-up flow of 23.0 ml/min, hydrogen at 30.0 ml/min, and air at 280 ml/min.

Subsequent analysis was performed with a Varian Saturn ion trap mass spectrometric detector. The same column was used but the temperature profile was modified to enable separation of all 22 herbicides. The modified program was: 40°C, hold for 5 min, then to 100°C at 30°C/min, then to 300°C at 5°C/min. The ion-trap manifold was held at 250°C, as was the transfer line. The mass spectrometer was tuned to FC-43 (perfluorotributylamine). The electron multiplier and automatic gain control target were set automatically. The mass range scanned was 45–400 a.m.u. The detector was turned off for the first 300 s to prevent overloading the electron multiplier from the solvent used in preparation of the herbicide standards (ethyl acetate).

The responses of the FID, NPD and MS detectors were calculated for each analyte by injection of the standard herbicide mixture at a minimum of five different concentrations. For the FID and NPD, area counts were plotted against the amount injected (ng) to produce a calibration curve. For the MS, the most abundant mass peak above 100 a.m.u. was chosen for quantification and calibration. The masses chosen were: EPTC, 128; Butylate, 146; Vernolate, 128; Pebulate, 204; Molinate, 126; Propachlor, 212; Cycloate, 154; Trifluralin, 306; Benfluralin, 292; Simazine, 202; Atrazine, 216; Propazine, 214; Profluralin, 318; Terbacil, 161; Metribuzin, 198; Bromacil, 207; Metolachlor, 162; Isopropalin, 280; Pendimethalin, 252; Oxadiazon, 258; Oxyfluorofen, 361; Hexazinone, 171.

2.4. Analytical procedure

Aliquots (4 ml) of standard solutions or samples were extracted from 4.6-ml vials sealed with hole-caps and Teflon lined septa. After addition of 4 ml to the vials and a stirrer bar, approximately 0.5 ml of headspace is left into which the needle is placed to prevent wicking of the sample during extraction. The fiber is then exposed to the aqueous phase for an appropriate time period with stirring and at room temperature. After extraction, the fiber is directly exposed to the hot injector of the GC for analysis.

2.5. Optimisation

Initial experiments focused on determining the time at which equilibrium was established between the analytes in the stationary and aqueous phases. Triplicate solutions were extracted for periods of time ranging from 10–120 min. The amount extracted at each time was then calculated and graphed against time. The equilibration times were determined by inspection and are listed in Table 1.

Optimisation of the desorption temperature and time was investigated by considering the amount desorbed from fibers after extraction of analytes from a solution of known concentration and the subsequent carryover at a range of temperatures and time periods. The optimised conditions were 5 min desorption at 230°C.

The linearity of the method was tested by analysing triplicate solutions over the range 0.1–1000 ng/ml, on the NPD, MS and FID. Each set of replicates was one tenth the concentration of the previous one. Amounts extracted were calculated by comparison with calibration curves and plotted against the initial concentration of the solution. The precision of the method was determined with the NPD and MS by extracting a minimum of seven replicate samples of 50 ng/ml and 10 ng/ml, respectively. The relative standard deviation (% R.S.D.) was calculated by dividing the standard deviation by the mean and multiplying by 100.

As a means of enhancing the extraction of analytes, the effect of ionic strength and pH was investigated. 4-ml solutions were analysed over the pH range 4–10 by addition of buffers. The low pH buffer was acetic acid–sodium acetate and the high pH buffer, sodium hydroxide–boric acid; both prepared according to Perrin and

Table 1
Selected nitrogen containing herbicides

Herbicide		Molecular formula	Solubility in water (mg/l)	Equilibration time (min)	K value
Class	Name				
Triazines	Atrazine	$C_8H_{14}ClN_5$	70	90	2000[a]
	Hexazinone	$C_{12}H_{20}N_4O_2$	330 000	10	300[a]
	Propazine	$C_9H_{16}ClN_5$	8.6	90–120	3000[a]
	Metribuzin	$C_8H_{14}N_4OS$	1200	50–90	200[a]
	Simazine	$C_7H_{12}ClN_5$	3.5	10	300[a]
Nitroanilines	Benfluralin	$C_{13}H_{16}F_3N_3O_4$	<1	50–90	7000[b]
	Isopropalin	$C_{15}H_{23}N_3O_4$	0.1	50	5000[b]
	Pendimethalin	$C_{13}H_{14}N_3O_4$	0.3	50	20 000[b]
	Profluralin	$C_{14}H_{16}F_3N_3O_4$	0.1	30	7000[b]
	Trifluralin	$C_{13}H_{16}F_3N_3O_4$	20	50	8000[b]
Substituted Uracils	Bromacil	$C_9H_{13}BrN_2O_2$	815	30	400[a]
	Terbacil	$C_9H_{13}CN_2O_2$	710	50–90	200[a]
Thiocarbamates	EPTC	$C_9H_{19}NOS$	365	90	4000[a]
	Molinate	$C_9H_{17}NOS$	800	50–90	2000[a]
	Cycloate	$C_{11}H_{21}NOS$	85	90	7000[a]
	Butylate	$C_{11}H_{23}NOS$	45	90	3000[a]
	Pebulate	$C_{10}H_{21}NOS$	60	90	4000[a]
	Vernolate	$C_{10}H_{21}NOS$	107	90	10 000[a]
Others	Metolachlor	$C_{15}H_{22}ClNO_2$	530	50	4000[a]
	Oxyfluorofen	$C_{15}H_{11}ClF_3NO_4$	0.1	30	3000[b]
	Oxadiazon	$C_{15}H_{18}Cl_2N_2O_3$	0.7	50	20 000[b]
	Propachlor	$C_{11}H_{14}ClNO$	700	50	1000[a]

[a,b] K values determined under optimum conditions; overnight extraction, 4 M NaCl ([a]) or unsalted ([b]).

Dempsey [23]. Subsequently, pH 2 and pH 11 were tested by simply using appropriate concentrations of acetic acid (1 M) and NaOH (0.01 M) respectively. Ionic strength was tested by addition of NaCl (2 M, 4 M, and supersaturated) to triplicate solutions. The effect of a combination of salt and pH was investigated by combining pH 2 and 4 M NaCl. In all cases triplicates were analysed together with triplicate neutral control solutions with which comparisons were made.

Detection limits are defined as the concentration of an analyte in a sample which gives rise to a peak with a signal-to-noise ratio (S/N) of 3. Solutions were analysed at subsequently lower levels until they approached the limit of quantification, at which point the limits of detection were calculated. For mass spectral analysis, the ratio of the quantification mass peak to the noise was used. If lower detection limits are required, analysis of more than one characteristic mass peak can be used to improve the signal-to-noise ratio at low concentrations. For the FID analysis, an area count of 1000 was chosen as a conservative estimate of the smallest detectable peak. This area count corresponds to three times the typical noise reading, which ranges from 400 to 600. For the NPD, the noise was measured before each run and was typically equivalent to a signal of 13 area counts, therefore the lowest detectable peak was defined as having an area greater than 40 area counts.

2.6. Sample analysis

Soil samples were analysed qualitatively by taking 0.3 g soil and adding approximately 4 ml of water, to ensure that the sample could be stirred. Wine samples were directly analysed by taking 4-ml aliquots. The standard addition method was used to quantify the amount of any herbicide present in real samples analysed with the MS. Samples were first analysed and herbicides identified if their mass spectrum and retention times were the same as those found for standards. Subsequently, triplicate real samples, together with triplicate spiked samples were analysed and the results calculated for those herbicides previously identified. Spike concentrations were 10 and 20 ng/ml.

3. Results and discussion

Solid-phase microextraction involves the partitioning of analytes between the sample matrix and a polymeric stationary phase according to their partition coefficients, K. This process can be defined by the following equation [16]

$$n_s = \frac{K V_s V_{aq} C^o_{aq}}{K V_s + V_{aq}} \quad (1)$$

where n_s is the amount extracted by the fiber coating, K is the partition coefficient, V_{aq} and V_s are the volumes of the aqueous and stationary phases, respectively and C^o_{aq} is the initial concentration of analytes in the aqueous phase. It can be seen from Eq. 1 that the sensitivity of the method and the linear range are dependent upon the volume of the stationary phase and the partition coefficient. The choice of an appropriate stationary phase is thus extremely important. Currently two coated fibers are available commercially, the poly(dimethylsiloxane) and poly(acrylate). The herbicides analysed here are predominantly polar analytes with small octanol–water partition coefficients (log P_{ow}) [24], and generally high solubility in water. These analytes should therefore partition more favourably into a polar stationary phase than a non-polar one. This is exemplified by the analysis of phenols, a group of polar analytes which are poorly extracted from water by the poly(dimethylsiloxane) fiber but which are successfully extracted with the poly(acrylate) [20]. Preliminary experiments, conducted to compare the two coatings, indicated that the poly(acrylate) was capable of extracting all the analytes, whilst the poly(dimethylsiloxane) was not.

The rate at which the extraction process reaches equilibrium is primarily dependent upon the rate of mass transfer in the aqueous phase [25], and is improved by stirring. Therefore, all extractions were performed under stirred conditions. The time profiles obtained for the target herbicides enabled determination of the equilibration times shown in Table 1. Equilibration times ranged from 10 to 120 min with more than half of the analytes reaching equilibrium by 50 min. The optimised GC separation is also 50 min in duration, thus a 50-min extraction time ensures optimal time efficiency for the SPME method. The two factors which have the potential to be affected by choosing an extraction time that is less than the time required for equilibrium are precision and sensitivity. The former could be adversely affected if the extraction time is not carefully monitored since slight deviations in the extraction time imply large deviations in the amount extracted when equilibrium has not been established. Therefore extractions were performed for 50 ± 2 min. The latter is only likely to be affected if the K values are small and equilibrium has not been reached. Fortunately, the analytes with smaller K values generally have equilibration times less than 50 min thus the overall sensitivity of the method will not be affected. Fig. 1 shows a chromatogram obtained from extraction of a 100 ng/ml sample of the 22 herbicides using these conditions, with MS (a) and NPD (b) detection.

The amount of each analyte extracted by a 95 μm poly(acrylate) coated fibre was determined at equilibrium and used to calculate the K values from Eq. 1. The results are presented in Table 1 together with literature values for the analytes' solubility in water. It is immediately clear that there is a correlation between solubility in water

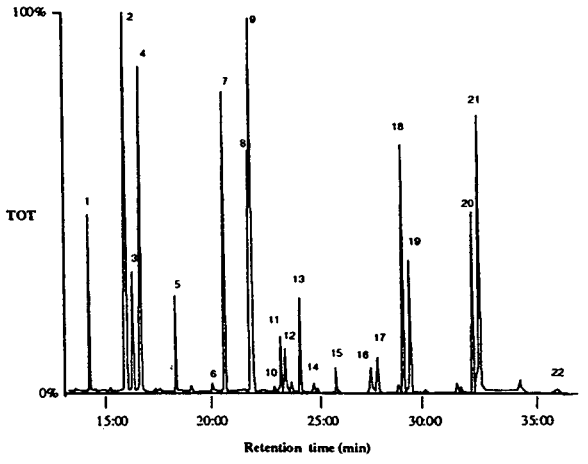

(a)

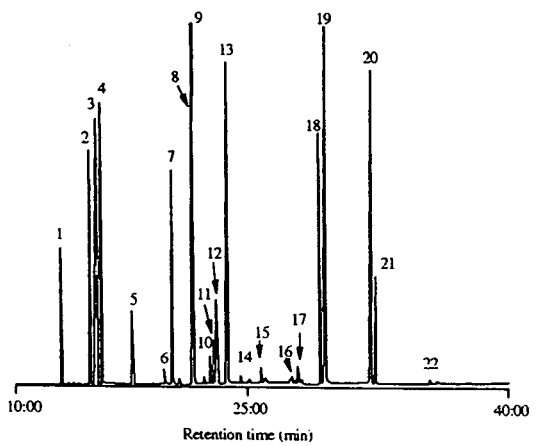

(b)

Fig. 1. Chromatograms of 50-minute extractions of 100 ng/ml herbicide standards. (a) Mass spectral detection, total ion plot; (b) nitrogen–phosphorous detection. Peak identification: 1 = EPTC; 2 = Butylate; 3 = Vernolate; 4 = Pebulate; 5 = Molinate; 6 = Propachlor; 7 = Cycloate; 8 = Trifluralin; 9 = Benfluralin; 10 = Simazine; 11 = Atrazine; 12 = Propazine; 13 = Profluralin; 14 = Terbacil; 15 = Metribuzin; 16 = Bromacil; 17 = Metolachlor; 18 = Isopropalin; 19 = Pendimethalin; 20 = Oxadiazon; 21 = Oxyfluorofen; 22 = Hexazinone.

and K values, the more soluble an analyte the lower the K. Therefore, by decreasing the solubility of a given analyte in water, the amount extracted can be increased. There are several ways that this could be achieved, including addition of salt to the matrix, variation of the matrix pH, or formation of derivatives. Consequently, both the effect of ionic strength and pH were determined. The effect of varying the ionic strength was tested by comparing three concentrations of NaCl. The addition of salt at each concentration generally caused an increase in the amount extracted, with the exception of the nitroanilines, oxadiazon and oxyfluorofen. The investigation of pH effect was undertaken with the aim of finding a pH at which the extraction of these compounds was enhanced and at which the extraction of the other classes was not significantly decreased. Varying the pH from 4 to 11 had no significant effect on the extraction of any of the analytes, however, at pH 2 the extraction of the nitroanilines and oxyfluorofen was enhanced. The success of salt and pH 2 individually warranted extraction of the analyte mixture under conditions of salt and pH 2, to optimise extraction of all analytes. The results are shown in Fig. 2 and indicate that although the combination is effective for the extraction of most triazines, substituted uracils and thiocarbamates, it is not as effective as salt alone. Furthermore, the combination is detrimental to the extraction of nitroanilines, oxyfluorofen and oxadiazon which are best extracted under neutral or pH 2 conditions. Not surprisingly, different classes of analytes have different conditions under which optimum extraction occurs, however even under neutral conditions, the limits of detection (Table 3) are sufficiently low with the GC–MS to enable determination of all the analytes at low to sub ng/l levels.

The precision of the method was investigated for a set of seven replicates using both the MS and NPD detectors (Table 2). Differences in the precision achieved with the two detector systems are primarily due to the difficulty in accurately integrating small, broad peaks on the NPD. The majority of analytes were extracted with precision ranging from 2–20%. Since the US EPA only requires that methods which are to be accepted as standard methods have R.S.D. values below 30%, the precision of the new method

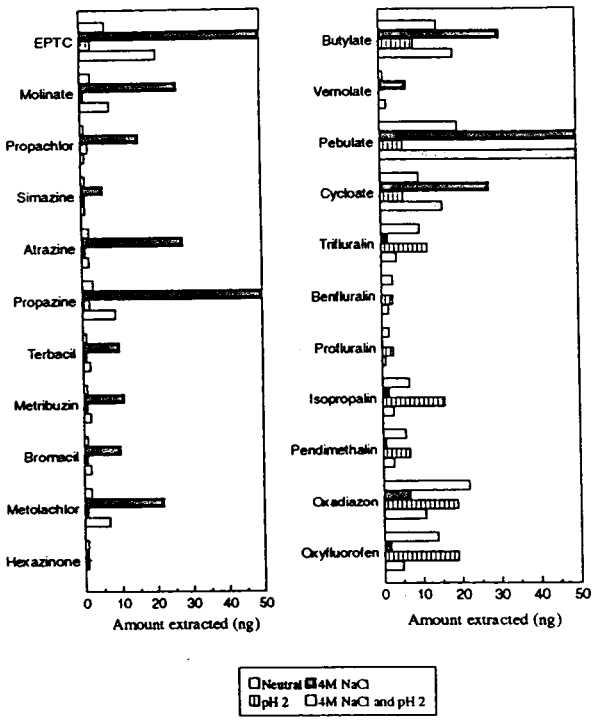

Fig. 2. The effect of salt, pH 2 and combined salt and pH 2. Triplicate standards (100 ng/ml) extracted for 50 min.

Table 2
Precision data obtained from 50-minute extractions of selected herbicides

Herbicide	Amount extracted[a] (ng)	% R.S.D. (NPD)	% R.S.D. (MS)
EPTC	1.9	9	10
Butylate	4.1	13	13
Vernolate	1.5	12	13
Pebulate	12	12	13
Molinate	1.7	7	12
Propachlor	1.2	9	5
Cycloate	4.4	12	14
Trifluralin	5	13	16
Benfluralin	1.6	13	11
Simazine	0.42	9	2
Atrazine	1.1	14	9
Propazine	0.7	12	14
Profluralin	1.5	7	7
Terbacil	0.54	10	13
Metribuzin	0.52	9	13
Bromacil	0.58	22	10
Metolachlor	0.6	10	15
Isopropalin	2.8	20	21
Pendimethalin	2.5	14	17
Oxadiazon	4	18	22
Oxyfluorofen	7	14	14
Hexazinone	0.34	22	4

[a] Average of seven replicates, containing 10 ng/ml of each analyte.

can be considered good. It is expected that precision will be improved with the use of an autosampler.

The linearity of the method has been investigated over the range 0.1–1000 ng/ml, with the GC–MS, GC–NPD and GC–FID. Of the 22 analytes analysed, 21 had correlation coefficients greater than 0.99 when linear regression analysis is performed, both when the y intercept is fixed at 0, or when it is allowed to vary.

The calculated limits of detection are presented in Table 3. The values were calculated from 100 ng/ml, 1 ng/ml and 0.01 ng/ml extractions for the FID, NPD and MS, respectively and refer to the concentration of a sample from which a sufficient quantity will be extracted by the fiber to be detected. The limits of detection are generally improved by three orders of magnitude with the MS when compared with the FID. The predominant difference in the limits of detection using the FID and NPD actually stems from the very low noise levels found in the NPD chromatograms rather than from a significant improvement in area counts for analytes. The limits of detection for US EPA methods 507 and 508 are shown for comparison, they are estimated detection limits [3] of the respective methods, obtained with GC–NPD and GC–ECD. All the relevant herbicides analysed by SPME–GC–MS had limits of detection well below those required by the EPA. Most of the analytes are also sufficiently extracted to provide NPD limits of detection which would be satisfactory for the EPA.

After the method development stage was complete, real samples were analysed with the GC–MS. Both contaminated soil and commercial wine samples were analysed. The soil samples were suspended in water and analysed as a

Table 3
Limits of detection for 50-minute extraction of selected herbicides

Herbicide	FID[a] (ng/l)	NPD[b] (ng/l)	MS[c] (ng/l)	EPA 507/508[3] (ng/l)
EPTC	2000	50	0.8	200
Butylate	1000	20	0.1	100
Vernolate	1000	20	0.5	100
Pebulate	1000	20	1	100
Molinate	2000	60	0.3	100
Propachlor	6000	800	15	500
Cycloate	800	20	0.05	200
Trifluralin	400	30	0.02	20
Benfluralin	300	30	0.4	NA[d]
Simazine	1000	70	1	100
Atrazine	7000	40	3	100
Propazine	10 000	50	0.3	100
Profluralin	200	30	0.1	NA
Terbacil	15 000	200	1	4500
Metribuzin	14 000	200	3	100
Bromacil	19 000	400	0.1	2500
Metolachlor	1000	200	0.01	700
Isopropalin	300	10	0.1	NA
Pendimethalin	200	20	0.1	NA
Oxadiazon	300	30	0.01	NA
Oxyfluorofen	200	300	6	NA
Hexazinone	2000	6000	1	800

[a] Determined from 100 μg/l solutions.
[b] Determined from 10 μg/l solutions.
[c] Determined from 10 ng/l solutions.
[d] NA = Not Applicable, i.e. not analysed by EPA 507 or 508.

purely qualitative experiment by the new procedure. Fig. 3 shows a portion of the GC–MS chromatogram obtained from extraction of a sample taken from a lawn to which a common herbicide had been applied. The total ion plot and two selected ion plots (292 and 335) are shown. The retention time and mass spectrum of the peak at 22:26 min are both indicative of the presence of Benfluralin (M_r 335, base peak, 292) in the soil sample. Several wine samples were analysed by the standard addition procedure after initial screening with the method indicated the presence of some herbicides. An example is the identification of nine of the twenty-two herbicides in a white wine from the Rhone valley, France. The herbicides found, together with their concentration in the sample, are given in Table 4. Concentrations ranged from 0.4 to 3.1 ng/ml. However, since the samples were spiked at 10 and 20 ng/ml, the accuracy of the calculated results for some analytes is limited. It is however indicative of the ability of the method to successfully analyse real samples.

4. Conclusions

This paper has demonstrated SPME to be a precise, reproducible technique for the analysis of nitrogen-containing herbicides from clean water. The new method is linear over several orders of magnitude, with either FID, NPD or MS detection. The detection limits required by EPA methods 507 and 508 are easily achieved with the use of the ion-trap MS in the total ion current mode. The use of salt enables substantial

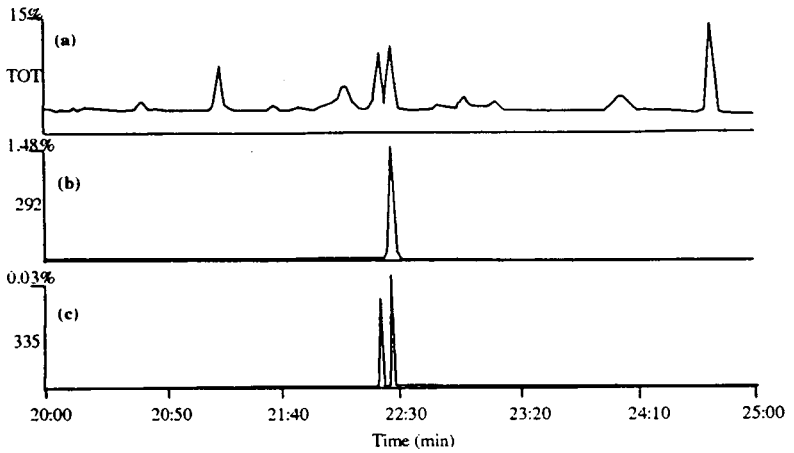

Fig. 3. GC–MS of pesticide residues extracted from soil by SPME. (a) Total ion plot, (b) selected ion plot, base peak = 292, (c) selected ion plot, $M^+ = 335$.

increases in the amount extracted of most analytes and can be used to improve the limit of detection if sub-ppt levels need to be detected with the NPD or FID.

Analysis of herbicide standards from more complex matrixes, such as those found in wine, have also been successfully performed. The standard addition procedure, combined with MS detection, enabled identification and quantitation of herbicides already present in the samples.

Table 4
Herbicides found in a wine sample

Herbicide	Concentration (ng/ml)[a]
Butylate	0.7
Pebulate	3.7
Trifluralin	2.2
Benfluralin	2.0
Profluralin	3.1
Isopropalin	0.8
Pendimethalin	0.9
Oxadiazon	0.4
Oxyfluorofen	1.0

[a] Triplicate samples quantified by standard addition at three concentrations.

The application of the method to the analysis of solid samples was exemplified by the identification of herbicides in contaminated soil.

Acknowledgements

The authors wish to gratefully acknowledge financial support from the Natural Sciences and Engineering Research Council of Canada, Varian Inc., and Supelco Inc.

References

[1] J. Tronczynski, C. Munschy, G. Durand and D. Barceló, Sci. Total Environ., 132 (1993) 327.
[2] H. Kobayashi, K. Ohyama, N. Tomiyama, O. Jimbo, O. Matano and S. Goto, J. Chromatogr., 643 (1993) 197.
[3] D. Barceló, J. Chromatogr., 643 (1993) 117.
[4] W.E. Pereira and C.E. Rostad, Environ. Sci. Technol., 24 (1990) 1400.
[5] R. Frank and Ll. Logan, Arch. Environ. Contam. Toxicol., 17 (1988) 741.
[6] W.E. Preiera, C.E. Rostad and Th.J. Leiker, Anal. Chim. Acta, 228 (1990) 69.
[7] K.A. Caldwell, V.M.S. Ramanujan, Z. Cai and M.L. Gross, Anal. Chem., 65 (1993) 2372.

[8] T.S. Steinhelmer, R.L. Pfeiffer and K.D. Scoggin, Anal. Chem., 66 (1994) 645.
[9] S. Durand, R. Forteza and D. Barceló, Chromatographia, 28 (1989) 597.
[10] G. Durand and D. Barceló, Anal. Chim. Acta, 243 (1991) 259.
[11] J.E. Patrick, Pesticides in Ontario Drinking Water from Surface Sources, 1988, Ontario Ministry of Agriculture and Food, September 1990.
[12] W.E. Johnson, N.J. Fendinger and J.R. Plimmer, Anal. Chem., 63 (1991) 1510.
[13] A. Di Corcia, R. Samperi, A. Marcomini and S. Stelluto, Anal. Chem., 65 (1993) 907.
[14] J.C. Molto, Y. Pico, G. Font and J. Manes, J. Chromatogr., 555 (1991) 137.
[15] C. Arthur and J. Pawliszyn, Anal. Chem., 62 (1990) 2145.
[16] Z. Zhang, M.J. Yang and J. Pawliszyn, Anal. Chem., 66 (1994) 847A.
[17] C. Meng, C.L. Arthur, P. Pawliszyn, R.P. Belardi and K.F. Pratt, Analyst, 118 (1993) 1501.
[18] C.A. Arthur, K. Pratt, S. Motlagh and J. Pawliszyn, Environ. Sci. Technol., 26 (1992) 979.
[19] Z. Zhang and J. Pawliszyn, J. High Resolut. Chromatogr., 16 (1993) 689.
[20] K.D. Buchholz and J. Pawliszyn, Anal. Chem., 66 (1994) 160.
[21] D.W. Potter and J. Pawliszyn, Environ. Sci. Technol., 28 (1994) 298.
[22] K. Buchholz and J. Pawliszyn, Environ. Sci. Technol., 27 (1993) 2844.
[23] D.D. Perrin and B. Dempsey, Buffers for pH and Metal Ion Control, Chapman and Hall, London, 1974.
[24] A. Noble, J. Chromatogr., 642 (1993) 3.
[25] D. Lough, S. Motlagh and J. Pawliszyn, Anal. Chem., 64 (1992) 1187.

ELSEVIER

Journal of Chromatography A, 704 (1995) 173–178

JOURNAL OF CHROMATOGRAPHY A

Validation of quantitative chromatographic analysis on laboratory-prepared thin layers ☆

Mira Petrović*, Marija Kaštelan-Macan

Laboratory of Analytical Chemistry, Faculty of Chemical Engineering and Technology, Marulićev trg 20, 41000 Zagreb, Croatia

First received 13 October 1994; revised manuscript received 10 December 1994; accepted 5 January 1995

Abstract

Validation of the determination of amino acids on laboratory-prepared plates was performed on a mixed natural zeolite and microcrystalline cellulose sorbent. Chromatograms were recorded in the visible region using a Datacolor DC 3890 reflectance spectrometer, Camag Turner Fluorimeter 111 slit-scanning densitometer and Leco 2001 image analyser. The precision, detection limit and limit of quantification for each method were determined. A lower total R.S.D. was obtained by measuring colour remission with the Datacolor system (2.7% for high concentration and 3% for low concentration), with an instrumental R.S.D. of 0.1–0.2%. Densitometry and image analysis resulted in a lower precision, especially at low concentration (total R.S.D. > 10%), with a significant instrumental error.

1. Introduction

Commercial precoated TLC plates with performance and consistency acceptable for quantitative analysis are generally used by analytical chemists. However, in some instances, such as in the investigation of new or physically and chemically modified sorbents, laboratory-prepared layers are needed. Problems connected with quantitative analysis on such layers are numerous. The principal barrier is the noise component of the signal obtained by sophisticated scanning densitometers as a result of heterogeneity of the layer structure, low abrasion resistance and damages to the sorbent surface [1]. Application of precoated plates minimizes the error that is the result of the signal-to-noise ratio. However, the problem of diffuse and irregular spots is not restricted only to laboratory-made supports. On commercial precoated plates diffuse spots can appear when the analyte concentration is very low and large sample volumes are applied to the chromatographic plate. Irregular spots usually appear near the second solvent front. Additional problems occur when chromatograms are made visible by application of chromogenic reagents resulting in a coloured and non-uniform background. Therefore, the precision and accuracy of quantitative TLC analysis depend on the layer characteristics and the validation procedure should take these parameters into account.

The aim of this work was to validate the results of intra-laboratory studies dealing with

* Corresponding author.

☆ Presented at the *International Symposium on Chromatographic and Electrophoretic Techniques, Bled, Slovenia, 10–13 October 1994.*

0021-9673/95/$09.50
SSDI 0021-9673(95)00018-6

quantitative analysis on laboratory-prepared plates. For this purpose the following chromatographic system was used: sorbent, natural zeolite mixed with microcrystalline cellulose; and test samples, α-alanine and glycine. This system was chosen as a model system for the determination of limiting factors in the quantitative analysis of diffuse and irregular spots obtained on laboratory-prepared plates.

2. Experimental

2.1. Chromatographic system

Sorbent

A mixture of microcrystalline cellulose (Merck) and natural tuff (1:1, w/w) was suspended in water, homogenized with an electric stirrer and spread on glass plates (20 × 20 cm) with a Camag applicator. The natural tuff, originating from the vicinity of Donje Jasenje, Croatia, consisted mainly of clinoptilolite, a mineral of the zeolite group, with minor amounts of feldspar, illite, sepiolite and calcite. The tuff was previously sieved and the fraction with particle size <40 μm was used for the layer preparation. The thickness of the wet layer was 300 μm. All experiments were performed on layers dried at room temperature.

Sample

A mixed stock standard solution of α-alanine and glycine was prepared by dissolving accurate amounts of powdered amino acids (Merck) in ethanol–H_2O (1:1, v/v). This solution was suitably diluted to give a mass concentration of each compound in the range 5–500 μm/ml.

A 10-μl Hamilton syringe was used for sample spotting. Samples were applied either as a narrow band 15 mm long or as spots with an approximate diameter of 5 mm.

Developing system

Phenol (saturated with water)–ethanol–acetic acid–water (12:4:1:4, v/v) was used.

Detection reagent

Spots were detected by spraying with ninhydrin solution (1% in 1-butanol) and heating at 80°C for 20 min.

2.2. Apparatus and conditions for determination

The following were used:

1. Datacolor DC 3890 reflectance spectrometer (Datacolor, Switzerland) equipped with an IBM-PC XT/AT computer; monitoring range, 400–700 nm with 10-nm intervals; screen diameter, 18 mm; monitoring wavelength (remission minimum), alanine λ = 510 nm and glycine λ = 500 nm.
2. Leco 2001 image analyser (Leco, Germany) equipped with a 486XT computer and high-resolution CCD camera with zoom; calibration, 0.1609 μm per pixel; determination of spot area in manual mode.
3. Camag Turner fluorimeter 111 slit-scanning densitometer (Camag, Muttenz, Switzerland) equipped with a chart recorder; slit width, 1 mm; scanning speed, 20 mm/min; filter number, 826; λ = 510 nm; chart paper speed, 20 mm/min; range, 5 mV.

3. Results

3.1. Colour analysis–visible reflectance spectrometry

The reflectance intensity of reddish violet spots was measured using the Datacolor DC 3890 reflectance spectrometer. The on-plate remission spectrum was plotted for amino acid samples (Fig. 1). The wavelengths of the remission minimum (500 nm for glycine and 510 nm for alanine) were chosen for further determination. The calibration graphs of remission (%) against sample concentration, regression equations and correlation coefficients are given in Fig. 2.

The precision of quantitative analysis on zeolite layers was checked by applying on the same plate seven loadings of the mixed standard solutions (low concentration level, 30 μg/ml

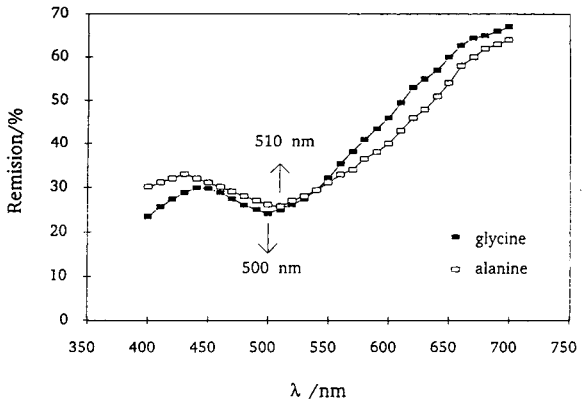

Fig. 1. Remission on-plate spectra of (□) alanine and (■) glycine obtained using the Datacolor DC 3890 visible reflectance spectrometer.

corresponding to 0.3 μg per spot; and high concentration level, 250 μg/ml corresponding to 2.5 μg per spot). Each spot was recorded five times and the relative standard deviation (R.S.D) was calculated. The results are summarized in Table 1. The error involved in the chromatographic and detection stages was estimated from the results of seven loadings (total R.S.D.). The instrumental R.S.D. corresponds to the error involved in the detection stage and it was obtained by multiple measurements of the same spot without resetting the screening position. This value represents the minimum error involved in the quantitative procedure and is attributable to the instrumentation system alone.

The detection limit (mass of substance that gives a response equal to twice the background) and the limit of quantification (mass of substance that allows the determination with 5% reliability) are given in Table 2. The results show that there is no significant difference between two amino acids and the values listed in table correspond for both alanine and glycine.

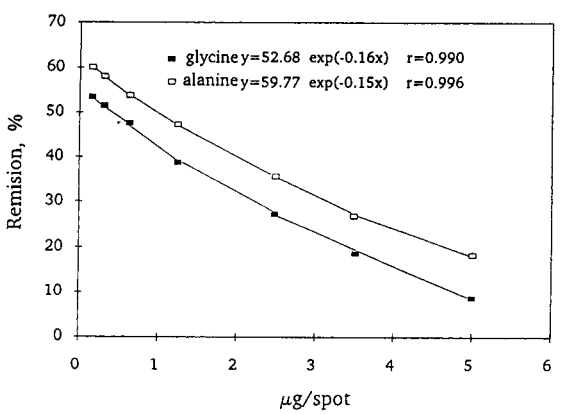

Fig. 2. Calibration graphs: colour analysis using the Datacolor DC 3890.

3.2. Image analysis

Calibration graphs of the spot area and spot intensity, determined with the Leco 2001 image analyser, as a function of sample concentration were plotted for each compound. Two sets of experiments were conducted. In one experiment samples were applied as a narrow band (length 15 mm) and in the other as a spot. The calibration graphs are given in Fig. 3A and B, respectively. Using an image analyser the chromatograms are imaged by a charged-coupled video camera and the information obtained is processed and documented in the form of a black-and-white picture. The spot area and spot intensity were determined using the "manual mode" software option for indication of spot edges. The measured value of the spot intensity is defined as the intensity of white colour in the spot within the range from 0 (100% black) to 255 (100% white).

3.3. Densitometry

For densitometric determination, calibration graphs of peak area against sample concentration were plotted (Fig. 4). A chromatogram of a mixed standard solution is given in Fig. 5. Each peak was recorded twice, and from the chromatographic profiles obtained areas under the chromatographic curves were determined using a planimeter as the mean value of three determinations. The R.S.D. of the planimetric determination of peak area was checked separately, and values of 0.5% for high concentration and 1.0% for low concentration were obtained on the basis

Table 1
Total and instrumental R.S.D. values

Method of quantification	R.S.D. (%)				
	Type	Alanine		Glycine	
		2.5 μg per spot	0.3 μg per spot	2.5 μg per spot	0.3 μg per spot
Color analysis: Datacolor 3890	Total	2.71	3.07	2.74	2.92
	Instrumental	<0.1	0.2	<0.1	0.2
Densitometry: Camag Turner Fluorimeter 111	Total	3.53	12.08	3.52	12.05
	Instrumental	1.53	8.99	1.40	8.80
Image analysis:	Spot area:				
Leco 2001, sample applied as band	Total	4.76	BDL[a]	4.67	BDL
	Instrumental	2.77	BDL	2.87	BDL
	Spot intensity:				
	Total	3.03	BDL	3.37	BDL
	Instrumental	0.45	BDL	0.40	BDL
Image analysis:	Spot area:				
Leco 2001, sample applied as a spot	Total	3.85	10.31	4.02	10.88
	Instrumental	2.00	7.40	2.10	7.00
	Spot intensity:				
	Total	3.80	9.45	3.65	9.00
	Instrumental	0.90	5.90	1.00	5.35

[a] BDL = below detection limit.

of seven measurements. Errors associated with the various steps in the densitometry are given in Table 1. The measurement error (instrumental R.S.D. was determined by multiple scanning (5×) of a single lane without changing any experimental variables between scans.

4. Discussion

Modern TLC has introduced sophisticated mechanical scanning densitometers, electronic scanners and video systems in daily laboratory practice [2]. One of the prerequisites for their meaningful and successful application is meeting detailed set criteria in preliminary stages of quantitative (QTLC). These criteria include the use of commercial precoated plates with strictly controlled performance. The question is how to perform, if it is necessary, quantitative analysis on laboratory-prepared layers. These layers cannot compete with precoated plates in term of consistency and homogeneity. Consequently, the spots obtained on laboratory-prepared plates are

Table 2
Detection limit and limit of quantification for the methods used

Method	Detection limit (μg per spot)	Limit of quantification (μg per spot)
Colour analysis	0.08	0.16
Image analysis:		
Sample applied as band	0.35	1.25
Sample applied as spot	0.20	1.00
Slit-scanning densitometry	0.20	0.50

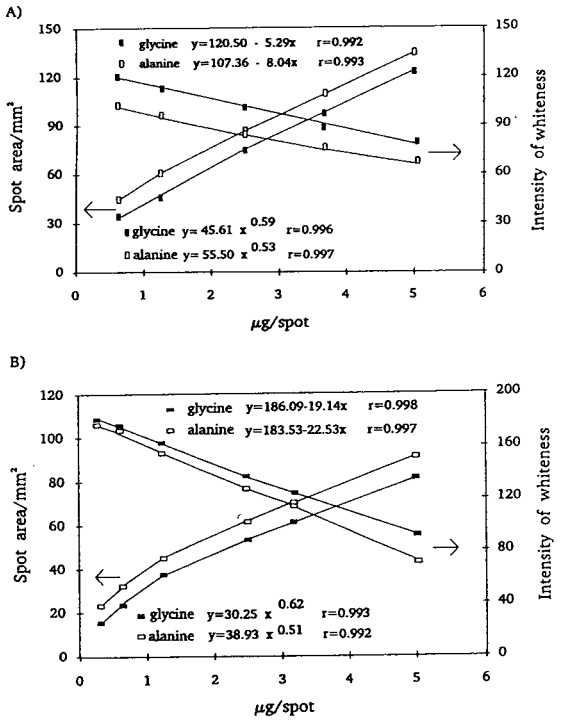

Fig. 3. Calibration graphs: image analysis using the Leco 2001 image analyser. (A) Sample applied as a 15-mm band; (B) sample applied as a spot.

more diffuse, making quantitative analysis more difficult even if an excellent separation is achieved.

The principal sources of error in QTLC are

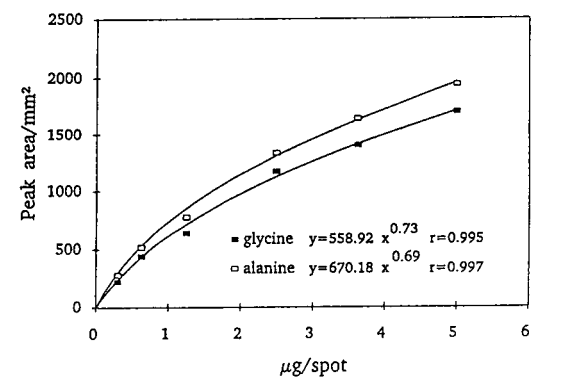

Fig. 4. Calibration graphs: densitometric scanning using Camag Turner Fluorimeter 111.

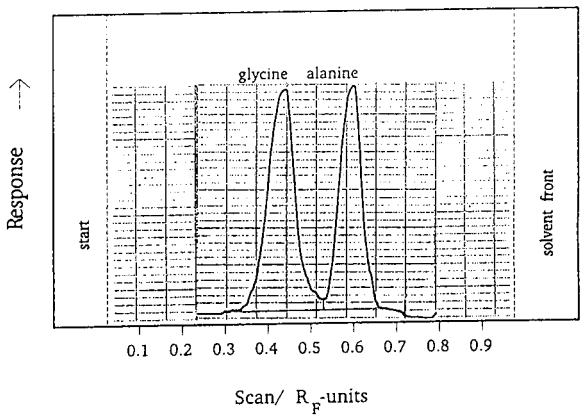

Fig. 5. Densitometric scan of a mixed standard solution Alanine and glycine concentrations, 0.25 µg/µl.

the reproducibility of sample application, reproducibility of the chromatographic conditions (heterogeneity of sorbent, deviations in layer thickness, non-linear solvent front) and reproducibility of the instrumental measurements.

The sample must be distributed homogeneously and the volume of sample applied to the layer must be accurately known. If possible, the sample application procedure should be automated using spray-on devices. However, many analytical laboratories, especially research laboratories dealing with small numbers of samples, use hand-held microsyringes. Although direct measurements of the precision of spotting procedure, relevant to this particular examination, were not conducted, some estimations on the basis of literature data can be made. The R.S.D. in spotting thin layers using a Hamilton microsyringe with a repeating dispenser, according to the literature [3,4], varies from 1.3 to 6.8% for delivery of 10 µl of ethanolic sample solution. This variation in the accuracy is due in part to the experience of the particular operator.

The difference between the total R.S.D. and instrumental R.S.D. corresponds to the error involved in the chromatographic stage. This error can be mainly attributed to the reproducibility of the spotting procedure, since the reproducibility of the chromatographic conditions was maintained by multiple determination

on a single plate. In all cases this value ranged between 2 and 3.3%.

A lower total R.S.D. was obtained by measuring reflectance with the Datacolor DC 3890: 2.7% for high concentration and 3% for low concentration with an instrumental R.S.D. of 0.1–0.2%. Transmission scanning (densitometry) and image analysis resulted in lower precision, especially at low concentration (total R.S.D. >10%), with a significant instrumental error.

The mechanical strength, durability and abrasion resistance of zeolite layers are comparable to those of conventional cellulose or silica gel layers. However, because of the considerably larger particle size of zeolite (<40 μm) and the high porosity of prepared layers, the spot edges were not sharp enough for automatic determination of spot size using the Leco 2001 image analyser. Working in the manual mode leads to a significant instrumental error and the results obtained are largely dependent on operator skill. An additional problem was associated with a reduced contrast between the spot and background due to the grey colour of the zeolite layer.

The main advantage of colour analysis using the Datacolor DC 3890 visible reflectance spectrometer is the possible analysis of irregular and diffuse spots. The parallel background colour analysis minimizes the problem of coloured and non-uniform layers. This method can be applied in laboratory practice for determination only in the visible range (λ = 400–700 nm), but with low sensitivity at the edge of the wavelength range (light yellow spots). The advantage is fast data acquisition, simple instrument design and possible analysis of two-dimensional chromatograms which are difficult to scan using conventional slit-scanning densitometers.

References

[1] C.F. Poole and S.K. Poole, Anal. Chem., 66 (1994) 27A.
[2] C.F. Poole and S.K. Poole, Chromatography Today, Elsevier, Amsterdam, 1991.
[3] B.R. Mullin, C.M.B. Poore and B.M. Rupp, in J.C. Touchstone and J. Sherma (Editors), Techniques and Applications of Thin Layer Chromatography, Wiley, New York, 1985.
[4] K.R. Brain and R. Hardman, J. Chromatogr., 38 (1968) 355.

ELSEVIER

Journal of Chromatography A, 704 (1995) 179–193

JOURNAL OF CHROMATOGRAPHY A

Direct and indirect chiral separation of amino acids by capillary electrophoresis

Hong Wan[1], Per E. Andersson, Anders Engström, Lars G. Blomberg*

Department of Analytical Chemistry, Arrhenius Laboratories for Natural Sciences, Stockholm University, S-106 91 Stockholm, Sweden

First received 6 December 1994; revised manuscript received 30 January 1995; accepted 31 January 1995

Abstract

Two approaches to the chiral separation of racemic mixtures of amino acids by means of capillary electrophoresis have been evaluated. These were indirect separation of diastereomers formed by derivatization with (+)- or (−)-1-(9-fluorenyl)ethyl chloroformate and direct chiral separation after derivatization with 9-fluorenylmethyl chloroformate.

Separation conditions were optimized by the application of a full factorial design. For indirect separation, concentration of sodium dodecyl sulphate (SDS) and pH were the most important separation variables, and for direct separation, concentration of isopropanol (IPA), β-cyclodextrin and SDS were the most prominent factors affecting separation. The presence of IPA was a prerequisite for chiral recognition.

With regard to selectivity, efficiency, analysis time and ease of method development the best results were provided by the indirect method. It should be noted, however, that the success of this approach is based on the availability of a derivatization reagent in high optical purity.

1. Introduction

Capillary electrophoresis is a rapidly expanding area of analytical chemistry. In a number of publications, it has been demonstrated that this technique, in the form of electrokinetic chromatography (EKC), is suitable for chiral separations [1–9]. Two different approaches to achieve such a separation can be distinguished. These are direct chiral separation and indirect separation of diastereomers. In general, derivatization is performed prior to the introduction of the sample into the separation capillary. The purpose of such a derivatization is twofold: to improve separation and detection [10,11]. When chirality is maintained after the derivatization, direct chiral separation is attempted on separation systems providing chiral selectivity. Diastereomeric derivatives are separated on non-chiral systems. However, the formation of diastereomers can also be utilized as a mechanism for chiral recognition in the separation capillary [12]. Further, a few examples of chiral separation of underivatized amino acids have been described [13–15].

With the current techniques for chiral separation by capillary electrophoresis, derivatization is of crucial importance. High demands are

* Corresponding author.

[1] On leave from Lanzhou Institute of Chemical Physics, Chinese Academy of Sciences, Lanzhou 73000, China.

0021-9673/95/$09.50
SSDI 0021-9673(95)00146-8

thereby made on the properties of the derivatization reagents. An ideal reagent should thus fulfil several requirements [16]. First, it should be stable and give rapid reactions in high yields at low temperatures and the reaction products should be sufficiently stable. Excess reagent or by-products from the reaction should not disturb the separation. Further, the reagent should be selective for the target analytes. In those cases where diastereomers are formed, the reagent must have a very high degree of chiral purity. A small impurity can lead to large errors, especially in the determination of enantiomeric excess (e.e.) [11]. Further, the reagent should contain or produce a strong chromophore or fluorophore. The reagent should be commercially available, and for chiral reagents, it is desirable that they are available in the L- as well as the D-form, so that elution orders can be reversed when required. In addition, the reagents should be inexpensive, although chiral reagents in high purity are inherently costly. A large number of derivatization reagents have been developed for application in connection with chiral separation in HPLC [10,11]. Many of these have been examined with regard to electrophoretic methods, but the performance of some promising reagents remains to be evaluated. In the present work, a reagent, FLEC, belonging to the latter group was tested for indirect chiral separation of D- and L-amino acids by micellar electrokinetic chromatography (MEKC).

Several examples of the direct separation of chiral derivatives of D- and L-amino acids have been presented. Dansylation is here the most commonly applied derivatization method [15,17–25]. Eggum and Sørensen have discussed the merits of dansylation [26]. Other types of derivatization reagents include: naphthalene dicarboxaldehyde (NDA) [22,27,28], phenylhydantoin (PTH) [29–31] and 4-fluoro-7-nitrobenz-2,1,3-oxadiazol [32]. Several types of separation systems providing chiral selectivity have been applied for the separation of this type of derivatives. The selectivity may thus occur in the form of chiral mixed micelles, cyclodextrins, crown ethers and bile salts.

Chiral separation can, as mentioned above, be achieved on the basis of the formation of diastereomeric interactions in the column. This approach is applied in ligand-exchange electrophoresis and when crown ethers are present in the buffer. When the chiral Cu(II)–aspartame complex was included in the background electrolyte, as many as 14 out of 18 dansyl amino acids could be resolved [33].

A few applications of the separation of diastereomers have been published. First, Tran et al. used 1-fluoro-2,4-dinitrophenyl-5-L-alanine amide (Marfey's reagent) for the formation of amino acid diastereomers [34]. After derivatization with 2,3,4,6-tetra-O-acetyl-β-D-glucopyranosyl isothiocyanate (GITC), Nishi et al. [35] were able to separate 19 D,L-amino acids; GITC was employed also by Lurie [36]. Van der Wal et al. prepared diastereomers by derivatization with *o*-phthalaldehyde (OPA) and N-acetylcysteine [37]. Similarly, Kang and Buck derivatized amino acids with (OPA) and either N-acetyl-L-cysteine or N-*tert.*-butoxycarbonyl-L-cysteine [38]. Derivatization with (+)-diacetyl-L-tartaric anhydride has been presented [39]. The advantages of the diastereomer approach are that optimization is simple and rapid and that the MEKC technique, in general, provides higher efficiency than direct chiral separation methods where complexation with the chiral selector often results in slow kinetics.

The aim of the present work was, in general terms, to compare the pros and cons of direct and indirect separation of racemic mixtures of amino acids (AAs) by capillary electrophoresis. For that purpose, comparison has been made, after optimization, of the separation of racemic amino acids after their derivatization by two chemically similar reagents, FLEC (**1**) and FMOC (**2**). For the determination of D- and L-amino acids, these reagents fulfil most of the above mentioned requirements.

1

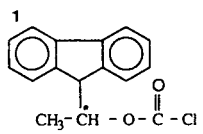

2

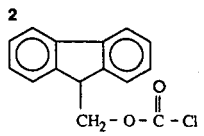

It has been demonstrated that the application of statistical techniques for the optimization of

the separation conditions in capillary electrophoresis is a fruitful approach [40–44], and in the present work, a full factorial design was employed for the optimization of the separation conditions.

2. Experimental

2.1. Apparatus

A Prince (Lauerlabs, Emmen, The Netherlands) electrophoresis instrument equipped with an on-column UV detector, CV[4] (ISCO, Lincoln, NE, USA), operated at 254 nm and a high voltage power supply, CZE 1000 R, 0–30 kV (Spellman High Voltage Electronics, Plainview, NY, USA) was used. Uncoated fused-silica capillary tubing (Polymicro Technologies, Phoenix, AZ, USA) 360 μm O.D. and 25 μm I.D. in different lengths was utilized. Samples were introduced by pressure. Chromatograms were recorded with an ELDS 900 laboratory data system (Chromatography Data System, Kungshög, Sweden).

2.2. Reagents

The amino acids were obtained from Sigma (St. Louis, MO, USA). Sodium dodecyl sulphate (SDS) was obtained from Fluka (Buchs, Switzerland), (+)- and (−)-1-(9-fluorenyl)-ethyl chloroformate (FLEC) and 9-fluorenylmethyl chloroformate (FMOC) from Eka Nobel (Bohus, Sweden). Hydroxypropyl-β-cyclodextrin (HP-β-CD) was synthesised according to Armstrong et al. [45]. Other reagents for preparation of buffers were of analytical grade. Buffers were prepared daily. The buffers were filtered through a 50 μm porous filter (Supelco, Bellefonte, PA, USA) before use.

2.3. Derivatization procedures

Derivatization of amino acids with (+)-FLEC and (−)-FLEC was as described earlier [46]; 200 μl of 10 m*M* FLEC was thus added to 200 μl of 3 m*M* amino acid in 0.2 *M* borate buffer (pH 9.0). This mixture was kept for 2 min, then extracted with 0.5 ml pentane to remove excess of reagent. After dilution, ten times with water, the sample was ready for introduction. Derivatization of amino acids with FMOC was as for FLEC.

2.4. Conditions

When changing buffers, the capillary was first rinsed with 0.1 *M* NaOH for 5 min, then with water for 10 min and it was finally conditioned with buffer for 30 min before sample introduction. Between sample introductions, the capillary was rinsed with buffer for 5 min. The separation capillary was thermostatted at 25°C. Optimization computer program was Codex (AP Scientific Service, Sollentuna, Sweden). Abbreviations: amino acids are indicated by three-letter symbols according to current standards [26].

2.5. Evaluation procedures

Resolution was calculated according to

$$R_s = \frac{1.18\,\Delta t}{w_{(0.5)1} + w_{(0.5)2}} \quad (1)$$

where Δt is the difference in migration times and $w_{(0.5)1}$ and $w_{(0.5)2}$ are the peak widths at half peak height.

According to Terabe et al. [47] the separation factor, α, in MEKC is

$$\alpha = \frac{k_2'}{k_1'} = \frac{t_2 - t_0}{t_1 - t_0} \times \frac{1 - t_1/t_{mc}}{1 - t_2/t_{mc}} \quad (2)$$

where t_1, t_2, t_0 and t_{mc} are the migration times of the first and second analyte peak, the aqueous phase and the micelles respectively, and k' is the capacity factor. The micelle time is thus necessary for the calculation of α. However, the determination of t_{mc} is uncertain in cases when the buffer contains organic solvents [48] or cyclodextrin [23]. Therefore, the first term on the right hand side of Eq. 2 was utilized as a measure of selectivity. When applied to MEKC, this expression is always $< \alpha$, however, for

EKC, Eq. 2 is in accordance with the definition of α.

3. Results and discussion

3.1. Optimization

In CE, a number of variables has to be considered when optimal conditions are sought. Several of these are interrelated, and a univariate approach to the optimization, thus trying to optimize one variable at a time, will, in general, not result in optimal conditions. Further, non-linear models are often required to describe resolution as a function of the separation variables. For these reasons, a multivariate approach has to be adopted for the optimization [49].

As a first step in the optimization process, it is beneficial to perform a screening experiment, where a relatively large number of variables are examined concerning their significance. It is of interest, of course, to gain a maximum of information from a minimum number of experiments. In order to achieve this, an experimental design should be applied. Several types of designs are available, which could be adopted, and the choice of design depends on the number of variables involved and how detailed the information is to be. A full factorial design is a good choice when the number of variables are four or less. When more than four variables are of interest, a fractional factorial design is applicable. With more than fifteen variables, a Plackett–Burman design is the preferred choice. However, with Plackett–Burman, a linear model is assumed to be satisfactory, and in CE, non-linear models are, as mentioned above, often desired [49].

Of an experimental design, the most critical part is the selection of the low and high limits of the design. A good knowledge of the separation system is generally needed in order to apply the proper limiting values. In a situation where the high and low limits have been selected above and below optimal, the experiment will be misleading as to in which direction the optimum will be found.

3.2. Derivatization reagents

Comparing the analysis of some differently derivatized amino acids by capillary electrophoresis, Albin et al. [50] maintained that FMOC offered the greatest utility with respect to separation efficiency and concentration detection limit when using fluorescence detection with a xenon lamp as light source. Instrumentation for fluorescence detection, suitable for capillary electrophoresis, has, however, not been available to us, and therefore detection was by UV in the present work.

Absorptivity of primary amines derivatized with different chiral reagents was compared at five wavelengths by Houben et al. [37]. The highest absorption was in the low-UV region, but derivatization with Marfey's reagent resulted in relatively high absorption also at 340 nm. A drawback of Marfey's reagent is, however, that a relatively high temperature or a prolonged time is required for the reaction. FLEC showed good absorptivity at 254 nm, and this wavelength was selected for the present work, thus avoiding interferences. Other merits of FLEC include high optical purity, >99.0 e.e. according to the manufacturer, availability in the (+) and (−) forms, rapid reaction at room temperature, no racemization during reaction and the formation of stable derivatives [46,51].

3.3. Diastereomeric separation of FLEC-AAs

For the separation of amino acids derivatized with FLEC, two key factors, pH and SDS concentration were optimized by full factorial design as mentioned above. The applied low factors were: pH 7.8 and SDS concentration 20 m*M*. The high factors were: pH 9.2 and SDS concentration 80 m*M*. For the design, 10 experiments, including two centre points, were performed utilizing a mixture of 4 different FLEC(−)-AAs (Thr, Ile, Val and Phe). The results obtained from optimization indicated that a high pH was necessary for the chiral resolution

of these 4 FLEC-AAs and that the different AAs showed optimal chiral separation at different SDS concentrations. For example, the first eluted analyte, Thr, had a relatively high optimal SDS concentration, ca. 60 m*M*, Fig. 1A. In contrast, for the last eluted amino acid, Phe, the SDS concentration should be as low as possible, Fig. 1B. This could be explained by the fact that Phe is more hydrophobic and the partition into the micelle phase would thus be more extensive for this amino acid. As a consequence, a lower SDS concentration should be needed. A buffer containing an intermediate concentration of SDS, 20 m*M*, and a high pH, 9.2, was thus selected in order to facilitate separation of a maximum number of FLEC(−)-AAs. As a result, 11 of 19 FLEC(−)-AAs examined were baseline separated. The amino acids, Arg, Asp, Cys, Glu, Lys, Pro, Trp, Tyr were not resolved. Much longer migration times were observed for these amino acids; thus, a buffer concentration of 20 m*M* SDS was too high for chiral separation of these amino acids.

When an organic modifier, acetonitrile (ACN), was added to the buffer, the separation of early eluted AAs such as Ser, Ala and Thr

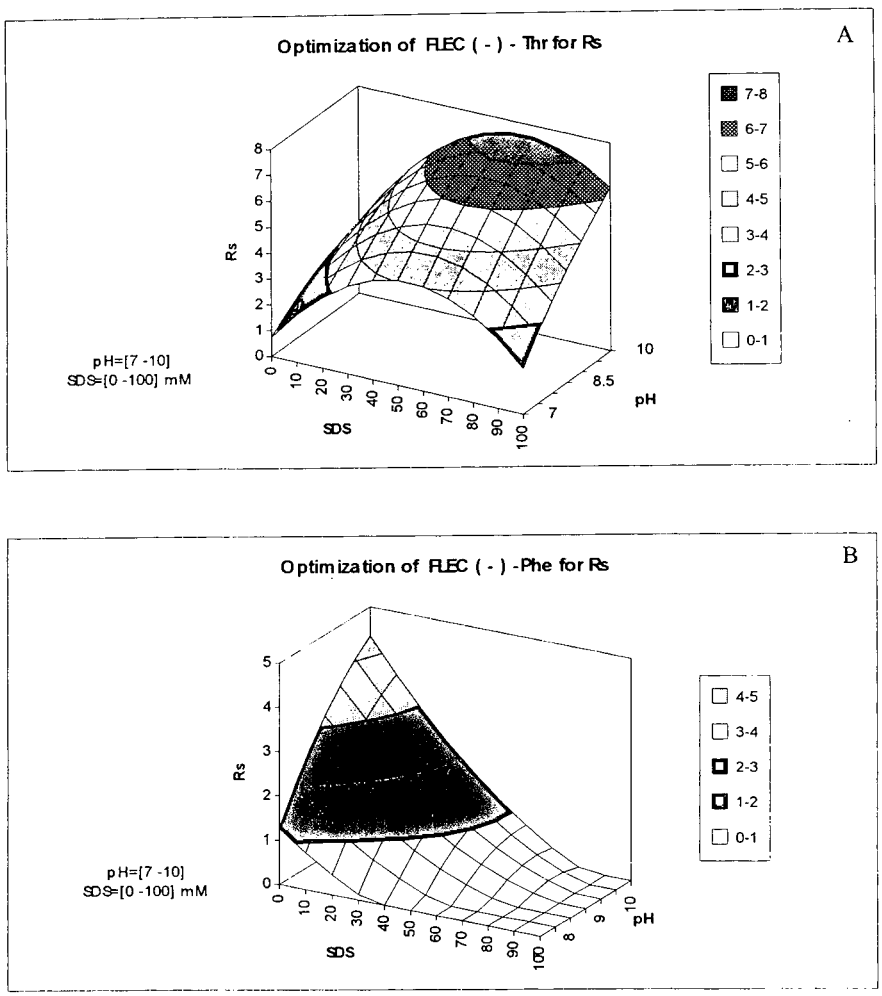

Fig. 1. Three-dimensional peak resolution surface for amino acids derivatized with (−)-FLEC, A = threonine; B = phenylalanine, as a function of the SDS concentration and the pH.

Table 1
Diastereomeric separation of FLEC(−)-AAs by MEKC

Amino acid	0% ACN				10% ACN			
	t (min)[a]	R_s	$\alpha >$	N/m ($\times 10^5$)	t (min)[a]	R_s	$\alpha >$	N/m ($\times 10^5$)
Ala	5.39	2.71	1.038	8.80	6.18	2.67	1.036	11.0
Arg	10.42	0	1	14.1	14.57	2.09	1.015	12.1
Cys	10.16	0	1	14.3	14.41	4.90	1.038	11.1
His	5.95	0.96	1.012	4.67	6.11	0	1	2.73
Ile	7.03	3.86	1.045	8.16	7.23	8.19	1.100	10.4
Leu	7.51	2.05	1.020	10.6	7.53	7.02	1.086	9.11
Lys[b]	–	–	–	–	5.01	4.76	1.159	6.91
Met	6.81	1.54	1.017	8.76	6.83	4.18	1.052	10.7
Nleu	7.68	3.62	1.035	9.00	7.79	9.23	1.100	11.0
Nval	6.49	3.98	1.047	9.40	6.76	6.40	1.082	10.8
Phe	8.26	2.71	1.021	13.2	8.60	8.84	1.107	8.44
Ser	5.18	3.33	1.040	9.11	5.94	2.03	1.029	9.60
Thr	5.32	5.70	1.080	9.64	5.92	4.00	1.064	9.29
Trp	10.01	0	1	13.4	10.86	2.01	1.019	12.1
Tyr[c]	–	–	–	–	6.97	1.23	1.023	5.22
Val	6.03	6.66	1.083	8.29	6.48	8.02	1.108	10.5

Conditions: buffer; 20 m*M* borate–15 m*M* phosphate (pH = 9.2) containing 20 m*M* SDS; separation column, 62.5 cm × 25 μm I.D. (effective length 45 cm); applied voltage, 25 kV; current, 9.0 μA; 8.2 μA for 10% ACN
[a] Migration time for the D form.
[b] 10 m*M* SDS and 30% ACN.
[c] 10 m*M* SDS and 50% ACN.

was less satisfactory, Table 1. This is because the optimal SDS concentrations required for Ser, Ala and Thr should be higher than 20 m*M* and thus, addition of ACN decreased the resolutions. However, the separation of later eluted AAs, Met, Ile, Leu, Nleu and Phe, was improved, Table 1. When 10% ACN was included in the buffer, Arg and Trp were resolved. After decreasing the SDS concentration to 10 m*M*, maintaining ACN at 10%, a small decrease in resolution, cf. Table 1, was observed for Trp (R_s = 1.30), and Arg (R_s = 1.33) with a seriously tailing peak. Further increasing the ACN concentration to 15% resulted in an improved separation of Trp (R_s = 1.70) and also a good peak shape for Arg (R_s = 1.05).

The amino acids Tyr and Lys were separated at 10 m*M* SDS when ACN concentrations were increased to 30% and 50%, respectively, Table 1. The application of these buffers resulted in a decrease in the number of theoretical plates, Table 1. This was most likely due to operation close to the critical micellar concentration (CMC). In the absence of any additives, the CMC for SDS in aqueous solutions at 25°C is 8.1 m*M* [52]. It has been demonstrated that, in the presence of a phosphate–borate buffer, micelle formation takes place at lower SDS concentrations, 5 m*M* [53]. However, it is also known that the CMC is increased in the presence of high concentrations of organic solvents [52].

The amino acids Pro, Glu and Asp could not be separated in this type of buffer, which is probably due to poor efficiency for Pro and electrostatic repulsion interactions for Glu and Asp. In addition, it was observed that the FLEC(−)-His derivative was unstable at room temperature since apparent changes in migration times or even the absence of a peak were observed a few hours after derivatization.

These results suggest that it is difficult to separate all AAs under the same conditions, since it is evident that partition coefficients and interactions differ too much. However, by op-

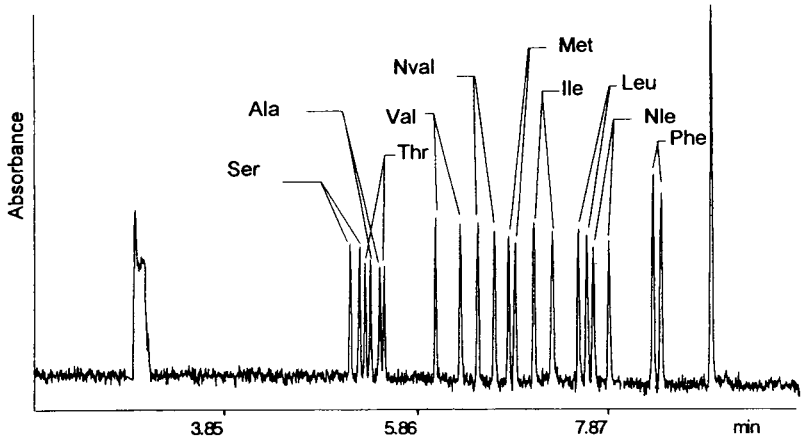

Fig. 2. Chromatogram, UV detection, of 10 amino acids derivatized with (−)-FLEC. Separation capillary, fused silica; 350 μm O.D., 25 μm I.D., total length 62.5 cm, effective length 45 cm; background electrolyte, 20 m*M* borate–15 m*M* phosphate (pH = 9.2), 20 m*M* SDS; applied voltage, 25 kV; current, 9.0 μA; temperature, 25°C.

timization, baseline separation of a mixture of 10 AAs has been achieved in one run in less than 10 min, Fig. 2. The D-form was eluted first when the AAs had been derivatized with (−)-FLEC. Reversal of elution order was, as expected, easily realized with (+)-FLEC. In order to be able to separate a wider range of amino acids in one run, the application of a mobile phase gradient would be necessary. Systems for the performance of such gradients have been presented by Sepaniak and co-workers [54,55].

3.4. Enantiomeric separation of FMOC-AAs

For the separation of FMOC-AAs, β-CD and HP-β-CD have been evaluated as chiral selectors. First, separation was attempted with HP-β-CD as chiral selector. In the capillary zone electrophoresis-mode (CZE), 7 FMOC-AAs (Thr, Phe, Leu, Met, Val, Nval and Nleu) were separated using a buffer containing 2.5 m*M* HP-β-CD and 100 m*M* phosphate at pH 6.0, Table 2. It was observed that an increase in buffer ionic strength resulted in enhanced resolution for these FMOC-AAs, but efficiencies were decreased. For instance, FMOC-Phe had a resolution of 0.87 and plate numbers of 5.69×10^5/m in a buffer containing 25 m*M* phosphate; but a resolution of 1.29 and plate numbers of 3.13×10^5/m in a buffer containing 100 m*M* phosphate. The decrease in efficiencies observed when increasing the ionic strength may be due to the decrease in electroosmotic flow. Further, since the selectivity was increased, an increase in analyte–CD interactions may be suspected, and this could also lead to band broadening. The Joule heating was 1.37 W/m. Taking into account that there was an active cooling of the capillary and that the diameter was only 25 μm, it may be concluded, on the basis of published data [53,56,57], that band broadening due to thermal effects ought to be quite small in this case. It was recently considered that the interaction between analyte and CD is impeded by buffer salts and water molecules, which would result in low enantioselectivities [58]. However, the present results demonstrate that buffer salts may have a positive effect on the chiral selectivity.

Separation of 4 FMOC-AAs under these conditions is shown in Fig. 3. Surprisingly, no chiral separation was observed when HP-β-CD was employed in MEKC, even though a wide range of conditions was investigated. The parameters pH, HP-β-CD and SDS concentrations were thereby varied. Further, the presence of three different organic modifiers, methanol, ACN and

Table 2
Separation data for FMOC-AAs and FLEC-AAs

Amino acid	Separated AAs	Method[a]	Migration time (min)	Selectivity α	Resolution	Plate height (μm)
FMOC-[d]	Ile	1	11.81	1.031	1.53	2.8
	Leu	1	12.26	1.023	1.24	3.6
	Met	1	12.88	1.025	1.31	3.8
	Nleu	1	12.41	1.020	0.94	4.0
	Nval	1	11.83	1.018	0.99	4.5
	Phe	1	11.68	1.025	1.29	3.1
	Thr	1	13.75	1.019	0.97	3.9
	7		11–14[f]	1.018–1.031[f] 1.023[b]	0.94–1.53[f] 1.18[b]	2.8–4.5 3.6[b]
FMOC-	15	2	18–32[f]	1.024–1.074[f] 1.044[b,e]	1.06–4.12[f] 2.35[b]	1.8–5.8[f] 2.3[b]
FLEC-	16	3	5–11[f]	1.012–1.159[f] 1.064[b,c,e]	0.97–6.66[f] 3.25[b,c]	0.7–3.6[f] 1.0[b,c]

[a] Methods: 1 = EKC-HP-β-CD; 2 = MEKC-β-CD; 3 = MEKC-indirect.
[b] Mean values for separated amino acids.
[c] For FLEC-AAs with ACN as in Table 1.
[d] Conditions: Buffer, 100 m*M* phosphate (pH = 6.0) containing 2.5 m*M* HP-β-CD; separation column, 62 cm (effective length 45 cm) × 25 μm I.D.; applied voltage, 30 kV; current 28.4 μA.
[e] α larger than given data.
[f] Range.

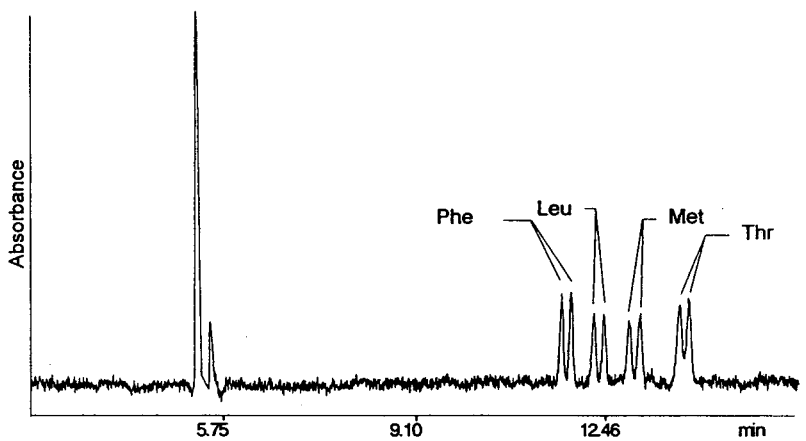

Fig. 3. Electropherogram, UV detection, of 4 amino acids derivatized with FMOC. Separation capillary, fused silica, 360 μm O.D., 25 μm I.D., total length 62 cm, effective length 45 cm; background electrolyte, 100 m*M* phosphate (pH = 6.02), 2.5 m*M* HP-β-CD; applied voltage, 30 kV; current, 28.4 μA; temperature 25°C.

IPA in the buffer was examined with negative results.

When β-CD was used as chiral selector, chiral separation was observed only with one type of organic modifier, IPA, in the CZE-mode as well as in the MEKC-mode. In the CZE-mode, 6 FMOC-AAs, Phe, Leu, Met, Thr, Asp and Glu, were examined, all of these being separated at pH 5.5 with 10 m*M* β-CD and 10% IPA. Migration times of Phe, Leu, Met and Thr were in the same range. For Glu and Asp, which were not resolved by diastereomeric separation, baseline separation was obtained with resolutions of 2.71 and 1.69.

It was noted that the resolutions of the FMOC-AAs were largely unchanged when the pH was raised from 5.5 to 7.0. This indicated that the pH had less effect on enantioselectivity in this case and that the pH could be kept unchanged during further optimization.

In order to obtain optimized conditions, and to separate as many AAs as possible by MEKC, an optimization by means of a full factorial design which contained 3 factors. The low factors employed were, SDS concentration 8 m*M*, CD concentration 3 m*M* and 5% isopropanol. The high factors were, SDS concentration 15 m*M*, CD concentration 10 m*M* and 15% isopropanol. For the factorial design 16 experiments including two centre points, were performed at pH 7.0 with a mixture of 6 FMOC-AAs. The optimization showed that all 6 FMOC-AAs had similar optimal conditions, which was completely different from the result obtained from the optimization of FLEC-AAs. This result suggests that more than one analyte should be considered in optimization so as to obtain optimal conditions that are suitable for many analogous analytes. In Figs. 4 A–C are shown an example of optimization for Phe-FMOC. It can be seen from Fig. 4, that the concentrations of β-CD and IPA were the most important parameters, and that optimal SDS and β-CD concentrations were dependent on the IPA concentration used. Additionally, the model prediction indicated maximum resolution for 18% IPA, 12 m*M* β-CD and 18 m*M* SDS. Considering that analysis time is increased when high IPA and SDS concentrations are employed, 15% IPA, 12 m*M* β-CD and 15 m*M* SDS were adopted as optimal conditions for testing all FMOC-AAs. Under these conditions, 15 of 19 FMOC-AAs were separated, Table 3. Only Ala, Cys, Tyr and Lys could not be separated. The system showed a good selectivity for the separation of FMOC-derivatized proline isomers. These analytes were, however, eluted as relatively broad bands, Table 3, baseline separation could therefore not be achieved in this case. In Fig. 5 is shown a typical chromatogram of the separation of a 7 FMOC-AAs mixture in the MEKC-mode. The D-form was first eluted, thus indicating that the L-form is more strongly bound to β-CD than the D-form. This elution order is beneficial in the determination of large enantiomeric excess for natural L-AAs, since the D-enantiomer is usually considered as an impurity and its elution prior to the large peak favours quantitation.

3.5. Effect of organic modifiers on chiral recognition

Addition of organic solvents could change the inclusion complex formation constant, thus affecting the optimum concentration of CD; separation may thereby be improved or worsened [59,60]. As mentioned above, chiral recognition for FMOC-AAs was found with β-CD only in the presence of IPA. The presence of isopropanol resulted in greatly decreased electroosmotic flow (EOF) as compared with methanol and ACN, as has been reported earlier [61–64]. Only low amounts of IPA, 5%, were required for enantioselectivity. The benefit of small amounts of a modifier, strongly binding to the β-CD, in the buffer for the moderation of the analyte–CD interaction was recently reported [65]. Armstrong et al. [66,67] demonstrated that chiral recognition could not be obtained by HPLC when the mobile phase contained water, but separation could be achieved in water-free systems. It was concluded that the presence of water forced the FMOC-part of the derivative into the cavity of the CD, when the interaction of the chiral part of the derivative, the amino acid, with the CD would thereby be insufficient

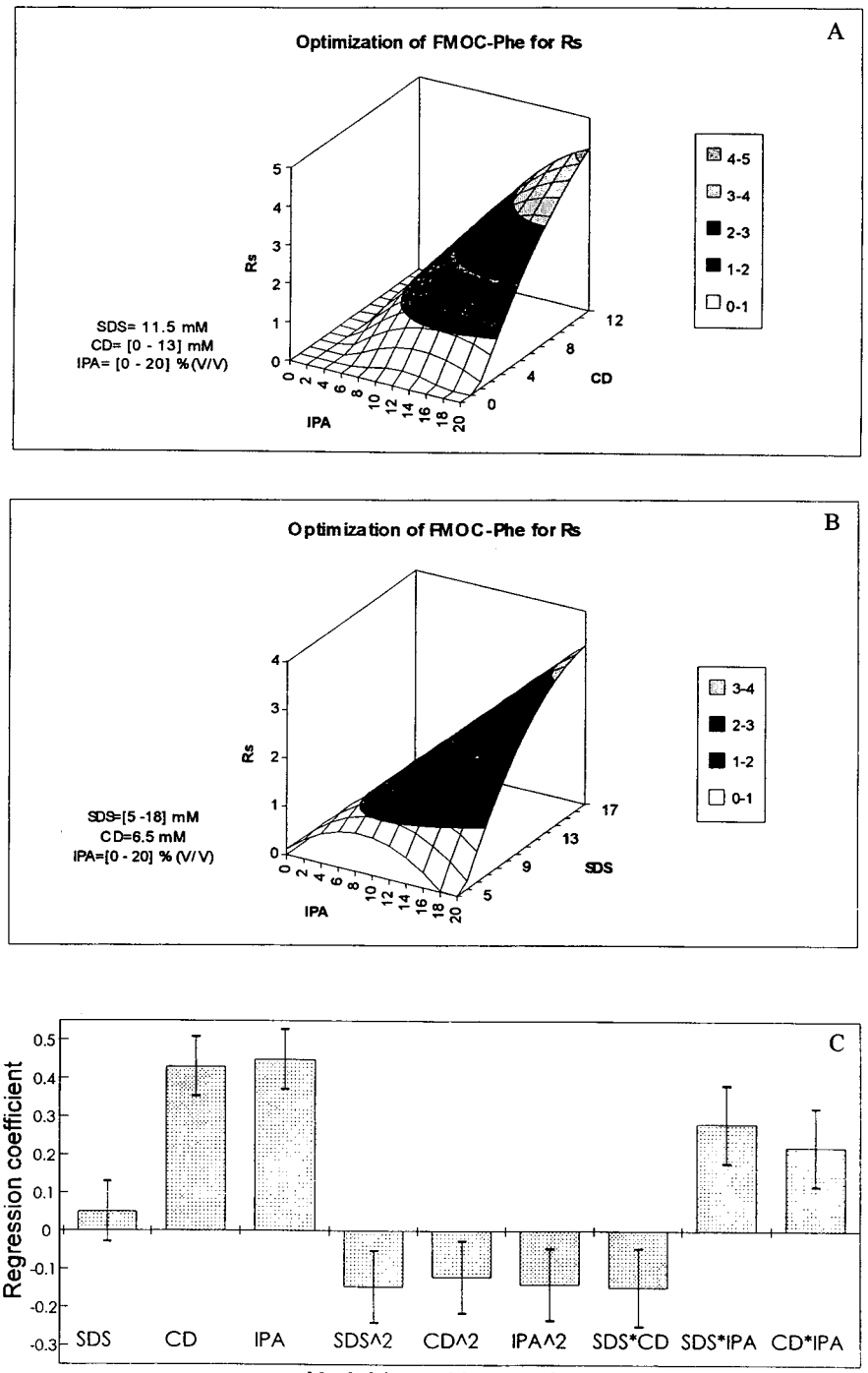

Fig. 4. Three-dimensional peak resolution surface phenylalanine derivatized with FMOC as a function of IPA and β-CD concentrations (A) and IPA and SDS concentrations (B). C is a bar chart for the regression coefficient and interaction effects of the three main variables for the resolution of phenylalanine derivatized with FMOC.

Table 3
Enantiomeric separation of FMOC-AAs by CD-MEKC

Amino acid	t (D-isomer) (min)	Selectivity $\alpha >$	R_s	N/m ($\times 10^5$)
Arg	21.99	1.040	1.10	2.26
Asp	32.64	1.026	1.68	3.24
Glu	30.30	1.051	3.20	3.36
His	18.60	1.040	1.80	4.80
Ile	20.85	1.074	4.14	5.20
Leu	22.07	1.022	2.72	5.28
Met	20.47	1.034	1.82	5.40
Nleu	23.34	1.039	2.38	4.40
Nval	20.88	1.037	1.83	3.70
Phe	23.68	1.062	4.12	5.52
Pro	21.75	1.033	1.08	1.72
Ser	19.07	1.024	1.06	3.64
Thr	19.14	1.027	1.41	4.94
Trp	25.13	1.048	3.31	4.92
Val	19.73	1.076	3.52	4.16

Conditions: buffer, 45 mM phosphate (pH = 7.0) containing 15 mM SDS, 12 mM β-CD and 15% IPA; separation column, 70 cm × 25 μm I.D. (effective length 50 cm); applied voltage, 25 kV; current, 6.8 μA.

for enantioselectivity. In water-free systems, with acetonitrile as the main mobile phase component, it was anticipated that ACN occupied the internal part of the CD, the AAs derivatives thus having to interact chirally with the external parts of the CD. It may be speculated that isopropanol, being less polar than methanol and ACN, has a similar role in the present system. For the 7 investigated FMOC-AAs, the effect of IPA concentration on the resolution of different

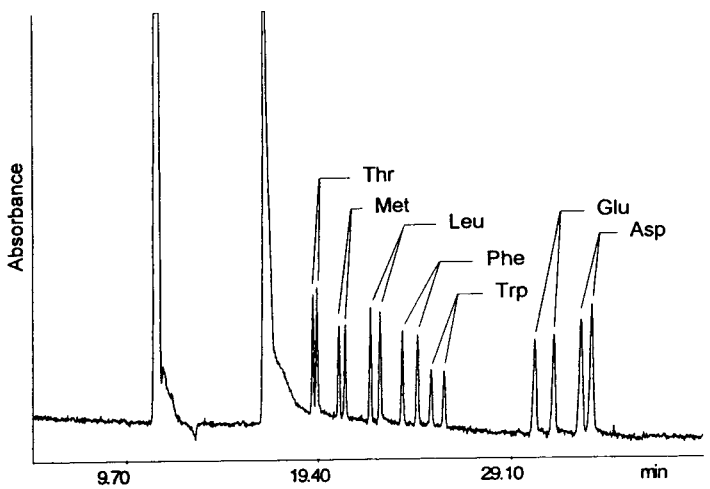

Fig. 5. Chromatogram, UV detection, of 7 amino acids derivatized with FMOC. Separation capillary, fused silica 360 μm O.D., 25 μm I.D., total length 70 cm, effective length 50 cm; background electrolyte, 45 mM phosphate (pH = 7.0), 15 mM SDS, 12 mM β-CD, 15% (v/v) IPA; applied voltage, 25 kV; current, 6.8 μA; temperature, 25°C.

FMOC-AAs is shown in Fig. 6 (top). It is evident that the best resolution for most of these FMOC-AAs was found at 15% IPA. This is also in good agreement with the conditions suggested above. On the other hand, the best efficiency was observed with 10% IPA, Fig. 6 (bottom). Further increasing the IPA concentration resulted in decreased efficiencies. This is because slow EOF led to a slow overall migration rate, which in turn resulted in increased band broadening by means of longitudinal diffusion [68]. Furthermore, the separation efficiencies of FMOC-AAs in the presence of either β-CD or HP-β-CD, were, in general, lower than the efficiencies obtained with the diastereomers, Table 2. This suggests that slow kinetics in the

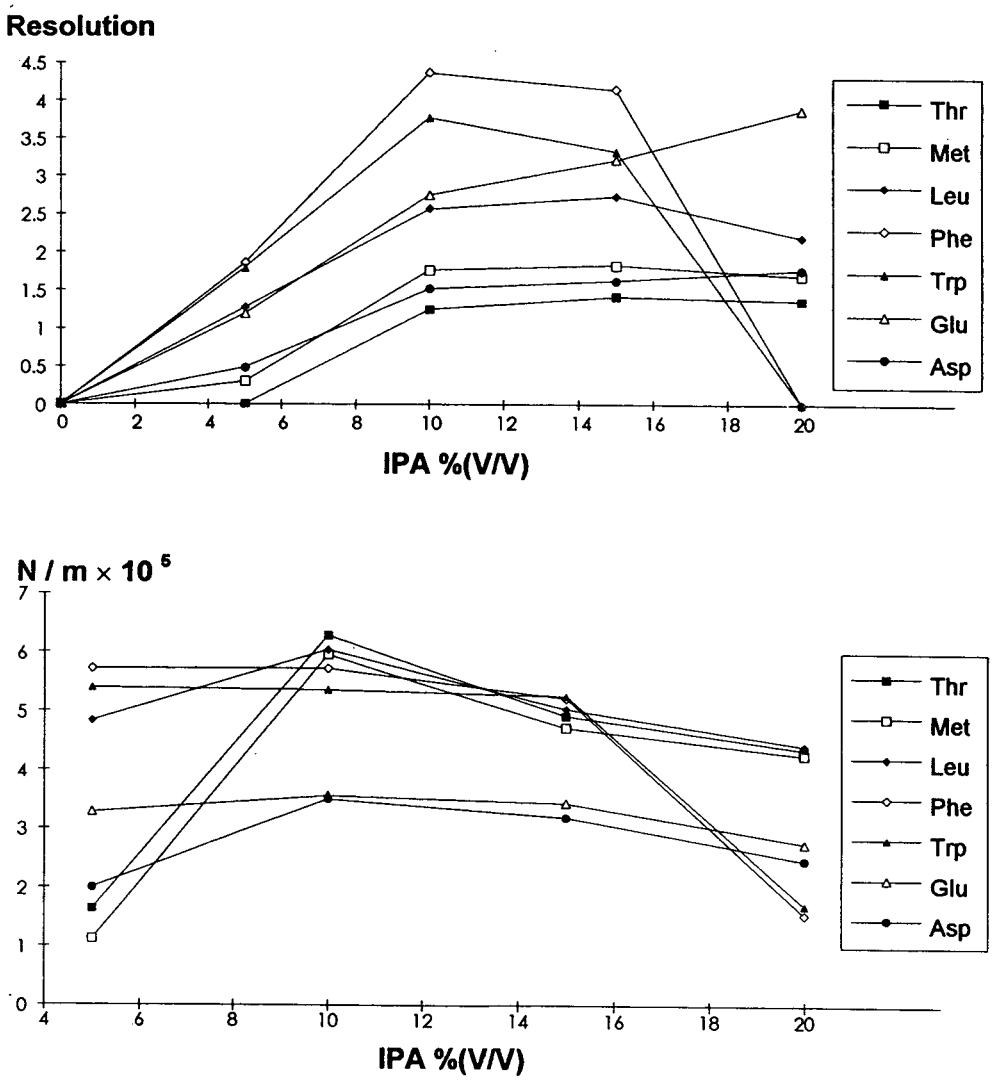

Fig. 6. Graphs of the resolution (top) and separation efficiency (bottom) of 7 FMOC derivatized amino acids as a function of % isopropanol. Separation capillary, applied voltage and temperature as in Fig. 5. Background electrolyte, 45 m*M* phosphate (pH = 7.0), 15 m*M* SDS, 12 m*M* β-CD and different % of isopropanol.

formation of inclusion complexes between analytes and cyclodextrins could also contribute to the band width.

Conclusions

The results are summarized in Table 2. The chiral separation of 19 amino acids has been examined and ca. 80% of these could be resolved by direct as well as by indirect methods. Indirect separation offered higher separation efficiencies than direct separation with or without micelles. The average plate heights were thus, 1.0, 2.3 and 3.6 μm, respectively. Moreover, the average resolution was higher for separation of diastereomers, 3.25, than for chiral separation with micelles, 2.35, or without micelles, 1.18. The speed of separation was higher for indirect separation, the separation time for the direct method using micelles was three times longer.

The number of variables that has to be optimized, depends on the separation task. In the examples given, two variables were optimized in the indirect approach, and three variables in the direct method. However, for the separation of late eluting diastereomers, an organic co-solvent was needed, which led to a three variable optimization also in this case. According to our opinion, the main difference in the method development of the two approaches concerns the scouting that precedes the optimization. As a starting point for the optimization, conditions must be found that result in, at least, some separation. This can be accomplished relatively easily in the indirect method, while the scouting experiments can be quite extensive in connection with the direct separation method. A good knowledge of the function of the significant variables is required for efficient scouting. In conclusion, for the analytical systems investigated, the best performance was achieved with the indirect separation method.

Optimization with different analytes could result in different optimal conditions, especially for diastereomeric separation of FLEC-AAs where the SDS concentration was the most significant factor influencing the separation. In comparison with the diastereomeric separation of amino acids derivatized with Marfey's reagent and GITC by means of MEKC, much lower SDS concentrations were required for the resolution of FLEC-AAs. In the direct separation mode, β-CD showed a wide range of enantioselectivities for FMOC-AAs. The other chiral selector tested, HP-β-CD was less useful.

The FMOC-AAs derivatives are somewhat hydrophobic, and a particular organic modifier, IPA, was found indispensable for the chiral separation of these derivatives. In the presence of IPA, variations in pH had, within limits, only a small effect on the chiral recognition. Due to the low SDS concentrations employed in the chiral separation of FMOC-AAs and FLEC-AAs, relatively high separation efficiencies were obtained with MEKC. Finally, it should be mentioned that the basis for the successful application of the chiral derivatization reagent is its high optical purity. The chiral recognition mechanism for FMOC-AAs with β-CD and its derivatives is being further investigated.

Acknowledgements

This work was supported by the Swedish Natural Science Research Council. A grant from the Chinese Academy of Science is gratefully acknowledged.

References

[1] K. Otsuka and S. Terabe, Trends Anal. Chem., 12 (1993) 125.
[2] T.L. Bereuter, LC-GC Int., 7 (1994), No. 2, 78.
[3] S. Terabe, K. Otsuka and H. Nishi, J. Chromatogr. A, 666 (1994) 295.
[4] M.M. Rogan, D.M. Goodall and K.D. Altria, Chirality, 6 (1994) 25.
[5] R. Kuhn and S. Hoffstetter-Kuhn, Chromatographia, 34 (1992) 505.
[6] M. Novotny, H. Soini and M. Stefansson, Anal. Chem., 66 (1994) 646A.
[7] T.J. Ward, Anal. Chem., 66 (1994) 633A.
[8] S. Fanali and F. Kilar, J. Cap. Elec., 1 (1994) 72.
[9] H.J. Issaq, Instrum. Sci. Technol., 22 (1994) 119.

[10] M.W. Skidmore, in K. Blau and J.M. Halket (Editors), Handbook of Derivatives for Chromatography, Wiley, New York, 1993, Ch. 10, p. 215.
[11] M. Ahnoff and S. Einarsson, in W.J. Lough (Editor), Chiral Liquid Chromatography, Blackie, Glasgow, 1989, Ch. 4, p. 39.
[12] J. Jacques, A. Collet and S. Wilen, Enantiomers, Racemates and Resolutions. Wiley, New York, 1981, Ch. 5, p. 251.
[13] R. Kuhn, F. Erni, T. Bereuter and J. Häusler, Anal. Chem., 64 (1992) 2815.
[14] R. Kuhn, F. Stoecklin and F. Erni, Chromatographia, 33 (1992) 32.
[15] A. Werner, T. Nassauer, P. Kiechle and F. Erni, J. Chromatogr. A, 666 (1994) 375.
[16] R. Weinberger, Practical Capillary Electrophoresis, Academic Press, Boston, 1993, p. 184.
[17] S. Terabe, M. Shibata and Y. Miyashita, J. Chromatogr., 480 (1989) 403.
[18] A. Guttman, A. Paulus, A.S. Cohen, N. Grinberg and B.L. Karger, J. Chromatogr., 448 (1988) 41.
[19] S. Terabe, Trends Anal. Chem., 8 (1989) 129.
[20] G.N. Okafo, C. Bintz, S.E. Clarke and P. Camilleri, J. Chem. Soc., Chem. Commun., 17 (1992) 1189.
[21] M.J. Sepaniak, R.O. Cole and B.K. Clark, J. Liq. Chromatogr., 15 (1992) 1023.
[22] G.N. Okafo and P. Camilleri, J. Microcol. Sep., 5 (1993) 149.
[23] S. Terabe, Y. Miyashita, Y. Ishihama and O. Shibata, J. Chromatogr., 636 (1993) 47.
[24] M. Tanaka, M. Yoshinaga, S. Asano, Y. Yamashoji and Y. Kawaguchi, Fresenius' J. Anal. Chem., 343 (1992) 896.
[25] M. Yoshinaga and M. Tanaka, J. Chromatogr. A, 679 (1994) 359.
[26] B.O. Eggum and H. Sørensen, in M. Friedman (Editor), Absorption and Utilization of Amino Acids, Vol. III, CRC Press, Boca Raton, FL, 1989, Ch. 17, p. 265.
[27] T. Ueda, F. Kitamura, R. Mitchell, T. Metcalf, T. Kuwana and A. Nakamoto, Anal. Chem., 63 (1991) 2979.
[28] T. Ueda, R. Mitchell, F. Kitamura, T. Metcalf, T. Kuwana and A. Nakamoto, J. Chromatogr., 593 (1992) 265.
[29] K. Otsuka and S. Terabe, J. Chromatogr., 515 (1990) 221.
[30] K. Otsuka, J. Kawahara, K. Tatekawa and S. Terabe, J. Chromatogr., 559 (1991) 209.
[31] K. Otsuka, K. Karuhaka, M. Higashimori and S. Terabe, J. Chromatogr. A, 680 (1994) 317.
[32] H. Ruyters and Sj. van der Wal, J. Liq. Chromatogr., 17 (1994) 1883.
[33] P. Gozel, E. Gassmann, H. Michelsen and R.N. Zare, Anal. Chem., 59 (1987) 44.
[34] A.D. Tran, T. Blanc and E.J. Leopold, J. Chromatogr., 516 (1990) 241.
[35] H. Nishi, T. Fukyama and M. Matuso, J. Microcol. Sep., 2 (1990) 234.
[36] I.S. Lurie, J. Chromatogr., 605 (1992) 269.
[37] R.J.H. Houben, H. Gielen and Sj. van der Wal, J. Chromatogr., 634 (1993) 317.
[38] L. Kang and R.H. Buck, Amino Acids, 2 (1992) 103.
[39] W. Schützner, S. Fanali, A. Rizzi and E. Kenndler, J. Chromatogr., 639 (1993) 375.
[40] S.F.Y. Li, Capillary Electrophoresis (J. Chromatogr. Library, Vol. 52), Elsevier, Amsterdam, 1992, Ch. 6.5, p. 316.
[41] J. Vindevogel and P. Sandra, Anal. Chem., 63 (1991) 1530.
[42] M. Castagnola, D.V. Rosetti, L. Cassiano, R. Rabino, G. Nocca and B. Giardina, J. Chromatogr., 638 (1993) 327.
[43] M.M. Rogan, K.D. Altria and D.M. Goodall, Chromatographia, 38 (1994) 723.
[44] K.D. Altria and S.D. Filbey, Chromatographia, 39 (1994) 306.
[45] D.W. Armstrong, W. Li, C.-D. Chang and J. Pitha, Anal. Chem., 62 (1990) 914.
[46] S. Einarsson and G. Hansson, in C.T. Mant and R.S. Hodges (Editors), HPLC of Peptides and Proteins: Separation, Analysis and Conformations, CRC Press, Boca Raton, FL, 1991, pp. 369–378.
[47] S. Terabe, K. Otsuka and T. Ando, Anal. Chem., 57 (1985) 834.
[48] J. Vindevogel and P. Sandra, Introduction to Micellar Electrokinetic Chromatography, Hüthig, Heidelberg, 1992, p. 55.
[49] R. Carlson, Design and optimization in organic synthesis, Elsevier, Amsterdam, 1992.
[50] M. Albin, R. Weinberger, E. Sapp and S. Moring, Anal. Chem., 63 (1991) 417.
[51] S. Einarsson, B. Josefsson, P. Möller and D. Sanchez, Anal. Chem., 59 (1987) 1191.
[52] M.J. Sepaniak, A.C. Powell, D.F. Swaile and R.O. Cole, in P.D. Grossman and J.C. Colburn (Editors), Capillary Electrophoresis, Theory and Practice, Academic Press, San Diego, CA, 1992, Ch. 6, pp. 159–189.
[53] M.J. Sepaniak and R.O. Cole, Anal. Chem., 59 (1987) 472.
[54] M.J. Sepaniak, D.F. Swaile and A.C. Powell, J. Chromatogr., 480 (1989) 185.
[55] A.C. Powell and M.J. Sepaniak, Anal. Instrum., 21 (1993) 25.
[56] R.J. Nelson, A. Paulus, A.S. Cohen, A. Guttman and B.L. Karger, J. Chromatogr., 480 (1989) 111.
[57] M.W.F. Nielen, Anal. Chem., 65 (1993) 885.
[58] F. Kobor, D. Belder and G. Schomburg, Poster presented at the 16th International Symposium on Capillary Chromatography, Riva del Garda, Italy, September 27–30, 1994.
[59] S.A.C. Wren and R.C. Rowe, J. Chromatogr., 603 (1992) 235.
[60] S.A.C. Wren and R.C. Rowe, J. Chromatogr., 609 (1992) 363.

[61] J. Gorse, A.T. Balchunas, D.F. Swaile and M.J. Sepaniak, J. High Resolut. Chromatogr. Chromatogr. Commun., 11 (1988) 554.
[62] C. Schwer and E. Kenndler, Anal. Chem., 63 (1991) 1801.
[63] S. Terabe in N.A. Guzman (Editor), Capillary Electrophoresis Technology (Chromatographic Science Series, Vol. 64), Marcel Dekker, New York, NY, 1993, Ch. 2, pp. 65–87.
[64] G.M. Janini, K.C. Chan, J.A. Barnes, G.M. Muschik and H.J. Issaq, Chromatographia, 35 (1993) 497.
[65] S.G. Penn, E.T. Bergström, D.M. Goodall and J.S. Loran, Anal. Chem., 66 (1994) 2866.
[66] J. Zukowski, M. Pawlowska and D.W. Armstrong, J. Chromatogr., 623 (1992) 33.
[67] J. Zukowski, M. Pawlowska, M. Nagatkina and D.W. Armstrong, J. Chromatogr., 629 (1993) 169.
[68] J.W. Jorgenson and K.D. Lukacs, J. Chromatogr., 218 (1981) 209.

ELSEVIER

Journal of Chromatography A, 704 (1995) 195–201

JOURNAL OF CHROMATOGRAPHY A

Determination of synthetic colours in confectionery and cordials by micellar electrokinetic capillary chromatography

Catherine O. Thompson, V. Craige Trenerry*

Australian Government Analytical Laboratories, 338–340 Tapleys Hill Road, Seaton 5023, Australia

First received 13 September 1994; revised manuscript received 3 February 1995; accepted 3 February 1995

Abstract

A rapid method for the determination of a number of commonly used synthetic colours permitted in confectionery and cordial in Australia by micellar electrokinetic capillary chromatography (MEKC) is described. The synthetic colours, green S, brilliant blue, erythrosine B, allura red, indigo carmine, sunset yellow, azorubine, amaranth, ponceau and tartrazine are well separated in less than 20 min using a 65 cm × 50 μm uncoated fused-silica capillary column with a buffer comprising of 15% acetonitrile and 85% 0.05 *M* sodium deoxycholate/0.005 *M* potassium dihydrogenorthophosphate/0.005 *M* sodium borate pH 8.6 operating at 30 kV. The compounds are detected with UV detection at 214 nm. Quinoline yellow and brilliant black can also be determined using this system. The levels of synthetic colours in a variety of confectionery items and cordials were in good agreement with those determined by high-performance liquid chromatography (HPLC). The level of reporting for the MEKC procedure is 5 mg/kg. This procedure is faster and less costly to operate than the HPLC method currently used in our laboratory.

1. Introduction

Analytical procedures based on the relatively new technique of micellar electrokinetic capillary chromatography (MEKC) are rapidly gaining acceptance as rugged analytical methods [1–5]. MEKC separations exhibit superior resolution to high-performance liquid chromatography (HPLC) separations, have the same order of repeatability and are faster and less costly to operate than HPLC methods [6]. MEKC was introduced by Terabe et al. [7] in 1984. With this technique, an electrophoretic buffer is modified with an ionic surfactant to provide a phase for chromatographic separation. Both anionic and cationic surfactants have been used as micelle modifiers to separate mixtures that cannot be easily separated using traditional capillary zone electrophoresis (CZE) [6]. Sodium dodecyl sulphate (SDS) and cetyltrimethylammonium bromide (CTAB) are commonly used as surfactants for MEKC. Bile salts (e.g. sodium cholate, sodium deoxycholate, sodium taurodeoxycholate) can also be used as anionic surfactants. These compounds exhibit different structural and aggregation properties to the other anionic surfactants and so affect the separations differently [8]. Nishi et al. [9] reported the separation and determination of the ingredients of a cold medicine by MEKC using sodium cholate and sodium deoxycholate as buffer modifiers. The separations were superior to when SDS was used as the

* Corresponding author.

0021-9673/95/$09.50
SSDI 0021-9673(95)00165-4

buffer modifier. We recently reported that buffers containing sodium deoxycholate gave better separation of *l*-ascorbic acid and *d*-erythorbic acid in fruit juices and wines than buffers modified with SDS when analysed by MEKC [5]. The addition of an organic solvent, (e.g. methanol, acetonitrile, tetrahydrofuran, dimethyl sulphoxide, dimethylformamide) to the buffer can also affect the separation of complex mixtures and buffers modified with various solvents have been used in a number of applications [6]. We have separated heroin, cocaine and related compounds in illicit drug seizures with buffers modified with acetonitrile [1,2]. We have also used a buffer modified with dimethyl sulphoxide to achieve the separation of a number of amphetamines [10], and we are currently investigating the separation of morphine alkaloids with a buffer modified with dimethylformamide [11]. Texts by Li [6], Weinberger [12] and by Kuhn and Hoffstetter-Kuhn [13] provide detailed descriptions of MEKC as well as many other examples of this technique.

A number of methods for the quantitative determination of synthetic colours using HPLC with UV–Vis detection as the determinative step have been reported in the literature [14–16]. Clarke and Wells [17] recently reported the separation of a number of synthetic colours by MEKC using a 75 cm × 50 μm I.D. uncoated fused-silica capillary column with a buffer comprising of 15% acetonitrile and 85% 0.05 *M* SDS/0.01 *M* sodium borate pH 9.2. The compounds were detected by UV at 214 nm. The separation was used to demonstrate the excellent separating potential of MEKC but was not used to quantitatively determine the levels of the colours. The related technique of isotachophoresis with conductivity detection has been used to quantitatively determine a number of synthetic colours in foods [18].

This paper describes the separation of green S, brilliant blue, erythrosine B, allura red, indigo carmine, sunset yellow, azorubine, amaranth, ponceau and tartrazine by MEKC using a phosphate/borate buffer modified with sodium deoxycholate and acetonitrile with the subsequent quantitation of the colours in some confectionery and cordial samples available in Australia. Azorubine, which is rarely used as an artificial colorant, was used as the internal standard for these determinations. Two other artificial colours, quinoline yellow and brilliant black, can also be determined using this electrophoretic system.

2. Experimental

2.1. Reagents

Amaranth, tartrazine, erythrosine B, indigo carmine, sodium deoxycholate, sodium cholate and SDS were obtained from Sigma (St. Louis, MO, USA). Brilliant blue, allura red and azorubine were obtained from Tokyo Kasei Kogyo (Tokyo, Japan). Green S, sunset yellow, ponceau, quinoline yellow, brilliant black, brown HT and chlorophyll copper complex were gifts from Dr. David Briggs and Ms. Geraldine Keogh, Faculty of Health and Behavioural Sciences, Deakin University, Geelong, Australia. Tetra-*n*-butylammonium hydroxide solution (40%) was obtained from Fisons (AAG) (Homebush, Australia). Tetrabutylammonium phosphate was obtained from Ajax Chemicals (Auburn, Australia). All other chemicals and solvents were analytical-reagent grade or HPLC grade and used without further purification.

2.2. MEKC buffer

A 2.16-g amount of sodium deoxycholate was dissolved in 100 ml of a 1:1 mixture of 0.01 *M* sodium borate and 0.01 *M* potassium dihydrogenorthophosphate. The pH of the solution was 8.6. A 15-ml volume of acetonitrile was added to 85 ml of the buffer and the solution filtered through a 0.8-μm PTFE filter disc before use.

2.3. Apparatus

MEKC

The samples were analysed with an uncoated fused-silica capillary column (65 cm × 50 μm I.D.) with an effective length to the detector of

40 cm (Polymicro Technologies, AZ, USA), using an Isco Model 3140 electropherograph (Isco, Lincoln, NE, USA) operating at 30 kV and at 25°C. The sample solutions were loaded under vacuum (vacuum level 2, 10 kPa s) and the colours were detected at 214 nm at 0.005 AUFS. The detector response was linear to 100 μg/ml. The capillary was flushed with running buffer for 2 min between analyses. Also, the running buffer was replaced after fifteen analyses. The capillary was cleaned on a weekly basis by washing with 0.1 *M* sodium hydroxide for 10 min followed by deionised water for 10 min before filling with running buffer. Electropherograms were recorded with either the ICE data management and control software supplied with the electropherograph or a HP 3350 laboratory data system (Hewlett-Packard, Palo Alto, CA, USA).

HPLC

The analyses were performed with a Model 600E HPLC pump, Model 712 WISP and a Model 490 programmable multiwavelength UV detector using a 4-μm C_{18} NovaPak 8 × 10 cm Radial-Pak cartridge equipped with a C_{18} precolumn (Waters Chromatography Division of Millipore, Milford, MA, USA) using gradient elution. The solvents were degassed before use.

Solvent A was deionised water. Solvent B was methanol and solvent C was 0.1 *M* tetra-*n*-butylammonium hydroxide in deionised water, neutralised with saturated potassium dihydrogenphosphate. Eluent flow-rate was 1.0 ml/min for 9 min, 1.5 ml/min from 10 to 15 min and returning to 1 ml/min after 17 min. The eluent composition was 45% A, 50% B and 5% C for the first 5 min (curve 1), changing to 15% A, 80% B and 5% C to 6 min (curve 6). This eluent composition was maintained to 15 min when it was changed to 45% A, 50% B and 5% C (curve 6) to 17 min. The system was allowed to equilibrate for 20 min before the next sample solution was injected onto the column. The column eluate was monitored at two wavelengths; 475 nm for the yellow and red dyes and 600 nm for the blue and green dyes. The detector output was set at 0.2 AUFS. The chromatograms were displayed on a dual-pen Omniscribe chart recorder (Houston Instruments, USA). Peak areas obtained from a HP 3350 laboratory data system were used in the calculations.

2.4. Samples and standards

MEKC

Samples.

The confectionery and cordials were products available for purchase in Australia and were analysed within the recommended "use by" dates. The confectionery was pulverised in either a commercial food processor or with a mortar and pestle. A 5-g amount of the powdered confectionery sample was weighed accurately and mixed with 25 ml methanol–water (20:80) and the mixture shaken vigorously for 5 min. The solution was centrifuged at 1000 *g* for 5 min and the supernatant filtered through a 5-μm cellulose acetate filter disc. A 1-ml volume of 0.05 *M* tetra-*n*-butylammonium phosphate solution was added to the supernatant and the solution passed through a C_{18} Sep-Pak cartridge which had been previously activated with methanol followed by 1% acetic acid in water. The retained colours were washed with 4 ml of water and then eluted from the C_{18} Sep-Pak cartridge with methanol. The methanol was removed with a stream of nitrogen. A 0.1-ml volume of azorubine solution (1000 μg/ml) was added to the residue and the mixture diluted to 2 ml with deionised water. The solutions were filtered through a 0.45-μm cellulose acetate filter disc before analysis. The cordials were treated in the same way except that 5 ml was used.

Standards.

Standard solutions were prepared in deionised water with azorubine as the internal standard at a final concentration of 50 μg/ml. The solutions were filtered through a 0.45-μm cellulose acetate filter disc before analysis.

HPLC

The sample solutions were prepared as described for the MEKC analyses, except that the final volume was 20 ml. The standard solutions

were prepared by dissolving the colours in deionised water. No internal standard was used for the HPLC analyses.

3. Results and discussion

Clarke and Wells [17] recently reported the separation of a number of synthetic colours using a 75 cm × 50 μm I.D. uncoated fused-silica capillary column with a buffer comprising of 15% acetonitrile and 85% 0.05 *M* SDS/0.01 *M* sodium borate with an applied voltage of 25 kV and a temperature of 25°C. We attempted to use this buffer with a 65 cm × 50 μm I.D. uncoated fused-silica column and an applied voltage of 30 kV to separate green S, brilliant blue, erythrosine B, allura red, indigo carmine, sunset yellow, azorubine, amaranth, ponceau and tartrazine. These compounds are the most commonly used synthetic food colours permitted for use within Australia [19]. The separation is displayed in Fig. 1A. This buffer was unsuitable as azorubine, amaranth and ponceau comigrated. However, the other compounds were well separated within 15 min. Separation was complete when 0.01 *M* sodium borate was replaced with a 1:1 mixture of 0.01 *M* potassium dihydrogenorthophosphate and 0.01 *M* sodium borate pH 8.6 (Fig. 1B). A similar separation was achieved when SDS was replaced with sodium deoxycholate (Fig. 1C). The peak shape for sunset yellow improved using this buffer, however the peak shape for tartrazine now showed tailing. Peak shapes similar to tartrazine are not uncommon in capillary electrophoretic separations, and can be used for quantitative determinations [20]. Sodium cholate was unsuitable as a micelle modifier as tartrazine migrated as a very broad peak and allura red split into two poorly resolved peaks (Fig. 1D). The peak shapes change from the SDS buffer to the sodium deoxycholate and sodium cholate buffers. These changes could be due to the interactions between the analytes and the micelle/organic solvent in the buffer. We use a number of MEKC/CZE methods in our laboratory in which the analytes are dissolved in water without any problems with poor peak shapes.

The buffer containing sodium deoxycholate as the micelle modifier was used for the quantitative analyses as this gave the best separation and the best peak shapes for the majority of the compounds. The separation of the ten compounds and the ratio of the migration times to the migration time of the internal standard (azorubine) were reasonably consistent over twenty repetitive injections using this buffer. Also, the peak shapes were maintained over twenty repetitions. This was in contrast to the buffer modified with SDS, where allura red and indigo carmine became quite broad with time. The repeatability data (relative standard deviations, R.S.D.s) for seven consecutive injections of a number of standards of different concentrations were satisfactory (e.g. green S, 10 μg/ml, R.S.D. 4.3%; 25 μg/ml, R.S.D. 2.0%; 50 μg/ml, R.S.D. 2.1%; 100 μg/ml, R.S.D. 2.1%; tartrazine, 10 μg/ml, R.S.D. 4.1%; 25 μg/ml, R.S.D. 2.8%; 50 μg/ml, R.S.D. 1.9%; 100 μg/ml, R.S.D. 2.5%).

The addition of 15% acetonitrile and 0.05 *M* sodium deoxycholate to the phosphate/borate buffer was necessary to achieve the desired separation. Electropherograms showing the separation of the colours with the different buffers are displayed in Fig. 2. Replacing acetonitrile with either methanol or dioxane in the buffer resulted in poor peak shapes and long run times. Dimethylformamide and dimethyl sulphoxide, which have been used successfully in our laboratory to assist in the separation of complex mixtures [10,11] were unsuitable as they absorb UV light at the detection wavelength used for this analysis (214 nm). The compounds were detected at a common wavelength of 214 nm as it was not possible to detect the synthetic colours in the visible region of their spectra with the instrument used for the analyses.

A range of confectionery items and cordials were analysed by MEKC and the levels of the colours in the products were compared with the levels obtained from the HPLC procedure that is currently used in our laboratory [21]. Azorubine was not present in any of the confectionery samples and so was used as the internal standard for the MEKC analyses. Azorubine was also

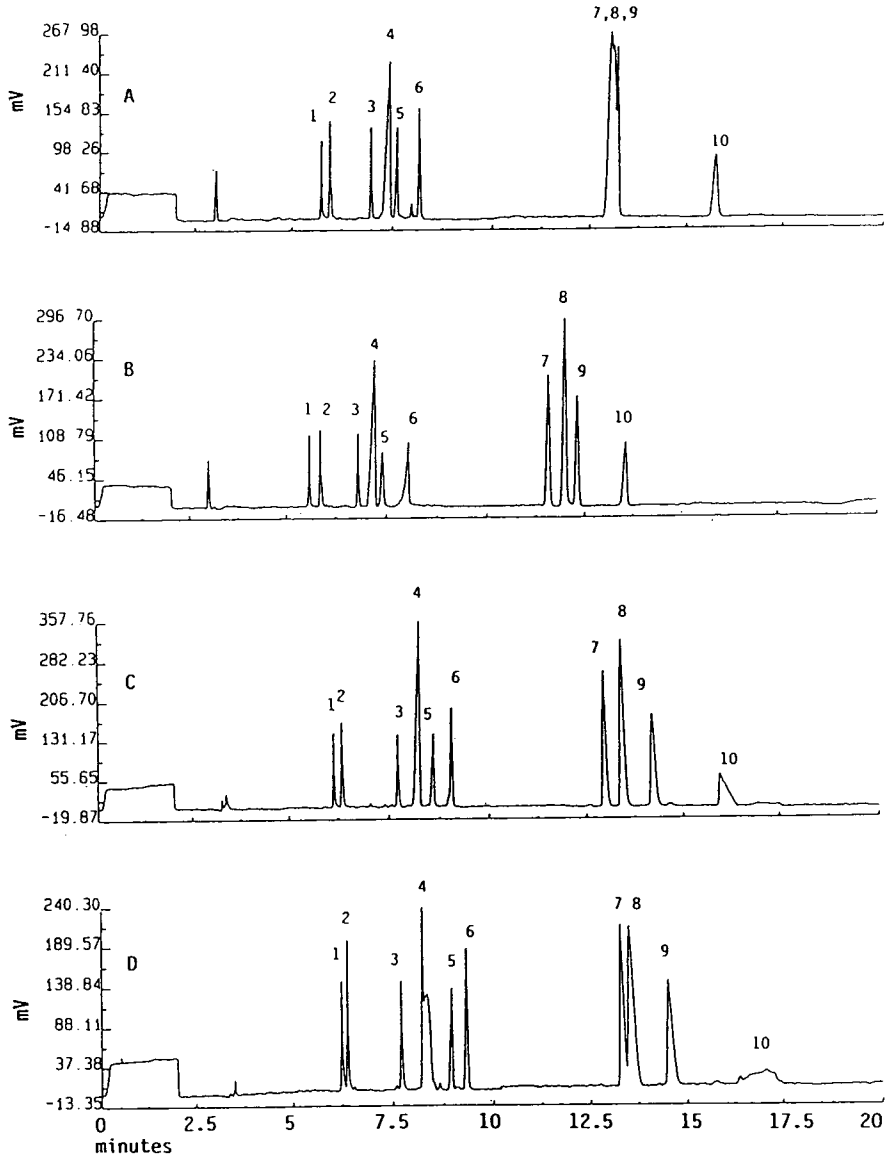

Fig. 1. Electropherograms showing the separation of green S (1), brilliant blue (2), erythrosine B (3), allura red (4), indigo carmine (5), sunset yellow (6), azorubine (7), amaranth (8), ponceau (9) and tartrazine (10) for (A) 15% acetonitrile and 85% 0.05 *M* SDS/0.01 *M* sodium borate buffer, (B) 15% acetonitrile and 85% 0.05 *M* SDS/0.005 *M* potassium dihydrogenorthophosphate/0.005 *M* sodium borate buffer, (C) 15% acetonitrile and 85% 0.05 *M* sodium deoxycholate/0.005 *M* potassium dihydrogenorthophosphate/0.005 *M* sodium borate buffer and (D) 15% acetonitrile and 85% 0.05 *M* sodium cholate/0.005 *M* potassium dihydrogenorthophosphate/0.005 *M* sodium borate buffer.

used as the internal standard for the cordials, except for one sample, where sunset yellow was used as the internal standard.

The levels of synthetic colours in five samples of confectionery and three cordials were in good agreement with the HPLC data. The instrument repeatability data (R.S.D.s) for the standard and sample solutions for the MEKC determinations

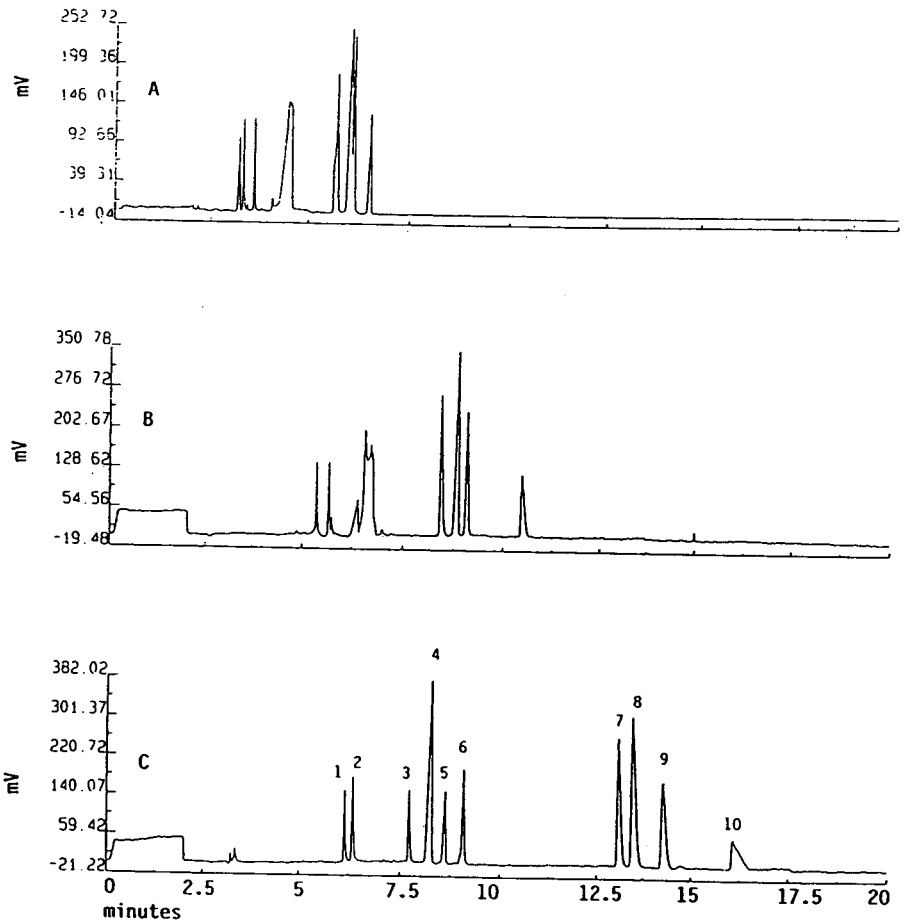

Fig. 2. Electropherograms showing the separation of green S (1), brilliant blue (2), erythrosine B (3), allura red (4), indigo carmine (5), sunset yellow (6), azorubine (7), amaranth (8), ponceau (9) and tartrazine (10) for (A) 0.005 *M* potassium dihydrogenorthophosphate/0.005 *M* sodium borate buffer, (B) 0.05 *M* sodium deoxycholate/0.005 *M* potassium dihydrogenorthophosphate/0.005 *M* sodium borate buffer and (C) 15% acetonitrile and 85% 0.05 *M* sodium deoxycholate/0.005 *M* potassium dihydrogenorthophosphate/0.005 *M* sodium borate buffer.

were also satisfactory. The electropherograms of the cordials were more complex than the confectionery due to the other additives present in samples. All of the cordials contained benzoic acid as a preservative. Benzoic acid and sorbic acid, which are permitted for use as preservatives in Australia [19] were well separated from the synthetic colours, however, the artificial sweetener saccharin, which is present in one sample of cordial, has the same migration time as allura red. Changing the detection wavelength to the absorption maxima for the colours in the visible region would eliminate these other components from the electropherograms. Citric acid, which is also present in the cordials, does not absorb strongly enough at 214 nm to cause a problem with the analyses.

Quinoline yellow, brilliant black, brown HT and chlorophyll copper complex are also permitted for use as synthetic colours in Australia [20]. Quinoline yellow appears as two peaks with similar migration times to green S and brilliant blue, while brilliant black migrates between amaranth and ponceau. The two peaks for quinoline yellow correspond to the two components in the synthetic colour preparation [21].

The ratio of the migration times of quinoline yellow and brilliant black to the internal standard (azorubine) are consistent over 20 repetitive injections. Both quinoline yellow and brilliant black are linear to 100 μg/ml and could therefore be determined quantitatively by this procedure. Brown HT and chlorophyll copper complex are not pure compounds and so appear as a mixture of peaks.

The analysis time is reduced from 37 min for HPLC to 18 min for MEKC procedure. Also, the procedure is less costly to operate than HPLC as MEKC is frugal in its use of chemicals and solvents and no costly columns are employed.

4. Conclusions

A rapid method for the separation and determination of commonly used synthetic colours in confectionery and cordials by MEKC is described. The separation of the compounds and the peak shapes were more consistent with a buffer modified with sodium deoxycholate than with a buffer modified with SDS. The instrument repeatability was acceptable, and the levels of the synthetic colours were in good agreement with the levels determined by the HPLC procedure currently used in our laboratory. The MEKC procedure is also faster and less costly to operate than the HPLC method.

Acknowledgements

The authors wish to thank Mr. Con Pyromallis for determining the levels of synthetic colours by HPLC, Dr. Robert Wells, Mrs. Robyn Clarke and Ms. Geraldine Keogh for their assistance and the Australian Government Analyst, Dr. C.J. Dahl, for his permission to publish.

References

[1] V.C. Trenerry, R.J. Wells and J. Robertson, *J. Chromatogr. Sci.*, 32 (1994) 1.
[2] V.C. Trenerry, R.J. Wells and J. Robertson, *Electrophoresis*, 15 (1994) 103.
[3] I. Pant and V.C. Trenerry, *Food Chem.*, in press.
[4] C.O. Thompson and V.C. Trenerry, *Food Chem.*, in press.
[5] P.A. Marshall, V.C. Trenerry and C.O. Thompson, *J. Chromatogr. Sci.*, in press.
[6] S.F.Y. Li, *Capillary Electrophoresis —Principles, Practice and Applications* (*Journal of Chromatography Library*, Vol. 52), Elsevier, Amsterdam, 1992.
[7] S. Terabe, K. Otsuka, K. Ichikawa, A. Tsuchiya and T. Ando, *Anal. Chem.*, 56 (1984) 111.
[8] R.O. Cole and M.J. Sepaniak, *LC·GC*, 10 (1991) 380.
[9] H. Nishi, T. Fukuyama, M. Matsuo and S. Terabe, *J. Chromatogr.*, 498 (1990) 313.
[10] V.C. Trenerry, R.J. Wells and J. Robertson, *J. Chromatogr. A*, in press.
[11] V.C. Trenerry, R.J. Wells and J. Robertson, in preparation.
[12] R. Weinberger, *Practical Capillary Electrophoresis*, Academic Press, San Diego, CA, 1993.
[13] R. Kuhn and S. Hoffstetter-Kuhn, *Capillary Electrophoresis —Principles and Practice*, Springer, Berlin, Heildelberg, 1993.
[14] M.L. Puttemans, L. Dryon and D.L. Massart, *J. Assoc. Off. Anal. Chem.*, 64 (1981) 1.
[15] J.F. Lawrence, F.E. Lancaster and H.B.S. Conacher, *J. Chromatogr.*, 210 (1981) 168.
[16] J.P. Chaytor and R.L. Heal, *J. Chromatogr.*, 368 (1986) 450.
[17] R. Clarke and R.J. Wells, presented at the *12th Australian Symposium on Analytical Chemistry, Perth, October 1993.*
[18] J. Karovicova, J. Polonsky, A. Pribela and P. Simko, *J. Chromatogr.*, 545 (1991) 413.
[19] *Australian Food Standards Code*, Australian Government Publishing Service, Canberra, 1994.
[20] B.F. Kenny, *J. Chromatogr.*, 546 (1991) 423.
[21] G.F. Keogh, *M.HN. Thesis*, Faculty of Health and Behavioural Sciences, Deakin University, Australia.

ELSEVIER

Journal of Chromatography A, 704 (1995) 203–210

JOURNAL OF CHROMATOGRAPHY A

Determination of cyclamate in low joule foods by capillary zone electrophoresis with indirect ultraviolet detection

Catherine O. Thompson, V. Craige Trenerry*, Bridget Kemmery

Australian Government Analytical Laboratories, 338–340 Tapleys Hill Road, Seaton 5023, Australia

First received 9 November 1994; revised manuscript received 25 January 1995; accepted 15 February 1995

Abstract

A rapid method for the determination of cyclamate in low joule cordials and other low joule foods by capillary zone electrophoresis (CZE) with indirect ultraviolet (UV) detection at 254 nm is described. Sorbic acid, which is often added to low joule cordials as a preservative, can also be determined with this procedure. Cyclamate and sorbate are well separated from the other components in the foods in less than 5 min using an uncoated fused-silica capillary column with an electrolyte consisting of 1 m*M* hexadecyltrimethylammonium hydroxide, 10 m*M* sodium benzoate operating at a voltage of −20 kV. Alpha-hydroxyisobutyric acid was used as the internal standard. The levels of cyclamate determined by CZE were in good agreement with those determined by the AOAC gravimetric method. The artificial sweeteners aspartame, acesulphame-K, alitame and saccharin can also be separated using this procedure. Saccharin and benzoic acid, which are often added with cyclamate to low joule cordials, and caffeine, which is added to low joule colas containing cyclamate, cannot be determined quantitatively with this system.

1. Introduction

Cyclamate, as the sodium or calcium salt, is added as an artificial sweetener to a variety of low joule foods and beverages available in Australia [1]. A number of methods based on wet chemical and HPLC procedures for the quantitative determination of cyclamate in a variety of low joule foods have been reported in the literature.

Cyclamate can be determined using the gravimetric or colourimetric procedures outlined in the Official Methods of Analysis of the Association of Official Analytical Chemists [2]. Unfortunately, these two procedures are labour intensive and time-consuming. Traditional high-performance liquid chromatography (HPLC) is not suited for the determination of cyclamate as cyclamate does not absorb in the usable UV range (above 200 nm). Herrmann et al. [3] used HPLC with indirect photometry to determine the level of cyclamate in a variety of low joule foods. The artificial sweeteners saccharin, dulcin and aspartame could also be determined with this procedure. Ion chromatography with conductivity detection has also been used to determine cyclamate, saccharin and acesulphame-K in a number of low joule foods [4] and cyclamate and saccharin in table top sweeteners [5]. HPLC has also been used to determine cyclamate after oxidation to cyclohexylamine and with pre-column derivatisation to a fluorescent derivative [6]

* Corresponding author.

0021-9673/95/$09.50
SSDI 0021-9673(95)00210-3

and after conversion to N,N-dichlorcyclohexylamine [7].

Methods based on capillary zone electrophoresis (CZE) are rapidly gaining acceptance as rugged analytical procedures [8,9]. Recently, CZE with indirect UV detection has been used to determine a number of different anions [10] and organic acids in a variety of samples [11]. CZE procedures exhibit greater chromatographic resolution, have the same order of repeatability and are often less costly to operate than HPLC [8,9]. It was of interest to see whether CZE could be used to provide a fast and robust method for the determination of cyclamate in low joule foods.

This paper describes a rapid CZE method for the determination of cyclamate in a variety of low joule foods using indirect UV detection at 254 nm. Alpha-hydroxyisobutyric acid was used as the internal standard. The accuracy of the procedure was evaluated by comparing the levels of cyclamate in the foods with those determined by the gravimetric procedure described in the literature [2]. The artificial sweeteners aspartame, acesulphame-K, alitame and saccharin can also be separated using this procedure.

2. Experimental

2.1. Reagents

Aspartame, sodium saccharin, potassium sorbate, alpha-hydroxyisobutyric acid, sodium cyclamate, hexadecyltrimethylammonium bromide (CTAB) and sodium benzoate were obtained from Sigma (St. Louis, MO, USA). OFM Anion-BT reagent was obtained from Waters Millipore (Milford, MA, USA). Hexadecyltrimethylammonium chloride was obtained from Aldrich (Milwaukee, WI, USA) and hexadecyltrimethylammonium hydroxide hydrate was obtained from Fluka Chemie (Buchs, Switzerland). Acesulfame-K and alitame were gifts from Hoechst (Frankfurt, Germany) and Pfizer (Groten, CT, USA), respectively. Caffeine was obtained from the Curator of Standards, Australian Government Analytical Laboratories, 1 Suakin Street, Pymble, NSW, Australia. All other chemicals and solvents were AR grade or HPLC grade and used without further purification.

2.2. CZE buffer

A 36.5-mg amount of hexadecyltrimethylammonium hydroxide hydrate was dissolved in 100 ml of 10 m*M* sodium benzoate. The solution was filtered through a 0.8-μm cellulose acetate filter disc before use.

2.3. Apparatus

CZE

The samples were analysed with an uncoated fused-silica capillary column (75 cm × 75 μm I.D.) with an effective length to the detector of 50 cm purchased from Polymicro Technologies (AZ, USA), with an electrolyte consisting of 1 m*M* hexadecyltrimethylammonium hydroxide and 10 m*M* sodium benzoate pH 6.6. An Isco Model 3140 electropherograph (Isco, Lincoln, NE, USA) operating at −20 kV and at 28°C was used for all determinations. The solutions were loaded under vacuum (vacuum level 2, 20 kPa s) and were detected at 254 nm with indirect detection and were determined quantitatively at 0.005 AUFS. The capillary was flushed with running buffer for 2 min between analyses. The capillary was cleaned on a weekly basis by washing with 0.1 *M* sodium hydroxide for 10 min followed by deionised water for 10 min before filling with running buffer. Electropherograms were recorded with the ICE Data Management and Control Software supplied with the electropherograph.

HPLC

The apparatus and conditions for the determination of sorbate in the cordial sample are based on those described by Lawrence and Charbonneau [12] and are detailed in a separate report [13].

2.4. Gravimetric analysis

The level of cyclamate in the cordials, soft drink and jam were determined by the method described in the AOAC Official Methods of Analysis No. 20.180 [2].

2.5. Samples and standards

Samples

The samples were purchased from local outlets and analysed within the recommended "use by" dates. The cordials and soft drinks were diluted with an appropriate amount of deionised water. The jam was blended with deionised water using a commercial food processor, the solution filtered through a Whatman No. 1 filter paper and made to volume with deionised water. The concentration of cyclamate in the final solutions should be less than 100 μg/ml. Alpha-hydroxyisobutyric acid was used as the internal standard at a final concentration of 50 μg/ml. The solutions were filtered through a 0.45-μm cellulose acetate filter disc before analysis.

Standards

Standard solutions were prepared in deionised water with alpha-hydroxyisobutyric acid as the internal standard at a concentration of 50 μg/ml. The solutions were filtered through a 0.45-μm cellulose acetate filter disc before analysis. The detector response for cyclamate was linear to 100 μg/ml.

3. Results and discussion

The analysis of cyclamate by traditional HPLC methods has limited application as cyclamate does not show absorption in the usable UV range (above 200 nm). HPLC with indirect photometry [3] and ion chromatography with conductivity detection [4,5] have been used to determine cyclamate in a number of foods. Recently, CZE using indirect UV detection, has been used to separate and quantify a number of compounds that do not absorb in the usable UV range. These include anions, cations and organic acids [10,11]. To achieve the separation of anions and organic acids, a cationic surfactant is added to the UV absorbing electrolyte causing the electroosmotic flow to move towards the anode, forcing the anions to migrate in the same direction as the electroosmotic flow from the injection end to the detector end of the instrument. This mode of CZE using OFM Anion-BT reagent as the cationic surfactant has been well documented by Jandik and Jones [14]. Anions are well separated using a chromate electrolyte containing OFM Anion-BT reagent, whilst phthalate and benzoate electrolytes containing OFM Anion-BT reagent have been used for the analysis of organic acids [10,11]. These analyses are easy to perform, have reasonable sensitivity (ppm range) and have short run times. Cyclamate (cyclohexane sulphamate) (Fig. 1) which is negatively charged and does not absorb in the usable UV range is well suited for this type of analysis.

Initial experiments with a 10 m*M* sodium chromate electrolyte containing 1 m*M* OFM Anion-BT reagent resulted in poor peak shapes for cyclamate and alpha-hydroxyisobutyric acid (added as an internal standard) even though the migration times were less than 5 min. Replacing sodium chromate in the electrolyte with sodium benzoate resulted in much sharper peaks for cyclamate and alpha-hydroxyisobutyric acid even though the migration times for cyclamate and alpha-hydroxyisobutyric acid remained the same.

The separation of cyclamate and alpha-hydroxyisobutyric acid was maintained over twenty repetitive injections and the detector response for cyclamate was linear to 100 μg/ml. To test the suitability of the system for quantitative purposes, standard solutions of different concentrations were analysed seven times and the peak area repeatability data (C.V., %) for cyclamate determined. The C.V. data were acceptable

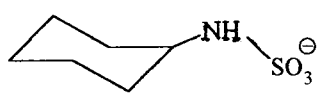

Cyclamate

Fig. 1. Structure of cyclamate.

(standard concentration, 5 μg/ml, C.V. 1.8%; 10 μg/ml, C.V. 1.6%; 20 μg/ml, C.V. 1.5%; 50 μg/ml, C.V. 2.3%; 100 μg/ml, C.V. 1.2%). The levels of cyclamate in a number of samples were then determined by CZE. The amounts of cyclamate present in the samples were in good agreement with those determined by the standard AOAC gravimetric procedure [2]. (Cordial 1 CZE 2.5 g/l, AOAC 2.6 g/l; cordial 2 CZE 6.5 g/l, AOAC 6.5 g/l; cordial 3 CZE 3.1 g/l, AOAC 3.2 g/l; cola CZE 0.7 g/l, AOAC 0.7 g/l; jam CZE 8.1 g/kg, AOAC 8.1 g/kg). None of the samples had any naturally occurring compounds that comigrated with the internal standard when analysed by CZE. The recoveries of added cyclamate and the peak area repeatability (C.V., %) data for cyclamate for seven replicate determinations were also excellent (cordial 1, recovery 101%, C.V. 1.2%).

The electropherogram of cordial 2 contained a negative peak which migrated before cyclamate and was assigned as sorbate. The peak appears in the opposite direction to the other peaks in the electropherogram as sorbate absorbs UV light more strongly than the benzoate electrolyte. The separation of sorbate and cyclamate was only marginal with this electrolyte and so other cationic surfactants were trialled in order to improve the separation and therefore the accuracy of the quantitation. Replacing OFM Anion-BT reagent with hexadecyltrimethylammonium chloride had little effect on the separation, whist the separation was only marginally better when OFM Anion-BT reagent was replaced with hexadecyltrimethylammonium bromide. Replacing OFM Anion-BT reagent with hexadecyltrimethylammonium hydroxide gave a greater separation of cyclamate and sorbate. The separation of cyclamate, sorbate and alpha-hydroxyisobutyric acid was maintained over twenty repetitive injections and the detector response for cyclamate was linear to 100 μg/ml, whilst the detector response for sorbate was linear to 5 μg/ml. The electropherograms showing the separation of cyclamate and sorbate with electrolytes containing Anion OFM-BT reagent and hexadecyltrimethylammonium hydroxide as the cationic surfactants are displayed in Fig. 2A,B.

To test the suitability of this system for quantitative purposes, standard solutions of different concentrations were analysed seven times to evaluate the peak area repeatability data (C.V., %) for cyclamate and sorbate. As with the previous system, the data were acceptable (cyclamate, standard concentration 5 μg/ml, C.V. 4.6%; 10 μg/ml, C.V. 1.7%; 20 μg/ml, C.V. 2.1%; 50 μg/ml, C.V. 1.6%; 100 μg/ml, C.V. 2.4%; sorbate, standard concentration 0.2 μg/ml, C.V. 3.9%; 0.5 μg/ml, C.V. 2.5%; 1.0 μg/ml, C.V. 1.7%; 2.0 μg/ml, C.V. 0.4%; 5.0 μg/ml, C.V. 2.1%).

The levels of cyclamate in three samples of low joule cordial and a sample of low joule cola were then determined using this electrolyte, with one cordial (sample 5) being analysed seven times for area repeatability (C.V., %) data. The electropherogram for cordial 5 is displayed in Fig. 2C. The levels of cyclamate in the samples were in good agreement with those determined by the AOAC gravimetric procedure [cordial 3, CZE 3.0 g/l, AOAC 3.2 g/l; cordial 4, CZE 2.2 g/l, AOAC 2.5 g/l; cordial 5, CZE 5.5 g/l (C.V. 1.0%), AOAC 5.5 g/l; cola, CZE 0.7 g/l, AOAC 0.7 g/l]. The sorbate content of cordial 5 compared favourably with the level determined by HPLC [12] (CZE 85 mg/l, HPLC 90 mg/l).

The results indicate that cyclamate can be determined quantitatively by CZE with either OFM Anion-BT reagent or hexadecyltrimethylammonium hydroxide as the cationic surfactant. However, a better separation of sorbate and cyclamate is seen with hexadecyltrimethylammonium hydroxide as the cationic surfactant. This would result in a more accurate quantitation, and is therefore the preferred electrolyte for the analysis.

Other food additives could also be separated with this CZE procedure. The artificial sweeteners, aspartame, alitame, acesulphame-K and saccharin also migrate with this buffer (Fig. 3). Acesulphame-K appears as a negative peak, while aspartame and alitame appear as positive peaks. Saccharin appears as a broad negative peak in the electropherogram. Saccharin is present in cordial 5 and in the diet cola and it was of interest to see if saccharin could be determined

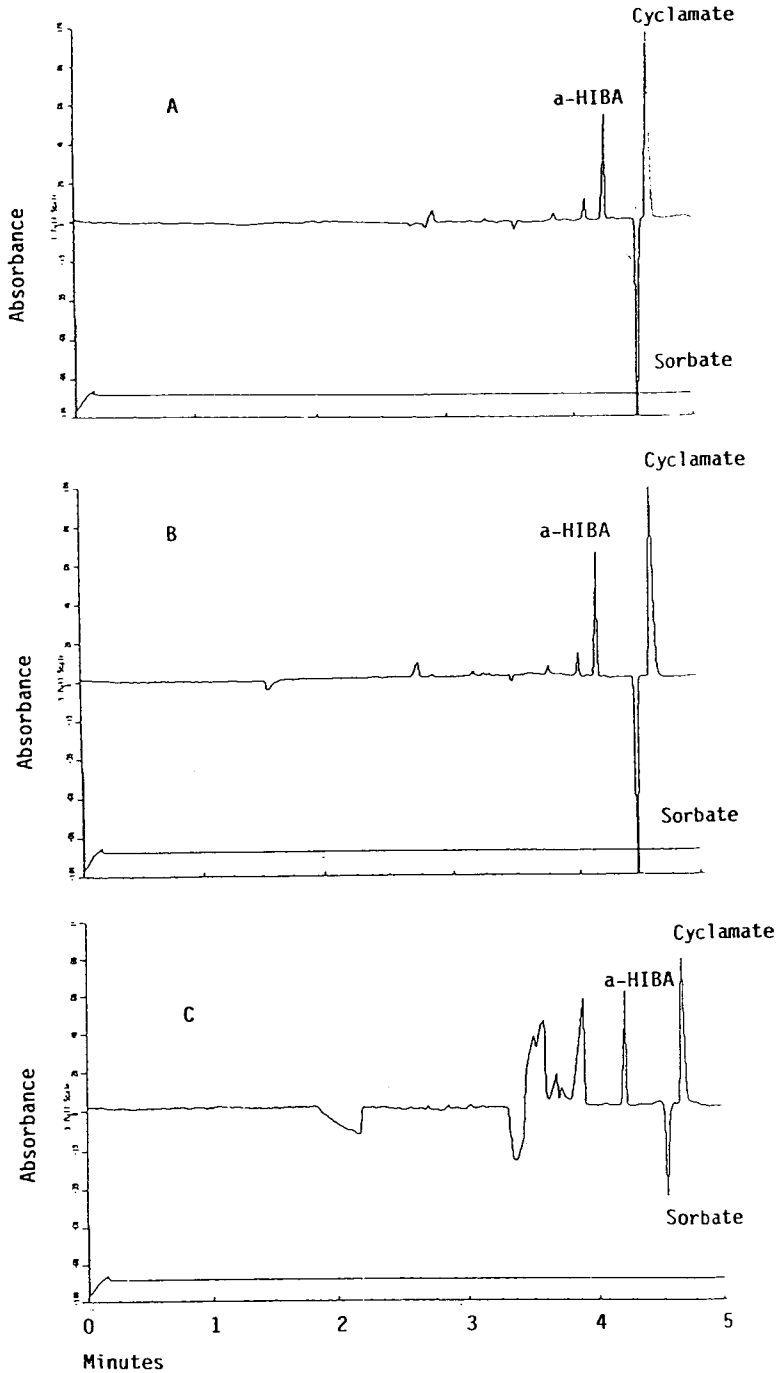

Fig. 2. Electropherograms of (A) standard solution containing cyclamate and sorbate using a 10 m*M* sodium benzoate, 1 m*M* OFM Anion-BT reagent electrolyte, (B) standard solution containing cyclamate and sorbate using a 10 m*M* sodium benzoate, 1 m*M* hexadecyltrimethylammonium hydroxide electrolyte, and (C) cordial 5 containing cyclamate and sorbate using a 10 m*M* sodium benzoate, 1 m*M* hexadecyltrimethylammonium hydroxide electrolyte. Alpha-hydroxyisobutyric acid (a-HIBA) was used as the internal standard. The *x*-axis gives the migration time in minutes.

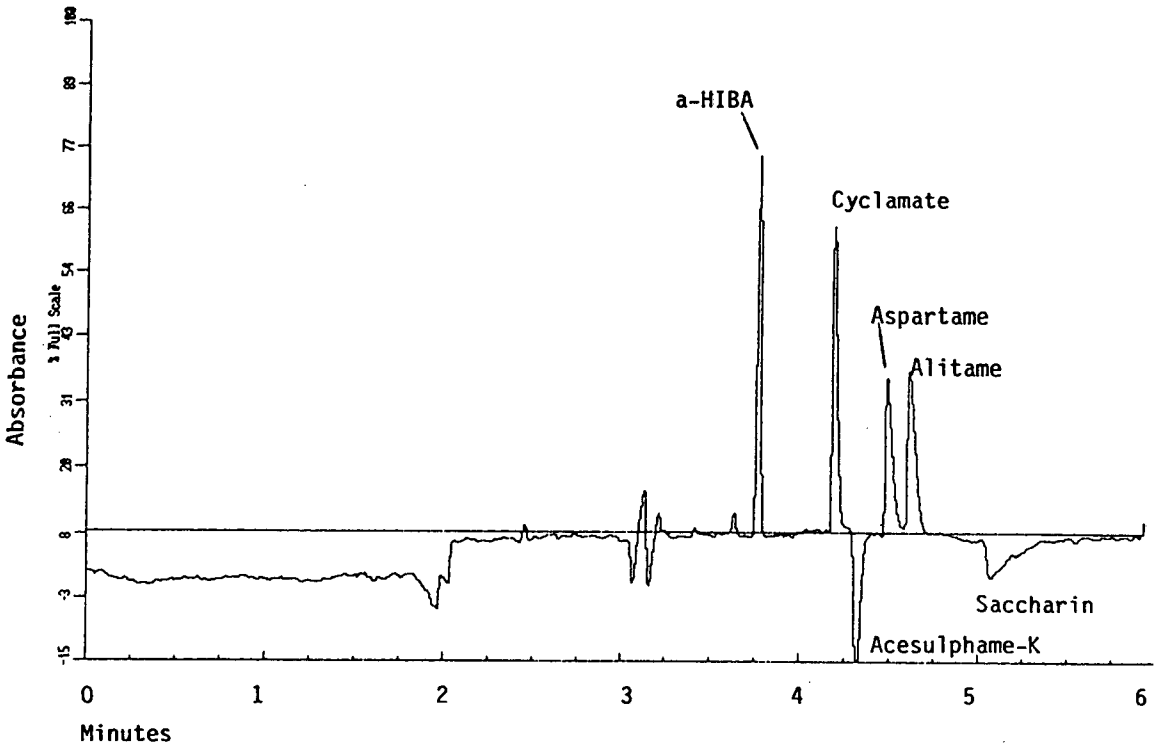

Fig. 3. Electropherogram showing the separation of cyclamate, acesulfame-K, aspartame, alitame, and saccharin using a 10 m*M* sodium benzoate, 1 m*M* hexadecyltrimethylammonium hydroxide electrolyte. Alpha-hydroxyisobutyric acid (a-HIBA) was used as the internal standard. The *x*-axis gives the migration time in minutes.

in the same analysis. However, this could not be done due to the poor detector response for saccharin. The diet cola also contains caffeine and benzoic acid. Caffeine does not migrate with this system and benzoic acid cannot be determined as the electrolyte contains sodium benzoate.

Cyclamate, saccharin and alpha-hydroxyisobutyric acid are well separated with an electrolyte consisting of 10 m*M* potassium hydrogen phthalate and 1 m*M* OFM Anion-BT reagent. In this instance, saccharin appeared as a positive peak in the electropherogram. However, as with the previous system, the detector response for saccharin was too small to be of any use for quantitative purposes.

In an earlier report, saccharin, caffeine, benzoic acid, sorbic acid and a number of other artificial sweeteners were separated and determined in diet drinks and cordials by micellar electrokinetic capillary chromatography (MEKC) [13]. The separation was achieved using a fused-silica capillary with the same dimensions as the one used in the present work and with a buffer consisting of 0.05 *M* sodium deoxycholate, 0.01 *M* sodium borate and 0.01 *M* potassium dihydrogen orthophosphate, pH 8.6. The analyses were performed at 20 kV and at 28°C with the compounds being detected by UV at 220 nm. Cyclamate and saccharin (and the other food additives) can therefore be determined in the same sample using the same column with different buffers and detector settings. After cyclamate has been determined, the column is washed with 0.1 *M* sodium hydroxide, refilled with the MEKC buffer and the detector settings optimised for the other analyses. Fig. 4 shows consecutive electropherograms for the

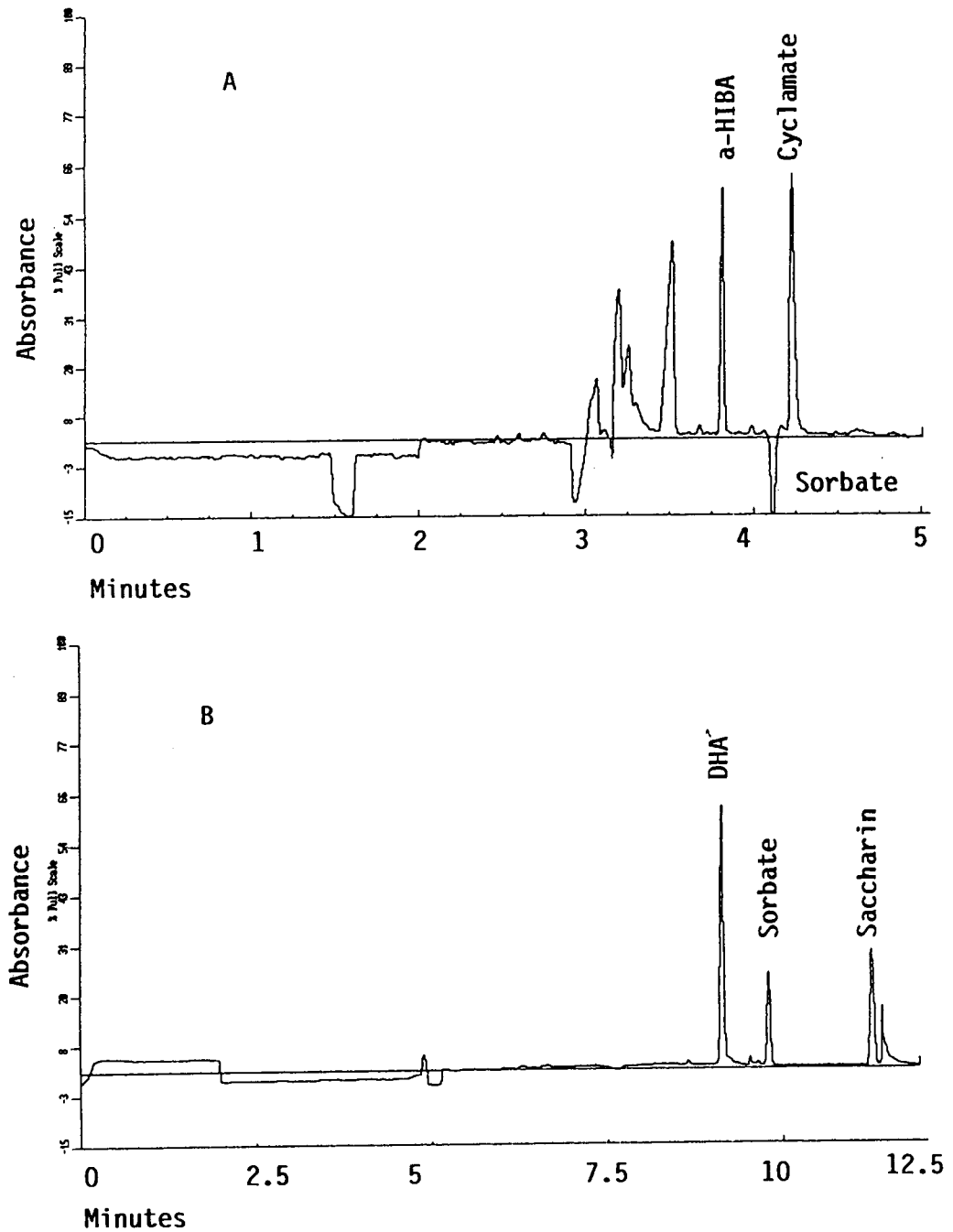

Fig. 4. Electropherograms of cordial 5 containing cyclamate, sorbate and saccharin using (A) a 10 m*M* sodium benzoate, 1 m*M* hexadecyltrimethylammonium hydroxide electrolyte with alpha-hydroxyisobutyric acid (a-HIBA) as the internal standard, and (B) using a 0.05 *M* sodium deoxycholate, 0.01 *M* potassium dihydrogen orthophosphate, 0.01 *M* sodium borate buffer pH 8.6 with dehydroacetic acid (DHA) as the internal standard. The *x*-axis gives the migration time in minutes.

determination of cyclamate, saccharin and sorbate in cordial 5. Although this is not as convenient as determining the analytes in one run, it is a practical alternative and shows the versatility of capillary electrophoresis as an analytical tool. This process can be fully automated with the ISCO Model 3140 electropherograph and other automated instruments.

4. Conclusion

A rapid method for the determination of cyclamate in low joule cordials, diet cola and low joule jam by capillary zone electrophoresis (CZE) is described. The levels of cyclamate were in good agreement with those determined by the standard AOAC gravimetric procedure. Sorbic acid, which is often added to low joule cordials as a preservative, can also be accurately determined with this procedure. Other food additives, e.g. saccharin and benzoic acid, which are often added to low joule cordials containing cyclamate, and caffeine, which is present in low joule colas containing cyclamate, cannot be determined quantitatively with this system. However, the amounts of the additives can be accurately determined in these samples by using a different MEKC system with the same capillary column.

Acknowledgement

The authors wish to thank the Australian Government Analyst, Mr. R. Hogg, for his permission to publish this work.

References

[1] Australian Food Standards Code, 1994. Australian Government Publishing Service, Canberra, Australia.
[2] Official Methods of Analysis, Association of Official Analytical Chemists, 14th edn., 1984, No. 20.180.
[3] A. Herrmann, E. Damawandi and M. Wagmann, J. Chromatogr., 280 (1983) 85–90.
[4] T. Biemer, J. Chromatogr., 463 (1989) 463–468.
[5] U. Haldna and J. Kois, Proc. Estonian Acad. Sci. Chem., 41 (2) (1992) 69–72.
[6] J. Ruter and D.I. Ulrich Raczek, Z. Lebensm. Unters. Forsch., 194 (1992) 520–523.
[7] M. Lehr and W. Schmid, Deutsche Lebensmittel-Rundschau, 89 (1993) 43–45.
[8] V.C. Trenerry, R.J. Wells and J. Robertson, J. Chromatogr. Sci., 32 (1994) 1.
[9] V.C. Trenerry, R.J. Wells and J. Robertson, Electrophoresis, 15 (1994) 103.
[10] J. Romano, P. Jandik, W.R. Jones and P.E. Jackson, J. Chromatogr., 546 (1991) 411–421.
[11] B. Kenny, J. Chromatogr., 546 (1991) 423–430.
[12] J.F. Lawrence and C.F. Charbonneau, J. Assoc. Off. Anal. Chem., 71 (1988) 934–937.
[13] C.O. Thompson, V.C. Trenerry and B. Kemmery, J. Chromatogr. A, 704 (1995) 195.
[14] P. Jandik and W.R. Jones, J. Chromatogr., 546 (1991) 431–443.

ELSEVIER

Journal of Chromatography A, 704 (1995) 211–216

JOURNAL OF CHROMATOGRAPHY A

Short communication

Counter-current chromatographic separation of polyunsaturated fatty acids

Olivier Bousquet*, François Le Goffic

Laboratoire de Bioorganique et Biotechnologies, associé au CNRS, Ecole Nationale Supérieure de Chimie de Paris, 11 Rue P. & M. Curie, 75231 Paris Cedex 05, France

Received 10 November 1994; accepted 14 December 1994

Abstract

Hexadecatrienoic acid (C16:3), octadecatetraenoic acid (C18:4), eicosapentaenoic acid (C20:5) and docosahexaenoic acid (C22:6) were purified in two steps by counter-current chromatography (CCC). The selected liquid phases were heptane–acetonitrile–water for the first step and heptane–methanol–water for the second. The upper non-polar phase was kept stationary in the coil of the instrument by a rotational force field. The separation was followed by UV detection at 210 nm and by analysing the eluted fractions by gas chromatography after esterification. The purity of the fatty acids therefore purified was checked by capillary gas chromatography. CCC may be an alternative to HPLC for the preparative-scale purification of such compounds.

1. Introduction

The ω-3 fatty acids possess a number of properties that make them valuable molecules in the biomedical and nutrition fields [1,2]. Eicosapentaenoic acid (C20:5, EPA) and docosahexaenoic acid (C22:6, DHA) have in particular been studied in oils containing large amounts of the acids or as ethyl esters in the presence of large amounts of other fatty acids methyl esters. According to Holman [3], these essential fatty acids are active in the growth and maintenance of human skin.

Their full purification is very difficult owing in particular to their easy peroxydation. It has been more or less achieved on a preparative scale, however, by the combination of different techniques such as solvent extraction, molecular distillation [4], urea inclusion [5], counter-current distribution (CCD) [6,7], counter-current chromatography (CCC) [8–10], thin-layer chromatography on a silver nitrate-coated plate [11], high-performance liquid chromatography (HPLC) [12,13], supercritical fluid extraction [14], supercritical fluid chromatography [15], organic synthesis [16] and enzymology [17].

We present here a two-step method for the purification of these fatty acids on a semi-preparative scale. The results can be extended to the preparative scale provided that a suitable instrument is available.

2. Experimental

2.1. Materials

A mixture of fatty acids was prepared by

* Corresponding author.

0021-9673/95/$09.50
SSDI 0021-9673(94)01233-4

saponification of an oil extract from microalgae (*Skeletonema costatum*) which was cultured under industrial fermentation conditions [18–20]. It was stabilized with butylated hydroxytoluene (BHT).

2.2. CCC system

The chromatographic system consisted of a Waters (Milford, MA, USA) M45 isocratic constant solvent-delivery pump, a six-way injection valve with a sample loop, a Waters Model 486 UV–visible spectrophotometer with a semi-preparative cell and an ISCO 328 fraction collector. The CCC apparatus was a multi-layer coil separator extractor (P.C. Potomac, MD, USA). The column was a 61.4 m × 1.6 mm I.D. PTFE tube wound on a 10-cm diameter holder [21]. The rotational speed was constant during elution and was controlled with a stroboscope. Detection was carried out at 210 nm and the fractions were analysed by GC and GC–MS after esterification of the fatty acids to methyl esters [22,23].

The fatty acid fraction was injected into the RP-CCC system with heptane as the stationary phase and acetonitrile–water as the mobile phase. Elution was performed at room temperature at a flow-rate of 2 ml/min. Fractions were collected every 5 min (10 ml). After analysis, the different fractions were pooled and the solvent was evaporated; an aliquot was esterified to methyl esters and analysed by GC. The separation of these essential fatty acids, in the third- and fourth-eluted fractions, was then studied with the biphasic system heptane–methanol–water.

In order to obtain a better separation, the resolution was increased by optimization of the CCC parameters, viz., the composition of the mobile phase, the flow-rate, the rotational speed and the injection loop volume.

2.3. Semi-preparative scale CCC

In order to improve this separation method for further purification, we injected into the column gram levels of material with a 9-ml sample loop. On-line detection was not possible and analysis of the fractions by GC was applied.

2.4. Identification methods

Esterification was performed with methanol in the presence of BF_3 (14%, w/v). The chromatograph (Shimadzu GC-14A) was equipped with a flame ionization detector and connected to an integrator (Shimadzu, Chrompack C-R5A). The column (Chrompack CP-Sil-5-CB) was a fused-silica megabore type (25 m × 0.25 mm I.D.). The conditions were as follows: column temperature, increased from 140 to 230°C at 3°C/min; injector and detector temperatures, 240°C; carrier gas, helium with a split of 40 ml/min. Before analysing the fatty acid methyl ester fractions by GC, it is possible to remove undesirable compounds from the esterification reaction and repurify the polyunsaturated fatty acids by described methods [9,10,24], i.e., a CCC run of the methyl esters with heptane–acetonitrile as a biphasic system.

For identification by GC–MS, experiments were performed on a Nermag R10-10C instrument combined with a gas chromatograph controlled by a Digital PDP11-23 Plus system (Delsi-Nermag, Argenteuil, France). The same column and temperature conditions as mentioned above were used. The retention times and mass spectra of the samples were compared with those obtained with standard C20:5ω3 and C22:6ω3 methyl esters (Sigma).

The free and methyl ester fatty acids were stored in solution in the dark with BHT as an antioxidant.

3. Results and discussion

3.1. Recovery of fatty acids from marine source

The analysis by GC of the total fatty acids of *Skeletonema costatum* shows a large number of fatty acids in the starting extracted oil. Dried algae could also be directly saponified with alcoholic KOH to recover the fatty acids quickly with the same ratios [25].

3.2. Purification of essential fatty acids

In this first CCC step, purification was carried out with RCOOH prepared directly from microalgae. All the saturated fatty acids were eliminated by a first CCC step with heptane–acetonitrile–3% water as a biphasic system. The main advantage of CCC is its efficiency, which allows one to remove all the non-essential fatty acids. In the microalgae we used, the recovered polyunsaturated fatty acids constituted about 20–40% (w/w) of the total fatty acids.

3.3. Chromatographic studies and separation

The equivalent chain length (ECL) of a fatty acid is defined as $ECL = N - 2n_{(C=C)}$, where N is the number of carbon atoms and $n_{(C=C)}$ is the number of double bonds in the fatty acid [26]. The ECL value for C16:3, C18:4, C20:5 and C22:6 is 10; the separation of these four compounds, with the same ECL, from marine oils is a challenging task.

In the reversed-phase mode, where heptane was the stationary phase and methanol–water was the mobile phase, the configuration was analogous to that in an octadecylsilyl (C_{18}) reversed-phase adsorption liquid chromatographic system. Polyunsaturated fatty acids have a COOH end, which could be ionized during elution, thus causing distortion of chromatograms. In order to suppress this ionization, a small amount of hydrochloric acid was added to the mobile phase. The elution mechanism depends on the alkyl chain length and the degree of unsaturation of the individual fatty acids.

In CCC we have $V_c = V_0 + V_s$ [27] with V_0 and V_s known (V_c = column volume; V_s = stationary phase volume); the general equation of chromatography, $V_R = V_0 + KV_s$, can also be written as $K = (V_R - V_0)/(V_C - V_0)$, so from the chromatograms, we can calculate directly the partition coefficients and the selectivity coefficients. As in HPLC, with an increasing proportion of water in the mobile phase to retain the compounds in the column better, the separation was increased as shown in Fig. 1. For each biphasic composition,

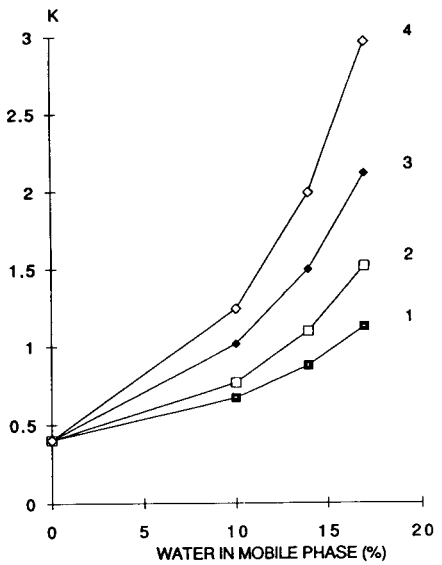

Fig. 1. Partition coefficients of four critical pairs of fatty acids versus the percentage of water in the mobile phase in RP-CCC. 1 = C16:3; 2 = C18:4; 3 = C20:5; 4 = C22:6.

the K values are a logarithmic function of the carbon chain length (Fig. 2).

Two parameters, the flow-rate of the mobile phase and the composition of the biphasic system, were important for optimizing the separation. Baseline resolution between EPA and DHA was obtained with 17% water in the mobile phase and after optimization of the chromatographic parameters, i.e., decreasing the flow-rate to 2.0 ml/min [21], increasing of the coil column rotational speed to 850 rpm and using a 0.5-ml injection loop [28]. For this separation (Fig. 3), the K and α values were as reported in Table 1.

The spectrophotometer response is a function of the degree of unsaturation in the carbon chain; for this reason, the mass ratio could not be obtained by comparison of peak areas without a calibration graph for each fatty acid.

The large range of flow-rate that can be used in CCC allows one to achieve the separation quickly at a high flow-rate and then to increase the resolution by decreasing the flow-rate.

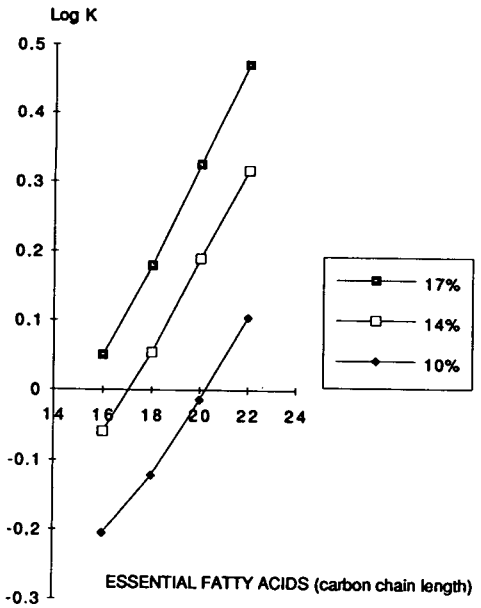

Fig. 2. Partition coefficients of four polyunsaturated fatty acids (critical pairs) from marine oil with different chain lengths with heptane–methanol containing different percentages of water as a biphasic system.

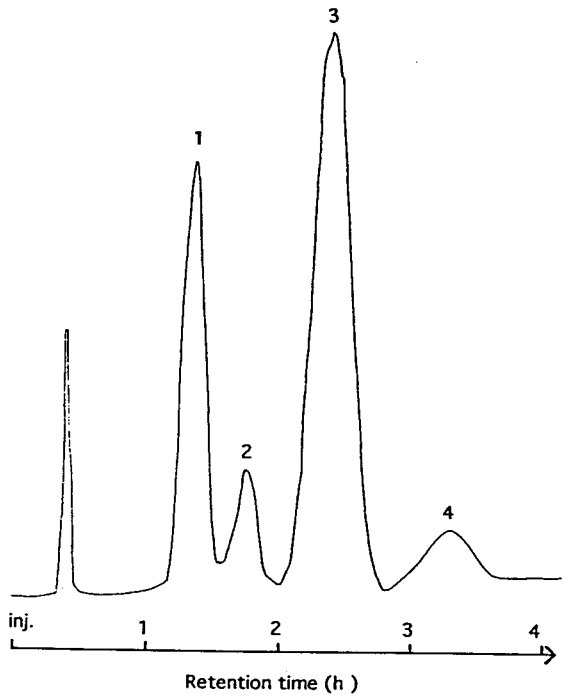

Fig. 3. RP-CCC of four essential fatty acids from *Skeletonema costatum*. 1 = C16:3; 2 = C18:4; 3 = C20:5; 4 = C22:6. $R_{s(EPA-DHA)} > 1$.

3.4. Semi-preparative scale

The high stationary volume increases the injection capacities in comparison with HPLC and decreases the saturation broading effects. The limiting factor is mainly due to the decrease in the stationary phase from variations of physical parameters such as viscosity and density difference when injection is being made. The crude sample is then eluted without separation occurring, but it can be totally recovered, e.g., through evaporation of solvents by a rotary evaporator under reduced pressure. Gram-level separations were achieved with a bench-top apparatus; we injected 2.4 g of total fatty acids into the 143-ml column and recovered 1 g of essential fatty acids (C16:3 43%, C18:4 7.5%, C20:5 45%, C22:6 4.5%).

Instruments with a larger column volume are available: an injection of 130 g of fatty acid esters was made with a 6.8-l apparatus. The liquid stationary phase makes the filling of the column faster and prevents irreversible adsorption phenomena with the support.

These results are encouraging for the separation of essential fatty acids on an industrial scale. Long-chain unsaturated fatty acids, which

Table 1
Partition coefficients of four essential fatty acids in the biphasic system heptane–methanol–water (500:415:85, v/v/v) used in counter-current chromatography

Fatty acid[a]	K	Selectivity factor
C16:3	1.1	
C18:4	1.5	$\alpha_{12} = 1.3$
C20:5	2.1	$\alpha_{23} = 1.4$
C22:6	2.9	$\alpha_{34} = 1.4$

[a] C20:5 = EPA and C22:6 = DHA.

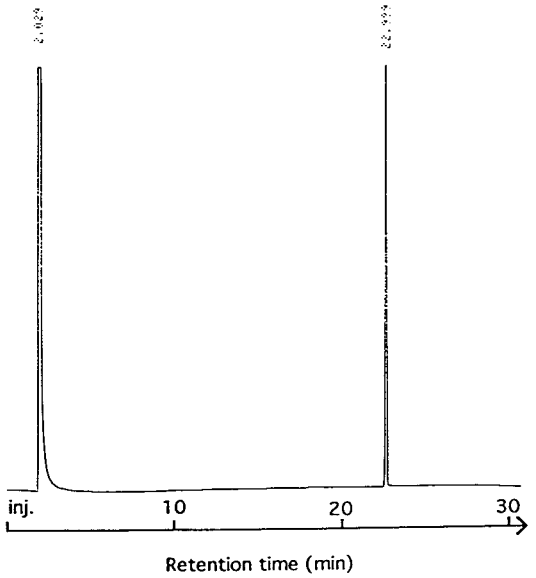

Fig. 4. GC of EPA methyl esters from microalgae purified by CCC. GC column, CP-Sil-5CD, 30 m × 0.25 mm I.D.; column temperature, increased from 140 to 230°C at 3°C/min; carrier gas, helium; flame ionization detection.

are generally susceptible to oxidation on a catalytic surface, are readily purified by CCC.

3.5. Peak identification

During elution when studying the chromatographic conditions for separation, the CCC fractions were systematically analysed, after esterification, by GC. The peaks of the fatty acid methyl esters were identified by comparison of retention times and mass spectra. Peak identification for the C20:5ω3 and C22:6ω3 esters was confirmed by comparison with the data for commercial standards. Fig. 4 shows the EPA and DHA purity, monitored by GC, after esterification to methyl esters.

4. Conclusions

CCC has been widely applied to the separation of various organic and inorganic materials, as an alternative and a complement to HPLC. CCC becomes especially attractive with increase in the column capacity and for the purification of labile compounds. Therefore, these results indicate that a separation process with a CCC instrument in order to obtain different compounds from microalgae is practicable and that this process will compete favourably with classical processes such as liquid and supercritical fluid extraction. Further experiments will be performed in order to increase the separations of different biological compounds from microalgae which are widely exploited and studied particularly for active molecule screening.

Acknowledgements

We are grateful to Mr. C. Goyer, Station Marine de l'Île Grande (Pleumeur-Bodou, France) for the gift of algae, to Dr. W. Klagba, Vegatec Society (Villejuif, France) for the loan of the countercurrent chromatographic device and to Mrs. J. Mauroy for the GC–MS analyses.

References

[1] J. Dyerderg, H.O. Bary, E. Stofferson, S. Moncada and J.R. Vane, *Lancet*, ii (1985) 117.
[2] W. Yongmanitchai and O.P. Ward, *Process Biochem.*, 24 (1989) 117.
[3] R.T. Holman, in W.H. Kunars and R.T. Holman (Editors), *Polyunsaturated Fatty Acids*, American Oil Chemist's Society, 1977, p. 163.
[4] N. Haagsma, C.M. van Gent, J.B. Luten, R.W. de Jong and E. van Doorn, *J. Am. Oil Chem. Soc.*, 59 (1982) 117.
[5] R.G. Ackman, W.M.N. Ratnayake and B. Olsson, *J. Am. Oil Chem. Soc.*, 65 (1988) 136.
[6] H.J. Dutton, in R.T. Holman, W.O. Lundberg and T. Malkin (Editors), *Progress in the Chemistry of Fats and Other Lipids*, Pergamon Press, Oxford, 1954, Ch. 7, p. 292.
[7] C.F. Allen, P. Good, H.F. Davis, P. Chisum and S.D. Fowler, *J. Am. Oil Chem. Soc.*, 43 (1966) 223.
[8] A.P. Foucault, *Anal. Chem.*, 63 (1991) 569A.
[9] W. Murayama, Y. Kosuge, N. Nakaya, Y. Nunogaki, K. Nunogaki, J. Cazes and H. Nunogaki, *J. Liq. Chromatogr.*, 11 (1988) 283.
[10] J.G. Alvarez, J. Cazes, J.C. Touchstone and R.L. Grob, *J. Liq. Chromatogr.*, 13 (1990) 3603.
[11] P.A. Dudley and R.E. Anderson, *Lipids*, 10 (1975) 113.

[12] J.M. Beebe, P.R. Brown and J.G. Turcotte, *J. Chromatogr.*, 468 (1989) 225.
[13] C.B. Ching, K. Hidajat and N.S. Rao, *J. Liq. Chromatogr.*, 16 (1993) 527.
[14] W.B. Nilsson, E.J. Gauglitz Jr, J.K. Hudson, V.F. Stout and J. Spinelli, *J. Am. Oil Chem. Soc.*, 65 (1988) 109.
[15] A. Nomura, J. Yamada, K. Tsunoda, K. Sakaki and T. Yokoshi, *Anal. Chem.*, 61 (1989) 2076.
[16] E.J. Corey and S.W. Wright, *Tetrahedron Lett.*, 25 (1984) 2729.
[17] P. Langholz, P. Andersen, T. Forskov and W. Schmidtsdorff, *J. Am. Oil Chem. Soc.*, 66 (1989) 1120.
[18] J. Folch, M. Lees and G.H.S. Stanley, *J. Biol. Chem.*, 226 (1957) 497.
[19] E.G. Bligh and W.J. Dyer, *Can. J. Physiol.*, 37 (1959) 911.
[20] W.M.N. Ratnayake, B. Olsson, D. Matthews and R.G. Ackman, *Fat. Sci. Technol.*, 90 (1988) 381.
[21] O. Bousquet, A.P. Foucault and F. Le Goffic, *J. Liq. Chromatogr.*, 14 (1991) 3343.
[22] T. Araki, T. Ariga and T. Murata, *Biomed. Mass Spectrom.*, 3 (1976) 261.
[23] I. Horman and H. Traitler, *Biomed. Environ. Mass Spectrom.*, 18 (1989) 1016.
[24] O. Bousquet, N. Sellier and F. Le Goffic, *Chromatographia*, 39 (1994) 40.
[25] G. Lepage and C.C. Roy, *J. Lipid Res.*, 25 (1984) 1391.
[26] T.K. Miwa, K.L. Mikolajezak, F.R. Earle and I.A. Wolff, *Anal. Chem.*, 32 (1960) 1739.
[27] Y. Ito, in N.B. Mandava and Y. Ito (Editors), *Countercurrent Chromatography, Apparatus and Practice*, Marcel Decker, New York, 1988, Ch. 4, p. 443.
[28] O. Bousquet and F. Le Goffic, in preparation.

ELSEVIER

Journal of Chromatography A, 704 (1995) 217–223

JOURNAL OF CHROMATOGRAPHY A

Short communication

Direct high-performance liquid chromatography resolution on chiral columns of tiaprofenic acid and related compounds in bulk powder and pharmaceutical formulations

R. Ferretti[a], B. Gallinella[a], F. La Torre[a,*], C. Villani[b]

[a]*Istituto Superiore di Sanità, Laboratorio di Chimica del Farmaco, Viale Regina Elena 299, 00161 Rome, Italy*
[b]*Dipartimento di Studi di Chimica e Tecnologia delle Sostanze Biologicamente Attive, Università "La Sapienza", Piazzale A. Moro 5, 00185 Rome, Italy*

First received 1 November 1994; revised manuscript received 29 December 1994; accepted 5 January 1995

Abstract

High-performance liquid chromatography (HPLC) was employed for the separation and determination of impurities [5-benzoyl-2-acetylthiophene (BAT), 5-benzoyl-2-ethylthiophene (BET) and (*RS*)-5-benzoyl-α-methyl-3-thiopheneacetic acid (3-isomer of tiaprofenic acid) contained in bulk racemic tiaprofenic acid and pharmaceutical formulations. Chiral columns containing the 3,5-dimethylphenylcarbamate of cellulose and amylose were used. The effect of the organic modifier, 2-propanol, in the mobile phase was studied. The HPLC method gave good performances from qualitative and a quantitative standpoints, allowing the enantiomeric ratios of tiaprofenic acid and its 3-isomer to be determined together with the related impurities BAT and BET.

1. Introduction

Stereochemistry is a major determinant of both pharmacodynamic and pharmacokinetic properties of non-steroidal anti-inflammatory drug derivatives of arylpropionic acids [1,2]. In fact the (*S*)-enantiomers of this class have a consistently higher pharmacological activity than the (*R*)-enantiomers; further, the (*R*)-(−)-enantiomers of ibuprofen and naproxen were found to be converted in vivo into the corresponding (*S*)-(+)-enantiomers [3–6]. However, only naproxen and flunaxaprofen are administered as the pure (*S*)-(+)-enantiomer.

Two methods are currently used to achieve the chiral chromatographic separation of racemic mixtures: (i) formation of diastereoisomeric derivatives before HPLC separation or addition of a chiral selector to the mobile phase and (ii) use of chemically bonded chiral stationary phases (CSPs). The second approach seems to be more promising, as the drawbacks arising from optically impure reagents or different rates of formation of the diastereoisomers are avoided.

Racemic mixtures of amides or anilides of arylpropionic acids have been resolved by means of HPLC on a CSP composed of (*R*)-N-(3,5-dinitrobenzoyl)phenylglycine or a variant of this chiral selector covalently bonded to silica [7–10]. In another study, a series of 1-naphthalenemethylamides derivatives of anti-inflammatory agents was separated either on microbore or

* Corresponding author.

0021-9673/95/$09.50
SSDI 0021-9673(94)00027-5

normal columns using as chiral selector the N,N′-3,5-dinitrobenzoyl derivative of (*R*,*R*)-diaminocyclohexane bonded to a siliceous matrix [11,12].

Underivatized anti-inflammatory agents have been separated on a chiral α_1-acid glycoprotein column [13]; the influence of N,N′-dimethyloctylamine added to the mobile phase was studied. With the same CSP, ketoprofen, ibuprofen and fenoprofen were determined in plasma [14] and the effects of the mobile phase composition, pH and temperature on the chiral resolution were studied.

Furthermore, racemic tiaprofenic acid was resolved using immobilized human serum albumin as the CSP [15]. Recently, the enantiomers of ibuprofen, ketoprofen and naproxen were separated using α-chymotrypsin absorbed or covalently bonded on silica as the CSP [16].

Pirkle and co-workers [17,18] utilized the principle of reciprocity for preparing a new promising CSP able to separate underivatized non-steroidal anti-inflammatory drug enantiomers.

Currently, tiaprofenic acid is dispensed and administered as a racemic mixture for the treatment of acute and chronic arthritis and osteoarthritis. In view of the increasing legislative concern regarding the development and use of chiral drugs, enantioselective analytical methods are required to study the pharmacokinetics and pharmacodynamics of each of the enantiomers.

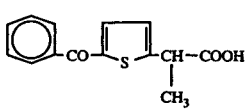

Tiaprofenic acid (1)

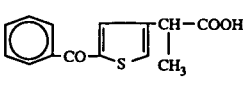

3-isomer of tiaprofenic acid (2)

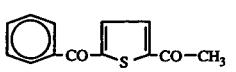

BAT (3)

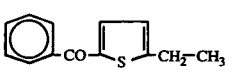

BET (4)

Fig. 1. Structures of tiaprofenic acid and its impurities.

In this paper, we describe a simple, isocratic method for the simultaneous separation, identification and measurement of enantiomers of *rac*-tiaprofenic acid and its *rac*-3-isomer, together with the achiral impurities 5-benzoyl-2-acetylthiophene (BAT) and 5-benzoyl-2-ethylthiophene (BET) (Fig. 1) in bulk powder and pharmaceutical formulations. Chiral columns containing cellulose and amylose derivatives adsorbed on the silica surface were used.

2. Experimental

2.1. Materials

Stainless-steel Chiralcel OD and Chiralpak AD columns (250 × 4.6 mm I.D.) (Daicel Chemical Industries, Tokyo, Japan) were used. HPLC-grade solvents were purchased from Carlo Erba (Milan, Italy). Trifluoroacetic acid (TFA) of Uvasol grade was obtained from Merck (Darmstadt, Germany). *rac*-Tiaprofenic acid was kindly supplied by Roussel-Pharma (Milan, Italy). The impurities (BAT, BET and the *rac*-3-isomer of tiaprofenic acid) were obtained from Roussel-Uclaf (Paris, France).

2.2. Apparatus

Chromatography was performed using a Waters (Milford, MA, USA) M 510 HPLC pump, a Rheodyne (Cotati, CA, USA) Model 7125 injector with a 20-μl sample loop, and a Model 991 programmable multi-wavelength diode-array detector (Waters).

2.3. Operating conditions

The following chromatographic conditions were used: with Chiralcel OD mobile phase, *n*-hexane–2-propanol–TFA (98.5:1.5:0.1) degassed in an ultrasonic bath before use; flow-rate, 1 ml/min; with Chiralpak AD, mobile phase, *n*-hexane–2-propanol–TFA (94.0:6.0:0.1)

degassed in an ultrasonic bath before use; flow-rate, 0.5 ml/min; column temperature, 20°C volume injected, 20 μl; and detection wavelength 296 nm. The columns were carefully washed every day with 60 ml of *n*-hexane. In this way, no decrease in efficiency was observed throughout the work.

2.4. Linearity of detector response

Calibration graphs were obtained by injecting the impurities BET, BAT and 3-isomer in the concentration range 0.2–4.0 μg/ml and tiaprofenic acid in the range of 50.0–2000.0 μg/ml.

2.5. Samples preparation

Tablets

In a mortar, ten tablets (previously weighed) were pulverized and, taking into account the average mass of the same, an amount of powder corresponding to 300 mg of tiaprofenic acid was weighed exactly. The powder was suspended in methanol (3 × 20 ml) and stirred for 30 min. The methanol was then filtered through a filter-paper and dried with a gentle stream of nitrogen and the residue was dissolved in 20 ml of *n*-hexane–2-propanol (9:1). A 1-ml volume of this solution was diluted to 5 ml before injection.

Injectable ampoules

The lyophilized content of a single ampoule (200 mg of tiaprofenic acid) was dissolved in 5 ml of deionized water and the solution was acidified to pH 3 with 0.1 *M* HCl. The aqueous solution was then extracted with diethyl ether (4 × 15 ml) in a separating funnel and the organic layer was washed with water (2 × 15 ml). The organic phase was dried over anhydrous Na_2SO_4, then concentrated to dryness with a gentle stream of nitrogen. The residue was dissolved in 20 ml of *n*-hexane–2-propanol (9:1). A 1-ml volume of this solution was diluted to 5 ml before injection.

Following the extraction procedures described above, we obtained recoveries of 91% for tablets and 98% for ampoules.

3. Results and discussion

Currently HPLC methods are employed for the determination of tiaprofenic acid and its impurities in bulk products and pharmaceutical formulations. These methods, however, do not permit the evaluation of the enantiomeric ratio of the compounds containing a stereogenic centre (tiaprofenic acid and its 3-isomer) together with the achiral impurities BAT and BET. The aim of this work was the determination of the enantiomeric ratio of tiaprofenic acid and its 3-isomer and, at the same time, the determination of the related compounds BAT and BET in bulk products and pharmaceutical formulations.

Cellulose- and amylose-based CSPs (Chiralcel OD and Chiralpak AD) have been successfully employed to separate directly the enantiomers of ibuprofen [19], ketoprofen and tiaprofenic acid [20]; nevertheless, the enantiomeric resolution of the *rac*-3-isomer of tiaprofenic acid, as far as we know, has never been attempted. We adapted the method described by Okamoto et al. [20] to obtain the separation of the enantiomers of tiaprofenic acid and its 3-isomer from the remaining impurities BAT and BET.

Both racemic mixtures of tiaprofenic acid and its 3-isomer were efficiently resolved on Chiralcel OD and Chiralpak AD columns (Figs. 2 and 3); however, the order of elution of the enantiomers of tiaprofenic acid and the 3-isomer were not determined owing to the lack of a single enantiomer.

The enantioselectivity factors (α), obtained with the Chiralcel OD column, showed a dependence on eluent composition; higher values of α were observed with the decreasing 2-propanol content in the mobile phase (Table 1). Small amounts of 2-propanol (less than 1.5%) in the mobile phase resulted in too long elution times of tiaprofenic acid and its isomer, whereas poor enantioseparation of the 3-isomer of tiaprofenic

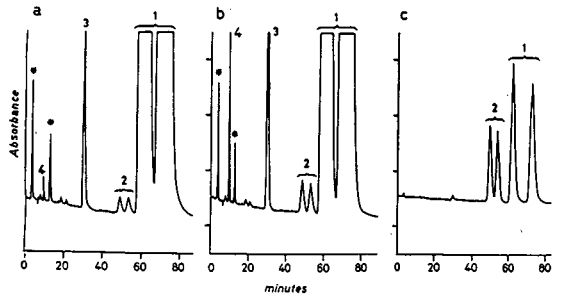

Fig. 2. HPLC of the compounds in Fig. 1. Eluent, *n*-hexane–2-propanol–TFA (95.0:5.0:0.1); column, Chiralcel OD; detection wavelength, 296 nm. (A) Overloaded tiaprofenic acid (10 μg); (B) overloaded tiaprofenic acid (10 μg) spiked with BAT (42 ng), BET (42 ng) and 3-isomer (42 ng); (C) resolution of the enantiomers of tiaprofenic acid and 3-isomer. Asterisks indicate unknown impurities.

acid was obtained with 2-propanol content in the mobile phase higher than 5%.

The amylose-based column was more effective and the separation (α) and resolution factors (R) were better than those obtained with the cellulose-based column (Tables 1 and 2); in addition, the shorter retention times and slower flow-rates obtained with the Chiralpak AD column gave savings in time and solvents. Surprisingly, good values of the resolution of the enantiomers of tiaprofenic acid and its 3-isomer were obtained with the Chiralpak AD column all the whole range of 2-propanol concentrations used

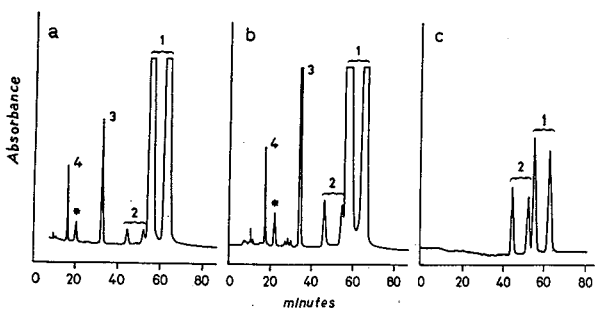

Fig. 3. HPLC of the compounds in Fig. 1. Eluent, *n*-hexane–2-propanol–TFA (94.0:6.0:0.1); column, Chiralpak AD; detection wavelength, 296 nm. (A) Overloaded tiaprofenic acid (10 μg); (B) overloaded tiaprofenic acid (10 μg) spiked with BAT (42 ng), BET (42 ng) and 3-isomer (42 ng); (C) resolution of the enantiomers of tiaprofenic acid and 3-isomer. Asterisks indicate unknown impurities.

Table 1
Chromatographic data for tiaprofenic acid and the 3-isomer on a Chiralcel OD column

Compound	k_1'[a]	α[b]	R_s[c]	Eluent[d]
Tiaprofenic acid	1.97	1.12	1.38	A
	4.17	1.13	1.72	B
	7.52	1.13	1.91	C
	19.93	1.18	2.60	D
3-Isomer	1.77	1.00	No resolution	A
	3.53	1.05	0.62	B
	7.88	1.06	1.00	C
	15.62	1.09	1.51	D

[a] Retention factor of the first-eluted enantiomer.
[b] Enantioselectivity factor.
[c] Resolution factor.
[d] Eluents: (A) *n*-hexane–2-propanol–TFA (90.0:10.0:0.1); (B) *n*-hexane–2-propanol–TFA (95.0:5.0:0.1); (C) *n*-hexane–2-propanol–TFA (97.0:3.0:0.1); (D) *n*-hexane–2-propanol-TFA (98.5:1.5:0.1).

in the mobile phase (Table 2). Nevertheless, the 2-propanol content in the mobile phase was optimized to improve the regioselectivity between the more retained enantiomer of the 3-

Table 2
Chromatographic data for tiaprofenic acid and the 3-isomer on a Chiralpak AD column

Compound	k_1'[a]	α[b]	R_s[c]	α[d]	Eluent[e]
Tiaprofenic acid	2.47	1.21	3.02	1.02	A
	3.59	1.19	2.62	1.05	B
	5.13	1.17	3.17	1.05	C
	6.99	1.16	3.07	1.13	D
	8.05	1.16	3.23	1.06	E
3-Isomer	1.89	1.28	3.90		A
	2.76	1.24	3.69		B
	3.99	1.22	3.70		C
	5.30	1.16	4.17		D
	6.23	1.21	3.93		E

[a] Retention factor of the first-eluted enantiomer.
[b] Enantioselectivity factor.
[c] Resolution factor.
[d] Regioselectivity factor calculated as k_1' (tiaprofenic acid)/k_2' (3-isomer).
[e] Eluents: (A) *n*-hexane–2-propanol–TFA (85.0:15.0:0.1); (B) *n*-hexane–2-propanol–TFA (90.0:10.0:0.1); (C) *n*-hexane–2-propanol–TFA (92.5:7,5:0.1); (D) *n*-hexane–2-propanol-TFA (94,0:6.0:0.1); (E) *n*-hexane–2-propanol–TFA (95.0:5.0:0.1).

isomer and the less retained isomer of tiaprofenic acid (Table 2); this was of great importance in obtaining the separation of the 3-isomer impurity from tiaprofenic acid, mainly in pharmaceutical formulations (Fig. 4).

From this point of view, the Chiralcel OD column showed a higher regioselectivity than the amylose-based column (Tables 1 and 2); in fact, no resolution was obtained between the less retained enantiomer of tiaprofenic acid and the more retained 3-isomer when the Chiralpak AD column was overloaded to detect the 3-isomer impurity in commercial samples (Fig. 3). For this reason, we deemed the Chiralcel OD column more appropriate than the Chiralpak AD for the present problem.

Addition of a small amount of TFA to the mobile phase had a beneficial effect on the separation and the resolution, as it minimizes the ionization of the carboxylic groups of the analytes (tiaprofenic acid and its 3-isomer) and reduces their interaction with the polar sites of the CSPs.

The detection limits obtained with this chromatographic system, using the Chiralcel OD column, were ca. of 5 ng for the 3-isomer of tiaprofenic acid and 1 ng for BAT and BET, calculated on a response of twice the noise level,

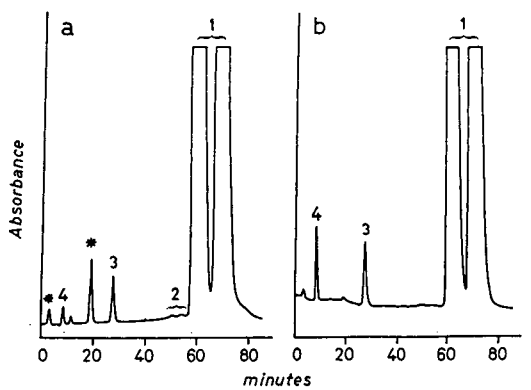

Fig. 4. HPLC of pharmaceutical formulations: (a) tablets and (b) injectable ampoules. Sample injected 10 μg of tiaprofenic acid; eluent *n*-hexane–2-propanol–TFA (95.0:5.0:0.1); column, Chiralcel OD; detection wavelength, 296 nm. Asterisks indicate unknown impurities. The recoveries are 91% for tablets and 98% for ampoules.

and they appeared adequate for application to industrial products.

The calibration graphs (seven points for the impurities and tiaprofenic acid) showed good linearity with a correlation coefficient of 0.9986 for BAT ($c = 0.010A + 0.850$), 0.9992 for the BET ($c = 0.012A + 0.661$), 0.9987 for the 3-isomer of tiaprofenic acid ($c = 0.017A - 0.940$) and 0.9990 for the tiaprofenic acid ($c = 1.651 \cdot 10^{-5}A + 0.192$) ($c$ = sample concentration in μg/ml, A = area counts). Table 3 shows the accuracy and precision data at each individual standard concentration.

The use of a linear photodiode-array detector turned out to be useful in confirming that the chiral separation of a pure racemic compound had, in fact, taken place. As enantiomers behave identically in symmetrical environments, they will absorb non-polarized light in exactly the same way, giving identical spectra (Fig. 5).

4. Conclusions

The HPLC method described for the determination of impurities BAT, BET and the 3-isomer of tiaprofenic acid in bulk product and pharmaceutical formulations appears to be easy to use, reproducible and sensitive. The main advantage is that a single chromatographic run allows the simultaneous determination of the impurities in tiaprofenic acid together with the enantiomeric ratio of tiaprofenic acid and its 3-isomer.

The Chiralcel OD column was preferred to the Chiralpak AD because of the higher regioselectivity shown towards *rac*-tiaprofenic acid and its 3-isomer.

No derivatization of the compounds containing a stereogenic centre (tiaprofenic acid and the 3-isomer) is required for the separation, and therefore the drawbacks due to racemization or different rates of reaction of the single enantiomer or side-reactions of the impurities, which do not contain a stereogenic centre (BAT and BET), with the derivatizing agent are avoided.

In conclusion, with the increasing interest in enantiomerically pure drug formulations in both the pharmaceutical industry [21] and regulatory

Table 3
Inter-day precision and accuracy for BET, BAT, 3-isomer and tiaprofenic acid standards

Compound	Parameter[a]	Amount of samples injected (ng per 20 μl)						
		84	63	42	31.5	21	10.5	5.25
BET	*M*	83.5	62.9	41.3	30.9	21.4	9.8	6.1
	R.S.D. (%)	1.2	0.9	3.5	5.6	2.0	11.7	0.2
	R.E. (%)	−0.6	−0.2	−1.7	−1.9	+1.9	−6.7	+16.0
BAT	*M*	83.7	63.6	42.2	30.9	21.8	10.0	6.3
	R.S.D. (%)	0.6	1.1	1.8	7.0	4.7	11.8	4.9
	R.E. (%)	−0.3	+0.9	+0.5	−1.9	+3.8	−4.7	+20.0
3-Isomer	*M*	83.3	63.9	46.9	31.9	22.5	10.2	6.5
	R.S.D. (%)	1.5	1.4	2.4	3.5	11.6	11.5	19.9
	R.E. (%)	−0.8	+1.4	+11.7	+1.3	+7.1	−2.8	+23.8
		Amount of samples injected (μg per 20 μl)						
		40	20	10	8	4	2	1
Tiaprofenic acid	*M*	40.0	19.9	10.5	7.2	3.8	2.2	1.3
	R.S.D. (%)	3.7	4.8	2.4	6.6	10.7	3.9	9.9
	R.E. (%)	+0.07	−0.2	+5.4	−10.2	−6.0	+9.0	+35.0

[a] *M* = mean value; R.S.D. = relative standard deviation; R.E. = relative error; $n = 3$ in each instance.

authorities [22–25], a chromatographic method able to determine simultaneous chiral and achiral impurities is suitable for quality control of pharmaceutical formulations and for investigations of stereoselective pharmacokinetics and biotransformations.

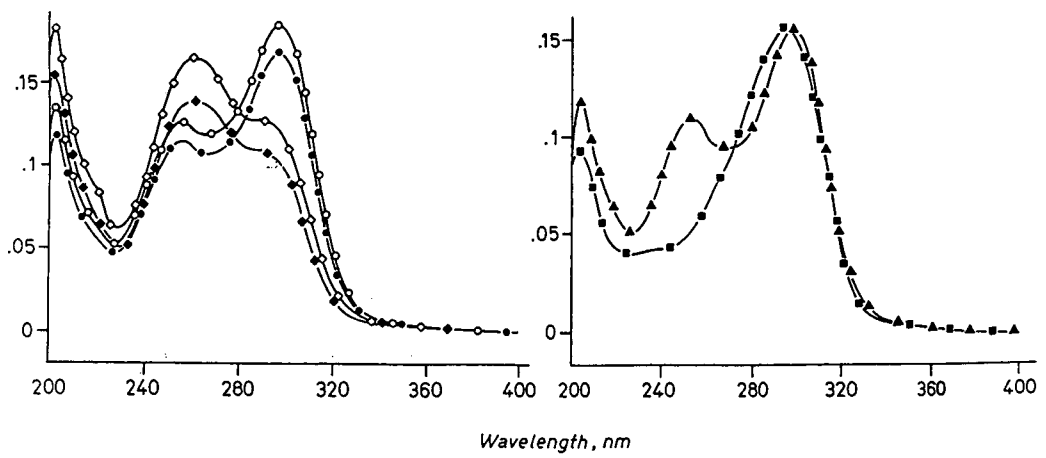

Fig. 5. UV spectra of the compounds in Fig. 1, ○, ● = Tiaprofenic acid; ◇, ◆ = 3-isomer; ▲ = BAT; ■ = BET. Left, open and filled symbols: 1st and 2nd eluted enantiomers, respectively.

References

[1] A. Avgerinos and A.J. Hutt, *Chirality*, 2 (1990) 249.
[2] E.G. Ariens, *Med. Res. Rev.*, 6 (1986) 451.
[3] D.G. Kaiser, G.J. Reischer and W.J. Wechter, *J. Pharm. Sci.*, 65 (1976) 269.
[4] J. Caldwell, A.J. Hutt and S. Fournel-Gigleux, *Biochem. Pharmacol.*, 37 (1988) 105.
[5] F. Jamali, *J. Drug Metab. Pharmacokinet.*, 13 (1988) 1.
[6] J. Goto, N. Goto and T. Nambara, *J. Chromatogr.*, 239 (1982) 559.
[7] I.G. Wainer and T.D. Doyle, *J. Chromatogr.*, 284 (1984) 117.
[8] W.H. Pirkle and J.E. McCune, *J. Chromatogr.*, 471 (1989) 271.
[9] D.M. McDaniel and G. Sneider, *J. Chromatogr.*, 404 (1987) 123.
[10] W.H. Pirkle and J. Welch, *J. Liq. Chromatogr.*, 14 (1991) 3387.
[11] F. Gasparrini, D. Misiti, F. La Torre, M. Sinibaldi and C. Villani, *J. Chromatogr.*, 457 (1988) 235.
[12] F. Gasparrini, D. Misiti, F. La Torre, M. Pierini and C. Villani, *J. Chromatogr.*, 633 (1993) 81.
[13] J. Hermansson and M. Eriksson, *J. Liq. Chromatogr.*, 9 (1986) 621.
[14] Menzel-Soglowek, G. Geisselinger and K. Brune, *J. Chromatogr.*, 532 (1990) 295.
[15] N. Muller, F. Lapicque, E. Drelon, P. Gillet, C. Mont, B. Poletto and P. Netter, *J. Chromatogr.*, 616 (1993) 261.
[16] I. Marle, A. Karlsson and C. Pettersson, *J. Chromatogr.*, 604 (1992) 185.
[17] W.H. Pirkle, C.J. Welch and B. Lamm, *J. Org. Chem.*, 57 (1992) 3854.
[18] W.H. Pirkle and C.J. Welch, *J. Liq. Chromatogr.*, 15 (1992) 194.
[19] M. Ueji and C. Tomizawa, *J. Pestic. Sci.*, 11 (1986) 447.
[20] Y. Okamoto, R. Aburatani, Y. Kaida, K. Hatada, N. Inotsume and M. Nakano, *Chirality*, 1 (1989) 239.
[21] M.N. Cayen, *Chirality*, 3 (1991) 94.
[22] H. Shindo and J. Caldwell, *Chirality*, 3 (1991) 191.
[23] A.J. Hutt, *Chirality*, 3 (1991) 161.
[24] W.H. De Camp, *J. Pharm. Biomed. Anal.*, 11 (1993) 1167.
[25] A.G. Rauws and K. Groen, *Chirality*, 6 (1994) 72.

ELSEVIER

Journal of Chromatography A, 704 (1995) 224–227

JOURNAL OF CHROMATOGRAPHY A

Short communication

Rapid detection of high-molecular-mass dienes in beeswax

Angelo G. Giumanini[a,*], Giancarlo Verardo[a], Paolo Strazzolini[a], Howard R. Hepburn[b]

[a]*Department of Chemical Sciences and Technologies University of Udine, I-33100 Udine, Italy*
[b]*Department of Zoology and Entomology, Rhodes University, 6140 Grahamstown, South Africa*

First received 12 October 1994; revised manuscript received 27 January 1995; accepted 31 January 1995

Abstract

A rapid procedure for the detection of high-molecular-mass dienes in waxes, using a combination of chromatographic separations and direct inlet mass spectrometric determinations, allowed the determination of the presence of and the approximate relative concentrations on C_{31}–C_{35} dienes in some beeswaxes.

1. Introduction

Beeswax is a complex mixture of organic compounds belonging to a number of chemical classes. Aliphatic saturated and monounsaturated compounds have been described in several papers [1]. A mixture of alkanes and alkenes can be easily separated from more polar components by means of column absorption chromatography, using silica gel as the stationary phase and hexane as the eluent. Subsequent separation of the alkenes can be carried out by reversible complex-forming column chromatography on silica gel impregnated with silver nitrate. Whereas GC–MS analysis, using high-resolution capillary columns and electron impact ionization, allows the separation of several alkenes present in the mixture and the determination of their molecular masses, evidence for the presence of dienes could not be obtained. Higher molecular mass conjugated dienes and dienes with isolated double bonds may be expected to exhibit longer retention times because of their lower volatility. Therefore, it was necessary to develop a rapid procedural variation for the resolution of dienes in beeswax.

2. Experimental

The total hydrocarbon (TH) fraction from beeswax was obtained as described in a previous paper [2]. An alkene fraction was obtained by rechromatographing the TH fraction on a silica gel thick layer (Merck, PSC-Fertigplatten Kieselgel 60 F_{254}, layer thickness 2 mm) impregnated with silver nitrate using hexane as the eluent [3]. The spot containing the unsaturated hydrocarbons was detected with iodine, scraped off and extracted with hot hexane. The extract was deposited on the solid introduction system of a mass spectrometer, from which it was slowly fully evaporated into the ion source. Mass spectral data were continuously recorded and stored in a computer, from which it was possible to

* Corresponding author.

0021-9673/95/$09.50
SSDI 0021-9673(95)00145-X

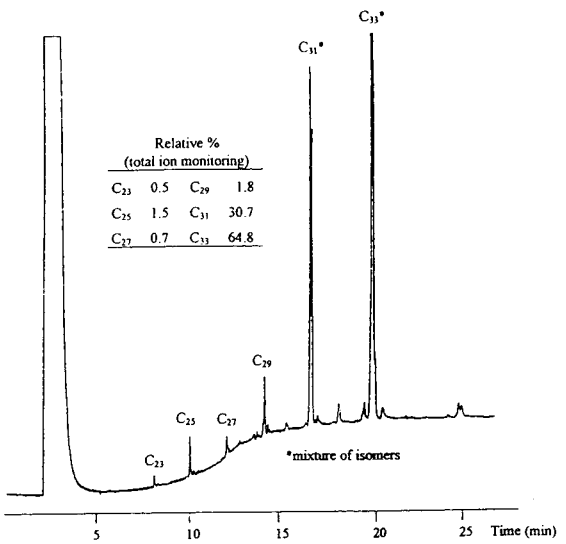

Fig. 1. Typical GC profile (MS detector, positive ions, total ion current, SPB-5 fused-silica capillary column, 30 m × 0.32 mm I.D., 0.25-μm film thickness, temperature programme, 100–300°C at 10°C min^{-1}) of the unsaturated fraction of hydrocarbons from a European beeswax.

obtain single-ion traces of the evaporated components.

GC–MS and MS measurements were obtained using a Finnigan Model 1020 gas-chromatograph–mass spectrometer, with electron impact ionization in the positive-ion mode (70 eV electron energy).

3. Results and discussion

A typical GC profile of the unsaturated hydrocarbon present in beeswax is shown in Fig. 1. Fig. 2 shows the electron impact (EI) mass spectrum at 70 eV of the peak corresponding to $C_{31}H_{62}$ alkene ($M^+ = 434$ u).

The whole unsaturated mixture was slowly vaporized into the electron impact ion source of the mass spectrometer at 120°C. Under these conditions there was a definite fractionation into two otherwise unresolved mixtures, one made up of the alkenes and a quantitatively much smaller one containing dienes of molecular mass corre-

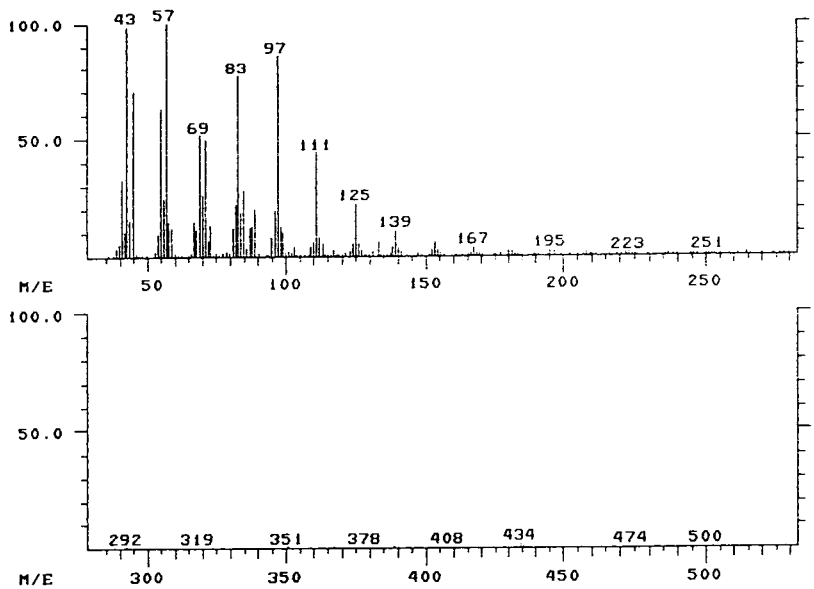

Fig. 2. Typical mass spectrum of an eluate ($C_{31}H_{62}$) from the capillary GC separation of the components of the alkene fraction of beeswax hydrocarbons.

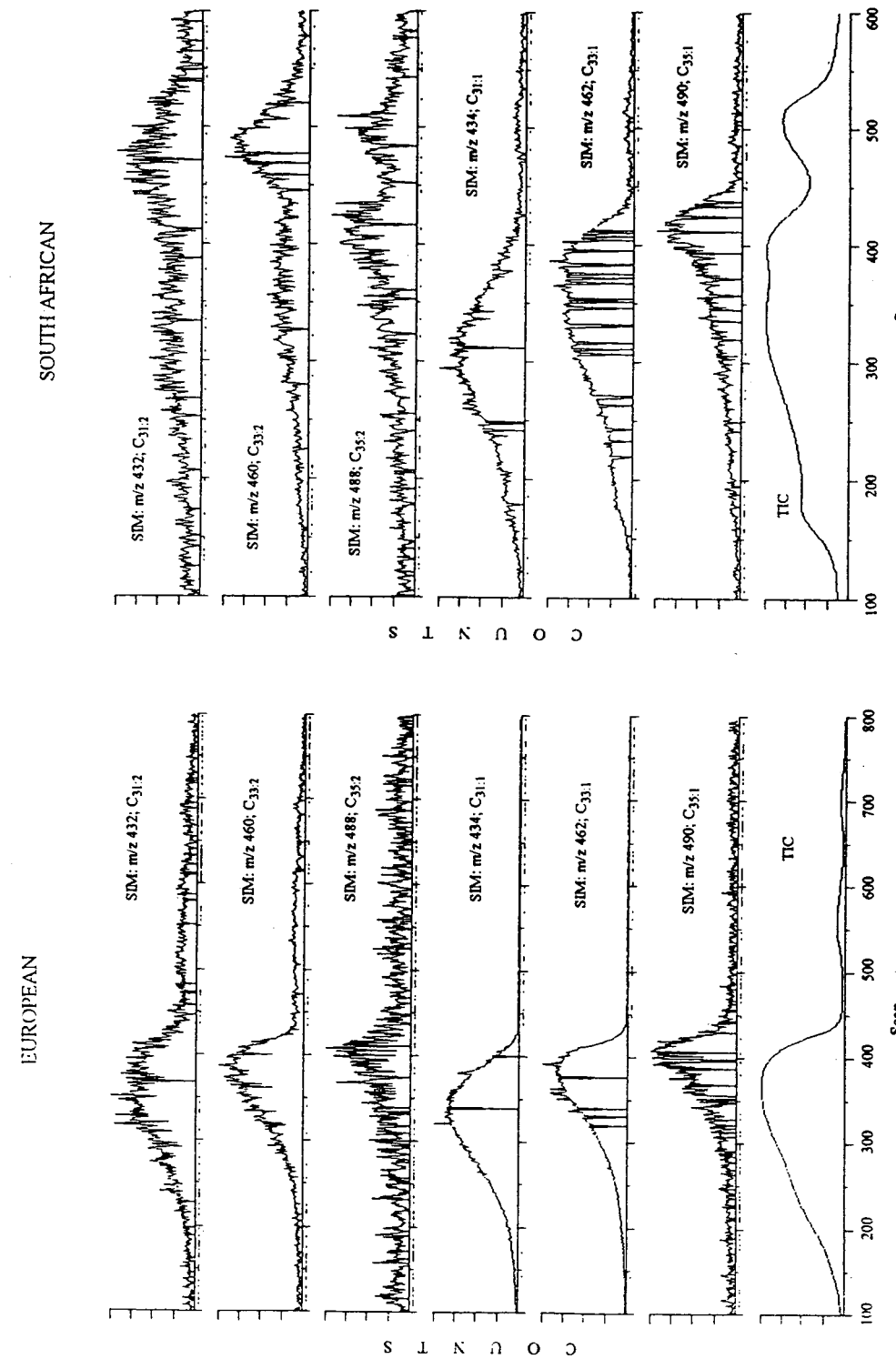

Fig. 3. SIM and total ion current (TIC) of the bulk evaporated unsaturated hydrocarbons in a European and a South African beeswax.

Table 1
Relative abundance of dienes in European and South African beeswax

Carbon No.	European		South African	
	Rel. %	Dienes (%)[a]	Rel. %	Dienes (%)[a]
C_{31}	25	1.4	19	2.9
C_{33}	65	3.5	60	9.2
C_{35}	10	0.7	21	3.2

[a] In unsaturated hydrocarbon fraction.

sponding to the GC-detectable alkenes. Single-ion monitoring (SIM) of the molecular ions for individual alkenes and dienes (Fig. 3) plotted against time confirmed the concentration of the dienes in the sublimate at longer times. Integration of the M^+ ions profiles led to an approximate evaluation of a ratio of 100:6 of the relative molar concentration of alkenes to dienes for a European wax. Also, the ratio of the integrated SIM of the individual parent peaks of the alkenes and dienes allowed the evaluation of their relative abundances (Table 1). The ratios thus obtained for the alkenes matched fairly well with the results of the GC using the MS as a total ion monitor (TIC) (Table 2).

Table 2
Relative abundances determined on GC-separated alkenes (EI-MS) and bulk vaporized alkenes (EI-MS, SIM parent ion) from a South African wax

Carbon No.	GC–MS (%)	SIM (%)
C_{23}	2	5
C_{25}	4	9
C_{27}	3	8
C_{29}	3	7
C_{31}	14	16
C_{33}	57	42
C_{35}	17	13

Our procedure, in its present form, does not provide structural information on the dienes. A complete study may be effected by double methyl sulfenation of the double bonds, followed by capillary GC–MS [4]. Dienes with internal bonds were found in propolis [5] and in some other material waxes both of animal and plant origin. At least one bond was internal. The type of partial separation obtained in the vaporization process, presenting the C_{31}–C_{35} alkenes on the far side of the vaporization peak, allows one to infer the structure of unconjugated internal alkenes. The beeswax from the African Cape bee *Apis mellifera capensis* was found to be richer in dienes than that of the European beeswax from *Apis mellifera* var. *ligustica* × *carnica*.

Acknowledgements

This work was supported by the Italian National Research Council (CNR) grants 92.01213.CT06 and 93.02434.CT06 and the Italian Ministry for Universities Research and Technology grants 1991–94, 40–60% to A.G.G. Some of the experimental work was carried out by Miss Barbara Griguol.

References

[1] P.E. Kolattukudy, *Chemistry and Biochemistry of Natural Waxes*, Elsevier, Amsterdam, 1976, Ch. 1.
[2] G. Bonaga, A.G. Giumanini and G. Gliozzi, *J. Agric. Food Chem.*, 34 (1986) 319–326.
[3] J.G. Kirchner, *Techniques of Chemistry, Vol. XIV: Thin-Layer Chromatography*, Wiley, New York, 2nd ed., 1978.
[4] D.A. Carlson, C.S. Roan, R.A. Yost and J. Hector, *Anal. Chem.*, 61 (1989) 1564–1571.
[5] M. Seifert and E. Haslinger, *Liebigs Ann. Chem.*, 11 (1989) 1123–1126.

ELSEVIER

Journal of Chromatography A, 704 (1995) 228–233

JOURNAL OF CHROMATOGRAPHY A

Short communication

Capillary gas–liquid chromatography of 6-hydroxylated bile acids

Ashok K. Batta[a,*], Suresht K. Aggarwal[a], G. Stephen Tint[b], Manju Batta[b], Gerald Salen[a,b]

[a]*Department of Medicine, and Sammy Davis, Jr. Liver Institute, University of Medicine and Dentistry of New Jersey, New Jersey Medical School, Newark, NJ 07103, USA*

[b]*Veterans Administration Medical Center, East Orange, NJ 07019, USA*

First received 29 November 1994; revised manuscript received 8 February 1995; accepted 9 February 1995

Abstract

Gas–liquid chromatographic separation of several bile acids with a hydroxyl group at C-6 is described on two capillary columns, CP-Sil-19 CB and CP-Sil-5 CB. The gas–liquid chromatographic retention indices of bile acids with 6α- and 6β-hydroxyl groups are compared with those of bile acids without the C-6 hydroxyl group and the effect of the C-6 hydroxyl group on the retention indices of bile acids is determined. Both 6α- and 6β-hydroxyl groups increase the retention index of a bile acid. The retention indices of 6α- or 6β-hydroxyl derivatives of chenodeoxycholic acid were found to be higher than those of the corresponding 6-hydroxy derivatives of cholic acid on the CP-Sil-19 CB column but lower on the CP-Sil-5 CB column. Although all 6-hydroxylated derivatives of lithocholic, chenodeoxycholic and cholic acids were not completely resolved on either column alone, combining the two columns resulted in the complete separation of all these compounds.

1. Introduction

Bile acids hydroxylated at C-6 have been isolated from the bile of several animal species, e.g., α-, β- and ω-muricholic acids in rat [1] and hyodeoxycholic acid and hyocholic acid in the pig [2][1]. Substantial amounts of these compounds are excreted in the urine of patients with hepatobiliary diseases (see Ref. [3], and references therein) and it is considered that hydroxylation at C-6 may facilitate hepatic clearance of excessive amounts of toxic endogenous bile acids during these diseases [4]. In order to make a sensible correlation between the presence of these compounds and the disease, it is important to have available analytical methods that can be

* Corresponding author.

[1] The following abbreviations were used: lithocholic acid, 3α-hydroxy-5β-cholanoic acid; chenodeoxycholic acid, 3α,7α-dihydroxy-5β-cholanoic acid; deoxycholic acid, 3α,12α-dihydroxy-5β-cholanoic acid; hyodeoxycholic acid, 3α,6α-dihydroxy-5β-cholanoic acid; cholic acid, 3α,7α,12α-trihydroxy-5β-cholanoic acid; hyocholic acid, 3α,6α,7α-trihydroxy-5β-cholanoic acid; α-muricholic acid, 3α,6β,7α-trihydroxy-5β-cholanoic acid; β-muricholic acid, 3α,6β,7β-trihydroxy-5β-cholanoic acid; ω-muricholic acid, 3α,6α,7β-trihydroxy-5β-cholanoic acid; GLC, gas–liquid chromatography; rrt, relative retention time; RI, retention index (Kovats value); TMS, trimethylsilyl.

0021-9673/95/$09.50
SSDI 0021-9673(95)00183-2

used for the detection of the various 6-hydroxy bile acids from biological fluids. We report herein the gas–liquid chromatographic (GLC) characteristics of the trimethylsilyl (TMS) ethers of several 6α- and 6β-hydroxy bile acid methyl esters and their GLC retention indices are compared with those of the corresponding bile acid derivatives without a hydroxyl group at C-6. Since most of the bile acid derivatives studied are well resolved on the columns employed, we hope that the method will be useful for characterization of 6-hydroxy bile acids in biological fluids.

2. Experimental

Cholic acid, chenodeoxycholic acid, deoxycholic acid, lithocholic acid and 3α,6β-dihydroxy-5β-cholanoic acid were purchased from Steraloids (Wilton, NH, USA). Hyodeoxycholic acid and hyocholic acid were from Canada Packers (Toronto, Canada). Ursodeoxycholic acid (3α,7β-dihydroxy-5β-cholanoic acid) and ursocholic acid (3α,7β,12α-trihydroxy-5β-cholanoic acid) were gifts from Tokyo Tanabe, Japan. The 12β-hydroxy bile acids were prepared via reduction of the corresponding 12-oxo derivatives with potassium/*tert.*-amyl alcohol [5]. The α-, β- and ω-muricholic acids were synthesized from chenodeoxycholic acid and 3α,6α,7α,12α-, 3α,6β,7α,12α-, 3α,6β,7β,12α- and 3α,6α,7β,12α-tetrahydroxy-5β-cholanoic acids were synthesized from cholic acid following literature methods [6–8]. The 3α,6β,7α,12β- and 3α,6β,7β,12β-tetrahydroxy-5β-cholanoic acids were synthesized from 3α,12β-dihydroxy-5β-chol-6-enoic acid following methods previously published [9]. Methyl esters of the bile acids were prepared by addition of 0.5–1 ml of 3% anhydrous methanolic hydrochloric acid (Aldrich Chemical Co., Milwaukee, WI, USA) to 5–20 mg of the respective bile acid and keeping at room temperature for 2 h. Solvent was then evaporated at 55°C under N_2 and the methyl ester was crystallized from either pure methanol or from aqueous methanol. All compounds were >98% pure as judged by gas–liquid chromatography and all synthesized compounds exhibited mass spectral fragmentation patterns compatible with their structures. Sil-Prep (hexamethyldisilazane–trimethylchlorosilane–pyridine, 3:1:9) was used for preparation of trimethylsilyl ether derivatives of the bile acids and was purchased from Alltech Associates (Deerfield, IL, USA).

2.1. Gas–liquid chromatography

A Hewlett-Packard Model 5880A gas chromatograph equipped with a flame ionization detector and an injector with a split/splitless device for capillary columns was used for all separations. The chromatographic column consisted of a chemically bonded fused-silica CP-Sil-19 CB (stationary phase, 85% dimethyl, 7% cyanopropyl, 7% phenyl and 1% vinylsiloxane) or CP-Sil-5 CB (stationary phase, 100% dimethylsiloxane) capillary column (25 m × 0.22 mm I.D.) (Chrompack, Raritan, NJ, USA) and helium was used as the carrier gas. The GLC operating conditions were as follows. Injector and detector temperatures were 260°C and 290°C, respectively. After injection, the oven temperature was kept at 100°C for 2 min, then programmed at a rate of 35°C/min to a final temperature of 265°C when using a CP-Sil-19 CB column and 278°C when using a CP-Sil-5 CB column [10].

2.2. Derivatization

The bile acid methyl esters (5–10 μg) were reacted with 100 μl of Sil-Prep for 20 min at 55°C. Solvents were evaporated at 55°C under N_2 and the trimethylsilyl (TMS) ether derivatives formed were redissolved in 100 μl of hexane. One μl was injected onto the GLC column simultaneously with 5α-cholestane, the internal standard. The retention times of the various bile acids (RRT) were calculated relative to that of 5α-cholestane. Also, the retention index values (Kovats) for the derivatized bile acids were determined by comparison with the retention times of C_{29}–C_{37} *n*-alkanes [11].

3. Results and discussion

Both 6α- and 6β-hydroxylated bile acids are native to several animal species and are excreted in substantial amounts in patients with cholestatic liver disease. It is important to have a reliable GLC method for the detection and quantitation of 6α- and 6β-hydroxylated bile acids in the presence of the endogenous bile acids found in biological fluids and for the metabolic studies of these 6-hydroxylated bile acids. We have examined the GLC behavior of the methyl ester-TMS ethers of several common bile acids with epimeric hydroxyl groups at C-7 and C-12 on a relatively less polar CP-Sil-5 CB capillary column and a more polar CP-Sil-19 CB column and compared the effect of an added 6α- or 6β-trimethylsilyloxyl group. Retention times of all bile acid derivatives were highly reproducible on both columns. For amounts of bile acids ranging from 5 to 100 ng injected onto each column, the detector response, as shown by the integrator, was linear. Furthermore, the peak areas of the various compounds were similar to that obtained for 5α-cholestane when similar amounts were injected onto the column.

Table 1 lists the retention indices of the TMS ethers of various bile acid methyl esters epimeric at C-7 and C-12 on CP-Sil-5 CB and CP-Sil-19 CB columns. As can be seen, derivatives of 12β-hydroxy bile acids have lower retention indices than those of the corresponding 12α-hydroxy epimers on both columns. In contrast, the 7β-hydroxy epimers were eluted significantly later than their 7α-hydroxy counterparts, the more polar CP-Sil-19 CB column showing greater resolutions between the corresponding pairs. A TMS group at C-7 or C-12 significantly increases the retention index of a 3α-trimethylsilyloxy bile acid methyl ester, the effect being most pronounced with the 7β-TMS substituent and only minor with a 12β-TMS substituent. However, when occurring together in the same compound, these groups do not show an additive effect. In fact, on the more polar column, bile acid derivatives with 7α,12α-dihydroxy groups

Table 1
GLC retention indices of methyl ester-trimethylsilyl ethers of bile acids epimeric at C-7 and C-12 on CP-Sil-19 CB and CP-Sil-5 CB capillary columns

5β-Cholanoic acid	Relative retention time		Retention index	
	CP-Sil-19	CP-Sil-5	CP-Sil-19[a]	CP-Sil-5[b]
3α-Hydroxy-	1.59	1.34	3339	3157
3α,7α-Dihydroxy-	1.73	1.49	3397	3244
3α,7β-Dihydroxy-	1.85	1.57	3439	3279
3α,12α-Dihydroxy-	1.67	1.45	3373	3221
3α,12β-Dihydroxy-	1.60	1.39	3345	3191
3α,7α,12α-Trihydroxy-	1.69	1.53	3381	3261
3α,7β,12α-Trihydroxy-	1.85	1.62	3440	3303
3α,7α,12β-Trihydroxy-	1.66	1.49	3370	3240
3α,7β,12β-Trihydroxy-	1.85	1.62	3438	3305

Retention times are expressed relative to that of 5α-cholestane. Retention time of 5α-cholestane was 11.65 min on CP-Sil-19 CB column and 13.20 min on CP-Sil-5 CB column. Retention indices (Kovats values) were determined by previous injection of a hydrocarbon mixture C_{31}–C_{37} under identical GLC conditions.

[a] The retention times of the various *n*-alkanes on CP-Sil-19 CB column were as follows: C_{31}, 13.52 min; C_{32}, 15.26 min; C_{33}, 17.46 min; C_{34}, 20.22 min; C_{35}, 23.71 min; C_{36}, 28.12 min; and C_{37}, 33.67 min.

[b] The retention times of the various *n*-aklanes on CP-Sil-5 CB column were as follows: C_{31}, 16.49 min; C_{32}, 18.61 min; C_{33}, 21.24 min; C_{34}, 24.50 min; C_{35}, 28.54 min; C_{36}, 33.56 min; and C_{37}, 39.79 min.

Table 2
GLC retention indices of methyl ester-trimethylsilyl ethers of 6-hydroxylated bile acids on CP-Sil-19 CB and CP-Sil-5 CB capillary columns

5β-Cholanoic acid	Relative retention time		Retention index	
	CP-Sil-19	CP-Sil-5	CP-Sil-19	CP-Sil-5
3α,6α-Dihydroxy-	1.80	1.52	3422	3256
3α,6β-Dihydroxy-	1.71	1.49	3389	3242
3α,6α,7α-Trihydroxy-	1.94	1.69	3471	3336
3α,6β,7α-Trihydroxy-	1.64	1.50	3359	3246
3α,6α,7β-Trihydroxy-	2.44	2.01	3608	3453
3α,6β,7β-Trihydroxy-	1.99	1.72	3486	3348
3α,6α,7α,12α-Tetrahydroxy-	1.86	1.70	3445	3340
3α,6β,7α,12α-Tetrahydroxy-	1.58	1.52	3338	3254
3α,6α,7β,12α-Tetrahydroxy-	2.29	1.99	3570	3447
3α,6β,7β,12α-Tetrahydroxy-	1.93	1.63	3468	3310
3α,6β,7α,12β-Tetrahydroxy-	1.59	1.49	3342	3243
3α,6β,7β,12β-Tetrahydroxy-	1.93	1.74	3467	3356

Retention times are expressed relative to that of 5α-cholestane. Retention indices (Kovats values) were determined as described above. Retention times of 5α-cholestane and C_{31} to C_{37} hydrocarbons in both columns are shown in Table 1.

are consistently eluted before those of the corresponding bile acids with a 7α-hydroxy group (Tables 1 and 2). This seems to be a general phenomenon since a similar relationship has been observed for bile alcohols with hydroxyl groups at the 7α- and 12α-positions where the TMS ethers of bile alcohols with a 7α,12α-dihydroxy structure were always eluted before the TMS ethers of the corresponding bile alcohols with only a 7α-hydroxyl group on the more polar CP-Sil-19 CB column and later on the less polar CP-Sil-5 CB column [12].

Both 6α- and 6β-TMS groups increase the retention index of a bile acid. However, their effect is greatly influenced by the presence of the vicinal TMS group at C-7 (Tables 2 and 3). Thus, while the axial 6α-TMS group exerts an additive effect on the retention index of the bile acid with either a 7α- or 7β-TMS group, the effect of an equatorial 6β-TMS group is greatly suppressed (e.g., hyocholic acid and ω-muricholic acid vs. α- and β-muricholic acids; Tables 2 and 3). Further, the effect of a TMS group at the 12α-position is generally small and compounds with a 12α-TMS group had shorter retention indices than the corresponding compounds without the 12α-TMS group when chromatographed on the CP-Sil-19 CB column (Table 2) as observed for bile acids or bile alcohols without the hydroxyl group at C-6. However, on the less polar CP-Sil-5 CB column, though the two tetrahydroxy compounds with a 7α,12α-grouping eluted from the column later than α-muricholic acid and hyocholic acid as one would expect, the other two compounds with a 7β,12α-grouping in fact eluted before β- and ω-muricholic acids.

Although the methyl ester-TMS ethers of hyocholic acid and the muricholic acids and their 12α-hydroxy derivatives can be well resolved on both columns, overlap occurs when compounds of the two series are co-chromatographed. A GLC chromatogram of all eight epimers is shown in Fig. 1. As seen from the figure, resolutions between the various pairs are generally better on the CP-Sil-19 CB column and the methyl ester-TMS ethers of hyocholic acid and ω-muricholic acid that do not show baseline resolution from the corresponding 12α-hydroxy compounds on the CP-Sil-5 CB column are completely resolved on the CP-Sil-19 CB column. On the other hand, the methyl ester-TMS ether of hyocholic acid could not be resolved from the corresponding

Table 3
Comparative effects of TMS groups at C-6, C-7 and C-12 on the retention index of methyl ester-TMS ether of lithocholic acid on CP-Sil-5 CB and CP-Sil-19 CB columns

Trimethylsilyloxyl substituent	ΔRI value	
	CP-Sil-19 CB	CP-Sil-5 CB
6α	83	99
6β	50	85
7α	58	87
7β	100	122
12α	36	64
12β	6	34
7α,12α	43	96
7β,12α	102	146
7α,12β	31	83
7β,12β	99	148
6α,7α	132	179
6β,7α	20	89
6α,7β	269	296
6β,7β	147	191
6α,7α,12α	106	185
6β,7α,12α	−1	97
6α,7β,12α	231	290
6β,7β,12α	129	153
6β,7α,12β	3	86
6β,7β,12β	128	199

The ΔRI values for the epimeric hydroxyl groups were calculated by subtracting the retention index for the TMS ether of methyl lithocholate from that of the methyl ester-TMS ether of the given bile acid.

derivative of 3α,6β,7β,12α-tetrahydroxy-5β-cholanoic acid on CP-Sil-19 CB column. However, the two compounds were well resolved on the CP-Sil-5 CB column. Thus, a combination of the two columns is necessary for complete resolution of all eight compounds.

The application of retention indices on polar and non-polar columns has recently been demonstrated by Iida et al. [13] for several bile acid methyl ester-TMS ethers. An important advantage of using our capillary columns is that the retention indices for compounds with chenodeoxycholic acid ring hydroxylations are consistently higher than those for bile acids with cholic acid ring hydroxylations on the more polar CP-Sil-19 CB column and they are consistently lower on the less polar CP-Sil-5 CB column. This was found to be true even when a 6α- or 6β-hydroxyl group was also present with the exception of the 7β-hydroxy compounds, β- and ω-muricholic acids and their 12α-hydroxy derivatives, 3α,6α,7β,12α-tetrahydroxy-5β-cholanoic acid and 3α,6β,7β,12α-tetrahydroxy-5β-cholanoic acid, on the CP-Sil-5 CB column (Table 2). We hope that the GLC method presented here will be useful for characterization of new 6-hydroxylated bile acids and for the routine analysis of serum and urinary bile acids in patients with cholestatic liver diseases, where gas–liquid chromatography–mass spectrometry may be the only means of characterization.

Acknowledgement

This work was supported by U.S. Public Health Service grants HL-17818, DK-18907, and DK-26756.

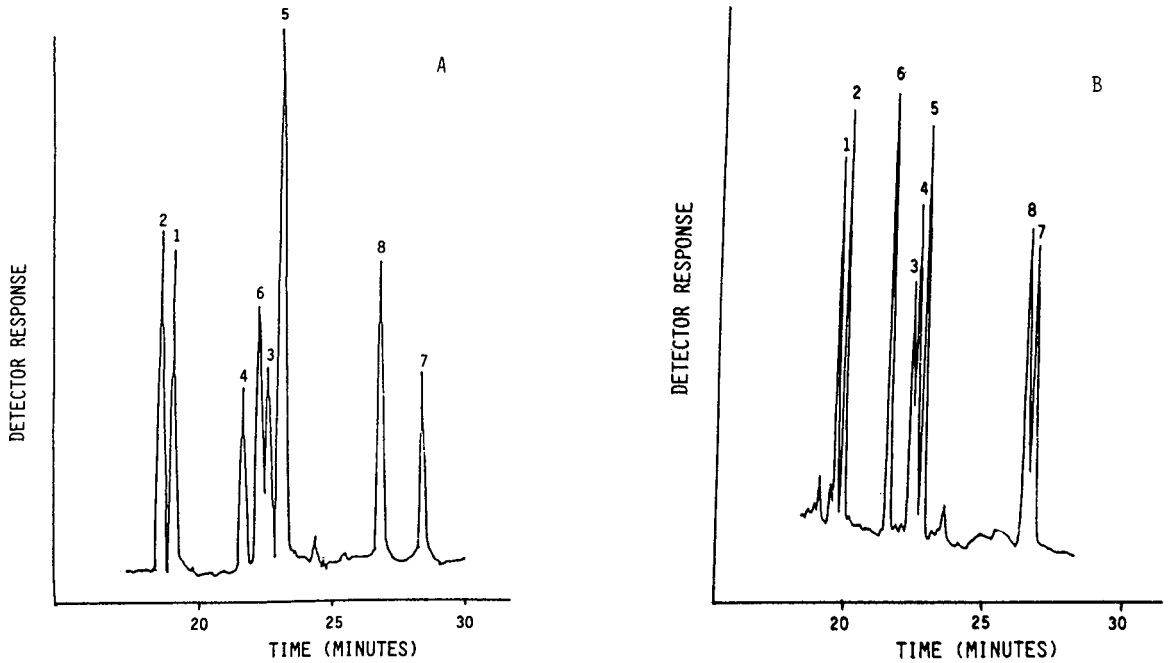

Fig. 1. GLC chromatogram of the methyl ester-TMS ether derivatives of 6-hydroxy bile acids. (A) CP-Sil-19 CB column; (B) CP-Sil-5 CB column. Peak identification, methyl ester-TMS ether of: 1 = 3α,6β,7α-trihydroxy-5β-cholanoic acid; 2 = 3α,6β,7α,12α-tetrahydroxy-5β-cholanoic acid; 3 = 3α,6α,7α-trihydroxy-5β-cholanoic acid; 4 = 3α,6α,7α,12α-tetrahydroxy-5β-cholanoic acid; 5 = 3α,6β,7β-trihydroxy-5β-cholanoic acid; 6 = 3α,6β,7β,12α-tetrahydroxy-5β-cholanoic acid; 7 = 3α,6α,7β-trihydroxy-5β-cholanoic acid; 8 = 3α,6α,7β,12α-tetrahydroxy-5β-cholanoic acid; I.S. = internal standard (5α-cholestane).

References

[1] G.A.D. Haslewood, Biochem. J., 62 (1956) 637.

[2] S.L. Hsia, in P.P. Nair and D. Kritchevsky (Editors), The Bile Acids: Chemistry, Physiology and Metabolism, Vol. 1 (Chemistry), Plenum Press, New York, 1971, p. 95.

[3] G. Salen, G.S. Tint and A.K. Batta, in G. Gitnick (Editor), Current Hepatology, Vol. 13, Mosby–Yearbook, St. Louis, MO, 1992, Ch. 9, p. 269.

[4] J. Shoda, T. Osuga, R. Mahara, M. Tohma, K. Matasuura, N. Tanaka, Y. Matsuzaki and H. Miyazaki, J. Chromatogr., 488 (1989) 315.

[5] A.K. Batta, S.K. Aggarwal, G. Salen and S. Shefer, J. Lipid Res., 32 (1991) 977.

[6] T. Iida, T. Momose, T. Tamura, T. Matsumoto, F.C. Chang, J. Goto and T. Nambara, J. Lipid Res., 30 (1989) 1267.

[7] T. Kurosawa, R. Mahara, H. Nittono and M. Tohma, Chem. Pharm. Bull. (Tokyo), 37 (1989) 557.

[8] T. Iida, I. Komatsubara, S. Yoda, J. Goto, T. Nambara and F.C. Chang, Steroids, 55 (1990) 530.

[9] S.K. Aggarwal, A.K. Batta, G. Salen and S. Shefer, Steroids, 57 (1992) 107.

[10] A.K. Batta, R. Arora, G. Salen, G.S. Tint, D. Eskreis and S. Katz, J. Lipid Res., 30 (1989) 1953.

[11] L.S. Ettre, Anal. Chem., 36 (1964) 31A.

[12] A.K. Batta, S.K. Aggarwal, G. Salen, R. Mirchandani and S. Shefer, J. Lipid Res., 33 (1992) 1403.

[13] T. Iida, T. Momose, T. Tamura, T. Matsumoto, J. Goto, T. Nambara and F.C. Chang, J. Chromatogr., 389 (1987) 155.

ELSEVIER

Journal of Chromatography A, 704 (1995) 234–237

JOURNAL OF CHROMATOGRAPHY A

Short communication

Enantiomeric resolution of anionic *R*/*S*-1,1′-binaphthyl-2,2′-diyl hydrogen phosphate by capillary electrophoresis using anionic cyclodextrin derivatives as chiral selectors

Bezhan Chankvetadze[1], Gabriele Endresz, Gottfried Blaschke*

Department of Pharmaceutical Chemistry, University of Münster, Hittorfstr. 58–62, 48149 Münster, Germany

Received 6 December 1994; accepted 10 February 1995

Abstract

The enantioseparation of racemic 1,1′-bi-2-naphthol (1), 1,1′-binaphthyl-2,2′-diyl hydrogen phosphate (2) and 1,1′-binaphthyl-2,2′-diamine (3) using native β-cyclodextrin (β-CD) and its anionic derivatives such as carboxymethyl-β-CD (CM-β-CD), sulfoethyl ether of β-cyclodextrin (SEE-β-CD) and sulfobutyl ether of β-cyclodextrin (SBE-β-CD) has been studied. The successful resolution of 2 in the anionic form using negatively charged cyclodextrin derivatives shows that the role of the Coulombic interactions is not critical for the chiral guest–host recognition in capillary electrophoresis (CE). The application of SEE-β-CD as a chiral selector in CE has been demonstrated for the first time. Comparison of the enantioseparation efficiencies of SEE-β-CD and SBE-β-CD shows that the spacer length and the substitution pattern are factors with rather low importance and that the resolution efficiency is mainly determined by the counter-current mobility of the chiral selector.

1. Introduction

Cyclodextrins (CDs) belong to the most commonly used chiral selectors in analytical chemistry, particularly for gas chromatographic (GC), high-performance liquid chromatographic (HPLC), supercritical fluid chromatographic (SFC) and capillary electrophoretic (CE) enantioseparations. The role of electrostatic forces has been recognized to be very important for the chiral selector–selectand interactions with charged cyclodextrins in CE [1–3,5]. Therefore neutral chiral selectors or chiral selectors carrying a charge opposite to that of the racemic solutes are commonly used for CE enantioseparations. In our previous study the CE enantioseparation of the neutral thalidomide molecule was achieved using very low concentrations of the anionic SBE-β-CD as a chiral selector [4]. No measurable electrostatic interactions exist between the neutral racemic guest and the ionic

* Corresponding author.

[1] Permanent address: Department of Chemistry, Tbilisi State University, Chavchavadze ave 1, 380028 Tbilisi, Republic of Georgia.

0021-9673/95/$09.50
SSDI 0021-9673(95)00186-7

chiral host. This result prompted us to investigate the possibility of chiral recognition in pairs where the racemic solute and the chiral selector both are negatively charged.

2. Experimental

2.1. Equipment

A Grom capillary electrophoresis system 100 (Herrenberg, Germany), equipped with a Linear Instruments (Reno, NV, USA) UVIS 200 detector and a HP 3396 A integrator (Hewlett-Packard, Avondale, PA, USA) was used with (a) an untreated fused-silica capillary (Grom) 41 cm effective length × 50 μm I.D and (b) a polyacrylamide coated capillary with 41 cm effective length × 50 μm I.D. Electric field strength was 400 V/cm, temperature 21 ± 1°C. The racemic samples were introduced hydrostatically (10 cm) for 5 s at the anodic end. Detection of the solutes was carried out at 210 nm. The anode and cathode buffers had the same pH and molarity as the run buffer but contained no chiral selector.

2.2. Chemicals and reagents

The racemic compounds 1,1′-bi-2-naphthol (1), 1,1′-binaphthyl-2,2′-diyl hydrogen phosphate (2) and 1,1′-binaphthyl-2,2′-diamine (3) were purchased from Aldrich (Aldrich-Chemie, Steinheim, Germany). Tris(hydroxymethyl)-aminomethane (Trizma base) was from Sigma (Sigma, St. Louis, MO, USA). Methacrylic acid-3-trimethoxysilylpropylester, Tris-borate-EDTA-buffer, acrylamide, ammoniumpersulfate and N,N,N′,N′-tetramethylethylendiamine used for preparation of polyacrylamide coated capillaries following the procedure described in Ref. [6] were all from Fluka (Fluka Chemie, Buchs, Switzerland). SBE-β-CD (substitution degree approx. 3.14, $M_r = 1684$) was a gift from Prof. J.F. Stobaugh and Prof. V.J. Stella (Center for Drug Delivery Research, The University of Kansas, Lawrence, KS, USA), SEE-β-CD (substitution degree approx. 0.4) and CM-β-CD (substitution degree approx. 0.3) were gifts from Wacker Chemie (Munich, Germany). Analytical grade KH_2PO_4, Na_2HPO_4, H_3PO_4 and NaOH were purchased from Merck (Darmstadt, Germany).

2.3. Buffer and sample preparation

Stock solutions of 50 m*M* KH_2PO_4 and 30 m*M* benzoic acid were prepared in double distilled, deionized water. The pH was adjusted with 0.5 *M* H_3PO_4 or 0.5 *M* NaOH for phosphate buffer and 0.1 m*M* Trizma base for the benzoic acid buffer. The run buffers for the chiral separations were prepared accordingly after the addition of appropriate amounts of the chiral selectors. All solutions were filtered and degassed by sonification before use. Stock solutions of 1 mg/ml of the racemic compounds 1, 2 and 3 were stored at 4°C and diluted to 60 μg/ml before use. CD derivatives were injected into the capillary as 10 mg/ml solutions in the 30 m*M* benzoic acid buffer. The composition and the electrophoretic profile of the chiral anionic selectors were characterized using a polyacrylamide coated capillary. The latter was used to exclude the contribution of electroendoosmotic flow (EOF) in the total mobility of the cyclodextrin derivatives. The 30 m*M* benzoic acid buffer at pH 6.0 was used to detect the CD derivatives at 254 nm (indirect detection mode, due to the shift of the UV absorption of the benzoic acid in the cyclodextrin complexes).

3. Results and discussion

All anionic CD derivatives used are heterogenous mixtures of components with different degrees of substitution and as a consequence with different anionic mobilities at pH 6.0 characterized by CE in a polyacrylamide coated capillary (Fig. 1).

The enantioseparations were carried out using all four chiral selectors at pH 3.0 and 6.0 to ensure that both 2 and 3 are resolved as anionic and cationic species respectively. The existence of 2 in an anionic form under the experimental

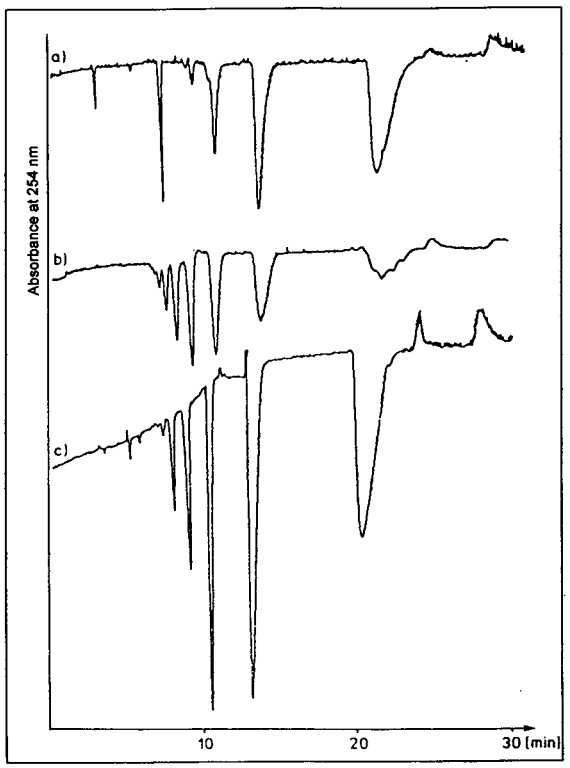

Fig. 1. Electropherograms of CM-β-CD (a), SBE-β-CD (b) and SEE-β-CD (c) used as chiral selectors. Polyacrylamide coated fused-silica capillary with 41 cm effective length was filled with 30 m*M* benzoic acid buffer at pH 6.0. Solutions (5 m*M*) of the CD derivatives were injected hydrostatically on the cathodic end and detected using indirect detection technique at 254 nm. The field strength was maintained at −345 V/cm.

conditions used, but without cyclodextrins, has been additionally confirmed by comparison of the mobility with the EOF, which has been measured as the migration time of the neutral marker mesityl oxide (MSO). The migration times of MSO and compound 2 were 6.2 and 21.3 min, respectively.

The results of the enantioseparations are shown in Fig. 2 and Table 1. These results illustrate that contrary to the expectations the anionic chiral selector SBE-β-CD more effectively separates the enantiomers of the negatively charged compound 2 than those of the corresponding neutral analyte 1 at pH 6.0. This result was confirmed with the other negatively

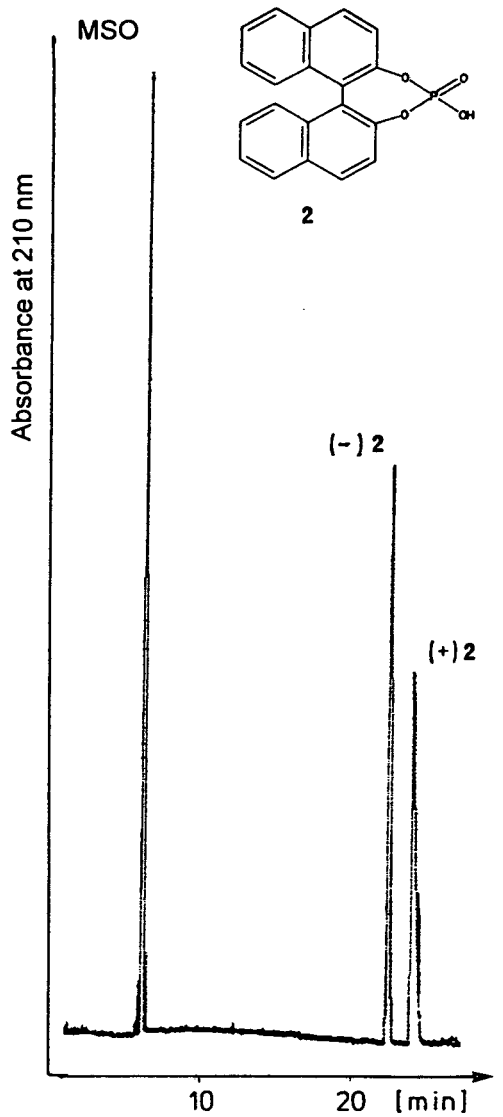

Fig. 2. Electropherogram of 1,1′-binaphthyl-2,2′-diyl hydrogen phosphate 2. Uncoated fused-silica capillary with 43 cm effective length was filled with 0.5 m*M* SBE-β-CD/50 m*M* phosphate buffer at pH 6.0. The field strength was maintained at 400 V/cm. The sample was injected hydrostatically at the anode. The EOF was measured as the migration time of mesityl oxide (MSO).

charged CD derivatives SEE-β-CD and CM-β-CD. Amine 3 exists at pH 6.0 as a neutral substance and is resolved as such. However the enantioseparation is more efficient at pH 3.0.

Table 1
Enantioseparation parameters

Solute	pH	α_{rel}			
		SBE-β-CD	SEE-β-CD	CM-β-CD	β-CD
1	6.0	poor chiral recognition			no separation
2	6.0	1.03	1.02	1.06	no separation
3	3.0	1.05	1.04	1.14	1.09

The latter result can not necessarily be ascribed to a more stereospecific binding of the protonated form of 3 to SBE-β-CD in comparison with the neutral form. Another explanation is the strongly inhibited EOF at low pH while the EOF does not favor the enantioseparation [4,5]. The results given in Table 1 confirm that negatively charged CD-derivatives resolve the enantiomers not only of neutral and cationic, but also of anionic racemates.

In conclusion, the anionic cyclodextrin derivatives such as CM-β-CD, SEE-β-CD and SBE-β-CD exhibit a chiral recognition ability not only to positively charged and neutral analytes but also for negatively charged analytes. On the basis of this finding the role of the Coulombic interactions in the host–guest complexation using CD-hosts seems not to be critical. Additionally, SEE-β-CD has been used as a chiral selector in CE for the first time and it exhibited a chiral recognition ability comparable to that of SBE-β-CD (Table 1). These two derivatives have a different spacer length and degree of substitution but surprisingly they are characterized by a quite similar electrophoretic profile (Fig. 1). Also the CM-β-CD proved to be a mixture of several compounds. This result leads to the conclusion that the role of the spacer length and the substitution pattern seem to be factors of rather low importance and that the efficiency of the enantioseparation is determined mainly by the counter-current mobility of the chiral selectors as already emphasized in previous studies by us [4,7] and others [5,8].

Acknowledgements

The authors thank Heinrich-Hertz-Stiftung for a stipend (B.Ch.), the Deutsche Forschungsgemeinschaft for financial support, Prof. J.F. Stobaugh and Prof. V.J. Stella, University of Kansas (Lawrence, Kansas, USA) for a sample of SBE-β-CD and Wacker Chemie (Munich, Germany) for a sample of SEE-β-CD and CM-β-CD.

References

[1] A. Nardi, A. Eliseev, P. Bocek and S. Fanali, J. Chromatogr., 638 (1993) 247.
[2] Th. Schmitt and H. Engelhardt, Proceedings of the 15th International Symposium on Capillary Electrophoresis (P. Sandra, Editor), 1993, p. 1163.
[3] Th. Schmitt and H. Engelhardt, Chromatographia, 37 (1993), 475.
[4] B. Chankvetadze, G. Endresz and G. Blaschke, Electrophoresis, 15 (1994) 804.
[5] R.J. Tait, D.O. Thompson, V.J. Stella and J.F. Stobaugh, Anal. Chem., 66 (1994), 4013.
[6] S. Hjerten, J. Chromatogr., 347 (1985) 191.
[7] B. Chankvetadze, G. Endresz and G. Blaschke, J. Chromatogr. A, 700 (1995), 43.
[8] I.S. Lurie, R. Klein, T.A. Dal Cason, M.J. LeBelle, R. Brenneisen and R.E. Weinberger, Anal. Chem., 66 (1994) 4019.

ELSEVIER

Journal of Chromatography A, 704 (1995) 238–241

JOURNAL OF CHROMATOGRAPHY A

Short communication

Suppression of chiral recognition of 3-hydroxy-1,4-benzodiazepines during micellar electrokinetic capillary chromatography with bile salts

S. Boonkerd, M.R. Detaevernier, Y. Michotte*, J. Vindevogel

Department of Pharmaceutical Chemistry and Drug Analysis, Pharmaceutical Institute, Vrije Universiteit Brussel, Laarbeeklaan 103, 1090 Brussels, Belgium

Received 15 December 1994; accepted 23 January 1995

Abstract

During the development of a micellar electrokinetic chromatographic screening method for 1,4-benzodiazepines, peak splitting and broadening were observed for some 3-hydroxy-1,4-benzodiazepines (oxazepam, lorazepam, temazepam and lormetazepam). This phenomenon occurred when the micellar phase consisted of bile salts and can be ascribed to the chiral nature of these surfactants. As the bile salts were applied in order to reduce the capacity factors to an appropriate level, enantiomer separation was not an objective and even disturbing. By increasing the analysis temperature, the chiral recognition of these compounds could be suppressed.

1. Introduction

Capillary electrophoretic techniques have been applied in pharmaceutical analysis with great success [1]. Separations of heterogeneous drug mixtures, containing a few benzodiazepines, have been reported [2,3] but only a limited number of studies were specifically dedicated to 1,4-benzodiazepines [4–7]. Except for the analysis of a few cationic species, which can be electrophores in an acidic buffer [4], neutral to mildly alkaline buffers containing an anionic surfactant have been applied [2,3,5–8]. However, with sodium dodecyl sulphate (SDS), the most popular surfactant in micellar electrokinetic capillary chromatography (MEKC), the capacity factors are high, generally above 20 [9]. Therefore, they elute close to the t_{mc} (retention time of the micelle) and resolution is limited. Some have organic modifiers added to the buffer to reduce capacity factors [3,5–8] but, through the reduction of the electroosmotic flow, this also leads to prolonged analysis times [6]. Another way to reduce k' values is to replace SDS with a less solubilizing surfactant, such as bile salts [10]. However, being chiral, bile salts also have the ability to interact differently with enantiomers [11]. This can lead to unwanted peak broadening or peak splitting. Pure 3-hydroxy-1,4-benzodiazepine enantiomers are difficult to isolate, are quickly racemized in aqueous medium [12,13] and are clinically used in racemic forms [14]. Therefore, enantiomeric recognition is not required for drug quality control or screening

* Corresponding author.

0021-9673/95/$09.50
SSDI 0021-9673(95)00098-4

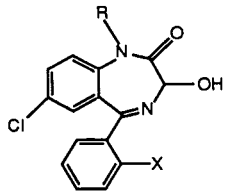

	R	X
Oxazepam	H	H
Temazepam	CH_3	H
Lorazepam	H	Cl
Lormetazepam	CH_3	Cl

Fig. 1. Benzodiazepines used in this study.

purposes, and is in fact a complicating factor. In this paper it will be shown that, for the 3-hydroxy-1,4-benzodiazepines (Fig. 1), chiral recognition can be simply suppressed by increasing the temperature during the MEKC analysis with bile salts.

2. Experimental

Electrokinetic chromatography was performed on a P/ACE 2100 system (Beckman, Palo Alto, CA, USA). Fused-silica capillaries (Beckman) were of 75 μm I.D., 375 μm O.D., 57 or 97 cm long, with the detection window 7 cm from the capillary outlet. The capillaries were liquid cooled at the temperatures indicated.

Temazepam, lorazepam, oxazepam and lormetazepam were obtained from Wyeth Labs. (Maidenhead, Berks., UK). Borate and borate–phosphate buffers were prepared with deionized water (Seralpur Pro 90 CN, Seral, Germany) and contained various amounts of the surfactants sodium cholate (SC) or sodium deoxycholate (SDC) (Sigma, St. Louis, MO, USA). All the buffer solutions were filtered through a 0.2-μm membrane filter.

Samples were introduced by pressure for 2 s, analysed with an applied voltage of 20 kV, unless stated otherwise, and detected at 214 nm. Between runs the capillary was flushed for 2 min with buffer and left to equilibrate for 5 min.

3. Results and discussion

During initial attempts at the MEKC analysis of a set of fourteen derivatives of 1,4-benzodiazepines with bile salts [9], some broadened peaks were observed. After having eliminated sample matrix effects, by preparing the sample in the separating buffer, and recognizing that the unusual peak shapes occurred only for the 3-hydroxy derivatives, it was obvious that chiral selectivity could be the reason for the peak broadening and splitting. The 3-hydroxybenzodiazepines were the only racemates in the mixture. From the literature, it is known that the enantiomers are easily racemized [12,13,15]. It is also known that, when the time scales of racemization and separation are comparable, typical peak interconversion profiles are obtained in which the signal between the elution of the two enantiomers forms a plateau [16], rather than returning to the baseline. This is caused by the fact that, during the analysis, a fraction of the enantiomer species is converted into its mirror image. They will therefore migrate during the first part of the analysis with the characteristics of one enantiomer, and during the remaining time with the characteristics of the other. This phenomenon has been observed in gas chromatography [16] and liquid chromatography [17] and in the MEKC analysis of diastereomeric rotamers [18,19].

By increasing the analysis time (by decreasing the applied voltage or, more efficiently, by increasing the column length, Fig. 2), the split and broadened peaks could be transformed into these typical interconversion patterns. The fact that the same relative intensities in those patterns were observed at four different wavelengths (200, 214, 254 and 280 nm) further contributes to the proof that the observed effects are related to enantiomeric recognition by the bile salt micellar phase. In those cases where peak splitting occurred, the second peak always had a higher intensity. It is known [13,14] that the racemization half-lives of 3-hydroxybenzodiazepines are increased in a less polar, aprotic medium. The hydrophobic micellar interior is enriched with the more retained enantiomer, which can be assumed to have, on average, an increased half-life. Consequently, the formation of a small enantiomeric excess during analysis can be expected.

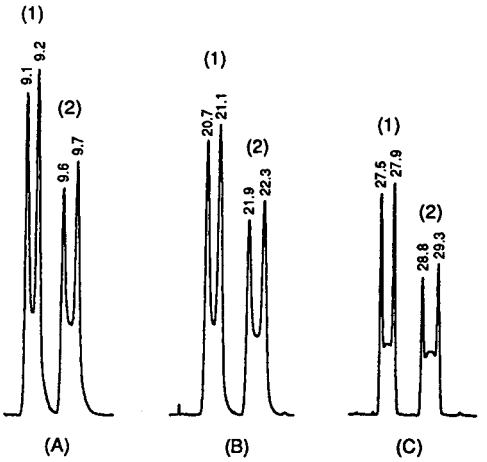

Fig. 2. MEKC separation of (1) temazepam and (2) oxazepam in a bile salt buffer as a function of analysis time [20 m*M* borate–phosphate (pH 8.0), 60 m*M* SC, 20°C]. (A) 20 kV, column length 57 cm; (B) 10 kV, 57 cm; (C) 20 kV, 97 cm.

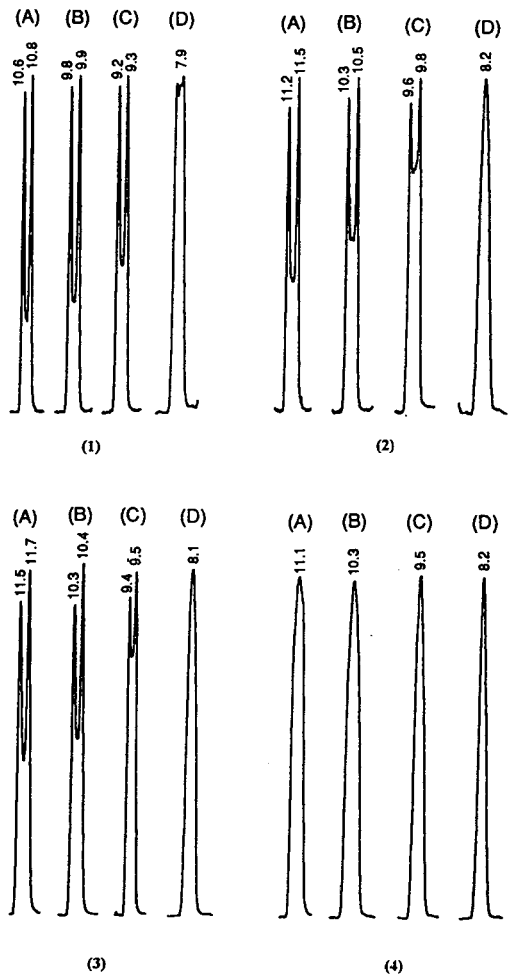

Fig. 3. MEKC separation of (1) temazepam, (2) oxazepam, (3) lorazepam and (4) lormetazepam in a bile salt buffer as a function of temperature [20 m*M* borate (pH 8.0), 50 m*M* SC, 20 kV, column length 57 cm]. Temperature: (A) 20; (B) 22; (C) 25; (D) 30°C.

In contrast, increasing the temperature leads to an increase in the racemization speed. Once fast enough, in relation to the analysis time, chiral recognition is no longer observed and single, sharp peaks are obtained (Fig. 3). The results shown were obtained with SC as surfactant, but comparable results have also been obtained with SDC. Among the four species, lormetazepam enantiomers are known to have the shortest half-life (0.7 min at 37°C and pH 7.5 [15]), and this benzodiazepine is also the easiest to obtain as a sharp single peak. The reported half-lives for the other species at 37°C and pH 7.5 (oxazepam 3.0 min, lorazepam 1.3 min, temazepam 3.4 min [15]) do not correlate well with the degree of peak splitting that is observed. Of course, apart from the different temperature and pH conditions in our experiments, differences in enantioselectivity and capacity factors will also play a role. For lorazepam the half-life at 23°C (also at pH 7.5) was reported to be 5.0 min [15]. This is comparable to the time scale of the analyses shown in Fig. 3.

In the series shown in Fig. 3, some peak splitting can still be observed for temazepam. This could be avoided by further increasing the temperature to 33°C, at which a single, sharp peak was obtained at any pH investigated from 7 to 11. Fig. 4 shows the separation of four 3-hydroxybenzodiazepines after optimization in 20 m*M* borate buffer (pH 10.2) containing 50 m*M* SC and 10% acetonitrile with a fused-silica capillary of length 57 cm at 33°C.

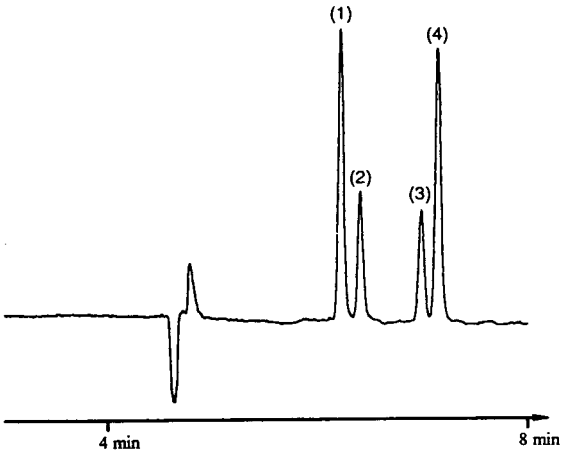

Fig. 4. MEKC separation of 3-hydroxybenzodiazepines [buffer, 20 m*M* borate (pH 10.2), 50 m*M* SC, 10% acetonitrile; 20 kV, column length 57 cm, 33°C]. Peaks: 1 = temazepam; 2 = lormetazepam; 3 = oxazepam; 4 = lorazepam.

References

[1] K.D. Altria, J. Chromatogr., 646 (1993) 245.
[2] P. Wernly and W. Thormann, Anal. Chem., 63 (1991) 2878.
[3] P. Wernly and W. Thormann, Anal. Chem., 64 (1994) 2155.
[4] I.M. Johansson, R. Pavelka and J.D. Henion, J. Chromatogr., 559 (1991) 515.
[5] M. Tomita, T. Okuyama, S. Sato and H. Ishizu, J. Chromatogr., 621 (1993) 249.
[6] M. Schrafroth, W. Thormann and D. Allemann, Electrophoresis (Weinheim), 15 (1994) 72.
[7] I. Bechet, M. Fillet, P. Hubert and J. Crommen, Electrophoresis (Weinheim), 15 (1994) 1316.
[8] M.A. Evenson and J.E. Wiktorowicz, Clin. Chem., 38 (1992) 1847.
[9] S. Boonkerd, M.R. Detaevernier and Y. Michotte, in preparation.
[10] H. Nishi, T. Fukuyama, M. Matsuo and S. Terabe, J. Chromatogr., 513 (1990) 279.
[11] S. Terabe, M. Shibata and Y. Miyashita, J. Chromatogr., 480 (1989) 403.
[12] Y. Aso, S. Yoshioka, T. Shibazaki and M. Uchiyama, Chem. Pharm. Bull., 36 (1988) 1834.
[13] S.K. Yang and X.L. Lu, Chirality, 4 (1992) 443.
[14] T.B. Vree, A.M. Baars and E.W. Wuis, Pharm. Weekbl. Sci. Ed., 13 (1991) 83.
[15] X.L. Lu and S.K. Yang, J. Chromatogr., 535 (1990) 229.
[16] V. Schurig and W. Burkle, J. Am. Chem. Soc., 104 (1982) 7573.
[17] H. Fujima, H. Wada, T. Miwa and J. Haginaka, J. Liq. Chromatogr., 16 (1993) 879.
[18] X.Z. Qin, D.P. Ip and E.W. Tsai, J. Chromatogr., 626 (1992) 251.
[19] B.R. Thomas and S. Ghodbane, J. Liq. Chromatogr., 16 (1993) 1993.

ELSEVIER

Journal of Chromatography A, 704 (1995) 242–246

JOURNAL OF CHROMATOGRAPHY A

Short communication

Determination of palladium(II) as a chloro complex by capillary zone electrophoresis

Hong-Wei Zhang, Li Jia, Zhi-De Hu*

Department of Chemistry, Lanzhou University, Lanzhou, Gansu 730000, China

First received 30 June 1994; revised manuscript received 24 January 1995; accepted 25 January 1995

Abstract

A novel method of separating and determining palladium as the chloro complex $PdCl_4^{2-}$ in the presence of rhodium(III), ruthenium(III), osmium(III) and iridium(III) chloro complexes by capillary zone electrophoresis (CZE) is described. On-column direct UV detection was achieved at 214 nm and the detection limits were lower than 20 ppb. By adding a suitable long-chain cationic surfactants, 0.2 m*M* cetyltrimethylammonium bromide, to the carrier electrolyte to create a layer of positive charges at the capillary wall and by reversing the polarity of the CZE system (cathodic injection and anodic detection scheme), analyte anions were caused to migrate in the direction of the electroosmotic flow, and thus the analysis time (3.0 min) was shortened. The effect of sample stacking on the plate number was investigated.

1. Introduction

Owing to its extremely high separation efficiency, capillary electrophoresis (CE) has proved to be a powerful tool for the determination of inorganic ions and inorganic ion complexes. As long ago as 1967, Hjérten [1] demonstrated the first application of CE to inorganic cations, namely the separation of bismuth and copper cations. Sixteen years later, Tsuda et al. [2] separated copper and iron cations. In 1987, Huang et al. [3] described the separation of rubidium, potassium, sodium, lithium and alkylamines. It is only in the last few years that CE has rapidly expanded to encompass various classes of ions. In 1992 Jones and Jandik [4] listed 129 ionic species found to be separable by CE, including inorganic and organic anions, short-chain anionic surfactants, Group I and II metals, some transition metals (manganese, iron, cobalt, nickel, copper, zinc, cadmium, mercury and lead) and some lanthanides.

However, relatively little attention has been devoted to separating and determining the platinum group metals ruthenium, rhodium, palladium, osmium, iridium and platinum. As we know so far only Buchberger et al.'s work [5] relates to the separation of cyanide complexes of palladium(II) or platinum(II) and some non-platinum group metals, cadmium(II), zine(II), cobalt(II) and cobalt(III). The difficulty in the determination of platinum group metals by CE is that they exist in the form of metal complexes in water, which are stable in solutions of high ligand concentration, which leads to a high ionic strength and great Joule heating.

In this paper, the separation and determination of Pd(II) as chloro complexes are de-

* Corresponding author.

0021-9673/95/$09.50
SSDI 0021-9673(95)00121-2

scribed for the first time. We found the following advantages of determination of platinum group metals as chloro complexes by CZE. First, chloride complexes of platinum group metals are the basis of the qualitative and quantitative analysis of platinum group metals [6] and platinum group metals are usually dissolved in $HCl–HNO_3$, so it is important to determine platinum group metals as chloro complexes. Second, we found that the separation and determination of Pd chloro complexes by CZE in the optimum system gave excellent results i.e., a good detection limit and linear range, compared with the above-mentioned method [5]. Third this method can determine Pd(II) in the presence of Rh(III), Ru(III), Os(III) and Ir(III) chloro complexes and Cu(II), Ni(II), Fe(II), Co(II) and a large amount of Cl^-.

2. Experimental

2.1. Instrumentation

The CE system employed as a Quanta 4000 (Waters Chromatography Division of Millipore, Milford, MA, USA) with a negative power supply. Direct UV detection was achieved with the use of a Zn lamp and a 214-nm optical filter. Waters AccuSep fused-silica capillaries (52.2 cm × 75 μm I.D.) were used throughout. Data acquisition was carried out with a Maxima 820 chromatography workstation (Waters) with a system interface module connecting the CE system to the station. Collection of electrophoretic data was initiated by a signal cable connection between the Quanta 4000 and the system interface module.

2.2. Reagents and carrier electrolytes

All chemicals were of analytical-reagent grade. A palladium(II) stock standard solution (1.00 mg/ml) was prepared by dissolving 0.1000 g of palladium metal in aqua regia, fuming the solution to dryness with hydrochloric acid and diluting to 100 ml with 1 *M* hydrochloric acid. The stock standard solution was diluted to 10.00 μg/ml Pd with deionized water. Further dilution was carried out as required by using a solution containing at least a 200-fold stoichiometric excess of Cl^- to ensure sufficient chloride to form the Pd(II) chloro complex. Rh(III), Ru(III), Os(III) and Ir(III) stock standard solutions (100 μg/ml) were prepared by exactly weighing on an analytical balance the appropriate salt, $(NH_4)_2OsCl_6$, which required the addition of 5.0 g of ascorbic acid as reducing agent for dissolution, $(NH_4)_2Rh(H_2O)Cl_5$, $(NM_4)_2Ru(H_2O)Cl_5$ and $(NH_4)_3IrCl_6 \cdot H_2O$ (Aldrich), then dissolving them in 20 ml of 6 *M* HCl and finally diluting to 100 ml with deionized water.

Carrier electrolytes of 50 m*M* HCl–KCl (50 m*M* Cl^-) containing 0.2 m*M* cetyltrimethylammonium bromide (CTAB) were prepared by mixing appropriate volumes of 50 m*M* HCl containing 0.2 m*M* CTAB and 50 m*M* KCl solution containing 0.2 m*M* CTAB, and then if necessary titrating with KOH solution to achieve the required pH. The electrolyte was prepared daily, degassed and filtered through a 0.45-μm membrane prior to use.

2.3. Procedure for electrophoresis

Gravity injection was used. A 3-min capillary purge was performed prior to all injections. The purge was accomplished by a 12–15 p.s.i. vacuum applied to the receiving electrolyte vail. The sample was injected at the cathode and the detector was placed 7.25 cm from the receiving electrolyte end. The electroosmotic flow μ_{eo} was determined from the migration time of formamide.

3. Results and discussion

3.1. Effect of pH on electrophoretic mobility

Fig. 1 shows the effect of pH on electrophoretic mobility μ_e of Pd(II) chloro complex for 50 m*M* HCl–KCl carrier electrolyte containing 0.2 m*M* CTAB. The pH range is from 2.80 to 5.95 because the electric current hardly changes within this range, and thus the effect of

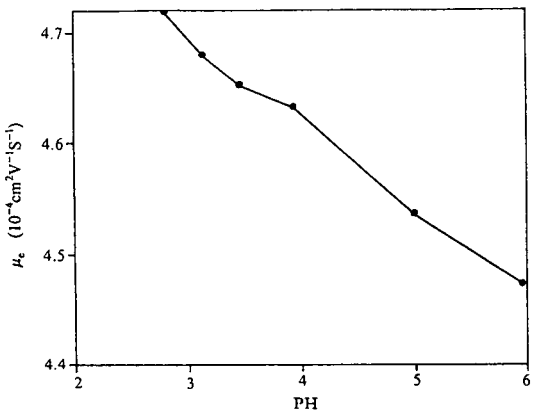

Fig. 1. Effect of pH on the electrophoretic mobility μ_e of the Pd(II) chloro complex. Carrier electrolyte, 50 m*M* HCl–KCl containing 0.2 m*M* CTAB at different pH values; untreated fused-silica capillary, 52.2 cm × 75 μm I.D.; applied voltage, 15 kV.

electric current can be eliminated. Fig. 1 shows that the electrophoretic mobility decreases with increasing pH. The $PdCl_4^{2-}$ complex slightly hydrolyses with increasing pH. The hydrolysates are complicated, and may be $PdH_2OCl_3^-$, $PdOHCl_3^{2-}$, etc. The average number of Cl^- ligands decreases with increasing pH, so the effective electrophoretic mobility of the Pd(II) complex decreases. This conclusion was further confirmed by the following experiment.

3.2. Influence of the concentration of Cl^- on migration time, plate number and peak area

We found that the Cl^- concentration of the carrier electrolyte influences the migration time of the Pd(II) chloro complex. Considering that zones do not travel at the same velocity for different Cl^- concentrations of the carrier electrolyte, we corrected the peak area for the differences in zone velocity to obtain the actual influence of concentration of Cl^- on peak area. We refer to the general peak area, with units of peak response (μV s), as the temporal peak area, S_t. The correction involves simply multiplying the temporal peak area S_t by the zone velocity. Thus the influence of zone velocity on peak area is eliminated. We refer to the corrected peak area, with units of the peak response (μV cm), as the spatial peak area, S_l. A similar correction for band width was made by Huang et al. [7] to analyse the contributions of the various factors to band width.

From Table 1, the Cl^- concentration of the carrier electrolyte influences the migration time, peak height, plate number and temporal peak area, but hardly influences the spatial peak area. Generally, increasing the concentration of carrier electrolyte increases the migration time owing to the decreased electroosmotic mobility [8]. For the Pd(II) chloro complex, with increasing Cl^- concentration of the carrier electrolyte, the electroosmotic mobility also decreases, but the migration time decreases. The decreased migration time is due to the change in the degree of complexation: the average ligand number and effective negative charge of the Pd(II) chloro complex increase with increasing ligand Cl^- concentration, which results in an increase in the effective electrophoretic mobility. Therefore, it can be concluded that the larger the degree of

Table 1
Influence of Cl^- concentration (C) of carrier electrolyte on migration time (t), peak height (H), plate number (N), temporal peak area (S_t) and spatial peak area (S_l) of Pd(II) chloro complex

C (m*M*)	t (min)	H (μV)	N ($\times 10^{-4}$)	S_t (μV s)	S_l (μV cm)
5	4.220	349	0.54	2752	489
10	4.130	655	1.9	2728	495
25	3.838	1025	4.7	2511	490
50	3.327	1409	8.8	2198	495

Conditions: voltage, 15 kV; carrier electrolyte, HCl–KCl of different concentrations containing 0.2 m*M* CTAB at pH 3.0; capillary, 52.2 cm × 75 μm I.D.

complexation of Pd(II) with Cl^-, the larger the effective electrophoretic mobility becomes, which is the same conclusion as in the above discussion about the effect of pH on electrophoretic mobility.

Whereas the effect of Cl^- concentration on migration time is small, it significantly and favourably influences the plate number: with increasing Cl^- concentration, the peak becomes higher and narrower, but the spatial peak area remains almost unchanged. The reason is sample stacking, which is a powerful technique in narrowing the analyte zone length and increasing the number of theoretical plates in capillary ion analysis (CIA). Sample stacking (concentration of the analyte zone) is the process that occurs when a voltage is applied along a capillary tube containing a sample plug with an electric resistivity higher than that of the surrounding carrier electrolyte. From our recent work [9], the "stacking force" (ΔE) is the difference between the field strength along the sample zone E_1 and running carrier electrolyte E_2:

$$\Delta E = E_1 - E_2 = \frac{V}{l_0 + \frac{L}{\rho_0/\rho_2 - 1}} \quad (1)$$

where V is the applied voltage, L is the total length of the capillary, l_0 is the initial length of introduced sample zone, ρ_0 is the electric resistivity of the introduced sample solution and ρ_2 is the electric resistivity of the running carrier electrolyte. From Eq. 1, the smaller is ρ_2, the greater the "stacking force" becomes. The electric resistivity of a strong electrolyte solution is inversely proportional to the solution concentration. Therefore, a general increase in plate number was observed with increasing concentration of Cl^- of the carrier electrolyte. Obviously an increasing Cl^- concentration in the carrier electrolyte has several advantages: the migration time decreases and the peak height and plate number increase.

3.3. Selection of optimum conditions

Based on the above analyses, it is in a solution of low pH and high chloride concentration that the Pd(II) chloro complex is stable and not easy to hydrolyse, which requires the chloride concentrations of both the sample solution and the carrier electrolyte to be high. Moreover, to prevent the band from spreading, the chloride concentration of the carrier electrolyte must be higher than that of the sample solution owing to the "stacking effect'. However, the increase in the chloride concentration and the decrease in the pH of the carrier electrolyte are subject to limits because a solution of low pH and high chloride concentration has a high ionic strength, which results in high conductivity, large current and large Joule heating. Based on the experimental results, 50 m*M* HCl–KCl carrier electrolyte at pH 3.0 was selected as the optimum condition. Further, 0.2 m*M* CTAB, which was also determined by experiment, was added in carrier electrolyte to cause the electroosmotic flow to move in the same direction as $PdCl_4^{2-}$ (towards the anode).

3.4. Limits of detection and quantitative analysis

Based on a peak height of twice of the baseline noise, the detection limit was determined for hydrostatic injection, where the sample was raised by 10 cm for 20 s. The detection limit of $PdCl_4^{2-}$ was 20 ppb for 50 m*M* KCl–HCl carrier electrolyte containing 0.2 m*M* CTAB at pH 3.0. Quantitative determination using hydrostatic injection can be carried out on the basis of a linear relationship between peak area and sample concentration. The linear range was two orders of magnitude above the limit of detection (the correlation coefficient for the calibration curve is 0.9998). The relative standard deviation of the peak area for $PdCl_4^{2-}$ was 3.1% ($n = 8$).

Our experiments showed that $PdCl_4^{2-}$ can be determined in the presence of 20 ppm of Ir(III), Os(III), Rh(III) and Ru(III), 100 ppm of Cu(II), NI(II), Fe(II) and Co(II) and a large amount of Cl^- (see Fig. 2). The cations Cu(II), Ni(II), Fe(II) and Co(II) do not influence the determination of Pd since they travel in the opposite direction to the cathode, and so Fig. 2 does not contain the peaks of Cu(II), Ni(II),

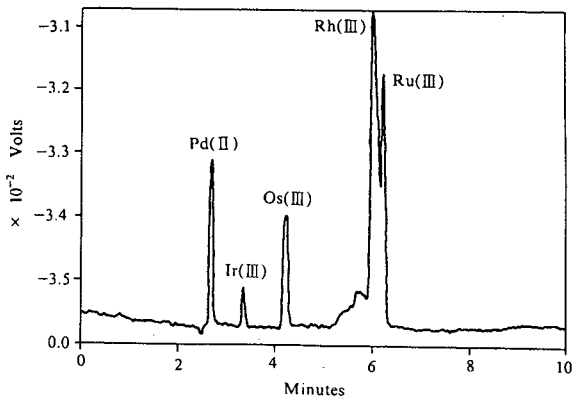

Fig. 2. Electropherogram for the determination of Pd(II) in the presence of 20 ppm each of Ir(III), Os(III), Rh(III) and Ru(III) chloride complexes and 100 ppm each of Cu(II), Ni(II), Fe(II) and Co(II). Carrier electrolyte, 50 m*M* HCl–KCl containing 0.2 m*M* CTAB at pH 3.0. Applied voltage 17 kV. Other experimental conditions as in Fig. 1.

Fe(II) and Co(II). At pH 3.0, Ir(III), Os(III), Rh(III) and Ru(III) chloro complexes easily hydrolyse and they migrate more slowly than the Pd(II) chloro complex (see Fig. 2), so they also do not influence the determination of Pd. Studies are currently being carried to improve the separation selectivity of platinum group metals, such as the simultaneous determination of Pd(II) and Pt(II) as chloro complexes. The potential application of the method, such as in the precious metal mining industry and in the control of waste water from synthetic rubber plants, is great.

Acknowledgement

Thanks are expressed to the National Natural Science Foundation of China for its financial support.

References

[1] S. Hjérten, Chromatogr. Rev., 9 (1967) 122.
[2] T. Tsuda, K. Nomura and G. Nakagawa, J. Chromatogr., 264 (1993) 385.
[3] X. Huang, T.K.J. Pang, M.J. Gordon and R.N. Zare, Anal. Chem., 59 (1987) 2747.
[4] W.R. Jones and P. Jandik, J. Chromatogr., 608 (1992) 385.
[5] W. Buchberger, O.P. Semenove and A.R. Timerbaev, J. High Resolut. Chromatogr. Chromatogr. Commun., 16 (1993) 153.
[6] S.X. Zai and C. Huang, Analysis of Precious Metals, Metallurgical Industries Press, Beijing, 1988, p. 23.
[7] X.H. Huang, W.F. Coleman and R.N. Zare, J. Chromatogr., 480 (1989) 95.
[8] B.B. Van Ormann, G.G. Liversidge, G.L. McIntire, T.M. Olefirowicz and A.G. Ewing, J. Microcol. Sep., 2 (1990) 176.
[9] H.W. Zhang, X.G. Chen and Z.D. Hu, J. Chromatogr. A, 677 (1994) 159.

PUBLICATION SCHEDULE FOR THE 1995 SUBSCRIPTION

Journal of Chromatography A and *Journal of Chromatography B: Biomedical Applications*

MONTH	1994	J	F	M	A	M[a]	J	
Journal of Chromatography A	Vols. 683–688	689/1 689/2 690/1 690/2	691/1 + 2 692/1 + 2 693/1 693/2	694/1 694/2 695/1 695/2	696/1 696/2 697/1 + 2 698/1 + 2	699/1 + 2 700/1 + 2 702/1 + 2 703/1 + 2	704/1 704/2 705/1 705/2	The publication schedule for further issues will be published later.
Bibliography Section				713/1			713/2	
Journal of Chromatography B: Biomedical Applications		663/1 663/2	664/1 664/2	665/1 665/2	666/1 666/2	667/1 667/2	668/1 668/2	

[a] Vol. 701 (Cumulative Indexes Vols. 652–700) expected in October.

INFORMATION FOR AUTHORS

(Detailed *Instructions to Authors* were published in *J. Chromatogr. A*, Vol. 657, pp. 463–469. A free reprint can be obtained by application to the publisher, Elsevier Science B.V., P.O. Box 330, 1000 AH Amsterdam, Netherlands.)

Types of Contributions. The following types of papers are published: Regular research papers (full-length papers), Review articles, Short Communications and Discussions. Short Communications are usually descriptions of short investigations, or they can report minor technical improvements of previously published procedures; they reflect the same quality of research as full-length papers, but should preferably not exceed five printed pages. Discussions (one or two pages) should explain, amplify, correct or otherwise comment substantively upon an article recently published in the journal. For Review articles, see inside front cover under Submission of Papers.

Submission. Every paper must be accompanied by a letter from the senior author, stating that he/she is submitting the paper for publication in the *Journal of Chromatography A* or *B*.

Manuscripts. Manuscripts should be typed in **double spacing** on consecutively numbered pages of uniform size. The manuscript should be preceded by a sheet of manuscript paper carrying the title of the paper and the name and full postal address of the person to whom the proofs are to be sent. As a rule, papers should be divided into sections, headed by a caption (*e.g.*, Abstract, Introduction, Experimental, Results, Discussion, etc.). All illustrations, photographs, tables, etc., should be on separate sheets.

Abstract. All articles should have an abstract of 50–100 words which clearly and briefly indicates what is new, different and significant. No references should be given.

Introduction. Every paper must have a concise introduction mentioning what has been done before on the topic described, and stating clearly what is new in the paper now submitted.

Experimental conditions should preferably be given on a *separate* sheet, headed "Conditions". These conditions will, if appropriate, be printed in a block, directly following the heading "Experimental".

Illustrations. The figures should be submitted in a form suitable for reproduction, drawn in Indian ink on drawing or tracing paper. Each illustration should have a caption, all the *captions* being typed (with double spacing) together on a *separate sheet*. If structures are given in the text, the original drawings should be provided. Coloured illustrations are reproduced at the author's expense, the cost being determined by the number of pages and by the number of colours needed. The written permission of the author and publisher must be obtained for the use of any figure already published. Its source must be indicated in the legend.

References. References should be numbered in the order in which they are cited in the text, and listed in numerical sequence on a separate sheet at the end of the article. Please check a recent issue for the layout of the reference list. Abbreviations for the titles of journals should follow the system used by *Chemical Abstracts*. Articles not yet published should be given as "in press" (journal should be specified), "submitted for publication" (journal should be specified), "in preparation" or "personal communication".

Vols. 1–651 of the *Journal of Chromatography*; *Journal of Chromatography, Biomedical Applications* and *Journal of Chromatography, Symposium Volumes* should be cited as *J. Chromatogr.* From Vol. 652 on, *Journal of Chromatography A* (incl. Symposium Volumes) should be cited as *J. Chromatogr. A* and *Journal of Chromatography B: Biomedical Applications* as *J. Chromatogr. B.*

Dispatch. Before sending the manuscript to the Editor please check that the envelope contains four copies of the paper complete with references, captions and figures. One of the sets of figures must be the originals suitable for direct reproduction. Please also ensure that permission to publish has been obtained from your institute.

Proofs. One set of proofs will be sent to the author to be carefully checked for printer's errors. Corrections must be restricted to instances in which the proof is at variance with the manuscript.

Reprints. Fifty reprints will be supplied free of charge. Additional reprints can be ordered by the authors. An order form containing price quotations will be sent to the authors together with the proofs of their article.

Chromatography in the Petroleum Industry

Edited by **E.R. Adlard**

Journal of Chromatography Library, Volume 56

Petroleum mixtures consist primarily of relatively unreactive complex hydrocarbons covering a wide boiling range. Such mixtures are difficult to separate by most analytical techniques. Therefore, the petroleum industry has for many years played a leading role in the development of chromatographic methods of analysis. Since the last book specifically concerned with chromatographic analysis of petroleum appeared 15 years ago, numerous advances have been made including developments in liquid and supercritical fluid chromatography, the advent of silica capillary columns with bonded stationary phases and the commercial availability of new selective detectors.

The current book contains chapters written by experts concerning the analysis of mixtures ranging from low boiling gases to waxes and crude oils.

Although the volume is specifically aimed at the petroleum analyst, there is much information of general interest which should be of benefit to a very wide readership.

Contents:

©1995 452 pages Hardbound
Price: Dfl. 435.00 (US$ 255.75)
ISBN 0-444-89776-3

ELSEVIER
An imprint of Elsevier Science

ORDER INFORMATION

ELSEVIER SCIENCE B.V.
P.O. Box 330
1000 AH Amsterdam
The Netherlands
Fax: +31 (20) 485 2845

For USA and Canada:
P.O. Box 945, New York
NY 10159-0945
Fax: +1 (212) 633 3680

US$ prices are valid only for the USA & Canada and are subject to exchange rate fluctuations; in all other countries the Dutch guilder price (Dfl.) is definitive. Customers in the European Union should add the appropriate VAT rate applicable in their country to the price(s). Books are sent postfree if prepaid.